Regional Water and Soil Assessment for Managing Sustainable Agriculture in China and Australia

中国与澳大利亚区域农业持续发展中的水土资源评价

Editors: Tim R. McVicar, Li Rui, Joe Walker, Rob W. Fitzpatrick and Liu Changming

Australian Centre for International Agricultural Research
Canberra, Australia 2002

The Australian Centre for International Agricultural Research (ACIAR) was established in June 1982 by an Act of the Australian Parliament. Its mandate is to help identify agricultural problems in developing countries and to commission collaborative research between Australian and developing country researchers in fields where Australia has a special research competence.

Where trade names are used this does not constitute endorsement of, nor discrimination against any product by the Centre.

ACIAR Monograph Series

This peer-reviewed series contains the results of original research supported by ACIAR, or material deemed relevant to ACIAR's research objectives. The series is distributed internationally, with an emphasis on developing countries.

McVicar, T.R., Li Rui, Walker, J., Fitzpatrick, R.W. and Liu Changming, eds. 2002. Regional Water and Soil Assessment for Managing Sustainable Agriculture in China and Australia. ACIAR Monograph No. 84, 384p.

ISBN 1 86320 325 7 (printed)
ISBN 1 86320 326 5 (electronic)

Technical editing and production management: Hilary Cadman and Sue Mathews, Biotext, Canberra, Australia
Design: Peter Nolan, Clarus Design, Canberra, Australia
Chinese translations: Li Lingtao, Canberra, Australia
Printing: Brown Prior Anderson, Melbourne, Australia

Cover photographs:

Background photograph: a test area of upland rice grown on the North China Plain (Lu Zhang).

Front cover inset photographs representing the four main sections of this book (Water balance modelling, Soil-environment impacts, Spatial information systems and Technology transfer):

Top: The array of micro-lysimeters used to measure crop transpiration and soil evaporation at Changwu Agro-ecological Research Station in the tableland area of the Loess Plateau. (Lu Zhang)

Second: Soil erosion, with solutes and colloids being released into waterways in the Mount Lofty Ranges, which form the western edge of the Murray-Darling Basin in southeastern Australia. (Jim Cox)

Third: How winter wheat regional water use efficiency for the North China Plain varies in space and time. (Tim McVicar et al; see Chapter 18)

Bottom: Technology transfer in action as scientists from China and Australia examine soils before discussing findings with the farmer. (Rob Fitzpatrick)

Back cover inset photographs:

Left: Agricultural land typical of southeastern Australia. (Jim Cox)

Right: The rounded mountains and gullies typical of the hilly region of the central Loess Plateau. (Lu Zhang)

1 Water Balance Modelling: Concepts and Applications

Lu Zhang,[*] Glen R. Walker[†] and Warrick R. Dawes[*]

Abstract

Many environmental problems are caused by changes in aspects of the hydrological cycle. Water balance modelling combined with field experiments can give us a better understanding of the components of the hydrological cycle from which to develop appropriate management options. Water balance models can be constructed at any level of complexity. In simple 'bucket' models only the most important processes are represented. When appropriately used, bucket models can provide useful insights into the functional behaviour of a system. Complex models are needed to understand complex feedbacks and interactions among different processes of the system. However, increasing the complexity of a model does not necessarily lead to a more accurate model and it is essential that model complexity matches the availability of data. The key to successful water balance modelling is to have a clearly defined objective and to select an appropriate model. This chapter outlines the principles of water balance modelling and explains how models can be used in crop management.

水文循环要素的变化引起了许多环境问题。水量平衡模型结合野外试验，可以更好地了解水文循环各组成成分、选择合适的管理方式。水量平衡模型可以建造在任意复杂的程度上。简单的“桶式”模型只考虑了最重要的水文循环过程，有助于了解系统内部的功能。如果要理解系统内部过程间的复杂反馈以及相互作用，则需要复杂的模型。不过，增加一个模型的复杂性并不一定就增加了它的精确性，模型的复杂程度必须与能得到的数据相匹配。有一个明确的目标，选择一个合适的模型是建模成功的关键。本文概述了水量平衡模型化的原则，并说明了如何将模型应用在农作物管理方面。

[*] CSIRO Land and Water, PO Box 1666, Canberra, ACT 2601, Australia. Email: lu.zhang@csiro.au

[†] CSIRO Land and Water, Adelaide, SA 5064, Australia.

Lu Zhang, Walker, G.R. and Dawes, W.R. 2002. Water balance modelling: concepts and applications. In: McVicar, T.R., Li Rui, Walker, J., Fitzpatrick, R.W. and Liu Changming (eds), *Regional Water and Soil Assessment for Managing Sustainable Agriculture in China and Australia*, ACIAR Monograph No. 84, 31–47.

THE MOVEMENT of water through the continuum of the soil, vegetation and atmosphere is an important process central to energy, carbon and solute balances. The system is integrated, so changes in one part of the system will affect the others and we need to consider the dynamic interactions and feedback between the processes.

Most current environmental problems arise from tampering with one, or a few, aspects of the system with no understanding of the function of the system as a whole. In Australia, much environmental degradation, including salinisation, is associated with changes in the near-surface water balance induced by massive clearing of native vegetation. These changes have led to significant increases in groundwater recharge, which in turn have led to rising watertables and salinisation. In contrast, the groundwater tables on the North China Plain (NCP) have declined significantly due to overuse of groundwater for irrigation. This presents a serious problem for sustainable agricultural development in the region because there is no reliable surface water for irrigation.

Field techniques alone cannot identify optimal or appropriate land use, because changes occur over a large area and a long time. Also, field experiments are expensive and only a limited number of land-use options can be trialled. For similar reasons, there is a limit to the range of soils and catchments that can be used for field trials. One way to overcome the problem is to combine field experiments with water balance modelling. Modelling takes account of climate variability because it can be used to objectively analyse climatic data and to extrapolate results from short-term field trials over periods of many years. It can also provide an insight into feedbacks and linkages, and help set priorities for field experimentation and data collection.

This chapter deals with the concepts of surface water balance modelling and the processes involved. It briefly describes the WAVES (water, atmosphere, vegetation, energy, soil) model and its application to the NCP and the Australian Mallee region.

Understanding the Hydrological Cycle

The natural occurrence of water circulation near the surface of the Earth, the hydrological cycle, is illustrated in Figure 1. Radiant energy from the sun is the driving force of the cycle, which is generally considered to begin with the evaporation of water from oceans. The resulting water vapour is transported to the atmosphere, where, with favourable conditions, it may produce precipitation. Precipitation may:

- be intercepted by vegetation and evaporated directly back to the atmosphere;
- infiltrate the soil and evaporate from the soil surface or be transpired by vegetation;
- become surface runoff; or
- drain through the soil to form groundwater recharge.

Vegetation influences the hydrological cycle through the exchange of energy, water, carbon and other substances and is therefore critical for many hydrological processes, in particular transpiration, infiltration and runoff. The land phase of the hydrological cycle is of particular interest to those studying the problem of deep drainage.

The movement of water through the hydrological cycle varies significantly in both time and space. Australia, the driest continent, has the highest variability in rainfall and runoff and is therefore a difficult system to model. Torrential rains can flood even the driest part of the continent, while in adjacent areas the story may be very different. The hydrological cycle emphasises the four phases of interest to hydrologists: precipitation, evapotranspiration, surface runoff and groundwater. However, in the context of dryland salinity and recharge control, it is also important to

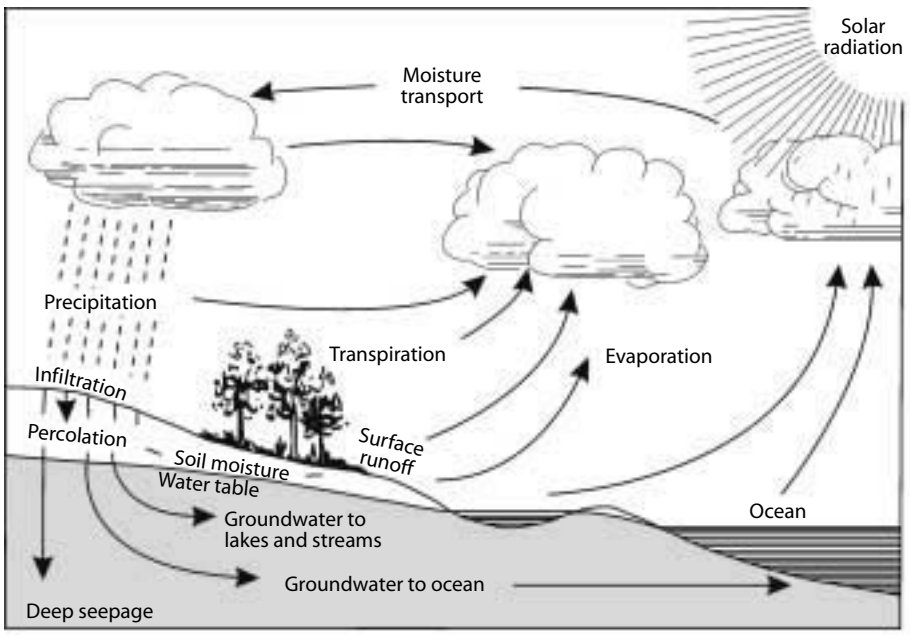

Figure 1. The hydrological cycle.

determine deep drainage and changes in soil water storage. In addition, there can be different relationships between surface water and groundwater. For example, a stream or stream reach can receive groundwater as baseflow or discharge to groundwater. Understanding these relationships can help us to estimate catchment-scale water balance.

Figure 2 shows the three components of the runoff from a catchment:

- surface runoff or overland flow (Q_1)
- subsurface runoff or interflow (Q_2)
- groundwater runoff or baseflow (Q_3).

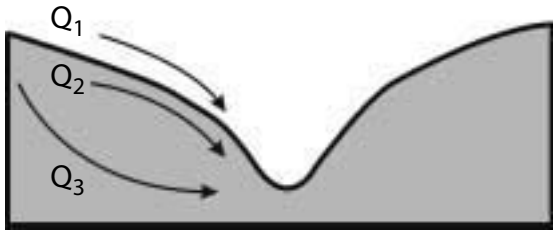

Figure 2. Runoff components.

Surface runoff or overland flow is the water that travels over the surface of the ground towards the stream channel. It can be generated by two mechanisms: infiltration excess runoff (Hortonian overland flow) and saturation excess runoff (Dune and Black overland flow) (Freeze 1974). Infiltration excess runoff often occurs from patches where soils become saturated at the surface. This happens when rainfall intensity exceeds the infiltration capacity of the soils. Hortonian overland flow is an important runoff mechanism in arid and semiarid regions, where rainfalls tend to be intensive and surface infiltration rates low. Saturation excess runoff is generated by rainfall on areas where the soil is already saturated from below. This mechanism of surface runoff generation occurs primarily on the lower slopes of the catchment and along valley bottoms adjacent to stream channels.

Subsurface runoff or interflow represents that portion of infiltrated rainfall that moves laterally through the upper soil layers until it reaches the stream channel. Subsurface runoff moves more slowly than surface runoff. The proportion of total runoff that occurs as subsurface runoff or interflow depends on space–time properties of rainfall and

physical characteristics of the catchment. A thin soil layer overlying more impermeable soil layers tends to promote subsurface runoff or interflow, whereas uniformly permeable soil encourages downward movement of infiltrated rainfall.

Subsurface runoff has always been a popular concept amongst forest hydrologists — indeed amongst humid temperate hydrologists generally. Dunne (1978) termed it subsurface stormflow and used physical models and hydrograph data to show that, even on small catchments, this flow peaked some hours, or even days, after the cessation of rainfall. The real problem is how to model water movement laterally through the soil on hillslopes down to the streamline in real soils. Because this principally occurs in forest with deep litter layers, it has been suggested that most water moves through this litter (see Dunne 1983). However, Beven (1981) has suggested that in fact extensive exfiltration at low rates can create a very shallow flow moving at reasonable speed that meets the time requirements. This is particularly the case where topographic convergence concentrates both the subsurface and exfiltrated water.

Thus, in sloping situations, particularly if there is a reduction in permeability with depth, lateral flow can develop in both the litter layer and the upper soil zone. Water then flows laterally downslope, mostly in a temporarily saturated zone, giving rise to the streamflow element termed interflow or intermediate response flow. The flow emerges in lower parts of the landscape or in the banks of channels and streams to contribute to the streamflow as interflow.

Groundwater runoff, or baseflow, is that portion of infiltrated rainfall that reaches watertables and then discharges into streams. It responds much more slowly to rainfall and does not fluctuate rapidly. It represents the drainage of water to the streamline from the regional or deep groundwater, or both. A minimum catchment area is often needed for such a response to be evident or for the regional groundwater surface to reach the stream incision level. Where we have seasonal rainfall we find that there is virtually an annual hydrograph of baseflow, with levels building up and peaking towards the end of the wet season. If the total outflow is low, then the baseflow may be intermittent or seasonal.

It should be clear that the distinctions between the three components of total runoff are arbitrary. These components can occur separately or simultaneously with varying magnitudes, depending on a combination of climatic and physical conditions of the catchment.

Water Balance

Water balance is based on the law of conservation of mass: any change in the water content of a given soil volume during a specified period must equal the difference between the amount of water added to the soil volume and the amount of water withdrawn from it. In other words, the water content of the soil volume will increase when additional water from outside is added by infiltration or capillary rise, and decrease when water is withdrawn by evapotranspiration or deep drainage. The control soil volume for which the water balance is computed is often determined arbitrarily. In principle, a water balance can be computed for any soil volume, ranging from a small sample of soil to an entire catchment. For the purpose of recharge estimation, it is generally appropriate to consider the root zone as the control volume and express the water balance per unit area.

Figure 3 depicts the water balance for a root zone. The processes represented form a part of the overall hydrological cycle (Fig. 1). Much of the rain that falls during the first part of a storm is intercepted by the canopy and evaporates directly back to the atmosphere. Rainfall that reaches the ground may either infiltrate the soil or run off. Some of the water that infiltrates the soil evaporates directly from the soil surface or is transpired by plants; some may be stored in the soil profile. Water that moves laterally

across the B horizon of the soil is known as subsurface flow; water that moves vertically is known as deep drainage. Deep drainage should not be confused with infiltration. Infiltration is the amount of water that enters the soil; deep drainage is the flux of water below the rooting depth.

The root zone water balance is usually expressed as:

$$\Delta S = P - I - E - T - RO - DD \quad (1)$$

where ΔS is the change in root zone soil water storage over the time period of interest, P is precipitation, I is interception loss, E is direct evaporation from the soil surface, T is transpiration by plants, RO is surface runoff or overland flow, and DD is deep drainage out of the root zone. All quantities are expressed in terms of volume of water per unit land area or equivalent depth of water over the period considered.

The recharge to the groundwater system can be calculated as:

$$R = DD - SSF \quad (2)$$

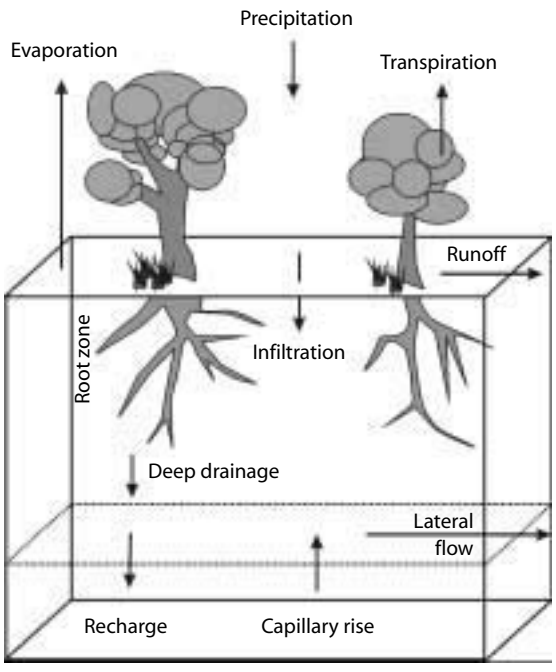

Figure 3. Schematic diagram of the water balance for a root zone.

where SSF is the lateral subsurface flow calculated according to Darcy's law (see 'WAVES' section below).

When the control volume is the entire catchment (Fig. 4), the surface water balance equation can be expressed as:

$$\Delta\langle S\rangle = \langle P\rangle - \langle ET\rangle - \langle Q\rangle - \langle R\rangle \quad (3)$$

where $\Delta\langle S\rangle$ is the change in spatially averaged catchment water storage, $\langle P\rangle$ is the spatially averaged precipitation, $\langle ET\rangle$ is the spatially averaged evapotranspiration, $\langle Q\rangle$ is the spatially averaged catchment surface runoff, and $\langle R\rangle$ is the spatially averaged catchment recharge.

The root zone water balance shown in Figure 3 can be considered as a plot-sized profile in a catchment, as shown in Figure 4. It is tempting to think of the catchment as a collection of such plots, with recharge estimates from each plot being simply added to yield the total recharge for the catchment. A few catchments do operate this way, but most exhibit complex lateral redistribution of water, so it is difficult to estimate catchment scale recharge. One should not assume that recharge estimates from a plot-scale water balance equal the catchment-scale estimates unless thorough hydrogeological investigations are undertaken: plots and catchments differ in terms of hydrological processes, recharge pathways and spatial heterogeneity of soil properties.

Evaluation of Water Balance

The root zone water balance presented by equations (1) and (2) is the basis of water balance modelling. The main advantages of the method are that it uses available data (rainfall, runoff) and has a clear conceptual basis. It seems simple in principle, but in practice it is difficult to measure or estimate each of the components. The evaluation of the water balance equation requires information about the system considered and adequate data.

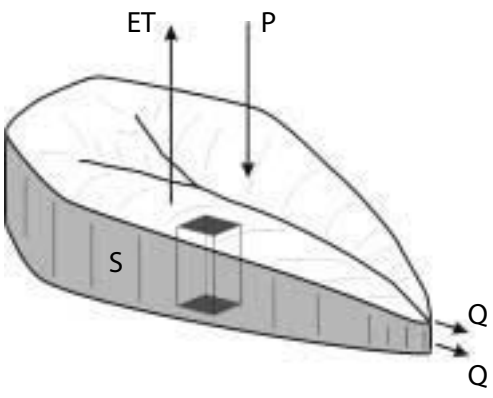

Figure 4. Schematic diagram of a catchment. The box indicates the control volume shown in Figure 3. S = water balance; ET = evapotranspiration; P = precipitation; Q = water runoff or water flow.

Precipitation is often the largest term in the water balance equation and can be measured directly using rain gauges. Interception loss is a complex process affected by factors such as rainfall regime and canopy characteristics. Interception loss can be measured directly in the field or estimated using the method of Horton (1919). Soil evaporation is often lumped together with plant transpiration as total evapotranspiration, which forms the second or third largest term in the water balance equation. Evapotranspiration can be estimated from meteorological and soil moisture data or measured directly. In agricultural fields, the amount of surface runoff generally is considered negligible. However, at catchment scale, runoff may be significant compared to the major components of the water balance; evaluation of this term can be difficult due to different runoff components. The evaluation of the storage term depends on the time period over which the water balance is computed. On an annual basis, the change in water content of the root zone is likely to be small in relation to the total water balance and can be neglected. Over a shorter period, the change in the soil water storage can be significant and must be considered. Different techniques such as the neutron meter and time domain reflectometry (TDR) can be used to measure soil water content. Deep drainage is often only a small fraction of the precipitation — 5% is a typical figure.

Water Balance Modelling

A water balance model can be considered as a system of equations designed to represent some aspects of the hydrological cycle. Depending on the objectives of the study and data availability, modelling can have different levels of complexity, although the model is a simplification of the real world, no matter how complex it may be. A simple bucket model may be suitable for some purposes; in other cases more complex models may be required. It is important to recognise that increasing model complexity does not necessarily improve accuracy (Walker and Zhang 2001).

Simple bucket models

Conceptualisation of the system is based on our understanding of the hydrological cycle and the different pathways that water can take within a catchment. In the simplest case, the control volume (e.g. paddock) is considered as a bucket that is filled up by rainfall and emptied by evapotranspiration. When the bucket is full, extra water is assumed to become deep drainage. The only input data required by this model are rainfall, actual evapotranspiration estimated from potential evapotranspiration and soil water content, and the available water storage capacity. An example of such a model is shown in Walker and Zhang (2001). There are a number of variations to the simple bucket model depending on conceptualisation of the system and methods for estimating evapotranspiration (Walker and Zhang 2001; White et al. 2000; Sophocleous 1991; Rowell 1994; Lerner et al. 1990; Scotter et al. 1979).

Complex models

More complex models are available that deal with soil moisture dynamics — feedback between plant growth and soil moisture (Walker and Zhang 2001). These models are designed to simulate complex interactions within the system, to explore sensitivities to different assumptions and to provide more rigorous analysis of experimental results.

Most have been reasonably well documented and people can be trained to use the models (Walker and Zhang 2001).

However, there are tradeoffs in choosing between complex models and the simple bucket models. One of the drawbacks in using more complex models is that they require more data and more time on the part of the user to understand them. Using a complex model without understanding its general structure, parameter space and input variables can cause problems, and interpreting results from such a model can be difficult because of feedback between processes. There is little point in selecting a complex model if sufficient data are not available. The key to successful modelling is to have very clear objectives, a good understanding of the system and a clear identification of appropriate representations (i.e. a clear conceptualisation of the system and matching of model complexity with data availability). Practical issues associated with complex models are discussed in detail by Hook et al. (1998) and Walker and Zhang (2001).

Matching model complexity with data availability

The present array of different water balance models exists because model users have different applications and purposes, and because of the variety in landscapes and climatic conditions. For some purposes, very simple single bucket water balance models are suitable, but other uses require greater functionality — for example, the ability to predict plant growth and grain yield. With greater functionality comes greater complexity. More complex models often require greater effort in parameterisation, more computing power, and additional work in interpreting results. Perhaps more significant is that error propagation can be more difficult to understand and detect. When selecting a model for a particular application a user needs to balance the desired functionality against complexity and data requirements.

The purpose of water balance modelling is generally to improve our understanding of the critical processes that influence the hydrological cycle and to extend knowledge from field or laboratory experiments to quantitative predictions for other sites and climates. The models are always a simplification of the field processes, but they attempt to account for the most important factors that influence the water balance. Adding predictions of less important processes might give diminishing returns if the costs in greater model complexity start to outweigh the extra value from additional functionality. Different models are just different balances between functionality and complexity; users need to chose a tool with an appropriate balance for their particular purpose. In general, a good rule of thumb is to avoid unnecessary complexity and to achieve a level of process detail consistent with the importance of the process for the application in question. There is not much point in having relatively unimportant processes represented in great detail.

In achieving a balance between simplicity and complexity, users should be aware of two types of modelling errors. The first is 'systematic error' resulting from simplifying assumptions (for example, not considering runoff or macropore flow). As we add more processes to the model and increase its complexity (see Fig. 5), we generally decrease the systematic error. The second type of error is 'calibration error' and results from our lack of knowledge of the parameters that are needed for the model. Generally, as complexity increases, there is greater risk of parameterisation error increasing. There is a need to reach some type of balance. However, it is not easy to quantify the systematic error, so it is not always easy to define exactly the balance between simplicity and complexity. As a guiding principle, a relatively simple model is likely to be required if there are limited data. The simplest model that we can usefully apply is one that captures only those factors that are critical to the processes that are being investigated.

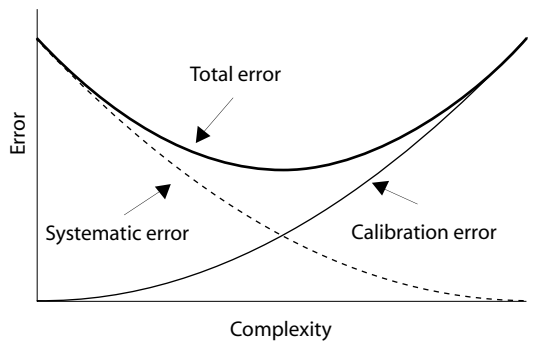

Figure 5. Schematic diagram showing systematic and calibration error.

Model parameterisation

With a significant increase in model complexity there is generally an increase in the number of parameters that are needed. Rainfall and evapotranspiration data are often available. The use of measured data to parameterise models (*direct estimation)* is ideal, but is not always possible. For example, detailed measurements of saturated or unsaturated hydraulic conductivity are usually not available away from research sites. Moreover, we often want to infer measurements over large areas. Where do we obtain these parameters?

One approach is to use more readily available information to estimate the attributes of interest. This is known as *knowledge-based estimation.* For example, there are predictive relationships between soil texture and a range of soil hydraulic properties. These can be combined with information on the distribution of different soil types to make spatial predictions of soil properties. So there is a range of methods for predicting well-defined and measurable *physical parameters*. However, some models contain *process parameters* that are artefacts of the model and not quantities that can be directly measured. Examples of *physical parameters* include water content and saturated hydraulic conductivity; *process parameters* include effective roughness, leaf mortality coefficients, or coefficients that control the rate of water movement between layers in a tipping bucket model. Such *process parameters* can be determined only through *model calibration*.

Model calibration is the process of inferring input parameter values by fitting model outputs to a set of detailed measurements. This constitutes the careful tuning of a model so that its output matches measurements. This should be avoided where possible as it is less desirable than either direct measurement or knowledge-based estimation. If calibration is necessary, the number of parameters that are calibrated should be kept to a minimum and researchers should ensure that the exercise does not result in the model getting the right answers (i.e. matching the measured data) for the wrong reasons. An incorrect mix of input parameter values might enable adequate matching of one set of data but the process description might still be inadequate and fail completely when applied in another set of conditions. Error due to poorly fitted parameters is called *calibration error.* It is desirable in any calibration to consider the function of different submodels separately, rather than just calibrating against integral model outputs such as profile water content.

Generally, models are parameterised using a combination of direct measurement, knowledge-based estimation and a minimum of calibration. Available data for parameterisation are often at the wrong spatial or time scale and sometimes inputs are highly correlated. It is important to have a good knowledge of the sensitivity of the model outputs to the parameterisation data. Then the user will know where to put the most effort into parameterisation through direct measurement, and will have a better understanding of the potential errors in model predictions.

Model testing and sensitivity analysis

Model testing is an essential step in any model development. In a strict sense, no model can be validated. Models are a simplification of reality, so it is necessary to build assumptions into the model. However, the more consistent a tested model is with measured information, the greater the confidence we may have in the tested model. If one is using the

model as an educational or explorative tool, it may not matter that the parameter values do not match reality exactly, as long as they are approximately right. However, if we are using the model for predictions, we must have confidence in the key parameters (Walker and Zhang 2001).

For this reason, we must understand how the conclusions relate to the assumptions of the model and the data used in the model parameterisation. A tested model that is useful for a given objective is one in which the conclusions are robust to both the assumptions and the data. Testing of a model involves a number of steps:

- testing whether assumptions are reasonable;
- testing whether code matches conceptualisation;
- testing the sensitivity of the model to input data and model parameters; and
- testing model outputs against observed data that were not used in model parameterisation.

In going through these steps, it is clear that model testing will always be partly subjective. The simplest method of sensitivity analysis is to vary input parameter values by a set amount or percentage, and evaluate the resulting changes in model output. This provides information about the propagation of error from input data to conclusions. If parameters are changed independently, some important interactions between parameters may be missed. These interactions occur when the response of the model to a change in a particular parameter depends on the values chosen for other parameters. The choice of output variable to use as a measure of model sensitivity is not trivial. Conclusions about the sensitivity or uncertainty analysis will usually change depending on which output parameter was chosen, whether the average, maximum or minimum was chosen, and which spatial and temporal condition was chosen.

WAVES—An Integrated One-Dimensional Energy and Water Balance Model

The WAVES model is designed to simulate energy, water, carbon and solute balances of a one-dimensional soil–canopy–atmosphere system (Dawes and Short 1993; Zhang et al. 1996). It is a process-based model that integrates soil and canopy–atmosphere with a consistent level of process detail. WAVES predicts the dynamic interactions and feedbacks between the processes. Thus, the model is well suited to investigations of hydrological and ecological responses to changes in land management and weather, such as those discussed above.

WAVES models the following processes on a daily time step:

- interception of rainfall and light by the canopy;
- surface energy balance;
- carbon balance and plant growth;
- soil evaporation and canopy evapotranspiration;
- surface runoff and infiltration;
- saturated/unsaturated soil moisture dynamics (soil water content with depth);
- drainage (recharge);
- solute transport of salt (NaCl); and
- watertable interactions.

The WAVES model is based on five balances:

- ***energy balance****:* partitions available energy into canopy and soil for plant growth and evapotranspiration (Beer's law);
- ***water balance****:* handles infiltration, runoff, evapotranspiration (Penman–Monteith equation), soil moisture redistribution

(Richards equation), drainage, and watertable interactions;

- ***carbon balance**:* calculates carbon assimilation using integrated rate methodology (IRM), dynamically allocates carbon to leaves, stems and roots, and estimates canopy resistance for plant transpiration;
- ***solute balance***: estimates conservative solute transport within the soil column and the impact of salinity on plants (osmotic effect only); and
- ***balance*** of complexity, usefulness, and accuracy.

Energy balance

The energy balance module calculates net radiation from incoming solar radiation, air temperature and humidity, then partitions it into canopy and soil available energy using Beer's law. Evapotranspiration is calculated using the Penman–Monteith equation (Monteith 1981) with available energy, vapour pressure deficit, and air temperature as inputs. The Penman–Monteith equation is a 'big leaf' model based on the combination of energy balance and aerodynamic principles. It requires estimation of aerodynamic and canopy resistances. The aerodynamic resistance is estimated from wind speed and surface roughness, while canopy resistance is calculated as a function of net assimilation rate, vapour pressure deficit, and carbon dioxide concentration. WAVES couples canopy and atmospheric data using the approach proposed by Jarvis and McNaughton (1986); it handles multilayer canopies explicitly.

WAVES assumes that the canopy and ground surface temperatures are equal to the average daily air temperature. This assumption does not introduce much error into the energy balance for relatively dense plant stands with nonlimiting water supply (Zhang et al. 1996). The ground heat flux is neglected in the energy balance equation because over land surfaces the daily mean value of the ground heat flux is one or more orders of magnitude smaller than the net radiation.

Water balance

The soil water balance module handles rainfall infiltration, overland flow, soil and plant water extraction, moisture redistribution, drainage (recharge), and watertable interactions. Soil water movement in both the unsaturated and saturated zones is simulated using a fully implicit finite-difference numerical solution of a mixed form of Richards' equation (Richards 1931; Dawes and Short 1993; Short et al. 1995). A full description of the solution to Richards' equation can be found in Dawes and Short (1993). Overland flow can be generated when the rainfall rate exceeds the infiltration rate of the soil, and when rain falls on a saturated surface. Both of the mechanisms are considered explicitly in WAVES. A watertable may develop anywhere within the soil profile. If nonzero slope is specified as input, then lateral subsurface flow occurs via any saturated watertable at a soil layer boundary, and is described by Darcy's law. Researchers can specify a regional groundwater depth, which may be changed daily according to changes in weather, and which can be used to interact with the WAVES soil column. Evaporation and transpiration draw water out of the soil; when the internal saturated water level is below the regional watertable, leakage into the column occurs and may bring salt with it. Conversely, when the internal water level is above the regional watertable, due to plant inactivity or large amounts of infiltration, water may leak out of the column and leach salts.

To solve Richards' equation, the analytical soil model of Broadbridge and White (1988) is used to describe the relationships among water potential, volumetric water content and hydraulic conductivity. This soil model has five parameters: saturated hydraulic conductivity, volumetric soil moisture content at saturation, air-dry volumetric water content, soil capillary length scale, and a soil structure parameter. The Broadbridge and White (1988) soil model can realistically represent a comprehensive range of soil moisture

characteristics, from highly nonlinear associated with a well-developed capillary fringe, to weakly nonlinear associated with highly structured soil and macropores.

The assumptions of Richards' equation are that the soil is incompressible, non-hysteretic and isothermal, and that moisture moves in a single phase only. The equation also assumes that flow is via the soil matrix only, and not via macropores and larger preferred pathways. The soil is assumed to be isotropic for the formulation of Darcy's equation for lateral movement. Any water ponded on the surface can either be left to pond, or appear as runoff within the time step. Soil air flow is ignored.

Carbon balance

The carbon balance and plant growth module calculates daily carbon assimilation from a maximum value and the relative availability of light, water and nutrients. The limiting effects of temperature and salt in the soil water on assimilation are modelled explicitly. It is assumed that the actual growth rate depends on the potential growth rate and the level of the available resources. To combine the three limiting factors on plant growth into a single scalar, we use the IRM of Wu et al. (1994), which allows other limiting factors, such as atmospheric carbon dioxide concentration, to be easily included. Once carbon assimilation is calculated, it is used as input to the dynamic allocation of carbon to leaves, stems and roots, and into the calculation of canopy resistance to transpiration.

Solute balance

Solute transport within the soil column is solved with a convection–dispersion equation, in the same way as soil moisture dynamics (Dawes and Short 1993). It is assumed that the solute concentration does not interact with soil hydraulic properties, so water fluxes and contents are constants with respect to the solutes, and that salt never crystallises out of solution. This makes the solution of solute dynamics explicit. The feedback of salinity to plants is through the reduction in apparent available water due to the osmotic potential induced by dissolved salt (NaCl) alone.

Overall model balance

WAVES emphasises the physical aspects of soil water fluxes and the physiological control of water loss through transpiration. It can be used to simulate the hydrological and ecological effects of scenario management options (e.g. for recharge control). The model strikes a good balance between generality, realism and accuracy, and provides a powerful tool for recharge study.

In what follows, we show how the WAVES model was used to investigate the effects of management on the water balance of irrigated crops on the NCP and to evaluate deep drainage under different cropping rotations in the Australian Mallee region.

Example 1: Modelling the water balance of irrigated crops on the North China Plain

Wang et al. (2001) used the WAVES model to analyse data obtained from field experiments at Luancheng Eco-Agro-System Experimental Station on the NCP and also to simulate the effect of irrigation management on crop growth in the region. Most rain falls in summer so irrigation is required during the winter wheat growing season, when the difference between rainfall and evapotranspiration is large. Corn grows during summer, but some irrigation is still required.

A relevant issue in irrigated agriculture is the relative importance of soil evaporation and transpiration. Results obtained from WAVES modelling suggest that before canopy closure—where the leaf area index (LAI) is less than 1—soil evaporation accounted for 50–90% of total evapotranspiration. There appears to be some scope to improve irrigation efficiency by altering the balance between these two fluxes. One strategy is to reduce soil evaporation by mulching. Covering the

surface with plant residues can reduce radiation and wind at the surface and hence reduce soil evaporation. Reduction of soil evaporation during the first stage when the soil is wet and evaporation is controlled by atmospheric demand can provide the crops with an opportunity to use the moisture in the top soil layers. During the second stage, when the soil is dry and evaporation is controlled by the moisture content, the rate of evaporation is usually much lower than during the first stage and the effect of mulching is likely to be small. The field experiments showed that mulching reduced soil evaporation by 50% under winter wheat (Fig. 6); this is equivalent to 80 mm of water over the entire growing season. In terms of irrigation efficiency, this means that we can reduce irrigation water by 25% over the entire growing season.

To further investigate the effect of irrigation on crop yield (growth), we conducted several scenario simulations using WAVES. The amount of water applied in each irrigation varied from 0–80 mm; Figure 7 shows the resulting leaf area development. It should be noted that irrigation had no impact on crop growth in wet years; in dry years it enhanced crop growth significantly, but the benefit became less obvious as irrigation water supply increased. The results suggest that current irrigation practices in the area tend to overirrigate crops. Given the limited water available for irrigation in the region, resulting in falling groundwater levels, irrigation cannot be maintained sustainably at current levels.

Example 2: Simulating episodic recharge under different crop rotations

Zhang et al. (1999a,b) described two field experiments conducted at Hillston (New South Wales) and Walpeup (Victoria) to see whether changing land use and agronomic practices could reduce groundwater recharge. Various crop and pasture rotations involving fallow, field pea, Indian mustard, wheat, oats, lucerne and medic pastures were considered. The WAVES model was calibrated with the field data and then used to simulate soil moisture content, plant growth and recharge under these rotations.

The WAVES model was able to accurately simulate soil moisture contents at both sites throughout the study period (Fig. 8). The depths were chosen to represent different soil layers and root zones at the two sites. The model was able to reproduce seasonal variations in soil moisture for different soil types under various cropping rotations. To further evaluate the performance of the model in simulating soil water dynamics, we compared calculated and

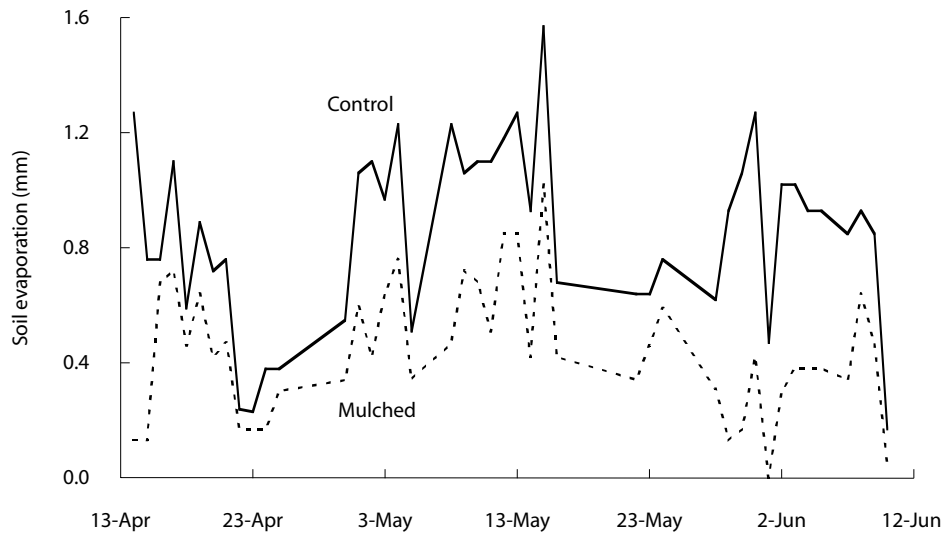

Figure 6. Effect of mulching on daily soil evaporation under winter wheat, 1996.

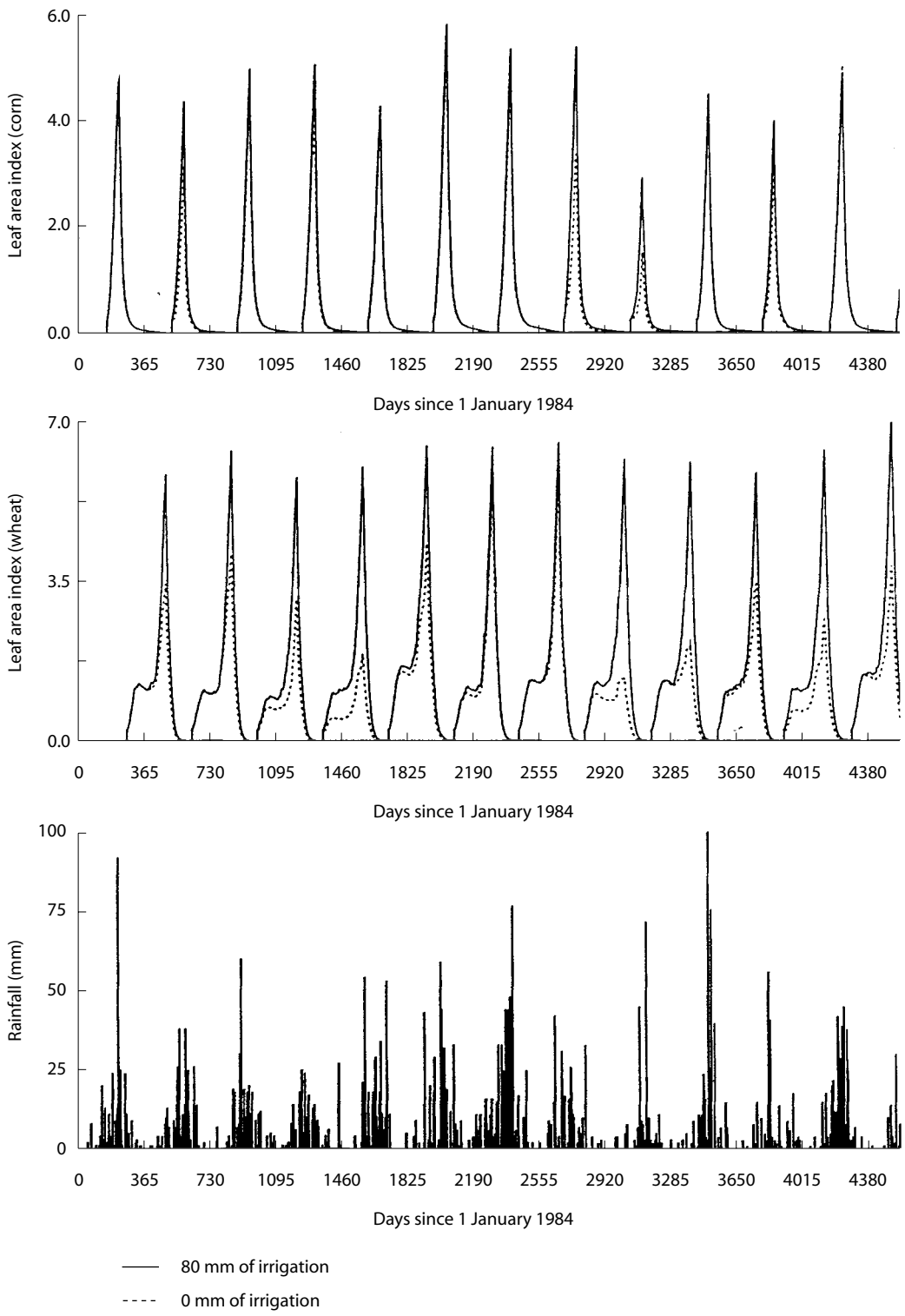

Figure 7. Effects of irrigation on leaf area development as simulated by WAVES.

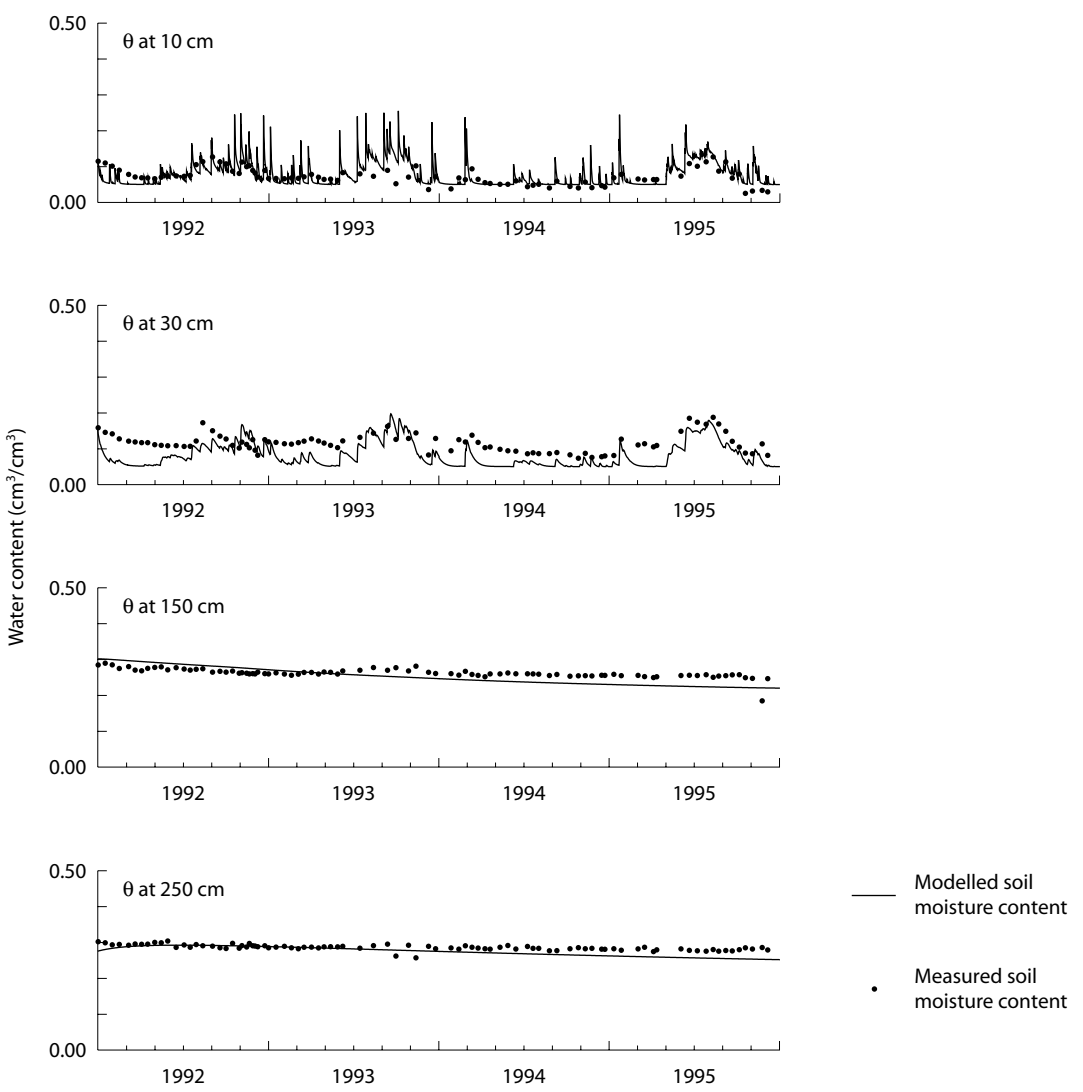

Figure 8. Comparison between modelled and measured soil moisture content at Hillston.

measured soil moisture profiles for different periods. The model agreed very well with the measurements throughout the soil profile (Fig. 9). At Hillston, throughout the study period, there was a drying front associated with maximum rooting density at approximately 1 metre, below which the soil water remained relatively constant.

At Hillston, the simulated recharge rate at 4.0 metre depth increased dramatically after 10 years for the medic rotation but not for the lucerne rotation, which continued to decrease (Fig. 10a). The recharge under medic rotation appeared to respond to the cumulative rainfall anomaly. At Walpeup, a similar trend was observed for the fallow rotation with shallow rooting depth. However, an increase in simulated recharge occurred after 20 years with deep-rooted plants (Fig. 10c). The nonfallow rotation was not sensitive to the cumulative rainfall anomaly, but the fallow rotation was (Figs 10b and 10c). The difference in simulated recharge under fallow and nonfallow rotations is significant.

These results suggest that changes in agronomic practice (for example, fallowing and crop rotation) may take a considerable period of time (more than

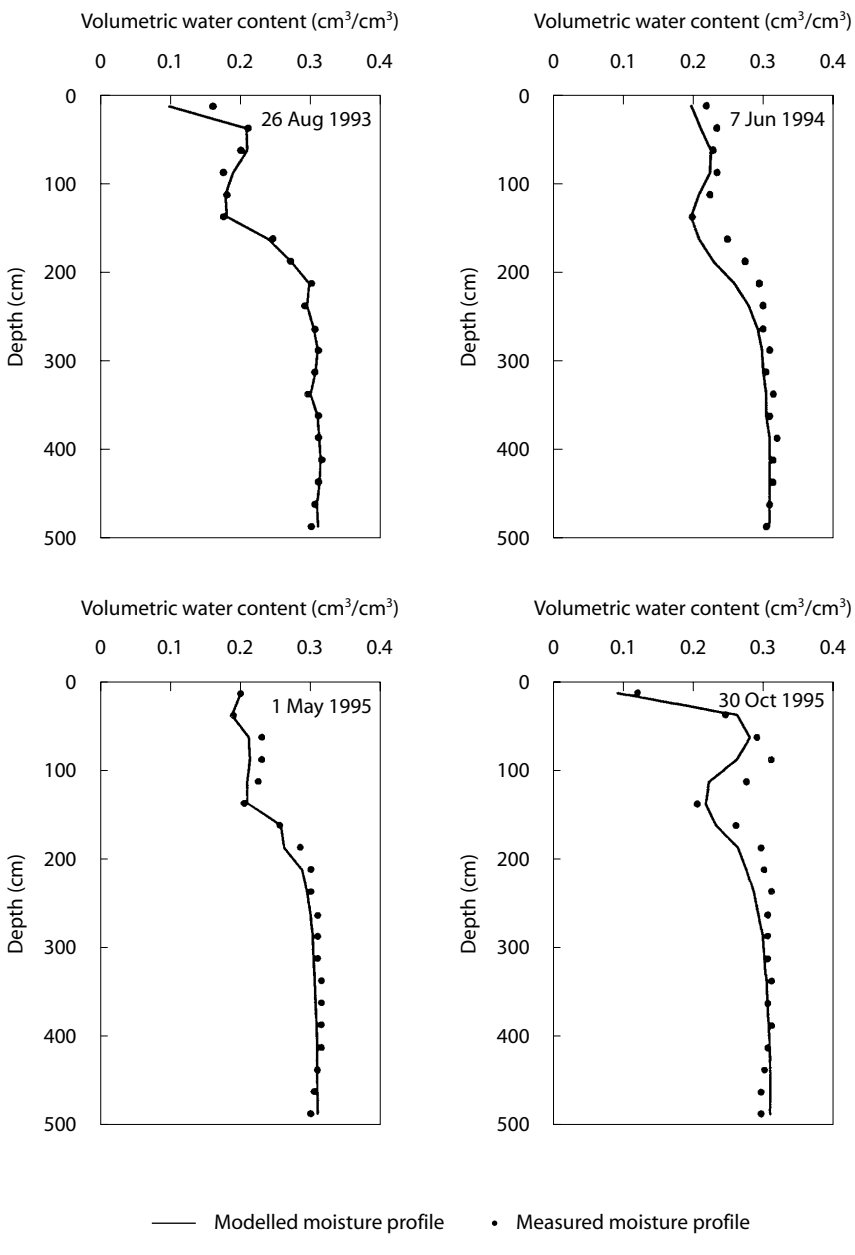

Figure 9. Modelled and measured soil moisture profiles at Walpeup for the selected dates.

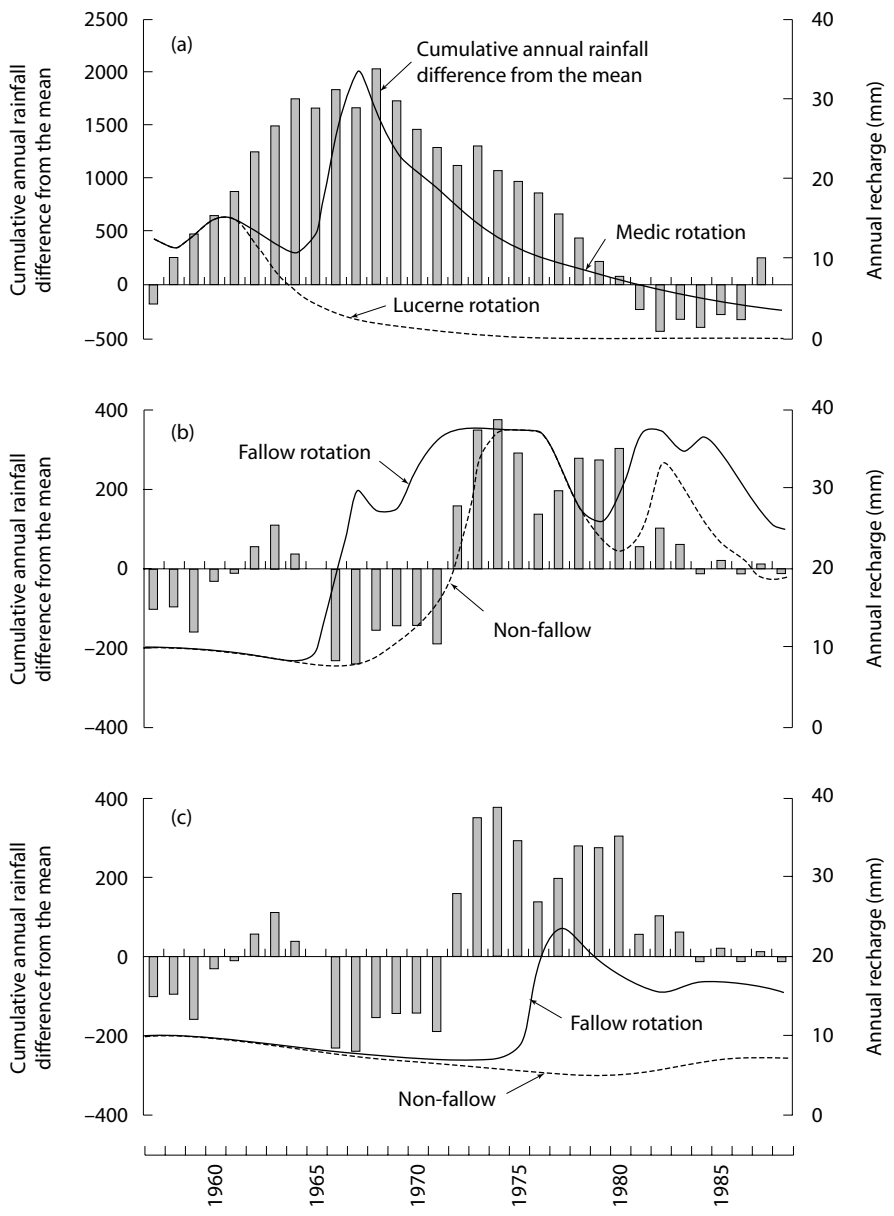

Figure 10. Cumulative annual rainfall differences from the mean and annual recharge rates at 400 cm depth for (a) Hillston under lucerne rotation (- - -) and medic rotation (—); (b) Walpeup with a rooting depth of 50 cm under nonfallow (- - -) and fallow rotation (—); and (c) Walpeup with a rooting depth of 100 cm under nonfallow (- - -) and fallow rotation (—).

10 years) to have any noticeable impact on recharge. The results also showed that deep-rooted plants have better control of recharge, but that the degree of control is modified by soil characteristics and the prevailing weather conditions.

The results showed that the recharge just below the root zone is episodic: it occurs infrequently and its magnitude is significant. Given the fact that plants can only use water in the root zone, the effect of current agronomic practices on episodic recharge is limited. During large rainfall events, the root zone (generally considered as a buffer zone) became saturated and significant recharge occurred. Episodic recharge can therefore substantially reduce the effectiveness of land management options in controlling recharge. This is more so for sandy soils than for clay soils because of low water holding capacity and high infiltration rates.

Acknowledgments

This project was supported by ACIAR (LWR1/95/07).

References

Beven, K. 1981. Kinematic subsurface stormflow. Water Resources Research, 17, 1419–1424.

Broadbridge, P. and White, I. 1988. Constant rate rainfall infiltration: a versatile nonlinear model. 1. Analytic solution. Water Resources Research, 24, 145–154.

Dawes, W.R. and Short, D.L. 1993. The efficient numerical solution of differential equations for coupled water and solute dynamics: the WAVES model. Canberra, CSIRO Division of Water Resources, Technical Memorandum 93/18,.

Dunne, T. 1978. Field studies of hillslope flow processes. In: Kirkby, M.J., ed., Hillslope Hydrology. Chichester, Wiley, 227–294.

Dunne, T. 1983. Relation of field studies and modeling in the prediction of storm runoff. Journal of Hydrology, 65, 25–48.

Freeze, R.A. 1974. Streamflow generation. Reviews of Geophysics and Space Physics, 12, 627–647.

Hook, R.A., Fleming, P.M. and Thomas, C. 1998. Understanding models. In: Willams, J., Hook, R.A. and Gascoigne, H.L., eds, Farming Action—Catchment Reaction: the effect of dryland farming on the natural environment. Melbourne, CSIRO Publishing.

Horton, R.E. 1919. Rainfall interception. Monthly Weather Review, 47, 603–623.

Jarvis, P.G. and McNaughton, K.G. 1986. Stomatal control of transpiration: scaling up from leaf to region. Advances in Ecological Research 15, 1–49.

Lerner, D.N., Issar, A.S. and Simmers, I. 1990. Groundwater recharge—a guide to understanding and estimating natural recharge. Hannover, International Association of Hydrogeologists, Heise.

Monteith, J.L. 1981. Evaporation and surface temperature. Quarterly Journal of the Royal Meteorological Society, 107, 1–27.

Richards, L.A. 1931. Capillary conduction of liquids through porous media, Physics, 1, 318–333.

Rowell, D.L. 1994. Soil Science: methods and applications. New York, John Wiley & Sons, Inc.

Scotter, D.R., Clothier, B.E. and Turner, M.A. 1979. The soil water balance in a fragiaqualf and its effect on pasture growth in Central New Zealand. Australian Journal of Soil Research, 17, 455–465.

Short, D.L., Dawes, W.R. and White, I. 1995. The practicability of using Richards' equation for general purpose soil-water dynamics models. Environment International, 21, 723–730.

Sophocleous, M.A. 1991. Combining the soilwater balance and water-level fluctuation methods to estimate natural groundwater recharge: practical aspects. Journal of Hydrology, 124, 229–241.

Walker, G.R. and Zhang, L. 2001. Plot-scale models and their application to recharge studies. In: Zhang, L. and Walker, G.R., eds, Studies in Catchment Hydrology: the basics of recharge and discharge. Melbourne, CSIRO Publishing.

Wang, H.X., Zhang, L., Dawes, W.R. and Liu, C.M. 2001. Improving water use efficiency of irrigated crops in the North China Plain—measurements and modelling. Agricultural Water Management, 48, 151–167.

White, R.E., Helyar, K.R., Ridley, A.M., Chen, D., Heng, L.K., Evans, J., Fisher, R., Hirth, J.R., Mele, P.M., Morrison, G.R., Cresswell, H.P., Paydar, Z., Dunin, F.X., Dove, H. and Simpson, R.J. 2000. Soil factors affecting the sustainability and productivity of perennial and annual pastures in the high rainfall zone of south-eastern Australia. Australian Journal of Experimental Agriculture, 40, 267–283.

Wu, H., Rykiel Jr., E.J., Hatton, T. and Walker, J. 1994. An integrated rate methodology (IRM) for multi-factor growth rate modelling. Ecological Modelling, 73, 97–116.

Zhang, L., Dawes, W.R. and Hatton, T.J. 1996. Modelling hydrological processes using a biophysically based model—application of WAVES to FIFE and HAPEX-MOBILHY. Journal of Hydrology, 185, 147–169.

Zhang, L., Dawes, W.R., Hatton, T.J., Hume, I.H., O'Connell, M.G., Mitchell, D.C., Milthorpe, P.L. and Yee, M. 1999a. Estimating episodic recharge under different crop/pasture rotations in the Mallee region. 2. Recharge control by agronomic practices. Agricultural Water Management, 42, 237–249.

Zhang, L., Hume, I.H., O'Connell, M.G., Mitchell, D.C., Milthorpe, P.L., Yee, M., Dawes, W.R. and Hatton, T.J. 1999b. Estimating episodic recharge under different crop/pasture rotations in the Mallee region. 1. Experiments and model calibration. Agricultural Water Management, 42, 219–235.

2

Simulation of Field-Scale Water Balance on the Loess Plateau Using the WAVES Model

Ming'an Shao,* Mingbin Huang,* Lu Zhang † and Yushan Li*

Abstract

The Loess Plateau is an important agricultural area in China; its productivity is limited mainly by available water. To achieve sustainable development it is essential to improve crop water use efficiency (WUE). This study describes field experiments on winter wheat that were conducted in 1984–94 at Changwu Agro-ecological Station, which is representative of the highland areas on the Loess Plateau. The study collected data on water and energy balance components, crop growth and yield. A model based on biophysical measurements—WAVES—was used to predict water cycling and crop growth for one-year and 10-year periods. The predictions agreed well with the field measurements. The study showed that WUE on the plateau can be improved by increasing soil fertility (mainly through fertiliser application). The WAVES model provides a useful tool for improving regional WUE for crop production.

黄土高原是中国重要的农业生产区，其生产能力主要受有效水分的制约。作物水分利用效率（WUE）的提高，有助于实现农业持续发展的目标。本章介绍了长武农业生态试验站 1984 到 1994 年间冬小麦的田间试验。该研究收集了水分能量平衡要素、作物生长及产量数据，采用了基于生物物理测量的 WAVES 模型来预测一年期和十年期的水分循环和作物生长。预测结果与野外实测值吻合很好。研究表明黄土高原水分利用效率可通过增加土壤肥力（主要是施肥）来提高。WAVES 模型有助于提高区域作物生产的 WUE。

* State Key Laboratory of Soil Erosion and Dryland Farming, Institute of Soil and Water Conservation, Chinese Academy of Sciences and Ministry of Water Resources, Yangling, Shaanxi 712100, PRC. Email: mashao@ms.iswc.ac.cn

† CSIRO Land and Water, PO Box 1666, Canberra, ACT 2601, Australia.

Ming'an Shao, Mingbin Huang , Lu Zhang and Yushan Li. 2002. Simulation of field-scale water balance on the Loess Plateau using the WAVES model. In: McVicar, T.R., Li Rui, Walker, J., Fitzpatrick, R.W. and Liu Changming (eds), *Regional Water and Soil Assessment for Managing Sustainable Agriculture in China and Australia*, ACIAR Monograph No. 84, 48–56.

THE LOESS Plateau of China is a mainly semiarid area that has some of the most serious soil erosion problems on the globe. Both crop production and environmental quality depend on good water management. For crop production, the objective of water management is to improve water use efficiency (WUE) (Chapter 4 discusses the definition of WUE). WUE involves the transport of water in the soil–plant–atmosphere continuum (SPAC). For example, it is influenced by hydrological and field water balance processes such as precipitation, runoff, infiltration, water uptake by roots, evapotranspiration and drainage. It is easy to measure precipitation and runoff, but evaporation and transpiration are difficult to determine exactly. Many equations and models have been developed to describe water transport processes in SPAC, but most focus on a single process. For example, Eagleson (1978a, b, c, d, e, f, g) focused on statistical-dynamic analysis but this had limited application to areas with striking topographic features and strongly varying seasonal precipitation patterns. Horton (1940) and Philip (1954) described infiltration processes but did not link them with the vegetation. Gardner (1960), Molz and Remson (1970) and Shao et al. (1987, 1988) developed models for water uptake by roots but the models are of limited use for predicting plant growth. Van den Honert (1948) and Shao (1992) used the relationships between electrical current and water flow to develop models for water transport in a soil–plant system, but these models still need to be improved for field conditions.

The existing equations and models cannot describe the material (e.g. water and carbon) cycling and energy balance in SPAC. The WAVES — water, atmosphere, vegetation, energy, soil — model has been described by Zhang et al. (1996), Dawes et al. (1997), Zhang and Dawes (1998) and Zhang et al. (1999). It is an integrated energy and water balance model based on the biophysical processes in SPAC. Chapter 1 provides further information about the WAVES model. In this study, we used the WAVES model to predict water balance in a typical highland area of the Loess Plateau. The main emphasis was on the processes of soil water movement and crop evapotranspiration.

The Overview provides background information about the Loess Plateau. The plateau has an average annual rainfall of 400–600 mm, falling mainly in July, August and September. The annual potential evaporation is 800–1000 mm. Dryland farming is the main form of agriculture. Soils are formed from loess parent materials and have fairly uniform profiles. Most have less than 1% organic matter. Soils have considerable water holding capacity because they are both deep and porous. Groundwater is 20–120 m below the soil surface and is not usually involved in the field water balance. The maximum rooting depth for winter wheat is about 3 m. To this depth, there are fairly significant changes in soil water; below it, the soil water content is relatively constant.

In this chapter, we validate the WAVES model for the highland area on the Loess Plateau by comparing its predictions with field measurements and to identify ways to improve the WUE of crops in the area.

Field Experiments and Data

Changwu Agro-ecological Station is located in the southern part of the Loess Plateau (see Figure 4 of the Overview). The climate is that of the continental monsoon temperate belt. The average annual temperature is 9.1°C and the annual mean precipitation is 587 mm. The accumulated temperature greater than 10°C is 3029°C. There are 171 frost-free days per year. The rainfall is concentrated between July and September. The soil is mapped as Heilou soil. Table 1 shows the particle composition and hydraulic properties of the soil.

Field experiments were carried out on six plots of winter wheat subjected to various degrees of fertiliser application (Table 2). Treatment 1 (T1) had the highest level of fertiliser application; no additional fertiliser was applied to treatment 6. Each

plot had an area of 10.26 × 6.5 m^2. Winter wheat was sown on about 20 September each year and the crop was harvested on about 2 July the following year. Soil water content, leaf area index and crop yield were measured during the growing season. The experiments began in 1984.

Table 1. Properties of Heilou soil at Changwu.

(a) Particle composition

Particle size (mm)	Proportion in soil (%)
> 0.25	0.14
025–0.05	5.86
0.05–0.01	52.80
0.01–0.005	9.10
0.005–0.001	13.60
< 0.001	18.50
< 0.0001	41.20

(b) Hydraulic properties

Property	
Saturated water content (cm^3/cm^3)	0.49
Field capacity (cm^3/cm^3)	0.297
Water content at permanent wilting point (cm^3/cm^3)	0.122
Mean bulk density (g/cm^3)	1.35

Table 2. Experimental fertiliser treatments for winter wheat, Changwu, 1984–present.

Treatment	Nitrogen (kg/ha)	P_2O_5 (kg/ha)	Organic material (kg/ha)
T1	120	60	75,000
T2	120	60	0
T3	0	60	0
T4	120	0	0
T5	0	0	75,000
T6	0	0	0

T1 etc. = treatment 1 etc. (see text for details of treatment)

Soil water content

We used two methods to measure the soil water content in the soil profile — the gravimetric method at 0–30 cm and a neutron probe at 30–300 cm. The measurement interval was 10 cm for the upper 100 cm and 20 cm for the lower 100–300 cm. Measurements were made twice a month for the high fertiliser treatment (T1) and twice a growing season for the other treatments. One measurement was made before sowing, the other after harvest.

Leaf area index

Thirty plants were randomly sampled during every stage of the growing period between September 1985 and July 1986. The length and width of each leaf were measured manually and the results used to calculate the leaf area index (LAI).

Meteorological data

The meteorological data were recorded at Changwu meteorological station next to the experimental plot. The station provides daily maximum and minimum air temperatures, wind velocity, sunshine hours, precipitation, mean daily saturated vapour pressure, and actual vapour pressure. We used the daily meteorological data from 1 September 1984 to 2 July 1994.

Model Calibration

In order to obtain the model parameters, the WAVES model was first run by using the meteorological data between September 1985 and July 1986. We selected vegetation parameters for winter wheat from Zhang et al. (1996) but adjusted the accumulated temperatures and the maximum root depth according to local conditions. The maximum rooting depth for winter wheat was set to 3 m. There were two types of lower boundary conditions. For short-period simulations (one year), the lower boundary was either a drainage

boundary (with a rate of 0.01 mm/day) for a rainy year or zero-flux boundary for a dry year. For long-period simulations (10 years), the lower boundary was assumed to be a zero-flux boundary. This selection of the lower boundary conditions was based on the specific characteristics of the water balance with winter wheat in the area.

The experimental site has a fairly uniform soil profile, so we assumed bulk density to be 1.35 g/cm^3 through the 3 m profile. We also assumed that the soil has just one layer. Table 3 lists the Broadbridge–White soil parameters (Broadbridge and White 1988) from the calibration run for the soil.

Results and Discussion

Leaf area index

Figure 1 shows the LAI predicted by the WAVES model and the measured LAI. The predicted values agreed well with the measurements during the whole growing season. Moreover, the model could predict the peak LAI, which is difficult to obtain by measurement. In the Loess Plateau region, winter wheat has a fairly long growing period. The plants are dormant during winter, when temperatures are low, so both predicted and measured LAI values showed little change between the end of November and March the next year (days 90–200 in Figure 1). From mid-March the crop grew again as temperatures increased. The model simulated well the change of leaf area with time. Figure 2 shows the results for a long-period run. The predictions of LAI by the model were sensitive to the amount of annual precipitation — that is, leaf area increased as rainfall increased, as expected. The peak index values for the 10 years of the simulation ranged from 3.5 to 5.6.

Soil water content

In order to validate the WAVES model for soil water predictions, the model was run for two growing seasons. Figure 3 shows that the predictions were better for short runs than for longer simulations. The relative errors for the 295-day run and the 380-day run were 4.84% and 5.44%, respectively. However, the errors for the 441-day run and the 671-day run were 8.23% and 6.74%, respectively. The largest errors occurred in the upper layer (0–50 cm) of the soil profile; the model underestimated the soil water content in the upper part of the profile

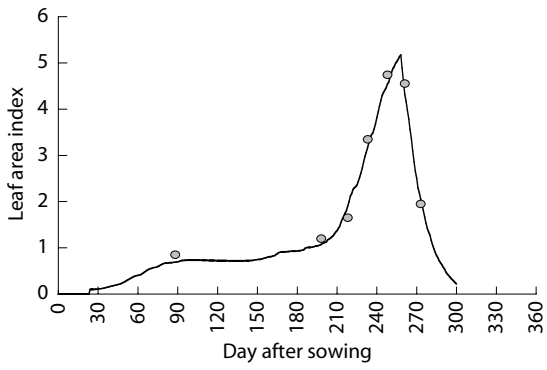

Figure 1. Comparison between predicted (—) and measured leaf area index (LAI) (o) for winter wheat, Changwu.

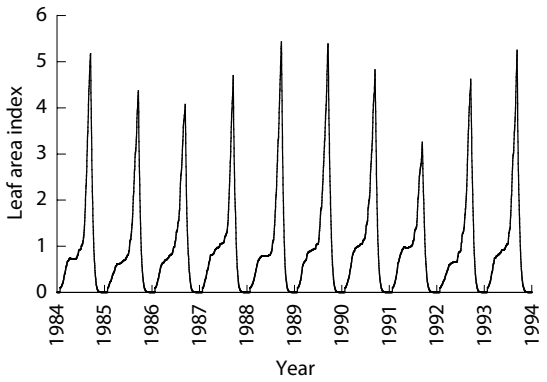

Figure 2. Leaf area index prediction for winter wheat, Changwu, 1984–94.

Table 3. The Broadbridge–White soil parameters for Heilou soil in Changwu.

Layer	Texture	Depth	K_s(m/d)	θ_s (cm^3/cm^3)	Θ_d (cm^3/cm^3)	λ_c(m)	C
1	Loam	0–300 cm	0.45	0.491	0.121	0.45	1.022

K_s = saturated hydraulic conductivity; θ_s = saturated soil water content; Θ_d = air-dry soil water moisture content; λ_c = characteristic length; C = shape parameter related to soil texture and structure

and overestimated it in the lower part of the profile. The reason may be water uptake by the crop roots: relatively deep-rooted winter wheat may take up more water in the lower soil profile than is predicted by the WAVES model because there are more effective roots than expected to extract water from the lower soil layers. For the upper soil profile the result is just the opposite. The WAVES model may be modified for relatively deep-rooted systems by adding more restrictive rules about water uptake by plant roots or by adjusting the weighting factor for the pattern of root distribution.

The model simulated the changes in soil water content at different depths (50 cm, 100 cm and 200 cm). Figure 4 shows that the model could predict changes of soil water content with time for the simulated 10-year period. The relative errors for the three depths were 13.60%, 12.19% and 11.17%, respectively. We stress that the model is good enough for water management for this long period. This will be very useful for making decisions to increase WUE on the Loess Plateau.

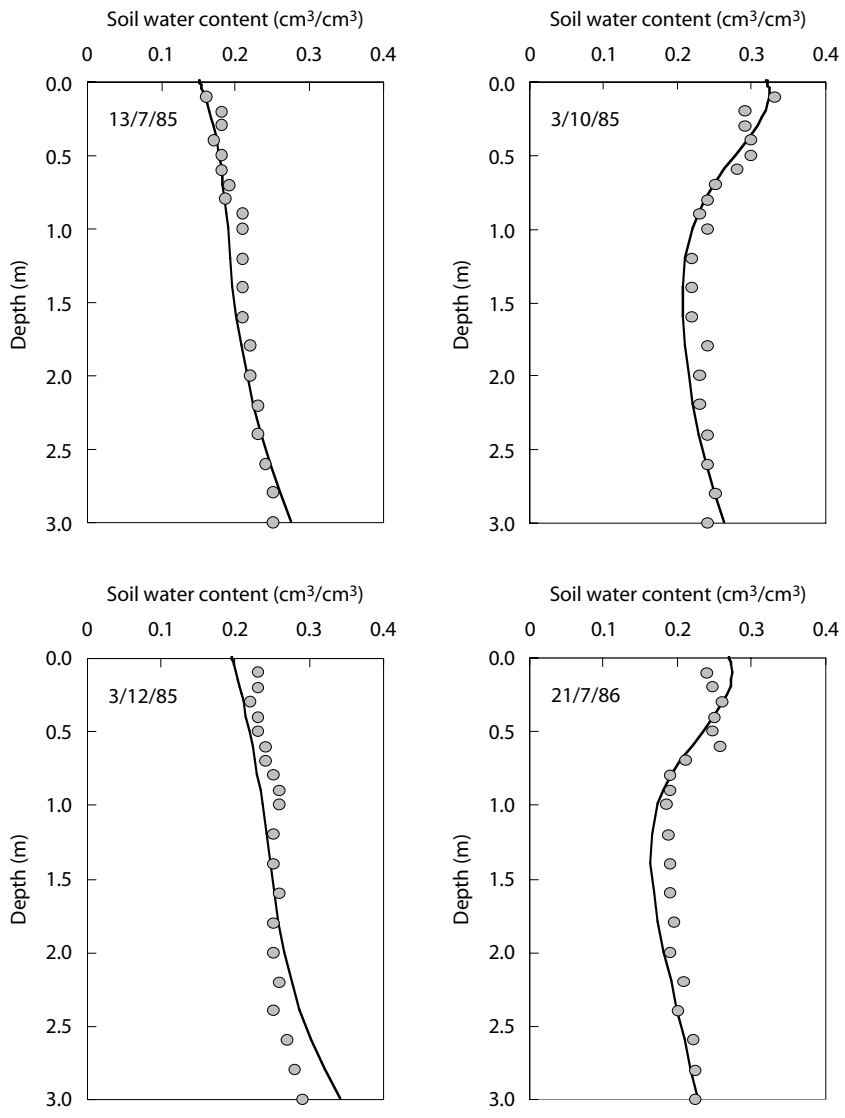

Figure 3. The observed (o) and predicted (–) values of soil water content (cm^3/cm^3) for winter wheat for different simulation periods.

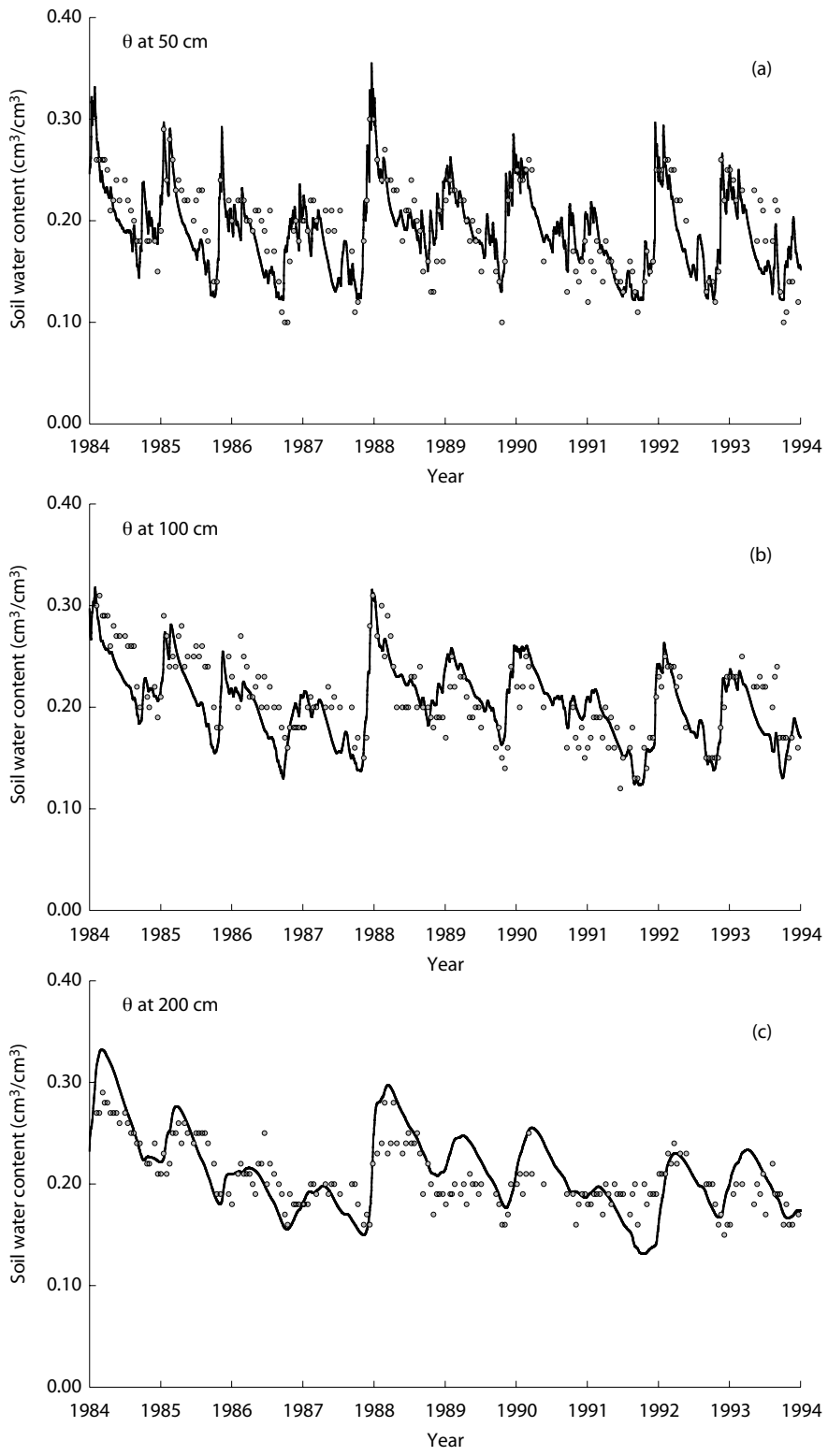

Figure 4. Times series of measured (o) and modelled (–) soil water content, Changwu, 1 September 1984 to 2 July 1994: (a) at 50 cm depth; (b) at 100 cm depth; (c) at 200 cm depth.

Coupling effects of soil water and soil fertility on water balance prediction

Crop production is affected by light, water and nutrients. The WAVES model takes soil nutrient levels into consideration. Nutrients are weighted relative to light (W_N) and the relative availability of nutrients (X_N). Dang (1995) suggested that there is a coupling effect of soil water and soil fertility on crop production. He showed that in a wet year reasonably high fertiliser application could remarkably increase the crop yield; in a dry year the result could be the opposite. The effect of the fertiliser will itself influence water balance and WUE. The water balance prediction of the model does not take this coupling effect into account. We used data from our long-term field experiments to test the ability of the WAVES model to deal with the coupling effect. In the simulation, we assumed $W_N = 1.0$ (Zhang et al. 1996). We calculated X_N from the amount of fertiliser applied, and the degree of optimal combination of light, water and crop yield. Table 4 shows the X_N values, together with simulation results for 1992 (a dry year) (Table 4a) and 1993 (a relatively wet year) (Table 4b).

For all six treatments, the model predicted the water balance better in a wet year than in a dry year. The relative errors were 0.37–5.29% for the wet year and 7.63–12.87% for the dry year. In other words, the effect of fertiliser on crop production appears to depend on the amount of precipitation. This effect is complicated but it would be useful to describe it quantitatively in order to improve the ability of the WAVES model to predict water balance and crop production. More research is needed on this topic.

Crop yield and WUE

Crop yield and WUE are critical issues for agriculture in the Loess Plateau region because of the water shortage there. We used long-term experimental data to study the relationships between crop yield, WUE and the amount of water used. Figure 5 shows the results for treatment 1 (the highest fertiliser application) and treatment 6 (no fertiliser application). Figure 5a shows that there is a

Table 4a. Predicted and measured water balance for experimental fertiliser treatments, Changwu, 18 September 1991 to 18 September 1992.

Treatment	T1	T2	T3	T4	T5	T6
Fertility index	0.87	0.69	0.22	0.42	0.56	0.32
Initial water storage (mm)	521.77	611.13	739.09	658.58	656.53	715.99
Precipitation (mm)	537.50	537.50	537.50	537.50	537.50	537.50
Canopy interception (mm)	10.46	10.71	7.39	9.44	10.33	8.65
Net precipitation (mm)	527.04	526.80	530.11	528.06	527.17	528.86
Evaporation (mm)	288.90	316.46	374.36	338.81	331.77	359.61
Transpiration (mm)	128.04	135.75	89.98	119.83	131.84	108.68
Evapotranspiration (mm)	416.94	452.21	458.64	458.64	463.61	468.28
Drainage (mm)	0	0	0	0	0	0
Predicted final water storage (mm)	631.86	685.72	804.87	727.99	720.09	776.56
Measured final water storage (mm)	699.44	742.37	829.85	826.64	826.45	843.62
Error of the prediction (%)	9.66	7.63	8.17	11.93	12.87	7.95

T1 etc. = treatment 1 etc. (see text for details of treatment)

Table 4b. Predicted and measured water balance for experimental fertiliser treatments, Changwu, 16 September 1992 to 16 September 1993.

Treatment	T1	T2	T3	T4	T5	T6
Fertility index	0.87	0.69	0.22	0.42	0.56	0.32
Initial water storage (mm)	591.91	623.54	712.60	731.41	734.44	728.77
Precipitation (mm)	628.00	628.00	628.00	628.00	628.00	628.00
Canopy interception (mm)	30.767	29.76	20.20	26.59	25.92	24.11
Net precipitation (mm)	597.24	598.24	607.80	601.40	599.09	603.89
Evaporation (mm)	259.47	265.86	302.71	283.01	276.40	290.34
Transpiration (mm)	271.95	267.65	198.50	248.68	265.05	229.74
Evapotranspiration (mm)	531.42	533.51	501.22	531.69	541.44	520.08
Drainage (mm)	25.43	35.17	80.04	84.51	84.06	85.54
Predicted final water storage (mm)	632.30	653.10	739.15	716.62	708.02	727.04
Measured final water storage (mm)	629.8	660.0	780.4	712.5	689.0	744.5
Error of the prediction (%)	0.40	1.05	5.29	0.37	2.75	2.35

T1 etc. = treatment 1 etc. (see text for details of treatment)

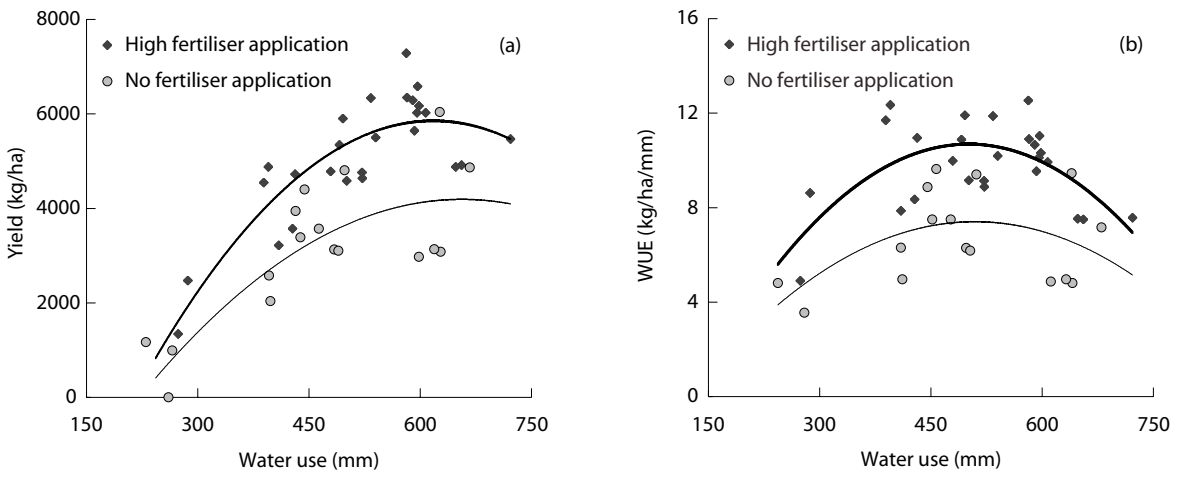

Figure 5. Relationships between water consumption and crop yield (a) or water use efficiency (b), for winter wheat, Changwu.

significant difference in crop yield between the two treatments based on the measurements of eight-year field experiments. Treatment 1 almost always had a higher crop yield than did treatment 6. When water use was 250–500 mm, there was a linear increase of crop yield with water use; this range of water use was the most economically profitable. Crop yield reached a maximum when water use was about 600 mm, after which it decreased. However, Figure 5b shows that WUE reached a peak when water consumption was about 480 mm in the growing season for winter wheat. In other words,

the maximum crop yield does not correspond to the highest WUE. If both maximum crop yield and WUE are being taken into consideration, water management measures may therefore require a compromise. This is the case for agricultural practice on the Loess Plateau. On one hand, the large population requires a high crop yield; on the other hand, a higher WUE is required because water resources are limited.

Conclusions

The study showed that the WAVES model can be used to predict water balance and crop production in the highland areas of the Loess Plateau. Satisfactory predictions were made for both a one-year period and a 10-year period. The predictions for LAI agreed very well with observation. LAI is an important parameter for both water balance prediction and water management practice. However, the model is developed for crops with a relatively shallow root system; it needs to be modified to improve its ability to predict the soil water content for more deep-rooted systems such as winter wheat on the Loess Plateau. This may be achieved by adding more restricted rules about water uptake by roots or by adjusting the weighting factor for the pattern of root distribution.

Acknowledgments

This work was supported by the key projects of G2000018605 and KZCX2-411, NSFC (40025106 and 49871039), and by ACIAR.

References

Broadbridge, P. and White, I. 1988. Constant rate rainfall infiltration: a versatile nonlinear model. Water Resources Research, 24, 145–154.

Dang, T. 1995. Study on modes of fertilizer application of winter wheat in a dryland tableland area for different rainy years. Journal of Soil and Water Conservation, 15(6), 22–27 (in Chinese).

Dawes, W.R., Zhang, L., Hatton, T.J., Reece, P.H., Beale, G. and Packer, I. 1997. Evaluation of a distributed parameter ecohydrological model (TOPOG-IRM) on a small cropping rotation catchment. Journal of Hydrology, 191, 64–86.

Eagleson, P.S. 1978a. Climate, soil and vegetation. 1. Introduction to water balance dynamics. Water Resources Research, 14(5), 705–712.

Eagleson, P.S. 1978b. Climate, soil and vegetation. 2. The distribution of annual precipitation derived from observed storm sequences. Water Resources Research, 14(5), 713–721.

Eagleson, P.S. 1978c. Climate, soil and vegetation. 3. A simplified model of soil moisture movement in the liquid phase. Water Resources Research, 14(5), 722–730.

Eagleson, P.S. 1978d. Climate, soil and vegetation. 4. The expected value of annual evapotranspiration. Water Resources Research, 14(5), 731–740.

Eagleson, P.S. 1978e. Climate, soil and vegetation, 5. A derived distribution of storm surface runoff. Water Resources Research, 14(5), 741–748.

Eagleson, P.S. 1978f. Climate, soil and vegetation. 6. Dynamics of the annual water balance. Water Resources Research, 14(5), 749–763.

Eagleson, P.S. 1978g. Climate, soil and vegetation, 7. A derived distribution of annual water yield. Water Resources Research, 14(5), 765–775.

Gardner, W.R. 1960. Dynamic aspects of water availability to plants. Soil Science, 89, 63–73.

Horton, R.E. 1940. An approach toward a physical interpretation of infiltration-capacity. Soil Science Society of America Proceedings, 5, 399–417.

Molz, F.J. and Remson, I. 1970. Extraction term models of soil moisture use by transpiring plants. Water Resources Research, 6, 1346–1356.

Philip, J.R. 1954. An infiltration equation with physical significance. Soil Science, 377, 153–157.

Shao, M. 1992. On variability of time constant of electrical analog for water flow in soil–plant system. Chinese Science Bulletin, 37(14), 1208–1211.

Shao, M., Yang, W. and Li, Y. 1987. Mathematical model of soil moisture absorption by plant roots. Acta Pedologica Sinica., 24(4), 295–305 (in Chinese).

Shao, M., Yang, W. and Li, Y. 1988. A dynamic model of soil moisture availability to plants in the loessial region. Chinese Science Bulletin, 33(17), 1470–1473.

van den Honert, T.H. 1948. Water transport in plants as a catenary process. Discussions of the Faraday Society, 3, 146–153.

Zhang, L. and Dawes, W. 1998. WAVES—An Integrated Energy and Water Balance Model, CSIRO Land and Water Technical Report No. 31/98. CSIRO Land and Water.

Zhang, L., Dawes, W.R. and Hatton, T.J. 1996. Modelling hydrologic processes using a biophysically based model — application of WAVES to FILE and HAPEX-MOBILHY. Journal of Hydrology, 185, 330–352.

Zhang, L., Dawes, W.R., Slavich, P.G., Meyer, W.S., Thorburn, P.J., Smith, D.J. and Walker, G.R. 1999. Growth and ground water uptake responses of lucerne to changes in groundwater levels and salinity: lysimeter, isotope and modelling studies. Agricultural Water Management, 39, 267–284.

3 Linking Water Balance to Irrigation Scheduling: a Case Study in the Piedmont of Mount Taihang

Xiying Zhang*

Abstract

Irrigation scheduling could reduce the amount of water used to irrigate crops and help to achieve water balance in the piedmont of Mount Taihang on the North China Plain (NCP), where the two staple crops are winter wheat and summer corn. A study at the Chinese Academy of Sciences Eco-Agro-System Experimental Station in Luancheng on the NCP investigated the effect of different irrigation regimes on grain yield and water use efficiency (WUE) in these crops. Irrigation schedules for maximum yield or WUE were established. Yield and WUE did not appear to be linearly related to total evapotranspiration. Maximum profit from a crop was obtained using less water than was needed for maximum yield. High yield, efficient use of water and a net profit from winter wheat were achieved using one, two and three irrigations (60 mm of water per irrigation) in wet, normal and dry years, respectively. Thus, the general practice of irrigating winter wheat four times during the growth period could be changed to irrigating one to three times a year, depending on the rainfall during the winter growing season, a practice that would greatly reduce supplemental water use.

为了维持山前平原地下水采补平衡，减缓地下水位急剧下降的趋势，在太行山山前平原中部的中国科学院栾城生态农业系统试验站进行了冬小麦和夏玉米优化灌溉制度的试验研究。研究结果表明作物的总耗水量与产量的关系不是直线关系，随着耗水量的增加，产量增加，当总耗水量增加到一定程度，产量反而减少，存在着对于产量或水分利用效率的最优耗水量。根据试验结果，建立了灌溉水的生产函数。目前山前平原最大产量下的灌水量大于最大经济效益下的作物灌水量。根据试验结果，太行山山前平原高产区冬小麦常年灌溉次数在 3~4 水，如果实施优化灌溉制度，干旱年灌 3 水、平水年灌 2 水、湿润年灌 1 水，灌水定额 60 毫米，可减少生育期灌水次数 1~2 次，

* Institute of Agricultural Modernization, Chinese Academy of Sciences and Ministry of Water Resources, Shijiazhuang 050021, PRC.
Email: xyzhang1@public.sj.he.cn

Xiying Zhang. 2002. Linking water balance to irrigation scheduling: a case study in the piedmont of Mount Taihang. In: McVicar, T.R., Li Rui, Walker, J., Fitzpatrick, R.W. and Liu Changming (eds), *Regional Water and Soil Assessment for Managing Sustainable Agriculture in China and Australia*, ACIAR Monograph No. 84, 57–69.

冬小麦产量提高 8%-10%，水分生产效率提高 11%-24%，这对减缓本区地下水位的下降有重要意义。

THE NORTH China Plain (NCP) is one of the most important grain production bases in China, providing more than 15% of China's total annual grain production and over 19% of its total winter wheat production. However, the average water resource per capita and per area is about 14% of the average for China (Shi 1995) and the amount of groundwater available for irrigation is decreasing. The Overview provides background information about the region.

The piedmont (the area lying at the foot of a mountain range) of Mount Taihang is a region of high production on the NCP and covers some 50,000 km^2. The groundwater table in the region is currently declining at the rate of 1–1.5 m per year. If this situation continues, the shallow groundwater will run out within 20–30 years and irrigated agriculture will no longer be possible.

Despite the shortage of water, irrigation water is often wasted. Water use efficiency (WUE) and the profit gained from supplemental irrigation is low, due to poor decisions about *when* to irrigate and *how much* water to apply to a crop (Pereira 1999). Improved irrigation scheduling practices could increase yields and profits for farmers, save significant amounts of water, reduce the environmental impacts of irrigation and improve the sustainability of irrigated agriculture (Smith et al. 1996). Irrigation scheduling requires an understanding of the water requirements of a crop and the effect of water on yield. This study investigated the impact of the frequency and timing of irrigation on the yield and WUE of crops in order to establish appropriate irrigation scheduling and thus reduce water use.

Water Deficit in the Piedmont of Mount Taihang

Rainfall

The piedmont of Mount Taihang is in a monsoon climatic zone. Mean annual rainfall is about 480–500 mm but fluctuates greatly from year to year, with a relative variability of 24.4% (Fig. 1). The distribution within a year is also very uneven (Fig. 2), with about 70% of the total rainfall occurring during July to September, the growing season of summer crops. About 25% of the total rainfall occurs during the growing season for winter wheat (October to June) when supplemental irrigation is needed.

Water requirements of crops

In the piedmont of Mount Taihang, two crops are grown each year: winter wheat and summer corn. Winter wheat is usually sown at the beginning of October and harvested during the first 10 days of June; corn is planted in the wheat fields about 5–7 days before harvesting the wheat. Figure 3 shows the total evapotranspiration due to winter wheat and corn under full irrigation at the Chinese Academy of Sciences Luancheng Eco-Agro-System Experimental Station (hereafter referred to as Luancheng Station), located in the central part of the piedmont of Mount Taihang. Measurements were taken over five seasons (1995–2000), using a large-scale weighing lysimeter.

During the five seasons of the study, climate conditions were normal and rainfall was variable. Under full irrigation, the crops encountered no water deficit, so total evapotranspiration represents local evapotranspiration of these crops in normal years without water deficit. Average total transpiration was about 453 mm for winter wheat

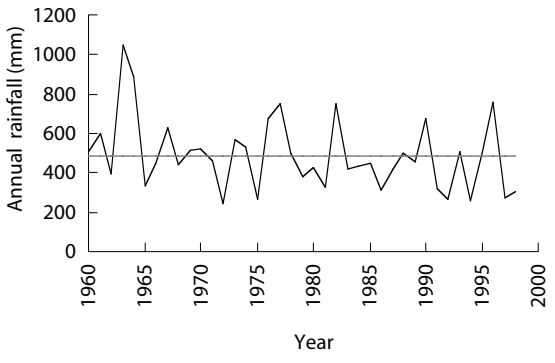

Figure 1. Fluctuation of annual rainfall in the piedmont of Mount Taihang (data averaged from several sites).

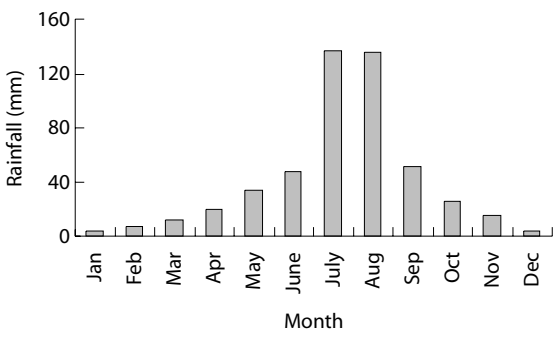

Figure 2. Average monthly rainfall in the piedmont of Mount Taihang (data averaged from several sites from 1961 to 1998).

Figure 3. The total evapotranspiration (mm) of winter wheat and summer corn measured by a large-scale weighing lysimeter from 1995 to 2000 at Luancheng Station. The large-scale weighing lysimeter is designed to contain the original (undisturbed) soil, which weighs 15 tonnes and is 3 m^2 in area and 2.5 m deep. Its metrical precision can reach 0.02 mm.

and about 423.5 mm for corn. The annual water requirements of the two crops in the region ranged from 830 mm (1998–99 season) to 927 mm (1996–97 season), with an average of 876 mm. Average seasonal rainfall is about 126 mm for winter wheat and 362 mm for summer corn. The average difference between water requirements and rainfall is 327 mm for winter wheat and 61 mm for summer corn. The average annual supplemental water required by the two crops can be as high as 388 mm. Irrigation is particularly necessary for winter wheat, because seasonal rainfall may provide less than one-third of the crop's water requirement.

Overdraft of groundwater

Groundwater is the source of most supplemental irrigation. In the piedmont of Mount Taihang, farmers generally irrigate winter wheat four or five times, and summer corn two or three times. As explained above, about 400 mm of supplemental irrigation is needed to ensure that crops in the region encounter no water deficit during the growing period. The quantity of groundwater recharged each year is about 200–250 mm (You 1998), giving a shortfall of 100–150 mm per year. Thus, current irrigation practices are rapidly depleting groundwater resources (Fig. 4). At present, WUE is 1.2–1.5 kg/m^3, well below the level of 2.0 kg/m^3 found in the developed world. It is vital to optimise irrigation scheduling in order to reduce irrigation water use and achieve water balance so that agriculture will be sustainable.

Effective Irrigation Scheduling

The relationship between crop yield and water use is complex. Both the timing of irrigation and the amount of water used can affect yield. The efficient use of irrigation water requires information on the optimum time to apply limited amounts of water to crops to obtain maximum yield and high quality (Al-Kaisi et al. 1997). Crops show different sensitivities to moisture stress at different stages of development (Doorenboss and Kanssan 1979; English and Nakamura 1989; Ghahraman and

Sepaskhah 1997). At some stages, moderate water deficit may not affect crops. Irrigation can be scheduled to take account of the responses of crops to water at different stages of development.

How evapotranspiration relates to grain yield and water use efficiency

In field experiments at Luancheng Station, the most frequent irrigation did not result in maximum yield or WUE. Figures 5 and 6 show how total water consumption for winter wheat and summer corn related to yield and WUE. The relationship was not as linear as reported by Turner (1990). Initially, increasing total water consumption led to an increase in yield and WUE. However, once yield and WUE peaked, any further increase in evapotranspiration led to a decrease in yield and WUE. The amount of water needed for maximum yield is greater than the amount needed for maximum WUE.

Sensitivity of crops to water stress at different stages of development

Crop sensitivity to water stress can be expressed as a mathematical relationship between relative yield and the relative amount of applied water (Jensen 1968):

$$\frac{Y}{Y_m} = \prod_{i=1}^{n} \left(\frac{ET_i}{ET_{i\max}} \right)^{\lambda_i} \qquad (1)$$

In Equation 1, Y is the actual yield under partial irrigation, Y_m is the yield under nonlimiting water use from full irrigation, n is the number of growth stages, ET_i is the actual amount of water used by the crop, ET_{imax} is the nonlimiting crop water use or potential water requirement and λ_i (sensitivity index) is the relative sensitivity of the crop to water stress during the ith stage of growth. The value of λ_i for a given crop is different at the various stages of growth: a more sensitive growth stage has a higher sensitivity index.

Figure 7 shows the effects of water stress on the yield of winter wheat at different growth stages. The highest reduction in yield occurred with water stress at jointing to booting, followed by stress at booting to heading. Water deficit when the crop was turning green or maturing did not affect yield. Equation 1

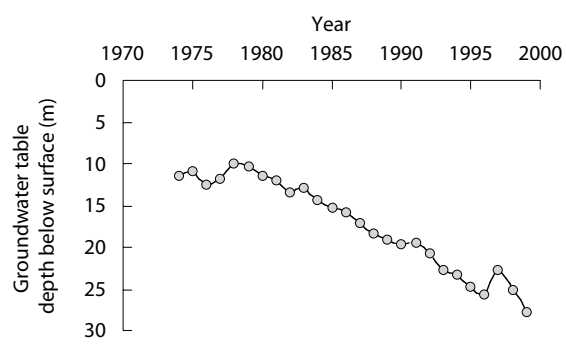

Figure 4. The rapid decline in the groundwater table at Luancheng Station.

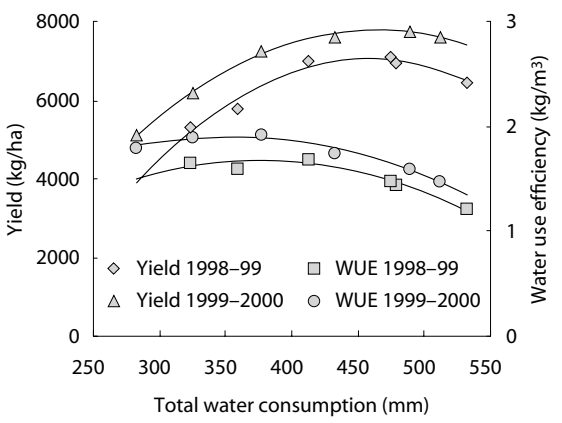

Figure 5. The relation of total water consumption, grain yield and water use efficiency of winter wheat from 1998 to 2000 at Luancheng Station.

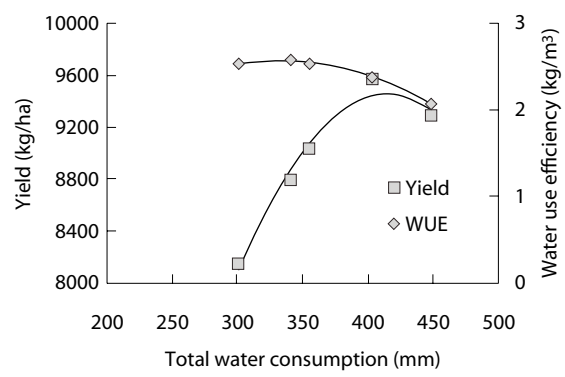

Figure 6. The relation of total water consumption, grain yield and water use efficiency of summer corn in the 1999 season at Luancheng Station.

was used to determine the sensitivity index of winter wheat and summer corn at various growing stages (Table 1). The highest index was at the jointing stage for winter wheat and at the heading to milky filling stage for corn. The negative sensitivity index for winter wheat when recovering (turning green) and maturing may indicate that at these stages moderate water stress is beneficial. The sensitivity index provides a means to determine the optimum time to apply limited amounts of water to obtain maximum yield.

Table 1. The sensitivity index (λ_i) of winter wheat and summer corn to water stress at various growth stages. Results are averaged from data accumulated over several years at Luancheng Station.

(a) Winter wheat

Growth stage	λ_i
Before over-wintering	0.0781
Recovering	–0.1098
Jointing	0.2984
Booting	0.2366
Heading to milky filling	0.1102
Maturing	–0.0541

(b) Summer corn

Growth stage	λ_i
Sowing to jointing	0.1496
Jointing to heading	0.2061
Heading to milky filling	0.3645
Milky filling to maturing	0.1116

Irrigation water efficiency

The irrigation production function describes the relationship between irrigation and crop yield. Researchers such as Zhang et al. (1993) have described this function with the following quadratic relationship:

$$Y = b_0 + b_1 W + b_2 W^2 \quad (2)$$

In Equation 2, Y is the crop yield, W is the total irrigation during the whole growth period of the crop, and b_0, b_1 and b_2 are coefficients.

The yield increase due to irrigation can be divided into three phases. In the first phase, marginal output value is greater than marginal cost; in the second, marginal output value is equal to marginal cost; in the third, marginal output value is lower than marginal cost. The following equations can express the situations:

$$\text{Phase one: } \Delta Y \times Py > \Delta W \times Pw \quad (3)$$
$$\text{Phase two: } \Delta Y \times Py = \Delta W \times Pw \quad (4)$$
$$\text{Phase three: } \Delta Y \times Py < \Delta W \times Pw \quad (5)$$

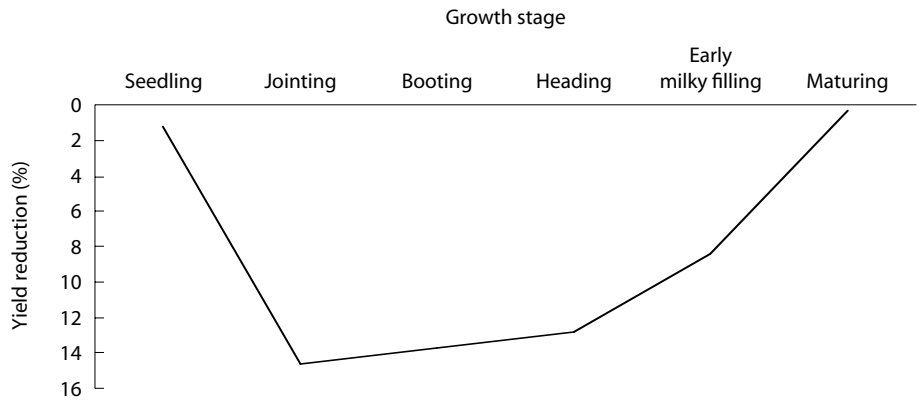

Figure 7. The yield reduction of winter wheat at different growth stages by water deficit in the 1996–97 season at Luancheng Station.

In Equations 3–5, ΔY is the yield increase by irrigation, *Py* and *Pw* are the respective unit prices of crop and water, and ΔW is the increase in amount of water used for irrigation.

In phase one, net output value will increase with irrigation; in phase two, net profit from irrigation is at a maximum; and in phase three, net profit from irrigation decreases. The amount of irrigation needed to obtain maximum profit can be calculated from the equation:

$$W = (Pw/Py - b_1)/2b_2 \qquad (6)$$

Table 2 shows the relationship between yield and irrigation at Luancheng Station. As maximum profit is obtained using less water than is needed for maximum yield, the general practice of irrigating for maximum yield in this region could be replaced by irrigation for maximum profit. If water prices increase in future, total irrigation quantity will need to be further reduced to obtain maximum profit.

Indicators for water stress

Irrigation scheduling should be based on soil water and plant water status (Stricevic and Caki 1997).

Soil water

There are many methods and measures to determine soil water status, which can act as an indicator for optimal irrigation scheduling. Significant crop stress occurs below a threshold value of soil water depletion. The threshold value varies with growth stage, due to variation in sensitivity to moisture stress. Thus, in winter wheat at jointing stage (the most sensitive stage to water stress), delaying irrigation for seven days caused a reduction in soil moisture content for the top 50 cm of soil from 22.5% to 17.4% by volume; yield was reduced by about 11%. In contrast, a decrease in soil moisture content to 16.5% by volume at maturing had no effect on yield in the 1996–97 season. Table 3 gives the critical soil moisture level (threshold) for various stages of winter wheat obtained from field experiments at Luancheng Station over several years.

Table 2. Relationship between yield and irrigation at Luancheng Station for winter wheat (1997–2000) and for summer corn (1999 season).

Crop	Season	Irrigation production function[a]	Irrigation at maximum yield (mm)	Irrigation at maximum profit (mm)[b]	
				Low water fee	High water fee
Winter wheat	1997–98	$Y = -0.0632\ W^2 + 12.421\ W + 5417.8$	98.3	90.4	58.7
	1998–99	$Y = -0.0499\ W^2 + 19.371\ W + 5161.9$	194.1	184.1	144.0
	1999–2000	$Y = -0.0489\ W^2 + 23.013\ W + 5075$	235.3	225.1	184.2
Corn	1999	$Y = -0.0309\ W^2 + 12.449\ W + 8139.5$	201.4	186.9	172.3

[a] Y = grain yield (kg/ha); W = total irrigation water (mm)
[b] When calculating irrigation with maximum profit, the price of winter wheat is taken as 1.0 yuan/kg and the price of corn as 0.9 yuan/kg (present price), the low water fee as 0.1 yuan/m^3 and the high water fee as 0.5 yuan/m^3 (US$1 = 8.5 yuan)

Table 3. Critical soil moisture level (threshold) for winter wheat at various growth stages at Luancheng Station.

Growth stage	Seedling	Turning green to start of noding	Jointing	Booting	Heading to early milky filling	Maturing
Percentage over field capacity	60	55	65	60	60	50

Leaf water potential

The water status of plants is a more reliable indicator of water stress than soil water content because it reflects the influence of both soil and climate on the plant (Berliner and Oosterhuis 1987). According to Hsiao (1990), the most effective indicator of plant water status for irrigation scheduling is leaf water potential (LWP), which is related to transpiration rate. Figures 8 and 9 show the daily LWP and transpiration rate for winter wheat and corn. During the day, LWP decreased with increasing transpiration.

The transpiration rate fluctuated but there was a significant correlation between LWP and meteorological factors. Figures 10 and 11 show diurnal LWP and air temperature, radiation and vapour pressure deficit (VPD) for winter wheat and summer corn. LWP is highest before dawn; as air temperature, VPD and radiation increase, LPW decreases. At noon, LWP is relatively constant for several hours; it then increases as temperature, VPD and radiation fall. There is a linear correlation between LPW and temperature, VPD and radiation. The relationship can be described using the equations in Table 4.

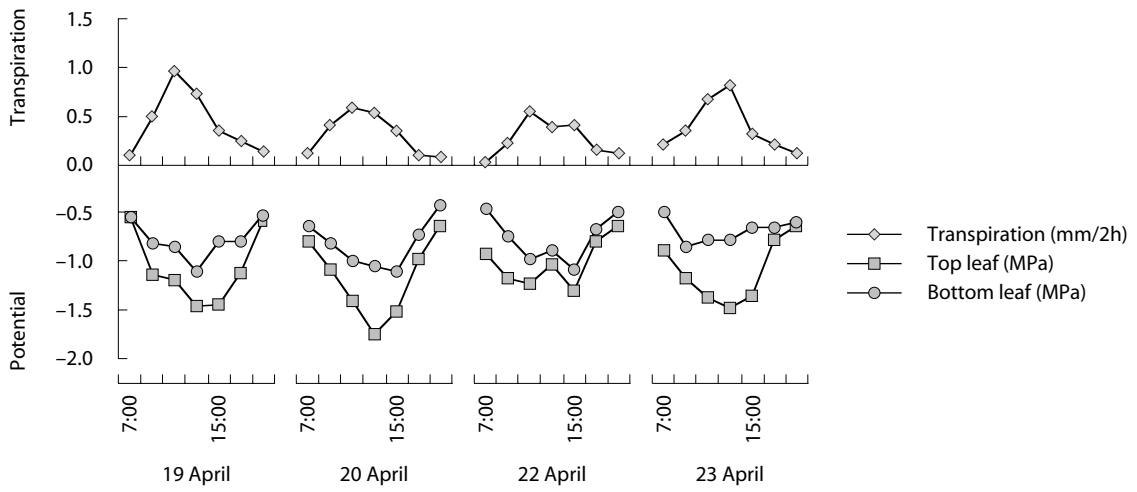

Figure 8. The diurnal change of leaf water potential with transpiration rate of winter wheat in 1996 at Luancheng Station.

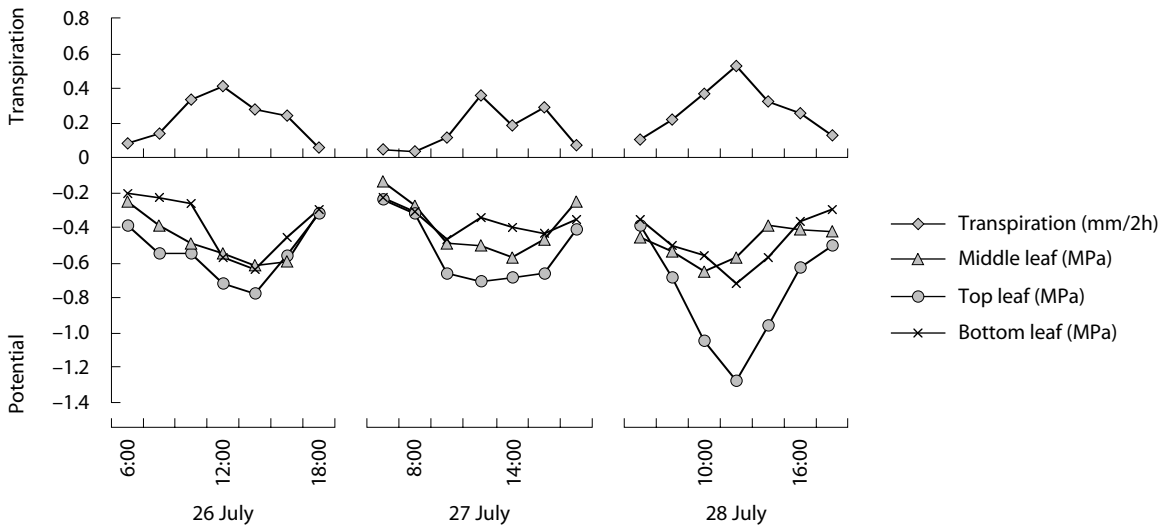

Figure 9. The diurnal change of leaf water potential with transpiration rate of summer corn in 1996 at Luancheng Station.

LWP has been used as an indicator for the crop water stress index (CWSI) (Sepaskhah and Kashefipour 1994) and to estimate evapotranspiration under water deficit (Kang et al. 2000). Figure 12 shows diurnal variation in LWP in well-watered and deficit-irrigated winter wheat. LWP was lower when soil moisture was lower. Early in the morning, the difference between LWP for well-watered plants and LWP for deficit-irrigated plants was greater than at any other time of the day.

During the evening, transpiration rate is low, so LWP can approach equilibrium with the effective soil water potential. At midday, transpiration is high and a leaf may lose water that cannot be immediately replenished even under well-watered conditions. Thus, variation in LWP between well-watered and water-deficit crops at midday may not reflect the true plant water status and predawn LWP appears to be the most effective indicator, a finding

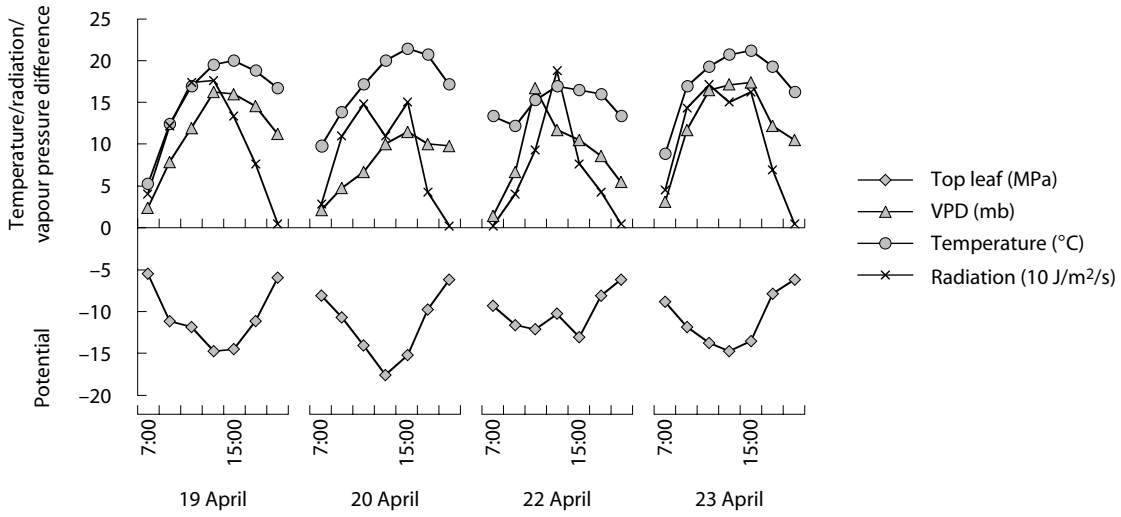

Figure 10. The diurnal change of leaf water potential with temperature, radiation and vapour pressure difference (VPD) of winter wheat in 1996 at Luancheng Station.

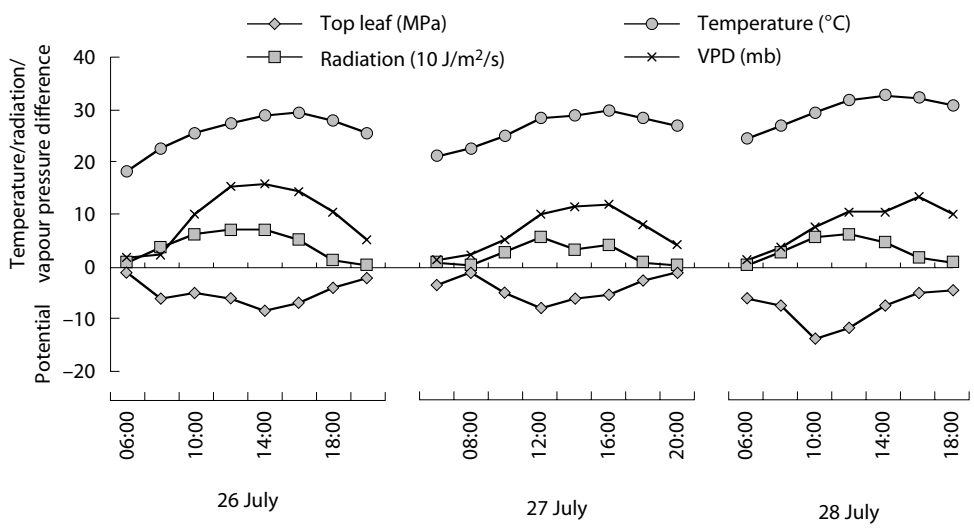

Figure 11. The diurnal change of leaf water potential with temperature, radiation and vapour pressure difference (VPD) of summer corn in 1996 at Luancheng Station.

that is consistent with other research (Nadler and Heuer 1997).

Table 5 shows the variation in LWP for winter wheat and summer corn at different levels of soil moisture, expressed as a percentage of field capacity. With decreasing soil moisture, variation in LWP usually increased. LWP can serve as an indicator of water stress for scheduling and control of irrigation.

Optimising the irrigation scheduling

Tables 6–10 show the results of different irrigation scheduling on yield, total water consumption and WUE for winter wheat and summer corn at Luancheng Station. Frequency and timing of irrigation affected grain yield and WUE, with irrigation important in improving yield. For example, in the 1999–2000 winter wheat season, when rainfall was scarce, the yield of the crop that was irrigated three times was almost 50% more than the crop without irrigation. However, the most frequent irrigation did not produce the maximum grain yield and gave the lowest (winter wheat) or almost the lowest (corn) WUE.

Because of the variation in rainfall, the frequency of irrigation needed to obtain maximum yield differed from one year to another. Generally a single

Table 4. Relation of leaf water potential to air temperature, radiation and vapour pressure difference in the absence of water stress at Luancheng Station.

Parameters	Winter wheat			Summer corn		
	Equation	*n*	*r*	Equation	*n*	*r*
Temperature (T, °C)	$\Psi L = 0.3279 + 0.0478T$	53	0.706	$\Psi L = 0.2012 + 0.01084T$	64	0.808
Vapour pressure deficit (VPD, mb)	$\Psi L = 0.7077 + 0.0384VPD$	53	0.762	$\Psi L = 0.1969 + 0.0592VPD$	64	0.812
Radiation ($J/m^2/s$)	$\Psi L = 0.733 + 0.00392R$	47	0.820	$\Psi L = 0.3666 + 0.01491R$	64	0.815

ΨL = absolute leaf water potential; *n* = number of measurements; *r* = correlation coefficient; mb = millibar; $J/m^2/s$ = Joules per square metre per second

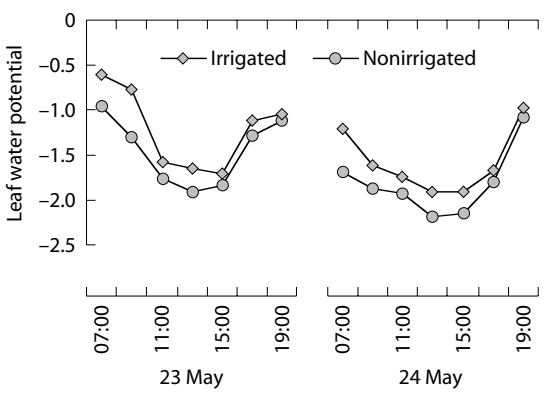

Figure 12. The difference of leaf water potential of summer corn under fully irrigated conditions and water-deficit conditions in 1996 at Luancheng Station.

Table 5. The variation of leaf water potential at different levels of soil moisture with full irrigation at Luancheng Station.[a]

Soil moisture	Difference in leaf water potential (kPa)	
	Winter wheat	Corn
80	0.1–0.2	0.1–0.2
60	0.3–0.45	0.3–0.4
45	0.5–0.67	0.45–0.6

[a] 0–50 cm soil moisture (percentage over field capacity)

irrigation in a wet year, two in a normal year and three in a dry year produced the maximum grain yield for winter wheat. For corn, three irrigations in a dry year produced the highest grain yield. Because the three seasons when corn was grown had less rainfall than in normal years, no results were obtained for wet or normal years. However, previous experiments suggested that for corn no irrigation was required when rainfall was high during the growing season (around 400 mm) and a single irrigation at seedling stage was sufficient in normal years.

Analysis of variance showed a significant difference in the effects of irrigation frequency and timing on yield and rate of water use. For example, in the 1998–99 season of winter wheat, five treatments were tested, all but two of which included two

Table 6. Yield, water use efficiency and total water consumption of different irrigation treatments for winter wheat at Luancheng Station, 1996–97.[a]

Number of irrigations	Timing of irrigation	Total irrigation (mm)	Total water consumption (mm)	Yield (kg/ha)	Water use efficiency (kg/m^3)
1	21 Nov	67.5	364.7	5500.6	1.51
2	21 Nov, 22 Apr	144.4	428.6	6900.8	1.61
2	21 Nov, 29 Apr	153.5	434.5	6164.3	1.42
3	21 Nov, 27 Mar, 22 Apr	171.4	428.9	6494.3	1.51
3	21 Nov, 27 Mar, 29 Apr	200.1	475.9	6308.6	1.33
3	21 Nov, 27 Mar, 7 May	186.7	460.0	6503.3	1.41
3	21 Nov,27 Mar, 14 May	193.7	476.1	6219.8	1.31
3	21 Nov, 18 Apr, 14 May	194.8	470.1	7170.0	1.53
3	21 Nov, 29 Apr, 22 May	176.7	413.2	6236.6	1.51
4	21 Nov, 27 Mar, 22 Apr, 14 May	252.5	474.7	6503.3	1.37

[a] All treatments were irrigated before over-wintering on 21 November

Table 7. Yield, water use efficiency and total water consumption of different irrigation treatments for winter wheat at Luancheng Station, 1997–98 season.

Number of irrigations	Timing of irrigation	Total irrigation (mm)	Total water consumption (mm)	Yield (kg/ha)	Water use efficiency (kg/m^3)
0	–	0.0	299.4	5413.8	1.81
1	15 April	84.7	333.7	6088.2	1.83
2	25 Mar, 21 Apr	95.0	338.4	5954.9	1.76
2	25 Mar, 20 May	151.3	366.0	5958.0	1.63
3	25 Mar, 21 Apr, 20 May	175.9	375.6	5650.7	1.50
3	7 Apr, 21 Apr, 20 May	166.6	389.8	6066.0	1.56

irrigations with 160 mm of water. Due to differences in the timing of irrigation, there was about 10% variation in WUE and yield. The results indicated that irrigation scheduling can be optimised for high yield and WUE.

Table 11 shows the irrigation scheduling for winter wheat that was developed from information about sensitivity to water stress, supplemental water available (200–250 mm annually) and experimental results. A single irrigation at the seedling stage is usually sufficient for summer corn, because the crop grows in the rainy season. Such irrigation would not exceed the amount of water available and would stop the decline in the groundwater table.

Table 8. Yield, water use efficiency and total water consumption of different irrigation treatments for winter wheat at Luancheng Station, 1998–99 season.

Number of irrigations	Timing of irrigation	Total irrigation (mm)	Total water consumption (mm)	Yield (kg/ha)	Water use efficiency (kg/m^3)
0	–	0	323.0	5325.8	1.65
1	16 Mar	80	366.4	7023.8	1.92
1	3 Apr	80	338.2	6697.5	1.98
1	24 Apr	80	370.4	7058.3	1.91
2	4 Mar, 24 Apr	160	444.2	7592.0	1.71
2	11 Mar, 24 Apr	160	438.4	7422.5	1.69
2	17 Mar, 6 May	160	399.0	6915.0	1.73
2	17 Mar, 14 May	160	403.9	7344.6	1.82
2	21 Nov, 24 Apr	160	400.3	6923.0	1.73
2	31 Mar, 5 May	160	442.5	7296.0	1.65
4	21 Nov, 31 Mar, 24 Apr, 5 May	240	478.5	6937.5	1.45

Table 9. Yield, water use efficiency and total water consumption of different irrigation treatments for winter wheat at Luancheng Station, 1999–2000 season.

Number of irrigations	Timing of irrigation	Total irrigation (mm)	Total water consumption (mm)	Yield (kg/ha)	Water use efficiency (kg/m^3)
0	–	0	282.9	5103.8	1.80
1	6 Apr	60	325.0	6180.8	1.90
2	2 Dec, 6 Apr	120	374.6	6810.0	1.82
2	25 Mar, 25 Apr	120	414.2	7092.9	1.71
3	2 Dec, 18 Apr, 10 May	180	432.6	7593.2	1.76
4	2 Dec, 6 Apr, 25 Apr, 15 May	240	487.7	6937.8	1.42

Discussion

For winter wheat, this study found that, in wet, normal and dry years, respectively, at a rate of 60 mm per irrigation, one, two or three irrigations of the crop were sufficient to obtain maximum profit and WUE. As winter wheat in this region is generally irrigated between three and five times each season, such an irrigation schedule could substantially reduce the use of groundwater. The amount of irrigation necessary for maximum profit was less than that required for maximum yield.

Table 10. Yield, water use efficiency and total water consumption of different irrigation treatments for corn at Luancheng Station, 1997, 1998 and 1999 seasons.

Year	Number of irrigations	Timing of irrigation	Total irrigation (mm)	Total water consumption (mm)	Yield (kg/ha)	Water use efficiency (kg/m^3)
1997	0	–	0	220.93	4114.5	1.86
	1	17 July	60	275.21	5611.1	2.03
	2	17 July, 14 Aug	120	349.36	5859.0	1.68
1998	0	–	0	290.40	5233.7	1.80
	1	16 July	60	364.60	6659.0	1.83
	2	16 Jul, 14 Aug	120	370.97	7118.4	1.92
1999	0	–	0	301.45	8155.5	2.52
	1	18 Jul	60	341.33	8794.5	2.58
	2	18 Jul, 7 Aug	120	355.46	9034.5	2.54
	3	18 Jul, 1 Aug, 23 Aug	180	402.73	9565.5	2.37
	4	18 Jul, 1 Aug, 23 Aug, 8 Sep	240	447.89	9280.5	2.07

Table 11. The optimised irrigation scheduling for maximum yield and water use efficiency of winter wheat with different types of seasonal rainfall under limited irrigation.

Type of seasonal rainfall[a]		Growth stage					Total (mm)
		Sowing to recovering	Jointing	Booting	Heading to milky filling	Maturing	
Dry	Average rainfall (mm)	30.7	3.5	6.3	12.9	6.4	59.8
	Simulated irrigation (mm)[b]	60	60	0	60	0	180
Normal	Average rainfall (mm)	52.3	10.9	17.4	16.3	8.1	105.0
	Simulated irrigation (mm)[b]	0	60	0	60	0	120
Wet	Average rainfall (mm)	67.9	17.4	22.8	34.2	12.1	154.4
	Simulated irrigation (mm)[b]	0	0	60	0	0	60

[a] Seasonal rainfall was analysed using the data from 1951 to 1999 in Luancheng County
[b] 'Simulated irrigation' is the irrigation amount used in the simulation model

In addition to irrigation scheduling, WUE can be improved by methods such as reducing soil evaporation. In the piedmont of Mount Taihang, about 30% of total water consumption in growing winter wheat and summer corn resulted from soil evaporation. Total soil evaporation was about 273 mm, equivalent to the amount needed for more than four irrigations of the crop. If this evaporation was reduced by even 50%, at least two irrigations of the crop could be saved. Thus, there is great potential for improving farmland WUE by reducing soil evaporation in the region, perhaps by the use of straw mulching.

References

Al-Kaisi, M., Berrada, A. and Stack, M. 1997. Evaluation of irrigation scheduling program and spring wheat yield response in southwestern Colorado. Agricultural Water Management, 34, 137–148.

Berliner, P. and Oosterhuis, D. 1987. Effect of root and water distribution in lysimeters and in field on the onset of the crop water stress. Irrigation Science, 8, 245–255.

Doorenboss, J. and Kanssan, A. 1979. Yield response to water. Food and Agriculture Organization (FAO) Irrigation and Drainage Paper 33. Rome, FAO, 193.

English, M. and Nakamura, B. 1989. Effects of deficit irrigation and irrigation frequency on wheat yields. Journal of Irrigation and Drainage, 115, 172–184.

Ghahraman, B. and Sepaskhah, R. 1997. Use of a water deficit sensitivity index for partial irrigation scheduling of wheat and barley. Irrigation Science, 18, 11–16.

Hsiao, T. 1990. Plant atmosphere interactions, evapotranspiration and irrigation scheduling. Acta Horticulture, 278, 55–65.

Jensen, M. 1968. Water consumption by agricultural plants. In: Kozlowski, T., ed., Water deficit and plant growth. New York, Academic Press, Vol. 2, 1–22.

Kang, S.Z., Cai, H.J. and Zhang, J.H. 2000. Estimation of maize evapotranspiration under water deficits in a semiarid region. Agricultural Water Management, 43,1–15.

Nadler, A. and Heuer, B. 1997. Soil moisture levels and their relation to water potentials of cotton leaves. Australia Journal of Agricultural Research, 48, 923–932.

Pereira, L.S. 1999. Higher performance through combined improvements in irrigation methods and scheduling: a discussion. Agricultural Water Management, 40, 153–170.

Sepaskhah, A. and Kashefipour, S. 1994. Relationship between leaf water potential, CWSI, yield and fruit quality of sweet lime under drip irrigation. Agricultural Water Management, 25, 13–22.

Shi, Y.F. 1995. The impacts of climatic change on the water resources of north and west part of China. Jinan, Shandong Science and Technology Publishing House, 369 pp (in Chinese).

Smith, M., Pereira, L.S., Beregena, J., Itier, B., Goussard, J., Ragab, R., Tollefson, L. and Van Hoffwegan, P., eds. 1996. Irrigation Scheduling: from theory to practice. FAO Water Report 8. Rome, Food and Agriculture Organization and International Commission on Irrigation and Drainage.

Stricevic, R. and Caki, E. 1997. Relationships between available soil water and indicators of plant water status of sweet sorghum to be applied in irrigation scheduling. Irrigation Science, 18, 17–21.

Turner, N. 1990. Plant water relations and irrigation management. Agricultural Water Management, 17, 59–73.

You, M.Z. 1998. The influences of water flux in a mountainous region on the water balance of the piedmont of Mt Taihang. In: You, M.Z., ed., Evaluation and Management of Agricultural Resources. Beijing, Meteorological Publishing House, 123–125 (in Chinese).

Zhang, H.P., Liu, X.N. and Zhang, X.Y. 1993. Theoretical bases for water-saving agriculture. In: Wang, Zhao, Chen, eds, Water-saving Agriculture and Water-saving Technologies. Beijing, Meteorological Publishing House, 163–178 (in Chinese).

4 Assessing Rainfed and Irrigated Farm Performance Using Measures of Water Use Efficiency

Jim W. Cox,* Tim R. McVicar,† Doug J. Reuter,* Huixiao Wang,‡ Jeremy Cape* and Rob W. Fitzpatrick*

Abstract

The aim of sustainable farming in both Australia and China is to achieve high water use efficiency (WUE), high profitability and minimal damage to the environment. High WUE is needed to minimise the overuse of scarce water resources. In this chapter, we review the many definitions of WUE that are in use in Australia and China. For example, in rainfed and irrigated zones of southern Australia, WUE or 'potential yield' is used as an index of production efficiency and its industry surrogates, whereas in China WUE is estimated as part of water-saving agricultural practices. We also look at why current measures of WUE are not appropriate for some cropping systems in Australia such as those in 'leaky' landscapes, where the crops cannot intercept and use all the water that reaches the root zone. A more encompassing measure of plant WUE may need to be developed for these systems and advocated to farmers. To maximise adoption by farmers, WUE must be based on easily measured parameters.

高效农业的目标是提高水分利用效率（WUE），增加收益，最大程度缩小植物水分低效利用对环境造成的不良影响，减少过度使用稀缺水资源。本文对中澳两国所采用的 WUE 的许多概念作了介绍和对比。例如，在南澳旱作和灌溉农业区，WUE 或潜在产量常作为产出效率指数，而在中国则是节水农业实践的一部分。本文也说明了目前这种 WUE 的计算对某些农作系统，如易渗漏地，并不适用，因为植被未能全部截留、利用到达根部的水分。对于这些系统，应有一个更周全的 WUE 计算方法，推荐给农民。其中的参数要易于测量，便于农民们采纳。

* CSIRO Land and Water, PMB 2, Glen Osmond, SA 5064, Australia. Email: jim.cox@csiro.au

† CSIRO Land and Water, PO Box 1666, Canberra, ACT 2601, Australia.

‡ Beijing Normal University, Institute of Environmental Sciences, Beijing, PRC.

Cox, J.W., McVicar, T.R., Reuter, D.J., Huixiao Wang, Cape, J. and Fitzpatrick, R.W. 2002. Assessing rainfed and irrigated farm performance using measures of water use efficiency. In: McVicar, T.R., Li Rui, Walker, J., Fitzpatrick, R.W. and Liu Changming (eds), *Regional Water and Soil Assessment for Managing Sustainable Agriculture in China and Australia*, ACIAR Monograph No. 84, 70–81.

SHORTAGE of water may restrict future regional agricultural productivity in both Australia and China. As the demand for high-quality irrigated produce increases in Australia and overseas, there is increasing competition for water between agriculture, urban users and the environment, where 'environmental river flows' are necessary to maintain aquatic and riparian ecosystems (Young 2001). In China, the demand for water is driven by industrialisation of the economy and rapid urbanisation of the population, particularly over the past two decades (Anderson and Peng 1998; Brown and Halweil 1998; Rosegrant and Ringler 2000). This competition for water puts the agricultural sector under pressure to maintain and increase production using less water. In spite of serious water shortage in both countries, large amounts of water are wasted due to poor irrigation methods, although in Australia this wastage has partly been addressed by the introduction of irrigation quotas. Hence, the agricultural sector must increase its water use efficiency (WUE). Where agricultural practices must change in response to new policies, regulatory bodies require methods for monitoring WUE and mechanisms for conflict resolution such as litigation, legislation, negotiated agreements and market mechanisms (Deason et al. 2001).

In China, the regional distribution of water resources does not match agricultural demand for irrigation. While some 44% of the population and some 58% of the cultivated land are in the northern and northeastern provinces, only 14% of the total water resources (surface runoff and groundwater) are found in those regions (Brown and Halweil 1998). Agricultural water consumption accounted for over 80% of the total water use; thus, 'water-saving agriculture' (the term used in China) is of great significance. Stanhill (1986) identified three main components of water-saving agriculture: reducing delivery losses in irrigation systems; improving transfer of water (from either irrigation or rainfall) to a depth where roots can access the water; and maximising WUE by crops.

Farm productivity (yield per hectare) and disposable farm income (net profit per hectare) are two parameters used widely to assess and compare the relative performance of farming enterprises within and between regions. In rainfed agriculture these two annually derived measures are highly variable, because production is dominated by prevailing weather conditions during each growing season. Economic returns from farming are also affected by commodity prices and other fluctuating economic variables, such as interest rates. Where irrigation is efficient, the impact of climate is less pronounced, because soil water deficits are prevented and production targets can be reached. On the other hand, overuse of irrigation water can depress yields and returns, and in the longer term can contribute progressively to insidious environmental risks, such as the rising saline groundwater levels found in parts of Australia (Walker et al. 1999).

In both rainfed and irrigated agriculture, farm yields and financial returns are also governed in the short to medium term by other factors, including:

- the quality of soil and land resources on the farm;
- the systems of land use and rotations that best suit the land resource and the climate; and
- how much money is invested in optimising economic returns and adopting improved farming practices to overcome constraints on yield.

In this chapter we assemble and evaluate practical indicators for assessing farm or field performance against benchmarks linked to the availability of soil water for plant growth — the factor that is the most yield limiting. Such indicators, which can be viewed as measures of WUE achieved during the growing season, have been prepared for rainfed and irrigated agriculture in both Australia and China. In this study we also assess landscapes where some of the seasonal rains bypass the soil–plant system due to

overland flow, lateral flows in subsurface soil horizons or drainage past the root zone. The relative importance of the processes operating within these systems are discussed in more detail in Chapters 1 and 5 of this volume.

Definitions of Water Use Efficiency

Stanhill (1986) defined WUE both hydrologically and physiologically; here we introduce the additional concept of economic WUE. Hydrological WUE is the ratio of evapotranspiration to the water potentially available for plant growth. It is expressed as a percentage or fraction (0–1). Physiological WUE measures the amount of plant growth for a given volume of water; it can be defined for different measures of 'plant growth' and 'volume of water'. Turner (1986) noted that care is needed when defining WUE. For example, 'plant growth' may be measured in units of net biomass (including roots) (Ritchie 1983; Tanner and Sinclair 1983; Turner 1997) or as crop yield (Tanner and Sinclair 1983; Turner 1997). Similarly, 'volume of water' can be measured as total transpiration (Tanner and Sinclair 1983; Turner 1997; French and Schultz 1984a,b), total evapotranspiration (Ritchie 1983; Tanner and Sinclair 1983; Turner 1997), total water input (Sinclair et al. 1984) or total growing-season precipitation plus initial soil water at the time of sowing (French and Schultz 1984a,b). Economic WUE attempts to gauge the value of different agricultural commodities by expressing WUE in units of wealth generated per volume of water used. Armstrong et al. (2000) developed a measure of WUE for dairy cattle farms, with the units being kilogram milk fat plus protein per millilitre of irrigation water applied. The different measures of WUE have different applications; for example, economic WUE is useful for regional planners, hydrological WUE is relevant to irrigation engineers and physiological WUE is valuable for those involved in plant, soil or atmospheric sciences.

Sinclair et al. (1984) introduced different timescales for several definitions of WUE, ranging from an instant to a day or a growing season. These temporal scales have now been linked to a range of spatial scales, which extend from a single leaf, through a canopy, field or farm to a region (see Table 1, Chapter 18). The scales are linked: leaf WUE (in the order of tens of square centimetres) will usually be measured over a short time (e.g. from one second to one day), whereas regional WUE (in the order of thousands of square kilometres) will usually be measured over a longer time (e.g. from one day to one growing season). To date, very little research has focused on farm-level or regional assessments of WUE; a study by Tuong and Bhuiyan (1999) is one of the few examples of a farm-level assessment. A report of regional monitoring of WUE over the North China Plain for 13 years is given in Chapter 18.

As there are a large number of current uses for the term WUE, all indexes of WUE need to be clearly defined. While some of these indexes are directly related to water use, others are indicators of production performance based on crop response to water supply. For a WUE index to be of practical value, it should be based on easily measured parameters such as volume of water delivered from headworks, river pumping station or farm bore; water volumes delivered at the farm gate; area of crop or pasture irrigated; commodity yield; and rainfall. A WUE index will be more precise if it includes measurements of soil water and crop water use.

Hydrologic WUE

Hydrologic WUE is determined by spatial considerations (e.g.the distance water is conveyed) and by the type of irrigation infrastructure used to deliver water to the farm gate (e.g. open channels or a piped system) and onto the irrigated area. Hydrologic WUE is expressed as a percentage or a fraction (0–1), without dimension. It is closely related to water saving during conveyance and

irrigation, and thus is important in research into field water balance, field water redistribution, canal seepage prevention, water conveyance works and new irrigation techniques.

The field water balance can be estimated from the following equation (Chen 1985):

$$E + T = P + I + U + W_1 - (R + D + W_2)$$

where P is precipitation; I is irrigation water supplied; E is soil evaporation; T is crop transpiration; evapotranspiration (ET) is the sum of E and T; U is upward capillary water; W_1 is the initial soil water storage at crop sowing; R is the surface runoff; D is deep drainage of soil water; and W_2 is the soil water storage when crop harvesting.

Three types of WUE indicators can be used to assess the efficiency with which irrigation water is diverted from a water source, transported and applied to a field.

Conveyance efficiency (Eff_c) takes into account channel seepage, spillage, and evaporative and any other water losses that occur during transport from the source to the point of delivery in the landscape. It can be expressed as:

$$Eff_c = (V_s/V_d) \times 100$$

where V_s is the total volume of water supplied to the target land area and V_d is the total volume of water diverted from the regional water body to the target land area.

The second indicator is termed distribution efficiency (Eff_d). It relates to the proportion of water received at the field inlets compared with the total outflow from the supply system and can be defined as:

$$Eff_d = V_r/V_{out}$$

where V_r is volume of water received at field inlets and V_{out} is the total outflow from the supply system.

The third indicator is application efficiency (Eff_a), which relates to the targeted land area.

$$Eff_a = V_{ap}/V_{wa}$$

where V_{ap} is the volume of water available within the plant-rooting zone (the volume supplied minus the sum of drainage, evaporative losses and nonrecycled tailwater) and V_{wa} is the volume of water applied from irrigation and rainfall. Application efficiency assumes that irrigation water is applied uniformly either by flood or pressurised systems.

Hydrologic efficiency can be measured on regional, farm or paddock scale; therefore, the scale should be made clear when efficiency estimates are reported. Efficiencies can also vary temporally and can be applied to single irrigation events or to longer periods such as months, growing seasons or years.

Hydrologic efficiency (Eff_h) of irrigation systems can be given as:

$$Eff_h = Eff_c \times Eff_d \times Eff_a$$

Having separate, yet interrelated, indicators of hydrologic WUE for an irrigation system allows managers to better monitor the system.

Physiological WUE

General

Physiological WUE is commonly used at several different levels: from molecular, through single leaf, canopy and field to regional levels. It can be called 'crop WUE'. As the spatial scale of the molecular level is outside the emphasis of this chapter, it will not be discussed further.

Single leaf level

At the single leaf level, WUE is defined as the net CO_2 uptake by leaf per unit of transpiration. It is expressed as the ratio of leaf photosynthesis rate to leaf transpiration rate, and could be the upper limit value for crop WUE. The water vapour and CO_2

fluxes can be expressed as the concentration gradient and diffusion resistance, which can be measured with gas exchange equipment. Thus, assuming that CO_2 and water vapour take identical paths between the leaf cell walls and bulk air, the WUE at this level could be calculated as follows (Fischer and Turner 1978);

$$WUE = \frac{\Delta c \times D_c\left(r_a + r_s\right)}{\Delta e \times D_e\left(r_a + r_s + r_i\right)}$$

where Δc and Δe are the leaf-to-air concentration gradients for CO_2 and water vapour, respectively; D_c and D_e are the diffusivities of CO_2 and water vapour, respectively; and r_a, r_s and r_i are the boundary layer, stomatal, and internal resistances to diffusion, respectively.

Assuming that the CO_2 concentration at the chloroplast is zero, r_i includes photorespiratory effects as well as other apparent and actual internal diffusive resistances to CO_2. As a result, Δc equals the concentration of CO_2 in the atmosphere, 0.58 mg/L at 25°C. Assuming that D_c/D_e is 0.6:

$$WUE = \left(\frac{360}{\Delta e}\right)\left(\frac{r_a + r_s}{r_a + r_s + r_i}\right)$$

with WUE in units of $mgCO_2/gH_2O$ and Δe mg/L. The intercellular air spaces of the leaf are assumed saturated with water vapour at the leaf temperature. The highest WUE that might be expected under any conditions can be calculated by assuming that r_i is zero, meaning that there is infinitely high photosynthetic affinity. At a leaf and air temperature of 25°C, an air relative humidity of 50% and air saturation deficit of 12 mg/L, WUE would be 30 $mgCO_2/gH_2O$. In reality, with the exception of crassulacean acid metabolism (CAM) plants, WUE values are usually substantially lower than this (Fisher and Turner 1978).

WUE is affected by environmental factors including air saturation deficit, air temperature, incident irradiance, leaf orientation and leaf movement. WUE also varies with genotypes, the leaf traits r_a, r_s and $r_{i,}$, and leaf water potential ψ_{leaf}.

Canopy (community) level

At the canopy level, WUE is defined as the ratio of a crop community's net CO_2 assimilation to its transpiration; that is, the ratio of the canopy CO_2 flux to the water vapour flux for the canopy transpiration. It can be expressed as follows:

$$WUE = \frac{F_c}{T}$$

where F_c is the canopy CO_2 flux and T is the water vapour flux for the canopy transpiration. The gas exchange theory has been extended to measure the fluxes of CO_2 and water vapour. The unit for WUE at this level should be the same as that for the single leaf. The canopy WUE can also be expressed on temporal scales as instantaneous, daily and seasonal WUEs.

Field level

At the field level, WUE is defined as the yield gained per unit of water used. The yield can be expressed as the net biomass Y_b (including roots) or the grain yield Y_e ($Y_b \times HI$, where HI is the harvest index). Field-level WUE is calculated as:

$$WUE = \frac{Y}{WU}$$

where Y is the dry matter yield (Y_b) or the grain yield (Y_e) in kg/ha; and WU (water use in mm) can be the total evapotranspiration, the irrigation water added or the precipitation, depending on the purpose of the analysis. For example, to show the effects of irrigation or precipitation on the accumulation of dry matter, the unit for WUE would be kg/ha/mm.

Regional level

At regional level, WUE is defined as the ratio of a region's annual yield (t) to its annual water use (m^3). Calculation of regional WUE is relatively complex because there are usually several crops growing in the same period and different kinds of landscapes within a region. Chapter 18 discusses regional WUE indicators.

Economic WUE

This index applies especially to irrigated agriculture and is used for assessing and comparing the financial benefits resulting from irrigation. The indicator is usually defined as:

$$\text{Economic WUE} = \frac{\text{operating surplus for the irrigated area (\$/ha)}}{\text{total water supplied to the crop in rainfall + irrigation (mm/ha)}}$$

Gross income or profit at full equity for the irrigated area could replace operating surplus as the numerator. In either case, the indicator is expressed as \$/ha/mm. Expressing WUE in these terms potentially allows economic policy to be the driving force for increasing WUE (Grimble 1999).

A ranking of sustainability indicators for assessing the economic performance of a farm business has recently been developed for Australia's cropping and pasture industries operating within rainfed regions (Pannell and Glenn 2000). In contrast, financially based indices are often volatile, being sensitive to changes in commodity prices and the effects of climatic conditions on crop yield and grain quality. Usually, data over several decades are required before trends can be discerned. However, an on-farm economic indicator has recently been proposed and assessed across major crop and pasture regions (Reuter et al. 1996). It links farm income per hectare (\$/ha) to annual rainfall received (mm) and thereby seeks to dampen the seasonal effects on economic performance. A variant, not yet tested, could link farm income to growing-season rainfall. This indicator, sometimes termed \$WUE in Australia, uses units of \$/ha/100 mm of annual rainfall.

Factors affecting WUE

Crop WUE is an important indicator for weighting the relationship between crop matter production and crop water use. Thus, factors affecting crop yield or water consumption will be reflected in a change in WUE. Factors affecting crop WUE vary both spatially and temporally, and can be divided into four categories:

- species or crop variety grown, encompassing plant breeding (Li et al. 1995) and genetic modification;
- soil conditions (Gong and Lin 2000), incorporating soil erosion, sodicity and salinisation (Rozelle et al. 1997);
- agricultural practices involving the use of fertilisers (Garabet et al. 1998), efficient irrigation management (Zhang and Oweis 1999; Zhang et al. 1998; Liu et al. 1998), time of planting and crop rotation (Li et al. 2000), planting density (Karrou 1998) and the use of mulch (Tolk et al. 1999) or plastic film (Jin et al. 1999) to reduce soil evaporation; and
- atmospheric factors including levels of incoming solar radiation, wind-speed conditions and the relative gradients of water vapour, both internal and external to the leaf.

Over a longer time frame, estimation of WUE will also be affected by changes in climate (Smit and Yunlong 1996, Loaiciga et al. 1996), including precipitation patterns (Thomas 2000) and CO_2 concentration (Hunsaker et al. 2000).

WUE Indicators for Rainfed Agriculture in Australia

For rainfed agriculture, we define WUE as 'the efficiency of crops or pastures in any year to acquire and use available soil water derived from seasonal

rainfall to produce harvested products'. In this context, 'harvested products' for annual crops refers to the grain or seed harvested at crop maturity, a measurement readily recorded by farmers. For grazed and ungrazed pastures, total pasture biomass can be estimated by a variety of procedures. The concept of potential yield, pioneered with wheat in the Mediterranean climatic zone of South Australia by French and Schultz (1984a,b), has proved to be a most innovative benchmarking system for ranking performance of rainfed farming crops and pastures. Their initial studies used 60 sets of data from field experiments and commercial crops, grown between 1964 and 1975, to relate grain in wheat to water use by the crop (French and Schultz 1984a).

Figures 1–4 show that crop water use increased as growing-season rainfall increased, resulting in a positive but variable trend between grain yield and crop water use. A boundary line (termed the 'potential yield line') was used to envelop all data points. For wheat, the intercept for this line was at 110 mm of water use, a value attributed to direct evaporative water losses from the soil surface and crop canopy. However, for hard-setting surface soils, evaporative losses were estimated to be higher (170 mm), because water infiltration into the root zone is slower, causing greater soil evaporative losses. The slope (20 kg/mm of water use) defined yield potential per millimetre of crop water use.

For practical reasons, farmers are unlikely to measure soil water changes between sowing and crop maturity; therefore, a surrogate estimate for crop water use has been determined (French and Schultz 1984b). The approach involved constructing relationships between grain yield and 'derived' growing-season rainfall (defined as April to October in South Australia). This term incorporated 30% of the measured rainfall falling in summer (i.e. before 1 April) and in late spring (i.e. after 31 October), based on the assumption that this rainfall increases grain yield. Through this step, farmers in any season could rank their crop yield relative to the potential benchmark yield from the simple equation:

$$\%\ \text{potential yield} = \frac{\text{actual yield}}{\text{potential yield}} \times 100$$

where the potential yield of wheat was defined as:

$$\text{potential yield (kg/ha)} = (\text{derived April–October rainfall} - 110\ \text{mm}) \times 20.$$

We then derived guidelines for assessing potential yield estimates in any field or season. For example, a potential yield of > 80% was judged to be approaching optimal productivity, where few, if any, constraints were limiting yield. On the other hand, a potential yield of < 50% was taken to indicate that grain yield was being seriously restricted by one or more factors such as weeds, disease, nutrient disorders or frost. The nature of these yield-limiting constraints then needed to be identified, either through field observations or the use of diagnostic procedures that identify particular field problems. In subsequent studies, potential yield lines were derived for other field crops and for pastures grown in South Australia (French 1992, 1995), and researchers in other Australian states developed relationships for other crops and environments. These regional variants have been summarised by Reuter et al. (1996). In Western Australia, a computer program (PYCAL) was developed to permit farmers to calculate and annually rank per cent potential yield for a range of crops; the program took into account variations in regional environments.

The potential-yield concept is relatively simple, and readily accessible parameters are used for the model based on principles of plant water use. Because of these characteristics, the approach was rapidly adopted by the grain industry in southern Australia for ranking yield performance at field and farm scales. However, farmers probably estimate potential yield using rainfall from April to October, rather than 'derived' growing-season rainfall. An

empirical index of plant water use remains an important cornerstone for site-specific management. The index can also now be linked to mapping of grain yield contours in fields using differential global positioning system (DGPS) grain yield monitors. The concept has also been used in South Australia to review and map temporal and spatial trends in cereal productivity, and the findings have influenced policy developments.

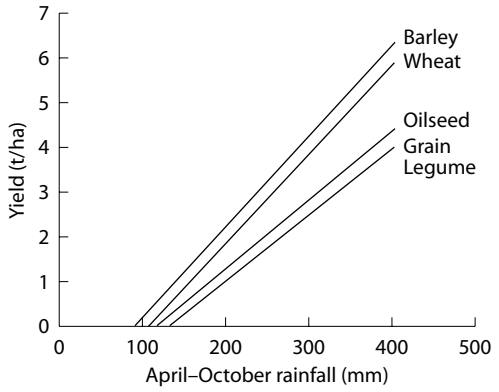

Figure 1 Relationships between potential grain yield and April–October rainfall (mm) for crops grown in South Australia (French 1995).

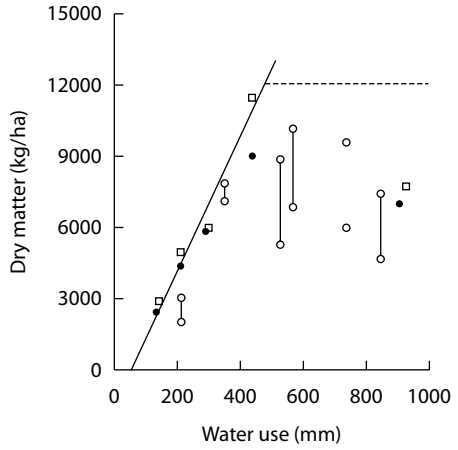

Figure 2 Relationships between growing-season water use (mm) and pasture dry matter production at experimental sites across Western Australia (from Bolger et al. 1993). Open squares represent values for maximum production systems (high fertiliser inputs, high seeding rates, good weed control); closed circles represent values for 'typical' production systems; open circles represent maximum and minimum values from Wesfarmers CSBP Ltd experimental sites.

Issues Arising from Estimating WUE under Irrigation

In irrigated agriculture, the aim of WUE is to optimise and sustain yield returns by matching water supply (rainfall plus applied water) to the amount of water needed by crops or pastures and to flush down salt accumulations within the root zone. In comparison to rainfed agriculture, irrigated

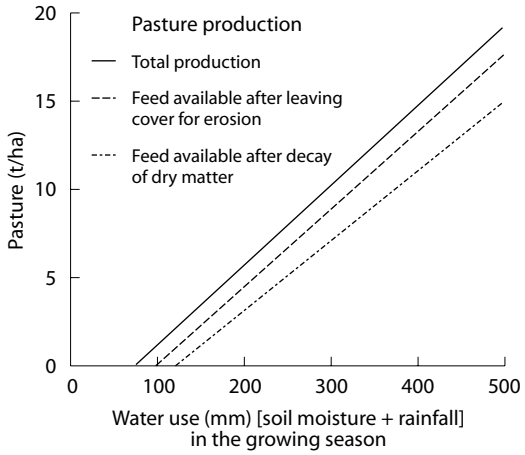

Figure 3 Relationship between water use in the growing season and pasture dry matter production in South Australia (after French 1992).

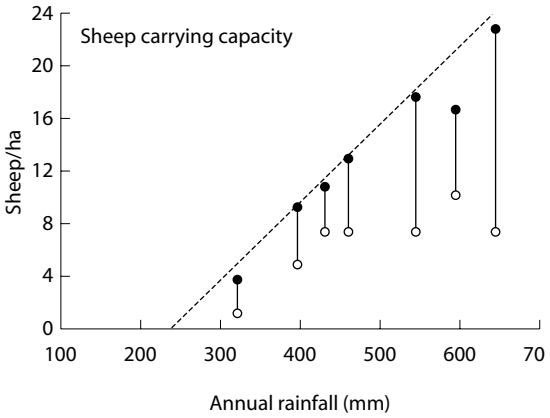

Figure 4 Relationship between annual rainfall and sheep carrying capacity derived from stocking rate experiments conducted at seven sites in South Australia (French 1992). Open circles represent minimum sheep carrying capacity; closed circles represent maximum sheep carrying capacity.

agriculture tends to have higher target yields and to use higher inputs such as fertilisers. However, the relative importance of factors such as crop water use, fertiliser requirements and salt accumulation will depend on the crop's root distribution, soil properties and the type of irrigation system used (e.g. flood, sprinkler, drip).

To obtain the full benefits from irrigation (by optimising WUE without adverse onsite or offsite effects), water management must be carefully controlled. Maximum production of dry matter, either per unit of water or per unit of land, is generally achieved through avoiding water stress by maintaining low water suction in the root zone. However, for some crops, one or more periods of water stress are necessary to maximise crop yield and product quality. In addition, an irrigation schedule that always maintains a fully charged root zone does not provide opportunities for taking advantage of rainfall and/or stored soil water. Also, if yields are to be maximised, irrigation must be managed to minimise salinity in the soil solution of the root zone.

Constraints to achieving high WUE in irrigated systems

With conventional flood irrigation systems, labour and operating costs are minimised by decreasing the frequency of irrigation. However, WUE and crop yields tend to be maximised when irrigation frequency is increased. Consequently, under irrigation, the most appropriate uses of land and water resources need to be balanced against economic feasibility and long-term sustainability.

Automated solid-set, centre-pivot sprinkler systems and trickle irrigation could increase WUE. Compared to flood irrigation systems, these systems offer opportunities to reduce water consumption without decreasing yield or income because they allow greater control of water application and require less labour. However, these benefits can only be achieved through increased capital costs and fuel consumption.

Flood irrigation systems can also be modified to permit closer control of water application. Laser-controlled precision land levelling allows better aerial distribution of water over the field and fewer applications of water. Combined with automation, major improvements in irrigation efficiency have been achieved in laser-level flooded systems. Closed conduits, rather than open waterways for lateral drains, allow for improved control and can make use of gravity to pressurise delivery systems or controls. In furrow-irrigated areas, furrow length can be reduced, intake distribution improved and tailwater eliminated.

Automated sensory systems for measuring soil and plant water status have recently become available. Often these systems incorporate data-loggers and sophisticated computing facilities, which can offer almost unlimited precision in controlling water supply. The benefit from such systems can be substantial and they offer scope for optimising WUE and product quality.

Numerous methods exist for modifying existing irrigation systems to increase WUE. However, to date, many of these have not found widespread application. One reason is lack of incentive, which can be linked to the pricing mechanism for irrigation water in Australia. Another problem is that many of these methods need adaptation and simplification to make them acceptable to growers. In addition, the basic irrigation infrastructure in many areas of Australia is old — a factor that often deters adoption of new technologies. Until capital inputs are available to revamp irrigation water delivery and handling systems, the potential for improving WUE will not be fully realised.

Another impediment to improved on-farm WUE is often the off-farm water distribution system. Typically, in most irrigated areas in Australia, water is distributed through large canals feeding laterals

that deliver water at the farm gate. The design and operation of the canal system dictates that (at best) water must be ordered some days in advance of supply, or (at worst) water is delivered on a fixed rotation scheme. Efficient on-farm water use requires an adequate supply of water, delivered on demand. This can also help schedule irrigations to individual fields, and provide sufficient feedback to improve the operation of the delivery system.

Need for efficient drainage systems

WUE will also be adversely affected by waterlogging. Excess application of irrigation water must be avoided. Therefore, irrigation systems should incorporate drainage systems that remove irrigation water applied in excess of crop needs and avoid excess salts accumulating in the root zone. Drainage systems must also minimise water entering adjacent fields through seepage from leaky canals and excess irrigation. Natural soil drainage rates need to be taken into account and supplemented by artificial drainage installations. Although flushing salts past the root zone is important to the long-term viability of an irrigation area, the increase in water volumes to either local or regional groundwater systems can cause other environmental problems, such as salinity, in areas removed from the primary area of irrigation.

Salinity and sodicity are major threats to optimum WUE in Australia. To avoid yield reductions from salinity, the downward flux of water through the root zone must be sufficient to avoid concentrating salts in the soil solution of the root zone. This flux is generally termed the 'leaching requirement'—the fraction of the total surface-applied water that must percolate through the root zone to prevent salinity levels in root zones from reaching harmful levels.

For typical irrigation water with an electrical conductivity of 1.8 dS/m (1,000 mg/L of dissolved solids), the leaching requirement for most crops is 0.05. In theory, this leaching requirement is easily met, even with the most efficient irrigation management, provided that there is uniform aerial distribution of irrigation water. However, in practice, uniform distribution is not easily achieved because some parts of a field always receive too much water and others do not receive enough water. Thus, drainage requirements are closely related to on-farm irrigation management and to the seepages and spills from the distribution system.

Estimating WUE in 'Leaky' Catchments

The term 'leaky catchment' refers to the lateral and vertical transport of water (and solutes) moving off-site from catchments (Cox and Fleming 1997; Cox and Pitman 2001). By definition, rainfed catchments harvest and partition seasonal rainfall into that which is available for plant growth and that which flows from the land into streams and subsequently into regional water bodies (Cox and Ashley 2000). Rain not intercepted and captured by the soil–plant system may move via overland and throughflow pathways towards streams, and by deep drainage to groundwater. Such losses to the soil–plant system are likely to be greater in areas of higher rainfall and in landscapes with sloping topography.

Where there are duplex soils, lateral transport of water and soil solutes is likely to be significant (Cox et al. in press). This may contribute to transient perched watertables and areas of waterlogging and salinisation, which develop, persist and expand within the landscape (including discharge and ponded areas at lower points in a catchment) (Cox and McFarlane 1995).

These processes have a definite seasonal incidence and may unbalance a catchment's hydrology. In any given year, the resident time of water (and solutes) varies at different points in the landscape (including the recharge and discharge areas). Within a growing season and in the longer term, cumulative effects may progressively occur that

impact on catchment hydrology and hence on the spatial use of water by plants.

Given the mobility of water within catchments, there is scant hope for using only growing-season or annual rainfall to estimate and compare WUE under different land management practices (e.g. comparing WUE under set-stocking or rotational grazing at varying grazing pressures). A more sophisticated model is required to quantify spatial contributions to catchment water balance. Such a model could in turn be used to estimate the proportion of rainfall that is intercepted or used by the soil–plant system.

In other words, we need to quantify the total environmental losses of water (i.e. water not intercepted or used by plants) before we move towards calculating WUE for a given farming system. We also need to recognise that WUE estimates are likely to vary spatially within a given catchment, and with the type of farming system used.

Conclusions

Various WUE indicators employed in China and Australia have been discussed. The type of WUE indicator used must be clearly stated because some are used to indicate production or economic performance rather than water use. To be widely adopted, an indicator of WUE must be practical and based on easily measured parameters.

Acknowledgments

This research was supported by contributions from ACIAR to Project LWR1/95/07, conducted by CSIRO Land and Water and the Chinese Academy of Sciences.

References

Anderson, K. and Peng, C.Y. 1998. Feeding and fueling China in the 21st Century. World Development, 26, 1413–1429.

Armstrong D.P., Knee, J.E., Doyle, P.T., Pritchard, K.E. and Gyles, O.A. 2000. Water-use efficiency on irrigated dairy farms in northern Victoria and southern New South Wales. Australian Journal of Experimental Agriculture, 40, 643–653.

Bolger, T.P., Turner, N.C. and Leach, B.J. 1993. Water use and productivity of annual legume-based pasture systems in the south-west of Western Australia. Proceedings of the XVII International Grasslands Congress, 174–275.

Brown, L.R. and Halweil, B. 1998. China's water shortage could shake world food security. World Watch, 11, 10–21.

Chen, Z.X. 1985. Field water balance. Advances in Soil Sciences 1, 26–30.

Cox, J.W. and Ashley, R. 2000. Water quality of gully drainage from texture-contrast soils in the Adelaide Hills in low rainfall years. Australian Journal of Soil Research, 38, 959–972.

Cox, J.W., Chittleborough, D.J., Ashley, R. and Varcoe, J. In press. Seasonal changes in water chemistry along a toposequence of texture-contrast soils. Australian Journal of Soil Research.

Cox, J.W., and Fleming, N.K. 1997. Understanding landscape processes. Property and Catchment Planning, Issues, Challenges and Professional Responsibilities. Proceedings of an Australian Institute of Agricultural Science and Technology Symposium Waite Institute, 16 September, 1997, Adelaide.

Cox, J.W. and McFarlane, D.J. 1995. The causes of waterlogging in shallow soils and their drainage in south-western Australia. Journal of Hydrology 167, 175–194.

Cox, J.W. and Pitman, A. 2001. Chemical concentrations in drainage from perennials grown on sloping duplex soils. Australian Journal of Agriculture Research, 52, 211–220.

Deason, J.P., Schad, T.M. and Sherk, G.W. 2001. Water policy in the United States: a perspective. Water Policy, 3, 175–192.

Fischer, R.A., and Turner, N.C. 1978. Plant productivity in the arid and semiarid zones. Annual Review of Plant Physiology, 29, 277–317.

French, R.J. 1992. Looking forward: a vision. Proceedings of the 33rd Annual Conference of the Grassland Society of Victoria Inc., 105–113.

French, R.J. 1995. Multidisciplinary teams to conduct integrated research on farming systems: a challenge. Australian Journal of Soil Research, 33, 659–671.

French, R.J. and Schultz, J.E. 1984a. Water use efficiency of wheat in a Mediterranean-type environment. I. The relation between yield, water use and climate. Australian Journal of Agricultural Research, 35, 743–64.

French, R.J. and Schultz, J.E. 1984b. Water use efficiency of wheat in a Mediterranean-type environment. II. Some limitations to efficiency. Australian Journal of Agricultural Research, 35, 765–775.

Garabet, S., Ryan, J. and Wood, M. 1998. Nitrogen and water effects on wheat yield in a Mediterranean-type climate. I. Growth, water-use and nitrogen accumulation. Field Crops Research, 57, 309–318.

Gong, J. and Lin, H. 2000. Sustainable development for agricultural region in China: case studies. Forest Ecology and Management, 128, 27–38.

Grimble, R.J. 1999. Economic instruments for improving water use efficiency: theory and practice. Agricultural Water Management, 40, 77–82.

Hunsaker, D.J., Kimball, B.A., Pinter, P.J.J., Wall, G.W., LaMorte, R.L., Adamsen, F.J., Leavitt, S.W., Thompson, T.L., Matthias, A.D. and Brooks, T.J. 2000. CO_2 enrichment and soil nitrogen effects on wheat evapotranspiration and water use efficiency. Agricultural and Forest Meteorology, 104, 85–105.

Jin, M., Zhang, R., Sun, L. and Gao, Y. 1999. Temporal and spatial soil water management: a case study in the Heilonggang region, PR China. Agricultural Water Management, 42, 173–187.

Karrou, M. 1998. Observations on effect of seeding pattern on water-use efficiency of durum wheat in semi-arid areas of Morocco. Field Crops Research, 59, 175–179.

Li, F., Zhao, S. and Geballe, G.T. 2000. Water use patterns and agronomic performance for some cropping systems with and without fallow crops in a semi-arid environment of northwest China. Agriculture, Ecosystems and Environment, 79, 129–142.

Li, J., Liu, X., Zhou, W., Sun, J., Tong, Y., Liu, W., Li, Z., Wang, P. and Yao, S. 1995. Technique of wheat breeding for efficiently utilizing soil nutrient elements. Science in China, 38, 1313–1320.

Lin, J.Y. 1997. Institutional reforms and dynamics of agricultural growth in China. Food Policy, 22, 201–212.

Liu, Y., Teixeira, J.L., Zhang, H.J. and Pereira, L.S. 1998. Model validation and crop coefficients for irrigation scheduling in the North China Plain. Agricultural Water Management, 36, 233–246.

Loaiciga, H.A., Valdes, J.B., Vogel, R., Garvey, J. and Schwarz, H. 1996. Global warming and the hydrologic cycle. Journal of Hydrology, 174, 83–127.

Pannell, D.J. and Glenn, N.A. 2000. A framework for the economic evaluation and selection of sustainability indicators in agriculture. Ecological Economics, 33, 135–149.

Reuter, D.J., Moore, A.D., Khanna, P.K., Tennant, D., McLean, G.D., French, R.J. and Hingston, F.J. 1996. Indicators of farm productivity and financial performance. In: Walker, J. and Reuter, D.J., eds, Indicators of Catchment Health: a technical perspective. CSIRO Publishing, Australia, 47–66.

Ritchie, J.T. 1983. Efficient water use in crop production: generality of relations between biomass production and evapotranspiration. In: Taylor, H.M., Jordan, W.R. and Sinclair, T.R., eds, Limitations to Efficient Water Use in Crop Production. American Society of Agronomy, Madison, 29–44.

Rosegrant, M.W. and Ringler, C. 2000. Impact on food security and rural development of transferring water out of agriculture. Water Policy, 1, 567–586.

Rozelle, S., Huang, J. and Zhang, L. 1997. Poverty, population and environmental degradation in China. Food Policy, 22, 229–251.

Sinclair, T.R., Tanner, C.B. and Bennett, J.M. 1984. Water-use efficiency in crop production. BioScience, 34, 36–40.

Smit, B. and Yunlong, C. 1996. Climate change and agriculture in China. Global Environmental Change, 6, 205–214.

Stanhill, G. 1986. Water use efficiency. Advances in Agronomy, 39, 53–85.

Tanner, C.B. and Sinclair, T.R. 1983. Efficient water use in crop production: research or re-search ? In: Taylor, H.M., Jordan, W.R. and Sinclair, T.R., eds, Limitations to Efficient Water Use in Crop Production. American Society of Agronomy, Madison, 1–28.

Thomas, A. 2000. Climatic changes in yield index and soil water deficit trends in China. Agricultural and Forest Meteorology, 102, 71–81.

Tolk, J.A., Howell, T.A. and Evett, S.R. 1999. Effect of mulch, irrigation, and soil type on water use and yield of maize. Soil and Tillage Research, 50, 137–147.

Tuong, T.P. and Bhuiyan, S.I. 1999. Increasing water-use efficiency in rice production: farm-level perspectives. Agricultural Water Management, 40, 117–122.

Turner, N.C. 1986. Crop water deficits: a decade of progress. Advances in Agronomy, 39, 1–51.

Turner, N.C. 1997. Further progress in crop water relations. Advances in Agronomy, 58, 293–338.

Wallace, J.S. 2000. Increasing agricultural water use efficiency to meet future food production. Agriculture, Ecosystems and Environment, 82, 105-119.

Walker, G., Gilfeder M., Williams, J. 1999. Effectiveness of current farming system in the control of dryland salinity. CSIRO Land and Water Publication, 16.

Young, W. (ed). 2001. Rivers as Ecological Systems: The Murray–Darling Basin. Murray–Darling Basin Commission, Canberra, Australia.

Zhang, H. and Oweis, T. 1999. Water-yield relations and optimal irrigation scheduling of wheat in the Mediterranean region. Agricultural Water Management, 38, 195–211.

Zhang, J., Sui, X., Li, B., Su, B., Li, J. and Zhou, D. 1998. An improved water-use efficiency for winter wheat grown under reduced irrigation. Field Crops Research, 59, 91–98.

5

The Water Balance of Pastures in a South Australian Catchment with Sloping Texture-Contrast Soils

Jim W. Cox* and Ashleigh Pitman†

Abstract

The water use of several pasture types was compared in a catchment in the Mount Lofty Ranges, South Australia. The study sites had sloping (less than 14%) texture-contrast soils. The aim was to delineate the water pathways (e.g. evapotranspiration, surface runoff, throughflow) in the catchment and to supply farmers with the best pasture option for minimising deep drainage.

Lucerne (*Medicago sativa* cv. Aquarius) produced more dry matter in summer and used more water than phalaris (*Phalaris aquatica* cv. Sirosa) on the mid- and upper slopes but was similar on the toe-slopes. The clay subsoils on the toe-slope were slightly saline, strongly sodic and sometimes affected by saline groundwaters in winter. After only one year's growth, the lucerne and phalaris pastures used more water than the existing cocksfoot (*Dactylis glomerata*) pasture on all parts of the slope. TOPOG-IRM modelling indicated that on all parts of the slope there was substantial deep drainage under the existing pasture (up to 29% of annual rainfall), with much-reduced deep drainage under phalaris and lucerne.

本文对比了几种牧草的水分利用壮况，以查明流域水分流失渠道(如蒸发蒸腾量，表面径流，壤中流等)，为当地农户找出最佳牧草种类，最大程度减少土壤水分深层渗漏。试验地点在南澳劳伏特山区，地面坡度<14%，土壤剖面质地不均，上层砂土或壤土，下层粘土。对比发现，苜蓿在夏季比苡草生产更多的干物质，在坡面的中上部也消耗更多的水分，但在坡面下部两者耗水量接近。坡下部的土壤粘土层有轻微盐化，严重碱化，冬季有时因地下盐

* CSIRO Land and Water, PMB 2, Glen Osmond, SA 5064, Australia. Email: jim.cox@csiro.au

† Department of Land and Water Conservation, PO Box 486, Moree, NSW 2400, Australia.

Cox, J.W. and Pitman, A. 2002. The water balance of pastures in a South Australian catchment with sloping texture-contrast soils. In: McVicar, T.R., Li Rui, Walker, J., Fitzpatrick, R.W. and Liu Changming (eds), *Regional Water and Soil Assessment for Managing Sustainable Agriculture in China and Australia*, ACIAR Monograph No. 84, 82–94.

水位升高而受到影响。在仅仅生长一年以后，在坡地的各个部位，苜蓿和苡草都能比当地原有的鸭茅草利用更多的水分。TOPOG－IRM 模型显示，鸭茅草下的土壤底层水分渗漏严重（可高达年降雨量的 29%），而在苜蓿和苡草下面则大大减少了。

LAND degradation is widespread in the agricultural regions of Australia, affecting vast areas of potentially productive land. Most land degradation (e.g. dryland salinity, waterlogging and erosion) has been caused by the widespread clearance of perennial native vegetation and its replacement with mainly annual crops and pastures (e.g. Saunders and Hobbs 1993). This has led to a drastic change in the hydrology of agricultural landscapes. It is widely acknowledged that recharge under introduced annual crops and pastures is significantly greater than that which occurs under natural vegetation (e.g. Kennett-Smith et al. 1993).

Duplex soils, sands or loams over clays occupy a large percentage of southern Australian agricultural regions (Chittleborough 1992). Their chemical and physical properties vary along a toposequence from crest to flat (Tennant et al. 1992). Duplex soils are particularly susceptible to land degradation when cleared for agriculture. Degradation on duplex soils is exacerbated by the development of rapidly fluctuating perched watertables on slowly permeable subsoil horizons (Cox et al. 1994; Cox and McFarlane 1995). On some sloping duplex soils, significant quantities of water can travel as throughflow on top of the B horizon (Cox and Fleming 1997; Fleming and Cox 1998). This can increase the risk of waterlogging on low slopes. On 'leaky' duplex soils, groundwater recharge can mobilise stored salts and bring them into the root zone, particularly in the toe-slopes and flats (Cox et al. 1996; Fitzpatrick et al. 1997). The chemical and physical properties of these duplex soils may change over time (Fitzpatrick et al. 2000).

It is apparent then that catchment water balances need to change so that less deep drainage occurs (Gregory et al. 1992). One option for achieving this may be changed agronomic practices. Lucerne (*Medicago sativa* L.), phalaris (*Phalaris aquatica* L.), and cocksfoot (*Dactylis glomerata* L.) are commercially available pasture species. Previous studies of these pasture species on flat land have shown considerable variation between species in their growth and soil water use (e.g. Whitfield et al. 1992; Crawford and Macfarlane 1995; Lolicato 2000).

The aim of this study was to compare the water balance under lucerne with that under phalaris in three parts of the landscape. In addition, the pastures were compared with the existing (cocksfoot-based) pasture. Although farmers are encouraged to sow perennial pastures as a means of recharge reduction, no study has looked at the differences in their water use on sloping duplex soils.

Materials and Methods

Site location, climate and soils

The experimental site was located in the Keynes catchment in the Mount Lofty Ranges, South Australia. The climate is Mediterranean and the mean annual rainfall is 544 mm, more than 75% falling between April and October. The catchment soils are typical of many in the > 500 mm rainfall region of the Mount Lofty Ranges (Fritsch and Fitzpatrick 1994; Cox et al. 1996). Slopes average 14%. The Overview provides background information about the area and Figure 5 of the Overview shows its location.

Pits were excavated along five toposequences in the catchment and soils were classified according to both Soil Survey Staff (1996) and Isbell (1996) criteria. Chemical properties of the soil horizons were measured on selected samples using standard techniques (Rayment and Higginson 1992). Saturated hydraulic conductivities (K_s) of the A, E and B soil horizons were measured at 12 sites in each of the upper, mid- and toe-slopes of the catchment, using a disc permeameter (Perroux and White 1988). At the same locations, intact cores (0.047 m diameter and 0.05 m height) were collected for measurement of soil water characteristics[1] and bulk density.

Experimental design

There were three pasture types: lucerne-based, phalaris-based, and the existing pasture comprising cocksfoot, subterranean clover (*Trifolium subterraneum* L.) and annual grasses and weeds. Each plot was approximately 0.2 ha. Lucerne *(Medicago sativa* cv. Aquarius) and phalaris (*Phalaris aquatica* cv. Sirosa) plots were sown in the first year of the trial (1996) and replicated at each of the three levels of the landscape (that is, there were two plots of each crop at each of the upper, mid-, and toe-slopes). The existing pasture surrounded the lucerne and phalaris plots; detailed measurements were collected from one plot location at each landscape level. Physical barriers prevented run-on; overland flow and throughflow were measured using v-notch weirs and tipping buckets installed in drains (Cox and McFarlane 1995). Further details are in Cox and Pitman (2001).

Measurement of soil water stored in the profile

Soil water storage was monitored regularly (2–3 times a week in summer, weekly in winter), from 1996 to 1997 using a neutron moisture meter (NMM) (CPN Corporation, California, USA). Readings were taken at 0.1, 0.2, 0.35, 0.5, 0.7, 0.9, 1.1, 1.4 and 1.7 m. The neutron probe was calibrated from measuring the water content of soil cores (623 cm^3) collected at various periods of the year. Cores were dried at 105°C for 24 hours; gravimetric soil water content was then calculated and linear regressions ($r^2 > 0.8$) established for each soil horizon. Probe readings were taken at the same time as core sampling for each access tube. The bulk density of each sample (and of samples from the soil pits) was calculated from the known core volumes; their respective volumetric water contents were then derived.

Plant production and root distribution

On four occasions, pasture was harvested for the calculation of pasture dry matter availability. About 18 months after lucerne and phalaris establishment, 10 soil cores were taken from each of the three existing pasture plots and from one lucerne and one phalaris plot at each of the three toposequence positions. One core from each site (taken from approximately 1 m downslope of the NMM access tube) was sectioned to correspond with the neutron probe reading depth, sealed in a plastic bag and used for additional NMM calibration. A second core was placed on a core tray, which was sealed and labelled for detailed profile description. The remaining eight cores were cut into 0.2 m sections and placed in plastic bags that were sealed, labelled, and stored for root washing. All samples were stored at < 4°C prior to analysis.

Roots were washed using the hydropneumatic elutriation method described by Smucker et al. (1982); this method reportedly recovers 15–25% more root dry weight than careful handwashing techniques (Mackie-Dawson and Atkinson 1991). The technique requires two sieve sizes (0.5 mm and 1.0 mm) to retain the roots. Further soil pits were excavated to allow analysis of root growth and distribution, including a qualitative description of root growth and penetration down the profile.

[1] Needed for the water balance modelling but not discussed in this paper.

Morphological measurements of length, area and root length density (RLD) were determined from scanned samples in the WinRHIZO™ package (Regent Instruments Inc., Quebec, Canada), using the method of Tennant (1975).

Hydrological modelling

Rainfall, solar radiation, wind speed, temperature and humidity were recorded hourly at an automatic weather station located in the catchment. TOPOG-IRM (a hydrological modelling package based on terrain analysis) (Dawes and Hatton 1993) simulations were run using the climatic, soil and vegetation data until soil water changes, overland flow and throughflow were correctly predicted. Actual evapotranspiration was derived from Penman–Monteith type equations (Monteith 1981) within TOPOG-IRM (Dawes and Hatton 1993). Deep drainage was determined by difference using the water balance equation for texture-contrast soils (Gregory et al. 1992).

Results

Soil types

From crest to flat, the soils were a sequence of Typic Palexeralfs to Aquic Palexeralfs to Natraqualfs; elsewhere the sequence was red and brown Chromosols to brown Sodosols to brown Dermosols. On the mid- and upper slopes, the topsoils were acidic (pH 6.2–6.7), nonsaline ($EC_{1:5}$ 0.01–0.06 dS/m)[2] and nonsodic (ESP < 5%).[3] The subsoils on the mid- and upper slopes had variable pH (6.5–7.6), were nonsaline ($EC_{1:5}$ 0.021–0.045 dS/m) and were usually nonsodic (ESP < 6%) except at depth (ESP was 10% at 1 m). On the toe-slopes, the topsoils were also acidic (pH 5.8–6.9) and nonsaline (0.015–0.045 dS/m) but were sometimes sodic (ESP 3–15%). The subsoils on the toe-slopes also had variable pH (6.6–7.8) and were often slightly saline ($EC_{1:5}$ <0.2 dS/m) and strongly sodic (< 21%).

Bulk density of the topsoil (0–0.4 m) was similar (1.5–1.7 g/cm^3) and not significantly different ($P < 0.05$) at all positions on the slope (Table 1). Bulk density of the subsoil was significantly ($P < 0.05$) higher on the toe-slope (< 2.0 g/cm^3 at 0.9 m) and lower on the upper slope (< 1.9 g/cm^3 at 1.50 m) than elsewhere. The change in the bulk density of the subsoil with depth was similar on the upper and middle slope but different on the toe-slope.

Table 2 shows the average K_s values. In general, K_s on the toe-slope was significantly ($P < 0.05$) lower than on the mid- and upper slopes in the A and B horizons (average 0.9 and 0.05 m/day, respectively) but was significantly ($P < 0.05$) higher in the E horizon (average 0.18 m/day).

Table 1. Bulk density of soil in a toposequence.

Depth interval (cm)	Mean bulk density (g/cm^3)[a]		
	Upper slope	Mid-slope	Toe-slope
0–20	1.503 (1.417–1.589)	1.570 (1.395–1.735)	1.490 (1.439–1.677)
20–40	1.738 (1.705–1.793)	1.717 (1.434–1.892)	1.627 (1.491–1.765)
40–60	1.659 (1.405–1.838)	1.796 (1.712–1.948)	1.823 (1.689–2.020)
60–80	1.631 (1.312–1.824)	1.741 (1.657–1.868)	1.973 (1.755–2.242)
80–100	1.665 (1.439–1.887)	1.825 (1.769–1.983)	2.030 (1.802–2.508)
100–120	1.820 (1.659–1.920)	1.925 (1.810–2.008)	2.012 (1.775–2.248)
120–140	1.856 (1.683–1.946)	1.818 (1.813–1.823)	1.976 (1.764–2.134)
140–160	1.894 (1.720–2.014)	1.892 (1.881–1.904)	1.843 (1.698–1.984)

[a] Figures in brackets indicate the range

[2] $EC_{1:5}$ is the electrical conductivity; dS/m = deciSiemens per metre.

[3] ESP is exchangeable sodium percentage.

Rainfall

The annual rainfall was 14% below average in the first year of the trial (when the lucerne and phalaris were sown), close to the average in the second year of the trial and 26% below average in the final year (Table 3). The rainfall from April to October followed a similar pattern, with a 12% reduction in the first year, a slight increase (3%) in the second year and a substantial (40%) decrease in the final year.

Soil water

Figure 1 shows the change in soil water content (SWC) over two years below three pasture types on the upper slope of the catchment (the darker the shading, the higher the SWC). The SWC of the A horizon (approximately 0–0.35 m) followed a similar pattern under all treatments, responding rapidly to rainfall events. The type of overlying pasture did not significantly affect SWC over time ($P < 0.05$) (Fig. 2). During each winter, a perched watertable developed to some degree on all treatments within the clay subsoil (at approximately 0.5–0.6 m depth).

In the soil profile below 0.35 m, changes in SWC were more gradual, and less influenced by the weather conditions. Under cocksfoot-based pasture, SWC at 0.35–1.7 m increased over the period of study at all slope positions (Table 4), based on end water content minus the initial water content (the amount of water used by the plant or drained). Under phalaris, SWC decreased at all slope positions, with the greatest water uptake in the upper slope position, followed by the mid- and toe-slopes. Under lucerne too, SWC decreased most in the upper slope region, followed by the mid- and toe-slopes. This trend was confirmed by solving the water balance to 1.8 m depth (Table 5). Lucerne on the mid- and upper slope and phalaris on the upper slope dried the soil profile over a two-year period. Over the same period, the SWC increased in all landscape positions under the cocksfoot. Thus, the greatest deep drainage occurred under cocksfoot; there was substantially less deep drainage under phalaris, and there was an uptake of soil water from below 1.8 m by the lucerne in the upper and mid-slope positions. In the toe-slope position, deep drainage was similar under lucerne and phalaris (Table 5).

Table 2. Average measured saturated hydraulic conductivity (*Ks*) used in the modelling of deep drainage (m/day).

Horizon	Toe-slope	Mid-slope	Upper slope
A	0.93	1.97	2.06
E	0.18	0.14	0.11
B	0.05	0.08	0.07

Dry matter production and root analysis

Lucerne-based pasture was significantly ($P < 0.05$) more productive than the phalaris-based or cocksfoot-based pasture in the upper and mid-slope positions. It was also more productive on the toe-slopes but not to the same degree. Toposequence position in this regard was highly significant ($P < 0.01$). Table 6 shows the summer

Table 3. Monthly rainfall at Keyneton township and seasonal rainfall for the Keynes catchment (mm).

	J	F	M	A	M	J	J	A	S	O	N	D	Total	Apr–Oct total
Average[a]	18	23	20	35	62	64	80	76	63	49	29	25	544	429
1996	48	15	13	37	37	67	121	9	48	58	9	5	467	377
1997	47	8	30	10	10	132	84	80	73	53	15	7	549	442
1998	10	61	2	7	56	24	12	85	73	0	35	39	404	257

[a] 78-year average data from Bureau of Meteorology

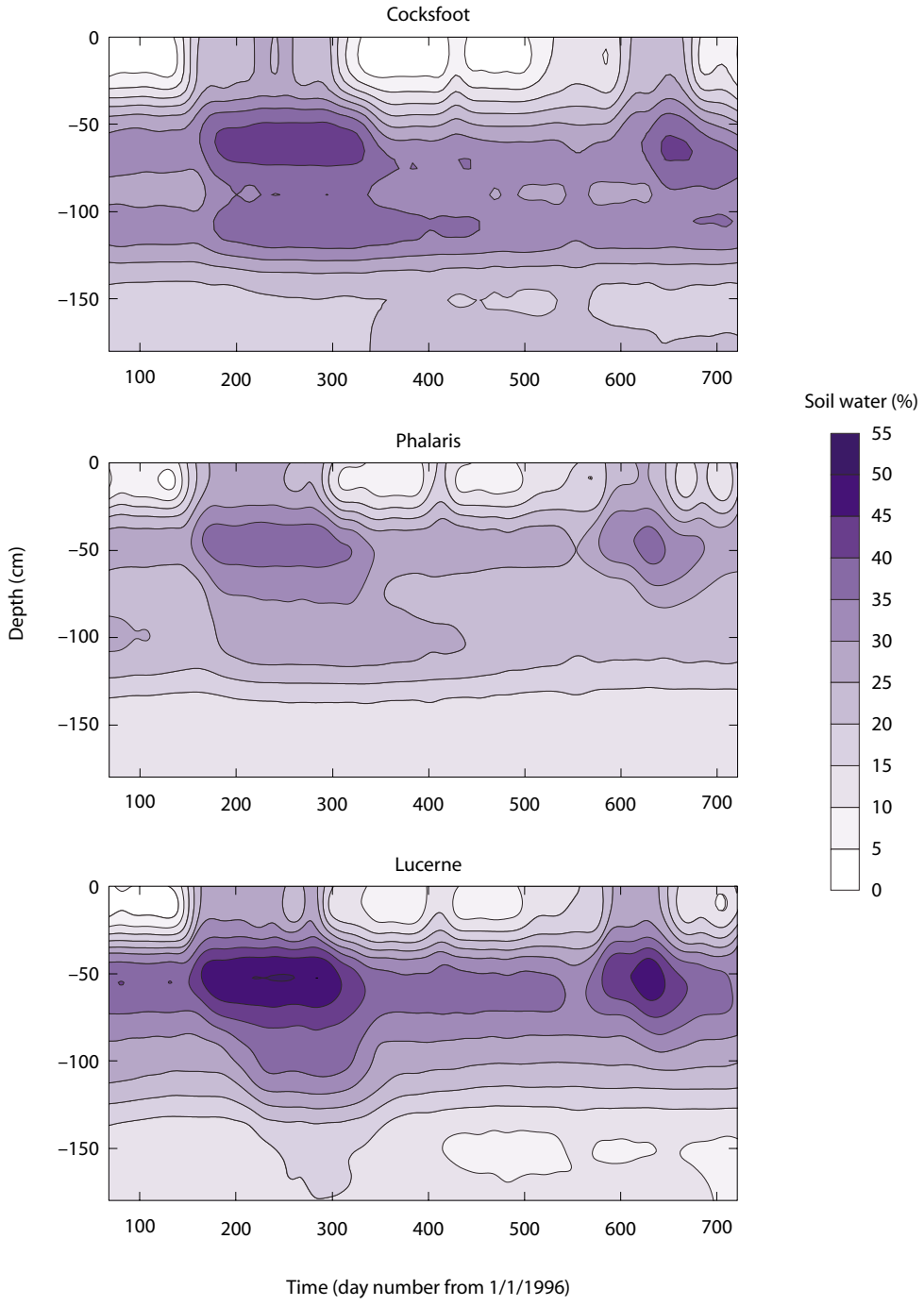

Figure 1. An example of soil water content (volume %) over a two-year period, under three pasture treatments on the upper slope, showing the development of perched watertables within the B horizon (average 35–75 cm).

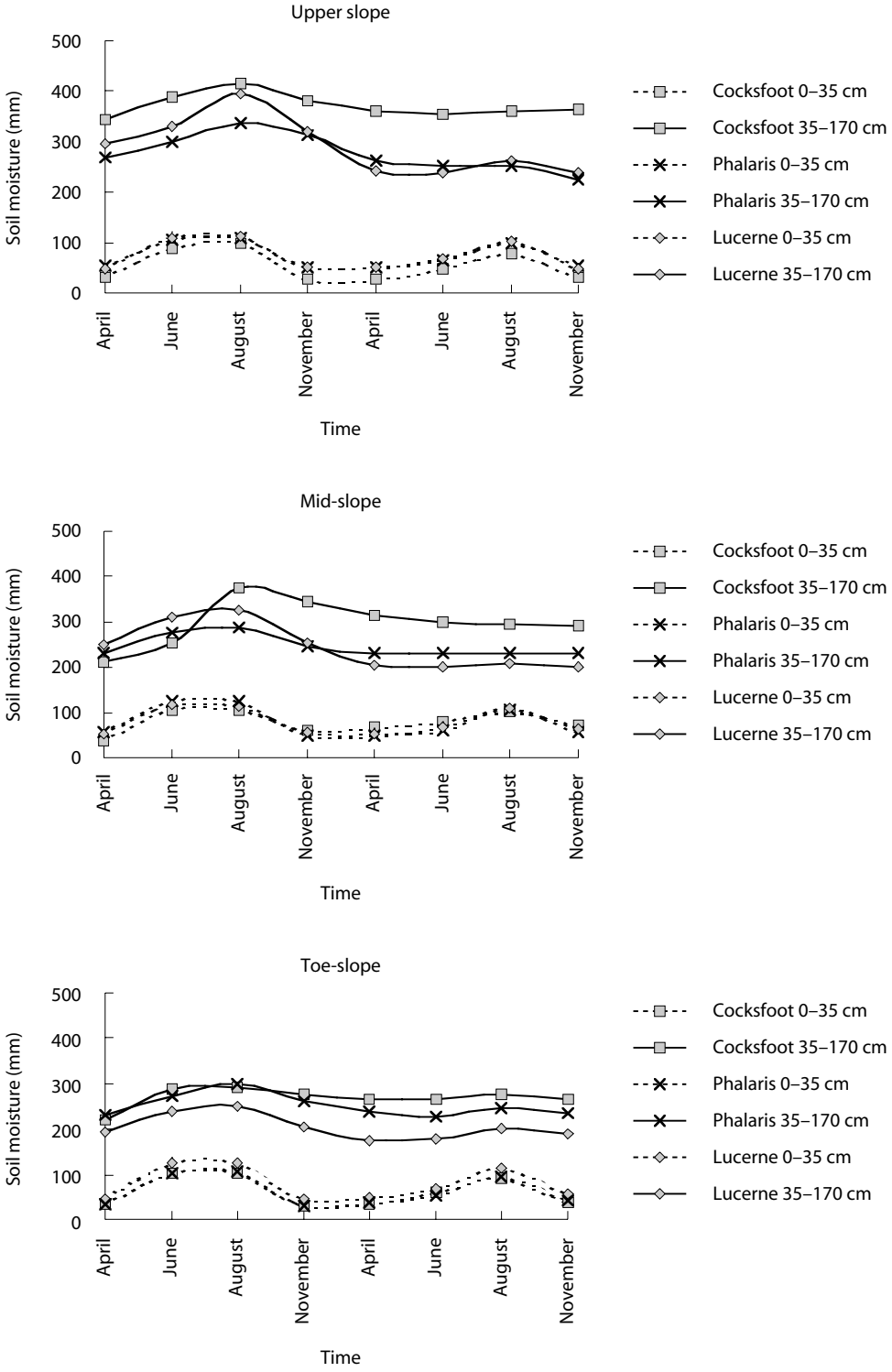

Figure 2. Average monthly soil water content (mm), from April 1997 to December 1998, under pasture.

growth advantage of the lucerne compared with the cocksfoot and phalaris-based pastures (the lucerne production in April 1997 was much higher than the other two pastures on all slope positions).

For all three pasture treatments, examination of roots in soil pits confirmed that most roots were in the top 0.3 m of the soil profile (Table 7); this is consistent with other studies (Evans 1978; Gregory 1998). Visual inspections revealed a dense mat of roots in the top 0.1 m under all treatments, but surface samples (0–0.1 m) were not analysed because it would have taken too long to prepare samples of such a large amount of extraneous organic material.

Table 4. Average change (initial–final) soil water content (mm), 35–170 cm soil depth, over a two-year period (1996 to 1997).

Pasture	Upper slope	Mid-slope	Toe-slope
Cocksfoot	14.9	81.8	48.9
Phalaris	58.0	11.2	1.8
Lucerne	74.8	57.8	10.5

Figure 3 shows mean data (from eight cores per treatment per slope position) for the scanned root samples. The cocksfoot samples were taken from the pre-existing pasture; the other samples were taken about 18 months after pasture establishment. Cores were taken to the maximum depth possible given soil conditions and the limitations of the drilling rig; most samples were no deeper than 1.4 m. As indicated in Figure 3, most of the cocksfoot and phalaris root material below approximately 0.9 m was dead.

Discussion

Soil water, deep drainage and water use

The soil water content of the A horizon was similar under all pasture types. In the autumn/winter of the first year of the trial, a perched watertable developed within the B horizon under all pastures and at all slope positions. By the autumn of the second year, the lucerne, and to a slightly lesser degree the phalaris, had begun to dry the profile below 0.35 m; this, combined with below average rainfall, reduced the development and duration of perching. Under the cocksfoot, the soil profile below 0.35 m had remained at a higher SWC; perching developed earlier and lasted longer than for the other two pasture treatments.

Table 5. Average water balance for different pasture/slope treatments (mm), 0–180 cm soil depth.

	Cocksfoot			Phalaris			Lucerne		
	Upper slope	Mid-slope	Toe-slope	Upper slope	Mid-slope	Toe-slope	Upper slope	Mid-slope	Toe-slope
Rainfall[a]	897	897	897	897	897	897	897	897	897
Evapotranspiration[b]	752	755	826	806	785	872	878	877	870
Surface runoff[a]	2	2	18	1	2	40	1	43	1
Throughflow[a]	8	18	74	8	44	14	13	13	29
Change in water storage[c]	–59	–141	–102	19	–32	–50	44	26	–49
Deep drainage[d]	194	263	81	63	98	21	–39	–62	46

[a] Actual measurements
[b] Actual evapotranspiration from TOPOG-IRM
[c] Initial–final soil water content
[d] Deep drainage is by difference in the water balance equation

Predicted deep drainage losses under cocksfoot were substantial over the two-year period, particularly in the upper and mid-slope positions. There was less drainage at the toe-slope position, because 73.5 mm of infiltration was removed via throughflow. Generally, throughflow increased downslope due to the increase in bulk density, and consequent lower porosities, of the sodic B horizon.

Deep drainage under the cocksfoot pastures ranged from 9% to 29% of annual rainfall over the two years. Under the phalaris treatments, deep drainage ranged from 21 to 98 mm, or 2–11% of the total rainfall for the period.

Phalaris persisted longer into summer than cocksfoot, broke dormancy earlier, had

Table 6. Mean dry matter production (kg/ha) of lucerne, phalaris and cocksfoot-based pastures, at three toposequence positions, over four time periods.

Slope	August 1996	October 1996	April 1997	October 1997	Total
Lucerne sites					
Upper	1211.6	2851.5	2393.9	2860.3	9317.3
Mid	1123.9	2954.2	1518.9	2461.1	8058.1
Toe	796.5	1871.2	1229.4	1796.7	5693.8
Phalaris sites					
Upper	1033.5	2732.4	936.1	2440.5	7142.5
Mid	902.2	2623.6	888.9	1491.4	5906.1
Toe	938.2	2618.4	905.0	1764.8	6226.4
Cocksfoot sites					
Upper	941.4	2904.6	552.1	1796.1	6194.2
Mid	902.8	2295.0	599.2	1667.1	5464.1
Toe	997.4	2098.6	767.9	1637.7	5501.6

Table 7. Root length densities at discrete depth intervals for the three pasture species tested.

	Root length density (cm/cm^3)		
Depth interval (cm)	Cocksfoot	Phalaris	Lucerne
10–30	3.7	6.0	6.5
30–50	0.9	1.8	1.9
50–70	0.5	0.8	0.7
70–90	0.2	0.4	0.5
90–110	0.2[a]	0.3[a]	0.3
110–130	0.1[a]	0.2[a]	0.3

[a] The bulk of root material in the cocksfoot and phalaris samples below 90 cm was dead

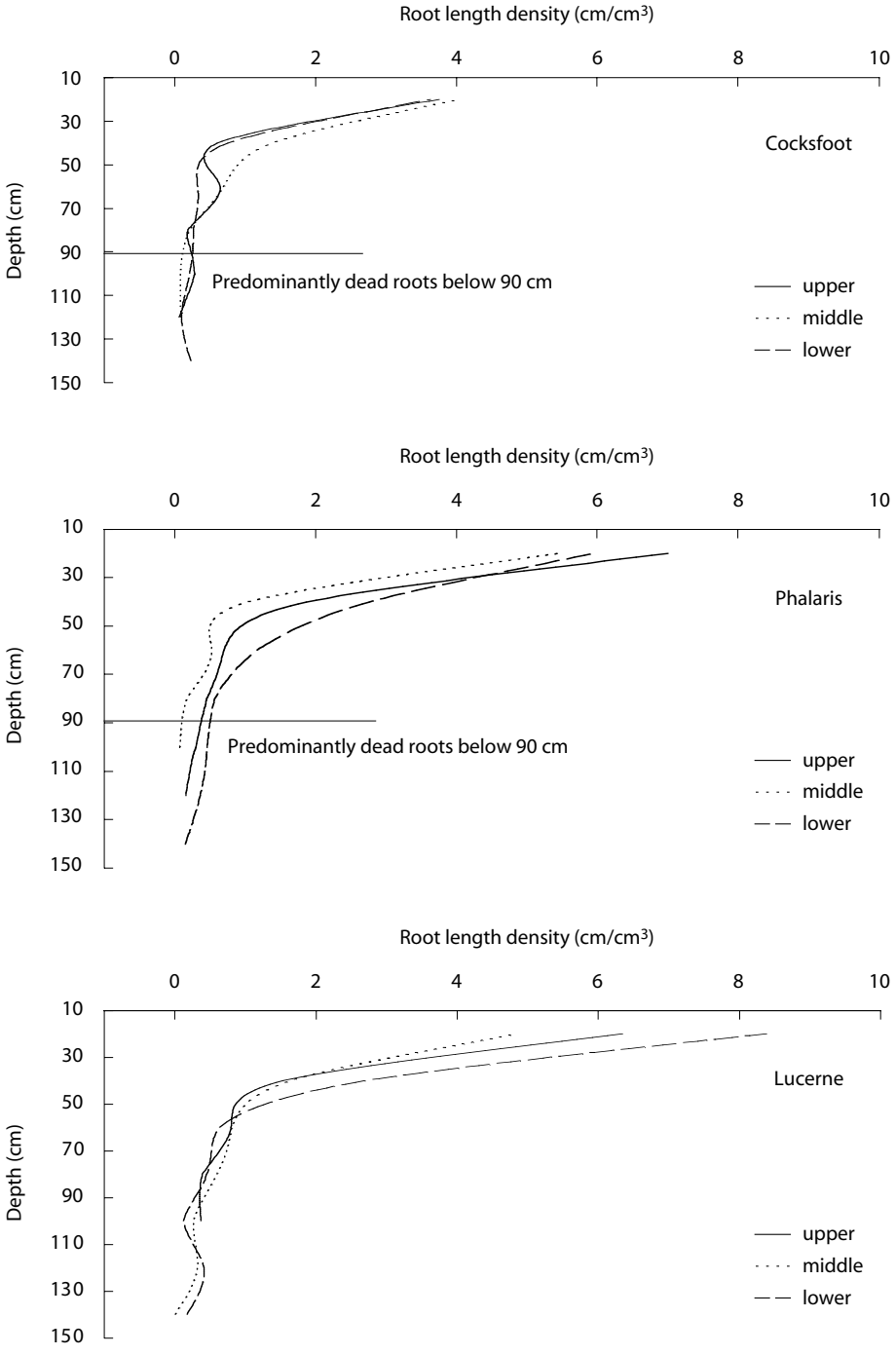

Figure 3. Root length density emphasising toposequence effects for cocksfoot, phalaris and lucerne.

proportionally more groundcover, and produced between 0.5 and 1.0 tonnes/ha more dry matter at each slope position. This additional growth resulted in increased evapotranspiration. These factors, and the substantially smaller increases in SWC under phalaris than under cocksfoot, suggest that farmers should be encouraged to sow phalaris rather than cocksfoot.

Modelling showed that under lucerne deep drainage occurred only on the toe-slope. At this point on the toposequence, 46 mm (5% of the total rainfall) passed below the 1.8 m profile boundary; groundwaters were shallow, so it probably contributed to recharge. In both the upper and mid-slope positions, soil water (44 and 26 mm respectively) was depleted from below 1.8 m by the lucerne. Numerous other studies, at smaller scale, support the ability of lucerne to extend its roots to a considerable depth, extract soil water from deep within the profile and reduce deep drainage. This study demonstrated that lucerne significantly reduces deep drainage on duplex soils at a small subcatchment scale, particularly at the upper and mid-slope positions. The main advantage of lucerne over the other pasture species tested appears to be the ability to extend roots into the subsoil and extract soil water stored deep in the profile, which would otherwise contribute to deep drainage. Lolicato (2000) reached a similar conclusion in his comparison of lucerne with cocksfoot, phalaris and birdsfoot trefoil (*Lotus corniculatus*). At the toe-slope position, where there was poor drainage and increased salinity, lucerne and phalaris both performed similarly, allowing deep drainage of 27–29 mm, in comparison to 63 mm at that position under cocksfoot.

Dry matter production and root analysis

Lucerne produced more dry matter over two years than the phalaris or cocksfoot in the upper and mid-slope positions. This was largely due to the summer dominant growth of lucerne. Phalaris and cocksfoot generally showed similar dry matter production, although phalaris production was slightly higher than that of cocksfoot over summer. Lucerne production was consistently lower than phalaris and cocksfoot on the toe-slopes where soils were slightly saline.

The decline in root material below 0.3 m in the catchment was quite marked for all species. Ridley and Simpson (1994) reported a study on a duplex red soil with a similar A/B horizon at approximately 0.3 m; they found a more gradual decline, with substantial root length density (RLD) to 0.5 m (approximately two-thirds of that in the 0.1–0.3 m interval). The Keynes catchment data suggested that a restrictive A/B horizon may encourage root proliferation in the surface soil.

Visual inspection of soil pits indicated distinct differences in rooting depth between species: cocksfoot roots were observed to 1.2 m, phalaris to approximately 1.5 m and lucerne to more than 2.0 m. The cocksfoot had been established for many years, so had probably established a maximum rooting depth for that environment. Soil pits dug some 18 months after the establishment of the lucerne and phalaris pastures showed that root extension to 2.0 m had already occurred. Subsequent pits did not indicate that phalaris was increasing its penetration to any extent. The lucerne root system could not be excavated to the full extent as its taproots followed cracks into the underlying sandstone. Both the phalaris and the lucerne roots had taken advantage of macropores, cracks and other faults to extend into lower depths. There was little evidence of roots elsewhere in the soil matrix at depth.

Figure 3 shows root length for each toposequence. The relatively low RLD of cocksfoot in the 0.1–0.3 m range is obvious. In the 0.3–0.7 m section of the soil profile, cocksfoot RLD is 0.25–0.5 cm/cm^3, whereas phalaris and lucerne are closer to 0.5–1.0 cm/cm^3. Phalaris and lucerne have more roots in the 0.1–0.3 m region; phalaris appears to show differences related to toposequence position, with a higher RLD below 0.3 m, in both the upper and toe-slope positions. This is consistent with pasture growth trends for phalaris,

with lower pasture cuts on the mid-slope. Lucerne RLD seems consistent below 0.5 m, at all topo-sequence positions; its main advantage over the other two pastures is that substantial live roots extend down the profile. At depth, many of these roots were still less than 1 mm in diameter compared to the fine, hair-like roots of both cocksfoot and phalaris. Decreases in SWC under the three pasture types are consistent with the densities and morphology of their root systems.

Conclusions

The results of this study show that both lucerne and phalaris will produce a higher amount of dry matter and use more water resulting in less deep drainage than the cocksfoot-based pastures that farmers are currently sowing. Lucerne is the best choice on mid- and upper slopes; phalaris is best for low slopes, where soil salinity and sodicity reduce the performance of lucerne.

Acknowledgments

Graham and Melanie Keynes allowed us to use their farm to do the research. Greg Rinder and Bob Schuster drafted some of the figures.

References

Chittleborough, D.J. 1992. Formation and pedology of duplex soils. Australian Journal of Experimental Agriculture, 32, 815–825.

Cox, J.W. and Fleming, N.K. 1997. Understanding landscape processes. Property and Catchment Planning, Issues, Challenges and Professional Responsibilities. Proceedings of an Australian Institute of Agricultural Science and Technology Symposium held at the Waite Institute, Adelaide, 16 September 1997.

Cox, J.W., Fritsch, E. and Fitzpatrick, R.W. 1996. Interpretation of soil features produced by modern and ancient processes in degraded landscapes: VII. Water duration. Australian Journal of Soil Research, 34, 803–824.

Cox, J.W. and McFarlane, D.J. 1995. The causes of waterlogging in shallow soils and their drainage in southwestern Australia. Journal of Hydrology, 167, 175–194.

Cox, J.W., McFarlane, D.J. and Skaggs, R.W. 1994. Field evaluation of DRAINMOD for predicting waterlogging intensity and drain performance in south-western Australia. Australian Journal of Soil Research, 32, 653–671.

Cox, J.W. and Pitman, A. 2001. Chemical concentrations in drainage from perennials grown on sloping duplex soils. Australian Journal of Agriculture Research, 52, 211–220.

Crawford, M.C. and Macfarlane, M.R. 1995. Lucerne reduces soil moisture and increases livestock production in an area of high groundwater recharge potential. Australian Journal of Experimental Agriculture, 35, 171–180.

Dawes, W. and Hatton, T.J. 1993. TOPOG-IRM. 1. Model Description. Division of Water Resources Technical Memorandum 93/5. Canberra, CSIRO.

Evans, P.S. 1978. Plant root distribution and water use patterns of some pasture and crop species. New Zealand Journal of Agricultural Research, 21, 261–265.

Fitzpatrick, R.W., Cox, J.W. and Bourne, J. 1997. Managing waterlogged and saline catchments in the Mt. Lofty Ranges, South Australia. Adelaide, Cooperative Research Centre for Soil and Land Management.

Fitzpatrick, R.W., Merry, R.H. and Cox, J.W. 2000. What are saline soils and what happens when they are drained? Journal of the Australian Association of Natural Resource Management, Special Issue, June, 26–30.

Fleming, N.K and Cox, J.W. 1998. Nutrient losses off dairy catchments located on texture contrast soils. Carbon, phosphorus, sulphur and other chemicals. Australian Journal of Soil Research, 36, 979–995.

Fritsch, E. and Fitzpatrick, R.W. 1994. Interpretation of soil features produced by ancient and modern processes in degraded landscapes. 1. A new method for constructing conceptual soil–water–landscape models. Australian Journal of Soil Research, 32, 889–907.

Gregory, P.J. 1998. Alternative crops for duplex soils: growth and water use of some cereal, legume, and oilseed crops, and pastures. Australian Journal of Agricultural Research, 49, 21–32.

Gregory, P.J., Tennant, D., Hamblin, A.P. and Eastham, J. 1992. Components of the water balance on duplex soils in Western Australia. Australian Journal of Experimental Agriculture, 32, 845–855.

Isbell, R.F. 1996. The Australian Soil Classification. Melbourne, CSIRO Publishing.

Kennett-Smith, A.K., Thorne, R. and Walker, G.R. 1993. Comparison of recharge under native vegetation and dryland agriculture near Goroke, Victoria. CSIRO Division of Water Resources and Centre for Groundwater Studies Report No. 49. Adelaide, CSIRO.

Lolicato, S.J. 2000. Soil water dynamics and growth of perennial pasture species for dryland salinity control. Australian Journal of Experimental Agriculture, 40, 37–45.

Mackie-Dawson, L.A. and Atkinson, D. 1991. Methodology for the study of roots in field experiments and the interpretation of results. In: Atkinson, D., ed., Plant Root Growth: An ecological perspective. Oxford, Blackwell Scientific Publications, 25–47.

Monteith, J.L. 1981. Evaporation and surface temperature. Queensland Journal of the Royal Meteorological Society, 107, 1–27

Perroux, K.M. and White, I. 1988. Designs for disc permeameters. Soil Science Society of America Journal, 52, 1205–1215.

Rayment, G.E. and Higginson, F.R. 1992. Australian Laboratory Handbook of Soil and Water Chemical Methods. Sydney, Inkata Press.

Ridley, A.M., White, R.E., Simpson, R.J. and Callinan, L. 1997. Water use and drainage under phalaris, cocksfoot, and annual ryegrass pastures. Australian Journal of Agricultural Research, 48, 1011–1023.

Ridley, A.M. and Simpson, R.J. 1994. Seasonal development of roots under perennial and annual grass pastures. Australian Journal of Agricultural Research, 45, 1077–1087.

Saunders, D.A. and Hobbs, R.J. 1993. Rural land management and the environment. Proceedings of the National Conference on Land Management for Dryland Salinity Control. Bendigo, Australia, La Trobe University, 18–23.

Smucker, A.J.M., McBurney, S.L. and Srivastava, A.K. 1982. Quantitative Separation of Roots from Compacted Soil Profiles by the Hydropneumatic Elutriation System. Agronomy Journal, 74, 500–513.

Soil Survey Staff. 1996. Keys to Soil Taxonomy. 7th edition. Washington DC, United States Department of Agriculture, United States Government Printing Office.

Tennant, D. 1975. A test of a modified line intersect method of estimating root length. Journal of Ecology, 63, 995–1002.

Tennant, D., Scholtz, G., Dixon, J. and Purdie, A.P. 1992. Physical and chemical characteristics of duplex soils and their distribution in the south-west of Western Australia. Australian Journal of Experimental Agriculture, 32, 827–844.

Whitfield, D.M., Newton, P.J. and Mantell, A. 1992. Comparative water use of dryland crop and pasture species. Proceedings of the 6th Australian Society of Agronomy Conference, Armidale, 262–265.

6

Simulation of Winter Wheat Yield and Water Use Efficiency on the Loess Plateau of China Using WAVES

Shaozhong Kang,* Lu Zhang,† Yinli Liang‡ and Warrick R. Dawes†

Abstract

Water availability is a major factor limiting crop yields on the Loess Plateau of China. As competition for water intensifies, it is essential to develop alternative irrigation schedules that maximise crop yield and water use efficiency (WUE) for a given level of water supply. A field experiment with winter wheat (*Triticum aestivum* L.) from 1995 to 1998 calibrated and tested a biophysically based model (WAVES) in terms of grain yield and WUE prediction. The data collected include water and energy balance components, biomass and grain yield. Comparisons between the measurements and the model predictions were made with three years of field data. Modelled grain yield and WUE based on biomass and harvest index were in better agreement with the measurements than those based on transpiration and harvest index. The model was sensitive to different irrigation treatments, and in reasonable agreement with field measured data. The highest irrigation treatment resulted in the greatest evapotranspiration but not the highest yield, so WUE was relatively low. Appropriately limited irrigation could improve the grain yield and WUE. Aiming only for maximum grain yield or for maximum WUE could lead to uneconomical irrigation management.

水分供应是黄土高原粮食产量的主要限制因素。由于用水竞争的加剧，选择能够在某一设定供水水平上，产量最高，水分利用效率（WUE）最高的灌溉方式就很重要。1995-98 年间进行的冬小麦田间试验，在作物产量和 WUE 方面校正、检测了基于生物物理原理的 WAVES 模型。收集了水分能量

* Key Laboratory of Agricultural Soil and Water Engineering in Arid and Semiarid Areas, Northwest Sci-Tech University of Agriculture and Forestry, Yangling, Shaanxi 712100, PRC.

† CSIRO Land and Water, PO Box 1666, Canberra, ACT 2601, Australia.Email: lu.zhang@csiro.au

‡ Institute of Soil and Water Conservation, Chinese Academy of Sciences and Ministry of Water Resources, Yangling, Shaanxi 712100, PRC.

Shaozhong Kang, Lu Zhang, Yinli Liang and Dawes, W.R. 2002. Simulation of winter wheat yield and water use efficiency on the Loess Plateau of China using WAVES. In: McVicar, T.R., Li Rui, Walker, J., Fitzpatrick, R.W. and Liu Changming (eds), *Regional Water and Soil Assessment for Managing Sustainable Agriculture in China and Australia*, ACIAR Monograph No. 84, 95–104.

平衡组分、生物量和粮食产量的数据，作了测量值和模型预测值的比较。以生物量和收获指数为基础预测的产量及 WUE 与实测值的吻合程度高于以蒸腾与产量指数为基础的数值。该模型对不同灌溉条件敏感性高，与实测值的吻合令人满意。灌溉最多，则蒸发最多，但产量不是最高，所以 WUE 相对较低，适当的有限灌溉能提高产量和 WUE。仅仅追求最大产量或最高 WUE 可能导致灌溉的经济效益不高。

THE LOESS Plateau, located in the middle reaches of the Yellow River, is one of the main agricultural regions in China. The Overview provides background information on this area; Figure 1 of the Overview shows its location. Winter wheat (*Triticum aestivum* L.) and summer corn (*Zea mays*) are the main crops in the area. Average annual rainfall ranges from 300 to 600 mm, with over 60% occurring from July to September. As rainfall is low and variable, water is the most important factor limiting agricultural production in the region. Crops are irrigated with water pumped from the Yellow River or from collected rainfall. However, the amount of available water in the Yellow River has declined rapidly in recent years, so there is an urgent need to reduce irrigation in order to sustain agriculture in this area (Kang and Li 1997). A challenge is to develop management techniques that increase water use efficiency (WUE) while optimising crop production. Chapter 4 discusses this in more detail.

When available water becomes limited, water deficits are unavoidable in some periods of the crop growing season. Irrigation scheduling then becomes more important and complex because irrigation decisions need to be based on the relationship between water use and grain yield and on WUE. This requires people to evaluate alternative irrigation schedules and choose a schedule that optimises crop yield and WUE for a given level of water supply. There are few detailed investigations on water use–grain yield relationships and WUE under different water supply conditions in the region, although many irrigation practices involve soil water deficit control.

In order to develop guidelines for farmers and/or decision makers to manage crop production, many irrigation practices under various conditions must be evaluated in terms of their effect on yield and WUE. Process-based models can provide useful information about different irrigation practices. For example, Hook (1994) and Kang et al. (1992) have used models to determine the best irrigation strategies. Models can also add value to decision making by transferring results from extensive field experiments to other areas (Cheeroo-Nayamuth et al. 2000; Cabelguenne et al. 1999; Jagtap et al. 1999; Sankaran et al. 2000; Alagarswamy et al. 2000).

Modelling crop yield and WUE is an important facet of crop water management and requires a good understanding of crop–water relationships. WAVES (water, atmosphere, vegetation, energy and soil) is an integrated energy and water balance model based on the biophysical processes in the soil–plant–atmosphere continuum (Zhang et al. 1996). A detailed description of WAVES can be found in Zhang and Dawes (1998) and in Chapter 1 of this volume. The model was successfully applied to the Loess Plateau to model the processes of water dynamics, crop evapotranspiration, and biomass accumulation (Huang et al. 2001), but was not tested for crop yield prediction.

The objective of this chapter is twofold: to evaluate two different methods for predicting crop yield and WUE within the WAVES model, and to evaluate optimal water management practices for improving crop yield and WUE under limited water supply on the Loess Plateau.

Field Experiments and Data

Site description

We conducted field experiments in Changwu, Shaanxi Province, during 1995–98. The Overview provides background information about the area; Figure 4 of the Overview shows its location. The study site has an elevation of 1206 m and has a semiarid to warm temperate climate with an average annual rainfall of 542 mm, concentrated from July to September. Annual averages are 2226 hours for sunshine duration, 9°C for temperature and 1552 mm for potential evaporation. The groundwater table is 50–80 m below the surface. The soil is a dark loess soil with a loam texture; it has been intensively cultivated over many centuries. Table 1 shows the major physical properties of the soil. The top 30 cm contains 1.55% total organic matter, 0.106% nitrogen (Bremner and Mulvaney 1982) and 0.095% available phosphate (Olsen and Sommers 1982). The lysimeters were 3 m × 2 m in area and 3 m deep, separated by waterproof concrete walls buried up to the soil surface.

The soil was irrigated, fertilised and well mixed in the top 30 cm before sowing. In each plot, an aluminium tube, 2 m long, was installed for moisture measurements. A mobile plastic rain shelter was installed above the lysimeters to control soil water status. Winter wheat (cultivar Changwu 89-134[1]) was sown in late September. Seedling density was controlled at 200 plants/m^2. There were seven treatments of irrigation deficit each year with three randomly designed replicates (Table 2). All plants were harvested in early July in the year following planting.

Measurements and statistical treatment

A neutron moisture meter (CPN503, United States) was used to measure water content every 10 cm to a depth of 2 m, with measurements taken weekly. In controlling soil water deficit, average soil water content for the top 40 cm and 60 cm was monitored using a time-domain reflectometer (Trase system, Soil Moisture Equipment Corporation, United States). When soil water content dropped to the lower limit of the designated range (see Table 2), the plot was irrigated to its field capacity. The amount of irrigation water in each lysimeter was recorded and used to calculate total water consumption. At the end of the winter growing season, plants were harvested and the dry mass and final grain yield calculated. All data were statistically analysed and treatments were compared using Duncan's multiple range test.

Meteorological data were recorded by a standard weather station located at the experimental site. Daily values of maximum and minimum temperature, maximum vapour pressure deficit and average wind speed were recorded.

[1] This cultivar is widely used by farmers in the region.

Table 1. The particle composition and hydraulic properties of soils at Changwu.

Size (mm)	Particle composition						θ_s	θ_F	θ_{wilt}	γ_d
	>0.25	0.25–0.05	0.05–0.01	0.01–0.005	0.005–0.001	<0.001 mm				
%	1.1	2.4	57.0	8.6	17.7	13.2	0.486	0.255	0.1	1.21

θ_s = saturated soil water content (cm^3/cm^3); θ_F = field capacity (cm^3/cm^3); θ_{wilt} = water content at permanent wilting point (cm^3/cm^3); and γ_d = mean bulk density (g/cm^3)

Table 2. Controlled minimum soil water content of different treatments in the winter wheat growing season.

No.	Treatment[a]	Minimum soil water content maintained (% of field capacity)				
		Seeding to before winter freezing	Regrowth to stem elongation	Booting to heading	Flowering to milk ripeness	Maturity to harvest
1	LLLLL	45	45	45	45	45
2	LLLHM	45	45	45	70	55
3	LHMLL	45	70	55	45	45
4	LMHMH	45	55	70	55	70
5	MMHHL	55	55	70	70	45
6	HMHHM	70	55	70	70	55
7	HHHHH	70	70	70	70	70

[a] The growing season was divided into five periods and soil water content in the top 60 cm (40 cm before the jointing stage) was maintained during different stages at one of three levels: high soil moisture content (H) (no soil water deficit); medium (M) (mild soil water deficit); or low (L) (severe soil water deficit). When soil water content approached the minimum values, water was supplied up to field capacity.

Using the WAVES Model

WAVES can be used to predict crop yield and WUE. Crop yield is estimated from the carbon balance, determined by calculation of evaporation and transpiration demand for a given day. These fluxes are based on the soil conditions at the start of the day. A portion of the energy balance is used to estimate the stresses on the vegetation (Zhang and Dawes 1998), and carbon balance is then used to calculate assimilation based on those stresses. Finally, evaporative demand is calculated using a conductance based on the assimilation rate. In this way a complete cycle between the atmosphere, soil and vegetation can be made. The WAVES plant growth model is a generic algorithm using rate-based equations, physical principles and empirical results (Wu et al. 1994). WAVES does not attempt to model discrete phenological growth stages or to predict yield. The model treats a plant as three separate carbon sinks representing leaves, stems and roots. Each of these is assumed to occupy the conceptual site fully (i.e. leaves are evenly spread across each square metre, stem numbers are not determined but are uniformly spread and roots totally explore the depths to which root carbon is allocated).

Engineering estimates of crop yield can be made from knowledge of above-ground biomass and actual and potential transpiration, based on empirical relationships (Charles-Edwards 1982). The simplest equation uses the harvest index:

$$Y = HI \times DM \quad (1)$$

where Y is crop yield (kg/ha), HI is the harvest index, and DM is the total above-ground dry matter (kg/ha). Transpiration data can be used to make alternative yield estimates (de Wit 1958):

$$Y = HI \times m \frac{ET_a}{ET_p} \quad (2)$$

where m is a crop factor dependent on variety and species (kg/ha), ET_a is actual transpiration, and ET_p is average potential transpiration rate over the growing season. Within WAVES, the values of ET_a and ET_p are stored and can be used for these calculations with a user-specified harvest index and m parameter.

Harvest index is related to water supply level (Austin et al. 1980; Perry and D'Antuono 1989; Siddique et al. 1989). Based on Kang et al. (2000),

the harvest index for winter wheat was set to 0.25 (rainfed), 0.30 (limited irrigation), 0.40 (middle irrigation) or 0.35 (full irrigation). The crop factor *m* was set to 140 in all the simulations (Kang et al. 2000). Crop WUE was calculated as grain yield divided by seasonal evapotranspiration.

Calibration was done manually (i.e. without the use of software that optimises parameters for least squares or other error criteria). The calibration approach required a compromise between the degree to which a parameter could be adjusted for an individual plot, and the degree of parameter variation across plots. In order to obtain model parameters, the WAVES model was first run using the meteorological data between September 1995 and July 1996 and treatment 1 (full irrigation). Vegetation parameters for winter wheat were selected from the work of Zhang et al. (1996), with the accumulated temperatures and the maximum root depth adjusted according to local conditions. The soil in the experimental site has a fairly uniform profile and was assumed to have only one layer. The maximum rooting depth for winter wheat was set to 2 m under limited irrigation. The bottom of the soil column had a draining boundary with a maximum rate of 0.01 mm/day. This selection of the lower boundary condition is based on the specific characteristics of water balance with a winter wheat crop.

Results and Discussion

Grain yield prediction

Figure 1 shows a comparison of simulated and measured grain yield during the period 1995–98, using Equations 1 and 2 (Figs. 1a and 1b, respectively). Simulated grain yield using Equation 1 agreed well with the measurements. The best-fit slope through the origin was 0.97, with a correlation coefficient of 0.93. Grain yield simulated by Equation 2 also compared reasonably well with the measurements. The best-fit slope was 1.00 with a correlation coefficient of 0.82. These results indicate that grain yield can be approximated from estimates of above-ground dry matter and crop transpiration.

The harvest index and crop factor must be known to predict grain yield using the above methods. For winter wheat on the Loess Plateau of China, the harvest index varies from 0.25 to 0.40, depending on water availability (Kang et al. 2000). In water-limited crops that rely predominantly on stored water, the harvest index is roughly proportional to the amount of water available after anthesis (Nix and Fitzpatrick 1969). This is not the case for crops that rely predominantly on current rainfall (Passioura 1986). In other words, the harvest index varies with available soil water and other factors; it cannot be considered as an independent variable. The success of grain yield predictions using

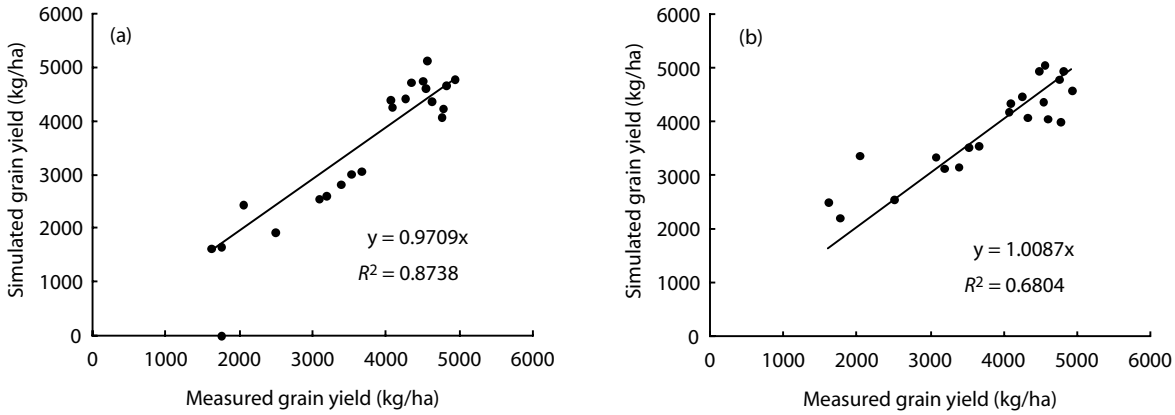

Figure 1. Effectiveness of WAVES in predicting grain yield for winter wheat, Changwu. (a) Prediction based on above-ground matter. (b) Prediction based on transpiration.

Equations 1 and 2 relies on accurate estimates of the harvest index. The results shown in Figure 1 support the findings of Zhang et al. (1999) and Wang et al. (2001), that the WAVES model can accurately simulate plant biomass under various soil moisture conditions.

The crop factor *m* is considered to be dependent only on variety and species (Hanks 1983). It can be applied to both water-limited and well-watered situations (de Wit 1958). We used a constant value in all simulations. Relationships represented by Equations 1 and 2 are attractive because they are simple; however, they are really useful only if we are able to estimate crop transpiration independently. This often means that a detailed model of a soil–crop–atmosphere system is required.

Water use efficiency

Figure 2 shows the comparison of the simulated WUE by the WAVES model and the measured values. The results obtained using Equation 1 agreed reasonably well with the measurements. The best-fit slope through the origin was 0.95, with a correlation coefficient of 0.75. The results using Equation 2 showed poor correlation with the measured values. Mathematically, WUE is estimated by dividing Equation 2 by actual evapotranspiration and shows the variation in potential evapotranspiration. Since this quantity is independent of crop growth, little correlation can be expected. Where potential evapotranspiration, and therefore atmospheric demand, becomes the most limiting factor in crop growth, the relationship shown in Equation 2 may yield better estimates of WUE.

Figure 3 illustrates how evapotranspiration relates to simulated grain yield and WUE, using the WAVES model. Grain yield and evapotranspiration increased simultaneously when evapotranspiration was below a critical value; the slope increased as evapotranspiration decreased and became negative when evapotranspiration was larger than the critical value (about 500 mm). However, the maximum WUE was reached when evapotranspiration was at 440 mm and did not correspond to the maximum grain yield. When evapotranspiration was relatively low, an increase in water use by a crop could result in large increases in both grain yield and WUE. However, at maximum WUE, an increase in crop water use could still lead to an increase in grain yield, but could only reduce WUE.

Simply aiming for maximum grain yield under limited irrigation will require too much water. However, aiming for maximum WUE will result in

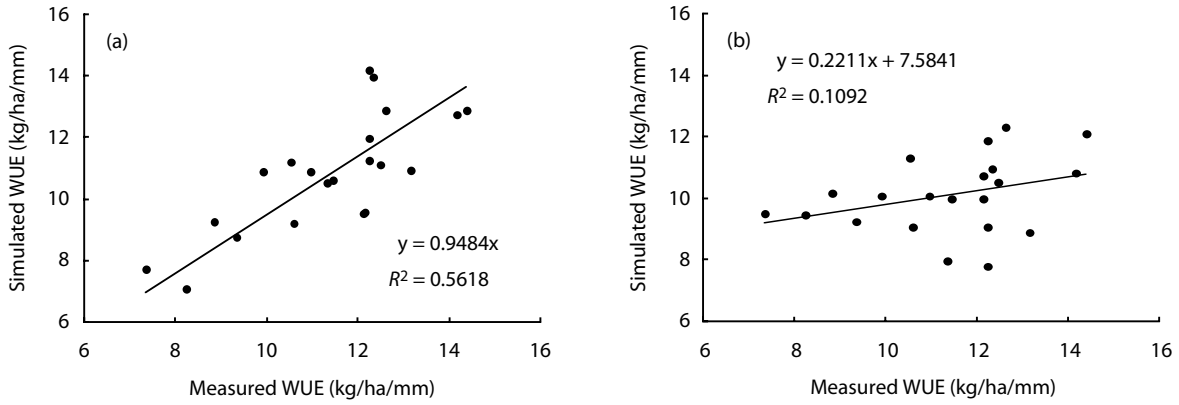

Figure 2. Effectiveness of WAVES in predicting water use efficiency (WUE) for winter wheat, Changwu. (a) Prediction based on above-ground matter. (b) Prediction based on transpiration.

a lower grain yield. Thus, it is necessary to consider both yield and WUE when irrigating. The association of high WUE with high yields has important implications for efficient use of water resources on the semiarid Loess Plateau of China.

Table 3 shows total evapotranspiration, grain yield, biomass and WUE calculated by summation of daily output from simulations over the whole growing season from 20 September to 2 July for three years, together with irrigation water use and rainfall. Simulated seasonal evapotranspiration varied between 234 and 526 mm. Simulated biomass was between 8800 and 12,600 kg per hectare (kg/ha). The simulated grain yield was 1600–5140 kg/ha, and 2200–5040 kg/ha, using Equations 1 and 2 respectively. Crop WUE was 6.16–12.87 kg/ha/mm and 7.78–12.33 kg/ha/mm for yield simulated by Equations 1 and 2 respectively.

Clearly, evapotranspiration, biomass and grain yield were lower under rainfed conditions than under irrigation. Evapotranspiration and yield depend on applied irrigation. Both evapotranspiration and biomass were maximised by full irrigation treatment, and were correspondingly lower without irrigation. However, the maximum grain yield occurred in treatment 5, in which applied irrigation water was 300 mm, reduced by one-third compared with the full irrigation treatment, with the deficit of evapotranspiration between 7% and 13%. The simulated results indicated that WUE of winter wheat could be improved by limited irrigation. Table 3 also indicates that the maximum WUE usually occurred in treatment 4. It suggests that the limited irrigation scheme has practical value for winter wheat production in this semiarid area.

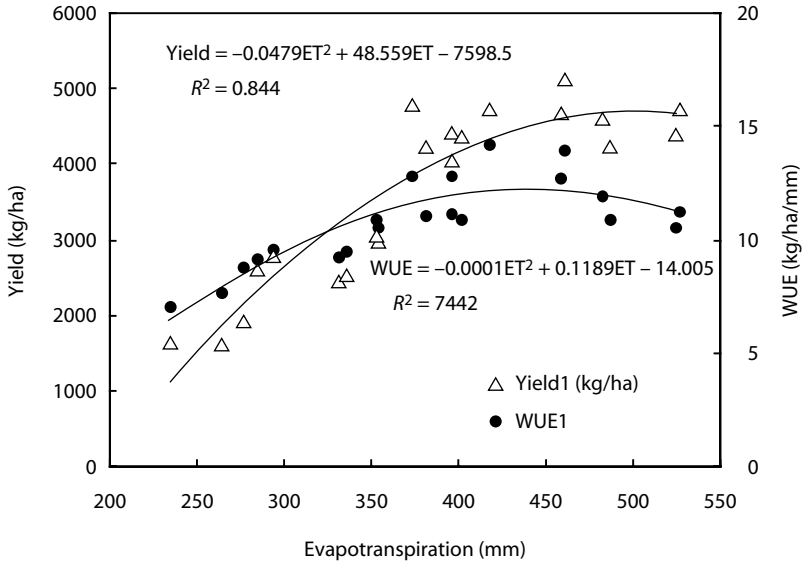

Figure 3. Effectiveness of WAVES in predicting the relationship between seasonal evapotranspiration (ET), water use efficiency (WUE) and grain yield for winter wheat in Changwu.

Table 3. Winter wheat evapotranspiration, biomass and grain yield simulated by the WAVES model, Changwu, 1995–98.

Years	Treatment no.	Rainfall[a] (mm)	Irrigation water (mm)	No. of irrigations	ET[a] (mm)	Biomass (kg/ha)	Yield 1 (kg/ha)[b]	Yield 2 (kg/ha)[c]	WUE1[d] (kg/ha/mm)	WUE2[e] (kg/ha/mm)
1995–96	1	239.6	0	0	234	8840	1660	2210	7.1	9.46
	2		100	1	284	10,400	2610	3120	9.2	9.09
	3		100	2	294	10,500	2810	3150	9.57	10.73
	4		200	3	395	11,175	4430	4470	11.21	11.32
	5		300	4	372	11,475	4790	4590	12.87	12.33
	6		400	4	380	11,438	4233	4003	11.13	10.52
	7		450	5	402	11,563	4375	4047	10.9	10.08
1996–97	1	137.0	0	0	263	10,000	1620	2500	7.7	9.50
	2		100	1	330	11,200	2450	3360	9.28	10.18
	3		100	2	335	11,167	2550	3350	9.52	10.00
	4		200	3	395	11,975	4070	4790	12.86	12.11
	5		300	4	458	12,400	4680	4960	12.76	10.83
	6		400	4	487	12,406	4255	4342	10.93	8.91
	7		450	5	523	11,938	4408	4178	10.53	7.98
1997–98	1	267.4	0	0	276	10,240	1940	2560	78.78	9.26
	2		100	1	354	11,767	3000	3530	10.6	9.98
	3		100	2	353	11,833	3070	3550	10.88	10.06
	4		200	3	417	12,373	4740	4949	14.2	11.86
	5		300	4	460	12,600	5140	5040	13.96	10.95
	6		400	4	482	12,500	4617	4375	11.98	9.08
	7		450	5	526	11,686	4736	4090	11.25	7.78

[a] ET and rainfall are evapotranspiration and rainfall in the growing season of winter wheat respectively
[b] Yield 1 is the simulated grain yield by Equation 1
[c] Yield 2 is the simulated grain yield by Equation 2
[d] WUE1 is the water use efficiency based on yield 1
[e] WUE2 is the water use efficiency based on yield 2

Conclusion

The WAVES model can be used to predict grain yield of winter wheat on the Loess Plateau. The simulated grain yield based on biomass and harvest index showed better agreement with the measurements than that based on transpiration and harvest index. The simulated WUE using grain yield from biomass and the harvest index agreed reasonably well with the measured values. However, when the grain yield obtained from crop transpiration and the harvest index was used to calculate WUE, the results estimated from the model showed poor correlation with the measurements. The model was very sensitive to different irrigation treatments. The harvest index is an important parameter for grain yield prediction. The model was developed with a constant harvest index for different irrigation treatments. However, the values of harvest index were similar but not constant for different irrigation treatments, and related water supply level.

WUE in this region can be improved by irrigation scheduling. Evapotranspiration was the highest when most irrigation water was applied, but WUE was relatively low. Appropriately controlled irrigation could improve the grain yield and WUE. Aiming only for maximum grain yield or for maximum WUE could lead to uneconomical irrigation management.

Acknowledgments

We are grateful for financial assistance from the Chinese National Natural Science Foundation (projectS 49725102 and G1999011708), as well as from ACIAR (project LWR1/95/07).

References

Alagarswamy, G., Singh, P., Hoogenboom, G., Wani, S.P., Pathak, P. and Virmani, S.M. 2000. Evaluation and application of the CROPGRO-Soybean simulation model in a Vertic Inceptisol. Agricultural Systems, 63, 19–32.

Austin, R.B., Bingham, J., Blackwell, R.D., Evans, L.T., Ford, M.A., Morgan, C.L. and Taylor, M. 1980. Genetic improvement in winter wheat yields since 1980 and associated physiological changes. Journal of Agricultural Science, 84, 675–689.

Bremner, J.M. and Mulvaney, C.S. 1982. Nitrogen–total. In: Page, A.L., Miller, R.H. and Keeney, D.R., eds, Methods of Soil Analysis, Part 2, Chemical and Microbiological Properties. Madison, WI, American Society of Agronomy, 595–624.

Cabelguenne, M., Debaeke, P. and Bouniols, A. 1999. EPICphase, a version of the EPIC model simulating the effects of water and nitrogen stress on biomass and yield, taking account of developmental stages: validation on maize, sunflower, sorghum, soybean and winter wheat. Agricultural Systems, 60, 175–196.

Chang, Y.Y. and Corapcioglu, M.Y. 1997. Effect of roots on water flow in unsaturated soils. Journal of Irrigation and Drainage Engineering, 123, 202–209.

Charles-Edwards, D.A. 1982. Physiological Determinants of Crop Growth. Sydney, Academic Press.

Cheeroo-Nayamuth, F.C., Robertson, M.J., Wegener, M.K. and Nayamuth, A.R.H. 2000. Using a simulation model to assess potential and attainable sugar cane yield in Mauritius. Field Crops Research, 66, 225–243.

Dawes, W.R., Zhang, L., Hatton, T.J., Reece, P.H., Beale, G. and Packer, I. 1997. Evaluation of a distributed parameter ecohydrological model (TOPOG-IRM) on a small cropping rotation catchment. Journal of Hydrology, 191, 64–86.

de Wit, C.T. 1958. Transpiration and crop yields. Veersl. Landbouwk. Onderz. 64.6 Institute of Biological and Chemical Research on Field Crops and Herbage, Wageningen, The Netherlands.

Feedes, R.A., Bresler, E. and Neuman, S.P. 1974. Field test of a modified numerical model for water uptake by root systems. Water Resources Research, 10, 1199–1206.

Feedes, R.A., Kowalik, P.J. and Zaradny, H. 1979. Simulation of field water use and crop yield. Wageningen, The Netherlands.

Hanks, R.J. 1983. Yield and water-use relationships: an overview. In: Taylor, H.M., Jordan, W.R. and Sinclair, T.R., eds, Limitations to efficient water use in crop production. American Society of Agronomy, Crop Science Society of America, Soil Science Society of America.

Hook, J.E. 1994. Using crop models to plant water withdrawals for irrigation in drought years. Agricultural Systems, 45, 271–289.

Huang Mingbin, Shao Mingan and Li Yushan. 2001. Comparison of a modified statistical–dynamic water balance model with the numerical model WAVES and field measurements. Agricultural Water Management, 48(1), 21–25.

Jagtap, S.S., Abamu, F.J. and Kling, J.G. 1999. Long-term assessment of nitrogen and variety technologies on attainable maize yields in Nigeria using CERES-maize. Agricultural Systems, 60, 77–86.

Jones, H.G. and Tardieu, F. 1998. Modelling water relations of horticultural crops: a review. Scientia Horticulturae, 74, 21–46.

Kang, S.Z., Liu, X.M., Gao, X.K. and Xiong,Y.Z. 1992. Simulation of water transportation in soil–plant–atmosphere continuum. Journal of Hydraulic Engineering, 3, 1–12 (in Chinese).

Kang, S.Z., Liu, X.M. and Zhang, G.Y. 1993. Simulation of soil water and heat movement with crop canopy shading. Journal of Hydraulic Engineering, 3, 11–17 (in Chinese).

Kang, S.Z., Liu, X.M. and Xiong, Y.Z. 1994. Theory of water transport in soil-plant-atmosphere continuum and its application. Water Resources and Hydro-Power Press of China, Beijing, 228 pp.

Kang, S.Z. and Li, Y.J. 1997. Tendency and countermeasure of 21st century water-saving agriculture development in China. Transactions of the Canadian Society of Association Executives, 13, 1–7.

Kang, S.Z., Zhang, L., Liang, Y.L. and Caia, H.J. 2000. Effects of limited irrigation on yield and water-use efficiency of winter wheat in the Loess Plateau of China. Field Crops Research (submitted).

Leenhardt, D., Lafolie, F. and Bruckler, L. 1998. Evaluating irrigation strategies for lettuce by simulation: 1. Water flow simulations. European Journal of Agronomy, 8, 249–265.

Nimah, M. N. and Hanks, R. J. 1973. Model for estimating soil water, plant and atmospheric interrelations: 2. Field test of model. Soil Science Society of America Proceedings, 37, 528–532.

Nix, N.A. and Fitzpatrick, E.A. 1969. An index of crop water stress related to wheat and grain sorghum yields. Agricultural Meteorology, 6, 321–337.

Olsen, S.R. and Sommers, L.E. 1982. Phosphorus. In: Page, A.L., Miller, R.H. and Keeney, D.R., eds, Methods of Soil Analysis, Part 2, Chemical and Microbiological Properties. Madison, WI, American Society of Agronomy, 403–448.

Passioura, J.B. 1986. Resistance to drought and salinity: Avenues for improvement. Australian Journal of Plant Physiology, 13, 191–201.

Perry, M.W. and D'Antuono, M.F. 1989. Yield improvement and associated characteristics of some Australian spring wheats introduced between 1860 and 1982. Australian Journal of Agricultural Research, 40, 458–472.

Sankaran, V.M., Aggarwal, P.K. and Sinha, S.K. 2000. Improvement in wheat yields in northern India since 1965: measured and simulated trends. Field Crops Research, 66, 141–149.

Siddique, K.H.M., Belford, R.K., Perry, M.W. and Tennant, D. 1989. Ear:stem ratio in old and modern wheat cultivars; relationship with improvement in number of grains per ear and yield. Field Crops Research, 21, 59–78.

Wang, H.X., Zhang, L., Dawes, W.R. and Liu, C.M. 2001. Improving water use efficiency of irrigated crops in the North China Plain—measurements and modelling, Agricultural Water Management. 48, 151-167.

Wu, H., Rykiel, E.J. Jr., Hatton, T. and Walker, J. 1994. An integrated rate methodology (IRM) for multi-factor growth rate modelling. Ecological Modelling, 73, 97–116.

Zhang, L., Dawes, W.R. and Hatton, T.J. 1996. Modelling hydrologic processes using a biophysically based model—application of WAVES to FIFE and HAPEX- MOBILHY. Journal of Hydrology, 185, 147–169.

Zhang, L. and Dawes, W. 1998. WAVES—An integrated energy and water balance model, CSIRO Land and Water Technical Report No. 31/98.

Zhang, L., Dawes, W.R., Slavich, P.G., et al. 1999. Growth and ground water uptake responses of lucerne to changes in groundwater levels and salinity: lysimeter, isotope and modelling studies. Agricultural Water Management, 39, 267–284.

7

Effects of Limited Irrigation on Yield and Water Use Efficiency of Winter Wheat on the Loess Plateau of China

Shaozhong Kang,* Lu Zhang,‡ Yinli Liang† and Huanjie Cai*

Abstract

Crop yields on the Loess Plateau of China are mainly limited by available water. A field experiment was conducted for winter wheat (*Triticum aestivum* L.) during 1995–98 to evaluate the effects of limited irrigation on crop yield and water use efficiency (WUE). The results showed that evapotranspiration, grain yield, biomass, WUE and harvest index depended on soil water content. The effect of irrigation on yield varied considerably due to differences in soil moisture content and irrigation scheduling between seasons. High moisture treatment gave the greatest evapotranspiration and biomass, but did not produce the highest grain yield and gave relatively low WUE. Appropriately controlled soil water content could improve grain yield, WUE and harvest index. Consistently high values of grain yield, WUE, and harvest index were obtained under conditions of mild water deficit at the seedling and start of regrowth to stem-elongation stages, with further soil drying at the physiological maturity to harvest stage. We therefore suggest that for winter wheat periods of mild soil drying in the early vegetative growth period together with severe soil drying in the maturity stage is an optimum limited-irrigation regime in this region.

黄土高原粮食产量很大程度上受水分供应的制约。在 1995 到 1998 年进行了冬小麦田间试验，以评价有限灌溉对作物产量和水分利用效率（WUE）的影响。结果显示土壤水分含量决定了水分蒸发量、粮食产量、生物量、WUE 和收获指数。灌溉对产量的影响因不同季节不同的土壤水分含量和灌溉方式而有相当大的变化。水分多产生的蒸发多，生物量多，但是产量不是最

* Key Laboratory of Agricultural Soil and Water Engineering in Arid and Semiarid Areas, Northwest Sci-Tech University of Agriculture and Forestry, Yangling, Shaanxi 712100, PRC.

† Institute of Soil and Water Conservation, Chinese Academy of Sciences and Ministry of Water Resources, Yangling, Shaanxi 712100, PRC.

‡ CSIRO Land and Water, Canberra, PO Box 1666, ACT 2601, Australia. Email: lu.zhang@csiro.au

Shaozhong Kang, Lu Zhang, Yinli Liang and Huanjie Cai. 2002. Effects of limited irrigation on yield and water use efficiency of winter wheat on the Loess Plateau of China. In: McVicar, T.R., Li Rui, Walker, J., Fitzpatrick, R.W. and Liu Changming (eds), *Regional Water and Soil Assessment for Managing Sustainable Agriculture in China and Australia*, ACIAR Monograph No. 84, 105–116.

多，WUE 相对较低。适当控制土壤水份含量能提高产量、WUE 和收获指数。在出苗、拔节初期轻度的水分亏缺，生理成熟至收获期再进一步的缺水可以获得高产量、高 WUE 和高收获指数。因此对于本地区的冬小麦而言，保持土壤在植物生长初期的轻度干燥和成熟期的严重干燥是一个合理的有限灌溉方式。

LIMITED irrigation means that the soil water deficit is controlled at certain stages of crop growth, a practice that has become more important in recent years in areas where water resources are limited. Water use efficiency (WUE) is defined here as the ratio between grain yield and total evapotranspiration during the growing season. For other definitions, see the review of WUE in Chapter 4. Studies on the effects of limited irrigation show that crop yield can be largely maintained and product quality can sometimes be improved while substantially reducing irrigation volume (Li 1982; Shan 1983; Fapohunda et al. 1984; Sharma et al. 1986; Singh et al. 1991; Zhang et al. 1999).

These studies also show that the relationship between crop yield and seasonal evapotranspiration can take different forms and that the empirical coefficients vary with climate, crop type and variety, irrigation, soil texture, fertiliser and tillage methods. The relationship between WUE and evapotranspiration or irrigation water use also shows large spatial and temporal variability. Aggarwal et al. (1986) reported that WUE decreased with increasing evapotranspiration, whereas Musick et al. (1994) found that WUE did not change with seasonal evapotranspiration. Under limited irrigation, reductions in grain yield due to restricted water availability depend on the degree, duration and timing of the imposed soil moisture deficit. The impact of soil moisture deficit on crop yield depends on the particular phenological stage of the crop, and the most sensitive stage can vary regionally (Singh et al. 1991). Because these differences relate to regional variability in environmental and agronomic practices, region-specific information is needed for developing and refining limited irrigation schemes.

The Loess Plateau is a vast arid and semiarid area with average annual rainfall ranging from 300 to 600 mm. Rainfall distribution is uneven, with more than 60% occurring from July to September. Total annual rainfall also varies significantly from year to year. Winter wheat (*Triticum aestivum* L.) and corn (*Zea mays*) are the main crops in the region. Available water is the most important factor limiting crop yields. During the last decade, irrigation water has been pumped from the Yellow River or from surface dams, and average crop yield has substantially increased. However, recently there has been a rapid decline in available water resources from the Yellow River; consequently, there is an urgent need for more efficient water use in order to sustain agriculture in the area (Kang and Li 1997). The Overview provides background information on the region; Figure 1 of the Overview shows the location of the Loess Plateau.

When the available water supply is severely limited, water deficits will be unavoidable during some periods of crop growth. Scheduling of irrigation times is then more complex because irrigation decisions must be based on the relationships between grain yield, crop growing phase and crop water use. Alternative irrigation schedules must be evaluated to determine which schedule maximises crop yield and WUE for a given level of water supply.

We lack adequate information on the relationships between grain yield and WUE under different irrigation regimes on the Loess Plateau; we also lack information about the degree of soil water deficit at different stages of growth, although many irrigation practices involve the control of soil water deficit.

The aim of this chapter was to study the effect of limited irrigation on crop yield and WUE for winter wheat in the field. The objectives were to:

- examine the impact of limited irrigation on crop yield;
- determine an optimum soil water deficit scheme under limited irrigation; and
- establish relationships between crop yield, WUE and the harvest index.

It was expected that the results of the study could be used to provide guidelines to farmers and irrigation managers on how to minimise water use while maintaining high wheat yields in the region.

Materials and Methods

Plant material and experimental design

The field experiments were conducted in Changwu, Shaanxi Province (see Figure 4 of the Overview) during 1995–98. The site is at an altitude of 1206 m, and has a semiarid, warm temperate climate with an average annual rainfall of 542 mm, falling mainly from July to September. Annual sunshine duration is 2226 hours, annual average temperature is 9°C and annual potential evaporation is 1552 mm. The groundwater table is about 50–80 m below the surface. The soil is a dark loess soil with a loam texture, which has been intensively cultivated over many centuries. Its major physical properties are given in Table 1. The top layer of the soil (30 cm) contains 1.55% total organic matter, 0.106% nitrogen (Bremner and Mulvaney 1982) and 0.095% available phosphate (Olsen and Sommer 1982). The experiments were carried out in lysimeters 3 m × 2 m in area and 3 m deep. Irrigation and fertiliser were applied to the top 30 cm before sowing. Each lysimeter had an aluminium tube 2 m in length installed for moisture measurements. During storms, a plastic rain shelter was installed above the lysimeters to control soil water status. Winter wheat (cultivar Changwu 89-134) was sown in late September. Seedling density was controlled to 200 plants/m^2. In total, 15 treatments of soil water deficit were included (Table 2) with three replicates. All plants were harvested in early July in the year following planting.

Measurements and statistical treatment

A neutron moisture meter (CPN503, United States) was used to measure water content every 10 cm to a depth of 2 m. Measurements were taken at weekly intervals. In controlling soil water deficit, average soil water content for the top 40 cm and 60 cm was monitored using time-domain reflectometry (Trase system, Soil Moisture Equipment Corporation, United States). When soil water content dropped to the lower limit of the designed range (see Table 2), the lysimeter was irrigated to its designated upper limit. The amount of irrigation water in each lysimeter was recorded and used to calculate total water consumption.

Table 1. Physical properties of the soils at Changwu.[a]

	Particle composition (mm)							
Size	>0.05	0.05–0.005	<0.005	Bulk density (g/cm^3)	Total pore space (%)	Field capacity (cm^3/cm^3)	Initial infiltration rate (mm/min)	Final infiltration rate (mm/min)
% in size class	3.5	65.6	30.9	1.21	50.6	0.255	5.9	1.6

[a] Data are the average value in the top 60 cm soil layer

A portable gas-exchange recording system (CID-301PS, CID Inc., Vancouver, WA, United States) was used to measure diurnal variations in the rate of photosynthesis and stomatal resistance on some clear days. The measurements were taken at hourly intervals from 7 a.m. to 7 p.m. At the end of each growing season, plants were harvested for estimation of dry matter in shoots and roots, and final grain yield.

Meteorological data — air temperature, air humidity, wind speed and rainfall — were recorded at a standard weather station located at the experimental site. Maximum and minimum temperature, maximum vapour pressure deficit and average wind speed were also recorded each day, as was daily potential evapotranspiration from an evaporation pan with a diameter of 601 mm.

All data were statistically analysed; Duncan's multiple range test was used to compare treatments.

Estimation of evapotranspiration, water use efficiency and harvest index

Crop evapotranspiration between two soil moisture content measurements or in the whole growing season was estimated from the equation:

$$ET = \Delta W + I + P + S_g - D - R_f \quad (1)$$

where ET is crop evapotranspiration, ΔW is the change in soil water storage between two soil moisture content measurements, I is irrigation, P is rainfall, S_g is capillary rise from the water table to the crop root zone, D is downward drainage from the crop root zone and R_f is surface runoff from the lysimeter.

Because the water table was below 50 m, capillary contribution from the groundwater can be ignored (Zhang et al. 1995). During heavy storms, a mobile plastic rain shelter eliminated runoff from the

Table 2. Controlled minimum soil water content of different treatments in the winter wheat growing season.

Treatment no.	Treatment type[a]	Soil water content maintained (% of field capacity)				
		Seeding to before winter freezing	Regrowth to stem elongation	Booting to heading	Flowering to milk ripeness	Maturity to harvest
1	LLLLL	45	45	45	45	45
2	LLLHM	45	45	45	70	55
3	LHMLL	45	70	55	45	45
4	HLMHM	70	45	55	70	55
5	MMMMM	55	55	55	55	55
6	LMLLM	45	55	45	45	55
7	MLLMH	55	45	45	55	70
8	MHLLH	55	70	45	45	70
9	MHMLL	55	70	55	45	45
10	HHLML	70	70	45	55	45
11	LMHMH	45	55	70	55	70
12	HHHHH	70	70	70	70	70
13	HMHLM	70	55	70	45	55
14	HMHHL	70	55	70	70	45
15	MMHHL	55	55	70	70	45

[a] The growing season was divided into five periods and soil water content in the top 60 cm (40 cm before the jointing stage) was maintained during different growth stages. When soil water content approached the minimum value, water was supplied up to field capacity. H = high soil moisture content (no soil water deficit); M = medium soil moisture content (mild soil water deficit); L = low soil moisture content (severe soil water deficit).

lysimeters. The measured rainfall during such events was applied as irrigation and allowed to infiltrate. Since irrigation water was applied to the topsoil and moisture content was controlled below field capacity (Table 2), deep drainage was assumed to be negligible.

Crop water use efficiency was calculated as grain yield divided by seasonal evapotranspiration. Harvest index was estimated as grain yield divided by total biomass.

Results and Discussion

Evapotranspiration, grain yield and biomass

Table 3 lists the average values of evapotranspiration, grain yield and biomass for different treatments in 1995–98. The growing season reference evapotranspiration calculated by a modified Penman equation was 534.2, 429.9, and 479.3 mm for the respective growing seasons. Actual evapotranspiration was considerably lower than for winter wheat in the Southern High Plains of the United States (Howell et al. 1995; Schneider and Howell 1997) or the North China Plain (NCP) (Zhang et al. 1999). The differences may be due to different climatic conditions.

The plants in treatment 1 were grown in rainfed conditions, with no irrigation in the growing season. Seasonal evapotranspiration varied from 213 to 267 mm. In 1996 and 1998, evapotranspiration was balanced by the growing-season rainfall. However, because of drought in 1997, 80 mm of stored soil water was used in addition to the seasonal rainfall. Grain yields varied between 1612 and 2493 kg/ha under rainfed conditions. In the irrigated treatments, seasonal evapotranspiration ranged from 227 to 519 mm and grain yield from 1771 to 4920 kg/ha, depending on the amount of water applied and the time of irrigation. Evapotranspiration and yield depend on the level of soil water deficit at different growth stages. In treatment 12 (high soil moisture), seasonal evapotranspiration was 358–519 mm during the three years of the study. These high values may have been due partly to relatively high soil evaporation resulting from more frequent wetting of the soil surface, especially early in the season, when crop cover was low.

The high soil moisture treatment did not produce the highest grain yield. In fact, the highest grain yield was attained in treatment 15, which was subject to mild water deficits at the seedling, regrowth and stem-elongation stages, followed by soil drying during the period from physiological maturity to harvest. Seasonal evapotranspiration in this treatment was 7.4–24.9% less than that in the high soil moisture treatment. Hence, this treatment combines the benefits of reduced irrigation water (7.4–24.9%) and higher grain yield (0.4–18.0%). The results are only a first indication for a single area, but they support the idea that water resources can be conserved through a process of mild soil drying in the early vegetative growing periods followed by severe soil drying in the maturity stage. This can assist in developing sustainable agriculture and may help in preventing further depletion of water resources. Thus, limited irrigation may be of real value in making winter wheat production part of a program of sustainable agriculture.

Table 4 shows that the regulated soil water deficit reduced leaf and stem development and stimulated root development. An advantage of smaller shoots is that crops consume less water. Canopy transpiration is largely a function of net energy absorbed by the leaves when available water is not limiting (e.g. Monteith 1981), and smaller leaf area will reduce light interception. In addition, soil water deficit may reduce water loss through physiological regulation, such as by reduced stomatal conductance (e.g. Davies and Zhang 1991). The data indicate that total water consumption was reduced by both smaller leaf area and lowered rate of leaf transpiration.

Table 3. Total evapotranspiration (ET), grain yield, harvest index and water use efficiency (WUE) of winter wheat plants, 1995–98.

Year	Treatment	Rainfall (mm)	Irrigation (mm)	ET (mm)	Biomass (kg/ha)	Grain yield (kg/ha)	Harvest index	WUE (kg/m^3)
1995–96	1	239.6	0	213	6000	1750	0.292	0.822
	2		97	300	9250	3180	0.344	1.060
	3		107	278	10251	3375	0.329	1.214
	4		269	385	11401	3905	0.343	1.014
	5		167	359	10451	3570	0.342	0.994
	6		183	291	10526	3505	0.333	1.204
	7		241	338	11426	3870	0.339	1.145
	8		281	387	13726	4020	0.293	1.039
	9		216	323	11901	4080	0.343	1.263
	10		268	389	12401	4230	0.341	1.087
	11		302	403	14551	4245	0.291	1.053
	12		408	519	16726	4200	0.251	0.809
	13		302	420	14051	4600	0.327	1.095
	14		383	383	12976	4775	0.368	1.247
	15		390	390	14351	4920	0.343	1.262
1996–97	1	137.0	0	220	6598	1612	0.244	0.734
	2		60	277	8294	3060	0.369	1.105
	3		112	231	7794	2039	0.262	0.883
	4		246	232	5598	1771	0.316	0.765
	5		158	310	9181	4079	0.444	1.315
	6		197	235	7984	2040	0.256	0.869
	7		280	296	8225	3060	0.372	1.036
	8		302	285	8026	2788	0.347	0.978
	9		235	254	9223	3076	0.334	1.212
	10		293	285	10746	3852	0.358	1.353
	11		284	227	6982	2045	0.293	0.902
	12		391	358	13001	4060	0.312	1.133
	13		306	330	12016	4749	0.395	1.439
	14		378	340	12717	4811	0.378	1.417
	15		361	329	10732	4792	0.447	1.458
1997–98	1	267.4	0	267	8726	2493	0.286	0.933
	2		88	308	8727	3520	0.403	1.143
	3		120	304	8409	3089	0.367	1.018
	4		217	310	9293	3533	0.380	1.138
	5		174	301	8126	3060	0.377	1.016
	6		198	339	9974	3506	0.352	1.035
	7		271	356	10314	3441	0.334	0.966
	8		296	370	10653	3659	0.343	0.990
	9		204	362	9860	3672	0.372	1.014
	10		253	305	9180	3680	0.401	1.205
	11		267	292	9066	3294	0.363	1.130
	12		350	399	13860	4533	0.327	1.135
	13		297	354	11334	4325	0.382	1.223
	14		324	367	11106	4485	0.404	1.224
	15		319	370	10314	4553	0.441	1.232

Under the rainfed conditions of treatment 1, minimum total above-ground biomass was 6000–8726 kg/ha (see Table 3); the maximum biomass was recorded in the high soil water conditions of treatment 12 (13,000–16,726 kg/ha). The linear curve fit through the data in Figure 1 indicates that early-season soil evaporation was about 28 mm. With limited irrigation and a controlled soil water deficit, the biomass was lower than with a high soil water content. However, the reduction in biomass was small in treatment 15 and even less in treatments 13 and 14 in 1997 and 1998. This was due to a compensatory effect of photosynthesis after rewatering under controlled soil water deficit (Table 5). Soil water deficit at the seedling stage substantially reduced leaf photosynthesis, but it recovered a few days after rewatering, suggesting that stomatal inhibition was the main reason (Cornic 1994). Further soil water deficit between the start of regrowth and stem elongation had less effect on the photosynthesis rate in treatment 15, especially for plants subjected to soil water deficit at the seedling stage. This could be related to a larger and deeper root system (Table 4) following soil drying at the seedling stage. A deep root system is beneficial under water-limited conditions as it allows water to be extracted from depth. Studies on dryland crops have shown that utilisation of water deep in the profile may be limited by root density (e.g. Jupp and Newman 1987; Zhang and Davies 1989; Kang et al. 1992; McIntyre et al. 1995).

Regression analysis shows that the relationship between grain yield and seasonal evapotranspiration is a quadratic function (Fig. 1). Grain yield did not increase when seasonal evapotranspiration exceeded a critical value: in this study about 434 mm, or approximately 84% of the measured maximum evapotranspiration. However, biomass increased linearly with evapotranspiration. Both biomass and grain yield showed good correlation with evapotranspiration (Fig. 1), but not with the amount of irrigation water applied (Table 3). These results suggest that the effect of irrigation on grain yield varied considerably due to differences in the soil moisture content and irrigation scheduling between seasons. A high soil moisture content throughout the season required a high water consumption but did not lead to higher grain yields. In some cases, high soil moisture content even resulted in lower grain yields (Table 3). Similar relationships have been reported for wheat, corn and cotton in Northwest China (Kang and Dang 1987), wheat in India (Rajput and Singh 1986;

Table 4. Distribution of root, stem, and leaf dry mass (%) at different development stages of winter wheat grown in the field under different treatments,[a] 1995–96.

Sampling date	Root			Stem			Leaf		
	LLLLL	MMMMM	HHHHH	LLLLL	MMMMM	HHHHH	LLLLL	MMMMM	HHHHH
4 Nov	22.6	22.6	22.6	38.0	38.0	38.0	39.4	39.4	39.4
6 Dec	19.6	12.3	10.1	35.8	40.0	34.8	44.6	47.7	55.1
6 Jan	19.9	14.2	12.0	45.6	42.6	32.0	34.5	43.3	56.0
6 Feb	16.3	15.2	13.8	40.8	39.7	34.1	42.9	45.1	52.1
13 Apr	14.6	14.9	14.1	53.2	49.2	49.1	32.1	35.9	36.8
21 May	12.4	11.0	8.7	69.2	67.6	73.5	18.4	21.4	17.8
29 May	13.4	12.0	7.2	60.6	61.8	58.9	10.4	11.9	12.0

[a] Table 2 shows details of treatments

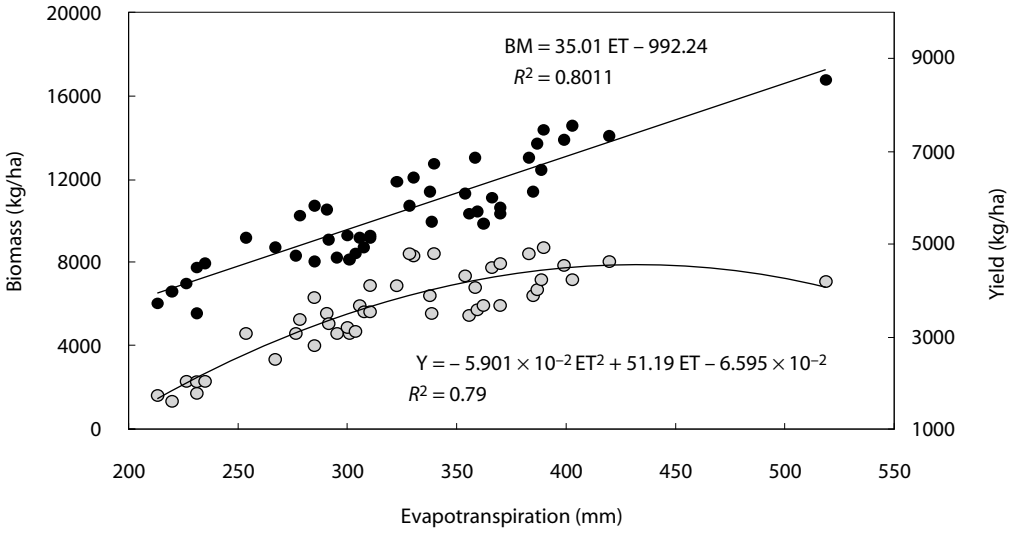

Figure 1. Relationships between growing season evapotranspiration (ET) and biomass (BM) and grain yield (Y) for winter wheat at Changwu.

Table 5. Photosynthesis rate (P_n) and relative photosynthesis (RP_n)[a] of winter wheat plants under different treatments.[b]

		Date (day/month)								
Variable	Treatment[c]	17/4	29/4	6/5	10/5	11/5	18/5	23/5	29/5	9/6
P_n (μmol/m²/s)	LLLLL	3.90	4.52	6.31	3.33	3.01	7.64	5.19	3.95	4.45
	MMMMM	6.10	6.67	8.27	5.12	5.49	8.04	6.26	4.25	4.95
	HHHHH	6.20	6.97	8.74	4.85	4.74	7.94	5.71	5.32	4.81
	HMHHL	6.01	6.37	7.12	4.85	5.03	8.53	6.40	5.93	4.71
	MMHHL	6.10	6.26	7.44	4.80	4.94	8.41	6.47	5.82	4.60
RP_n (%)	LLLLL	62.9	64.9	72.7	68.7	63.5	96.2	90.9	74.3	92.5
	MMMMM	98.4	95.7	94.6	105.6	115.8	101.3	109.6	79.9	102.9
	HHHHH	100	100	100	100	100	100	100	100	100
	HMHHL	96.9	91.4	81.5	100	106.1	107.4	112.1	111.5	97.9
	MMHHL	98.4	89.8	85.1	99.0	104.2	105.9	113.3	109.4	95.6

[a] Relative photosynthesis is the ratio of photosynthesis rates in each treatment to the rate of the control treatment (HHHH)
[b] Data are the daily average value of measurements in 1996. Values are means of replicates for each treatment.
[c] See Table 2 for details of treatments

Kumar and Khepar 1980), cowpea and corn in Nigeria (Fapohunda et al. 1984), and sorghum in Northeast Brazil (Sharma and Alonso Neto 1986).

It can be deduced from Figure 1 that grain yield required a minimum evapotranspiration of 152 mm for winter wheat. This value is lower than the 206 mm for dryland and irrigated wheat reported by Musick et al. (1994), and higher than the 84 mm for winter wheat on the NCP (Zhang et al. 1999), but very close to the 156 mm for wheat in the Mediterranean region (Zhang and Oweis 1999).

The relationship between grain yield and biomass is fitted with a quadratic function in Figure 2. Grain yield increased with biomass until it reached a value of 15,000 kg/ha, and then remained more or less constant, in line with the data in Figure 1.

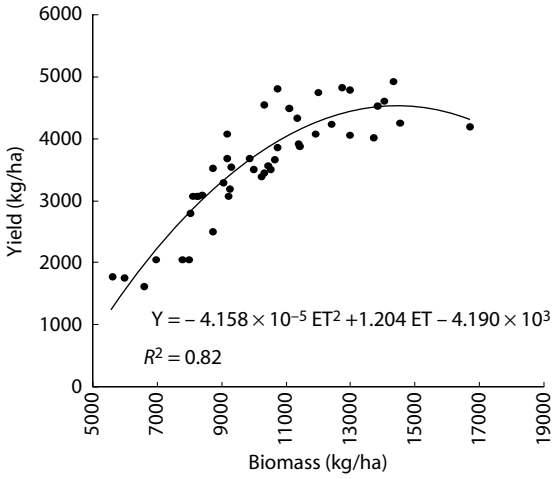

Figure 2. Relationship between biomass (BM) and grain yield (Y) for winter wheat at Changwu.

These relationships also indicate that the highest biomass was associated with maximum evapotranspiration, but not with the highest grain yield, which was reached by appropriately controlling soil water content and limiting evapotranspiration and biomass.

Water use efficiency and harvest index

WUE ranged from 0.73 to 0.93 kg/m^3 under rainfed conditions (Table 3) and from 0.77 to 1.46 under the irrigated treatments. The level of WUE depends on the controlled ranges of soil water deficit at different stages. WUE in the high soil moisture treatment (12) ranged from 0.81 to 1.14 kg/m^3 but the highest WUE values were recorded in treatment 15 (1.23–1.46 kg/m^3 over the three years of the study), as expected from the information on yield and seasonal evapotranspiration. The lower values for treatment 12 arose because seasonal evapotranspiration was the highest recorded in any treatment, but yield was not.

WUE values in our study were higher than those for winter wheat (0.40–0.88 kg/m^3: Howell et al. 1995; Schneider and Howell 1997) and for irrigated wheat (0.82 kg/m^3) in the US Southern Plains (Musick et al. 1994), but close to those (1.08–1.19 kg/m^3) for winter wheat in the Mediterranean region (Zhang and Oweis 1999) and for winter wheat (0.84–1.39 kg/m^3) on the NCP (Zhang et al. 1999).

The harvest index was 0.24–0.29 under rainfed conditions and 0.25–0.45 under irrigated conditions, meaning that appropriate irrigation and controlled soil water content can increase harvest index. Maximum harvest index was recorded in treatment 15. However, under treatment 12 (a high soil water treatment), the harvest index was only 0.25–0.33, much lower than under other irrigation treatments. This treatment resulted in high above-ground biomass (Table 4), causing lodging in the late growing stage, with adverse effects on grain filling. Sheng and Wang (1985) found that high soil moisture content during the grain-filling stage may result in lower 1000-seed weight and grain yield. Other investigators (e.g. Zhang et al. 1998) have reported similar results; it has been well established that remobilisation of carbohydrate reserves from the stem and the leaf sheath is a key factor for grain filling. In wheat, low soil moisture content during grain filling may lead to better use of the carbon reserves in stems and sheaths (Palta et al. 1994; Ricciardi and Stelluti 1995).

Regression analysis indicated a quadratic relationship between WUE and seasonal evapotranspiration (Fig. 3). WUE reached its maximum value at a seasonal evapotranspiration of 354 mm, then started to decrease with evapotranspiration. However, maximum WUE did not correspond to maximum grain yield (Figs 1 and 3). When evapotranspiration is relatively low, water availability is the limiting factor for grain yield and an increase in evapotranspiration results in significant increases in both grain yield and WUE. However, the rate of change starts to decrease as evapotranspiration further increases. Once WUE reaches its maximum value, an increase in total crop water use could still lead to a marginal increase in grain yield, but WUE would decrease. For example, at the maximum WUE the grain yield was 4134 kg/ha; a further increase of 20% in total crop water use would increase grain yield by only 8%. In economic

terms, grain yield response to total crop water use is a diminishing-return function. Therefore, aiming for maximum grain yield under limited water resources is not economical and should not be encouraged. These results also indicate that it is possible to maintain relatively high grain yield and WUE by limiting the duration and severity of plant water stress under limited irrigation.

The relation between harvest index and seasonal evapotranspiration is also nonlinear (Fig. 3). Maximum harvest index, like maximum WUE and grain yield, did not coincide with maximum seasonal evapotranspiration but was recorded when the seasonal evapotranspiration was about 346 mm. Therefore, the maximum value of the harvest index is attained under an appropriate evapotranspiration deficit.

The nonlinear curves fitted through the data in Figure 3 also indicate that WUE increases linearly with harvest index, in agreement with results from other studies (Austin et al. 1980; Perry and D'Antuono 1989; Siddique et al. 1989). Passioura (1977) and Fischer (1979) have suggested that in water-limited conditions a relatively high harvest index is needed to obtain high WUE. In our study, the highest harvest index occurred when evapotranspiration was about 70% of its maximum; the index then started to decrease with increasing evapotranspiration (Fig. 3). Improving the harvest index led to improvement in WUE under limited irrigation conditions.

Conclusions

Evapotranspiration, grain yield, biomass, WUE and the harvest index of winter wheat were all affected by controlled ranges of soil water content during growing seasons. Grain yield response to irrigation varied considerably due to differences in soil moisture content and irrigation scheduling between seasons. Evapotranspiration was highest under continuous high soil moisture conditions, as was above-ground biomass. However, grain yield was not the highest in these conditions, and WUE was relatively low due to inefficient use of the stored soil water. Maximum values of WUE and the harvest index occurred under appropriately controlled soil water conditions. WUE appears to increase linearly with harvest index; improvement in WUE under limited irrigation conditions is thus the consequence of an increased harvest index.

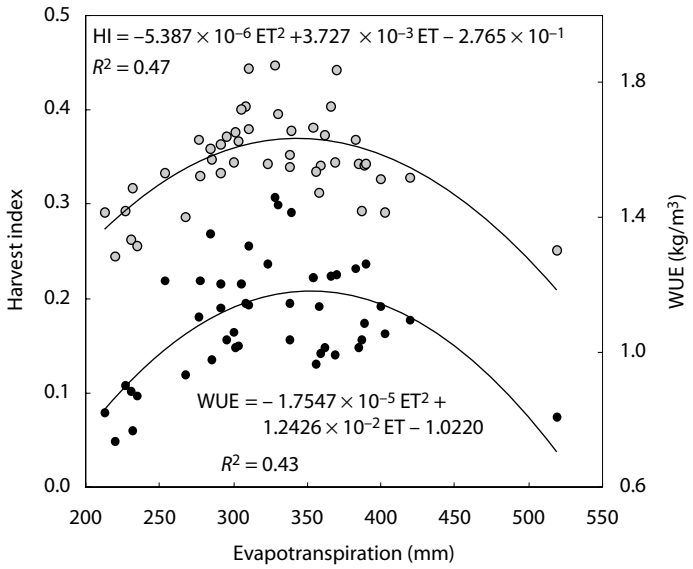

Figure 3. Relationships between seasonal evapotranspiration (ET) and water use efficiency (WUE) and harvest index (HI) for winter wheat at Changwu.

Appropriately limited irrigation and controlled soil water content level could lead to higher grain yield, WUE and harvest index. Compared to high water treatment, this practice has the advantage of lower above-ground biomass before flowering, greater net photosynthesis rates during grain filling, and larger grain yield. Hence, mild soil drying in the early vegetative growth period and severe soil drying in the maturity stage of winter wheat is an optimum limited irrigation regime in the Loess Plateau of China.

Acknowledgments

We are grateful for financial support from ACIAR (project LWR1/95/07). Kang Shaozhong is also grateful for the support of the Chinese National Nature Science Fund (No. 49725102) and project G1999011708.

References

Aggarwal, P.K., Singh, A.K., Chaturvedi, G.S. and Sinha, S.K. 1986. Performance of wheat and triticale cultivars in a variable soil-water environment. II. Evapotranspiration, WUE, harvest index and grain yield. Field Crops Research, 13, 301–315.

Austin, R.B., Bingham, J., Blackwell, R.D., Evans, L.T., Ford, M.A., Morgan, C.L. and Taylor, M. 1980. Genetic improvement in winter wheat yields since 1980 and associated physiological changes. Journal of Agricultural Science, 84, 675–689.

Bremner, J.M. and Mulvaney, C.S. 1982. Nitrogen-Total. In: Page, A.L., Miller, R.H. and Keeney, D.R., eds, Methods of Soil Analysis, Part 2, Chemical and Microbiological Properties, 595–624.

Cornic, G. 1994. Drought stress and high light effects on leaf photosynthesis. In: Barker, N.R. and Bowyer, J.R., eds, Photoinhibition of Photosynthesis: from molecular mechanisms to the field. Oxford, Bios Scientific Publishers, 297–313.

Davies, W.J. and Zhang, J. 1991. Root signals and the regulation of growth and development of plants in drying soil. Annual Review of Plant Physiology and Plant Molecular Biology, 42, 55–76.

Fapohunda, H.O., Aina, P.O. and Hossain, M.M. 1984. Water use–yield relations for cowpea and maize. Agricultural Water Management, 9, 219–224.

Fischer, R.A. 1979. Growth and water limitation to dryland wheat yield in Australia: a physiological framework. Journal of the Australian Institute of Agricultural Science, 45, 83–94.

Howell, T.A., Steiner, J.L., Schneider, A.D. and Evett, S.R. 1995. Evapotranspiration of irrigated winter wheat—Southern High Plains. Transactions of the American Society of Agricultural Engineers, 38, 745–759.

Jupp, A.P. and Newman, E.I. 1987. Morphological and anatomical effects of severe drought on the roots of *Lolium perenne* L. New Phytologist, 105, 393–402.

Kang, S.Z. and Dang, Y.H. 1987. Research on crop water production function and optimal irrigation scheduling. Water Resources and Hydraulic Engineering, 1, 1–12.

Kang, S.Z. and Li, Y.J. 1997. Tendency and countermeasure of 21st century water-saving agriculture development in China. Transactions of the Chinese Society of Agricultural Engineering, 13, 1–7.

Kang, S.Z., Liu, X.M. and Xiong, Y.Z. 1992. Research on the model of water uptake by winter wheat roots. Acta Agriculturae Boreali-Occidentalis, 20, 5–12.

Kumar, R. and Khepar, S.D. 1980. Decision models for optimal cropping patterns in irrigations based on crop water production functions. Agricultural Water Management, 3, 65–76.

Li, Y.S. 1982. Evaluation of field soil moisture condition and the ways to improve crop water use efficiency in Weibei region. Journal of Agronomy in Shaanxi Province, 2, 1–8.

McIntyre, B.D., Riha, S.J. and Flower, D.J. 1995. Water uptake by pearl millet in a semiarid environment. Field Crop Research, 43, 67–76.

Monteith, J.L. 1981. Evaporation and surface temperature. Quarterly Journal of the Royal Meteorological Society, 107, 1–27.

Musick, J.T., Jones, O.R., Stemart, B.A. and Dusek, D.A. 1994. Water-yield relationships for irrigated and dryland wheat in the US Southern Plains. Agronomy Journal, 86, 980–986.

Olsen, S.R. and Sommer, L.E. 1982. In: Page, A.L., Miller, R.H. and Keeney, D.R., eds, Methods of Soil Analysis, Part 2, Chemical and Microbiological Properties, 403–448.

Palta, J.A., Kobata, T., Turner, N.C. and Fillery, I.R. 1994. Remobilization of carbon and nitrogen in wheat as influnced by postanthesis water deficits. Crop Science, 34, 118–124.

Passioura, J.B. 1977. Grain yield, harvest index and water use of wheat. Journal of the Australian Institute of Agricultural Science, 43, 117–120.

Perry, M.W. and D'Antuono, M.F. 1989. Yield improvement and associated characteristics of some Australian spring wheats introduced between 1860 and 1982. Australian Journal of Agricultural Research, 40, 458–472.

Rajput, G.S. and Singh, J. 1986. Water production functions for wheat under different environmental conditions. Agricultural Water Management, 11, 319–332.

Ricciardi, L. and Stelluti, M. 1995. The response of durum wheat cultivars and Rht1/rht1 near-isogenic lines to simulated photosynthetic stresses. Journal of Genetics and Breeding, 49, 365–374.

Schneider, A.D. and Howell, T.A. 1997. Methods, amount, and timing of sprinkler irrigation for winter wheat. Transactions of the American Society of Agricultural Engineers, 40, 137–142.

Shan L. 1983. Plant water use efficiency and dryland farming production in Northwest of China. Newsletters of Plant Physiology, 5, 7–10.

Sharma, P.N. and Alonso Neto, F.B. 1986. Water production function of sorghum for Northeast Brazil. Agricultural Water Management, 11, 169–180.

Sheng, H.D. and Wang, P.H. 1985. The relationship between the weight of 1000-seeds and soil water content in winter wheat season. Acta Agriculturae Boreali-Occidentalis, 13, 73–79.

Siddique, K.H.M., Belford, R.K., Perry, M.W. and Tennant, D. 1989. Ear:stem ratio in old and modern wheat cultivars; relationship with improvement in number of grains per ear and yield. Field Crops Research, 21, 59–78.

Singh, P.K., Mishra, A.K. and Imtiyaz, M. 1991. Moisture stress and the water use efficiency of mustard. Agricultural Water Management, 20, 245–253.

Zhang, J. and Davies, W.J. 1989. Abscisic acid produced in dehydrating roots may enable the plant to measure the water status of the soil. Plant, Cell and Environment, 12, 73–81.

Zhang, H. and Oweis, T. 1999. Water-yield relations and optimal irrigation scheduling of wheat in the Mediterranean region. Agricultural Water Management, 38, 195–211.

Zhang, S., Kang, S.Z., Liu, X.M. and Xiong, Y.Z. 1995. A study on the variation laws of field phreatic water evaporation and its calculation method. Water Resources and Hydraulic Engineering, 6, 9–15.

Zhang, J., Sui, X., Li, B., Li, J. and Zhou, D. 1998. An improved water-use efficiency for winter wheat grown under reduced irrigation. Field Crops Research, 59, 91–98.

Zhang, H., Wang, X., You, M. and Liu, C. 1999. Water-yield relations and water use efficiency of winter wheat in the North China Plain. Irrigation Science, 19, 37–45.

8

Land Degradation Processes

Rob W. Fitzpatrick*

Abstract

This chapter describes how saline, sodic, acid and eroded soils are formed. Using simplified schematic diagrams based on Australian examples, we illustrate the major processes involved and show how some soils may act as precursors to land degradation. We use photographic examples from China to illustrate each degraded soil–landscape type. The chapter also discusses some of the differences between transient salinity and primary, secondary and seepage salinity.

本章阐述了土壤盐化、碱化、酸化以及土壤侵蚀的形成。针对澳大利亚的实例，以图例表格形式，简要展示了其中的主要作用过程，解释了有些类型的土壤可作为土地退化的前兆。用来自中国的照片材料说明退化土壤景观的各种不同类型。本章也探讨了暂时性盐碱化、原生盐碱化、次生盐碱化以及出渗盐碱化间的一些区别。

Introduction

LAND degradation (soil salinity, sodicity, acidity and erosion) is the systematic decline in the quality of land resulting from a mismatch between land use and land quality. It is the consequence of different natural processes, but is usually accelerated by human activities. The result is declining function. Land undergoing degradation normally passes through three phases.

- Natural degradation is generally slow because a steady state develops between soil formation and soil degradation (usually loss). Natural degradation represents 'inherent land quality'.
- Induced degradation results from inappropriate land use and management. Soils decline in quality, but productivity can be maintained by applying artificial nutrients and by appropriate soil management. Induced degradation happens more quickly than natural degradation.
- Desertification occurs when the degree of degradation is such that the resilience of the land is impaired. In unmanaged systems, desertification is indicated by changes in the quality and quantity of biomass and the biota. In agricultural systems, the degree of productivity reduction normally sets the stage for abandonment of the land. This is particularly

*CSIRO Land and Water, PMB 2, Glen Osmond, SA 5064, Australia.Email: rob.fitzpatrick@csiro.au

Fitzpatrick, R.W. 2002. Land degradation processes. In: McVicar, T.R., Li Rui, Walker, J., Fitzpatrick, R.W. and Liu Changming (eds), *Regional Water and Soil Assessment for Managing Sustainable Agriculture in China and Australia*, ACIAR Monograph No. 84, 119–129.

the case when levels of productivity can no longer be economically maintained through management.

In several dryland areas in China and Australia, salinity, waterlogging, erosion (water and wind) and other forms of land degradation are becoming severe and are expected to worsen. For example, water quality is declining because salts, nutrients and sediments are being transported into rivers, streams and dams. Native ecosystems, especially wetlands, are under threat, with loss of habitat and declining biodiversity and soil function. There are many causes of environmental degradation, but in both China and Australia by far the most all-encompassing is the clearing of native vegetation and its replacement with inappropriate agricultural practices. Improved agricultural production systems and restoration of native vegetation could help to restructure these landscapes to establish patterns of water use and ecological function similar to those of the original landscape before clearing. However, such restructuring depends on having a good understanding of the soil–water–landscape processes that are causing the problems.

The studies described in this volume summarise the results of a collaborative project between Chinese and Australian scientists to increase agricultural productivity and sustainability in certain regions of China and Australia. This chapter introduces the section on soils. It focuses on four major types of degradation — salinity, sodicity, acidity and erosion. The processes described are relevant to both Australia and China. The other chapters on soils focus on particular regions (Chapters 10, 12, 13 and 14) or particular processes (Chapters 9, 11 and 15).

In many areas, changes in components of water balance have led to severe changes in the physical and chemical characteristics of soils. In southern Australia, these changes occur particularly on duplex soils — soils that have an abrupt textural boundary between the top layers and the relatively impermeable subsoil layers. Such soils occupy 80% of the high- to medium-rainfall zones of southern Australia, which include some of Australia's prime agricultural (crops, meat, wool, dairy) and horticultural lands, as well as major catchments for regional water supplies. Thus, degradation of soil and water resources poses serious threats to land use and to the quality of water harvested and stored in regional water bodies.

Salinity

Saline soils are those with relatively large amounts of soluble salts such as sodium chloride. Such soils occur naturally; this is referred to as primary salinity (Fig. 1).

Figure 1. Primary salinity in northern Hebei Province, China.

Secondary salinity results from human activities such as irrigation and land clearing in areas that are not irrigated (dryland salinity) (Ghassemi et al. 1995). Both primary and secondary salinity affect plant growth by causing dehydration.

Saline soils form under different environmental conditions and thus have diverse morphological, chemical, physical and biological properties. There is no universally accepted definition for saline soils:

the definition used depends on the discipline and the type of measurements taken. For example:

- hydrogeologists distinguish primary and secondary saline soils (e.g. Coram 1998; George et al. 1997a);
- plant and soil scientists use the distribution of salt-tolerant plant species and/or the approximate range of soil electrical conductivity (EC) levels to distinguish slightly, moderately or severely affected saline soils (e.g. Allan 1996); and
- scientists in other disciplines may use:
  - measurements of pH (3.5–8.5), exchangeable sodium percentage, the sodium adsorption ratio and EC to identify sodic–saline soils (e.g. Soil Survey Staff 1987);
  - measurements of pH (> 9), presence of sodium carbonate and high EC to distinguish alkaline saline soils; and
  - pH (< 3.5), presence of sulfur and high EC to distinguish acid sulfate saline soils (Fitzpatrick et al. 1996).

The definition is further complicated by the fact that salinity can be transient (i.e. not associated with a permanent saline groundwater table).

In Australia, most studies of salinisation processes focus on primary and secondary salinity (e.g. George et al. 1997a; Coram 1998; Macumber 1991) or the processes occurring in sodic soils (described below) (e.g. Isbell et al. 1983; Naidu et al. 1995; Rengasamy and Sumner 1998; Shaw et al. 1998).

The soluble salts found in saline soils are of three types: chlorides, sulfates and carbonates. Most saline soils in Australia have high amounts of chloride salts (Isbell et al. 1983). However, in parts of the Mount Lofty Ranges (Fitzpatrick et al. 1996), Dundas Tableland and the North China Plain (Fig. 2) extensive areas of saline soils also contain sulfate salts (Fig. 1) and sulfides at depth (Fig. 2).

Saline soils with high amounts of carbonates of sodium (sodium bicarbonate) may also occur and are usually associated with coarse-textured materials. These saline soils often exhibit a whitish surface crust when dry (Fig. 1).

Figure 2. Saline sulfidic (black mud) soil near Yangcheng Reservoir, coastal zone on the North China Plain, Hebei Province.

High salinity (as defined by high EC) dehydrates plant cells because the dissolved salts decrease the osmotic potential of soil water. Water flows from the high osmotic potential (low salt concentration in plant cell) to low osmotic potential (high salt concentration in soil). Thus, plants cannot extract water from soil when the soil solution has a lower osmotic potential than the plant cells. The effect on plants is similar to drought stress, with reduced plant growth and often death. For many crops, yields are reduced when the soil extract EC reaches 4 dS/m (US Salinity Laboratory Staff 1954) and decline proportionately as EC levels increase above that level. Some crops, such as sugar beets, are tolerant to EC levels between 4 and 8 dS/m. At an EC of 16 dS/m the growth and yields of most crops are affected. Figure 3 shows the hydrological processes and salinity development commonly found in cropping systems in Australia.

Sodicity

Sodic soils, like saline soils, contain relatively large amounts of sodium, but in this case the sodium is present as ions, not as salts. A soil is considered to

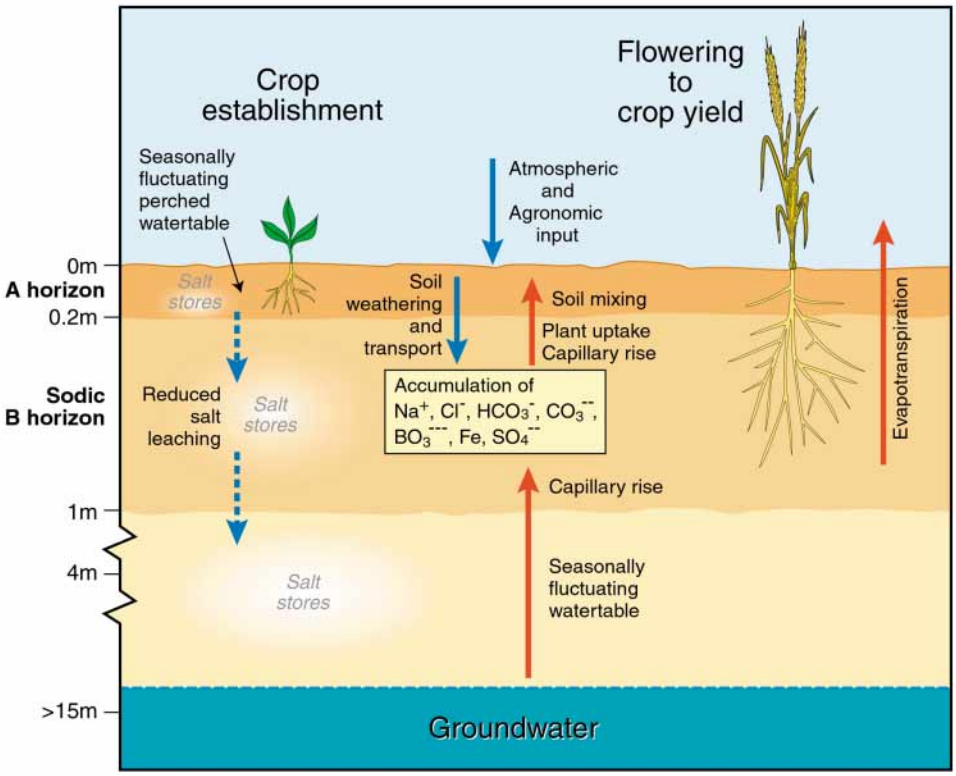

Figure 3. Hydrological processes and salinity development commonly found in cropping systems in Australia (from Fitzpatrick et al. 2001).

be sodic when the adsorbed sodium reaches a concentration where it starts to affect soil structure (Rengasamy and Sumner 1998). Sodic soils can result from drainage by erosion gullies or directly from the weathering of parent materials over thousands of years (Isbell et al. 1983).

Sodic soils have poor structure and low permeability, with adverse effects on plant growth (Fig. 2). Permeability allows water, gases (oxygen and carbon dioxide) and solutes to circulate easily to and from plant roots, which promotes plant growth. However, if a hard sodic dispersed clay layer occurs on the soil surface (Fig. 4) or close to the soil surface (e.g. the B horizon in Figs 3 and 5) it can act as a barrier to root development. The hard soil restricts root growth to either the cracks or topsoil above the claypan because movement of water, nutrients, and gases is too slow in sodic B horizons. In fact, when dry, the B horizon can be so hard that it is also a physical barrier to root penetration. The overall effect on plant growth is one of stress similar to that caused by extremely dry or saline conditions.

The rate and amount of downward percolation of salts are primarily controlled by soil texture and subsoil layer permeability. In coarse-textured horizons, water flows more quickly and the average pore diameter is larger than in fine-textured soils. Decreased water storage is directly related to greater pore diameter. As a result, deep percolation of water and salts is more likely to occur in coarse-textured soils. In some localities in Australia and China, relatively coarse-textured soils overlay impermeable sodic clay horizons. Under these circumstances, percolation leads to lateral flow of water and solutes along the surface of the impermeable layers. If the contact between the two different layers approaches the soil surface along a hill slope, as often happens, the laterally moving water will create a wet spot that eventually becomes saline as the water is evaporated (Fig. 6).

Figure 4. Sodicity development in surface soils. (Note damage to root development under the hard, dense, slowly permeable plate.)

Figure 5. Sodic subsoil formation. (Note that root development is restricted to the A1 horizon because roots find it difficult to penetrate the prismatic Bt horizon.)

Transient Salinity

Transient salinity is the term used for salinity that is not associated with a permanent saline groundwater table. Different forms of transient salinity are expressed in the subsoil and at the soil surface.

Transient salinity with subsoil expression

A recent survey of sodic soils in the South Australian wheat growing regions indicated slow accumulation of salts in the subsoil layers in small amounts that could be detrimental to crops. This phenomenon of 'subsoil transient salinity' in the root zones of sodic soils is different from the 'secondary' or 'seepage' salinity found in association with rising saline groundwater tables (Rengasamy and Sumner 1998; Shaw et al. 1998). When the upper layers of soil are sodic, water infiltration is very slow, because dispersed clay clogs soil pores. If the subsoils are sodic, downward movement of water is restricted, causing temporary waterlogging in the subsoil and the development of a 'perched watertable'. Salts accumulate above the perched watertable during the wet season and in the sodic subsoils following drying, due to water uptake by plant roots and evaporation. Although the rate of salt accumulation is not great, over time it can be detrimental to crops. Subsoil transient salinity fluctuates with depth and with season as the balance between downward and upward fluxes changes.

Generally the accumulated salts in the cereal-growing regions of southern Australia are sodium chloride. However, these salts may also include sodium carbonate and bicarbonate when soil becomes alkaline with a pH > 9.0 (i.e. alkaline-sodic saline soils) Studying salt accumulation in sodic subsoils in more detail will allow us to model this phenomenon and predict when and where it will occur.

Transient salinity with surface expression

The most extreme case of salt accumulation occurs when values range from 4 to 60 dS/m at the soil surface, often with salt efflorescences. These high levels of salt prevent crops from growing and can make the soil susceptible to scalding and erosion. This salinity is due to the localised mobilisation of salts by throughflow above slowly permeable sodic B horizons to topographic depressions. This so-called 'surface soil transient salinity' can occur in a variety of soil types and at all positions in undulating landscapes. It was first reported locally by Herriot (1942) and is commonly referred to as 'magnesia' patches in South Australia because of the

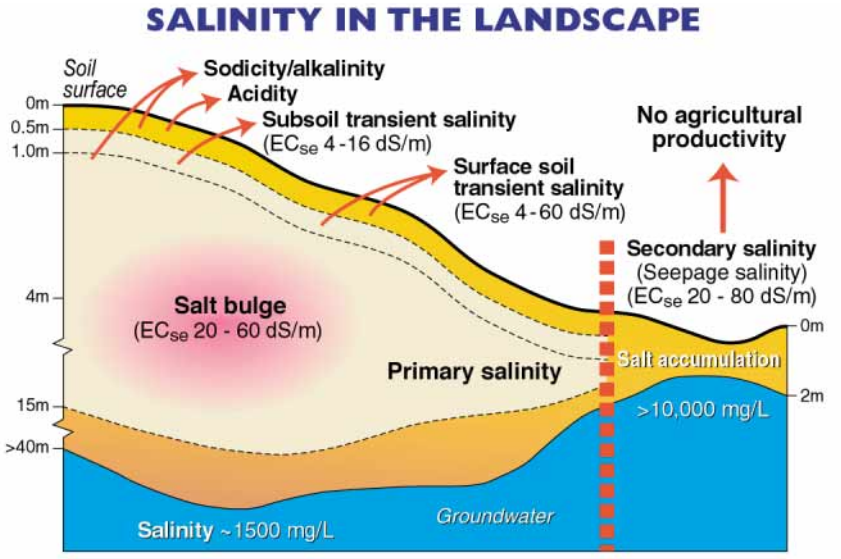

Figure 6. Landscape salinity, illustrating the development of primary salinity, salt bulges, subsoil transient salinity, surface soil transient salinity and secondary salinity (from Fitzpatrick et al. 2001).

presence of high magnesium, as well as sodium (in other words, magnesium is a natural part of the evaporation sequence).

Primary, Secondary and Seepage Salinity

Primary salinity

Primary salinity is caused when salts leach from the soil due to natural processes, eventually leading to the accumulation of salts in the groundwater, sometimes at levels of 2000 to 20,000 mg/L (Fig. 6). As long as the watertable is below 5 m, saline groundwater does not usually affect vegetation. Primary highly saline soils are usually found in foot slopes and topographic depressions, and near springs where the saline groundwater is naturally shallow (less than 1.5 m deep) (Figs. 1 and 6).

Salt stores in the regolith

Over many thousands of years, salt has been accumulating in older landscapes from the large quantities (20–200 kg/ha/year) of salt blown in from the ocean by wind and rain (e.g. Hingston and Gailitus 1976; Peck and Hurle 1976). In addition, salts have been generated by the weathering of rocks during soil formation and the leaching of connate salts trapped in the original sediments. For any particular situation, however, salinisation processes will depend on geology, climate, vegetation and changes superimposed by agriculture. For example, before agriculture in Australia, salts were leached down the profile by rain and accumulated within or below the root zones of native vegetation (Allison et al. 1990; Figs 3 and 6). In semiarid conditions there was not always sufficient rainfall to leach all incoming salts to the groundwater. The clay layers in deep subsoils often hindered the movement of water and salt, and a 'bulge' of salt accumulated at depths of 5–10 m (Fig. 6). Groundwater tables were usually 30 m or more below the surface and the quality of groundwater was frequently good (< 2000 mg/L salt). This is the present situation in the upper parts of the landscape in many cropping regions.

Secondary salinity

Secondary salinisation often follows land clearing, which causes groundwaters to rise and areas of primary saline soils to expand (Fig. 6). In Australia, the introduction of agriculture and the replacement

of perennial native vegetation with annual species have resulted in increased drainage, thereby disturbing the existing equilibrium of groundwater levels. This may 'recharge' the groundwater, resulting in raised groundwater pressures in low-lying discharge areas. The increased recharge may then discharge into low-lying areas and rivers (e.g. Wood 1924; Dyson 1990; Nulsen 1993; George et al. 1997b). At 2 m depth, the rate of salinisation is such that we can observe saline conditions in surface soils.

Seepage salinity

Salinity can occur through capillary rise from deeper (7 m) saline groundwater tables on silt loam soils. As water moves into the upper layers there will be a net mass flow of salt in solution in addition to capillary action bringing salts higher in the profile, closer to the evaporating surface or plant roots. This type of salinity is usually called seepage salinity. Over the past four decades it has affected an estimated 2.5 million ha of land and is predicted to increase fourfold over the next three to four decades (Coram et al. 2001).

Acidity

Soil acidity is a severe soil degradation problem that can greatly reduce the production potential of farming systems. Most occurs in productive agricultural zones. It causes production losses within paddocks, and also long-term and offsite effects, including:

- poor water use by plants (leading to higher recharge and erosion);
- increased leaching of nutrients and aluminium; and
- the irreversible breakdown of layer silicate minerals in soils.

Soil acidification can be determined by assessing the pH of a soil, which determines the concentration of hydrogen ions or acid in the soil. The pH is measured using a logarithmic scale: soils at pH 7 are neutral, those of pH < 7 are considered acidic. Soil acidity is not thought to restrict the growth of most crops or pasture until the pH drops to < 5.5–6.0 (pH_w) or < 5.0–5.5 (pH_{Ca}).

Development of acidity in soils is a natural process, especially in the high rainfall regions of southern Australia. Some soils are inherently acidic because of the high rates of leaching in these regions. Even in lower-rainfall cropping areas, some soil types have become acidic because they have no free lime in the profile. As soils become more acidic, plants and crops that cannot tolerate acidic conditions do not flourish, so productivity and yields decline. When conditions become severely acidic (e.g. pH < 4, such as in inland acid sulfate soils), biogeochemical processes start to break down the layer silicates in the soil, releasing aluminium, iron and manganese. This may lead to mineral toxicities and nutrient imbalances.

The natural rate of acidification is accelerated by the use of acidifying fertilisers, nitrogen fertilisers, the removal of agricultural products and nitrate leaching. The management of soil acidity involves the following requirements at the farm level:

- recognising paddock indicators of soil acidity
- monitoring soil pH
- knowing crop and pasture tolerances to acidity
- treating paddocks that have acidity problems.

Acid soils can be ameliorated by applying liming material or other types of neutralising agent, growing acid-tolerant plants or reducing the rate of acidification.

Erosion

Soil erosion by wind and water is a worldwide environmental problem that seriously threatens sustainability of agriculture. A recent study showed that the direct and indirect annual cost of erosion may be as high as $400 billion worldwide. This

translates to roughly $80 per year for every person on Earth. Some of the most eroded regions of the world — including the Loess Plateau in China (e.g. Xianmo Zhu and Mei'e Ren 2000; Lindstrom et al. 1990; Li and Lindstrom 2001; Figs. 7 and 8) — are located in semiarid areas where drought is a serious threat to sustainable agriculture.

Figure 7. Erosion gullies on the Loess Plateau, China.

Figure 8. Erosion gullies and terrasetts on the Loess Plateau, China.

The Loess Plateau is the thickest, most complete, loess deposition in the world (Figs. 7 and 8). The formation of the Loess Plateau is in essence the process of loess accumulation. Loess deposits and the Paleosols contained in them have a loose and porous structure, which has frameworks composed of sands and other coarse particles, filled with fine particles and microaggregates and strengthened by clayey materials. Such a porous medium is very susceptible to water erosion if not protected by plants. This is why soil and water losses are so severe in the Loess Plateau region. Without the protection of vegetation and stabilisation by root systems, raindrops impact and destroy the porous soil structure and cause a dramatic decrease in soil permeability. Improper tillage practices have also damaged the soil structure and reduced soil resistance to water erosion, often leading to severe soil erosion. Removal of natural vegetation and inappropriate land use leads to reduced soil permeability and an increase in soil water erosion. This is the main reason for high sediment loads in the Yellow River. Consequently, severe soil erosion is not a geological process, but a result of improper land use.

In areas with high erosion due to improper land use, research on wind erosion (Fig. 9) and water erosion, and on soil and water conservation and dryland farming, have led to the development of agricultural systems that could be sustainable. For example, comprehensive management schemes and reforestation of watersheds can result in water conservation and reduced wind and water erosion. Such improved productivity will raise farmers' income. The Loess Plateau is an example of this type of approach.

Figure 9. Wind erosion in northern Hebei Province, China.

In southern Australia, various incision and deposition cycles of sheet and streambank erosion have occurred in high winter rainfall areas (> 600mm) (Fitzpatrick et al. 1996). These erosion features may be associated with sodic soils (Natraqualfs or solodised solonetz soils) undergoing recent alteration caused by rising saline–sulfatic groundwater tables due to land clearing following European settlement approximately 120 years ago. Surface and subsurface pedological features, soil chemical, physical and hydrological measurements and remote sensing were used to study the age, onset and development of erosion in several key catchments in southern Australia (e.g. Prosser 1996). Aquic, saline and sulfidic conditions occur in seepage areas where saline and sulfatic groundwater rises to the surface from semiconfined aquifers. The almost bare surface that is formed is subjected to drastic alteration of soil structure during cycles of drying and wetting (Fitzpatrick et al. 1996). On drying, salts and iron minerals concentrate and crystallise at the surface by evaporation to form cemented impermeable soil materials. On wetting, salts are dissolved by rising groundwater and overland flow occurs. Rising saline water also flocculates clay particles, giving rise to low soil strength in the topsoil.

Saline sulfidic soils form in seepage areas with saline sulfatic aquifers and shallow watertables. The high sulfide and salt concentrations lead to the complete breakdown of soil structure and soil strength. Consequently, such seepage areas are highly prone to sheet erosion. Sheet erosion is produced by overland flow and controlled by salt concentration, which restricts the growth of the vegetation cover and reduces the structural stability of the topsoil. The saturated zone increases up the slope because of increased throughflow and overland flow and restriction of throughflow. The reasons for the restriction in throughflow include rising saline/sulfidic groundwaters, clay dispersion and iron oxide blockage of soil pores. Such conditions give rise to accelerated sheet erosion, which forms shallow incision zones and a thin deposition zone.

Conclusion

The three most important features that cause saline soils to differ are:

- hydrological status (presence or absence of groundwater);
- natural (primary) or induced (secondary) status; and
- soil chemical status (sodicity or type of soluble salt).

Several workers have attempted to categorise dryland saline soils using hydrology and water status (e.g. SCAV 1982 and Williams and Bullock 1989). We have further modified this concept and also included soil chemical status (Fig. 10). The important soil chemical features are halitic (sodium chloride dominant), gypsic (gypsum or calcium sulfate dominant), sulfidic (iron pyrite dominant), sulfuric (sulfuric acid dominant), and sodic (high exchangeable sodium on clay surfaces). Most of these terms are defined in Isbell (1996).

Acknowledgments

Funding support from ACIAR and NDSP2 is gratefully acknowledged. The author thanks the following people from CSIRO Land and Water: Greg Rinder, who prepared the figures and Richard Merry for information on soil acidity.

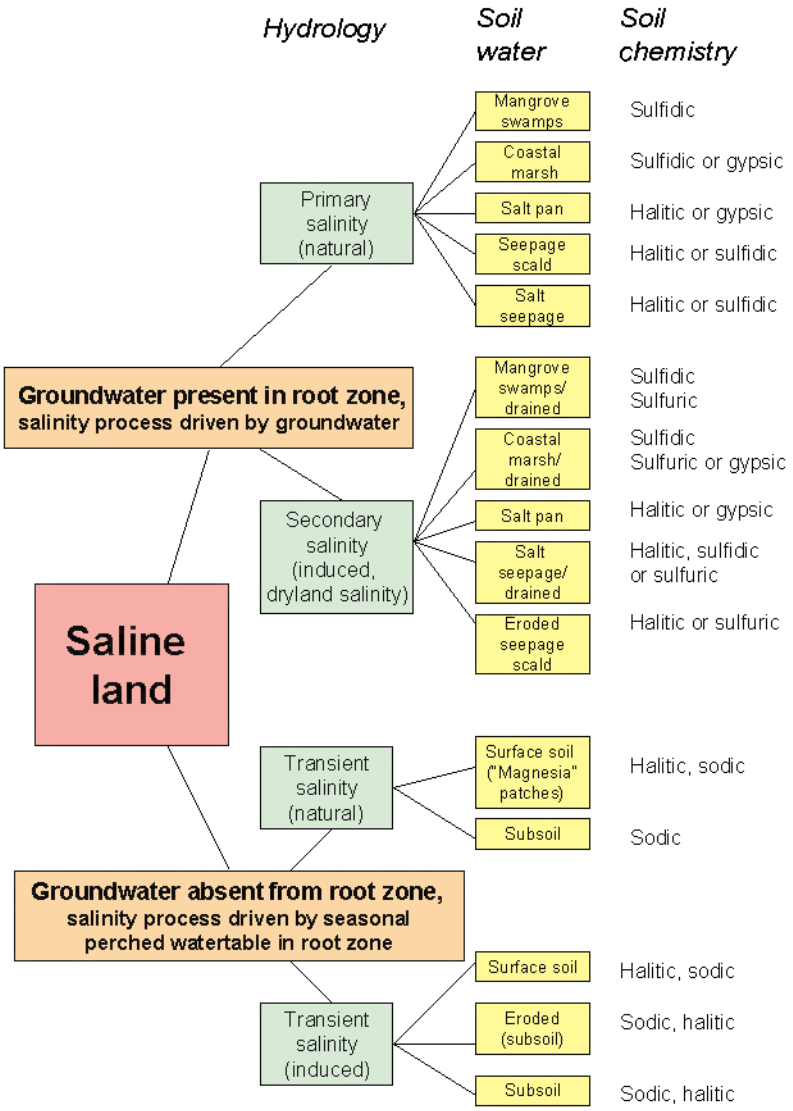

Figure 10. Categories of dryland saline soils as defined by hydrology, soil water status and soil chemistry (from Fitzpatrick et al. 2001).

References

Allan, M.J. 1996. Method for assessing dryland salinity in Victoria. Technical Report No. 34. Bendigo, Centre for Land Protection Research, Department of Conservation and Natural Resources.

Allison, G.B., Cook, P.G., Barnett, S.R., Walker, G.R., Jolly, I.D. and Hughes, M.W. 1990. Land clearance and river salinisation in the Western Murray Basin, Australia. Journal of Hydrology, 119, 1–20.

Coram, J. ed. 1998. National Classification of Catchments for land and river salinity control. A catalogue of groundwater systems responsible for dryland salinity in Australia. Report for the Rural Industries Research and Development Corporation, compiled by the Australian Geological Survey Organisation. Publication no 98/78 ISBN 0 6425 7884 2

Coram, J.E., Dyson, P.R., Houlder, P.A. and Evans, W.R. 2001. Australian Groundwater Flow Systems Contributing to Dryland Salinity. A Bureau of Rural Sciences Project for the National Land and Water Resources Audit's Dryland Salinity Theme. 77.

Dyson, P.R. 1990. The development, dynamics and management of groundwater systems and dryland salinity in the Uplands of south eastern Australia. In: Management of Soil Salinity in Southeastern Australia. Aust. Soc. Soil Sci., Riverine Branch, 253–267.

Fitzpatrick, R.W., Fritsch, E. and Self, P.G. 1996. Interpretation of soil features produced by ancient and modern processes in degraded landscapes: V Development of saline sulfidic features in non-tidal seepage areas. Geoderma, 69, 1–29.

Fitzpatrick, R.W., Rengasamy P., Merry R.H. and Cox J.W. 2001. Is dryland soil salinisation reversible? National Dryland Salinity Program. web site http://www.ndsp.gov.au.

Ghassemi, F., Jakeman, A.K. and Nix, H. A. 1995. Salinisation of land and water resources: human causes, extent, management and case studies. Chapter 2: Australia (143—212); Chaper 3: China (213—239). University of New South Wales Press Ltd, Australia and CAB International, UK.

George, R.J., McFarlane, D.J. and Nulsen, R.A. 1997a. Salinity threatens the viability of agriculture and ecosystems in Western Australia. Groundwater, 5, 6–21.

George, R.J., Speed, R. and Commander, P. 1997b. Hydrogeological models used for dryland salinity research and management: Western Australia. Unpublished paper prepared for the Conceptual Models Workshop held at the Australian Geological Survey Organisation in Canberra, 7 October 1997.

Herriot, R.I. 1942. The reclamation of highland 'Magnesia' patches, a preliminary note on work being conducted at Mt Bryan East. South Australian Journal of Agriculture, 94–95.

Hingston, F.J. and Gailitis, V. 1976. The geographic variation of salt precipitated over Western Australia. Australian Journal of Soil Research, 14, 319–335.

Isbell, R.F., Reeve, R. and Hutton, J.T. 1983. Salt and Sodicity in Soils: an Australian viewpoint. Division of Soils, CSIRO, 107–111. Melbourne, CSIRO/London, Academic Press.

Li Yand Lindstrom, M.J. 2001. Evaluating Soil Quality—Soil Redistribution Relationship on Terraces and Steep Hillslope. Soil Science Society of America Journal, 65,1500–1507.

Lindstrom, M.J., W.W. Nelson and T.E. Schumacher. 1990 Soil movement by soil tillage as affected by slope. Soil Tillage, 17, 225–254

Macumber, P.G. 1991. Interactions between Groundwater and Surface Systems in Northern Victoria. Victoria, Dept Conservation and Environment.

Naidu, R., Sumner, M.E. and Rengasamy, P. eds. 1995. Distribution Properties and Management of Australian Sodic Soils. Melbourne, Australia. CSIRO Publishing. 351.

Nulsen, R.A. 1993. Changes in soil properties. In: Reintegrating Fragmented Landscapes. New York, Springer-Verlag, 107–145.

Peck, A.J. and Hurle, D.H. 1976. Chloride balance of some farmed and forested catchments in south-western Australia. Water Resources Research, 9, 648–657.

Prosser I. 1996. Thresholds of channel initiation in historical and Holocene times, Southeastern Australia. In: Anderson, M.G. and Brooks, S.M., eds, Advances in Hillslope Processes. John Wiley & Sons. 687–708.

Rengasamy, P. 2000. Transient salinity in the root zones of sodic soils. Crop Science Society of South Australia, Newsletter No.187.

Rengasamy, P. and Sumner, M.E. 1998. Processes involved in sodic behaviour. In: Sumner, M.E. and Naidu, R., eds, Sodic Soils: Distribution, Properties, Management and Environmental Consequences. Oxford University Press, 35–50.

SCAV (Soil Conservation Authority of Victoria) 1982. Salting of non-irrigated land in Australia. Government Printer, Melbourne, Victoria.

Shaw, R.J., Coughlan, K.J. and Bell, L.C. 1998. Root zone sodicity. In: Sumner, M.E. and Naidu, R., eds, Sodic Soils: Distribution, Properties, Management and Environmental Consequences. Oxford University Press, 95–106.

Soil Survey Staff 1987. Sodic, sodic-saline, and saline soils of North Dakota. Miscellaneous Publication, Soil Conservation Service, United States Department of Agriculture, Bismarck, North Dakota.

US Salinity Laboratory Staff 1954. Diagnosis and improvement of saline and alkali soils. United States Department of Agriculture, United States Government Printing Office, Washington DC.

Williams, B.G. and Bullock, P.R. 1989. The classification of salt-affected land in Australia. CSIRO Division of Water Resources, Technical Memorandum 89/8.

Wood, W.E. 1924. Increase of salt in soil and streams following the destruction of the native vegetation. Journal of the Royal Society, Western Australia, 10, 35–47.

Xianmo Zhu and Mei'e Ren. 2000. The Loess Plateau- Its Formation, Soil and Water Losses, and Control of the Yellow River, Soil erosion and dryland farming Ed John M. Laflan. CRC Press, New York. 1–5.

9

Soil–Regolith Models of Soil–Water Landscape Degradation: Development and Application

Rob W. Fitzpatrick* and Richard H. Merry*

Abstract

Soil degradation (salinity, sodicity, waterlogging and acidity) in the high rainfall catchments in the Mount Lofty Ranges and Dundas Tablelands is a growing concern to property holders because of the rapid increase in waterlogged saline scalds. The objective of this study was to develop a systematic approach to constructing soil–regolith models that describe, explain and predict soil–water landscape degradation processes in a specific region.

The 'descriptive model' uses toposequences (soil landscape cross-sections) to describe the basic soil–regolith features and direction of soil water and solute movement. Here, we suggest that it is also necessary to produce models to explain and predict the relationships and behaviour of the soil–regolith system under study. Such models could explain and predict the processes giving rise to the vast range of complex and poorly understood saline, sodic and acid sulfate soils in catchments. Toposequence and catchment scales are the most suitable for constructing such models because each of the vertical and lateral changes can be linked to hydrological, physicochemical and biomineralogical processes.

This chapter describes several case studies that illustrate how the different types of soil–regolith model have been used to describe and predict degradation processes in salt-affected soils and adjacent stream waters, and to assist in generating maps at catchment and regional scales using geographic information systems. They have also been used to produce soil–landscape and vegetation field keys, which provide details of land-use options that can help to prevent the irreversible spread of saline and sodic conditions.

在劳伏特山区和邓达斯高原降水丰富的流域里，土地的快速退化（盐化、碱化、酸化以及渍涝），引起农场主的日益关注。本研究试图系统地构建土壤－风化层模型，以便解释和预报某个特定地区土壤－水分景观退化的过程。该描述性的模型用坡面层次（截面土壤景观）来描述基本的土壤－风

* CSIRO Land and Water/Cooperative Research Centre for Landscape Environments and Mineral Exploration, PMB 2, Glen Osmond, SA 5064, Australia. Email: rob.fitzpatrick@csiro.au

Fitzpatrick, R.W. and Merry, R.H. 2002. Soil–regolith models of soil–water landscape degradation: development and application. In: McVicar, T.R., Li Rui, Walker, J., Fitzpatrick, R.W. and Liu Changming (eds), *Regional Water and Soil Assessment for Managing Sustainable Agriculture in China and Australia*, ACIAR Monograph No. 84, 130–138.

化层特征，以及土壤水分和溶解物的移动方向。对于被研究的土壤－风化层系统，也有必要建造模型，以便解释和预报其间的关系和变化情况。对于导致流域大量出现复杂，人们了解甚少的盐碱化、酸化土壤的作用过程，这些模型可以作出解释、预报。因为每一个垂直方向或水平方向的变化都与水文、物理化学以及生物矿物过程有关，所以这样的模型最适合为一个坡面或者一个流域而建造。本章给出许多具体的研究实例，以说明不同类型的土壤－地表模型是如何解释、预测盐化土壤及其毗邻河流的退化过程，如何为采用地理信息系统在流域和区域范围制图提供辅助的。这些模型也可为土地保护组织制作野外土壤景观和植被的图例，详细提供土地利用的可能方式，以助于防止盐碱化的不可逆扩展。

FOUR questions frequently asked by the users of land resource information are:

- What soil properties are changing spatially with time?
- What are the most suitable approaches for characterising, monitoring, predicting and managing soil changes?
- What tools are required to make suitable predictions about soil and landscape conditions and sustainable land use?
- To what extent do soil processes and soil management influence water quality?

These four questions can be solved by integrating pedological, hydrological, biogeochemical and mineralogical data to develop various types of models that can identify and predict soil-landscape processes. This information can then be used to underpin and develop strategies for managing both spatial and temporal soil changes. Pedology is an integrative and extrapolative science because it builds an organisational framework to quantify and explain spatial variability within landscapes. It also provides a template, via mechanistic models, to understand biogeochemical processes at regional and global scales. Consequently, pedology provides an excellent framework for the extrapolation of spatial variability from detailed components of soils (hand specimens and horizons) to soil profile, toposequence, catchment, regional and global scales.

The objective of this chapter is to discuss the toposequence approach as a vehicle for presenting results of spatially-based conceptual models that can be used to develop:

- *descriptive models* to assess catchment-scale variability of saline, sodic and acid sulfate soils in order to develop practical solutions for ameliorating soils at farm scale (see Chapter 21);
- *explanatory models* to understand the relationships and behaviour of saline soil processes (including potential saline and acid sulfate soils) that can take into account changes in land management; and
- *predictive models* to predict changes in saline soils caused by drainage (e.g. erosion), which result in development of either sodic or acid sulfate soils.

Materials and Methods

The study area

Initial work was based on soil sampling and fieldwork in the Herrmann subcatchment near Mount Torrens, about 50 km northeast of Adelaide, South Australia (Fritsch and Fitzpatrick 1994). The Overview provides some background on the region and Figure 5 of the Overview shows its location. Figure 1 of Chapter 21 shows the location of the areas concerned. The landscape of much of the study area is undulating low hills; the altitude ranges from 400 to 500 m and local relief from about 30 to 50 m. The climate is Mediterranean, with most rain falling in winter (May to September) and hot, dry summers (December to February).

Soil–regolith models to describe, explain and predict landscape degradation

Salt-affected and waterlogged soils form under different environmental conditions and have diverse morphological, chemical, physical and biological properties. These soils can be grouped based on the types of electrolytes causing the salinity or their chemical and physicochemical properties (Szabolcs 1991). Three main types of characteristics are used:

- salt content, composition and distribution in the profile and (in some cases) also in the groundwater;
- exchangeable sodium percentage and sodium adsorption ratio (sodic soils); and
- pH conditions and the existence of sodium carbonate (alkaline sodic and saline soils).

Of all the continents, Australia has the highest proportion of salt-affected soils in relation to total surface area (Szabolcs 1991). Sodic and saline soils occupy almost 2 million and 0.39 million km^2, respectively (Northcote and Skene 1972). The sodic:saline ratio of 5.17 is 4.4–10.3 times that reported for other continents, and is consistent with the high proportion of sodium present in soil solutions and groundwaters. In Australia, most sodium-affected soils are the result of past inundations by brackish water, possibly supplemented by cyclic salt. The result is that in subsoils, Cl^- is the dominant anion and exchangeable Mg^{2+}:Ca^{2+} ratios are high.

The effects of adsorbed Na^+ on clay dispersion are most pronounced in the B horizon of dense alkaline subsoils, which comprise over 86% of Australian sodic soils (Northcote and Skene 1972). The impact of soil sodicity on the environment is an important land degradation issue in Australia. Both primary and secondary sodification can cause undesirable changes in soil structure, severe hillslope erosion, waterlogging and erosion of downstream watercourses.

Generally speaking, Australian soil-landscapes are extremely variable and complex; this is partly due to the great age of much of the continent. In adjacent landscape positions, one can be confronted with deeply weathered soils that contain ancient stored salt juxtaposed with very youthful soils on partly weathered rocks that are generating salt as a result of contemporary weathering processes. Much work has been done on the hydrogeology of dryland saline areas and soil sodicity, but there is little published material on the development of comprehensive biogeochemical and physical process models of saline and acid sulfate soils. One reason for the lack of data is that, until recently, saline and acid sulfate soils were not considered suitable for agricultural production. There is also little published information on the dynamics of saline, sodic and acid sulfate soils, in particular whether the changes are reversible if saline soils develop into sodic soils after drainage.

Soil–regolith models are a simplification or abstraction of the processes that may occur in a particular toposequence system under study so that the information can be more easily handled either manually or mentally for a specific purpose (e.g. Dijkerman 1974). Several kinds of simplification or abstraction may be used; for example, in creating

models that describe, explain or predict particular aspects of soil–regolith processes. Because more than one kind of simplification or abstraction is often used to design models, different models are not necessarily mutally exclusive. Here, we will show that the descriptive model is the precursor or framework for developing the explanatory model, which in turn is used to help develop the predictive model.

A systematic approach to describe topo-sequences: descriptive soil–regolith models

Chapter 21 provides a summary of how we described soils in toposequences and linked these soil-landscape features to the main soil and water processes operating within the landscape via toposequences.

In the toposequence shown in Figure 1, red soils of the middle and upper slopes principally have better drained, sandy and loamy A horizons overlying clayey B horizons (Palexeralfs). Lower slopes, terraces and valley floors frequently have more poorly drained, yellowish sodic (Natrixeralfs) and alluvial soils (Entisols), and wet, grey coloured soils (Aquents) in groundwater discharge areas. Discharge areas frequently support perched wetlands.

Soil colour as a key indicator in developing descriptive soil–regolith models

Soil colour can provide a descriptive indicator of redox status, and this relates to soil aeration, organic matter content and fertility. As described by Fitzpatrick et al. (1999b) and others, indicators of

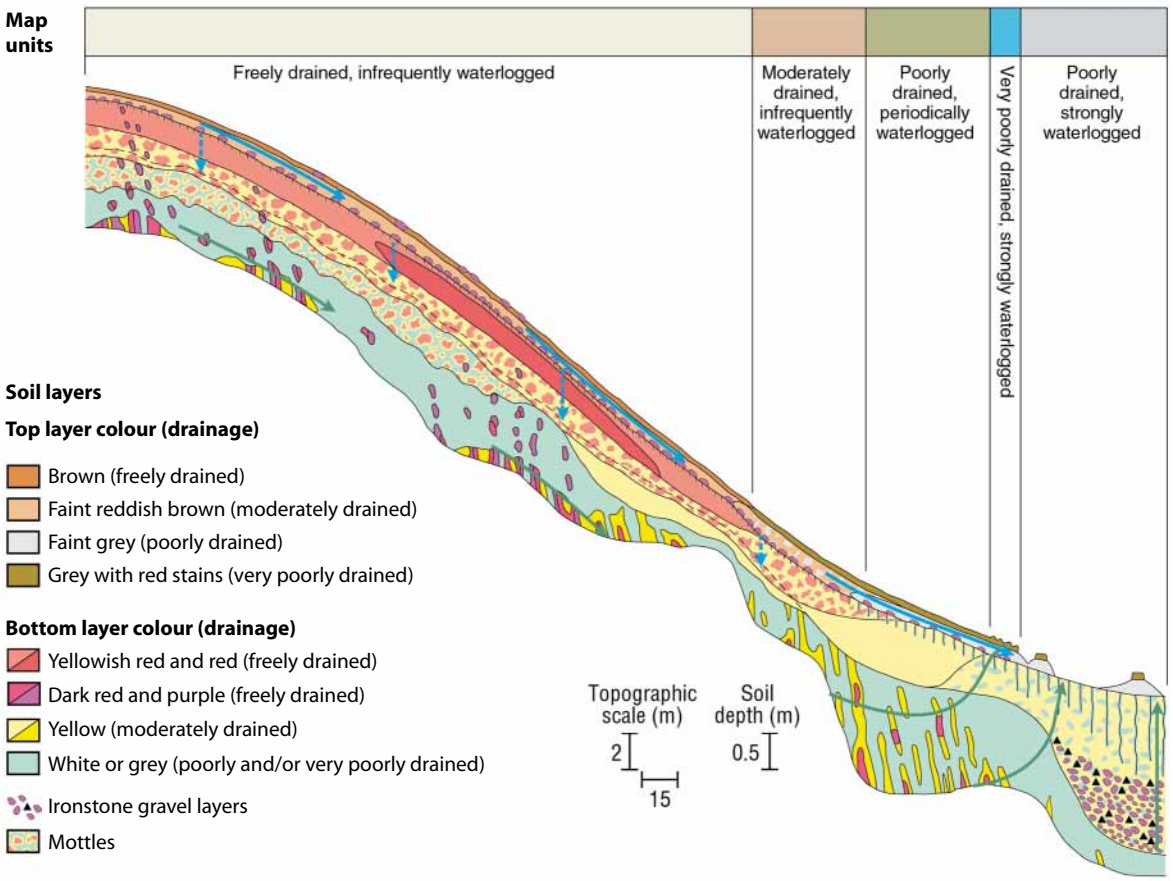

Figure 1. Descriptive soil–regolith model showing direction of perched fresh water flow and ground water flow. Modified from Fritsch and Fitzpatrick (1994).

good soil conditions for most forms of plant growth include the following:

- dark brown colours near the surface, often associated with high levels of organic matter, well-aggregated soil and above-average nutrient levels; and
- bright yellowish and reddish colours in subsoils, usually indicating oxidised conditions, suggesting good drainage. These coloured iron oxides also contribute to soils having good aggregation because of their strong surface charge properties. Aggregated soil materials are porous and contain sufficient air and water for root development.

Descriptive indicators of poor soil conditions include:

- mottles (blotches or specks) with dull yellow and orange colours in a grey, bluish or olive coloured material, indicating prolonged lack of soil aeration (seasonal or permanent waterlogging);
- rust-coloured specks and iron precipitates along fine roots, indicating prolonged or permanent waterlogging;
- very pale grey or white colours, indicating possible considerable leaching, low organic matter and low fertility;
- pale dense subsurface layers overlying dense clays (usually with mottled colours), indicating a perched watertable on the clay; and
- black mottles with the smell of hydrogen sulfide or mercaptan gases, which develop through anaerobic decay of organic matter, indicating severe waterlogging.

Figure 1 shows the distribution of these soil colour indicators in a toposequence.

Across large areas, it is expensive to monitor watertable depths (using piezometers or dipwells) to estimate water duration in soils. The field instrumentation installed down the toposequence is used to verify and quantify pathways and loads of water flow. Soil colour is a useful indicator for recognising and delineating waterlogged soils. Some visual indicators are obvious (e.g. occurrences of thick black accumulations of organic matter on soil surfaces), but some are more subtle (e.g. subsoil mottling patterns). Subsoil waterlogging can occur without any evidence on the surface. In Figure 1, we used mostly soil colour (together with other morphological, chemical and mineralogical indicators) and hydrology measurements (Cox et al. 1996) in the toposequence to construct the two-dimensional linkages that describe water flow paths and development of salinity (descriptive soil–regolith models).

Explanatory soil–regolith models

The descriptive model (Figure 1) was used to construct the explanatory soil-landscape model, which attempts to explain the contemporary geochemical dispersion and erosion processes present in the lower parts of the toposequence (Fig. 2).

In the catchments of the Mount Lofty Ranges and the Dundas Tableland, the codominant anions in saline groundwaters and soils are SO_4^{2-} and Cl^-. Chapter 11 describes the type of land degradation occurring in this particular landscape.

Predictive models

Development of potential acid sulfate soils

In many parts of inland Australia, the saline groundwater is rich in SO_4^{2-}, which can seep up through the soil, along with other ions in solution like Na^+, Mg^{2+}, AsO_4^{3-}, I^- and Cl^-. The SO_4^{2-} then concentrates by evaporation and forms various mineral precipitates within and on top of the soil (Figs 2 and 3a). The combination of rising sulfate-rich groundwaters, anaerobic conditions associated with saturated soils, agricultural activity and a

fractured rock geology rich in iron and sulfur can lead to the formation of saline soils with potential and actual acid sulfate soil conditions (Fitzpatrick et al. 1996, 2000). If the soil is wet and contains sufficient organic carbon, anaerobic bacteria use the oxygen associated with the SO_4^{2-} ions during the assimilation of carbon in organic matter. This process produces pyrite (FeS_2) and forms 'sulfidic materials'. The pyrite-enriched soils are termed potential acid sulfate soils because they have all the ingredients necessary to produce acid sulfate soils (Figs 2 and 3a).

Development of acid sulfate soils

Acid sulfate soils result when activity from animals, drainage works or other disruptions exposes the pyrite in the previously saturated soils to oxygen in the air. When this happens, pyrite is oxidised to sulfuric acid (H_2SO_4) and various iron sulfate-rich minerals, and acid sulfate soils form (Fig. 3b). When sulfuric acid forms, the soil pH can drop from neutral (pH 7) to less than 4 (we have measured values as low as 2) to form a 'sulfuric horizon' (Fig. 3b). The sulfuric acid dissolves the clay particles in soil, causing basic cations and associated anions (e.g. Na^+, Mg^{2+}, Ca^{2+}, Ba^{2+}, Cl^-, SO_4^{2-}, SiO_4^{4-}), trace elements, and metal ions such as iron and aluminium to be released on the soil surface and in stream waters.

As the regolith structure declines due to the accompanying sodicity, soils become clogged with clay and mineral precipitates and lose their permeability and groundcover. This prevents the groundwater below from discharging and forces it to move sideways or upslope (Fig. 3b). Soil around the clogged area eventually erodes, sending acid, metal ions and salts into waterways and dams, while a new area of potential acid sulfate soil develops upslope or adjacent to the original acid sulfate soil zone. If pugging by cattle or other activities continue to disturb the soil around the newly degraded area, it continues to expand (Fig. 3b). Bare, eroded, saline scalds surrounding a core of slowly permeable, highly saline, eroded acid sulfate soils (Fig. 3c) occur if these processes express on the surface of the soil. These saline landscapes are characterised by slimy red or white ooze and scalds with impermeable iron-rich crusts, and have been reported in South Australia, southwestern Victoria (Dundas Tableland), the Western Australian wheatbelt, the

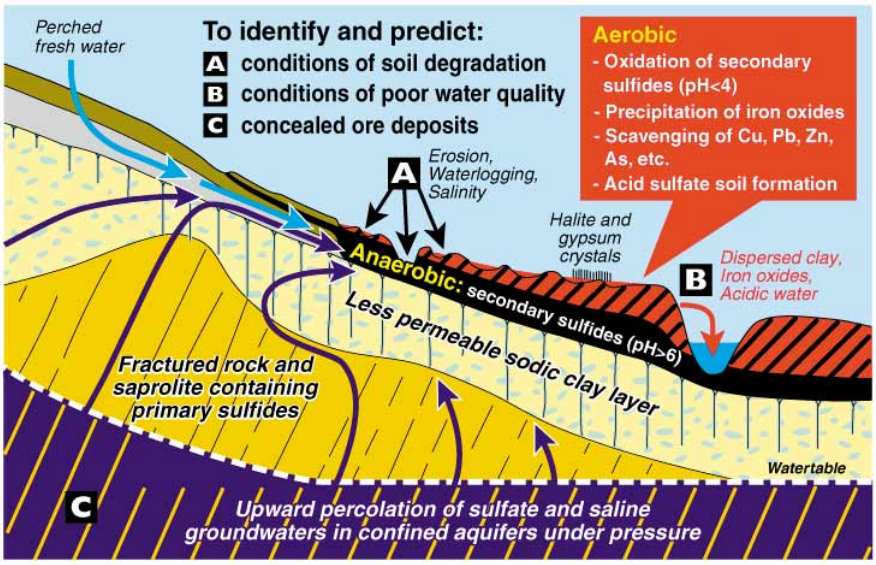

Figure 2. Explanatory soil–regolith model showing geochemical dispersion and erosion processes in saline landscapes and formation of secondary sulfides in potential acid sulfate soils in a perched wetland and actual acid sulfate soil along drainage lines.

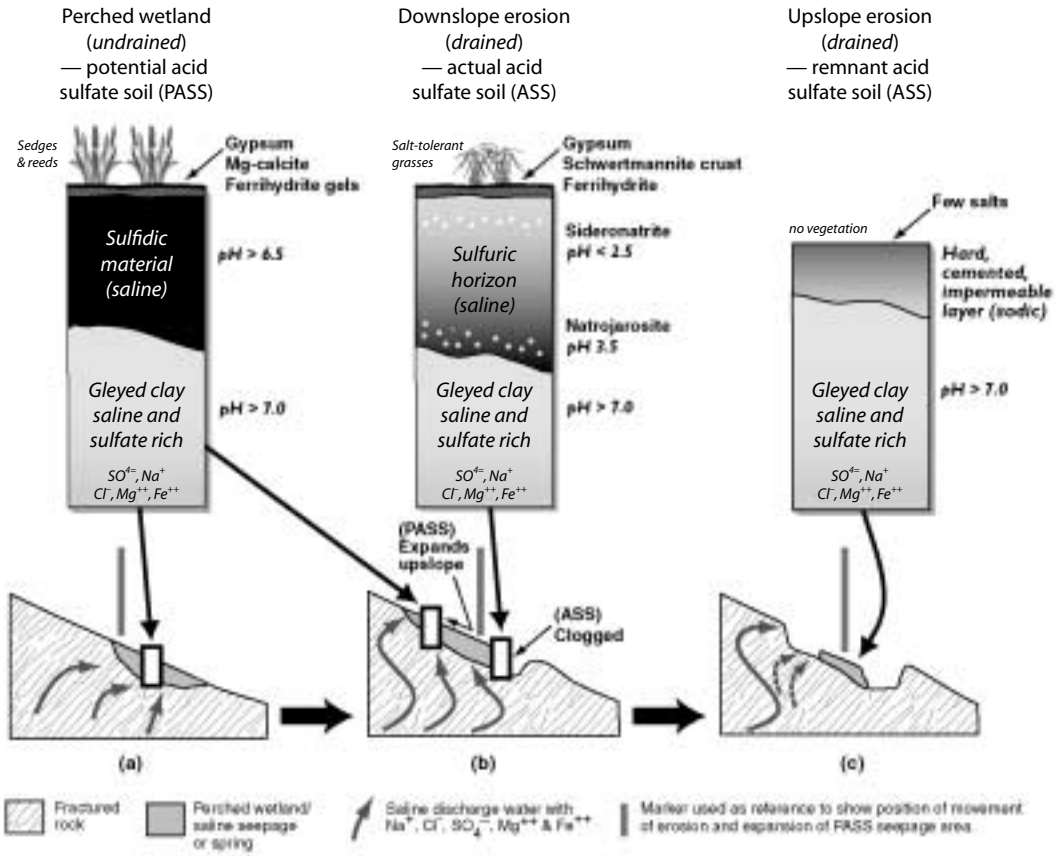

Figure 3. Predictive soil–regolith model showing the progressive transformation of saline potential acid sulfate soils in a perched wetland, via actual acid sulfate soils to eroded highly saline acid sulfate soils.

Yass valley in New South Wales and southeastern Queensland. While these reports suggest that saline acid sulfate soils are widely spread, the full extent, nature and severity of the problem are still unknown. This is because the discovery of saline inland acid sulfate soils is relatively recent (Fitzpatrick et al. 1996), although the problem has been studied in coastal areas since the 1980s.

Development of saline soils

In Australia there are extensive areas of naturally saline soils. The secondary saline soils that form following land clearing are more closely associated with processes leading to dryland salinity. Most of the saline soils found in Australia contain Cl^- as the dominant anion and Na^+ as the dominant cation (Fig. 4a). The accumulation of this stored salt is generally believed to originate from the ocean via rainfall and marine deposition in earlier geological periods (Isbell et al. 1983). Following the clearing of upland areas, saline seepages develop rapidly on slopes because of rising saline groundwater tables. When saline soils dry out, halite (sodium chloride) is often the main salt efflorescence formed (Fig. 4a). However, there is little information available on the nature of the soils and the salts that they contain.

Changes in salinity and development of sodicity

Sodic soils are believed to have developed from saline soils by freshwater leaching. Secondary sodic soils are known to develop from the drainage of saline soils (Fig. 4b). However, the formation of 'naturally' sodic soils is more uncertain: such soils could have formed directly from the weathering of certain parent materials thousands of years ago and may not necessarily have developed from saline

soils (Isbell et al. 1983). A case study conducted in the Mount Lofty Ranges of South Australia illustrated that a sodic soil with an exchangeable sodium percentage of more than 15% could develop from a saline soil (EC_{se} > 8 dS/m) when it was drained following the formation of a nearby erosion gully. Figure 4b illustrates freshwater leaching of a saline soil (Fritsch and Fitzpatrick 1994). The studies in the Mount Lofty Ranges have demonstrated the important interrelationships between salinity and sodicity in the context of soil–water–landscape processes and the flocculation and dispersion of clay particles (Fitzpatrick et al. 1994).

Changes in the mobility of colloids and clays

Freshwater throughflow in loamy or sandy surface horizons of drained saline soils in discharge areas leads to the development of sodic layers and to lateral movement of colloids into streams (Fig. 4b; Fitzpatrick et al. 1994). Such processes usually predominate in texture-contrast soils (duplex soils) in which dense, sodic, columnar B horizons (Btn, where 'B' is the subsoil horizon, 't' indicates clay accumulation and 'n' a sodic condition) occur. These layers restrict the downward movement of water, leading to waterlogging, tunnel erosion and enhanced lateral movement of water as surface runoff and as shallow groundwater flow in sloping land. Eventually a saline scald is formed (Fig. 4c).

Changes in decomposition and transformation rates of soil minerals

When saline soils are leached, salt efflorescenses on the soil surface are dissolved (Fig. 4b). Salt crystals develop at depth in sodic soils where saline groundwater discharges through the subsoil clay layer into the gully. This causes the banks to erode (salt weathering; Figs 4b and 4c). As shown in Figures 3a and 3b, when the potential acid sulfate soils undergo changes, different salt and iron minerals form because of differences in pH and salt concentrations (Fitzpatrick et al. 1996; Fitzpatrick and Self 1997). In the final stage of the acid sulfate soil formation, a hard soil layer remains, with few salts (Fig. 3c).

The acidification process accelerates the decomposition and formation of minerals in the soils and underlying rocks and can cause an increase in salinity and carbonate (Fitzpatrick and Merry 1999). Where salinity has surface expression, unsightly scalds develop; they are devoid of vegetation and contribute to poor quality water in the catchment.

Changes in greenhouse gas emissions

Saturated, saline soils are potential sources of greenhouse gases that have not been adequately researched. In a recent study of an area of about 80 km^2 in South Australia, Fitzpatrick et al. (1999a)

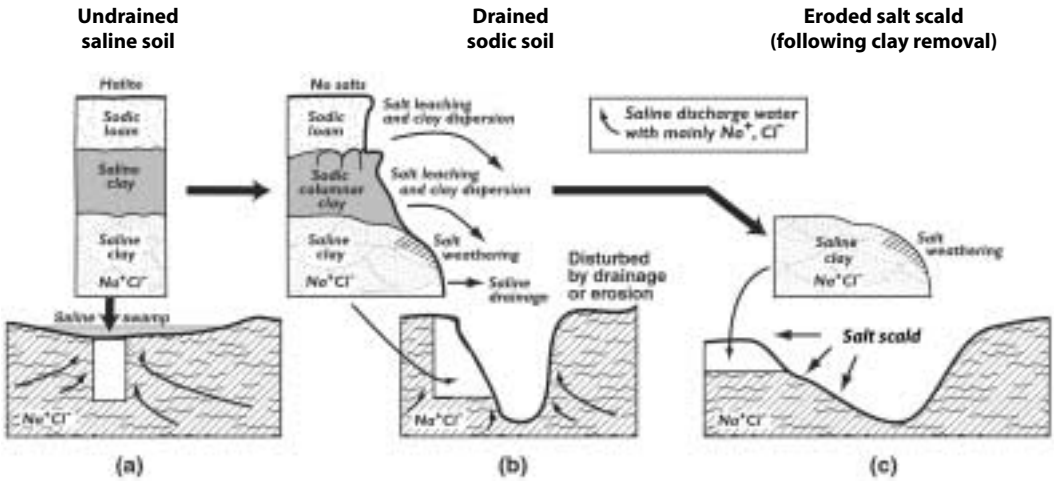

Figure 4. Predictive soil–regolith model showing the progressive transformation of saline soils, via sodic soils, to saline soils in salt scald.

used geographic information systems (GIS) to estimate that more than 10% of the area was strongly waterlogged and poorly drained, and a further 27% periodically waterlogged. A high proportion of the area was also characterised by saline discharge or potential acid sulfate soils. Depending on seasonal conditions, redox status and the nature of groundwaters (sulfidic, sulfatic or oxygenated), greenhouse gases such as carbon dioxide, nitrogen oxides and methane may be emitted. Drainage of these sites may decrease production of these greenhouse gases (Fitzpatrick and Merry 1999).

Conclusions

A systematic approach has been developed for constructing soil–regolith and water process models, which describe the toposequence system under study (descriptive model), and explain or predict the relationships and behaviour of the toposequence system under study (explanatory and predictive models). These models can be useful in generating maps at catchment and regional scales using GIS (see Chapters 11 and 21), and in producing practical soil-landscape and vegetation field keys from which to determine land-use options for preventing the irreversible spread of saline and sodic conditions (see Chapters 26 and 29).

Acknowledgments

The research was funded in part by ACIAR, Land and Water Australia, the National Landcare Program and the Natural Heritage Trust. We are grateful to members of the Tungkillo Landcare Group for their assistance. Scientists who contributed substantially to the study include Dr E Fritsch (ORSTOM), Dr P Self, Mr G Rinder and Ms Mary-Anne Fiebig (CSIRO).

References

Cox, J.W., Fritsch, E. and Fitzpatrick, R.W. 1996. Interpretation of soil features produced by ancient and modern processes in degraded landscapes: VII. Water duration. Australian Journal of Soil Research, 34, 803–824.

Dijkerman, J.C. 1974. Pedology as a science: The role of data, models and theories in the study of natural soil systems. Geoderma, 11, 73–93.

Fitzpatrick, R.W., Boucher, S.C., Naidu, R. and Fritsch, E. 1994. Environmental consequences of soil sodicity, Australian Journal of Soil Research, 32, 1069–1093.

Fitzpatrick, R.W., Fritsch, E. and Self, P.G. 1996. Interpretation of soil features produced by ancient and modern processes in degraded landscapes: V Development of saline sulfidic features in non-tidal seepage areas. Geoderma, 69, 1–29.

Fitzpatrick, R.W. and Merry, R.H. 1999. Pedogenic carbonate pools and climate change in Australia. In: Lal, R., Kimble, J.M., Eswaran, H. and Stewart, B.A. eds, Global Climate Change and Pedogenic Carbonates. Boco Raton, FL, CRC Press Lewis Publishers, 105–119.

Fitzpatrick, R.W., Bruce, D.A., Davies, P.J., Spouncer, L.R., Merry, R.H., Fritsch, E. and Maschmedt, D.J. 1999a. Soil Landscape Quality Assessment at Catchment and Regional Scale. Mount Lofty Ranges Pilot Implementation Project, National Land and Water Resources Audit. CSIRO Land and Water Technical Report 28/99, July 1999. www.clw.csiro.au/publications/technical99/tr28-99.pdf

Fitzpatrick, R.W., McKenzie, N.J., Maschmedt, D. 1999b. Soil morphological indicators and their importance to soil fertility. In: Peverell, K., Sparrow, L.A. and Reuter, D.J., eds, Soil Analysis: an interpretation manual. Melbourne, Australia, CSIRO Publishing, 55–69.

Fitzpatrick, R.W., Raven, M., Self, P.G., McClure, S., Merry, R.H. and Skwarnecki, M. 2000. Sideronatrite in acid sulfate soils in the Mt Lofty Ranges: First occurrence, genesis and environmental significance. In: Adams, J.A. and Metherell, A.K., eds, New Horizons for a New Century. Australian and New Zealand Second Joint Soils Conference Volume 2: Oral Papers. 3–8 December 2000, Lincoln University, New Zealand Society of Soil Science. 109–110.

Fitzpatrick, R.W. and Self, P.G. 1997. Iron oxyhydroxides, sulfides and oxyhydroxysulfates as indicators of acid sulfate surface weathering environment. In: Auerswald, K., Stanjek, H. and Bigham, J.M., eds, Soils and Environment: Soil Processes from Mineral to Landscape Scale, Advances in GeoEcology, 30, 227–240.

Fritsch, E. and Fitzpatrick, R.W. 1994. Interpretation of soil features produced by ancient and modern processes in degraded landscapes: I A new method for constructing conceptual soil-water-landscape models. Australian Journal of Soil Research, 32, 889–907; colour figures 880–885.

Isbell, R.F., Reeve, R. and Hutton, J.T. 1983. Salt and Sodicity: in Soils: An Australian viewpoint, McDonald, R.C., Isbell, R.F., Speight, J.G., Walker, J. and Hopkins, M.S. 1990. Australian Soil and Land Survey Field Handbook (2nd edn). Melbourne, Australia, Inkata Press, 87–183.

Northcote, K.H. and Skene, J.K.M. 1972. Australian soils with saline and sodic properties. CSIRO Soil Publication No. 27.

Szabolcs, I. 1991. Soil classification related properties of salt affected soils. In: Characterization, Classification, and Utilization of Cold Aridisols and Vertisols, Proceedings of sixth international soil correlation meeting (VI ISCOM). Lincoln, NE, United States Department of Agriculture, Soil Conservation Service, National Soil Survey Center.

10 Assessment of a Small Catchment on the Loess Plateau

Guobin Liu,* Mingxiang Xu,* Li Rui,* Joe Walker† and Weiyin Hu*

Abstract

The Loess Plateau is being redeveloped to achieve a healthy ecosystem. Taking a small watershed as an example, this study used an analytic hierarchy process to identify different land uses, soil characteristics, crop yield and income for assessment of ecosystem rehabilitation. Various physical and social indicators were also analysed on the catchment scale. The results showed that after about 20 years of soil conservation and restoration, the ecosystem health index of the watershed had improved from 0.178 in 1985 to 0.707 in 1999. The research introduced several new indicators (soil organic content, soil antiscourability, total income from industry and off-farm, and the efficiency of integrated control measures in decreasing soil loss) of physical characteristics of soil and suggested how these indicators should be weighted for calculation of the ecosystem health index.

本文以安塞纸坊沟小流域为对象，在对地块尺度和流域尺度的土壤物理特性指标、土地利用、植被状况和流域尺度的社会经济指标分析研究的基础上，利用层次分析法，选取林草覆盖度、基本农田面积、土壤抗冲性、土壤有机质含量、农业产投比、粮食单产、人均纯收入和综合治理减沙效率等反映流域生态经济生态功能评价指标，定量分析了黄土丘陵区安塞纸坊沟小流域进行水土保持型生态农业建设中生态系统恢复的过程。结果表明，该小流域经过近 20 年治理，经历了起始恢复、稳定发展阶段开始进入良性循环。其健康指数由 1985 年的 0.178 增加到 1999 年的 0.707。本研究中首次引入土壤抗冲性和有机质指标，并在评价中对生态系统恢复不同阶段给予各指标不同权重值，对方法进行了改进。

* Institute of Soil and Water Conservation, Chinese Academy of Sciences and Ministry of Water Resources, NWSUAF, Yangling, Shaanxi 712100, PRC. Email: gbliu@ms.iswc.ac.cn

† CSIRO Land and Water, GPO Box 1666, Canberra, ACT 2601, Australia.

Guobin Liu, Mingxiang Xu, Li Rui, Walker, J. and Weiyin Hu. 2002. Assessment of a small catchment on the Loess Plateau. In: McVicar, T.R., Li Rui, Walker, J., Fitzpatrick, R.W. and Liu Changming (eds), *Regional Water and Soil Assessment for Managing Sustainable Agriculture in China and Australia*, ACIAR Monograph No. 84, 139–154.

Soil erosion is a serious worldwide environmental problem and a major threat to the sustainability of agriculture. The Loess Plateau, with its deep, loose loess (a loam deposited by wind), is continuously losing soil and productivity due to severe soil erosion. Aware of the extent and severity of the problem, the Chinese government is promoting measures to control soil erosion and establish a healthy ecosystem in the Loess Plateau region. A successful approach is to focus on a small watershed that can act as a model for the development of similar watersheds. For example, three projects in the Zhi Fanggou catchment, each spanning five years, have produced significant economic, social and ecological benefits (Liu 1999). However, there is still no established method for assessing ecosystem health. Soil is a major ecosystem component, so its characteristics and dynamics are a useful index of health (Walker and Reuter 1996; Liu Guobin et al. 1999). In this study, we selected a catchment that had been managed for several years and measured several soil physical and chemical properties. We also developed a method to assess the health of the catchment.

The Zhi Fanggou catchment lies in the central area of the Loess Plateau in northern Shaanxi province. The catchment is 8.27 km^2 ranging from 1000 to 1350 m in altitude. Figure 4 of the Overview shows the main locations on the Loess Plateau.

There are significant topographic variations within the study area, with typical loess hills and gully landforms; 32% of land has a slope of more than 35°. The land is a mosaic of slope cropland, fallow land, grassland, shrubland, orchard land and woodland. Crops are mainly potatoes (*Solanum tuberosum*), beans (*Phaseolus valgaris*), corn (*Zea mays* L.) and millet (*Panicum miliaceum*). The artificial woods are dominated by locust trees (*Robinia pseudoacacia* L.). The grassland is mainly covered by annuals such as sweet wormwood (*Artemisia annua* L.), annual fleabane (*Erigeron annuus* Pers.) and sandy needlegrass (*Stipa glareosa* p. Smirn). Littleleaf peashrub (*Caragana microphylla*) is found in shrubland, and apple trees (*Malus pumila mill*) in orchards. Some land became fallow about two to three years ago when cultivated plots were abandoned.

The region has a semiarid continental climate with an average annual temperature of 8.8°C. Monthly mean temperatures range from 22.5°C in July to –7°C in January. Average annual precipitation is 485 mm, with 60% of rain falling between July and September. On average, there are 159 frost-free days and 2415 hours of sunshine each year.

Thick soils develop on loess parent material, averaging 50–80 m. The most common soil type in the catchment is loess with the texture of fine silt. The soil has little resistance to erosion and is being lost at the rate of about 10,000–12,000 t/km^2/year (Jiang and Fan 1990).

Materials and Methods

Soil characteristics

Twenty plots of different land-use types in the Zhi Fanggou catchment were selected in 1999. Table 1 shows the basic characteristics of the plots. Soil samples were taken for five layers at 10 cm intervals, from the soil surface to a depth of 50 cm. Soil antiscourability (the ability to resist detachment), stable rate of infiltration of water, aggregate stability and organic matter content were measured in these samples. Cohesion of surface soil when saturated was also measured.

Antiscourability

Soil antiscourability was measured by a washing method (Liu 1997), using specialised equipment referred to as an 'antiscouring mini-flume' (Fig. 1). Soil was placed in a groove and scoured with water at a rate of 1.4 L/minute, based on the premise that all the rainfall at 2 mm/minute (the maximum density in the Loess Plateau) in a standard plot of 5 × 20 m^2 would be lost as runoff. The soil sample was saturated before washing and the slope of the groove was regulated according to the selected plot.

Table 1. Basic characteristics of the experiment plots.

Land-use type	Vegetation type	No. of plots	Topography	Sampling date (1999)
Cropland	Foxtail millet	1	Steep slope	30 April–28 May 23–31 August 9–22 October
	Potato	3	Steep slope, terrace, gentle slope	
	Pearl millet	3	Gentle slope1, steep slope2	
	Soybean	2	Gentle slope, steep slope	
	Corn	1	Terrace	
Woodland	Poplar, acacia	3	Slope	29 June to 7 August
Shrubland	*Caragana korshinskii*	3		26 June to 14 August
Human-made grassland	Melilot	1		16 July
Natural grassland	*Bothriochloa ischaemum, Sophora viciifolia, Artemisia giraldii Stipa bungeana*	3		13 July to 7 August

Figure 1. Mini-flume for soil antiscourability test.

Four samples were taken at each of the five layers. Soil antiscourability was calculated from the following equation:

$$S_0 = \frac{Q \times T}{M}$$

where S_0 is soil antiscourability (L/min/g), Q is total runoff for scouring (mL), T is scouring time and M is the dry soil weight lost in the groove (g).

Steady infiltration rate

The soil infiltration rate was tested using an infiltration cylinder 12 cm in height and 10 cm in diameter. Soil samples were saturated for 12 hours before measurement and a constant head of water of 2 cm was maintained during measurement. The outflow was measured at three-minute intervals until the infiltration rate stabilised. Fifteen soil samples

were taken (three repeats in each of five layers). Soil steady infiltration rate was calculated as follows:

$$V = \frac{Qi}{S} \times \frac{10}{ti}$$

$$K_t = V \times \frac{L}{H + L}$$

$$K_{10} = \frac{K_{ti}}{0.7 + 0.03t}$$

where V is the soil steady infiltration rate (mm/min), Qi is the outflow from the cylinder during infiltrating time ti (mL), S is the area of the base of the cylinder (cm^2), L is the height of the soil sample (cm), H is the height of the water head (cm) and K_t is the infiltration coefficient when the water temperature is t (°C).

Aggregate stability

Aggregate stability was tested used a modification of the Yoder method (Zhu 1989). A set of sieves (5 mm, 2.5 mm, 1 mm, 0.5 mm and 0.25 mm) was prepared with larger mesh at the top and smaller mesh at the bottom. The saturated soil sample (wetted by capillary water to remove air in the soil) was placed in the sieves, which were then immersed in water and shaken for one minute. The aggregate in each sieve was weighed and the percentage of each particle class calculated. Mean weight diameter (MWD) of aggregate stability (Le Bissonnais 1996; Le Bissonnais 1997) was also calculated, using the following equation:

$$MWD = \sum_{i=1}^{n} X_i \cdot W_i$$

where MWD is mean weight diameter (mm), X_i is the average diameter of each particle class (mm) and W_i is the proportion of aggregate relating to X_i (%).

Soil cohesion

A pocket shear tester (Fig. 2) was used to measure soil surface cohesion (Brunori et al. 1989). Soil was first saturated using a sprinkler. A pocket vane tester was set at zero and inserted into the ground to a depth where the vanes were no longer visible. The tester was turned to the right until the soil failed. If the value was above 8, a smaller vane was used for further tests; if it was below 2, a larger vane was used.

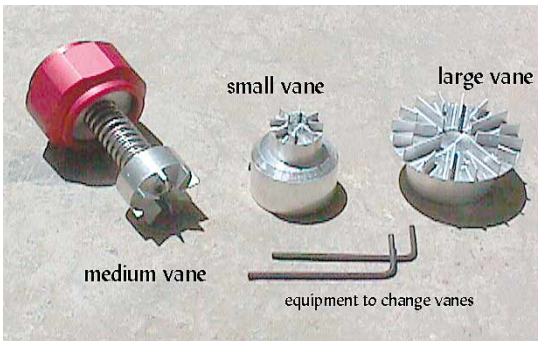

Figure 2. Shear tester with different vanes.

The average cohesion value (kg/cm^2) was calculated by multiplying by 0.02, 0.10 and 0.25 for the large, medium-sized and small vane respectively. Cohesion measurements were repeated 10 times in each plot.

The average of each parameter in each measuring period was calculated for each type of land use. A weighted average of each parameter in the whole catchment was calculated, based on the area used for each type of land use. An analysis of variance was calculated for each parameter from the measurements taken each year.

Organic matter content

Organic matter content was measured using the $K_2Cr_2O_7$ oxidation method.

Analytic hierarchy process

Soil characteristics were calculated on catchment scale (related to land use) and plot scale. The historical soil characteristics of the catchment were calculated from current land use and soil characteristics, based on the premise that soil characteristics differ markedly between different land uses and do not readily change within land-use classes.

The analytic hierarchy process (AHP) is a method to break a complex question into several different components, structure these components into layers, then rank the sequence of the components and weight them. The method described by Zhao Huancheng et al. (1986) was used to perform the following three tasks.

- *Construct an analytic hierarchy model.* A complex situation was divided into different components; structured into objective, criteria, index, scenario and measurement layers; and the relation between these layers structured by a graph.
- *Produce a matrix.* Components were sequenced by comparing the importance of each factor with the other factors and assigning them values as shown in Table 2. A matrix was produced based on these values, and the maximum eigenvalue and eigenvector of the matrix were calculated. The weighted values of the factors in one layer compared to those in a superior layer could then be calculated.

Table 2. Value assignment in the assessment matrix.

Value	Meaning
1	The two factors are equally important
3	One factor is slightly more important than the other one
5	One factor is obviously more important than the other one
7	One factor is intensively more important than the other one
9	One factor is extremely more important than the other one
2,4 6,8	Median of the respective values above

- *Test for consistency.* A single order consistency test was based on the following equation:

$$CR = \frac{CI}{RI} < 0.10 \qquad CI = \frac{\lambda_{max} - n}{n - 1}$$

where CI is the index of consistency, λ_{max} is the maximum eigenvalue of the matrix, n is the rank value of the matrix, RI is the mean random index of consistency and CR is the random consistency ratio. Table 3 shows the mean random index of consistency values.

The matrix is consistent if $CR < 0.10$. Otherwise, the matrix is not consistent and the matrix value should be adjusted.

An overall consistency test was conducted from the top layer of the matrix to the interior layers. The random ratio of consistency can be obtained using the following equation:

$$CR = \frac{CI_j}{RI_j}$$

where CI_j is the consistency index of the factors in the interior layer compared to factor j in the superior layer and RI_j is the corresponding mean random index of consistency. When $RI < 0.1$, the overall order of the hierarchy is consistent.

Table 3. Mean random index of consistency.

Value[a]	1	2	3	4	5	6	7	8	9
CR	0.00	0.00	0.58	0.90	1.12	1.24	1.32	1.41	1.45

CR = random consistency ratio
[a] See Table 2 for value assignments

Results and Discussion

Ecological indicators

Soil quality

Antiscourability

Table 4 shows the soil indicator characteristics in different land-use types. Soil antiscourability

differed significantly between different land uses in Zhi Fanggou catchment. Shrubland had the greatest antiscourability, followed in sequence by natural grassland, woodland, human-made grassland and farmland (Table 4). The antiscourability of shrubland and natural grassland was about 70–90 times greater than that of cropland. Two years after the conversion of slope cropland to grassland, the antiscourability had increased 10-fold, suggesting that soil antiscourability in slope cropland can improve rapidly when land use is changed.

Figure 3 shows soil indicator characteristics in soil profiles in the Zhi Fanggou catchment. The soil antiscourability profile for all types of land use decreased sharply from upper to lower layers except in cropland, where the highest value was found in the 10–20 cm layer, perhaps influenced by the presence of roots (Fig. 3a,b).

Infiltration rate

Infiltration is the process by which water enters the soil. It is an important link between precipitation, surface water, soil moisture and groundwater. Reduced infiltration can decrease crop yields as it leads to less water being stored in the soil for use by crops. Runoff associated with low infiltration is associated with soil erosion, particularly on slopes (Radford et al. 1992; Connolly et al. 1998). To build a healthy ecosystem in the Loess Plateau, increased infiltration capacity and reduced runoff are needed. Therefore, it is important to understand the characteristics of soil infiltration in soil and water conservation in the catchment.

Table 4 indicates that the infiltration rate varied widely among different types of land use and correlated positively with the MWD of soil, aggregate stability and organic matter content. Figures 3c and 3d show the organic matter content and steady infiltration rate, respectively, for different types of land use.

Vegetation can improve the antiscourability and infiltration of soil by increasing the content of organic matter and eliminating the effect of rainfall splash; plant roots can also increase antiscourability.

Aggregate stability

In general, soil aggregate stability correlates positively with organic matter content, which commonly declines under arable cropping, leading to soil degradation problems such as crusting, runoff and erosion (Bissonnais et al. 1997; Guerra 1994; Sullivan 1990). The MWD reflects the size of stable soil aggregate. In general, good soil structure has a higher MWD, making the soil porous with high infiltration ability.

In this study, MWD was highest in shrubland, followed by woodland, natural grassland, human-made grassland and cropland (Table 4). As a whole,

Table 4. Soil indicator characteristics in different land-use types.

Characteristic	Farmland	Woodland	Shrubland	Natural grassland	Planting grassland
Stable infiltration rate (mm/min)	0.65	1.11	0.85	1.93	0.78
OMC (%)	0.46	0.95	0.89	1.33	0.43
MWD of water stable aggregate (mm)	1.74	2.81	2.91	2.54	2.06
Antiscourability (L/min/g)	0.042	2.538	4.237	3.470	0.585
Cohesion (kg/cm^2)	0.082	0.111	0.082	0.111	0.119

MWD = mean weight diameter ; OMC = organic matter content
Note: The data in the table are the average of five layers from the soil surface to 50 cm down (saturated soil cohesion was measured only in the surface layer).

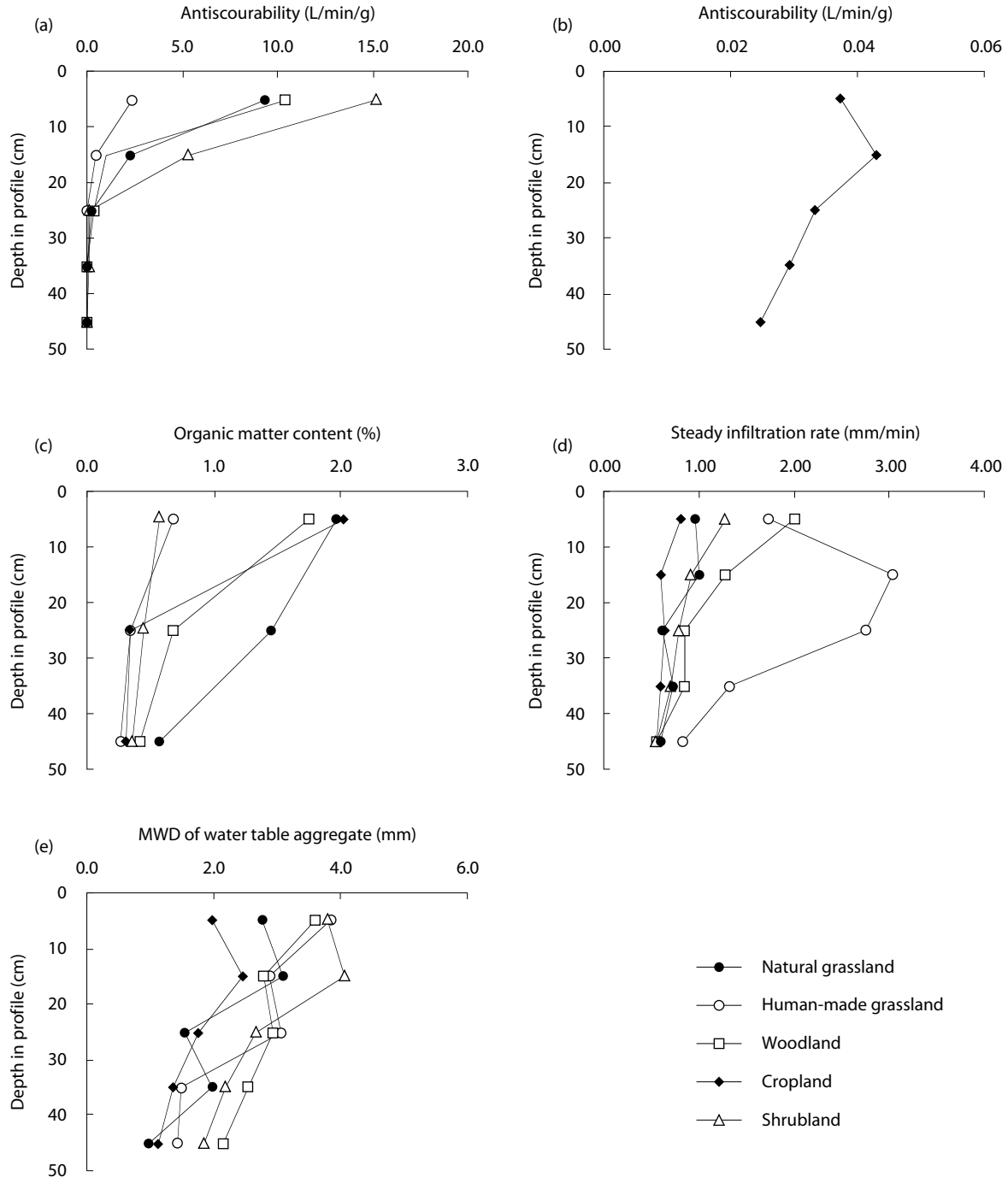

Figure 3. Soil indicator characteristics in soil profiles of the Zhi Fanggou catchment ecosystem: (a) and (b) antiscourability; (c) organic matter content; (d) steady infiltration rate; and (e) mean weight diameter.

MWD in the soil profile decreased from the upper to the lower layers (Fig. 3e), but was highest in the 10–20 cm layer in cropland, human-made grassland and shrubland, possibly due to farming activities on the topsoil.

Soil cohesion

Soil cohesion is an index of soil resistance related to the ability to resist external forces. Generally, soil erosion correlates negatively with soil cohesion, which is related to factors such as soil type, organic matter and soil water content (Brunori et al. 1989).

The study showed that soil cohesion for woodland and grassland was almost the same, and was much greater than that for shrubland and cropland (Table 4).

Plant roots, soil moisture content, bulk density, plasticity index and organic matter affect soil cohesion. Thus, saturated cohesion (cohesion of the soil when the soil is saturated) is low in the topsoil of cropland and shrubland.

Organic matter content

Soil organic matter is the basis of soil fertility and the formation of stable aggregate. In Zhi Fanggou catchment, different land-use types have significantly different soil organic matter content (Table 4). Levels are similar in cropland and human-made grassland, but about half to one-third of other land-use types. The sequence was natural grassland > woodland > shrubland > cropland and planting grassland (Table 4). The organic matter content decreased from the top of the soil to the lower layer (Fig. 3c).

There were significant positive correlations between the steady infiltration rate and the organic matter content:

$$y = 0.3583e1.0153x \quad R = 0.7973 \ (n=24)$$

where y is K_{10} and x is organic matter content.

The analysis showed that soil structure improved and the soil became more porous as the organic matter content increased, allowing an increase in infiltration capacity.

Spatial distribution

In order to better understand how soil environmental quality had changed after 20 years of environmental rehabilitation in the catchment, we analysed several soil characteristics at the plot scale in different land-use types. We then applied the plot-scale experimental results to the catchment and calculated the soil characteristic values for previous years using data from the year of the experiment. We made the following assumptions.

- We could ignore changes in soil characteristics over time, because they are much less significant than differences in characteristics for different forms of land use.
- We did not need to include water, bare rock, villages or roads in the total catchment area because these features occupied a negligible part of the total area and because we assumed that the area had not changed greatly in the previous 20 years.
- In calculating the total antiscourability of the catchment, we did not need to consider the antiscourability of terrace because soil is not usually lost from level terraces.

We classified cropland as either > 20° slope or ≤ 20° slope and calculated the soil characters of the catchment using the following equation:

$$V = \Sigma P_i \times V_i$$

where V is the value of the soil character on the catchment scale; P_i is the percentage area of land-use type i in the catchment area; and V_i is the value of the soil character in land-use type i at the plot scale.

For all the soil indicators we examined, we found that at 0–20 cm of the soil profile there were obvious

differences according to different land-use types (Fig. 3). In other words, soil characteristics in the upper layer (0–20 cm) of the soil profile are important and should receive more attention in indicator measurements.

Figure 4 shows several soil characteristics in the catchment for 1938, 1958, 1975 and 1997. For the same years, we also mapped the occurrence of these characteristics for different land-use types. Figures 5–10 show the spatial and temporal variation of several soil characteristics.

Temporal distribution

Figure 4 and Figures 5–10 show the temporal variation of several soil characters from 1938 to 1999. During the 1930s, the ecosystem was well developed because most sloping land was woodland, shrubland and grassland, with only a small area used for crops. The soil characters we analysed accordingly reached their highest values in 1938. In 1958, 'wasteland' was opened up, leading to degradation and maladjustment of the ecosystem. At this time, we found the lowest values for the soil characters we analysed. From 1958 to the 1970s values stayed the same or increased slowly. At about that time, integrated control measures were implemented in the catchment. These included changes in land use, the building of level terraces, vegetation rehabilitation, the development of cash crops and the planting of trees. Values rose quickly from the end of the 1970s to the 1990s, becoming steady in the early and mid-1990s and ascending again in 1997.

Vegetation

Vegetation plays a very important role in soil and water conservation. After the integrated control measures were put in place, the amount of vegetation cover in the catchment increased continuously — up to 57% in 1999, compared to 51% in 1938.

Primary cropland

As cropland is better managed and yields increase, it can be replaced by woodland and grassland, so that farming activities place less pressure on the environment. The target area for primary cropland per capita in Zhi Fanggou catchment is 3 mu (0.2 ha), which can provide sufficient food in normal years. We used the ratio of the present cropland per capita to the target figure of 0.2 ha to indirectly reflect the degree to which farming activities affect the environment.

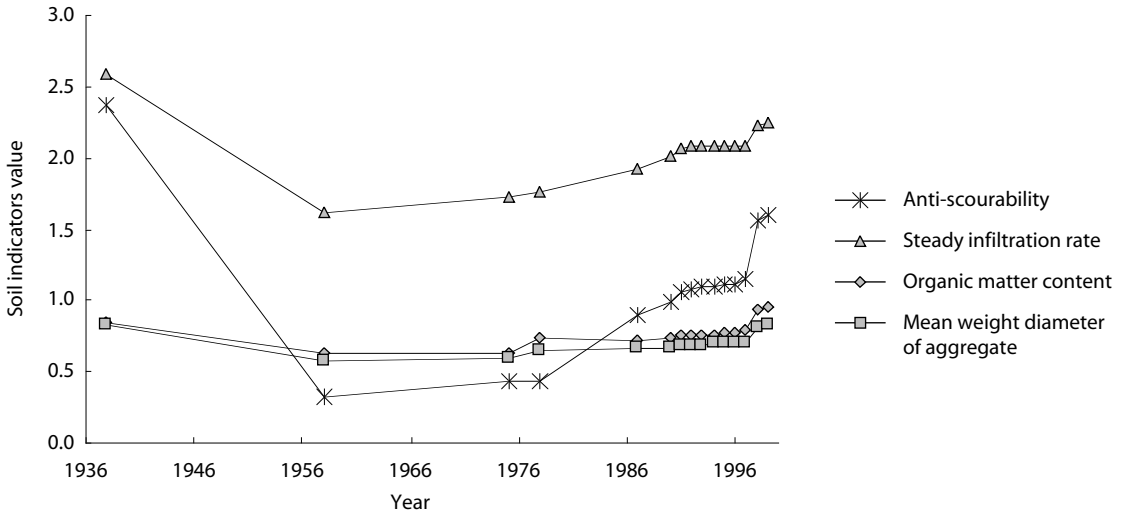

Figure 4. Soil trend indicators in the Zhi Fanggou catchment ecosystem, 1936–96.

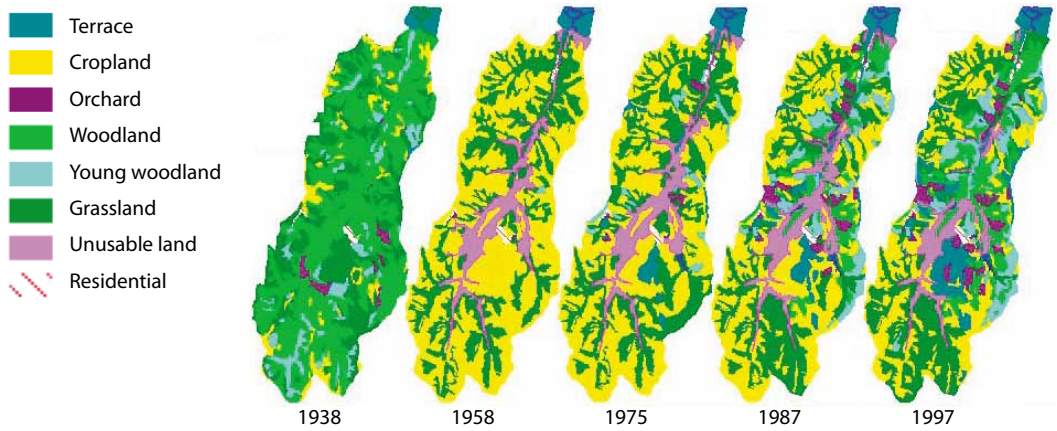

Figure 5. Land-use change in the Zhi Fanggou catchment ecosystem, 1938–97.

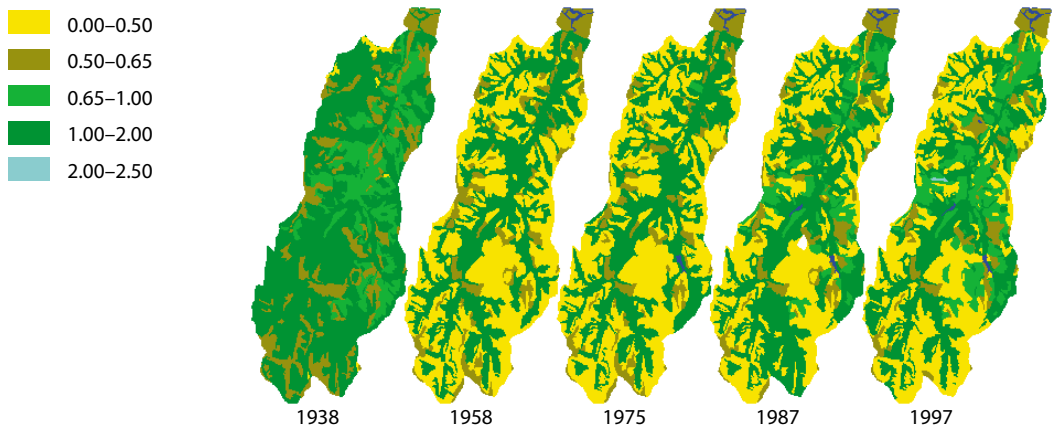

Figure 6. Organic matter content (%) in soils of the Zhi Fanggou catchment ecosystem, 1938–97.

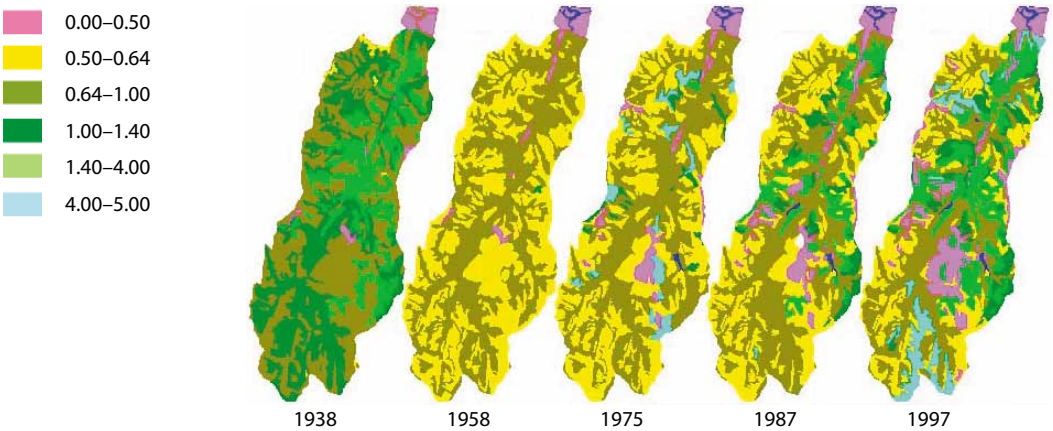

Figure 7. Infiltration (mm/min) in the Zhi Fanggou catchment ecosystem, 1938–97.

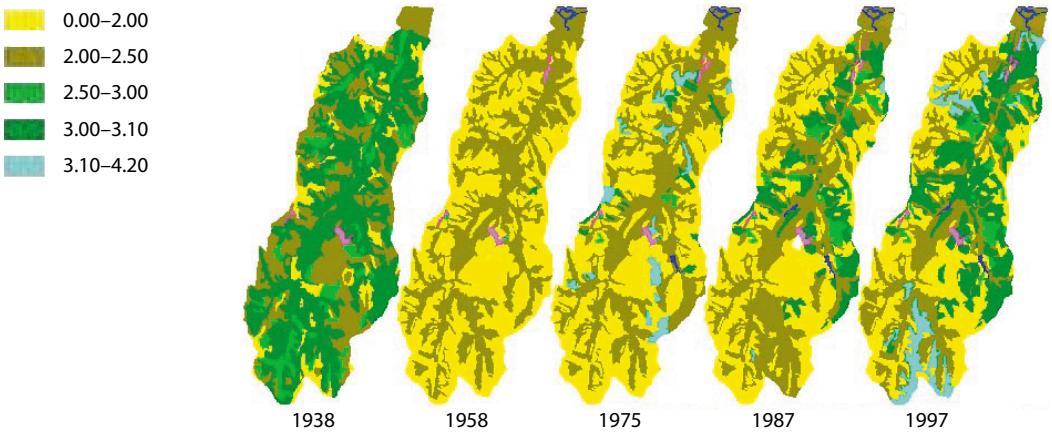

Figure 8. Mean weight diameter (mm) of aggregate in the Zhi Fanggou catchment ecosystem, 1938–97.

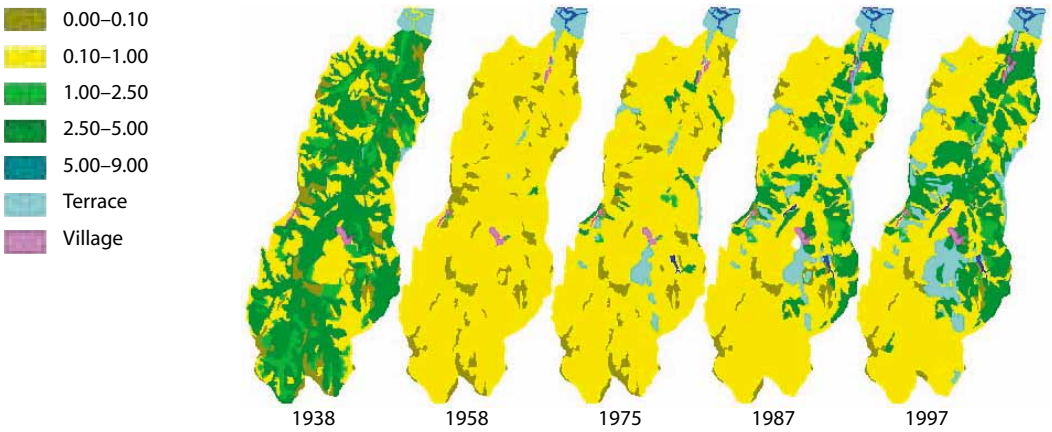

Figure 9. Antiscourability (L/min/g) in the Zhi Fanggou catchment ecosystem, 1938–97.

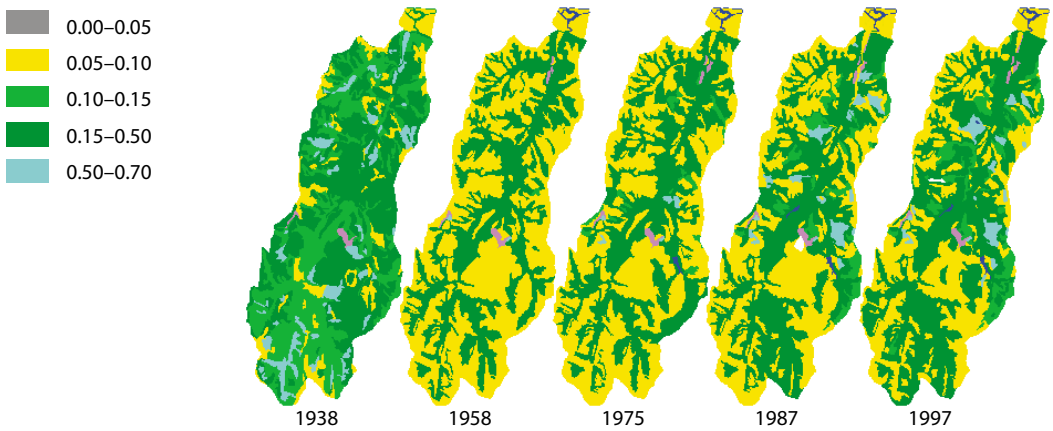

Figure 10. Cohesion (kg/cm^2)of soil in the Zhi Fanggou catchment ecosystem, 1938–97.

Socioeconomic indicators

Output/input ratio in agriculture

In agriculture the ratio of outputs to inputs can reflect the efficiency of capital and energy use. From 1984 the ratio decreased until the middle of 1990s, when it levelled off. Before integrated control measures were implemented, agriculture in the Zhi Fanggou catchment was carried out with little or no input. In the initial stage of the control measures, the output/input ratio was very high because soil productivity was low and potential productivity was great. When soil productivity increased, actual productivity was close to the potential and the output–input ratio stabilised.

Net income per capita

The net income per capita in the Zhi Fanggou catchment increased gradually from 1985 to 1999, although it decreased in 1991, 1996 and 1997 due to drought (Fig. 11a).

Realised potential yield

The realised potential yield (Fig. 11b) is the ratio of the current yield in the catchment to the potential maximum yield in the local climate, which is 5745 kg/ha (Liu et al. 1998). The realised potential yield reflected the industry structure of the Zhi Fanggou catchment and increases in soil productivity in the catchment. As a whole, the realised potential yield gradually increased from 1985 to 1999.

System function indicators

We used the following indexes to indicate how well the ecosystem was functioning in terms of its capacity to resist natural disasters and its ability to sustain stable development. The indicators demonstrated that, to some extent, damage to catchment ecosystems had slowed or ceased and that some recovery was occurring.

Ecosystem restoration

This indicator shows the extent of the effort to control the destruction of catchment ecosystems and to restore natural ecosystems. The indicator we used was the proportion of the actual control achieved as a percentage of the control that had been required.

Capacity to resist natural disasters

We measured the capacity of the catchment to resist natural disasters by calculating the production value in disaster years as a proportion of the mean production of recent years. The increasing trend in the capacity of the system to resist disasters (Fig. 12a) was a strong indication that integrated control measures in the Zhi Fanggou catchment had led to an improvement in the comprehensive functioning of the system.

Reduced soil loss

We measured the efficiency of the integrated control measures in decreasing soil loss by calculating the percentage soil loss before and after the introduction of integrated control measures. The intensity and amount of soil erosion in the Zhi

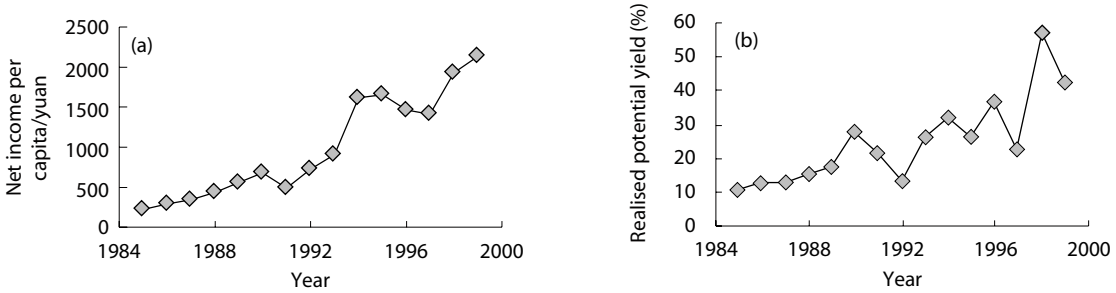

Figure 11. Changes in socioeconomic indicators in in the Zhi Fanggou catchment.

Fanggou catchment were reduced greatly after the introduction of the integrated control measures (Table 5). This was partly accounted for by a decrease in annual rainfall, but the figures in Table 5 have been adjusted to take account of this. Table 5 shows a gradual decrease in soil loss.

Industry and off-farm income

Total per capita income from industry and off-farm work in the catchment increased year by year from 1985 to 1999 (Fig. 12b). Agriculture in the region was seriously affected by the climate (especially drought). Sustainable economic development in the catchment should emphasise industry and off-farm work.

Catchment health assessment

The ultimate objective of watershed management is watershed 'health'. Diagnosing the health of a watershed is an important aspect of watershed management, which is linked to assessments of environmental quality. A healthy watershed system will have a relatively stable structure in which ecosystems function well and in which sustainable development can occur.

In order to appreciate the benefits of integrated control measures and establish corresponding ecosystem rehabilitation processes, it is necessary to assess watershed health. We used AHP to quantitatively assess the Zhi Fanggou catchment.

Identifying and selecting indicators

Health indicators should reflect the factors that influence sustainable development and should reveal the tendency of the ecosystem to change. Identifying and selecting indicators should therefore be objective and quantitative. In selecting indicators, we

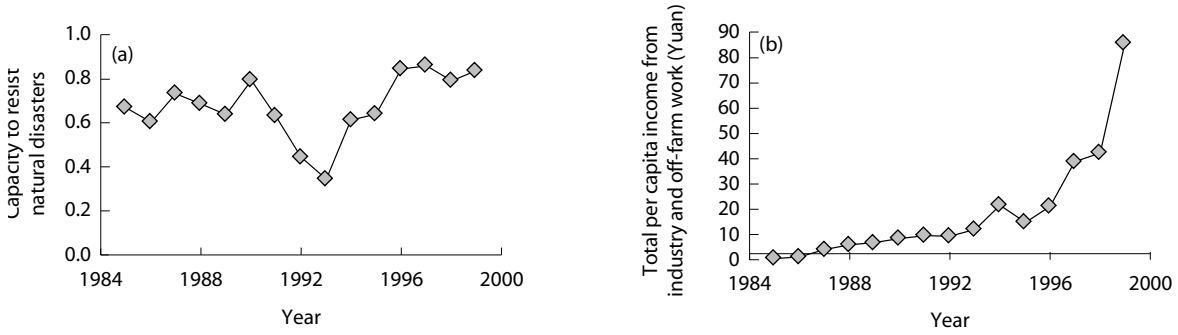

Figure 12. Dynamics of system function indicators.

Table 5. Efficiency of integrated control measures in decreasing soil loss.

Year	Soil erosion (t/km^2/year)		Reduction in soil loss (%)	Extent of control (%)[b]
	No control[a]	Control		
1991	13215.6	7168.0	45.8	44.0
1992	2393.3	1224.5	48.8	50.8
1993	–	0	–	54.0
1994	4160.7	1949.5	53.2	55.5
1995	5515.5	2624.2	52.4	57.7
1996	13198.4	5807.3	56.0	57.8
1997	23.1	6.0	74.0	60.1
1998	2621.7	1056.4	59.7	70.1
1999	5244.2	2087.2	60.2	72.4

[a] 'No control' measurements were obtained from the empirical formula
[b] The extent of the effort to control the destruction of catchment ecosystems and to restore natural ecosystems

considered the hilly and gullied nature of the Loess Plateau; the requirement for environmental rehabilitation; and the need for indicators to be objective, scientific, universal, independent and flexible. Figure 13 shows the indicators we selected.

Figure 14 shows how these indicators were used to assess health in the Zhi Fanggou catchment.

Weighting the indicators

We assumed that different factors were important at different stages of ecosystem rehabilitation. Table 6 shows the assessment matrix for weighting indexes in different periods of ecosystem rehabilitation. The matrix was graded by experimental experts in soil and water conservation according to various development stages (Lu Zongfan et al. 1990, 1997). Tests using the maximum eigenvalue and eigenvector of the matrix demonstrated that the matrix was consistent. The weight of indicators was calculated from the matrix.

Calculating a health index

In order to calculate the health index, the indicator unit must be uniform. The minimum and maximum values of the indicators (indicator criteria) were defined according to the research results on soil conservation and environmental rehabilitation, the historical and current values of the indicators in the catchment and national regional development policy. Table 7 shows the results.

The dimensionless values of the indicators were obtained from the marks of the unifying table. The health index (Table 8 and Fig. 14) was calculated as follows:

$$I = \Sigma W_{a1} \times V_{a1}$$

where I is the health index; W_{a1} is the weight of the indicator, *a1*, to the area of the catchment; and V_{a1} is the dimensionless value of the indicator, *a1*. The terms *a1*, *a2*,….*a10* identify the 10 indicators mentioned above.

Conclusions

Table 9 shows the health classification of the Zhi Fanggou catchment ecosystem. Before integrated control measures were introduced in the Zhi Fanggou catchment, catchment health was poor and there was a vicious circle in which increasing economic development led to reduced

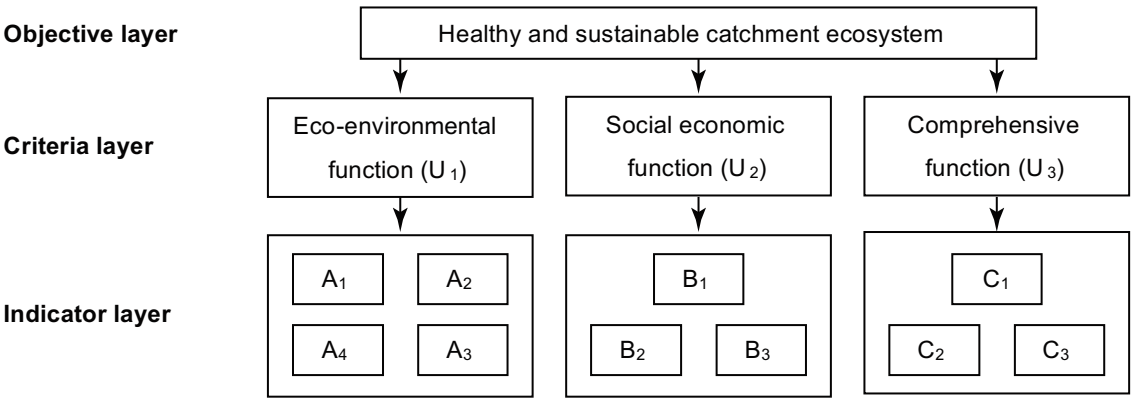

Figure 13. Structure of the analytic hierarchy model in assessing the ecosystem health of the Zhi Fanggou catchment. The indicators for environmental function include vegetation coverage (A1), ratio of primary cropland to targeted cropland area (A2), soil antiscourability (A3) and soil organic matter content (A4). The indicators for socioeconomic function include the ratio of outputs to inputs in agriculture (B1), the actual yield as a proportion of potential yield (B2) and the net income per capita (B3). The indicators for comprehensive function were the capacity to resist natural disasters (system resilience) (C1), the efficiency of integrated control measures in decreasing soil loss (C2) and the total income from industry and off-farm work(C3).

environmental quality (Zhao Chongyun 1996). After integrated control measures were introduced, the catchment ecosystem became relatively stable, with appropriate development.

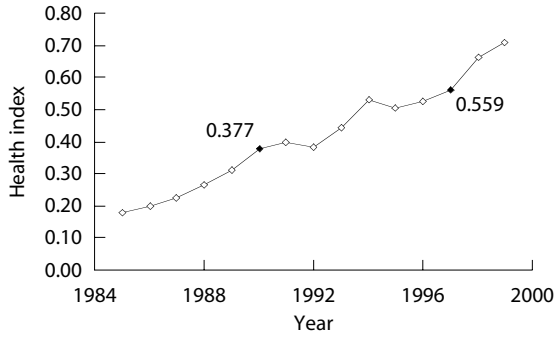

Figure 14. Changes in the health index of the Zhi Fanggou catchment ecosystem, 1984–2000.

Our research demonstrated that there have been three stages of ecosystem restoration in the Zhi Fanggou catchment: initial restoration (1985–88), with a health index of 0.25; stable improvement (1989–93), with a health index of 0.35–0.45; and a good development period (1994 on) with a health index of 0.45–0.70. The results provide scientific support for the theory that soil and water conservation measures can be gradually implemented in the Loess Plateau region. They also indicate that degraded ecosystems on the Loess Plateau can be restored with 20 years of integrated control measures.

Table 6. Assessment matrix for weighting indexes in different periods of ecosystem rehabilitation (see Figure 13 for an explanation of indexes).

	A1	A2	A3	A4	B1	B2	B3	C1	C2	C3
Initial restoration	0.0233	0.1129	0.0157	0.0314	0.0684	0.2762	0.2986	0.0186	0.0764	0.0783
Stable improvement	0.0349	0.1313	0.0338	0.0676	0.0555	0.2033	0.2086	0.0319	0.1185	0.1145
Good development	0.0510	0.1545	0.0437	0.0874	0.0513	0.1820	0.1723	0.0388	0.1119	0.1072

Table 7. Combined indicators.

		Value						
No.	Indicator[a]	1	2	3	4	5	6	7
A1	Vegetation coverage (%)	<5	10	15	20	35	50	>70
A2	Ratio of primary cropland to targeted cropland area (%)	<10	20	30	50	55	60	>75
A3	Soil antiscourability (min/L/g)[b]	<0.30	0.40	0.50	0.60	0.80	1.0	>2.0
A4	OMC (%)	<0.4	0.5	0.6	0.7	0.8	0.8	>1
B1	Output–input ratio in agriculture	11	10	9	8	7	6	5
B2	Yield as a proportion of potential yield (%)	<5	10	15	20	35	50	>75
B3	Net income per capita (yuan)	<100	200	500	1000	1500	2000	>3000
C1	System resilience (%)[c]	<5	10	15	20	35	50	>75
C2	Efficiency of integrated control measures in reducing soil loss (%)	<5	10	15	20	35	50	>75
C3	Total income from industry and off-farm work ($\times 10^3$ yuan)	<1	2	5	15	30	60	>140

OMC = organic matter content
[a] See figure 13 for an explanation of terms
[b] Volume of water (product of volume and time) needed to scour 1 g of dry soil
[c] The capacity to resist natural disasters

Table 8. Health indexes for the Zhi Fanggou catchment ecosystem, 1985–99.

Year	Health index
1985	0.178
1986	0.197
1987	0.224
1988	0.264
1989	0.310
1990	0.377
1991	0.400
1992	0.380
1993	0.441
1994	0.531
1995	0.503
1996	0.526
1997	0.559
1998	0.664
1999	0.707

Note: See text for explanation of how the index is calculated.

Table 9. Health classification of the Zhi Fanggou catchment ecosystem.

Item	Vicious circle	Frail	Relatively stable	Good	Well developed
Health index	<0.15	0.15–0.35	0.35–0.55	0.55–0.70	>0.70

References

Bissonnais, Y. Le and Arrouays, D. 1997. Aggregate stability and assessment of soil crustability and erodability: Application to humic loamy soils with various organic carbon contents. European Journal of Soil Science, 48, 39–48.

Brunori, F., Penzo, M.C. and Torri, Firenze, D. 1989. Soil shear strength: its measurement and soil detachability. Catena.

Connolly, R.D., Freebairn, D.M. and Bell, M.J. 1998. Change in soil infiltration associated with leys in south-eastern Queensland. Australian Journal of Soil and Research, 36, 1057–72.

Guerra, A. 1994. The effect of organic matter content on soil erosion in simulated rainfall experiments in W. Sussex, UK. Soil Use and Management, 10, 60–64.

Jiang Dingsheng and Fan Xingke. 1990. Study on the benefit and optimal disposition for measures of soil and water conservation in hilly and gully region in Loess Plateau. Studies on ecological agriculture with soil and water conservation in Loess Hilly Gully Region. Tianze Press, China, 87–100.

Le Bissonnais, Y. 1996. Aggregate stability and assessment of soil crustability and erodability: Theory and methodology. European Journal of Soil Science, 47, 425–437.

Le Bissonnais, Y. 1997. Aggregate stability and assessment of soil crustability and erodability: Application to humic loam soils with various organic carbon contents. European Journal of Soil Science, 48, 39–48.

Liu Guobin. 1997. Soil antiscourability research and its perspectives in Loess Plateau. Research on Soil and Water Conservation, 5, 91–101 (in Chinese).

Liu Guobin. 1999. Soil conservation and sustainable agriculture on the Loess Plateau: challenges and prospective. AMBIO, Sweden, 28(8), 663–668.

Liu Guobin and Zheng Fengli. 1998. Study on the system stability of soil and water conservational eco-agriculture in Zhifanggou small watershed in Ansai. Progress in Geography, 17(supplement), 48–54 (in Chinese).

Liu Guobin, Hu Chunsheng and Joe Walker (eds). 1999. A guide to environmental indicators. CSIRO Land and Water, Canberra (in Chinese).

Lu Zongfan, Liang Yiming and Wang Jijun. 1990. An approach to the division of period for ecological agriculture with soil and water conservation. In: Studies on ecological agriculture with soil and water conservation in Loess Hilly Gully Region. Tianze Press, 28–35.

Lu Zongfan, Liang Yimin and Liu Guobin (eds). 1997. Eco-agriculture in the Loess Plateau of China. Shaanxi Sci-tech Press, Shaanxi, China, 205–206 (in Chinese).

Radford, B.J., Gibson, G., Mielsen, T.G.H., Butler, D.G., Smith, G.D. and Orange, D.O. 1992. Fallowing practices, soil water storage, plant-available soil nitrogen accumulation and wheat performance in south west Queensland. Soil and Tillage Research, 22, 73–93.

Sullivan, L.A. 1990. Soil organic matter, air encapsulation and water-stable aggregation. Journal of Soil Science, 41, 529–534.

Walker, J. and Reuter, D.J. 1996. Indicators of Catchment Health: a technical perspective. CSIRO Publishing, Collingwood, Australia.

Zhao Chongyun, Zhang Jianming and Gu Hengyue (eds). 1996. Assessing method and model for the ecological benefit of integrated control to small watershed. Water Conservancy Press, Beijing, China, 135–140 (in Chinese).

Zhao Huancheng, Xu Shubuo and He Jingsheng (eds). 1986. Analytic Hierarchy Process—a new decision method for advice. Science Press, Beijing, China. (in Chinese)

Zhu Xianmo. 1989. Soil and agriculture in the Loess Plateau. Chinese Agricultural Press, 216–218.

11 Regional Prediction of Soil Profile Acidity and Alkalinity

Richard H. Merry,* Leonie R. Spouncer,* Rob W. Fitzpatrick,* Phil J. Davies* and David A. Bruce†

Abstract

The Mount Lofty Ranges lie northeast of Adelaide, South Australia. Soils in the region are being degraded through soil acidification and alkalisation, and the development of both potential and actual acid sulfate soils. These processes affect agricultural production and water quality. Soil testing and survey work in the area have shown significant acidification of acid sulfate and salt-affected soils in subcatchments. The spatial extent of these degraded soils has not been examined previously.

We have developed a method to determine the spatial distribution of soils with differing acidity and alkalinity (pH profiles) over an 80 km^2 region. The method involves using data from point, toposequence and subcatchment scales to develop simple mechanistic models and a geographic information system. We predicted soil profile pH classes for the 80 km^2 region and used these to plan the management of degraded soils. The data were also used as a soil degradation indicator for assessment of landscape quality at catchment and regional scale.

在阿德莱德东北方的劳伏特山区，土地的酸化和碱化以及硫酸性土壤的出现，影响水质和农作物产量。土壤分析与调查表明，该地区次级流域硫酸盐土壤和盐化土壤的酸化作用明显，不过，这些退化土壤的规模还未测定。我们采用一种方法来测量大范围（80 平方公里）土地上不同酸碱度（pH 值）土壤的空间分布。该方法采用收集到的点、坡面和次级流域不同尺度的数据，生成简单的机械模型和一个地理信息系统，预测了 80 平方公里内土壤的 pH 值等级，并以此制定退化土地的治理方案。该数据也作为土壤退化指标，用在流域和区域规模的景观质量评价工作中。

* CSIRO Land and Water, PMB 2, Glen Osmond, SA 5064, Australia. Email: richard.merry@csiro.au

† University of South Australia, Adelaide, SA 5001, Australia.

Merry, R.H., Spouncer, L.R., Fitzpatrick, R.W., Davies, P.J. and Bruce, D.A. 2002. Regional prediction of soil profile acidity and alkalinity. In: McVicar, T.R., Li Rui, Walker, J., Fitzpatrick, R.W. and Liu Changming (eds), *Regional Water and Soil Assessment for Managing Sustainable Agriculture in China and Australia*, ACIAR Monograph No. 84, 155–164.

THE UNDULATING, hilly landscape of the Mount Lofty Ranges, northeast of Adelaide, South Australia, supports agriculture ranging from extensive grazing to viticulture. A variety of soil and groundwater processes contribute to the development of soil acidity and alkalinity in the region. This soil degradation often occurs in specific parts of the landscape and is influenced by agricultural practices. For example, grazing and cropping of middle and upper slopes can lead to acidification in the upper parts of the soil profile. Alkaline, saline or sulfidic groundwaters can affect soil alkalinity and cause potential and actual acid-sulfate soils on lower slopes and valley floors. The chemistry and mineralogy of parent materials, especially Quaternary valley sediments and Cambrian metasediments containing pyrite, can also potentially influence soil acidity and alkalinity.

The objective of this study was to use mechanistic models and geographic information systems (GIS) to understand and predict spatially the processes that control soil profile pH in this landscape at point, toposequence, catchment and regional scales (80 km^2). The main aim was to better identify and manage those parts of the landscape where water quality may be degraded or where soil acidification could be remediated by liming.

Materials and Methods

The study area

Initial work was based on the soil sampling and fieldwork of Fritsch and Fitzpatrick (1994). We took field samples, principally in the Herrmann subcatchment (139° 01' E; 34° 53' S; area about 2 km^2) near Mount Torrens, about 50 km northeast of Adelaide. Sampling was also extended into the surrounding 80 km^2. We used the Herrmann subcatchment, with its detailed toposequences, to trial models designed to predict soil profile acidity and alkalinity over the broader region. Figure 1 of Chapter 21 shows the location of the areas concerned. The Overview provides some background information about the region; Figures 2 and 5 of the Overview show its location.

Landscape, soils and agriculture

Much of the study area comprises undulating low hills with altitudes of 400–500 m and local relief about 30–50 m (Fig. 1). The climate of the area is Mediterranean, with a pronounced maximum rainfall in winter (May to August) and hot, dry summers (December to February). Annual rainfall is topographically controlled; it decreases from southwest to northeast across the region, from about 700 mm to 550 mm. Stream channels have a normal tributary pattern and mostly erode soils, bedrock or the alluvial soils and sediments of valley floors, sometimes to depths of 2–3 m. The Herrmann subcatchment drains to the east into the Murray River system. The larger 80 km^2 area contains a drainage divide with about one-third draining to the west to the Torrens River system and the remainder to the east, to the Murray River system. Subcatchments vary in size from 2 to 5 km^2.

Figure 1. Undulating, hilly landscape of the study area, with eroding streamlines, perched wetlands (centre), sheep camps among groups of trees and agriculture that is mainly grazing and cropping on mid-slopes.

Soils of the middle and upper slopes in the study area mainly have sandy and loamy A horizons overlying clayey B horizons (Palexeralfs). Lower slopes, terraces and valley floors frequently have sodic (Natrixeralfs) and alluvial soils (Entisols), and wet soils (Aquents) in groundwater discharge areas with perched wetlands. Soils of the groundwater discharge areas are frequently saline and sulfidic — these are potential acid sulfate soils (Fitzpatrick et al. 1996). After oxidation of the sulfidic materials,

such soils become acid sulfate soils that contribute to degraded water quality through leakage of salts and acid weathering products. The clayey B horizons of sodic soils that have developed in areas where saline groundwater discharge has occurred often disperse and erode.

Land use in this area is predominantly sheep or cattle grazing on pasture. Increasingly, land is being used for more intensive purposes such as viticulture and cereal cropping. Commercial pine plantations have been established in areas of the Torrens River catchment, which is an important source of urban water supply.

Field soil sampling and mapping

Soil samples were obtained for three purposes:

- to establish boundaries for conventional soil mapping, using initial profile samples from toposequences within the Herrmann subcatchment and free sampling, largely as reported by Fritsch and Fitzpatrick (1994);
- to better characterise pH profiles that occur at specific points in the landscape that are subject to known acidification or alkalisation processes, using samples principally obtained from the Herrmann catchment; and
- to provide verification data for the predicted soil profile pH classes across the broader, 80 km^2 area, mainly using archived samples from previous field projects of CSIRO Land and Water (formerly the Division of Soils).

Using these samples, we produced sets of nested study areas that included georeferenced soil pH values at points and in toposequences. Georeferencing was mainly achieved using a global positioning system with positional accuracy of about 5 m. However, the sites from which the archived soil samples were obtained had been located on 1:50,000 topographic maps with cadastral overlay positioning; thus, they could only be accurate to within 50 to 150 m.

Soil pH analysis and profile classes

Soil pH was measured by standard procedures (Rayment and Higginson 1992), using a 1:5 soil to water suspension (pH_w).

As a basis for prediction across the broader region, nine soil acidity and alkalinity profile classes were established initially. The classes were then simplified to five categories, matching the profile classes known to occur in the catchment area. Solum (A and B horizons) depths of about 1 m were considered, or less where profiles were shallow. The classes were constructed along the lines of Northcote's 'soil reaction trends' (Northcote 1979), with modifications to separate potential and actual acid sulfate soils. The simplification was based on the profile classes found in topographic sequences or related to a specific topographic position within the Herrmann subcatchment.

In practice, some similar profiles proved to be difficult to discriminate and were therefore combined. The final classification, described below, clearly indicates soils in need of remediation or protection from degradation. However, the neutral, moderately acidic and moderately alkaline classes are still difficult to distinguish because of poor pH buffering and their susceptibility to change as a result of agricultural practices. There are other classes in the 80 km^2 area, but they were not included because the basis for prediction was restricted to the most common classes in the region.

The five profile pH classes used for broad-scale prediction are listed below.

- *Class a.* Alkaline ($pH_w > 7.5$) or neutral (pH_w 6.5–7.5) throughout and associated with lower slopes and valley floors. This class contains both potential and actual acid sulfate soils that are associated with waterlogged or groundwater discharge areas and may be prone to erosion if vegetation is lost. If denuded, these soils may develop high sodicity, salinity and bulk density.

- *Class b*. Moderately acidic surface (pH_w < 6.5), neutral or alkaline in the subsoil. This class includes soils affected by subsoil sodicity and alkalinity, which are are prone to clay dispersion, salinity and gully erosion.
- *Class c*. Neutral (pH_w 6.5–7.5) throughout. These soils were commonly shallower than 1 m and little affected by degradation or agricultural development.
- *Class d*. Moderately acidic (pH_w < 6.5) throughout. These soils were typically Palexeralfs of middle and upper slopes; they may be more acidic in the upper 10–20 cm due to agriculture and may be underlain by very acidic saprolite.
- *Class e*. Very acidic (pH_w < about 5) throughout most of the profile. This class is similar to Class d, but is considerably more acidic and likely to limit agricultural production through aluminium toxicity and nutrient deficiency. Liming of these soils should be considered a priority.

Figure 2 shows some typical pH profiles from the Herrmann subcatchment.

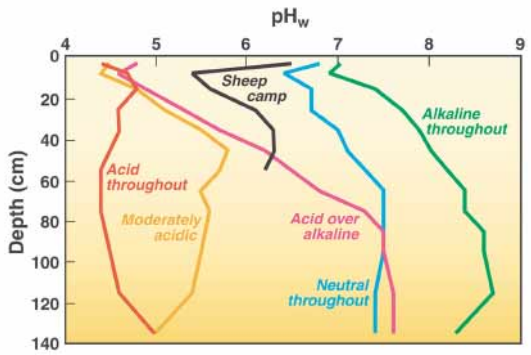

Figure 2. pH_w profile types found in the Herrmann catchment.

Spatial relationships

We used point data for profiles, hydrology and elevation to develop toposequences that were spatially matched with conventional soil maps for both a detailed (0.2 km^2) key area within the northeastern part of the Herrmann subcatchment and the subcatchment itself. The toposequence shown in Figure 3 illustrates the topographic relationships between soil pH profile and position in the landscape — the upper slope positions have acidic soil profiles and the lower slopes and valley floors have neutral and alkaline soil profiles. The pedological processes known to be operating in the area are long-term weathering and agricultural acidification on the middle and upper slopes; and salinity, alkalisation, sodification and development of saline and acid sulfate soils on the lower slopes (Fritsch and Fitzpatrick 1994; Fitzpatrick et al. 1996). Conventional mapping units were allocated to the appropriate pH class using both point and toposequence information, as shown in Figure 4 for the Herrmann subcatchment. These 'nested' maps and toposequences were then used to develop relationships as a basis for GIS prediction of soil pH profile over the 80 km^2.

The principal toposequence types were constructed from soil data at point sites; hydrology and elevation data; and structural analysis (Fritsch and Fitzpatrick 1994). Using the point data, linear weighted index models were derived for each of the different scales or areas of interest — subcatchment key area, subcatchment or region — depending on the availability of GIS data, as outlined below. We developed smaller scale, linear weighted models using data for the detailed parts of the catchment that were not available over the whole region.

The data used to develop the models and maps at the different scales are listed below (see also Fitzpatrick et al. 1999 for further detail).

- *Key area scale (0.2 km^2)*. Data were vegetation class maps developed from air photos and forward-looking infrared (FLIR) remote sensing, digital elevation models (DEMs) and soil mapping (not shown, see Fitzpatrick et al. 1999 and Chapter 21, this volume).

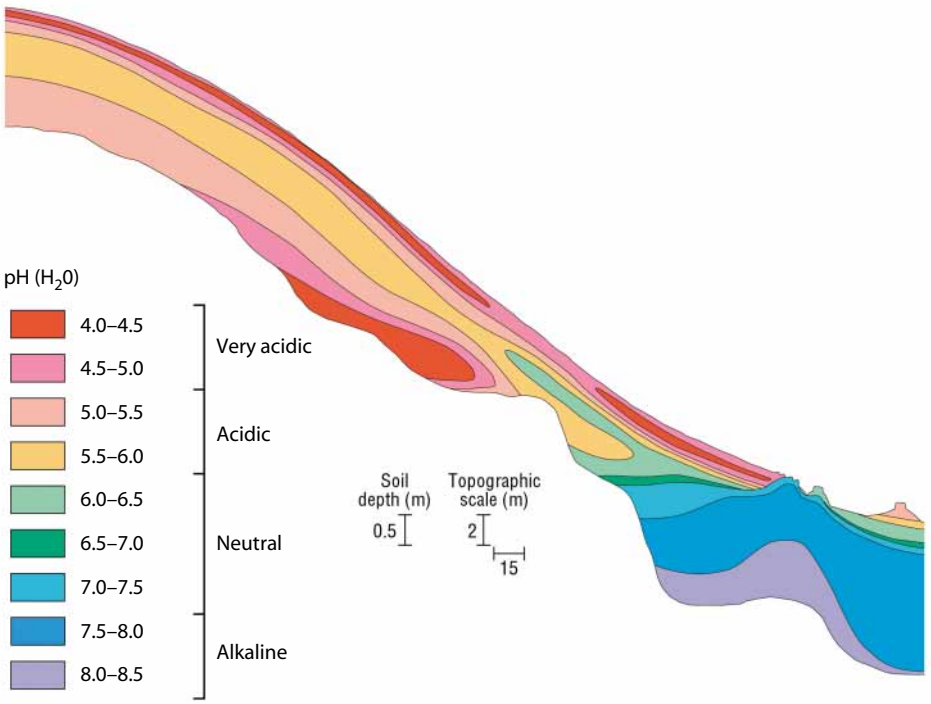

Figure 3. Acidity and alkalinity of soil layers along a typical toposequence from the Herrmann catchment.

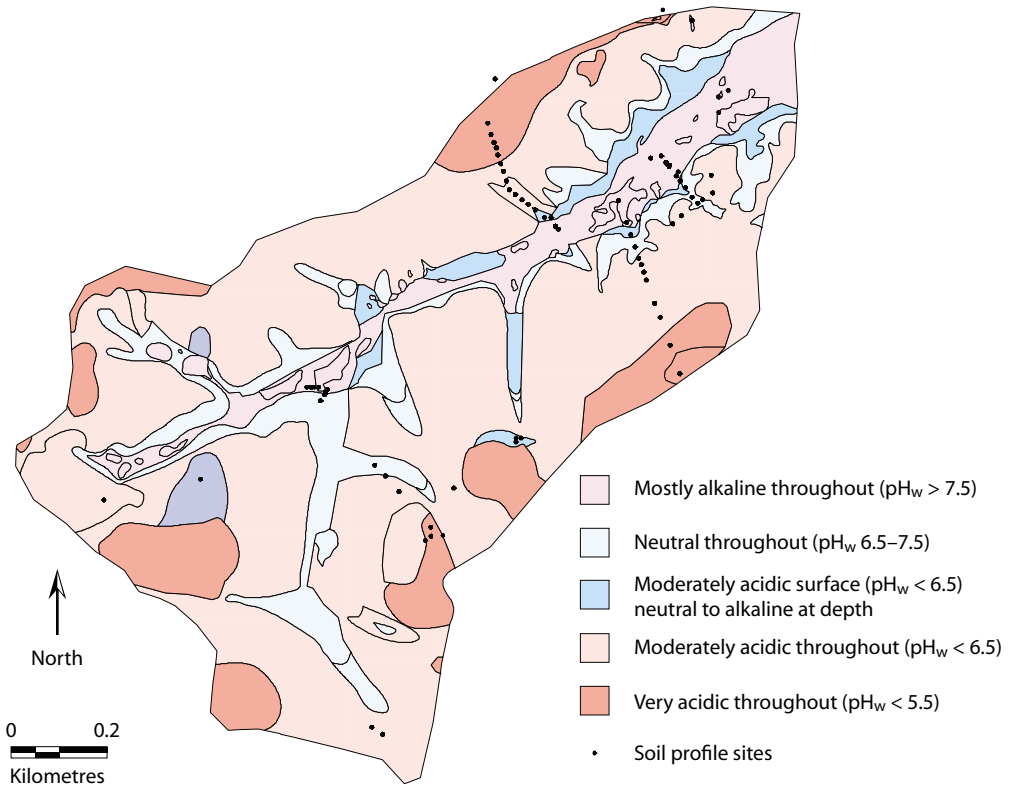

Figure 4. Conventional soil map of the Herrmann catchment (2 km^2) with soil units allocated to soil profile pH_w classes. Some point sample and toposequence locations are marked.

- *Subcatchment scale (2 km^2).* Two maps of soil pH class were developed at subcatchment scale (Figs 4 and 5). The map shown in Figure 4 was developed from conventional soil map boundaries, using toposequence and point pH profile data. Because the most reliable pH class data were obtained from subcatchment scale or below, the linear weight indexing used to model at that scale (Fig. 5) was adjusted for best fit with the conventional map (Fig. 4). The model was developed using a topographic index and land unit mapping of soil acidity classes at the 1:50,000 scale (compiled by D.J. Maschmedt of Primary Industries and Resources, South Australia). The topographic index was derived using the procedure of Hutchinson and Dowling (1992). The index can be represented as $\ln(A_s/\tan\beta)$, where A_s is the specific catchment area and $\tan\beta$ the local slope angle evaluated on a cell-by-cell basis from the DEM. The land unit mapping included both soil type and geology of the parent material — data that exist for the entire agricultural area of South Australia.

- *Region scale (80 km^2).* The map of the modelled best estimate of soil profile acidity and alkalinity for the larger region (Fig. 6) was generated by extrapolation of the model that produced Figure 5, using the same input data.

Verification of prediction of soil acidity/alkalinity profiles

To verify the models, we used two different approaches. First, because the same models were used to generate maps at the subcatchment and regional scales, we could verify the models to some extent by comparing the distribution of profile classes at the subcatchment scale (Fig. 5) with the conventional soil map (Fig. 4). Table 1 shows the results of this comparison.

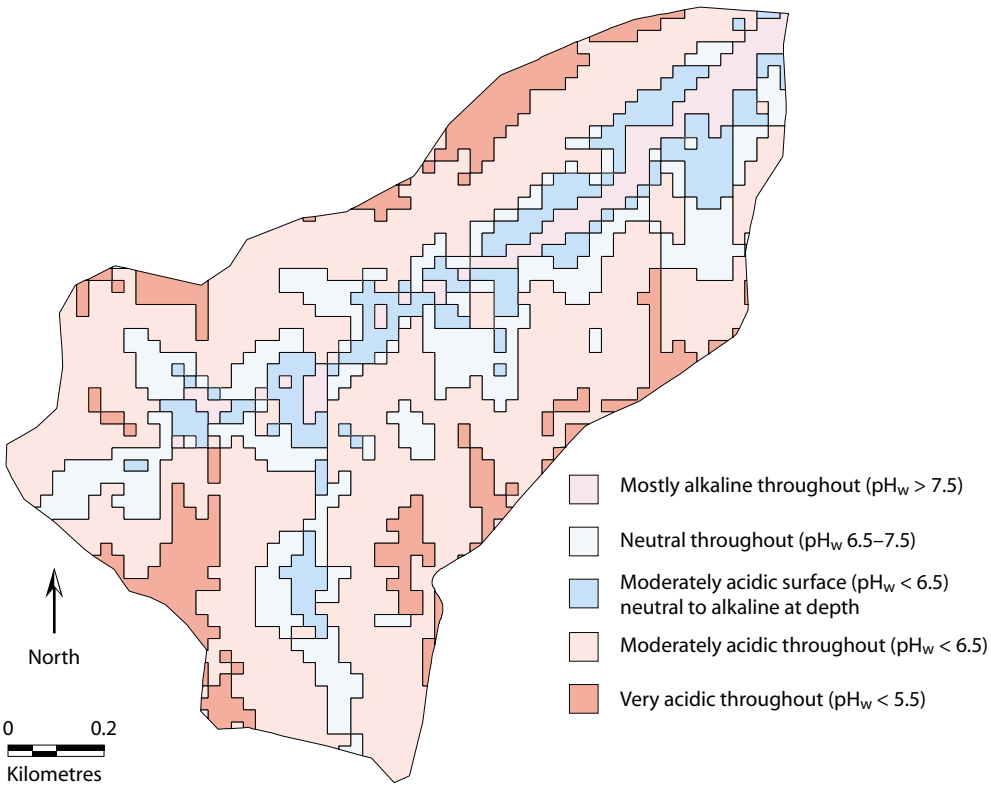

Figure 5. Modelled distribution of soil pH_w profile classes in the Herrmann (2 km^2) catchment. The modelling relied heavily on the GIS linear weighting index. Compare the spatial structure of Figure 4 and Figure 5.

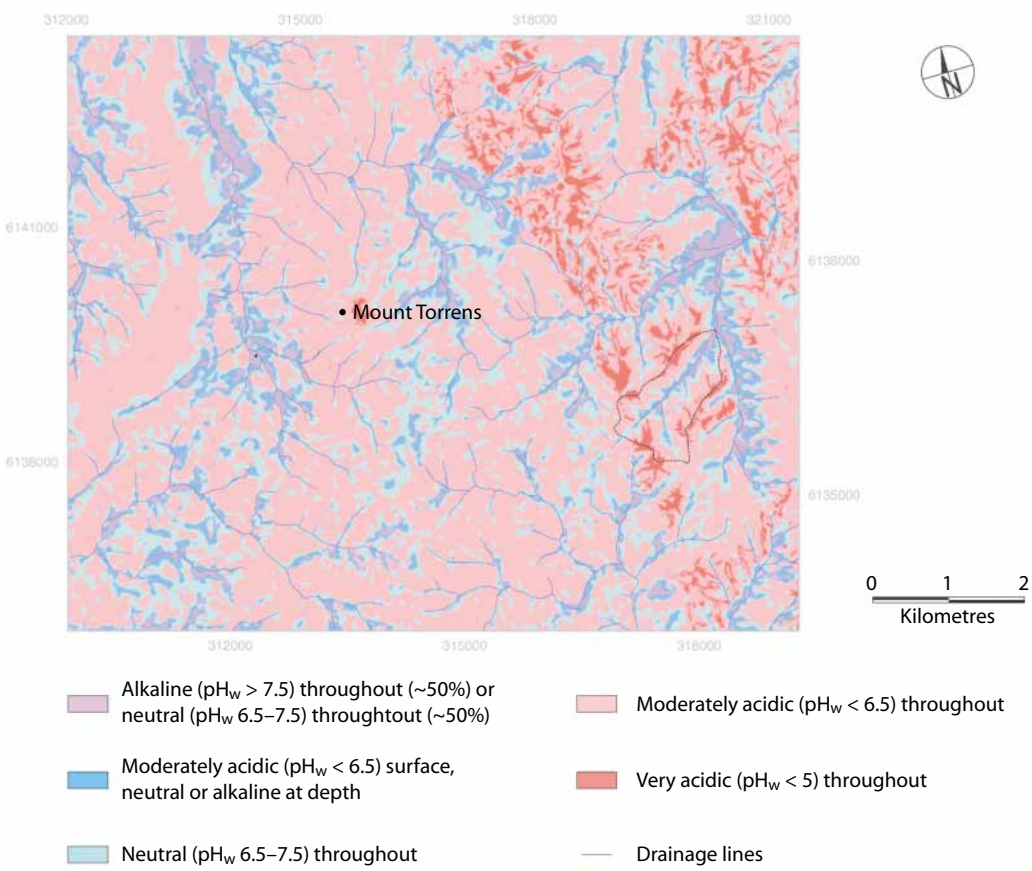

Figure 6. Best estimate of distribution of soil profile acidity and alkalinity classes for the 80 km^2 study region.

In the second approach, we collated archived data for 35 soil profiles with data for five profiles sampled as part of this project. Because the archived data were from sites georeferenced from a 1:50,000 scale topographic map, the positional accuracy is likely to be lower than the data collected for this project. Therefore, we drew a circle of scaled radius 100 m on the modelled regional map (Fig. 6), centred on the location obtained from the topographic map, and compared the classes that we predicted would occur within that circle with the profile used for verification.

Results and Discussion

Soil pH profiles and processes

Soils of the slopes and crests usually showed strong acidification in their A horizons (e.g. Fig. 2). This acidification is due to normal agricultural processes such as nitrate leaching of legume-fixed or fertiliser nitrogen, and removal of alkaline products such as hay, fodder or cereal grain. In samples taken to verify predictions in areas with sheep camps, we found that profiles were more alkaline than adjacent, moderately acidic soil profiles. This effect occurs because sheep camps, which are frequently located on or near hill crests, are the source of substantial alkaline input into the soil and thus result in near-neutral surface soils overlying acidic subsoils (Fig. 2). However, we did not include the location of sheep camps in our predictions because camps are not always related to particular features of the landscape or vegetation. Although terrain, remote sensing and vegetation analysis can identify sheep camps, such an exercise is probably not warranted because the aggregate area of the camps is quite small and they can be managed at a farm level.

The deeper subsoils in the middle and upper slopes on some parent materials were also highly acidified between 1 and 2 m and into the saprolite, illustrated in Figures 2 and 3. This is believed to result from soil formation on parent materials that contain significant sulfide minerals, either in bands or dispersed through the regolith. Oxidation of these sulfides has resulted in acidic profiles that are strongly weathered. These parent materials have been mapped as the Talisker Calc-Siltstone (containing the Nairne Pyrite Member), the Tapanappa and other unnamed formations of Cambrian age that occur in a broad band in the eastern Mount Lofty Ranges and on Kangaroo Island (Belperio et al. 1998). This pyrite is also the likely source of most of the sulfur of the potential and actual acid sulfate soils found associated with perched and relict wetlands in the study area (Fitzpatrick et al. 1996).

Table 1. Comparison of areas of modelled soil pH profile classes (Fig. 5) (a to e) for the subcatchment (2 km^2) scale with map classes developed from conventional soil mapping (Fig. 4).

Conventional soil mapping	Modelled soil classes	Area (m^2)	Area (%)[a]
Class a (alkaline throughout)	a	52,519	43
	b	41,361	
	c	23,151	
	d	5,045	
	e	18	
Class b (acidic surface, neutral to alkaline at depth)	a	2,866	
	b	22,404	36
	c	14,795	
	d	17,816	
	e	4,670	
Class c (neutral throughout)	a	5,502	
	b	41,205	
	c	58,949	36
	d	59,720	
	e	128	
Class d (moderately acidic throughout)	a	1,840	
	b	33,780	
	c	146,113	
	d	554,168	70
	e	52,512	
Class e (very acidic throughout)	c	1,162	
	d	84,770	
	e	90,127	51

[a] Indicates the percentage of the area allocated to a profile class by the model that coincides with the same class allocated from conventional soil mapping

On the lower slopes, soils were frequently alkaline (Fig. 3). The principal cause of alkalinity is the accumulation of sodium salts that results from concentration by evapotranspiration, and the subsequent development of sodic clays. Magnesic calcites are sometimes observed in these valley floor soils; they develop from evaporative concentration from groundwaters, sometimes in wetlands (Fitzpatrick and Merry 1999).

Prediction of pH profile

The GIS-based models were able to predict soil pH profiles at scales useful for land management. Verification indicated that the predictions were acceptable, especially where soils were acidic or alkaline throughout. Although saline, sulfidic soils were contained within Class a soils, their distribution was influenced by proximity to the pyritic parent materials mentioned above. Therefore, it is important to use geological data in the generation of the model at this scale. Soils that are acidic throughout (Class e) and generally in need of lime treatment are clearly associated with the older, more stable and weathered parts of the landscape. They were efficiently predicted using the topographic index and existing land unit maps containing geological information. Similarly, these predictors successfully identified alkaline and sodic soils of lower slopes and valley floors.

For the 80 km^2 region, the correct class or a neighbouring class was usually predicted. The inclusion of the DEM-based topographic index at this scale allowed us to link pH profile class with topographic position more reliably than by using conventional 1:50,000 acidity-class mapping.

Verification of models

Two approaches were used to verify the models. The first compared the areas of each soil pH profile class provided by the modelled data with the conventionally mapped areas of the Herrmann subcatchment (Table 1). For each conventionally mapped class other than Class c, the soil class predicted by the model was the same as the most common profile type in the mapping unit. For each conventionally mapped class, the next most common class (second in area, apart from Class c) predicted by modelling was always the class most similar to the predominant class. The modelled data were much more closely related to the subtleties of topography than was possible using conventional mapping, and real boundaries are usually continuums rather than sharp breaks. Therefore, the modelled spatial distributions of profile classes are considered more reliable than conventional soil mapping and point sampling.

The second approach of verification involved the comparison of soil profile data from 40 sites distributed across the larger region. A difficulty arose because the historical material used was georeferenced from 1:50,000 topographic maps. Soil pH profile classes were predicted for an area of 100 m radius, centred on the verification site as originally located from a topographic map. Of the 40 sites, 20 were the same class as the most common profile classes predicted for the 100 m radius circle; 11 had the same verification profile as the modelled subdominant class; 5 were in the adjacent class; and 4 were in another minor class. For all verification sites where the locations were approximate, the model always predicted the same pH class within the 100 m radius circle. These data also suggested that the mostly 'alkaline throughout' soil class (Class a) would probably not exist on parent rocks older than Cambrian in the western part of the region. This should be further investigated; if it is found to be true, the predictive model should be modified.

Conclusions

Where toposequence trends in soil profile pH were evident, GIS was able to predict soil profile pH types over relatively large regions with good effectiveness and to highlight those areas requiring specific management. Verification of the predictions indicated that the methodology was useful in identifying very acidic profiles requiring liming programs, or alkaline and sodic profiles requiring gypsum application and drainage management. Related work predicting the location of waterlogged and groundwater discharge areas (Davies et al. 2000) is also important as it helps to identify soils affected by alkaline and saline groundwaters, and potential acid sulfate soils that develop in wetlands. The spatial distributions of these acidic, alkaline and wetland soils are clearly related to topography and the geology of parent materials.

Soils with profile pH values in the moderately acidic, neutral or moderately alkaline range were less well discriminated. The pH values of the upper part of these soil profiles are more likely to be affected by agricultural management because they are usually less well buffered against pH change; they are also less likely to need lime or gypsum application.

Although the process of transfer of alkalinity by stock is well known, we were not aware of the number of sheep camps in this area and the extent to which they were contributing to soil alkalisation. The sheep camps require farm-level management to preserve soil fertility and conserve remnant vegetation.

The approach to prediction of the properties of soils in landscapes described here is expected to add value to existing land-unit mapping, improve regional planning of management of soil degradation processes and be a useful tool in agricultural extension. Strategic liming of selected parts of catchments has been shown to be effective in their management (see, for example, Adams and Evans 1989) with potential to improve plant and animal productivity and stream water quality.

Acknowledgments

The funding support of ACIAR and the Mount Lofty Ranges Pilot Implementation Project of the Australian National Land and Water Resources Audit is gratefully acknowledged. The late Mr Leon Herrmann and the Tungkillo Landcare Group provide ongoing access to sites and other support. Dr E. Fritsch of ORSTOM contributed both data and mapping from parts of the Herrmann subcatchment that were fundamental to the generation of ideas that led to this work. Mr David Maschmedt of PIRSA assisted through provision of land unit maps.

References

Adams, W.A. and Evans, G.M. 1989. Effects of lime applications to parts of an upland catchment on soil properties and the chemistry of drainage waters. Journal of Soil Science, 40, 585–597.

Belperio, A.P., Preiss, W.V., Fairclough, M.C., Gatehouse, C.G., Gum, J., Hough, J. and Burtt, A. 1998. Tectonic and metallogenic framework of the Cambrian Stansbury Basin—Kanmantoo Trough, South Australia. AGSO Journal of Australian Geology and Geophysics, 17, 183–200.

Davies P.J., Fitzpatrick R.W., Bruce D.A., Spouncer, L.R. and Merry, R.H. 2000. Use of spatial analysis techniques to assess potential waterlogging in soil landscapes. In: Adams, J.A. and Metherell, A.K., eds, Soil 2000: new horizons for a new century. Australian and New Zealand Second Joint Soils Conference. Volume 3: Poster Papers. 3–8 December 2000, Lincoln University. New Zealand Society of Soil Science.

Fitzpatrick, R.W., Bruce, D.A., Davies, P.J., Spouncer, L.R., Merry, R.H., Fritsch, E. and Maschmedt, D.J. 1999. Soil landscape quality assessment at catchment and regional scale. (Mount Lofty Ranges Pilot Implementation Project, National Land and Water Resources Audit) CSIRO Land and Water Technical Report 28/99, July 1999, 69 pp. (Also www.clw.csiro.au/publications/technical99/tr28-99.pdf).

Fitzpatrick, R.W., Fritsch, E. and Self, P.G. 1996. Interpretation of soil features produced by ancient and modern processes in degraded landscapes: V. Development of saline sulfidic features in non-tidal seepage areas. Geoderma, 69, 1–29.

Fitzpatrick, R.W. and Merry, R.H. 1999. Pedogenic carbonate pools and climate change in Australia. In: Lal, R., Kimble, J. and Stewart, B.A., eds, Global Climate Change and Pedogenic Carbonates. Advances in Soil Science. Proceedings of the International Workshop on Global Climate Change and Pedogenic Carbonates. Tunis, Tunisia. 13–17 October 1997. Boco Raton, CRC Lewis Publishers.

Fritsch, E. and Fitzpatrick, R.W. 1994. Interpretation of soil features produced by ancient and modern processes in degraded landscapes: I. A new method for constructing conceptual soil–water–landscape models. Australian Journal of Soil Research, 32, 889–907.

Hutchinson, M.F. and Dowling, T.I. 1992. A continental hydrological assessment of a new grid-based digital elevation model of Australia. In: Beven, K.J. and Moore, I.D., eds, Terrain Analysis and Distributed Modelling in Hydrology. Chichester, John Wiley.

Northcote, K.H. 1979. A Factual Key for the Recognition of Australian Soils. Fourth Edition. Adelaide, South Australia, Rellim Technical Publications, 124.

Rayment, G.E. and Higginson, F.R. 1992. Australian Laboratory Handbook of Soil and Water Chemical Methods. Melbourne, Inkata Press, 330.

12 Managing Soil Fertility for Sustainable Agriculture in Taihang Mountain Piedmont, North China

Chunsheng Hu*

Abstract

Soil fertility—the ability of soil reserves to supply adequate levels of essential nutrients needed for plant growth—affects agricultural productivity and sustainability as well as environmental health. For nearly 50 years, there have been great improvements in the balance of nutrient input and output in farmland in the piedmont of Mount Taihang. Soil surveys carried out in 1978, 1989 and 1998 showed that the levels of soil organic matter, total nitrogen (N), total phosphorus (P), available P and other trace elements have increased, but that available potassium (K) levels have not. These results are similar to those obtained by estimating the nutrient balance, which indicate that the characteristics of nutrient cycling depend on the system of fertiliser application in farmland. Soil chemical fertility according to the Chinese classification Standard for Soil Nutrients is good on the whole. In the piedmont of Mount Taihang, nutrient management should focus on reducing the N input and increasing K levels in order to ensure sustainable productivity and good environmental health.

土壤肥力是土壤供应作物生长所须养分的能力。土壤肥力影响农业的生产力、持续性及区域环境健康。近 50 年来，太行山前平原农田养分平衡有了极大的改善。除了钾素外，农田中氮素、磷素等投入量超过作物产品携出量，有机物投入量超过土壤有机质分解量，且盈余量越来越大，特别是肥料氮。1978 年、1989 年、1998 年在栾城县进行的三次土壤调查结果也表明，除了土壤速效钾外，土壤有机质、土壤全氮、土壤全磷、土壤速效磷及微量元素都有明显的提高，这与农田养分平衡估算的趋势是一致的。由此说明，农田施肥制度决定了农田养分循环格局，农田养分循环格局决定了土壤肥力的演替。根据中国土壤养分分级标准，从整体来看，栾城县土壤肥力较好、且向高肥力方向发展，但化肥氮投入过多及污染物的排放对农田环境健康构成潜在的影响。为了农业生产的持续性与区域环境安全，太行山前平原农田应减少氮素的投入、增加钾的投入。

* Shijiazhuang Institute of Agricultural Modernization, Chinese Academy of Sciences, Shijiazhuang, Hebei Province 050021, PRC.
Email: cshu@public.sj.he.cn

Chunsheng Hu. 2002. Managing soil fertility for sustainable agriculture in Taihang Mountain piedmont, North China. In: McVicar, T.R., Li Rui, Walker, J., Fitzpatrick, R.W. and Liu Changming (eds), *Regional Water and Soil Assessment for Managing Sustainable Agriculture in China and Australia*, ACIAR Monograph No. 84, 165–172.

Introduction

SOIL fertility is a measure of soil productivity. It can be broadly defined in terms of physical, chemical and biological factors: nutrient levels, water, air, heat, soil chemistry, soil physics and characteristics of the biome. More narrowly, it can be defined as the ability of soil to supply adequate levels of the nutrients that are essential for plant growth. The natural levels of these nutrients depend on factors associated with soil formation: parent materials, climate, vegetation, topography, time and other external forces such as erosion, deposition, accumulation and groundwater. Human activities also affect soil fertility in cultivated areas. We have known for 1000 years that applying animal and vegetable manure to the soil can restore its fertility (Tisdale and Nelson 1966). Conversely, unwise land use may lead to decreases in soil fertility and productivity. This paper focuses on the concept of soil fertility that is confined to nutrients — that is, the ability of the soil to supply adequate levels of essential nutrients for plant growth.

Since the 1960s, there has been a 20-fold increase in the amount of chemical fertiliser applied each year in China; the amount per area of farmland is now near that of developed countries. This has contributed to a threefold increase in grain production in 30 years. However, there are emerging problems in protecting the agricultural environment. Soil fertility acts as an indicator of both environment and soil quality.

We now know that applying fertiliser has ecological risks, especially when resources are not used carefully. Consequently, managing soil fertility for crop growth now focuses on the sustainable use of resources and protection of the environment rather on maximising yields and profits. For example, people now expect that manure and other nutrients from organic waste will be recycled rather than being allowed to seep into groundwater or other parts of the environment; people also expect that measures will be taken to prevent the degradation of soil fertility through over-consumption or a lack of balance of crop nutrients.

The management of soil fertility requires the rational application of fertiliser. This depends on the type of soil and the pattern of nutrient cycling in a particular agroecosystem. This chapter focuses on changes in the soils of the Taihang Mountain piedmont of North China over the past 50 years. It assesses nutrient input and output, and describes patterns of nutrient cycling and evolving soil fertility. It then draws some conclusions about the sustainable management of soil fertility in the region.

The study focuses on the balance between nutrient inputs and outputs. Inputs include chemical fertiliser, manure and straw, bionitrogen fixation and irrigation. Outputs include crop uptake, leaching from the soil, runoff on the soil surface, drainage, and nitrogen (N) loss through processes such as denitrification and ammonia emission. It is difficult to quantify some of these items. For example, the amount of N lost through leaching and denitrification depends on the net superfluous amount of inorganic N. Consequently, we use the constants of N loss after fertiliser application and N fixation.[1]

Changes in Applied Nutrient Levels

We selected Luancheng County as a typical study case for the Taihang Mountain piedmont, which is part of the North China Plain (NCP). The Overview provides further details of the NCP region. Over the past 50 years, nutrient inputs have increased very quickly, as shown in Figures 1–3 (Hu Chunsheng and Wang Zhiping 1999). For example, inorganic N increased from 0 kg/ha/year to 420.5 kg/ha/year; organic N increased at a slightly slower rate, from 36.0 kg/ha/year to 101.3 kg/ha/year over the past 50 years. In the past, N has been applied mainly as

[1] In other words, we assume that the nitrogen loss rate does not change as conditions change.

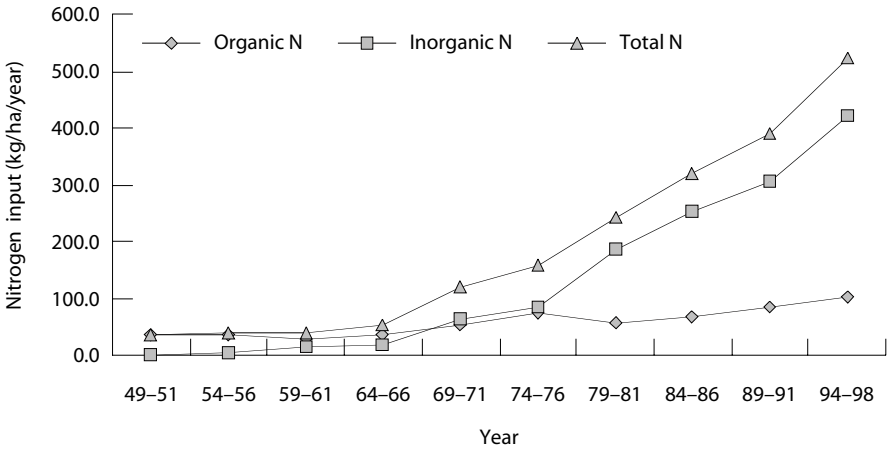

Figure 1. Nitrogen (N) input in farmland in Luancheng, 1949–98.

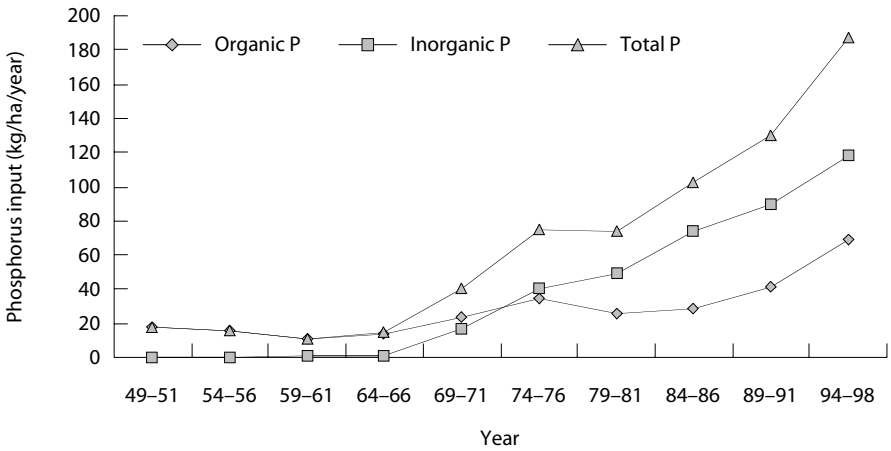

Figure 2. Phosphorus (P) input in farmland in Luancheng, 1949–98.

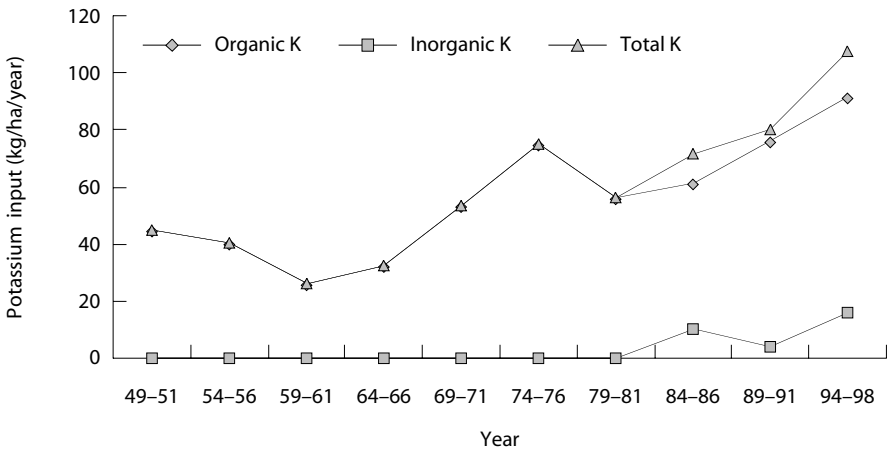

Figure 3. Potassium (K) input in farmland in Luancheng, 1949–98.

organic N, but inorganic N is now more important: applied inorganic N accounted for half of the total N applied in the 1960s, up to 60% in the 1970s, and is now 80%. Phosphorus (P) has followed a similar trend, but 5–10 years later: applied inorganic P accounted for half of the total applied P in the 1970s but up to 70% in the 1990s. Potassium (K) was applied as organic K until the late 1980s, since when the application of inorganic K has gradually increased.

The ratio of artificial nutrient input to product output[2] could be an indication of whether excess nutrients are being added to the soil. If the ratio is less than 1, the nutrient budget is negative; if the ratio is larger than 1, the nutrient budget is positive. The bigger the ratio, the greater the level in the soil of superfluous nutrients that could be lost to the environment.

Fertiliser is added to the soil to promote grain yield. For example, Table 1 shows that from 1949–51 to 1994–98 output N increased from 58.8 kg/ha/year to 519.8 kg/ha/year and input N increased from 58.9 kg/ha/year to 123.5 kg/ha/year. The ratio of N input to output increased from 0.88 to 1.74 over the same period. The N balance started to change from negative to positive in the early 1980s. From 1949–51 to 1994–98, output P increased from 15.8 kg/ha/year to 122.8 kg/ha/year and input P from 17.4 kg/ha/year to 187.0 kg/ha/year; the ratio of P input to output increased from 0.7 to 1.52. The P balance did not change from negative to positive until the 1970s. Nutrient K was abundant in the early 1950s, but there has subsequently been a deficit, with the ratio of input to output less than 1. Thus, fertiliser efficiency has gradually decreased with increasing crop yield. Increasing levels of nutrient input have been required, and inorganic nutrients have had to be applied at increasing rates as productivity increased.

[2] For example, straw and grain—that is, above-ground biomass.

The added nutrients have improved crop yield but have also accumulated in the soil. It is evident that fertiliser input is close to a maximum.

Soil Nutrient Content

Table 2 shows that soil fertility has improved with increased fertiliser input and better nutrient balance (Hu Chunsheng 1999). The data in the table represent the average of 32 soil samples from Luancheng County. Available K has obviously decreased rapidly as less K fertiliser has been added to soil during the past three decades; it will be essential to apply K to farmland in future if soil fertility is to be sustained in the Taihang Mountain piedmont.

Evaluating Soil Fertility

Crop production is based on the use of plant nutrients and on the physical characteristics of the soil. More plant nutrients have been added since 1960, but most crops continue to depend on 'mining' the soil for some or most nutrients. Soil diagnosis helps to determine when additions are needed. Both chemical and physical properties can be used as diagnostic indicators for soil fertility.

Classification of soil fertility

Table 3 shows the classification of soil fertility according to the Chinese standard classification (Shanmin Shen 1998). This is a general standard for the whole of China, discussing most crops and soil types. It is based on the effect of fertiliser application on yield at particular levels of soil nutrients. There are six grades. Grade 1 soil has excellent fertility; applying additional fertiliser to soil of this grade will not increase crop yield. Grade 6 soil has very poor fertility; applying additional fertiliser is likely to have a significant effect on crop yield. Grade 4 is the threshold level at which fertiliser must be applied to increase the yield.

Table 1. The structure and balance of nutrients in farmland, Luancheng county, 1949–98 (kg/ha/year).

Year	Nutrients[a]	Artificial inputs		Natural input	Output		Balance ratio[b]	Grain yield
		Organic	Inorganic		Product	Loss		
1949–51	N	36.0	0	22.9	44.4	14.4	0.81	2108
	P_2O_5	17.4	0	0	15.8	0	1.10	
	K_2O	44.8	0	0	36.8	0	1.22	
1954–56	N	34.5	3.3	23.1	53.4	15.5	0.71	2528
	P_2O_5	15.8	0	0	18.8	0	0.84	
	K_2O	40.1	0	0	41.5	0	0.97	
1959–61	N	27.5	12.3	22.8	43.0	15.9	0.93	2070
	P_2O_5	10.6	0.7	0	15.0	0	0.75	
	K_2O	26.2	0	0	34.4	0	0.76	
1964–66	N	34.6	18.8	22.3	60.5	21.3	0.88	2828
	P_2O_5	13.5	1.3	0	21.2	0	0.70	
	K_2O	32.7	0	0	48.8	0	0.67	
1969–71	N	54.3	64.4	21.5	101.3	47.5	1.17	4568
	P_2O_5	24.1	16.5	0	34.8	0	1.17	
	K_2O	53.6	0	0	76.3	0	0.70	
1974–76	N	73.2	83.8	21.2	137.6	62.8	1.14	7410
	P_2O_5	34.0	40.7	0	48.6	0	1.54	
	K_2O	74.8	0	0	91.5	0	0.82	
1979–81	N	55.9	186.2	21.6	160.6	96.9	1.51	8348
	P_2O_5	25.3	48.9	0	54.6	0	1.36	
	K_2O	56.5	0	0	108.7	0	0.52	
1984–86	N	65.6	252.0	21.9	202.0	127.0	1.57	9 690
	P_2O_5	28.6	74.3	0	68.3	15.6	1.23	
	K_2O	61.4	10.4	0	139.5	0	0.51	
1989–91	N	84.8	304.2	22.2	240.9	181.8	1.61	10,995
	P_2O_5	40.9	89.3	0	80.4	0	1.62	
	K_2O	76.4	4	0	166.6	0	0.49	
1994–98	N	101.3	420.5	22.2	300.3	219.5	1.74	13,650
	P_2O_5	68.6	118.4	0	122.8	0	1.52	
	K_2O	91.3	16	0	202.7	0	0.49	

[a] N = nitrogen; P_2O_5 = phosphorus oxide; K_2O = potassium oxide
[b] Balance ratio = artificial input divided by product output

Physical and chemical properties of the soil

We analysed soil fertility using the threshold guidelines for soil chemical indicators shown in Table 2 and the Australian standard soil physical indicators described by Walker and Reuter (1996). Soil fertility was evaluated according to the following criteria:

Physical factors

- soil consistency
- soil texture
- soil colour
- status of any roots
- presence of slaking and dispersion
- field capacity
- available water
- wilting point
- bulk density
- total porosity
- air-filled porosity

Table 2. Soil nutrient content in Luancheng, 1978–98.

	Total nutrient content (g/kg)								Available nutrient content (mg/kg)					
Year	OM	N	P	K	Zn	Cu	Pb	Cd	P	K	Fe	Cu	Zn	Mn
1978	11.5	0.78	1.5	22.8	–	–	–	–	7.77	141	8.27	1.03	0.67	8.20
1989	14.6	0.91	–	–	54.8	16	23.6	0.11	8.9	106.2	8.25	0.87	1.16	7.51
1998	15.0	1.03	0.8	12.2	58	19.4	12.8	0.63	16.0	88.1	9.0	2.03	1.67	9.0

Cd = cadmium; Cu = copper; Fe = iron; K = potassium; Mn = manganese; N = nitrogen; OM = organic matter; P = phosphorus; Pb = lead; Zn = zinc

Table 3. Classification of soil fertility (Chinese standard classification).

	Grade					
Soil component[a]	1	2	3	4	5	6
Organic matter (g/kg)	4	3–4	2–3	1–2	0.6–1	0.6
Total N (g/kg)	0.2	02–0.15	0.15–0.10	0.10–0.075	0.075–0.05	0.05
Total P (g/kg)	0.1	0.081–0.1	0.061–0.08	0.041–0.06	0.02–0.04	0.02
Olsen-P (mg/kg)[b]	40	40–20	20–10	10–5	5–3	3
Available K (mg/kg)	200	200–150	150–100	100–50	50–30	30
Available Zn (mg/kg)	3	1.1–3	0.51–1.0	0.31–0.5	0.3	
Available Fe (mg/kg)	20	10.01–20	4.51–10	2.51–4.5	2.5	
Available Mn (mg/kg)	30	15.1–30	5.1–15	1.1–5	1.0	
Available Cu (mg/kg)	1.8	1.01–1.8	0.21–1.00	0.11–0.2	0.11	
Available B (mg/kg)	2	1.01–2	0.5–1.0	0.26–0.5	0.25	
Available Mo (mg/kg)	0.3	0.21–0.3	0.16–0.2	0.11–0.15	0.10	
Indicators	Excellent	Very good	Good	Fair	Poor	Very poor

[a] Mo = molybdenum; B = boron; see Table 2 for explanation of other chemical abbreviations
[b] Olsen-P refers to the level of phosphorus measured using the Olsen analytical method

Chemical factors

- organic matter
- total N
- total P
- available P
- available K
- trace elements

Luancheng County typically has cinnamon soil with a thin humus layer and thick middle solum. Tables 4 and 5 show the main morphological and physical properties of the soil. In summary, soils are grey–yellow in morphology, sandy, loose, and good for storing water, but have a high bulk density and a plough pan. They have fair levels of total organic matter, total N, total P and available K, with good levels of trace elements; this suggests that soil fertility in Luancheng is in the middle range and that applying fertiliser every year is necessary to maintain soil fertility and sustain crop production. The results showed a potential deficiency in K; although current levels are not causing reduced crop yields, it is essential to start applying K fertiliser immediately.

Overall, soil fertility is judged to be fair to near good. Over the past 50 years, there has generally been a trend towards improved soil fertility, particularly for total organic matter, total N, available P and trace elements. Only in the total and available K content has there been a sharp reduction in levels: the average K content was at the lower end of the range (grade 3–4), suggesting the start of a trend to K deficiency. A serious problem is an increase in total cadmium (Cd), indicating probable soil pollution.

Conclusions for Sustainable Management

Successful management of soil fertility must meet the objectives of increasing production, being economically profitable and protecting the environment to enable the sustainable development of agriculture. The rational input of chemical fertiliser and manure must be emphasised for high-yield regions such as the Taihang Mountain piedmont. The basic approach should be to increase control over chemical fertiliser input, to increase the input of K fertiliser and to increase the level of manure returned to the soil.

The input of chemical N fertiliser is up to 420.5 kg/ha/year and there is a trend to continuously increase the amount for higher yields. The entry of superfluous N into the soil poses a serious ecological risk. In many places, the nitrate content

Table 4. Main morphological indicators of grey-yellow soil in Luancheng County.

					Root density (cm/cm^3)	
Layer[a]	Thickness (cm)	Consistency	Colour	Texture	Wheat	Corn
A_1	0–17	Soft	Grey–brown	Sandy loam	3.49	1.12
A_1B	17–30	Very hard	Light brown	Sandy loam	1.63	0.48
B_1	30–65	Firm	Dark brown	Loam	0.51	0.26
B_2	65–90	Firm	Dark brown	Loam	0.34	0.25
BK	90–145	Very hard	Light yellow	Light clay	0.16	0.12
B_3	145–170	Very hard	Grey yellow	Light clay	0.18	
BC	170–190	Very hard	Light yellow	Medium clay		

[a] Capital letters refer to soil horizons
Source: Report of the Luancheng County Natural Resources Survey and Agricultural Division, 1979.

Table 5. Main physical indicators of soil in Luancheng County.

Layer[a]	Thickness (cm)	Field capacity (%)	Wilting point (%)	Plant available water (%)	Bulk density (g/cm^3)	Total porosity (%)	Air-filled porosity (%)
A_1	0–17	36.35	9.63	26.73	1.41	46.42	10.07
A_1B	17–30	34.86	11.37	23.49	1.51	42.62	7.76
B_1	30–65	33.25	13.92	19.33	1.47	44.14	10.89
B_2	65–90	34.28	13.91	20.37	1.51	42.62	8.34
BK	90–145	34.36	12.95	21.41	1.54	41.48	7.12
B_3	145–170	38.98	13.87	25.11	1.64	37.68	1.42
BC	170–190	38.05	16.44	21.61	1.59	39.58	1.53

[a] Capital letters refer to soil horizons
Source: Report of the Luancheng County Natural Resources Survey and Agricultural Division, 1979.

of groundwater and vegetables is already more than prescribed by the National Hygienic Standard of Drinking Water and Food. Increasing levels of Cd in the soil may be due to the application of phosphate accompanied by Cd. Cadmium accumulation in the soil may lead to Cd pollution, a serious environmental issue. The ability of the soil to supply adequate levels of K for plant growth has decreased, as little K fertiliser has been applied in the past 50 years. K deficiency in the soil can reduce yields and reduce the efficiency of other fertilisers.

Farmers in the Taihang Mountain piedmont should emphasise the balanced application of fertilisers. In particular, policy makers should encourage the collection of manure and its return to soil.

References

Chunsheng, H. and Zhiping, W. 1999. The soil nutrient balance and fertilizer use efficiency in farmland ecosystems in Taihang Mountain Piedmont. Progress in Geography, 17 (supplement), 131–138.

Chunsheng, H. 1999. Physical and chemical indicators of soil health diagnostics and its application. Eco-Agriculture Research, 7(3), 16–18 (in Chinese).

Shen, S., ed. 1998. Soil fertility of China. Beijing, Chinese Agricultural Publishing.

Tisdale, S.L. and Nelson, W.L., eds. 1966. Soil fertility and fertilizer. New York, Macmillan Publishing Co. Inc.

Walker, J. and Reuter, D.J. 1996. Indicators of catchment health—a technical perspective. Melbourne, CSIRO Publishing.

13 Chemical Properties of Selected Soils from the North China Plain

Renzhao Mao,* Rob W. Fitzpatrick,† Xiaojing Liu* and Phil J. Davies†

Abstract

Saline and sodic soils occur in large areas on the North China Plain (NCP). This presents a serious problem for sustainable agricultural development in the area. This study identified and characterised saline, sodic and sodic-saline soils on the NCP and recommended some strategies to deal with salinity in the region. Three distinct regions were identified: the coastal, middle and western zones. The parent material of the soils is river alluvium. Illite (Hydromica) is the dominant layer silicate mineral; smectite, kaolinite and chlorite are subdominant.

华北平原大面积的盐碱土是区内农业持续发展所面临的一个严重问题。本研究提供了几个代表性盐化地点盐碱土的化学和矿物学性质的定量信息，提出了一些治理措施。该区可划分为滨海、中部和西部三个区。土壤母质属于河流冲积物。水云母为主导层状硅酸盐粘土矿物，蒙脱石、高岭石、绿泥石为次要矿物。

SOIL salinisation is a growing problem in agriculture worldwide. As we try to meet global needs for agricultural production, more and more countries are concerned about the increasing problem of salinity. China is one of the nations that have a serious problem with saline soils; the North China Plain (NCP), a major food production area, has especially suffered from this problem.

For instance, in the early 1950s the NCP had more than 2 million ha of saline soils; at the end of the 1950s, 4 million ha were affected, and in the mid-1980s only 2 million ha were affected. This overall decrease in extent of saline affected soils has been largely due to changes in irrigation practices and an associated fall in the depth of the groundwater table in the region. Areas where the extent of salinisation

* Shijiazhuang Institute of Agricultural Modernization, Chinese Academy of Sciences, Shijiazhuang 050021, PRC.
Email: renzhao.mao@china.com
† CSIRO Land and Water, PMB 2, Glen Osmond, SA 5064, Australia.

Renzhao Mao, Fitzpatrick, R.W., Xiaojing Liu and Davies, P.J. 2002. Chemical properties of selected soils from the North China Plain. In: McVicar, T.R., Li Rui, Walker, J., Fitzpatrick, R.W. and Liu Changming (eds), *Regional Water and Soil Assessment for Managing Sustainable Agriculture in China and Australia*, ACIAR Monograph No. 84, 173–186.

is still considered serious include the lower elevated plains of the Bo Gulf, the four lakes in the south of Shandong Province and the Huang (Yellow) River irrigation area in Henan Province.

The Cangzhou prefecture (115°42'–117°50'E and 37°28'–38°57'N) or subregion is a small part of the NCP adjacent to the Bo Sea in the lower-lying plain of the Hai River's southern reach downstream. With a total area of 14,056 km^2, the subregion is characterised by low and smooth relief, a deficient freshwater supply, waterlogged land, salty groundwater and a serious saline soil problem. It experiences frequent dry periods and its soils are saline-alkaline with low levels of nutrients. All these factors contribute to low crop yields (Mao and Liu 2000). The Overview provides some background information on the NCP.

The main objectives of our study were:

- to determine the chemical, distribution (dynamic changes) and mineralogical properties of salt-affected soils in the Cangzhou prefecture;
- to develop an understanding of the processes occurring in the soils; and
- to use an increased understanding of the conditions at Cangzhou to recommend strategies to ameliorate existing degradation and prevent further damage to soils elsewhere (the strategies would aim to improve the use and management of soil resources to increase crop yields and arrest the decline in soil quality).

Saline Soils on the North China Plain

Soil salinisation is the accumulation of soluble salts in the soil that results in some degree of decrease in soil productivity (see Chapter 8). Saline-alkali soils include solonchak and solonetz (alkaline soils), and various other soils affected by salt or sodium ions. Soil salinity, the concentration of soluble salts in soil, is commonly graded by considering the integrated biophysical effect on crops or the extent of damage to crops (Xiong and Li 1987). Poor plant growth can result from:

- toxicity due to high concentrations of ions, such as Cl^-, SO_4^{2-}, Na^+ and Mg^{2+};
- diminished absorption of nutrients because of poor ion balance;
- decreased water absorption by roots because high ion concentrations lead to water stress; and
- a decline in soil structure, particularly where Na^+ is the dominant cation to generate soils with high exchangeable sodium percentages (ESPs).

In the NCP, soil salinity and sodicity are strongly influenced by:

- the monsoon climate with annual wet and dry seasons;
- the chemistry and depth of groundwater and surface waters, which have changed substantially over the past two decades;
- topography; and
- soil type (in the NCP, the principal soil type is 'Chao soil', a Chinese term; other soil types found in the region include meadow and coastal solonchak, saline swamp, saline meadow, sandy and cinnamon).

Distribution of soil types

Saline soil types can be characterised by the ratio of the principal anions present (e.g. Cl^- and SO_4^{2-}) measured in centimoles (cmol). On the NCP, the soil types are broadly distributed between the following three geographical zones:

- the coastal zone, with 'Cl-type' soils, in which Cl^- is dominant (Cl^-:$SO_4^{2-} > 8$), and in which there is a wide range in the ratios both between different profiles and along the same profile;

- the western zone, with 'SO_4^{2-}Cl-type' soil, in which SO_4^{2-} is dominant (Cl^-:SO_4^{2-} < 2); and
- the middle zone, with 'mixed anions', in which there are roughly equal amounts of Cl^- and SO_4^{2-} (this zone is located between the coastal and western zones).

Figure 1 shows the ratio of Cl^-: SO_4^{2-} in soil profiles from the coastal and middle soil zones of the NCP. Table 1 shows anion data for two soil profiles with layers extending below 40 cm. Macun village is located in the coastal zone and the soil has a ratio of Cl^-: SO_4^{2-} > 8. The Cl^- in the upper layers is currently active and moves downwards and accumulates together with SO_4^{2-}. However, the soil from Wangsi village basically has a constant ratio (Cl^-:SO_4^{2-} = 1–2) in all layers, indicating that it is of mixed type.

Salt accumulation at the soil surface

Figure 2 illustrates the trend in total salt content with depth for representative soil types from the coastal and middle zones of the NCP. A total salt content of 2–6% was measured at 0–1 cm in both soil types from the middle zone, which decreased sharply to 1–2% at 1–5 cm and 0.8% at 5–10 cm. The salt concentration remained essentially constant, at around 0.5%, at depths below 40 cm. The saline soil in Dalangdian, Nanpi County, is considered to be a typical example of this kind of salt distribution. The soil solution contains a mixture of Cl^-, SO_4^{2-}, Na^+, Mg^+, HCO_3^- and K^+ ions, with the Na^+ cation being the dominant ion (concentrations of about 44 cmol/m^3 in the surface layer). The salt distribution in this soil progressively stabilises below depths of 50 cm, with total salt concentrations being 20–40 g/kg at 0–5 cm and 1–2 g/kg at 40–50 cm, though there was more Cl^- and Na^+ at 100–120 cm than in the upper layers.

Saline soils on the NCP are characterised by accumulated salts near the surface. This has occurred for a variety of reasons. Because of the critical depth to saline groundwater and intense evaporation, salts have progressively moved or wicked up from the saline groundwaters and lower-lying soils. Salinity has also expanded from lower topographic sites to higher sites because of uneven microtopography. The level of salinity in soils is closely correlated with crop development and yield because cultivation management, seed emergence and crop growth all occur in the plough layer (major rooting depth). Thus, salt content at the soil surface (0–20 cm) can be used to categorise the extent and nature of soil salinisation and provide a sound basis for rehabilitating saline-sodic soils. Good farming practices and appropriate biological approaches should enable salt to be redistributed and leached out of the soil.

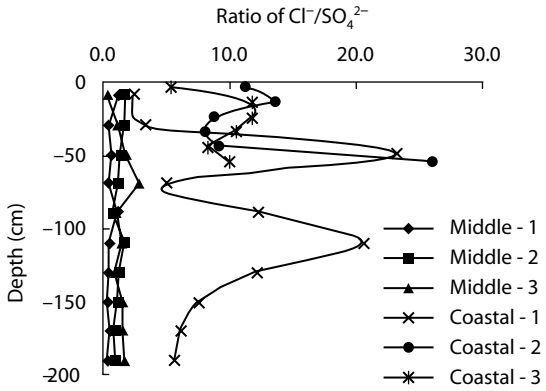

Figure 1. Ratio of Cl^-/SO_4^{2-} in coastal and middle zones of the North China Plain.

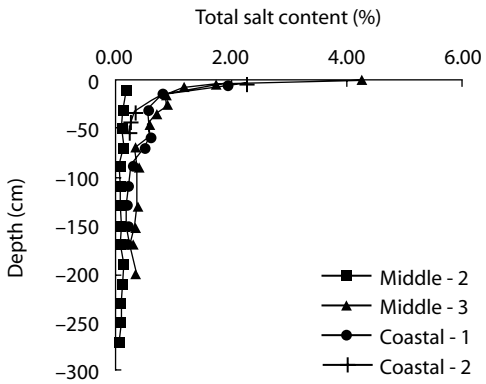

Figure 2. Trend in total salt content with depth in coastal and middle zones of the North China Plain.

Salt accumulation in subsoils and lower soil layers

In the 1980s, the leaching process was exacerbated by the lowering of the saline groundwater table in the western zone of the saline region of the NCP, causing salt to accumulate in subsoil horizons and lower layers of the soil. Consequently, there were changes in soil salinity in the 0–20 cm layer. In addition, there was a decrease in the area affected by salinity and in the level of salinity in the surface layers. For example, Figure 3 shows that salt accumulated significantly in the subsoil horizons

Table 1. Salt composition of soils from two locations in Cangzhou subregion, 1998–99.

Location	Depth (cm)	Ion concentration (cmol/kg)						Total salt content (%)	Cl^-/SO_4^{2-}
		HCO_3^-	Cl^-	SO_4^{2-}	Ca^{2+}	Mg^{2+}	$Na^+ + K^+$		
Wangsi village Nanpi County (98N-2)	0–1	0.55	60	23.05	2.93	21.65	57.5	6.34	2.6
	1–5	0.35	18	5.58	0.90	6.18	15.35	1.73	3.2
	5–10	0.4	11.8	3.78	0.98	3.95	9.9	1.17	3.1
	10–20	0.45	8.3	2.83	0.45	2.68	8.15	0.86	2.9
	20–30	0.45	9.1	2.80	0.53	3.20	7.7	0.90	3.3
	30–40	0.45	6.1	2.43	0.38	2.33	6	0.69	2.5
	40–50	0.45	4.95	2.00	0.35	2.05	4.6	0.57	2.5
	50–60	0.45	4.15	2.58	0.35	2.48	4.1	0.59	1.6
	60–80	0.45	3.4	1.10	0.30	1.55	2.35	0.36	3.1
	80–100	0.5	3.05	1.35	0.33	1.63	2.35	0.38	2.3
	100–140	0.5	2.9	1.33	0.35	1.48	2.4	0.37	2.2
	140–160	0.55	2.2	1.40	0.30	1.45	2.05	0.34	1.6
	160–180	0.35	2	1.15	0.33	0.98	2.05	0.29	1.7
	180–210	0.4	2.1	1.55	0.38	1.03	2.8	0.35	1.4
Macun village Yanshan County (99Y-1)	0–10	0.3	22.5	4.70	1.03	3.93	22.3	1.92	4.8
	10–20	0.3	10.2	1.55	0.40	1.55	9.7	0.81	6.6
	20–40	0.45	9.2	0.20	0.28	1.08	7.35	0.58	46.0
	40–60	0.4	8.1	0.83	0.35	1.38	6.7	0.59	9.8
	60–80	0.35	7.95	0.33	0.35	1.33	5.6	0.51	24.1
	80–100	0.35	5.1	0.13	0.23	0.85	3.55	0.33	39.2
	100–120	0.35	3.6	0.15	0.18	0.78	2.35	0.24	24.0
	120–140	0.3	3	0.20	0.18	0.63	2.1	0.22	15.0
	140–160	0.3	3	0.25	0.18	0.53	2.4	0.22	12.0
	160–180	0.3	3	0.28	0.20	0.63	2.2	0.23	10.7

(40–100 cm) of Heijian County. In 1990, the same process occurred in the middle zone of the region. Table 2 shows the mean total salt content for 43 profiles along the 20 km Daima Canal transect in Nanpi County and for 14 of these sites that were selected to represent the status of salt accumulation in subsurface and lower layers. The results are representative of the variation in soil salinisation for the middle zone of the NCP.

Seasonal salt movement

The NCP has a monsoon climate, with annual wet and dry seasons. Under natural conditions, salt leaches out in the wet season (July to September) but accumulates at the surface during the dry season, particularly from March to May. Water and salt movements vary with seasonal changes. In winter, salt and water are frozen and immobile; in spring salt accumulates in soils; in summer it leaches out; and in autumn it moves slowly to the soil surface. Hence, seasonal changes cause salts to be redistributed in soils, both vertically and laterally. Evaporation of the shallow groundwater has led to high salt concentrations in certain surface soils, but final concentrations depend on soil texture and heat.

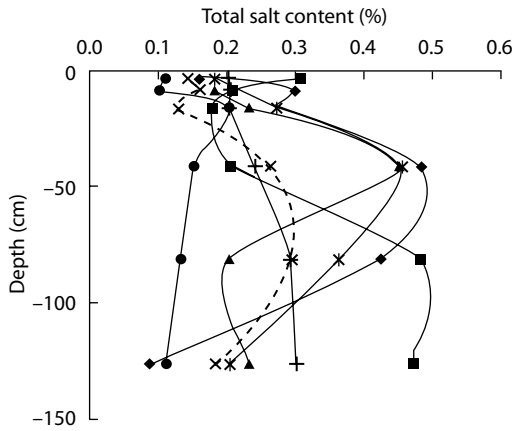

Figure 3. Distribution of salt content in seven different soil profiles in Heijian County.

Table 2. Soil salinity on a transect along Daima Canal, Nampi County, 1997.

	14 sites		43 sites	
Depth (cm)	Mean TSC (%)	SD	Mean TSC (%)	SD
0–10	0.12	0.04	0.13	0.05
10–20	0.11	0.03	0.12	0.06
20–30	0.11	0.04	0.12	0.08
30–40	0.14	0.06	0.13	0.11
40–60	0.25	0.36	0.15	0.22
60–80	0.23	0.24	0.15	0.15
80–100	0.20	0.15	0.13	0.10
100–120	0.25	0.22	0.15	0.14

SD = standard deviation; TSC = total salt content

Figure 4 shows salt content in the soil profile at Nanpi County (in the middle zone of the NCP saline region) at different times of the year. Salt in the 0–10 cm layer in this profile migrated upwards with capillary water, and accumulated in the upper soil layers in winter and spring. In July and August (summer), heavy rains leached salts to subsoil horizons or deep layers in the regolith and decreased the total salt content. This process tends to increase the levels of exchangeable Na^+ and Mg^{2+} in these soils, thus increasing soil sodicity.

In contrast, following the wet season, the total salt content increased rapidly in the profile as water evaporation increased. There was a sharp change in soil salt levels in the layer above 40 cm and a gradual

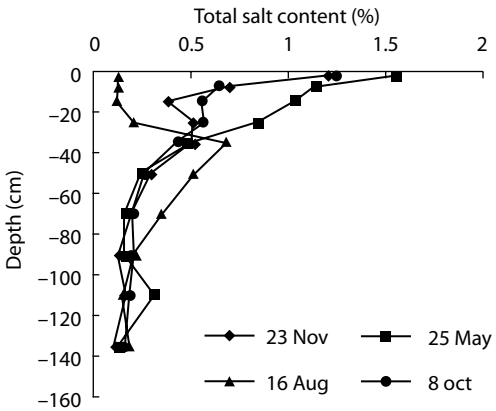

Figure 4. Salt distribution in the soil profile at Nanpi County at different times of the year.

change from 40–60 cm; below 100 cm, the level was relatively stable. For example, in 1998, 252 mm of rain fell in 24 hours, giving rise to large amounts of water in ponds and depressions (Mao and Liu 2000). Regional climatic data suggest that when there is about 300 mm of rainfall in 24 hours and a runoff volume of 24–85 mm, such conditions will occur. It is estimated that the root zone (about 2 m deep) could contain as much as 145 mm of precipitation. When there is more than 50 mm of rain at any one time, salt could accumulate in the 40–80 cm layer in the profile if it was carried with water seeping down under gravity. Salt loss occurs naturally only in the soil layers above 60 cm. In the coastal region, the groundwater is shallow and has a relatively high total salt content. The dynamics of salinisation in the coastal zone are considered to be basically the same as for Nanpi County.

Localised spatial distribution of salinisation

Figure 5 shows the nonuniform distribution of the salt ions among three saline soils in the Dalangdian depression, located 10 m apart from each other. We measured large differences in salt concentrations or accumulations at the surface of these profiles. For example, at the eastern point, the saline soil profile had an uneven distribution of salt concentration because of differences in the water–salt movement caused by variations in surface microtopography, soil compaction, soil texture, ditch arrangement and water allocation. Salt concentrations were variable or 'transient' depending on the groundwater level, ion activity or stage of salinisation and desalinisation.

Alkalisation

Primary alkalisation was uncommon in the three study regions on the NCP, but secondary alkalisation appeared to be an increasing problem because of 'artificial' or farming activities, even though there was less salinisation and a smaller area was affected. Alkalisation has occurred via two pathways. First, as the natural environment has altered, saline soils have begun to lose salt and have gradually transformed to more alkaline saline soils. Second, alkalisation has resulted from poor land management, such as applying high levels of fertilisers or irrigating with highly saline water. The commonly believed theory is that, as the groundwater level was lowered, salts moved from the upper to the lower layers in these soils and the Na^+ ion was adsorbed by complex colloids to form more alkaline soils when Na^+:(Ca^{2+}+Mg^{2+}) > 4 (in cmol/L).

Alkalisation and salinisation sometimes occur in the same zone. Alkalisation occurs mainly as a result of alkaline freshwater from deep groundwater areas around old rivers with high levels of Na^+, HCO_3^- and CO_3^{2-}. Soil colloids in contact with alternating Na^+-rich and fresh waters can develop sodic properties (colloid with high amounts of exchangeable Na^+ adsorbed on its surface) and can disperse as rain or surface water percolates through soils. This causes soil particles to move with the water and collect in holes or at low-lying sites, making it difficult for water to move through soils. Consequently, at lower-lying sites, after evaporation, soil tended to form a layer of 'tile-like' pieces about 1–5 cm thick, covered by a layer of blue-green algae. However, at higher sites, a gray, thin silt–sand layer about 0.5–1.0 cm (sometimes up to 3 cm) was formed on the soil surface, under which was a crust about 1 cm thick. There was a honeycomb-like layer 2–3 cm below the soil crust of 'tile-like pieces'; under

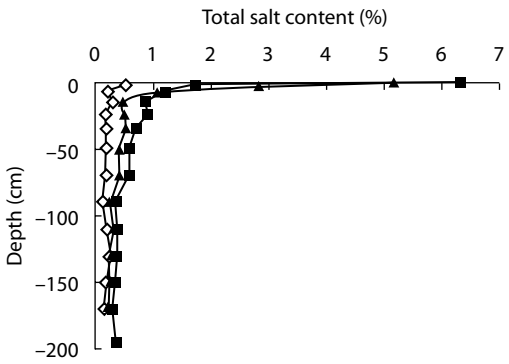

Figure 5. Salt distribution in the soil profile in three saline soils 10 m apart, near the Dalangdian depression.

that was a layer of 20–30 cm consisting of aggregated soil particles and sandy soil. Tables 3 and 4 show properties of sodic soil profiles in Hejian. An alkaline soil near Hejian has recently been found to have a pH of 8.5–9.1, and an ESP of 15–35%, with an HCO_3^- content of more than 0.7 cmol/km.

Alkaline soils were categorised into 'slightly sodic soils', 'moderately sodic soils', 'severely sodic soils' or 'solonetz soils', depending on the degree of alkalisation, the proportion of alkaline area and their toxicity to crops or plants. For example, if the sodic area was more than 60–70% and the degree of sodicity more than 40–50%, the soil was identified as solonetz. Alkaline soils were classified as coastal meadow sodic soils, meadow sodic soils or sodic Chao soils depending on whether they occurred in coastal or western inland zones.

Table 3. Properties of sodic soil in Heijian County.

Depth (cm)	pH	CEC (cmol/kg)	Exchangable Na^+ (cmol/kg)	ESP (%)
0–5	8.84	4.63	0.75	16.11
5–10	9.10	4.82	1.60	33.28
10–20	8.96	6.56	1.70	29.85
20–40	8.92	8.05	1.80	22.41

CEC = cation exchange capacity; ESP = exchangeable sodium percentage

Causes of Salinisation

Climate

The study region is semiarid with a continental monsoon climate. The average annual rainfall is 500–600 mm. Rainfall distribution is uneven in most years (coefficient of variation 30–40%), with 3% of the total rain falling from December to February, 16% from March to May, 79% from June to August, and 2% from September to November. Thus, the wet season lasts for three months, with the other months essentially remaining dry. Yearly potential evaporation is three to four times more than precipitation, so drought and waterlogging occur alternately. Waterlogging may be accompanied by salinisation. Water and salts accumulate in spring and decrease in summer. Climate strongly influences evaporation and concentration of salts in groundwaters, with mineralisation being 2–5 g/L. Consequently, salinisation occurs easily, with total soil salinity levels reaching 0.3–0.4%.

Topography and landform

Landform in the study region is strongly controlled by old river systems and includes flat highlands, sloping land, flat lowlands and wetland depressions. Surface runoff could drain away in flat highlands, recharging groundwater, raising the watertable and tending to cause soil salinisation.

Table 4. Salt composition of sodic soil in Heijian County.

Depth (cm)	Ion concentration (cmol/kg)							TSC (%)
	CO_3^{2-}	HCO_3^-	Cl^-	SO_4^{2-}	Ca^{2+}	Mg^{2+}	Na^++K^+	
0–5	0.05	1.00	0.30	0.33	0.05	0.09	1.35	0.14
5–10	0.00	0.99	0.40	0.06	0.10	0.04	3.14	0.16
10–20	0.00	0.60	0.52	0.16	0.13	0.17	2.00	0.13
20–40	0.00	0.36	0.63	0.30	0.18	0.14	2.57	0.14
40–60	0.11	2.04	1.14	0.10	0.21	0.11	3.04	0.26
60–100	0.05	0.76	2.60	0.42	0.07	0.07	4.78	0.29
100–150	0.05	0.76	2.03	0.15	0.10	0.14	1.74	0.18

TSC = total salt content

Parent materials

The parent material in the region is alluvium from the Huang and Hai rivers, which overflow and change course many times. Sandy loam soils develop because of their close proximity to rivers, whilst clayey soils may develop further away from rivers. Loamy soils occupy zones between the sandy loam and clayey soils. The stratification and variation of parent materials with certain salt minerals is the primary cause of saline soil formation in the study region. Table 5 shows the distribution of soil texture characteristics in the area. In 2-m profiles, silty clayey loams were relatively wide-ranging; this is a condition for salinisation. Silty clayey loams and clayey loams were dominant in topsoil; clayey soil occupied nearly one-third of the total area in the bottom soil. Clayey layers at depth could be an obstacle to salt movement.

Table 5. Distribution of soil texture characteristics in Cangzhou prefecture.

	Proportion of land (%)				
Depth (cm)	LS	SL	ZCL	CL	LC
0–20	0.08	1.77	45.49	41.66	11.01
20–60	0.33	2.89	41.35	31.92	23.51
60–100	1.29	4.83	36.46	24.67	32.75
100–200	5.64	11.93	46.00	5.74	30.68

CL = clayey loam; LC = loamy clay; LS = loamy sand; SL = sandy loam; ZCL = silty clay loam

Surface water and groundwater

Salinisation requires water to transport salts in and out of the regolith. Fresh surface water can transport salt from one catchment to another in floods. Saline groundwater can transport salts at or to certain critical depths, although the water moves slowly in a lateral direction. Runoff water is the main way in which groundwater in the study region is recharged. In some seasons, water can result in sustainable or secondary salinisation.

Sources of salt

The study region contains zones that are rich in various types of soluble salts. The dominant source is the shallow layer of salty groundwater. Water from the upland river systems played a major role in the past but its importance has decreased in the last 30 years and such water is no longer a source of salt.

Saline waters (2–3 g/L) and salty waters (> 3 g/L) occur in the groundwater systems that underlie most of the region (7230 km^2 or 51%). There are high levels of Cl^-, SO_4^{2-}, and Na^+; the total salt content depends directly on the concentrations of these ions. Groundwater was the most active cause of saline soils. However, saline soils have gradually decreased in extent because the groundwater levels have declined during the past 20 years.

Wind and air are other sources of salt accumulation in coastal zones. Salt from the sea can be carried long distances inland by wind as spindrift or can fall to the ground with rain after being carried by warm northwesterly winds.

'Desalted Chao soil' results from large-scale improvements in saline soils. Surface soils have gradually lost salt as water, fertiliser and salt regimes have changed. However, salt remains below the subsoil and is therefore a potential source of surface salt, which could accumulate if groundwater levels rise.

Clay Minerals in Soils of the North China Plain

Typical profile

Clay minerals (< 2 μm) in the study region consist of aluminosilicates and a range of oxides, hydroxides and oxyhydroxides. These minerals occur in most soils and exhibit colloidal properties, which make soils stable (prevent erosion), play a key role in nutrient mineralisation and control the physical and chemical processes of soil formation. No matter what they inherit from parent material or

develop in the process of soil formation, clay minerals all have a unique set of characteristics: they are stable, they are resistant to weathering, and they are very fine-grained. Research involving aluminosilicates (or clay minerals) is important in understanding the origin, classification and utilisation of soils.

There has been little research on the nature and properties of clay minerals of saline soil in the Haihe low plain; there are a variety of opinions about the composition of clay minerals. According to Xiong and Liu (1987), the major component of the Chao soil is Hydromica (illite), and the yellow Chao soil (a subclassification of Chao soil) is mainly composed of Hydromica, with chlorite and smectite as minor components. Xiong and Liu (1987) suggested that Chao soil is mainly composed of Hydromica (90%), with smectite, kaolinite and vermiculite as minor components. X-ray diffraction (XRD) and X-ray fluorescence (XRF) were used to obtain further information about the composition of these alluvial saline soils in typical soil profiles.

Determining the profile

Tables 6 and 7 and Figure 6 show properties of soil collected in Xiaowang village, Nanpi County. The soil is characterised as moderately saline Chao soil; there is a shallow watertable at about 4 m. Changes in soil texture in the profile are obvious because of the influence of the alluvium of old and modern rivers. The profile studied is typical of the region.

Composition of clay minerals

XRD and XRF were used to determine the clay mineral composition. Figure 7 shows the pattern of XRD of clay fractions from soil samples treated with magnesium-saturated glycerol and air-dried. Samples were taken from five soil layers. Hydromica or illite (1 nm), smectite (1.83 nm), chlorite or vermiculite (1.42 nm and 0.353 nm), kaolinite and microcrystal quartz (0.426 nm) were found in every layer. Hydromica is the major mineral in the soil in this region; minor minerals include kaolinite, chlorite and montmorillonite; and trace minerals are microcrystal quartz and vermiculite. Amorphous material was not considered in this study. The mineral composition of the clay mineral was not closely correlated with soil texture. Chlorite and vermiculite had four feature peaks at the same position, but the two kinds of minerals can be roughly diagnosed by peak intensity.

Table 6. Some properties of soils in Nanpi County.

Depth (cm)	Texture	Consistency	EC (dS/m)	pH
0–15	L	Firm	0.89	8.11
15–35	L	Firm	0.94	8.22
35–75	SL	Soft	1.64	8.20
75–160	ZC	Rigid	1.16	8.23
160–250	S	-	0.72	8.37

EC = electrical conductivity; L = loamy; S = sand; SL = sandy loam; ZC = silty clay

Table 7. Properties of Chao soil at Xiaowang village, Nanpi County.

	Proportion of soil components (%)									
Depth (cm)	SiO_2	Al_2O_3	Fe_2O_3	TiO_2	MnO	CaO	MgO	K_2O	P_2O_5	Other
0–15	47	23	9	0.56	0.16	0.56	4.8	3.7	0.3	11
15–35	48	22	9	0.6	0.15	0.86	4.4	3.6	0.3	11
35–75	48	22	9	0.56	0.13	1.08	4	3.5	0.3	11.5
75–160	47	22	8	0.53	0.11	1.27	3.4	3.3	0.2	14
160–250	49	21	10	0.56	0.1	0.42	4.6	3.9	0.5	10

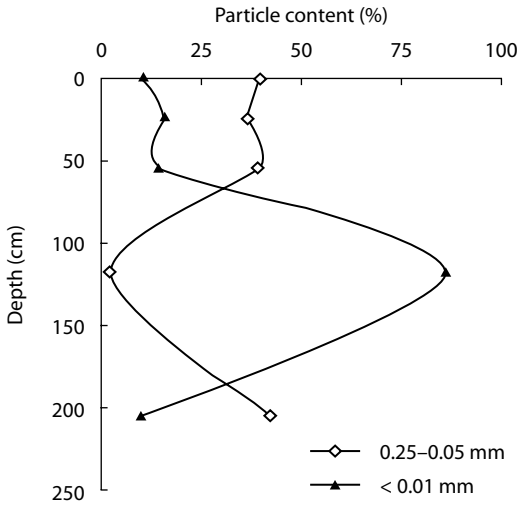

Figure 6. Distribution of different sized particles in Chao soil at Xiaowang village, Nanpi County.

A barium-saturated solution can also be used to see if the peak at 1.42 nm disappears or appears at 1.2 nm. Figure 8 shows the results for three soil layers. The peak beyond 1.42 nm disappeared, but peaks were otherwise similar to those in the magnesium–glycerin treatment: peak position did not change but peak intensity did. These data suggest that vermiculite is not very likely to occur in saline Chao soil.

Difference between soil layers

The theory of XRD requires the different peaks at 1.2, 1.4, 1.8, 2.4, and 3.2 nm to be adjusted by a weighting factor relative to the 1.0 nm peak so that peak intensities are strictly comparable. The PW 1800 XRD instrument (Philips) fitted with a variable automatic divergence slit can be used to approximately cancel out the influence of relatively broad peaks. The intensities of the diffractions of different layers suggested that the peaks of bottom-layer soil (160–250 cm) were the most intense and those of the clayey layer (75–160 cm) were the weakest in all layers. The data also indicated the decrease of crystallinity in finer grains. The peaks of higher-angle spacings were very weak or not obvious, which showed that crystallinity was poor and there were smaller amounts of interlayer minerals.

We examined the difference between the peaks of Ch_{d004} and Kl_{d002} in this diffraction. For clays in the bottom layer with a coarser texture, the intensity of the chlorite peak was higher than that of kaolinite; in other layers the reverse was true (see Figure 7). The clay minerals in each layer reflect the integrated effect of the parent material and the environment. The mineral composition and crystallinity in the bottom layer were similar to the loess parent material (Mao 1998), indicating that the material in this area came from the Loess Plateau. The clay minerals in the upper layers, however, were not very different from those in the bottom layer. The results also show that bioclimatic conditions have had little effect on the composition and changes of clay minerals during the short time for which there are records.

Effects of clay minerals on properties of saline soil

Aluminosilicate minerals with high amounts of exchangeable Na^+ (e.g. > 15%) can lead to dispersing in water. Illite (Hydromica) and smectites tend to disperse easily in soils with wide ranging electrolytic concentrations (Rengasamy and Sumner 1998). The content and properties (e.g. fine particle mixtures with < 0.2 μm) of the clay minerals in soils may influence the physical and chemical properties of colloids in soils. For example, in saline soils that are rich in available K^+, exchangeable Mg^{2+} may enhance the dispersion of illite by comparison with Ca. Soils of the NCP are known to tend to become alkaline in the process of losing salt; further research on the mechanism for this is needed.

Interpretation of Thematic Mapper Data

Thematic mapper (TM) data or images can provide information on the distribution of saline soils. Chapter 16 provides an introduction to Landsat Thematic mapper data. From previous work by Tian et al. (1995) using TM data from 1985, variation in the distribution and extent of saline

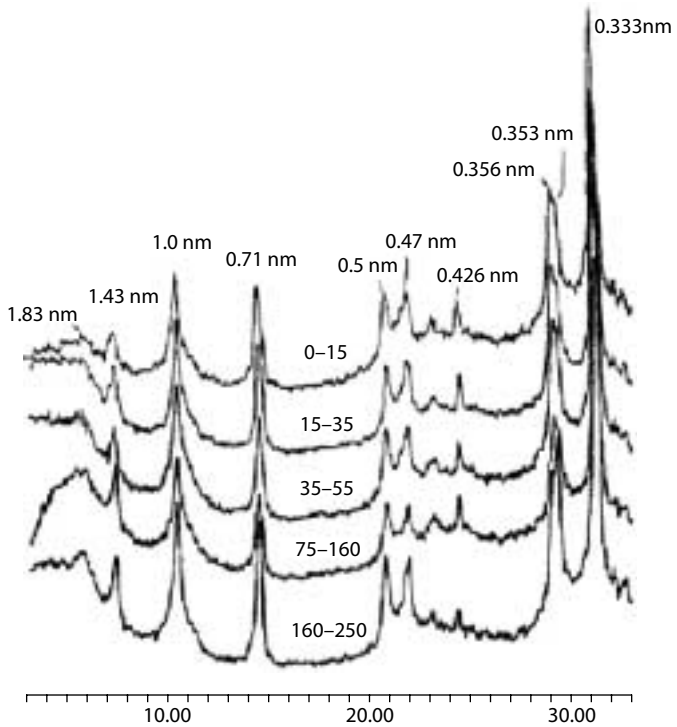

Figure 7. X-ray diffraction pattern of clay treated by magnesium–glycerol.

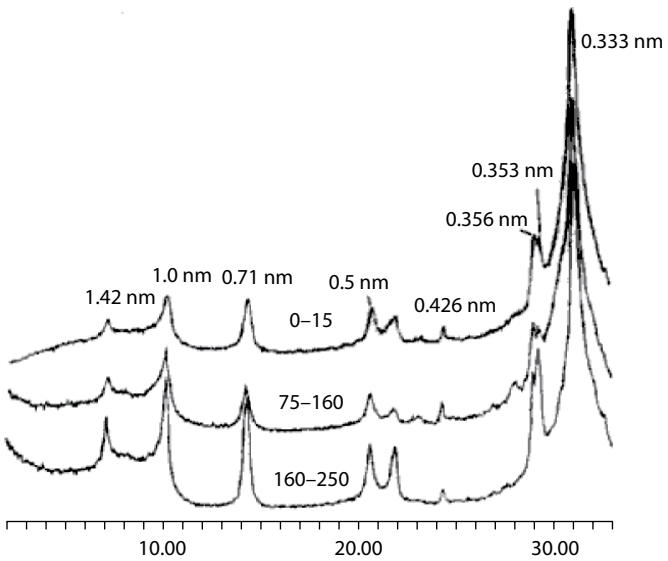

Figure 8. X-ray diffraction pattern of clay treated by barium.

soils patches was assessed for the Cangzhou prefecture from 1985 to 1997. After 1985, the area of the NCP covered by saline soils greatly decreased and salinity was reduced as water resources were fully used for irrigation. Table 8 shows the results of TM interpretation for an image acquired in 1997. In the southwest (Suning, Renqiu, Xian, Botou, Dongguang and Wuqiao), the dominant soils are slightly saline, accounting for 30% of the total area. In coastal areas (e.g. Huanghua, Haixing, Zhongjie and Dagang) there are large areas of moderately or severely saline soils.

Developing Strategies for Dealing with Saline Soils

The improvement and use of saline soils should take into account season, local conditions and type of crop, and combine specialised use with comprehensive control. Technical measures should be based on knowledge about the causes of saline soil and the principles of movement of water and water–salt. It is important to find solutions for the permanent control of salinisation as well as quick temporary solutions. Four main types of measures can be considered.

- *Controlling salt movement into soils*. The normal growth of crops prevents salt from going into the upper layers of the soil. Improved irrigation and drainage are required to control the rise of the groundwater table and environmental salt accumulation. For example, landwater could be irrigated with saltwater and freshwater alternately, surface mulch could be used or surface soils could be furrowed after rain.
- *Removing excessive salts*. In saline cultivated fields and/or grassland the normal growth of crops or grasses will be encouraged by measures that remove excessive salt from the soil — for example, using freshwater storage to leach salt out, removing the salt in the surface layer or replacing soil.

Table 8. Extent of soil salinity in Cangzhou Prefecture determined by Thematic mapper.

		Area affected (ha × 10^4)				
Location		Slightly saline	Moderately saline	Severely saline	Solonchak	Total
County	Huanghua	2.64	2.39	0.58	0.28	5.89
	Haixing	0.70	1.29	0.57	0.44	3.00
	Zhongjie	0.58	0.25	0.09	0.01	0.93
	Nandagang	0.43	0.43	0.14		1.00
	Yanshan	0.84	0.20			1.04
	Mengcun	0.62	0.22			0.84
	Qing	0.32	0.31	0.06	0.02	0.70
	Cang	1.03	0.23	0.04	0.03	1.33
	Nanpi	0.23	0.21	0.11	0.03	0.58
	Dongguang	0.29	0.13	0.03		0.45
	Wuqiao	0.11	0.03			0.14
	Botou	0.18	0.12			0.30
	Xian	0.52	0.37	0.08		0.97
	Hejian	0.42	0.24	0.01		0.67
	Renqiu	0.49	0.17			0.66
	Suning	0.14				0.14
Type of area	Coastal	7.12	5.31	1.48	0.78	14.68
	Middle and inland	2.42	1.28	0.23	0.03	3.96
	Total	9.54	6.59	1.71	0.81	18.65

- *Establishing a fertile soil layer*. An agronomic proverb says, 'The more fertiliser, the less saline-alkali soils.' Improving soil fertility and reducing salt in the surface layer will result in improvements in physical and chemical properties of the soil and in biological activity, with better soil structure, higher nutrient content and better self-regulating capacity. The movement of capillary water will also be restrained. Therefore it is necessary to reduce evaporation and salt accumulation in the surface soil to promote crop growth.

- *Adaptive cultivation of plants and crops*. Crops and grasses have different tolerance for salt in different water and salt environments, so selected crops or grasses must be cultivated on the basis of different types and salinities of soils. In addition, some agronomic measures are required — for example, delaying the time of seeding.

Using the appropriate technique for the degree of salinisation

Slightly salinised soils

Slightly salinised soils lie in the upper soil layers where there are good irrigation and drainage systems and surface or groundwater flows. In the study area, the groundwater was usually at 3–4 m, but sometimes at 5–8 m. Some shallow wells contain salty or slightly salty water that can be used to a limited extent. Cultivated lands that lack irrigation equipment could yield only 750–1500 kg/ha, in contrast to areas with irrigation systems that could yield about 6000 kg/ha. Poor physical properties are some of the main factors preventing crops from utilising saline soils. The key limiting factors are drought and reduced fertility. Techniques to improve the soil should therefore emphasise drought resistance, moisture preservation and soil fertility. Examples are:

- greatly exploiting water sources and water-saving irrigation, for instance by using moderately salty water, collecting local rainfall, introducing offsite water use or improving the capacity of the soil to retain moisture;

- fertilising soils to adjust the relationship between fertiliser and salt, for example by applying organic matter, feeding straw back to the soil, combining chemical fertiliser and manure or rotating cultivation to increase biomass and soil fertility;

- paying more attention to arid agricultural techniques to maximise crop yield under conditions of drought and salinisation, particularly by ploughing, harrowing and getting rid of weeds;

- regulating crop distribution, for example by selecting drought-resistant varieties or growing crops like corn, soybean, cotton and pasture; and

- covering the soil surface with plastic film to keep it warm and wet and to impede salt from moving up.

Moderately salinised soils

Moderately saline soils can be irrigated and drained to some extent, but cannot escape waterlogging in some wet seasons. The groundwater table in the study region was at about 2.5–3.5 m, with a large amount of salty water. Drought, low fertility and, especially, salinity were the main limiting factors. The following improvement techniques therefore concentrated mainly on cultivation and management in the better drainage systems:

- flattening land in order to reduce the effect of microrelief on salt accumulation;

- changing seeding practices to take better account of water and salt movements;

- applying fertiliser to soils to improve soil productivity and allow more suitable plants to be grown (e.g. the common green manure plants *Astragalus adsurgens* Pall, *Medicago sativa* L. and *Melilotus albus* Desr);

- regulating crop and grass distribution;
- covering the soil with plastic film and straw; and
- treating seeds with special biochemicals to protect seedlings from diseases and insect pests.

Severely salinised soils

Most severely salinised soils occur as large areas in coastal regions, but smaller patches are scattered away from the sea. These soils lie in low areas with poor drainage, where it is easy to accumulate water in wet seasons. The depth to groundwater was 0.5–1.5 m, but salty water that could not be used for irrigation was extensively distributed in the area. Improving the soil therefore focused on developing better drainage systems, pasture and husbandry rather than on crop cultivation. In particular, it focused on developing and using the existing natural pasture and introducing salt-tolerant plants for husbandry (e.g. *Puccinellia chinampoensis* Ohwi, reeds, *Bromus inermis* Leyss, *Elymus dahuricus* Turcz and *Festuca arundinacea* Schreb).

Developing Strategies for Dealing with Sodic Soils

In the past, the problem of sodic soil on the NCP seemed of low significance in comparison to the damage caused by salinity. Sodic soils have very poor physical and chemical properties and are more difficult to improve than saline soils. Therefore, integrated measures are needed to reclaim sodic soils, including the following measures:

- improving irrigation and drainage systems, and controlling the groundwater table;
- constructing field terraces (similar to bed farming) to conserve rainfall;
- applying fertilisers, in particular, combining chemical fertiliser with manure, to improve soil productivity;
- planting salt-tolerant grasses; and
- adding soil ameliorants (e.g. gypsum for neutralisation of sodicity).

Conclusions

Saline and sodic soils on the NCP present a serious problem for sustainable agricultural development. The area covered by saline soils has greatly decreased since 1980 but further improvements in soil and water management practices through both temporary and permanent measures are needed.

We need to develop a regional perspective that will allow the management of saline and sodic soils to be integrated into a comprehensive management package. This would aim to improve use of soil resources to increase crop yields and arrest the decline in soil quality. We can then develop models of soil processes and recommend strategies to ameliorate existing problems and prevent further damage to soils.

References

Mao, R. 1998. The clay mineral of Lou-soil in Wei-river basin and their spatial variations. Journal of Soil Erosion and Soil Water Conservation, 4(5), 92–97. (in Chinese)

Mao, R. and Liu, X. 2000. Study on the indicators for assessment of agro-eco-environmental quality in saline region of lower Haihe Plain. Eco-agriculture Research, 8(3), 59–62. (in Chinese)

Mao, R., Liu, X. and Han, S. 1999. The influence of water storage on groundwater and soil secondary salinization in Peri-Dalandian reservoir area. In: Tadano, T. and Tian, K. (eds.), Development of Technology for Sustainable Biological Production in Saline Soil Areas of Huang-Huai-Hai Plain in China. Proceedings of China-Japan Joint Symposium, Xian, China, 38–44.

Rengasamy, P. and Sumner, M.E. 1998. Processes Involved in sodic behaviour. 35–50. In: Sumner, M.E. and Naidu, R. (eds.). Sodic Soils: Distribution, Properties, Management and Environmental Consequences. Oxford University Press.

Tian, J., Mao, R., Matsumoto, S. and Yamazaki, S. 1995. Study on the evolution of the saline-alkaline land in Heilonggang region. ACTA Pedologica Sinica, 32(2), 228–234 (in Chinese).

Xiong, Y. and Li, Q. 1987. Soils in China. Beijing, Chinese Science Press (in Chinese).

14 The Effects of Soil Moisture and Nutrients on Cropland Productivity in the Highland Area of the Loess Plateau

Yinli Liang,* Shaozhong Kang† and Chenge Zhang*†

Abstract

Soil moisture and nutrient distribution, and their effect on cropland productivity in the tableland area of the Loess Plateau, were studied. For major crops, the following characteristics were investigated: sensitivity to water stress at different stages of growth, methods for improvement of crop water use efficiency and soil nutrient input and output of a cropland ecosystem in the tableland area of the Loess Plateau. This chapter discusses how soil fertility can be improved in a cropland ecosystem, the effects of fertiliser on crop productivity under different patterns of rainfall, how fertiliser use can be linked to productivity, optimum fertilisation and factors affecting the efficiency of fertiliser use. It describes key factors limiting cropland productivity and the main measures by which productivity can be increased in the tablelands of the Loess Plateau.

本文分析了黄土旱塬农田生产力的变化、土壤水分和养分分布特征及其对农田生产力的影响，研究了主要作物水分利用特征、不同生长阶段作物水分敏感性指数、以及提高作物水分利用率的途径；分析了黄土旱塬农田系统土壤养分的输入与输出特征，不同降雨年型肥料对作物生产力的效应；氮磷肥料的利用效率和影响因子，提出了改善农田生态系统土壤肥力的途径。最后，探讨了限制作物生产力的关键因子的变化以及提高农田系统生产力的主要措施配置，分析了黄土旱塬生产力的变化趋势。

* Institute of Soil and Water Conservation, Chinese Academy of Sciences and Ministry of Water Resources, Yangling, Shaanxi 712100, PRC.

† Key Laboratory of Agricultural Soil and Water Engineering in Arid and Semiarid Areas, Northwest Sci-Tech University of Agriculture and Forestry, Yangling, Shaanxi 712100, PRC. Email: kangshaozhong@163.net

Yinli Liang, Shaozhong Kang and Chenge Zhang. 2002. The effects of soil moisture and nutrients on cropland productivity in the highland area of the Loess Plateau. In: McVicar, T.R., Li Rui, Walker, J., Fitzpatrick, R.W. and Liu Changming (eds), *Regional Water and Soil Assessment for Managing Sustainable Agriculture in China and Australia*, ACIAR Monograph No. 84, 187–194.

THE HIGHLAND area of the Loess Plateau is situated in the central southern portion of the plateau. The Overview provides background information on the region; Figure 1 of the Overview shows its location. The climate is classified as a semihumid temperate zone with an average annual temperature of 7.0–13.5°C and a frost-free period of 140–230 days. Most areas can support three harvests over two years but some regions in the eastern part can achieve two harvests per year. Average annual precipitation is 500–600 mm, with wide variation between years and seasons, so the soil is frequently deficient in moisture. The area is a typical dryland farming area where agricultural production depends mainly on rainfall. Rainfall is concentrated in the period from July to September, so there is a water shortage in spring and winters are dry and cold. The soil is moderate loamy Heilu soil, formed from deep Malan loessial soil. It is suitable for dryland cultivation due to its porous nature and high capacity to hold water: 500–600 mm of rainfall can be stored in the top 2 m of soil in this region. The soil functions as a reservoir and is important in sustaining production of the staple crops, which are winter wheat and summer corn. These crops account for 70–80% of sowing in the region and 80–90% of food crop production.

Critical problems in agricultural production in the highlands are the small area of land available for growing crops, soil erosion, frequent drought and low crop yield.

The overall aims for ensuring food production in this small highland region, with many slopes and gullies, are:

- to improve the efficiency of water and land resource use, and increase productivity, by increasing fertiliser use through the combined application of manure, nitrogen (N) and phosphorus (P);
- to focus on soil moisture, nutrient cycling and nutrient balance in the cropland ecosystem;
- to investigate the theories and techniques of improving land productivity to promote development of the regional economy; and
- to investigate solutions to the problems of high population density, which places demands on land and water resources and the ecosystem.

The Effect of Soil Moisture on Cropland Productivity

Soil moisture characteristics

In the highland area of the Loess Plateau, most soil is loamy; its moisture capacity reaches 800–900 mm in the 0–200 cm layer because the soil has many interspaces. Precipitation is about 600 mm, so the soil's capacity to hold moisture constantly exceeds precipitation. The deep layer of water held in the soil makes the Loess Plateau a highly suitable environment for plant growth. To promote use of this deep soil moisture by crop roots requires an understanding of crop root growth and stage of development.

Productivity

The highlands of the Loess Plateau are typical dryland farming areas, where soil moisture and nutrients are the main factors limiting crop production. During 1986–90, crop productivity was low and the main limiting factor was soil fertility rather than soil moisture; yields were improved mainly by increasing fertiliser. During this period, lack of nutrients led to a decrease in the yield of winter wheat (by 29.3–54.6%) and of summer corn (by 5.2–35.6%). Fertiliser use gradually improved soil fertility and in 1991–95 low fertility was responsible for only a 1.6–2.8% decrease in yield, with soil moisture the main factor limiting productivity. In 1986–91, moisture shortage led to a fall in the yield of winter wheat (of 3.0–17.9%) and of summer corn (of 4.6–21.7%). However, in 1992–95, the effect of low soil moisture was greater, causing yield to fall by 5.9–75.2% in winter wheat and by 13.3–72.8% in summer corn.

Historically, fertiliser input in the Loess Plateau region has been low; in large areas of the region fertiliser input is currently insufficient because of economic constraints. Thus, nutrient stress is a limiting factor for improving productivity in the long term. However, water shortage is becoming more important than nutrient stress as a limiting factor for productivity, particularly in regions where initial productivity is high and the rural economy is relatively active.

The Effect of Soil Nutrient Distribution on Cropland Productivity

Soil nutrient distribution in the highlands of the Loess Plateau

Table 1 shows the soil nutrient distribution in the highlands of the Loess Plateau. The coefficient of variation for each nutrient is large, particularly for available P and potassium (K). Overall, the soil is low in organic matter, N and P, but rich in K.

Table 1. Soil nutrient distribution in croplands in the highlands of the Loess Plateau.

	Range	Average
Organic matter	4.78–13.94 g/kg	9.45 g/kg
Nitrogen	0.410–1.055 g/kg	0.75 g/kg
Available nitrogen	34.0–74.9 mg/kg	53.7 mg/kg
Available phosphorus	0–25.3 mg/kg	6.3 mg/kg
Available potassium	88.2–367.3 mg/kg	175.1 mg/kg

Effect of nutrient on cropland productivity

Use of N fertiliser improved the yield of winter wheat. Studies from 1984 to 1995 on Heilu soil showed that adding N increased winter wheat yield by 84.8–186.7% (average 135.5%) (Liang et al. 2000). The increase in wheat yield per kilogram of N was 6.9–27.1 kg (average 17.0 kg). However, as the quantity of added N increased, the impact on yield decreased. The effect of N fertiliser was also related to the quantity of P added. If enough P was used, N had a greater effect on yield and the decrease in impact with increasing amounts of N was less marked.

The use of P fertiliser improved winter wheat yield in Heilu soil by 0.3–48.4% (average 26.8%). The increase in wheat yield per kilogram of P was 6.3 kg. The effect of P was much greater if it was used together with N, as shown in Table 2. Similarly, the effect of N was greater when combined with P. N combined with P fertiliser produced a wheat yield of 2233–3495 kg/ha (average 3049 kg/ha) — an average increase of 139.6% when compared to using no fertiliser, of 25.4% compared to using only N and of 25.4% compared to using only P.

Table 2. Effect of combining nitrogen and phosphorus fertiliser.

	Increase in yield (%)		
	Nitrogen fertiliser (kg/ha)		
Phosphorus fertiliser (kg/ha)	0	90	180
90	0.3	29.5	39.1
180	2.2	34.9	48.4

Sensitivity of Different Growth Stages of Major Crops to Water Stress

Limited-water irrigation and optimal management of limited water resources is based on variation in the sensitivity of different growth stages of a crop to water stress. Little is known about the water sensitivity of different stages of winter wheat and summer corn on the semiarid Loess Plain. The Jensen multiplication model (Jensen 1986) describing water sensitivity is more sensitive and more practical than the addition model in China (Kang and Dang 1987). Hence, we used the Jensen multiplication model to determine the relation between crop yield and water consumption (Jensen

1986). Taking the relative evaporation at each growth stage (i) as the independent variable, the effect on crop yield can be expressed as follows:

$$\frac{Y_a}{Y_m} = \prod_{i=1}^{n} \left(\frac{ET_a}{ET_m} \right)_i^{\lambda_i} \quad (1)$$

where Y_a is actual crop yield, Y_m is maximum crop yield if sufficient water is present, n is the ordinal number of the growth stage, ET_a is actual evapotranspiration, ET_m is maximum evapotranspiration and λ_i is the crop water sensitivity index of each growth stage (that is, the extent to which crop yield is affected by any water deficit). For this model, a high value of λ_i indicates a large reduction in crop output. Hence, λ_i is the crucial parameter in the model.

The aim of this study was to determine changes in water sensitivity for winter wheat and summer corn during the entire growth season, and propose an optimum water supply schedule for these crops in the Loess Plateau region.

Field experiments were conducted in plots sheltered from rain, at the Changwu Agro-Ecological Station of the Chinese Academy of Sciences on the Loess Plateau during 1995–97. Figure 4 of the Overview shows the location of Changwu; the station is approximately 1200 m above sea level. The mean temperature is 9.0–9.5°C and mean annual precipitation is 548 mm.

The crops studied were winter wheat (variety Changwu 134) and summer corn (variety Danyu 13). For each crop, we investigated the soil moisture level and the stage at which the crop was irrigated. Three levels of soil moisture were tested: low (D) with a relative water content of 45–55%, medium (Z) with a relative water content of 55–70%, and high (G) with a relative water content of 75–85%. Water treatment stages differed for the two crops. Development of winter wheat was divided into five stages: seedling (early October to early March), vegetative (early March to early April), jointing (early April to early May), heading (early May to early June) and the milk phase. Development of summer corn was divided into four stages: jointing (mid-June to mid-July), preheading (mid-July to early August), flowering (early to late August) and the milk phase (late August to late September). A total of 15 different irrigation treatments were tested in winter wheat and summer corn, using a random design with two replications for each treatment. Plots were watered regularly according to soil moisture content. Before ploughing, N and P were sprinkled on the soil surface at rates of 138 kg/ha and 112.5 kg/ha, respectively.

Time-domain reflectometry (TDR) was used to measure the soil water content at 15-day intervals. Crop water use was calculated from the soil water content measured at each growth stage. Crop yield was determined at maturity. The least squares difference method was used to test significant difference and the Jensen model was used to calculate crop water sensitivity at different growth stages.

Determination of crop water sensitivity

Data from the field experiments were used to calculate relative evapotranspiration from different growth stages and relative yield from different irrigation treatments using the Jensen model and the following equations (Equation 2 is for winter wheat in 1995–96; Equation 3 is for summer corn in 1996–97):

$$\frac{Y_a}{Y_m} = \left(\frac{ET_{a1}}{ET_{m1}} \right)^{0.253} \times \left(\frac{ET_{a2}}{ET_{m2}} \right)^{0.024} \times \left(\frac{ET_{a3}}{ET_{m3}} \right)^{0.17} \times \left(\frac{ET_{a4}}{ET_{m4}} \right)^{0.07} \times \left(\frac{ET_{a5}}{ET_{m5}} \right)^{0.014} \quad (2)$$

$$\frac{Y_a}{Y_m} = \left(\frac{ET_{a1}}{ET_{m1}} \right)^{0.0936} \times \left(\frac{ET_{a2}}{ET_{m2}} \right)^{0.2097} \times \left(\frac{ET_{a3}}{ET_{m3}} \right)^{0.1989} \times \left(\frac{ET_{a4}}{ET_{m4}} \right)^{0.026} \quad (3)$$

Water sensitivity at different stages

Equation 2 shows that the water stress index λ_i varied greatly among the different growth stages of winter wheat. The stage from seedling to vegetative had a high λ_i value and was crucial for the crop. The λ_i value was lowest during the vegetative to jointing stage because the plants were relatively small at this stage and the temperature was low, so the plants grew slowly. Winter wheat grows rapidly from the jointing to the heading stage when leaves and stems and reproductive growth occur simultaneously. Leaf area increased rapidly at this stage and the weather became warmer, giving a high level of transpiration from the leaves. Thus, water deficit in this period greatly affected yield and the value of λ_i was high. The water stress index was also high from the heading to milk stage. This period is crucial for seed formation, so water deficit affects reproductive growth. During the milk to mature stage, plant leaves begin to turn yellow, transpiration decreases and the effect of water deficit on yield is reduced. The λ_i value at this stage was low; this was expected because oversupply of water in this period delays maturity. Overall, the seeding to vegetative stage was the most sensitive to water deficit, followed by the jointing to heading stage, the heading to milk stage, the milk to mature stage and the vegetative to jointing stage.

Equation 3 shows that the water stress index varied greatly among the different growth stages of summer corn. For the reasons given above for winter wheat, the λ_i value was low during the early period of nutritive growth before jointing but was high after jointing, due to nutritive and reproductive growth and increasing temperatures. The λ_i value was also high in the heading to milk stage, which is crucial to yield. During the milk to mature stage, the effect of water deficit on yield decreased, again for the reasons given above for winter wheat.

Irrigation efficiency and water use efficiency of crops under limited water supply

At different stages of growth, water deficit affects yield differently. Table 3 shows that a yield of 4500 kg/ha can be achieved with some water deficit. Controlled water deficit can benefit the output of winter wheat. For a target yield of 4500–5000 kg/ha, soil moisture should be sufficient before winter and at particular stages during the growth period. Of greatest benefit to output were alternate medium and high water treatments during the early period and water stress treatment during the late milk stage. For a target yield of 3750–4500 kg/ha, at least one stage of sufficient soil water during the whole growth period is needed. Alternate medium and high water treatments during earlier stages and water stress at a later stage were beneficial to yield. For a target output of less than 3750 kg/ha, there could be two stages of water stress treatment during the whole growth period.

Among the treatments in which the yield was higher than 3750 kg/ha, two alternating serious water-deficit stages gave a noticeably higher yield than did two continuous serious water-deficit stages. There were remarkable positive relationships between biomass and irrigation volume ($r = 0.82$, $n = 15$) and with grain yield and irrigation volume ($r = 0.82$, $n = 15$). During the seeding stage, there were also positive relationships between biomass and irrigation volume and between grain yield and irrigation volume ($r = 0.75$, $r = 0.74$, $n = 15$): irrigation during the seeding stage was important to promote early vigour, for the plant to live through winter safely and to gain high yield.

This was contrary to previous results, which showed two critical water sensitive stages for winter wheat: the first from the mother cell quartet of pollen to pollen forming stage, the second from the beginning of milk stage to the milk mature stage (Shan 1996). There are two possible reasons for this. First, the experimental treatments were different. Our study began water treatments before winter, when the seedling was incomplete; we used different drought degree treatments; and we divided the soil water treatment into five stages during the whole growth period. The previous study began most water treatments when the seedling was complete

Table 3. Effect of irrigation volume on irrigation efficiency (IE) and water use efficiency (WUE) of winter wheat, 1996–97.[a]

Treatment[b]	Yield (kg/ha)	Irrigation (mm)	WU[c] (mm)	IE (kg/ha/mm)	WUE (kg/ha/mm)
D-D-D-D-D	2025	97	213	20.88	9.5
D-D-D-G-Z	3180	187	300	17.00	10.6
D-G-Z-D-D	3375	167	278	20.21	12.1
G-D-Z-G-Z	3405	269	385	12.66	8.8
Z-Z-Z-Z-Z	3570	241	359	14.8	9.9
D-Z-D-D-Z	3705	183	291	20.2	12.7
Z-D-D-Z-G	3870	241	338	16.1	11.5
Z-G-D-D-G	4020	281	387	14.3	10.4
Z-G-Z-D-D	4080	216	323	18.9	12.6
G-G-D-Z-D	4230	268	389	15.8	10.9
D-Z-G-Z-G	4245	302	403	14.1	10.5
G-G-G-G-G	4500	408	519	11.0	8.7
Z-Z-G-G-D	4500	302	420	14.9	10.7
G-Z-G-D-Z	4575	257	383	17.8	11.9
G-Z-G-G-D	4920	306	390	16.1	12.6

[a] Each value is the mean of four measurements from separate plots
[b] D = low soil moisture with soil relative water content at 45–55%; Z = middle soil moisture with soil relative water content at 55–70%; G = high soil moisture with soil relative water content at 75–85% for the five winter wheat growth stages introduced previously.
[c] WU = water quantity used (mm)

(after winter and the start of vegetative growth) and strong, and used different periods and degrees of water treatment. Second, our study was conducted in highland and gully regions in the semiarid environment of the Loess Plateau; this area is typical dry farmland, and drought was the main obstacle to crop production. We considered it important for winter wheat to have early vigour, grow strongly, live through winter safely and give a high yield (Liang and Richards 1999). The previous study focused on high yield rather than on water saving and high water use efficiency. If a grain yield of more than 3750 kg/ha is desired, the total water use should be 320–420 mm, with an irrigation volume between 260 mm and 300 mm at the seedling stage and before flowering; this will produce a high yield and a high irrigation efficiency.

Table 4 shows that there were great differences in the grain yield of summer corn under different water treatments. The yield was lowest under sustained water stress and highest when there was sufficient irrigation during the total growth period of summer corn; the yield under light water stress was between these two extremes. Alternating water supply to the soil had different effects on grain yield in corn. Yield was lowest when plants suffered from serious water stress at all four growth stages; when three growth stages suffered from serious water stress, the yield was lower than when only two stages suffered such stress; similarly, when two stages suffered from serious water stress, the yield was lower than when one stage suffered from such stress during the growth period. Moreover, the yield depended on which stage was affected: water stress

Table 4. Effect of irrigation volume on irrigation efficiency (IE) and water use efficiency (WUE) of corn, 1995–96.[a]

Treatment[b]	Yield (kg/ha)	Irrigation (mm)	WU[c] (mm)	IE (kg/ha/mm)	WUE (kg/ha/mm)
D-D-D-D	4370	136	218	32.1	20.1
Z-D-D-D	5216	186	286	28.0	18.2
Z-D-D-Z	5643	174	256	32.43	22.4
D-Z-Z-Z	6219	254	342	24.5	18.2
Z-D-Z-Z	6228	270	360	23.1	17.3
Z-Z-D-Z	6572	335	416	19.6	15.8
Z-Z-Z-D	6905	220	322	31.4	21.4
Z-Z-Z-G	7497	259	357	28.9	21.0
Z-G-Z-Z	7497	277	370	27.1	20.3
G-Z-Z-Z	7641	383	473	20.0	16.2
Z-Z-Z-Z	7991	277	370	28.8	21.6
Z-Z-G-Z	8244	391	515	21.1	16.1
Z-G-G-G	8945	492	564	18.2	15.9
G-G-G-G	9371	554	661	16.9	14.2
Z-G-G-Z	10,062	447	526	22.5	19.1

[a] Each value is the mean of four measurements from separate plots
[b] D = low soil moisture with soil relative water content at 45–55%;
Z = middle soil moisture with soil relative water content at 55–70%;
G = high soil moisture with soil relative water content at 75–85% for the four summer corn growth stages introduced previously
[c] WU = water quantity used (mm)

had a greater effect on yield after jointing and from the heading to milk stage than from the milk to mature stage. Grain yields of more than 7000 kg/ha could be obtained for corn when there was only light water stress if no serious water stress occurred at any time during the growth period.

Discussion

In the areas where water was limited, the central task was to save water while obtaining a high yield efficiently. The main objective of optimising or managing limited water resources is to increase the economic yield per unit water volume (Aston and van Bavel 1972; Blank 1975; Liang and Richards 1999; Shan 1996; Steinberg and Henningger 1997).

The results showed an obvious relationship between yield and irrigation volume. Moreover, for wheat yield, irrigation volume produced different effects at different stages of plant growth. Yield was most affected when seedlings were irrigated before March; irrigation at the jointing to heading stage produced the next greatest effect. The effect of irrigation at the vegetative to jointing stage and after the milk stage was relatively unimportant.

Crop sensitivity to water stress was relatively high. The water stress sensitivity index, λ_i, was relatively large at the seedling stage but relatively low during the vegetative to jointing stage. The λ_i value increased after the jointing stage and was also high during the heading to milk stage, but began to decrease during the milk to mature stage (Equation 2). The reason may be that the seedling stage is the crucial stage for root elongation and root system development. Liang and Kang (2000) studied the relationship between photosynthetic and soil water

deficit at different growth stages; the highest ratio of photosynthetic sensitivity to soil water deficit occurred at the booting to heading stage. At this time, the temperature was relatively high, water consumption was relatively large, water requirements were urgent and there was an increased sensitivity to water deficit. This suggests that water deficit affects not only photosynthesis, but also grain yield. The yield would be little affected if water stress occurred after the vegetative or milk stages, but would be affected greatly if the water stress occurred after the jointing or heading stage. Thus supplementary irrigation should be arranged, if possible, for the seedling and jointing to heading stages. If soil water content during the seedling stage is sufficient for the formation of a strong seedling, irrigation should be applied if possible at the booting to heading stage rather than at other stages.

The water sensitivity index λ_i of summer corn also differed at different growth stages. It was relatively low before jointing, and it was high after the jointing stage and during the heading to milk stage; however, it began to decrease during the milk to mature stage. Water stress before jointing or after the milk stage had little effect on yield, but water stress after the jointing or heading stage affected the yield greatly. Hence, the heading stages should be given the highest priority for irrigation, followed by the after-jointing stage.

Soil nutrient input and output of cropland ecosystems

The soils of most cropland areas in the Loess Plateau region contain insufficient N for wheat and corn. In addition, there is not enough P available in the soil to satisfy crop needs. Consequently, both N and P are added in fertiliser. The soils of the Loess Plateau are rich in K, so K fertiliser is not usually applied.

Studies at Changwu Agro-Ecological Station from 1984 to 1995 have shown that the efficiency of fertiliser use depends on precipitation. The fertiliser use efficiency for N was 6.4–58.6% (average 35.3%, coefficient of variation 48.7%); for P, the figure was 3.7–19.8% (average 14.2%, coefficient of variation 39.5%).

The fertiliser use efficiency for N and P depended on the quantity of fertiliser used. For P fertiliser (phosphorus oxide, P_2O_5) applied at 90 kg/ha and N fertiliser applied at 45–180 kg/ha, the fertiliser use efficiency was 25.4–42.9% (average 36.3%) in wheat.

Main Conclusions

Long-term research on the Loess Plateau has shown that cropland productivity depends on many production factors. If fertility or water were limiting factors for the crop, the yield depended on time, space and productivity level. This was not the case for dryland farming areas, in which increased fertiliser application was the key to increasing yield and water use efficiency under certain water conditions. As productivity improves, water becomes more important in determining yield.

References

Aston, A.R. and van Bavel, C.H.M. 1972. Soil surface water depletion and leaf temperature. Agronomy Journal, 64:368–373.

Blank, H. 1975. Optimal irrigation decision with limited water. Colorado State University, PhD thesis.

Jensen, M.E. 1986. Water consumption by agricultural plants. In: Kozlowski, T.T., ed., Water Deficits and Plant Growth. New York, Academic Press, 1–122.

Kang, S.Z. and Dang, Y.H. 1987. Study on crop water production function and optimal irrigation scheme. Water Resource Sciences, Boreali-Occidentalia Sinica, 1, 1–11.

Liang, Y.L. and Richards, R.A. 1999. Seedling vigor characteristics among Chinese and Australian wheat. Communications in Soil Science and Plant Analysis, 30, 159–165.

Liang, Y.L. and Kang, S.Z. 2000. Effect of no full irrigation on physiological characters of wheat on Loess Plateau. In: J.M. Laflen, ed., Soil Erosion and Dryland Farming. US, CRC Press, 131–136.

Liang, Y.L., Dang, T.H. and Zhang, C.E. 2000. Cropland ecosystem productivity research on Loess Plateau. Xi'an, Shaanxi Science and Technology Press, 143–168.

Shan, L. 1996. The study on limited water efficient utilization in dry land. Research of Soil and Water Conservation, 3(1), 8–13.

Steinberg, S.L. and Henningger, D.L. 1997. Response of the water status of soybean to change in soil water potential controlled by the water pressure in micro-porous tubes. Plant Cell and Environment, 20, 1506–1516.

15 Element Mobility in a Mediterranean Environment

Jim W. Cox*

Abstract

When saline groundwater discharge areas are drained there is always concern over the level of salt within the discharge water. In this study, groundwater discharge rates and quality were measured in an erosion gully that drained a catchment with saline, sodic and acid sulfate-like soils (typical of discharge areas in the Mount Lofty Ranges, South Australia).

The research determined that contaminants other than sodium chloride will be of concern if discharge areas are drained. Even in very low rainfall years, drainage water contained up to 41 kg/ha/year of sodium but also 2 kg/ha/year of sulfur. Losses of sulfur, magnesium and calcium followed a similar trend to sodium losses. The losses of phosphorus were 0.005–0.007 kg/ha/year and nitrate losses were up to 0.002 kg/ha/year.

土地退化形成侵蚀沟，成为地下水渗出区的排水通道，水中含盐量的高低值得关注。在一个侵蚀沟测量了土壤水分的渗出率及其质量。该流域分布有盐土、碱土和硫酸类土，渗出的水流进入沟道排走。该沟在阿德莱德丘陵农业区具有代表性。研究发现，如果有排水系统，则除了氯化钠之外，其它的污染物也值得注意。即使在降水量很少的年份，水中钠的年含量高达每公顷 41 千克、硫的年含量为每公顷 2 千克。硫、镁、钙的流失趋势同钠的相似。磷年流失量是每公顷 0.005 – 0.007 千克，氮多达每公顷 0.002 千克。

THE VOLUME of sodium chloride that is discharged into streams as a result of rising saline groundwaters in the agricultural regions of southern Australia is well documented (e.g. Schofield et al. 1988). The transport of nutrients such as phosphorus (P) and nitrate from agricultural catchments to waterways has also received a lot of attention in the international literature because of their environmental implications (Costin 1980; Greenhill et al. 1983;

* CSIRO Land and Water, PMB 2, Glen Osmond, SA 5064, Australia. Email: jim.cox@csiro.au

Cox, J.W. 2002. Element mobility in a Mediterranean environment. In: McVicar, T.R., Li Rui, Walker, J., Fitzpatrick, R.W. and Liu Changming (eds), *Regional Water and Soil Assessment for Managing Sustainable Agriculture in China and Australia*, ACIAR Monograph No. 84, 195–202.

Haygarth and Jarvis 1996; Nash and Murdoch 1997). Of particular concern is the eutrophication of water bodies caused by P attached to clay (e.g. Sharpley and Syers 1979; Sharpley et al. 1994).

In the > 600 mm annual rainfall region of the Mount Lofty Ranges, salt and colloids have recently been shown to be transported both over and through texture-contrast soils via overland flow and throughflow, respectively (Fleming and Cox 1998; Stevens et al. 1999). In the region of the Mount Lofty Ranges with < 600 mm annual rainfall, Pitman et al. (1998) showed that, over three years with average rainfall or less, overland flow was less than 1% of annual rainfall and was shed only from the lower slopes (near the drainage gullies). Thus contaminants are infrequently transported in large quantities via overland flow in these environments.

The removal of evergreen native vegetation for grazing in the Mount Lofty Ranges has significantly increased recharge to the fractured rock aquifer. Up to 20% of annual rainfall leaches below the root zone, even in below-average years (Pitman et al. 1998). Groundwaters have risen to the land surface in low-lying areas and brought sodium (Na) and sulfur (S) from the weathered schist regolith (Cox et al. 1996). Highly corrosive, acid-sulfate conditions have then formed (Fitzpatrick et al. 1996; Brown 1997). These conditions reduce the stability of the soils and result in gully formation. The gullies then drain these soils (Cox 1998).

Engineering options (e.g. drainage schemes) are being installed in some areas to rapidly lower shallow saline groundwaters. However, the biogeochemical and physical processes that are taking place in saturated, saline soils in groundwater discharge zones will vary depending on soil type, the nature of the groundwaters and the period of saturation (Fitzpatrick et al. 2000).

This study assessed the likely impacts on water quality of draining waterlogged, saline, sodic and sulfidic soils in the Mount Lofty Ranges. The volume and quality of drainage water in an erosion gully cutting through a series of these soils were studied over three years. The aim was to gain a better perspective of the relative quantities of salt and colloids being exported from agricultural catchments in low-rainfall agricultural environments.

Materials and Methods

Site and climate

The Overview provides some background information on the Mounty Lofty Ranges. The study was carried out in the Keynes catchment, near Keyneton, from 1994 to 1996. The catchment is located in the uppermost western part of the Murray–Darling Basin. Drainage flows southwest out of the catchment, then east to the Murray River (a major water supply for Adelaide). Climate, vegetation, soils and landscape features are typical of those throughout the Mount Lofty Ranges. A pluviometer attached to a weather station continually monitored rainfall and also measured evaporation (Table 1). The long-term (previous 30 years) average rainfall at Keyneton is 544 mm (Bureau of Meteorology). From May to September, rainfall exceeds potential evaporation by a total of 185 mm.

Vegetation, soils and hydrology

Native vegetation has been cleared from most of the catchment. A mix of grasses, subterranean clover (*Trifolium subterraneum* L.) and cocksfoot (*Dactylis glomerata* L.), with invasions of salvation jane (*Echium plantagineum* L.), storksbill (*Erodium moschatum* L.) and soursob (*Oxalis pes-caprae* L.), is now grazed by sheep and cattle.

The texture-contrast soils (Northcote 1960; Chittleborough 1992) of the catchment have formed over metasediments. They consist of 30–40 cm of sandy loam (A horizon) overlying an argillic layer; the clay content of the B horizon is 20% greater than the overlying layer. The A horizon has

Table 1. 1994–96 and long-term (30-year average) rainfall and potential evaporation (mm) at Keyneton.

	J	F	M	A	M	J	J	A	S	O	N	D	Annual
Rainfall													
1994	20	1	4	6	28	119	18	27	25	29	22	5	304
1995	48	15	13	37	37	67	121	9	48	58	9	5	467
1996	47	8	30	10	10	132	84	80	73	53	15	7	549
Long-term rainfall (mm)[a]	18	23	20	35	62	64	80	76	63	49	29	25	544
Potential evaporation													
1994	183	139	149	81	50	21	40	44	68	100	101	168	1144
1995	150	126	95	47	20	16	9	21	47	66	98	112	807
1996	127	96	77	35	27	39	17	25	46	77	97	120	783
Potential evaporation (mm)	139	108	97	53	30	23	26	32	49	73	89	119	838

[a] Long-term rainfall and potential evaporation data from the Bureau of Meteorology

a low water-holding capacity and a high saturated hydraulic conductivity; it is acidic to neutral (McMurray 1994; Pritchard 1998). The B horizon has a fine texture and generally low permeability but in places is 'leaky' due to macropores (Kirkby et al. 1997; Pritchard 1998). The B horizons are alkaline. The soils in the catchment receive 15 kg/ha of superphosphate each year. The soils are mostly a series of Chromosols, Sodosols and Dermosols (Isbell 1996) or Xeralfs (Soil Survey Staff 1996), from Typic Palexeralfs on the crests through Aquic Palexeralfs on the mid-slopes to Natrixeralfs on the lower slopes and flats (McMurray and Cox 1995). A gully cuts through and drains areas of acid sulfate-like soils that have formed in the valley (Brown 1997).

A concrete triangular profile flat-V weir (Bos 1976) was installed in an erosion gully draining approximately 200 ha of the catchment (Fig. 1). Stage height was recorded every 10 minutes for three years using a Dataflow Pty Ltd capacitance probe attached to a single channel data-logger.

Flow rates were calculated in litres per second (L/s) using Equation 1 (Bos 1976):

$$Q = C_d C_v \frac{4}{15}(2g)^{0.5} \frac{B}{H_b}(h_e)^{2.5} \qquad (1)$$

where Q is the flow rate (L/s), C_d is the discharge coefficient (0.66), C_v is the approach velocity coefficient (1.0), g is the gravitational acceleration (9.8 m/s^2), B is the channel surface width (m), H_b is the height of the crest (m), and h_e is the adjusted height of water over the weir crest in metres calculated from the formula $h_e = h_1 – K_h$ where h_1 is the measured height of water in metres and K_h is a constant (0.0008 m).

Pitman et al. (1998) collected runoff and throughflow off fifteen 50 × 50 m plots in the catchment (Fig. 1) over a three-year period (which included the wettest year of this study). They showed that in years with average rainfall or less, overland flow in the catchment was less than 1% of annual rainfall, throughflow was up to 8% and

groundwater recharge reached 20%. Thus gully drainage must be predominantly groundwater discharge with some throughflow. We therefore measured groundwater levels continuously in a piezometer located in the valley, using a capacitance probe and data-logger (Dataflow Pty Ltd; Fig. 1).

Water chemistry and loads

Water samples were collected on 53 occasions at all stages of flow (from rising limb to recession) by grab sampling from the centre of the stilling well when the gully was flowing across the weir. Samples were prepared and analysed as per Cox and Pitman (2001). Total chemical loads were calculated by multiplying the chemical concentration by the discharges between sampling periods, and then by integration of the load versus time curve.

Results

Rainfall

In the first year of the trial, annual rainfall was 304 mm (44% below average), but June rainfall was twice the average due to one exceptionally large rainfall event (61 mm/day). In the second year of the trial, there was 468 mm of rain, which was 14% below average. Unusually high falls (up to 30 mm/day) were measured in January and February. The last year of the trial had the highest rainfall (548 mm), although it was only about average; the wettest month was June.

Groundwater levels

Groundwater levels were lowest (about 394 m above the Australian Height Datum) in May of each year. Seasonal rises in groundwater levels were 1.2, 1.4, and 1.9 m each year, reflecting seasonal rainfall levels for the respective years.

Gully flows

Below-average rainfall in the first year resulted in relatively low flows (< 100 L/second), with one exception. The maximum flows occurred at the beginning of July, which corresponded to the highest daily rainfall event of that year (61 mm).

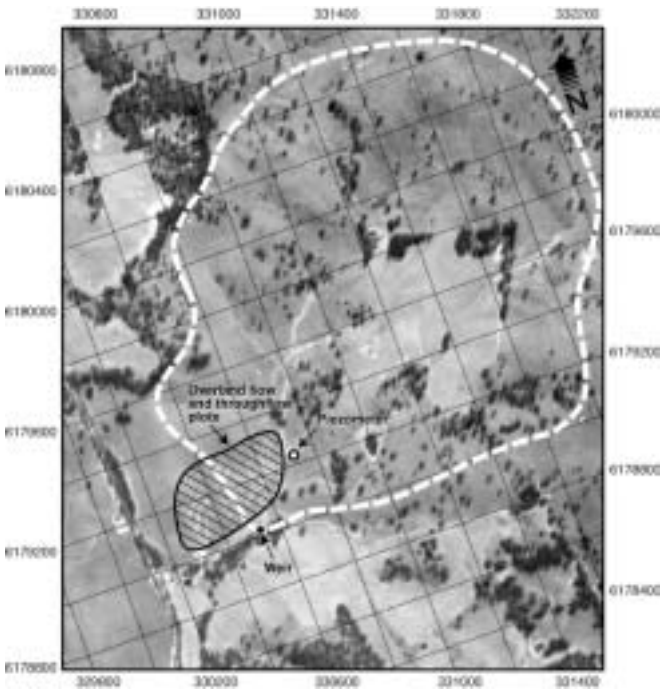

Figure 1. Location of catchment area, gully, weir, piezometer and overland flow/throughflow plots (from Cox and Ashley 2000).

Total flow in the first year was 9.8 megalitres (ML) (2.3% of catchment annual rainfall). Annual gully flow (***Flow***) was well correlated with seasonal changes in groundwater levels (***S***, m; Equation 2).

$$\boldsymbol{Flow} = 3.87 \times 10^6 \, e^{0.877 \cdot \boldsymbol{S}}, \; r^2 = 0.808 \qquad (2)$$

The impact of relatively high rainfall in January (48 mm) and July (121 mm) in the second year could be seen in the change in flows. Two relatively high flows were recorded in January (230 and 120 L/second); an extreme flow (710 L/s) was recorded on 23 July in the second year. Total flow was 15.7 ML (2.4% of catchment rainfall). Total flow in the last year was 19.5 ML (2.5% of catchment rainfall). The maximum flow occurred on 14 March (640 L/s).

The low r^2 values showed that, in general, there was no relationship between daily rainfall and daily flow over the three years [daily gully flow = 3.9 × daily rainfall (mm) + 15.1, $r^2 = 0.138$; daily gully flow = 2.78 × previous day rainfall (mm) + 17.4, $r^2 = 0.070$] or between monthly rainfall and flow. However, the relationship between annual gully flow (***Flow***) and annual rainfall (***P***, mm) (3 measurement points only) was clearer:

$$\boldsymbol{Flow} = 4.16 \times 10^6 \, e^{0.0028 \cdot \boldsymbol{P}}, \; r^2 = 0.999 \qquad (3)$$

The data imply that even in very low rainfall years the storage capacity of the highly weathered regolith is exceeded and the excess water is discharged through the gully system.

Seasonal changes in electrical conductivity and acidity of the discharge waters

The gully water was generally alkaline (around pH 8.5) but had slightly lower pH (about 8.3) in the wettest year. One rapid drop in pH (to 7.5) must have been due to a major volume of throughflow (fresh perched water) entering the gully, because it corresponded with the lowest electrical conductivity. At this time, discharge was high (310 L/s). Large changes were measured in the electrical conductivity of the gully drainage waters between winter and summer each year. Electrical conductivity was high at the start of each season — around 30 decisiemens per metre (dS/m) — but dropped to about 5 dS/m each winter. The electrical conductivity was lowest (2 dS/m) in the winter of the third year. Electrical conductivities generally tended to be lowest in the wettest winters and highest in the driest summers.

Chemical concentrations

Table 2 summarises the average total nutrient and chemical concentrations in gully flow. Concentrations of sodium (Na), magnesium (Mg), sulfur (S) and calcium (Ca) were always higher than those of other chemical species. Average Na concentrations in the first year were higher (2800 mg/L) than Mg (317 mg/L), S (198 mg/L), Ca (103 mg/L) or K (961 mg/L). This pattern was repeated each year. The average concentration of most contaminants was highest in the driest year (1994).

Table 3 is a summary of the annual loss (kg/ha/year) of chemicals in gully flow and shows that high chemical concentrations (Table 2) do not always mean high losses of these chemicals, because they can form during periods of low flow. The greatest losses of Na, Mg, S and Ca were 41, 4.5, 1.9 and 1.4 kg/ha/year, respectively. The trends in losses of Na, Mg and Ca over time were similar to that of S, which shows that the processes leading to loss of these chemicals are similar.

Na losses were highly correlated with Mg ($r^2 = 0.993$), S ($r^2 = 0.984$) and Ca ($r^2 = 0.804$); the relationships between these parameters were similar in all years (Table 4).

Average phosphorus (P) concentrations were similar each year (0.9, 0.6 and 0.5 mg/L; Table 2). Annual P loss was low, 5–7 g/ha (Table 3), but concentrations were of environmental concern. P loss was usually very high during the most intense gully flows, but there was no significant relationship

($P < 0.05$) between P loss and gully flow. In contrast to the other nutrients, the average nitrate nitrogen (NO_3-N) concentrations were clearly highest (0.6 mg/L) in the driest year and lowest (0.1 mg/L) in the wettest year. Annual NO_3-N losses were 2–10 g/ha. There was no relationship between daily NO_3-N loss and gully flow.

Discussion

Gully flow was very sporadic, with long periods of little or no flow. Some very high rainfall events caused high gully flow, but in general there was no relationship between daily rainfall and daily flow over the three years of monitoring. This was because most flow in the gully was groundwater discharge, with some throughflow. There are time lags between rainfall and the groundwater discharge and throughflow entering the gully. On one occasion, gully flow was due mostly to runoff (overland flow and throughflow) as groundwater levels were very low. Total annual gully flow (catchment discharge) was similar each year (2.3%, 2.4% and 2.5% of rainfall) and reflected both the slight differences in annual rainfall and the annual change in groundwater levels.

Table 2. Average total salt concentrations in gully discharge.

	Average concentration (mg/L)		
Chemical or nutrient	1994	1995	1996
Sodium	2797.7	1985.6	2020.5
Magnesium	316.8	232.3	215.7
Sulfur	198.1	112.3	103.3
Calcium	102.9	90.9	91.9
Potassium	60.9	46.4	44.2
Phosphorus	0.94	0.59	0.53
Boron	0.61	0.65	0.44
Nitrate	0.57	0.30	0.11
Iron	0.15	0.09	0.11
Zinc	0.13	<0.05[a]	<0.05[a]
Aluminium	<0.05[a]	0.26	<0.05[a]
Manganese	<0.05[a]	<0.05[a]	<0.05[a]

[a] Level of detection

Table 3. Total chemical and nutrient loads in gully discharge.

	Total load (kg/ha/year)		
Chemical or nutrient	1994	1995	1996
Sodium	23.7	41.4	23.4
Magnesium	2.70	4.49	2.85
Sulfur	1.34	1.93	1.16
Calcium	1.32	1.22	1.35
Potassium	0.51	0.87	0.53
Phosphorus	0.005	0.007	0.005
Boron	0.006	0.011	0.007
Nitrate	0.010	0.009	0.002
Iron	0.008	0.013	0.03
Zinc	0.002	0.002	0.002
Aluminium	0.011	0.018	0.004
Manganese	0.0008	0.005	0.001

Table 4. Relationships between sodium (Na) and magnesium, sulfur and calcium loads in gully discharge (g/ha/year).

Element	1994	1995	1996	All years
Magnesium	0.116xNa–0.997 r^2=0.997	0.107xNa+0.048 r^2=0.996	0.126xNa–0.064 r^2=0.998	0.120xNa–0.181 r^2=0.993
Sulfur	0.056xNa–0.045 r^2=0.991	0.044xNa+0.189 r^2=0.965	0.051xNa+0.010 r^2=0.995	0.049xNa+0.058 r^2=0.984
Calcium	0.077xNa–0.570 r^2=0.697	0.020xNa+0.408 r^2=0.548	0.064xNa+0.001 r^2=0.989	0.053xNa–0.185 r^2=0.804

The gully drainage chemistry changed markedly over the three years of the study, partly due to the water pathways (groundwater recharge, throughflow and some overland flow) and water residence (lag) times. Changes in pH of the gully drainage were sometimes very rapid. In contrast, there was relatively little change in electrical conductivity of the gully drainage each winter. However, considerable changes were measured at the start of each winter season (probably due to the flushing and evaporation of salt) and at the end of winter (probably due to the concentration of salt).

Concentrations of Na, Mg, S and Ca were far higher than those of other contaminants. The loss of Na was one order of magnitude higher than the levels reported by Fleming and Cox (1998) for runoff from dairy catchments in the high-rainfall zone of the Mount Lofty Ranges, whereas Mg, S and Ca losses were similar. Mg, S and Ca behaved like Na; losses of these chemicals can be predicted with good accuracy from measurement of Na only.

P losses (5–7 g/ha/year) were two orders of magnitude lower than those reported by Fleming and Cox (1998) and Nelson et al. (1996) for grazed catchments in the high-rainfall zone of the Mount Lofty Ranges. The annual P losses were one order of magnitude lower than those reported in agricultural runoff in New South Wales by Costin (1980), or by Greenhill et al. (1983) in overland flow from perennial pastures in Victoria. P was always in the soluble form, probably because it does not enter the gullies as overland flow but moves through the soil (in both throughflow and recharge) into the gullies. Also, the hypersaline conditions probably cause flocculation of P, which attaches to colloids and is trapped in the gully (the gully sediments are high in P). P concentrations were about 100 times higher than those considered acceptable for the health of upland stream ecosystems (ANZECC and ARMCANZ 1999).

Conclusion

Gully discharge from the Keynes catchment in the Mount Lofty Ranges in low rainfall years was hypersaline and, just as importantly, had high levels of S, P, NO_3-N and other elements. It is expected that in higher rainfall years, when overland flow causes erosion and scouring of the gully, losses of some of these contaminants will be orders of magnitude higher. Thus, if drainage systems are installed in discharge areas, they must be designed to regularly filter fine (solutional) contaminants in low rainfall years as well as colloidal material during (the less frequent) erosive events.

Acknowledgments

Graham and Melanie Keynes allowed us to use their farm for the research.

References

ANZECC (Australian and New Zealand Environment and Conservation Council) and ARMCANZ (Agriculture and Resource Management Council of Australia and New Zealand). 1999. Australian and New Zealand Guidelines for Fresh and Marine Water Quality. National Water Quality Management Strategy. Public comment draft, July 1999. Canberra, ANZECC and ARMCANZ.

Bos, E.G. 1976. Discharge Measurement Structures. International Institute for Land Reclamation and Improvements Publication 20. The Netherlands, International Institute for Land Reclamation and Improvements, 197–203.

Brown, B. 1997. Transportation of the salts required in the formation of acid sulphate soils through a saline rocky microcatchment. University of Adelaide, BSc Honours thesis.

Chittleborough, D. 1992. Formation and pedology of duplex soils. Australian Journal of Experimental Agriculture, 32, 15–25.

Costin, A.B. 1980. Runoff and soil and nutrient losses from an improved pasture at Gininderra, Southern Tablelands, New South Wales. Australian Journal of Agricultural Research, 31, 533–546.

Cox, J.W. 1998. Land clearance changes on the hydrology of a toposequence as predicted by soil morphology. Proceedings of the 16th World Congress of Soil Science, Montpellier, France, 20–26 August 1998. (CD-ROM)

Cox, J.W., Fritsch, E. and Fitzpatrick, R.W. 1996. Interpretation of soil features produced by modern and ancient processes in degraded landscapes: VII. Water duration. Australian Journal of Soil Research, 34, 803–824.

Cox, J.W. and Ashley, R. 2000. Water quality of gully drainage from texture-contrast soils in the Adelaide Hills in low rainfall years. Australian Journal of Soil Research 38, 959–972.

Cox, J.W. and Pitman, A. 2001. Chemical concentrations in drainage from perennials grown on sloping duplex soils. Australian Journal of Agriculture Research, 52, 211–220.

Fitzpatrick, R.W., Fritsch, E. and Self, P. 1996. Interpretation of soil features produced by ancient and modern processes in degraded landscapes: V. Development of saline sulfidic features in non-tidal seepage areas. Geoderma, 69, 1–29.

Fitzpatrick, R.W., Merry R.H. and Cox, J.W. 2000. What are saline soils and what happens when they are drained? Journal of the Australian Association of Natural Resource Management, June, 26–30.

Fleming, N.K. and Cox, J.W. 1998. Chemical losses off dairy catchments located on a texture-contrast soil: carbon, phosphorus, sulfur and other chemicals. Australian Journal of Soil Research, 36, 979–995.

Greenhill, N.B., Peverill, K.I. and Douglas, L.A. 1983. Nutrient loads in surface runoff from sloping perennial pastures in Victoria. New Zealand Journal of Agricultural Research, 26, 503–506.

Haygarth, P.M. and Jarvis, S.C. 1996. Pathways and forms of phosphorus losses from grazed grassland hillslopes. In: Anderson, M.G. and Brooks, S.M., eds, Advances in Hillslope Processes. Vol 1. London, John Wiley and Sons Ltd., 283–294.

Isbell, R.F. 1996. The Australian Soil Classification. Melbourne, CSIRO Publishing.

Kirkby, C.A.K., Smythe, L.J., Cox, J.W. and Chittleborough, D.J. 1997. Phosphorus movement down a toposequence from a landscape with texture-contrast soils. Australian Journal of Soil Research, 35, 399–417.

McMurray, L. 1994. Soil properties associated with waterlogging down concave and convex toposequences. Adelaide University, BSc Honours Thesis.

McMurray, L.S. and Cox, J.W. 1995. Soil morphological features down a convex toposequence: Keyneton, South Australia. Adelaide, South Australia, CRC for Soil and Land Management, Technical Report 2/95, 22.

Nash, D. and Murdoch, C. 1997. Phosphorus in runoff from a fertile dairy pasture. Australian Journal of Soil Research, 35, 419–429.

Nelson, P.N., Costsaris, E. and Oades, J.M. 1996. Nitrogen, phosphorus and organic carbon in streams draining two grazed catchments in the Mt. Lofty Ranges, South Australia. Journal of Environmental Quality, 25, 1221–1229.

Northcote, K.H. 1960. A factual key for the recognition of Australian soils. Adelaide, CSIRO.

Pitman, A., Cox, J.W. and Bellotti, W.D. 1998. Water usage and dry matter production of perennials down a duplex toposequence. Proceedings of the 9th Australian Agronomy Conference, Charles Sturt University, Wagga Wagga, 20–23 July 1998.

Pritchard, J. 1998. Modelling the water balance of duplex soils at Keyneton, Mt Lofty Ranges, SA. Adelaide University, BSc Honours Thesis.

Schofield, N.J., Ruprecht, J.K. and Loh, I.C. 1988. The impact of agricultural development on the salinity of surface water resources of south-western Australia. Perth, Water Authority of Western Australia, Report WS27, 69.

Sharpley, A.N. and Syers, J.K. 1979. Phosphorus inputs into a stream draining an agricultural catchment. Water Air and Soil Pollution, 11, 417–428.

Sharpley, A.N., Chapra, S.C., Wedepohl, R., Sims, J.T., Daniel, T.C. and Reddy, K.R. 1994. Managing agricultural phosphorus for protection of surface waters: Issues and options. Journal of Environmental Quality, 23, 437–451.

Soil Survey Staff. 1996. Keys to Soil Taxonomy. 7th edition. Washington DC, United States Department of Agriculture, United States Government Printing Office.

Stevens, D.P., Cox, J.W. and Chittleborough, D.J. 1999. Phosphorus, nitrogen and carbon movement over and through duplex soils in sub-catchments of the Adelaide Hills. Australian Journal of Soil Research, 37, 679–693.

16

An Introduction to Temporal-Geographic Information Systems (TGIS) for Assessing, Monitoring and Modelling Regional Water and Soil Processes

Tim R. McVicar* Phil J. Davies†, Yang Qinke‡ and Guanglu Zhang§

Abstract

In this chapter we introduce the concept of temporal-geographic information systems (TGIS). We first describe some nontemporal concepts of GIS, consider the issues of scale and of continuous and discrete data, and give a brief background to the basis of remote sensing measurements. Using the concept of the 'data construct' as a tool for understanding TGIS data structures, we explain the relationship between characteristics (extent, resolution and density) and domains (attribute, spatial and temporal) of each dataset. Finally, we discuss two emerging issues in TGIS: the assessment of spatial–temporal accuracy and uncertainty, and the use of metadata systems.

我们在本章引入了时态地理信息系统（TGIS）的概念。首先解说 GIS 的非时间概念，考虑了尺度问题、连续数据与离散数据问题，简单介绍了遥感测量的物理背景。从数据构建概念入手，说明 TGIS 数据结构。阐明了每套数据特性（范围、精度和密度）与域性（属性、空间和时间信息）的关系。最后，探讨了 TGIS 中的两个议题：时间空间精度的评估和不确定性，标准格式的数据系统的应用。

* CSIRO Land and Water, PO Box 1666, Canberra 2601, Australia. Email: tim.mcvicar@csiro.au

† CSIRO Land and Water, PMB 2, Glen Osmond, SA 5064, Australia.

‡ Institute of Soil and Water Conservation, Chinese Academy of Sciences and Ministry of Water Resources, No. 26 Xinong Road, Yang Ling, Shaanxi Province, 712100, PRC.

§ Chinese Academy of Sciences, Shijiazhuang Institute of Agricultural Modernisation, PO Box 185, Shijiazhuang 050021, PRC.

McVicar, T.R., Davies, P.J., Yang Qinke and Guanglu Zhang. 2002. An introduction to temporal-geographic information systems (TGIS) for assessing, monitoring and modelling regional water and soil processes. In: McVicar, T.R., Li Rui, Walker, J., Fitzpatrick, R.W. and Liu Changming (eds), *Regional Water and Soil Assessment for Managing Sustainable Agriculture in China and Australia*, ACIAR Monograph No. 84, 205–223.

IN THIS CHAPTER we provide background information on some of the techniques that are used to assess the sustainability of regional agricultural systems that are described in subsequent papers in this section. We introduce the concept of temporal-geographic information systems (TGIS) and explain how remote sensing data can be used to generate information for GIS monitoring.

Most readers of this book will have already heard the term 'GIS', which usually connotes analysis in the spatial domain. However, to assess the sustainability of agricultural systems, the temporal domain is also needed; we use the term TGIS to describe this concept. The benefit of using this slightly nonstandard term is that the reader immediately contemplates both the spatial and temporal domains. The concept of adding a temporal element is essentially similar to the notion of integrating remote sensing into GIS (IGIS), proposed by Quattrochi (1993). Theoretical and technical aspects of data integration arising from the inclusion of time in GIS are discussed in detail by Langran (1992), Peuquet (1994, 1995) and Mitasova et al. (1995).

Scale, resolution and extent

Many different definitions of the term 'scale' are in common use in the TGIS community (Quattrochi 1993; Bian 1997; Cao and Lam 1997), and among other agricultural scientists and policy makers who use output from TGIS. The confusion that this situation creates can sometimes be overcome by using the terms 'resolution' or 'extent' rather than scale. Below, we describe some of the different ways in which the term 'scale' is used, and show why alternative terms may be preferable or qualify what is meant by 'scale'.

- 'Cartographic scale' or 'map scale' refers to the ratio first used in the production of paper maps. For example, a cartographic scale of 1:1000 means that 1 mm on the map represents 1 m (1000 mm) on the ground; whereas 1:1,000,000 means that 1 mm on the map represents 1 km (1,000,000 mm) on the ground.
- 'Geographic scale' is a term often used by noncartographic scientists to describe area. In this sense, a large study area is said to have a large scale. The term 'extent' is preferable to 'scale' for describing the size of a study area (which is sometimes referred to by ecologists as the 'spatial domain').
- A third meaning of scale is that of resolution — the smallest element (or grain) that can be distinguished. For example, the resolution of an electronic microscope is much finer than that of a traditional optical microscope, and one minute is a finer measure of time than one hour.
- Finally, and most applicable to TGIS analysis and modelling, there is 'operational scale' or 'process scale'. For example, a single wheat plant operates on a smaller spatial extent than a wheat field.

Time can also be the scalar; for example, a tree will usually have a longer temporal extent than an individual wheat plant. Hence, in a spatial–temporal construct, a tree occupies a larger volume than does a wheat plant. Put simply, trees usually live longer and are bigger than wheat plants. Obviously, in this tree–wheat example, the different life forms are operating at different spatial and temporal scales. Thus, a model generated at one scale may not be totally applicable at another scale (i.e. a model generated for trees may not be applicable to wheat plants). Although this may be obvious in the above example, in complex environmental modelling it is not always easy to determine whether scaling up or down from one extent–resolution domain to another is appropriate. For example, is the model developed for a single tree relevant for modelling a stand of trees or a forest? The answer to this question depends on which process is modelled (which in part determines the transferability of the model across scales) and on data availability. Many models

developed for small spatial extents (usually short temporal extents) are 'data-hungry' and are not easily applied to larger spatial extents (usually longer temporal extents). Chapter 1 discusses the question of extrapolating from one scale to another with respect to water balance models.

An area of active research in the disciplines of pedology and hydrology is the aptness of 'upscaling' (going from small to large, in space and/or time, by crossing geographic scales) and 'downscaling' (from large to small). The terms 'upscaling' and 'downscaling' are not equivalent to the terms 'aggregating' or 'disaggregating', respectively (Bloschl and Sivapalan 1995). Upscaling and downscaling involve a fundamental change in approach in the TGIS modelling, whereas aggregating implies combining a scale of measurement and disaggregating implies splitting it. For example, crop yield can be aggregated from a district to a county level simply by adding the district level values together; this is routinely performed on the North China Plain (Chapter 18). Weekly rainfall totals can be disaggregated into daily values using some knowledge of rainfall patterns.

In the original definitions of scale relevant to TGIS (Lam and Quattrochi 1992), the concepts of resolution and extent were, by default, both included in 'geographic scale'. Later modifications (Bian 1997; Cao and Lam 1997) differentiated geographic scale into the related concepts of resolution and extent. To give a spatial example of the concept of extent, the whole of China is a large spatial extent (or 'patch of dirt'). The entire country could not be modelled using 10 m (fine resolution) grid data because the data volumes would be too large to store on current computing hardware and processing would take too long. It is more likely that China would be modelled with 1000 m (coarse resolution) grid data. In terms of temporal extent, processes of soil genesis, which occur over a long time (a large extent) obviously require coarser measurements and descriptions of temporal resolution than do within-season crop water-use processes, which occur over a period of a few months (a short extent).

In hierarchy theory — a type of multilevel modelling used in ecology and landscape ecology — temporal and spatial scales tend to covary in relation to one another. That is, processes that operate over large areas usually occur over long periods, and processes that operate over small areas usually do so over short periods (Bloschl and Sivapalan 1995), as in the tree–wheat example given above. However, this principle does not hold for all environmental sciences. For example, extreme climatic events such as hurricanes and typhoons occur over large areas and have a relatively short duration. Therefore, the cartographic notion of a minimum mapping unit, which is spatial, needs to be extended for TGIS to include a temporal component. The minimum element in TGIS, in both space and time, needs to be placed in the context of both the operational (or process) scale and the resolution (and hence extent) of the study. If the two are not matched, a trend may go undetected because any signal measured will be influenced by the overlay of processes occurring at different spatial and temporal resolutions (and hence extents). Thus, if the resolution in space or time is too small, the process studied will appear as noise and any trend in either time or space will not be evident. On the other hand, if the resolution is too large, an established process may only appear as a slowly varying trend.

TGIS has many different environmental applications. Recent reviews include urban systems (Mesev 1997), agrometeorology (Maracchi et al. 2000), rural land use and associated changes in soil condition (Sommer et al. 1998), drought (McVicar and Jupp 1998), aquatic botany (Lehmann and Lachavanne 1997), hydrologic processes (Gurnell and Montgomery 1998; Rango and Shalaby 1998), regional evapotranspiration (Kustas and Norman 1996), atmospheric processes (Bernard et al. 1998), geomorphology (Butler and Walsh 1998) and oceanographic fisheries (Santos 2000). A common

feature of most reviews is the extensive use of remote sensing for what are often considered as two different tasks: monitoring the environment and updating GIS. Here, we consider these two tasks as identical operations.

Geographic Information Systems

Geographic location is a key component of GIS, which themselves are a subset of information systems. There are many information systems that make little or no use of geographic location. For example, in those used by banks and other financial institutions the quantity (i.e. how much money there is) is the main attribute of interest (pardon the pun). However, as such systems become more complex, the temporal components (e.g. calculating interest rates and compound returns on long-term investment strategies) become more important, because quantity depends on factors such as time since a deposit was made or when a loan was established.

Types of data

In GIS, map-type data can be stored digitally, displayed visually and integrated with other data sets. One way to visualise data is as vectors. Vector data are commonly points, lines or polygons, with one, or more, attribute(s) associated with the geographic feature of interest. Examples of point data are meteorological data measurements (e.g. air temperatures, rainfall and solar insolation) and soil pH at a location accurately determined using global positioning system (GPS) technology. Linear data include features such as road, rail and river networks. Attributes associated with a road could be whether it is paved or not and how wide it is. Polygon data are usually thematic maps that include attributes such as administrative boundaries, land use and land cover. Point-based measurements can be interpolated[1] to generate polygon data. For example, soil pH data recorded at many points can be spatially interpolated to produce a map of soil pH.

GIS data are either continuous or discrete (discontinuous). For example, pH units, (which are continuous from 1 to 14) may be stratified into several discrete pH ranges (e.g. $<$ 5.0, 5.0–8.0 and $>$ 8.0) in order to assess the land capability for potential agricultural uses. Although the extent of any of the three domains (attribute, spatial and temporal) may be equal, the continuous or discontinuous nature of the data needs to be known if it is to be used effectively in spatial–temporal analysis (Heuvelink and Huisman 2000).

Spatial analysis

In GIS, different attributes for the same geographic area are separated to allow for spatial analysis. For example, Figure 1 shows five different attributes of the landscape (or 'real world' in GIS terminology) — climate, vegetation, soil, geology and digital elevation. When these five attributes are overlaid, and the landscape stratified into unique combinations, 14 different hydrothermal regions are identified.

An important distinction in GIS is that between land cover and land use. For example, in an area designated 'State forest', the land use is forestry; however, the land cover, which in this case would be mainly forest, may vary from 100% (e.g. old-growth forest) to 0% (e.g. roads or areas which have been clear-felled), with a range in between. Many of the variables mapped in GIS are exclusive; that is, the data are thematic, with each area belonging to one class or another. However, there are several examples where spatial data are not exclusive but depend on the user's perspective. For example, the most valuable asset of a State forest could be its provision of clean water or maintenance of biodiversity (through providing a habitat for flora and fauna). Thematic maps, simulation outputs and all products generated from TGIS need to be

[1] In GIS, the term 'interpolation' refers to values of an attribute at unsampled points being estimated from measurements made at surrounding sites.

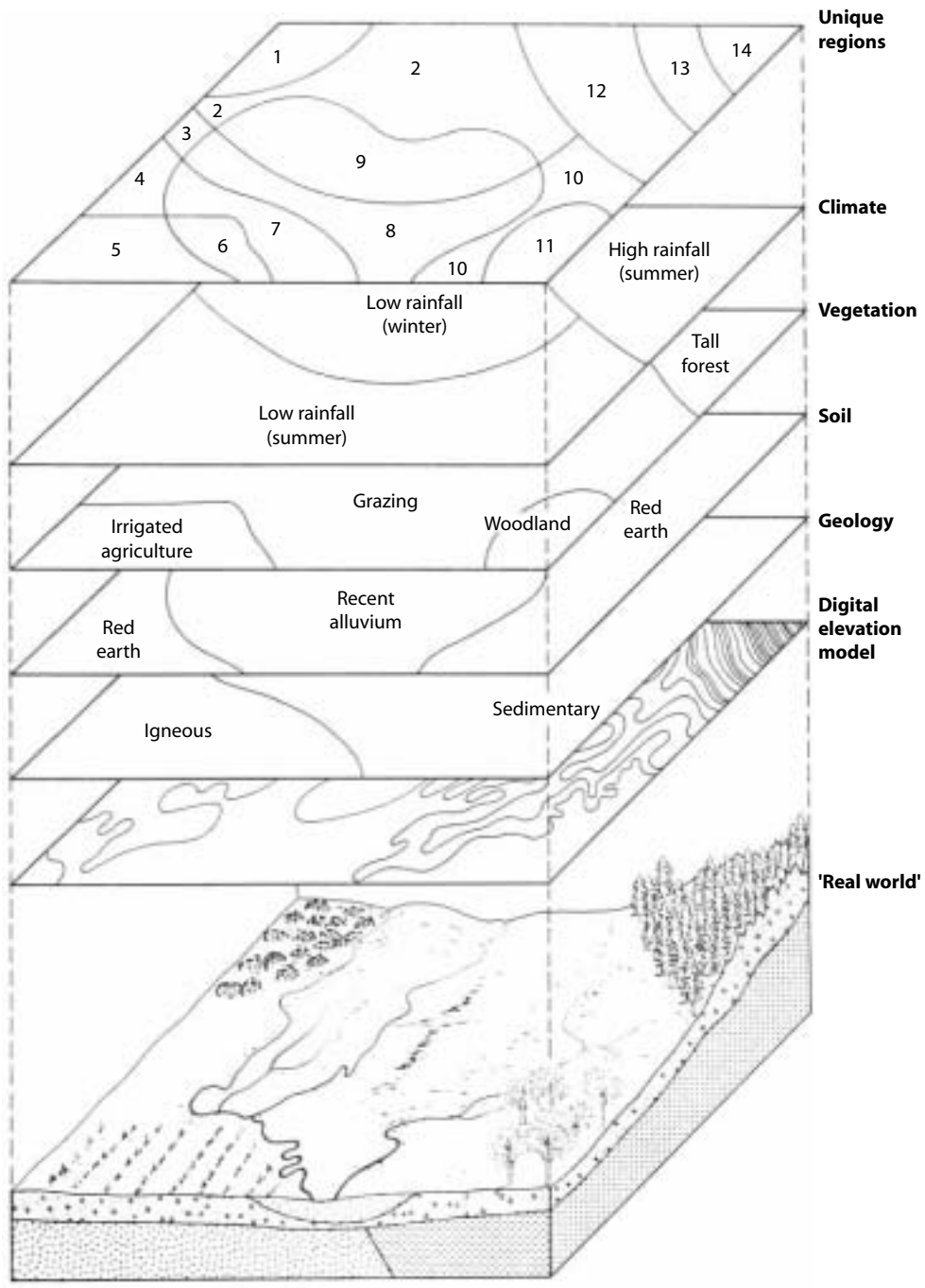

Figure 1. GIS landscape stratification of unique regions, based on five attributes (climate, vegetation, soil, geology and digital elevation model).

critically evaluated because the conclusions can be strongly influenced by the perspective of the user, the accuracy of the data and even the very nature of the data.

Currently, many researchers with point models wish to add a 'spatial dimension'. Three common ways to add a spatial dimension are described below.

- 'Area-weighting' (AW) was first used in the late 1960s and early 1970s; it is simply the multiplication of a response (e.g. crop yield), based on its proportion of a larger area, which is assumed to be homogeneous (Fig. 1).
- The 'interpolate then calculate' (IC) approach involves interpolating all driving parameters and variables, and simulating an output for an entire landscape by running the model at many points, with a given spatial resolution over a given spatial extent. This can be a daunting task given the resolution and extent of the study area, the time interval and length of simulation runs, and the number of parameters and variables.
- 'Calculate then interpolate' (CI) is a recent approach that is gaining popularity. Stein et al. (1991) introduced CI and found that it was preferable to the IC approach; Bosma et al. (1994) came to the same conclusion in the case of small samples. Bechini et al. (2000), estimating global solar radiation in northern Italy, reported that mean square errors using the CI approach were only about half those calculated using the IC method. Chapter 19 discusses the use of a CI approach to estimate moisture availability within the Murray–Darling Basin (MDB).

The AW approach allows remotely sensed data (discussed in detail below) to be classified to provide a potentially rich source of polygon data. Remotely sensed data are usually classified into discrete land-cover classes; these may be amalgamated to land-use classes and then integrated with other data layers in GIS. Remote sensing is stored in a raster (grid) data format; this type of format is most suited to spatially continuous data sets (where each grid cell can be thought of as a discrete element), such as those collected by remotely sensed data sources. Other interpolated data sets, such as digital elevation models (DEMs) or climate surfaces (e.g. monthly maximum and minimum air temperatures and rainfall), may also be stored as rasters.

Remote Sensing

'Remote sensing' is the term used for the acquisition of digital information describing characteristics of the Earth's surface. It involves measuring the electromagnetic spectrum (EMS) using satellite, aircraft or ground-based systems. Characteristically, the information is obtained at a distance (or 'remote') from the target — hence the name. Sensors on board numerous satellites and aircraft can be used in the assessment of sustainable agriculture. In this section we provide some general background information on remote sensing and describe different techniques involved, drawing heavily on material presented by McVicar and Jupp (1998).

Remote sensing data are obtained as digital recordings of the signal strength from specific portions (channels or bands) of the reflective, thermal or microwave portions of the EMS. Figure 2 shows how a satellite records such data. Some satellites orbit the Earth at approximately 700 km, while others are geostationary, located above the equator at some 36 000 km. Computer analysis of the digital images can highlight features of soils and vegetation. Each pixel (picture element) contributing to the image is a measurement of a particular wavelength of electromagnetic radiation at a particular spatial resolution for a particular location at a particular time (minute, hour, day, month and year).

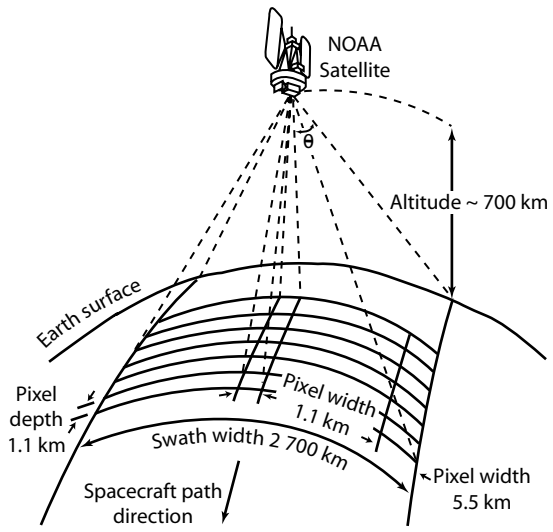

Figure 2. How satellites record data from the Earth's surface (adapted from Harrison and Jupp 1989), specifically NOAA-AVHRR, outlined in Table 1.

Remote sensors can distinguish different types of land cover (e.g. green grass, fine sandy loam and water) by their spectral properties, as shown in Figure 3. This allows the different land covers to be classified (i.e. mapped as separate classes). Remote sensing instruments vary in their ability to resolve the EMS signal. Figure 3 shows the spectral properties of different surfaces as measured by four different sensors. In two of the four cases (Hyperion and MSS) the attribute (spectral) response is continuous; however, because the resolution and extent of the data obtained are very different, the two sensors provide different attribute responses for any particular surface (Table 1). Hyperion, which records 196 calibrated channels, each with a 10 nm spectral resolution, is regarded as a hyperspectral sensor; while MSS is considered a broadband sensor.

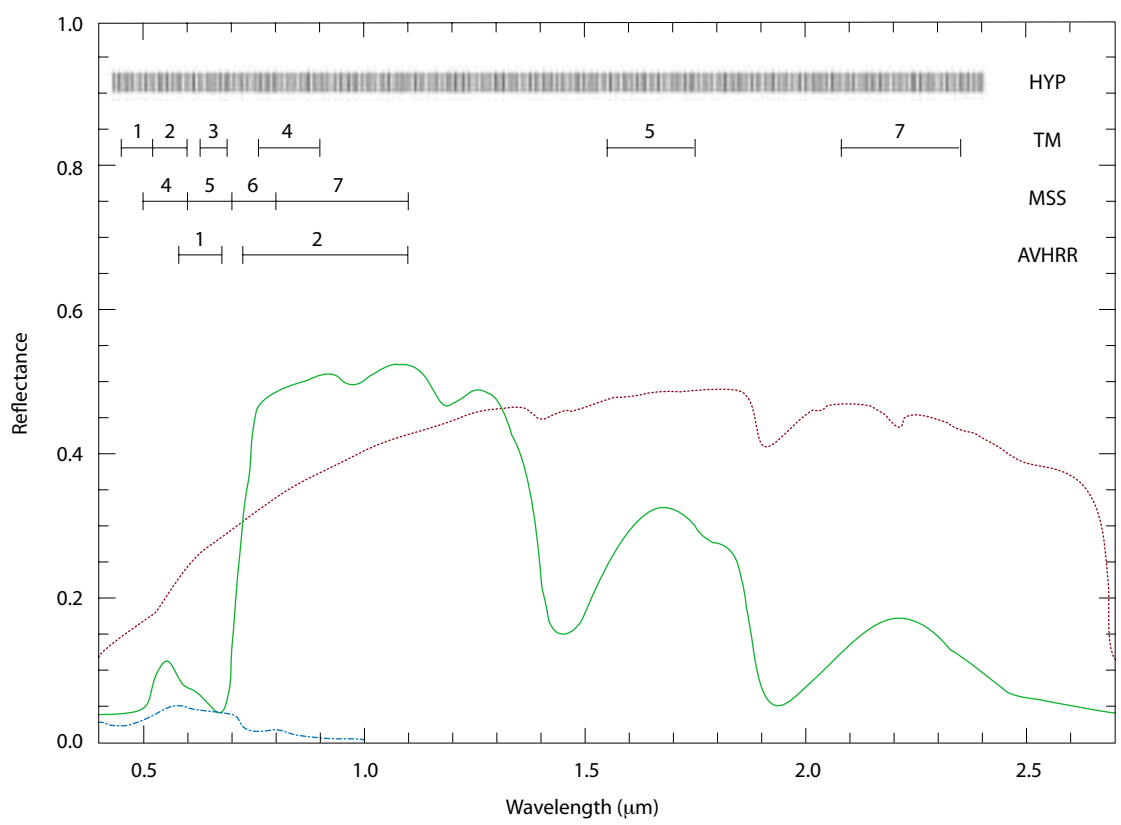

Figure 3. Idealised reflectance plots from 0.4 to 2.7 μm for green grass (solid line), fine sandy loam (dotted line), and water (dash-dot line). The figures show channel resolutions for some typical remote sensing instruments that are further discussed in Table 1. AVHRR = advanced very high resolution radiometer; Hyp = Hyperion; MSS = multispectral scanner; TM = Thematic mapper.

Table 1. General description of some current satellite optical remote sensing based sensors.

Satellite: sensor (quantisation)	Channel number	Spectral resolution	Spatial resolution (in m) at nadir	Sample swath	Repeat cycle	Lifetime
NOAA–AVHRR (10 bit)	1[a]	580–680 nm	1100	2700 km	Every 12 hours	1978 to present
	2	725–1100 nm				
	3	3.55–3.93 μm				
	4	10.5–11.3 μm				
	5	11.5–12.5 μm				
Landsat:MSS[b] (6 and 7 bit)	4	500–600 nm	80	185 km	Every 16 days[c]	1972 to present
	5	600–700 nm				
	6	700–800 nm				
	7	800–1100 nm				
Landsat:TM[d] (8 bit)	1	450–520 nm	30	185 km	Every 16 days	1983 to present
	2	520–600 nm				
	3	630–690 nm				
	4	769–900 nm				
	5	1.55–1.75 μm				
	7	2.08–2.35 μm				
	6	10.4–12.5 μm	120			
EO-1:Hyperion (12 bit)	242 in total	from 436 nm to 2405 nm	30	7.6 km	Every 16 days	Nov 2000 to Sept 2002

AVHRR = advanced very high resolution radiometer; EO = Earth observing; MSS = multispectral scanner; NOAA = National Oceanographic and Atmospheric Administration; TM = thematic mapper; Note 1000 nm = 1 μm.

[a] From 1978 to 1981 only the first four of these five channels were acquired.

[b] The Landsat:MSS is a multispectral sensor on board the Landsat satellites. Channels 4–6 are recorded as 7-bit and calibrated to 8-bit; channel 7 is recorded as 6-bit and calibrated to 8-bit.

[c] From 1972 to 1983, the repeat cycle for Landsat 1–3 was 18 days.

[d] Landsat:TM is the TM sensor on board Landsat 4 and 5. The channel numbers do not ascend in order of increasing wavelength due to the late inclusion of channel 7. The TM sensor was enhanced on Landsat 7, and is hence abbreviated as ETM. There is an additional 15 m panochromatic channel (520 to 900 nm), and the spatial resolution of the thermal channel (10.4-12.5 μm) has reduced from 120 m to 60 m. Landsat 7 was launched on 15 April 1999.

Remote sensing of the Earth's surface relies on the presence of atmospheric windows — wavelengths of the EMS where a signal generated from properties of the Earth's surface can pass with little, or no, interaction with the atmosphere. Certain areas of the EMS are not suitable for remote sensing because atmospheric constituents absorb all the electromagnetic radiation in particular wavelengths. For example, in Figure 3, Thematic mapper (TM) Channel 5 is in an atmospheric window that extends from around 1.5 to 1.7 μm. Either side of this window (1.45 and 1.95 μm) there is a relatively low reflectance for green grass due to a strong absorption of these wavelengths. Figure 4 shows the divisions of the EMS, some of which are discussed in more detail below.

Remote sensing measurements

The following background provides some discussion of the physical basis of remotely sensed measurements and how the flux of photons is converted into a digital image. The terms and concepts may be somewhat daunting to those not actively involved in remote sensing, and it may help

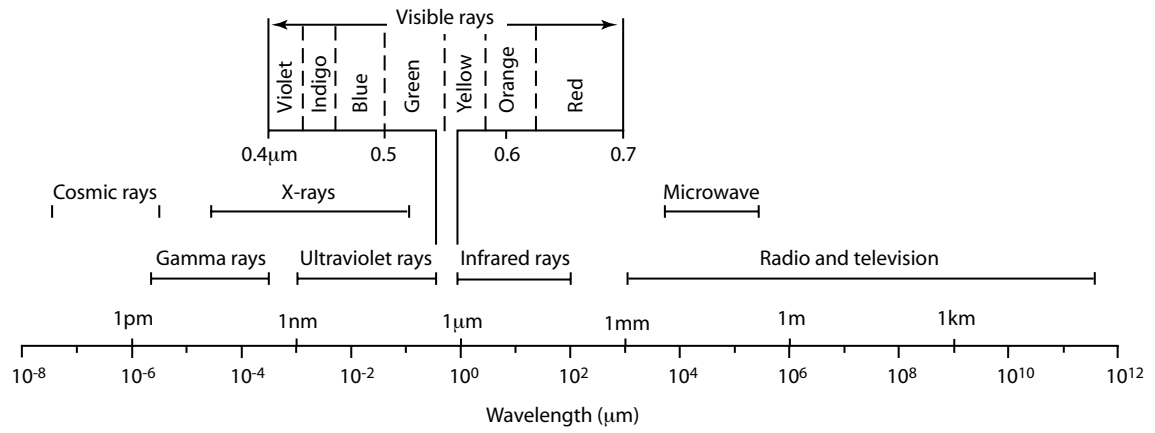

Figure 4. The parts of the electromagnetic spectrum (adapted from Harrison and Jupp 1989).

to think of remote sensing instruments as 'high-tech' cameras that record certain characteristics (extent, resolution and density) for each of the three domains (attribute, spatial and temporal).

Satellites and sensors

Table 1 gives characteristics for selected sensors and satellites on board a few of the Earth observing (EO) satellites used for assessing regional agricultural sustainability; these include NOAA (National Oceanographic and Atmospheric Administration), Landsat and EO satellites. The NOAA series of United States satellites carry the advanced very high resolution radiometer (AVHRR) sensor. The NOAA satellites orbit the poles at a height of some 700 km, similar to the height of the Landsat satellites. Data from NOAA are acquired over a large swath width when compared to the Landsat data; this is due to the wide scan angle (± 55°) of the AVHRR sensor. The local area coverage (LAC) pixel size is 1100 m at the subsatellite point, becoming 5400 m at the edge of the swath. The sensor also records global area coverage (GAC) data, which are a subset of the LAC data and nominally have a 5 km × 3 km resolution. GAC data are derived from LAC data on board the satellite and are recorded at the National Aeronautics and Space Agency (NASA) Goddard Space Flight Centre. Cracknell (1997) provides an extensive overview of the AVHRR sensor, the NOAA series of satellites and some applications of AVHRR data.

The Landsat series of satellites operate at a height of 700 km; they are polar-orbiting, sun-synchronous and pass a given latitude at the same solar time. Landsat 3 had a thermal channel. The main remote sensing system on Landsat 1–3 was the MSS sensor, while the TM sensor was included on Landsat 4.

EO-1 was launched on 21 November 2000 as part of NASA's 'New Millennium' program. One of the main aims of EO-1 is to demonstrate new technologies. The satellite carries three remote sensing instruments: Hyperion, Advanced Land Imager and Atmospheric Corrector. Hyperion is the first hyperspectral satellite-based sensor available for civilian applications; its spectral extent is from 436 nm to 2406 nm. The exact position of Hyperion's 7.6 km wide swath is determined by rolling the EO-1 spacecraft and pointing the instrument. Hyperion's ground resolution is nominally 30 m, similar to TM. To provide the opportunity to cross-validate with the enhanced TM carried by Landsat 7, EO-1 is in orbit one minute after Landsat 7.

Reflective remote sensing

The reflective portion of the EMS ranges nominally from 0.4 to 3.75 μm. Light of shorter wavelength than this is termed ultraviolet (UV). The reflective portion of the EMS can be further subdivided into the visible (0.4–0.7 μm), near-infrared (NIR) (0.7–1.1 μm), and shortwave-infrared (SWIR) (1.1–3.75 μm). Our remote sensing devices (eyes) allow

us to see in the visible portion of the EMS, and to distinguish colours through different properties of reflective surfaces. However, there are differences in the way people see shades of certain colours. For example, some people cannot sense subtle changes in colours — things are black or white, there are no shades of grey — whereas more perceptive people sense different shades of grey. In remote sensing, this is akin to the idea of 'quantisation', the term used to refer to the number of possible levels of response. Remote sensing converts an analogue photon flux to digital images, where the number of quantisation levels is a function of the number of bits used to represent the photon flux. The number of quantisation levels equals two to the power of the number of bits. Thus, 7-bit data provide 128 (2^7) levels of quantisation, 8-bit data 256 (2^8), 10-bit data 1024 (2^{10}) and 12-bit data 4096 (2^{12}). The ability of remote sensing measurements to distinguish different properties of the Earth's surface in the EMS is partly determined by the level of quantisation.

Many remote sensing instruments have channels situated in the red and NIR parts of the spectrum (see Table 1). These two reflective bands are often combined to produce vegetation indexes. The most common linear combinations are the simple ratio (NIR/red) and normalised difference vegetation index (NDVI), which is derived from (NIR–red)/(NIR+red). Several publications (Tian 1989; Kaufman and Tanre 1992; Thenkabail et al. 1994; Leprieur et al. 1996) provide comprehensive listings of vegetation indexes.

Figure 5 shows how a typical green leaf reflects light. Chlorophyll pigments in the leaf absorb red light. Radiation in the NIR portion of the spectrum is scattered by the internal spongy mesophyll leaf structure, leading to higher values in the NIR channels. This interaction between leaves and the light that strikes them is one determinant of the different responses in the red and NIR portions of reflective light shown in Figure 5.

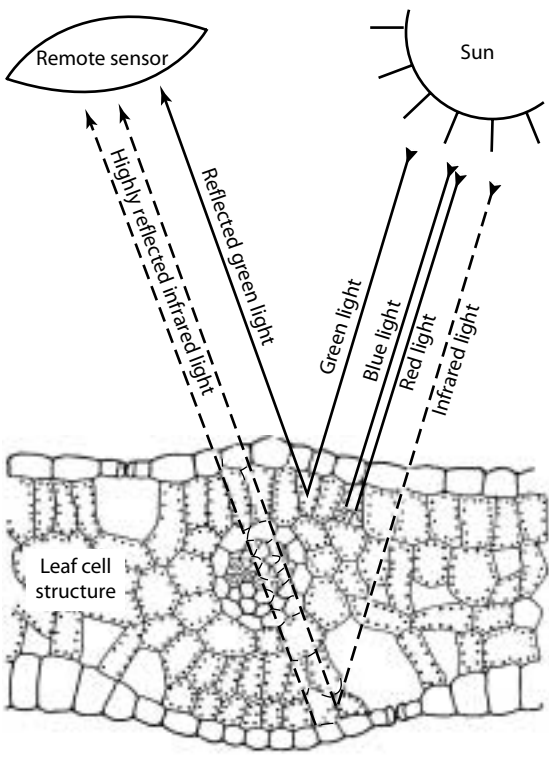

Figure 5. Reflectance of a typical green leaf in cross-section; chloroplasts reflect the green light and absorb red and blue light for photosynthesis. Near infrared light is highly scattered by water in the spongy mesophyll cells (adapted from Harrison and Jupp (1989).

There are positive correlations between NDVI and factors such as plant condition (Sellers 1985); foliage presence (including leaf area index (LAI)) (Curran et al. 1992; Tucker 1979; Nemani and Running 1989; McVicar et al. 1996a; McVicar et al. 1996b; McVicar et al. 1996c); and per cent foliage cover (Lu et al. 2001). Based on the relationship between LAI and NDVI, many previous studies have modelled crop yield by integrating the area under the NDVI curve (denoted ∫NDVI) for all or part of the growing season (Rasmussen 1998a; Rasmussen 1998b; McVicar et al. 2000; Honghui et al. 1999). Some researchers have used regression-based models developed from NDVI data acquired at specific times during the growing season (Maselli et al. 1992; Smith et al. 1995).

The amount of green leaf is one determinant of the signal strength in the reflective portion of the EMS. Several other important factors that affect the acquired value include soil colour and sun-target-sensor geometry.

The following discussion draws heavily on Roderick et al. (2000), whose work elegantly illustrated the effect of soil colour and quantisation on overall reflectance, and showed how change can be distinguished using remotely sensed measurements. The authors assumed a Lambertian surface (one that has no angular dependency), with no shade present and two soils, one dark (5% albedo[2]) and the other bright (30% albedo), with green grass (10% albedo) in the red portion of the EMS. Table 2 shows the simulated landscape's reflectance as the amount of simulated grass cover increases by 20% intervals from 0 to 100%.

On a dark soil, a 20% increase in green grass results in an overall 1% increase in albedo; on a bright soil it results in a 4% decrease. Hence, the albedo of the elements that make up the scene and their relative proportions are important to the overall albedo. We can invert this reasoning and ask 'How much change in green grass is needed to detect a change for different instrument quantisation?' Table 3 shows the results.

For dark soils sensed with a 7-bit instrument, a 15% change in cover is needed to change the recorded digital number by 1. This reduces to 0.5% for a 12-bit system. At the same level of quantisation, a larger relative difference between end-members requires a smaller change in per cent grass cover to detect change. This is because there is a greater difference in the albedo of the end-members when looking at bright soils (20% difference) than when considering the dark soil (5% difference) example.

Table 2. Overall reflectance (%) when the amount of green grass (10% albedo) increases by intervals of 20% cover over a dark (5% albedo) and bright (30% albedo) soil.

Green grass cover (%)	Overall reflectance (%) when on a dark soil	Overall reflectance (%) when on a bright soil
0	5	30
20	6	26
40	7	22
60	8	18
80	9	14
100	10	10

In reality, the land surface is not a perfect Lambertian reflector (Liang and Strahler 2000) — most surfaces in the optical (reflective and thermal) portions of the EMS are strongly anisotropic[3]. The geometry of sun, target and sensor, and the size, shape and spacing of elements (e.g. trees over bare ground) controls the amount of shadow contributing to the signal (Hall et al. 1995). This effect, termed the bidirectional reflectance distribution function (BRDF) (Burgess and Pairman 1997; Deering 1989), is characteristic of vegetation structure in reflective remotely sensed images. This means that in addition to the albedo of the scene elements and their relative proportions, the spatial distribution and the pixel size of observation affect the signal measured by remote sensing instruments (Jupp 1989ab; Woodcock and Strahler 1987; Walker et al. 1986; Jupp and Walker 1996). In addition, the match between the operational scale and the resolution partly controls the strength of relationships between surface properties and remote sensing (Friedl 1997). Image information content is minimal when the resolution is approximately equal to the operational scale (Woodcock et al. 1988ab). Other factors affecting

[2] Albedo is the fraction of light that is reflected by a body or surface.

[3] Anisotropic means having different physical properties in different directions.

Table 3. The change needed in amount of green grass to detect a change for different instrument quantisation levels.

Quantisation	Levels	Precision (1/level)	Change of green grass cover on dark soil (%)	Change of green grass cover on bright soil (%)
7-bit	128	0.007813	15.626	3.907
8-bit	256	0.003906	7.812	1.953
10-bit	1024	0.000977	1.954	0.489
12-bit	4096	0.000244	0.488	0.122

the reflective portion of the EMS include changes in the observed signal due to changes in the atmospheric component of the signal, including atmospheric precipitable water (Choudhury and DiGirolamo 1995; Hobbs 1997), and changes in the response of the sensor over time (Mitchell 1999).

Thermal remote sensing

The thermal portion of the EMS ranges nominally from 3.75 to 12.5 μm. The observed surface temperature is a function of the radiant energy emitted by the surface which is remotely sensed, be it land, ocean or cloud top. Models have been developed to allow surface temperature to be extracted from thermal remote sensing data. Prata et al. (1995) review the algorithms and issues, including land emissivity estimation, involved in the calculation of land-surface temperature, denoted T_s.

Thermal remote sensing is an observation of the status of the surface energy balance (SEB) at a specific time of day. The SEB is driven by the net radiation at the surface. During the daytime, the net radiation is usually dominated by incoming shortwave radiation from the sun, the amount reflected depending on the albedo of the surface. There are also longwave components that well up and down. At the ground surface, the net all-wave radiation is balanced between the sensible, latent and ground heat fluxes. The ground heat flux averages out over long periods of time; thus, the SEB represents the balance between the sensible and latent heat fluxes. During the day, T_s is partially dependent on the relative magnitude of the sensible and latent heat fluxes (Quattrochi and Luvall 1999; McVicar and Bierwirth 2001). This is exploited in the mapping of regional moisture availability for the MDB, as reported in Chapter 19.

Remotely sensed thermal data are also recorded at night. At this time, the SEB is dominated by the release from the ground of heat that was absorbed during daylight hours, which is governed by how much heat was absorbed during the day and the rate at which it is released after sunset. The environment's capacity to store heat depends on the amount of water it is storing.

Microwave remote sensing

The microwave portion of the EMS ranges nominally from 0.75 to 100 cm. Radio signals have wavelengths that are included in these bands. These systems can either be active (the sensor sends its own signal) or passive (the background signal from the Earth's surface is observed). This range of the EMS is further divided into five smaller sections that are used for remote sensing (Table 4).

Both passive and active microwave observations have been used to determine the near-surface soil moisture for a number of experimental field sites. Radar (radio detection and ranging), is an active system based upon sending a pulse of microwave energy and then recording the strength, and sometimes polarisation, of the return pulses. The way the signal is returned provides information to determine characteristics of the landscape. Radar has been used in the determination of near-surface soil moisture. Table 5 gives technical specifications of the current satellite radar systems — the Japanese

Earth Resources Satellite (JERS), the Earth Resource Satellite (ERS) and the RADARSAT. JERS observes the Earth's surface using eight spectral bands in the reflective portion of the EMS. ERS was launched and is operated by the European Space Agency. RADARSAT is a synthetic aperture RADAR (SAR) on board a Canadian satellite.

A 'Data Construct' Perspective

Within TGIS remotely sensed data, GIS data, point-based measurements and model outputs (either point and spatial) can all be integrated, as they all have spatial and temporal characteristics associated with the data attribute. Economic and social data can also be integrated as they too have temporal and (usually) spatial components. Some data used to assess regional agricultural sustainability are 'aspatial' in that they do not have a precise spatial reference (e.g. wool prices or interest rates), but the temporal nature of these variables can be incorporated into larger information systems.

The integration of several data types, usually with varying spatial–temporal characteristics, allows for more objective determination of agricultural sustainability. In the chapters in this section, the data used depend in part on the specific issue that is being modelled under the broad topic of 'regional agricultural sustainability'.

Temporal aspects of TGIS

Time plays a minimal part in some aspects of TGIS modelling. For example, in most environments there is little or no acknowledgment of the temporal attribute of DEMs — because it is generally temporally invariant, the time when the data was captured is of little relevance. However, in other aspects of TGIS modelling, time is an important component (e.g. in the case of active erosion, soil characteristics changing in response to changes in vegetation, soils becoming acidified, or crop water use and irrigation scheduling through the growing season).

Temporal component of DEM

Elevation varies with time in some circumstances; for example, in small, deep actively eroding gullies on the Loess Plateau (as described in Chapter 10). The DEM for these small parts of the plateau may need to be updated perhaps every two years, or possibly after heavy episodic rainfall events that instigate erosion. In contrast, the DEM for the entire plateau may be updated only when there are major technological and methodical advancements

Table 4. The parts of the microwave section of the electromagnetic spectrum used for remote sensing.

	Band				
	P	L	S	C	X
Wavelength (cm)	100–30	30–15	15–7.5	7.5–3.75	3.75–2.4

Table 5. Technical specifications of current satellite- based radar data.

Sensor	Wavelength	Pixel size (m^2)	Incidence angle	Polarisation	Swath width (km)	Recorded since	Current repeat cycle
JERS	L-band	18	35°	HH	75	June 1993	44 days
ERS	C-band	12.5	23°	VV	102.5	Sept 1991	35 days
RADARSAT	C-band	100	20–49°	HH	500[a]	Nov 1995	3 days

ERS = Earth Resource Satellite; JERS = Japanese Earth Resources Satellite; RADAR = radio detection and ranging

[a] The ScanSAR wide mode is reported here, as it has the largest swath width and therefore has the most potential for regional agricultural assessment through electrical conductivity. The large incidence angle means that the repeat cycle is only a few days. However, the entire 30º range may not be suitable for the accurate estimation of soil moisture.

in producing such measurements, perhaps every 20 years. The date when data are captured can be used to model rates of erosion (in units of cubic metres of soil lost per year) and to monitor the movement of gully fronts. On the Loess Plateau, authorities can use such data to ensure the long-term viability, based on geomorphic stability, of roads and rail networks. Massive expenditure is required to construct new highways and railways to support the increased transport of goods and services in China's rapidly developing economy. Therefore, it is important to ensure that transport pathways are not placed in positions where they will need constant maintenance (or even rebuilding) because of slump erosion in gullies after heavy rains.

Temporal components of soils

Temporal data can also be important for soils. Certain physical properties, such as water-holding capacity, may be considered temporally inert, and therefore may need to be mapped only once. However, TGIS scientists need to understand the processes that control the water-holding capacity of soils in order to take these processes into account. For example, there are plans to control erosion on the Loess Plateau and rising watertables in southeastern Australia by replanting vast tracks of land with deep-rooted perennial vegetation. This change in land use will have a range of effects (spatial and temporal) on the soil:

- The initial vegetation type replanted will depend on environmental considerations such as rainfall amount and seasonality, and may be a mix of trees, shrubs or grasses. The mix is likely to change with time, as soil conditions improve.
- Changing the land use from agricultural systems based on cropping or grazing to deeper-rooted perennial vegetation will usually, over time, result in increased levels of organic matter and nutrients (N, P and K) in the top layers of the soil.
- The changes to the top layers of soil are likely to change infiltration rates and soil water-holding capacity, especially for soils relatively close to the surface.
- If areas are replanted with shrubs, changes to the soil properties are unlikely to be constant because the plants will induce spatial variation: soil that is close to the shrub will be influenced more quickly and intensely than soil further away as a result of organic matter produced by the plant. This potential influence at the microscale will reduce with time, as the shrubs grow bigger and plant material is laterally distributed by water and wind flowing over the soil surface.

The concept of soils being in motion due to combinations of wind and water systems, operating at different space and time scales, with varying residence times between motions, can make it difficult to understand the origins of present-day soil properties (Gatehouse et al. 2001). TGIS can help to provide conceptual models of landscape evolution that can be used to assess the impact of possible management actions on a range of landscape functions.

A further example of the importance of time to soil spatial data is the identification and monitoring of soil degradation due to waterlogging, which in southeastern Australia leads to the development of acid sulfate soils. Knowing when data was captured allows scientists to assess the rate of change of acid sulfate scalds. More importantly, such monitoring will allow conceptual models of the processes governing the development of acid sulfate soils to be further refined.

Temporal components of water balance

Assessment of spatial–temporal patterns and trends in regional ecohydrology often involves the use of time-series data, such as in situ regional yield estimates, water use figures and remotely sensed data. Because it provides repeated measurements at a particular spatial resolution and electromagnetic

wavelength, remote sensing makes it possible to monitor dynamic environmental conditions. This is illustrated in Chapter 19 for assessing moisture availability in the MDB and in Chapters 18 and 20 for vegetation cover.

Data are usually integrated from several different sources, all with varying TGIS data constructs. In order to spatially monitor (or temporally map) an issue concerning regional agricultural sustainability, it is helpful to think of the data construct as a cube, in which two of the three dimensions are spatial (latitude and longitude) and one is temporal. To provide a culinary analogy, the data construct for monitoring moisture availability in a region (as in Chapter 19) could be thought of as pancakes of remotely sensed data intersected at right angles by skewers of point-based meteorological data. In some situations, more complex spatial–temporal data models are needed (e.g. event-driven and four–dimensional data models) (Peuquet 2001; Chen and Jiang 2000; Zhang and Hunter 2000). For example, in modelling the movement of pollutants in groundwater and the atmosphere, the extra dimension of elevation (or depth) must be included in the TGIS data construct. The most appropriate spatial–temporal data model to use will depend on the application, and there are subtle interactions between database design and utility that should be taken into account (Roddick et al. 2001; Abraham and Roddick 1999).

Linking remotely sensed data with meteorological data (as in Chapter 19) illustrates the concept of the 'data construct', as the two types of data have very different spatial, temporal and attribute characteristics. For example, cloud-free AVHRR data for the land surface may be available only weekly; whereas some meteorological variables are recorded as daily extremes (maximum and minimum air temperatures), daily averages (vapour pressure) or daily integrals (precipitation and solar radiation).

Spatial aspects of TGIS

Remotely sensed data are spatially dense because the image is a census at a particular spatial resolution and electromagnetic wavelength rather than a point sample. There is a contrast between spatial density of remote sensing and isolated meteorological stations or field sites. For example, meteorological stations may be 200 km apart but remotely sensed data might be measured at a spatial resolution of 1 km for each of those 200 km.

While GIS data may cover entire regions, they are often produced from the spatial interpolation (or extrapolation) of point samples; this is frequently the case for meteorological and soil data. In these instances, the spatial extent of the GIS data may appear to be complete, but in fact the spatial density of the input data is low. For example, a thematic map of soil classes may be developed from a series of observation points located every 5 km^2 for a 1000 km^2 area. The data from these 200 point samples are interpolated to characterise the soils for the larger area. Whether or not this is valid will depend on the spatial autocorrelation of the soil property being mapped. If the soil is uniform, only one observation may be needed to characterise the entire area, whereas if the soils vary considerably, the 200 observations may provide a poor representation. Soil maps are currently generated using stratified soil sampling based on continuous data sets. Where such data are radiometric or DEMs, they are usually obtained from interpolation of point or linear data, so it is important to track the density of the input data. Also, some error analysis of the interpolation process used to create the surface should be included in the associated metadata system.

To fully understand the data construct of all data sets being integrated in a TGIS for a specific application, it is useful to consider the characteristics of each data set in terms of a three-by-three matrix. The attribute (spectral), spatial and temporal characteristics can be defined in terms of the extent, resolution and density of the different

data sets (Table 6). In order to use TGIS effectively to assess and monitor the agricultural sustainability of a region, all the elements that make up this matrix need to be taken into account.

Emerging Issues

Accuracy and uncertainty assessments

For geospatial simulation modelling, including AW, IC and CI approaches, sensitivity analysis is needed to determine the uncertainty of the final output (Mowrer and Congalton 2000). Sources of uncertainty include both input data and the model itself (Heuvelink and Pebesma 1999). Recently, Gahegan and Ehlers (2000) provided a framework to model uncertainty when linking remotely sensed and GIS data, but they assumed that remotely sensed data would be used only in a thematic (or discontinuous) way. In analysing uncertainty and error propagation in GIS, positional accuracy is often forgotten; this may become an issue for institutionally available GIS data in Australia (Van Niel and McVicar 2001; Van Niel and McVicar 2002). There are many methods for assessing the accuracy of thematic maps derived from the classification of remote sensing data (Fenstermaker 1994); these should be used to estimate overall accuracy, user and producer accuracy for the map, and how each class can best be used in TGIS analysis.

Metadata

Awareness of the importance of metadata (data about data) in TGIS is increasing. As monitoring frameworks extend, any changes in the measurement system or processing must be recorded, to allow those undertaking retrospective analysis of such data sets to understand the genesis of the data. This is also true for data collected over large areas, possibly by many individuals. Operational agencies that collect and disseminate data routinely (e.g. national meteorological and national mapping agencies) allocate many resources to ensuring that metadata are collected, updated and readily available. A metadata system to comprehensively study long-term, large-area environmental issues is becoming a central part of any TGIS. In short, the metadata are at least as important as the data. In TGIS, if there are no metadata, there may as well be no data. A crucial part of a comprehensive metadata system is keeping track of where data are stored and of their current backup status. Assessing the quality of data is also

Table 6. Matrix showing characteristics of remotely sensed data sets in terms of their domain.

	Characteristic		
Domain	Extent	Resolution	Density
Attribute (spectral)	Portion of the EMS being sampled	Bandwidth	Number of bands in a particular portion of the EMS (e.g. hyperspectral sensors have higher spectral density than broadband instruments)
Spatial	Area covered by the image	Smallest pixel or picture element acquired	Complete[a]
Temporal	Recording period over which the data are available[b]	Period of data acquisition[c]	Repeat characteristics of the satellite (and, for some applications, the availability of cloud-free data)

[a] This contrasts with the potentially lower spatial density of point observations
[b] For some remotely sensed systems (e.g. Landsat MSS) data have been recorded for 25 years
[c] For remotely sensed systems this is a matter of seconds, which contrasts with point data such as the daily rainfall totals recorded at meteorological stations

important in developing TGIS. This is easier in the case of data collected directly by the TGIS developer than it is for data that are collected by others or obtained remotely and then integrated into the system. The issues of metadata and the data life cycle (Goodchild 2000) need to be comprehensively addressed, especially for institutionally maintained and distributed data.

TGIS researchers working alone or in small groups may have no or little understanding of issues relating to metadata. However, if they wish to become part of interconnected TGIS studies, they must give due consideration and resources to this issue. During the course of this ACIAR project (July 1997 to June 2001), there was a rapid increase in the number of databases available from the internet for China, Australia and other countries. Evidently, global 'interconnectedness' is only beginning.

Conclusions

The spatial–temporal data construct of regional databases can be used to monitor and assess the sustainability of agricultural production within the broader environmental context. Data are integrated from a variety of sources, and information extracted by empirical relationships, 'data-mining' and spatial–temporal process models.

For all geographic regions, spatial and temporal trend analysis of regional agricultural sustainability (and other variables) must be based on data. Currently, there is a mismatch between the data that are available and what is required to infer causal relationships between measures of regional agricultural sustainability and agricultural practices for large areas over long periods. The collection of data and the quality and availability of databases are major issues facing organisations involved in research and policy of regional agriculture. These issues need to be addressed by those managing agricultural, water and land resources.

Acknowledgments

This research has been supported with contributions from ACIAR Project LWR1/95/07 conducted by CSIRO Land and Water and the Chinese Academy of Sciences. More details can be found at www.eoc.csiro.au/aciar.

References

Abraham, T. and Roddick, J.F. 1999. Survey of spatio-temporal databases. GeoInformatica, 3, 61–99.

Bechini, L., Ducco, G., Donatelli, M. and Stein, A. 2000. Modelling, interpolation and stochastic simulation in space and time of global solar radiation. Agriculture, Ecosystems and Environment, 81, 29–42.

Bernard, L., Schmidt, B., Streit, U. and Uhlenküken, C. 1998. Managing, modeling, and visualizing high-dimensional spatio-temporal data in an integrated system. GeoInformatica, 2, 59–77.

Bian, L. 1997. Multiscale nature of spatial data in scaling of environmental models. In: Quattrochi, D.A. and Goodchild, M.F., eds, Scale in Remote Sensing and GIS. Boca Raton, CRC Press Inc., 13–26.

Bloschl, G. and Sivapalan, M. 1995. Scale issuses in hydrological modelling: a review. In: Kalma, J.D. and Sivapalan, M., eds, Scale Issuses in Hydrological Modelling. Chistester, John Wilet & Sons, 9–48.

Bosma, W.J.P., Marinussen, M.P.J.C. and van der Zee, S.E.A.T.M. 1994. Simulation and areal interpolation of reactive solute transport. Geoderma, 62, 217–231.

Burgess, W. and Pairman, D. 1997. Bidirectional reflectance effects in NOAA AVHRR data. International Journal of Remote Sensing, 18, 2815–2825.

Butler, D.R. and Walsh, S.J. 1998. The application of remote sensing and geographic information systems in the study of geomorphology: An introduction. Geomorphology, 21, 179–181.

Cao, C. and Lam, N. 1997. Understanding the scale and resolution effects in remote sensing and GIS. In: Quattrochi, D.A. and Goodchild, M.F., eds, Scale in Remote Sensing and GIS. Boca Raton, CRC Press Inc., 57–72.

Chen, J. and Jiang, J. 2000. An event-based approach to spatio-temporal data modeling in land subdivision systems. GeoInformatica, 4, 387–402.

Choudhury, B.J. and DiGirolamo, N.E. 1995. Quantifying the effect of emissivity on the relation between AVHRR split window temperature difference and atmospheric precipitable water over land surface. Remote Sensing of Environment, 54, 313–323.

Cracknell, A.P. 1997. The Advanced Very High Resolution Radiometer (AVHRR). London, Taylor & Francis.

Curran, P.J., Dungan, J.L. and Gholz, H.L. 1992. Seasonal LAI in slash pine estimated with Landsat TM. Remote Sensing of Environment, 39, 3–13.

Deering, D.W. 1989. Field measurements of bidirectional reflectance. In: Asrar, G., ed., Theory and Application of Optical Remote Sensing. New York, John Wiley and Sons, 14–65.

Fenstermaker, L.K. ed. 1994. Remote Sensing Thematic Accuracy: a compendium. American Society for Photogrammetry and Remote Sensing.

Friedl, M.A. 1997. Examining the effects of sensor resolution and sub-pixel heterogeneity in spectral vegetation indices: implications for biophysical modelling. In: Quattrochi, D.A. and Goodchild, M.F., eds, Scale in Remote Sensing and GIS. Boca Raton, CRC Press Inc., 113–139.

Gahegan, M. and Ehlers, M. 2000. A framework for the modelling of uncertainty between remote sensing and geographic information systems. Journal of Photogrammetry and Remote Sensing, 55, 176–188.

Gatehouse, R.D., Williams, I.S. and Pillans, B.J. 2001. Fingerprinting windblown dust in south-eastern Australian soils by uranium-lead dating of detrital zircon. Australian Journal of Soil Research, 39, 7–12.

Goodchild, M.F. 2000. Communicating the results of accuracy assessment: metadata, digital libraries and assessing fitness of use. In: Mowrer, H.T. and Congalton, R.G., eds, Quantifying Spatial Uncertainity in Natural Resources: theory and applications for GIS and remote sensing. Chelsea, Michigan, Sleeping Bear Press, 3–15.

Gurnell, A. and Montgomery, D. 1998. Preface: hydrological applications of GIS. Hydrological Processes, 12, 821–822.

Hall, F.G., Shimabukuro, Y.E. and Huemmrich, K.F. 1995. Remote sensing of forest biophysical structure using reflectance decomposition and geometric reflectance models. Ecological Applications, 5, 993–1013.

Harrison, B.A. and Jupp, D.L.B. 1989. Introduction to Remotely Sensed Data, CSIRO Publications.

Heuvelink, G.B.M. and Huisman, J.A. 2000. Choosing Between Abrupt and Gradual Spatial Variation ? In: Mowrer, H.T. and Congalton, R.G., eds, Quantifying Spatial Uncertainity in Natural Resources: Theory and Applications for GIS and Remote Sensing. Chelsea, Michigan, Sleeping Bear Press, 111–117.

Heuvelink, G.B.M. and Pebesma, E.J. 1999. Spatial aggregation and soil process modelling. Geoderma, 89, 47–65.

Hobbs, T.J. 1997. Atmospheric correction of NOAA-11 NDVI data in the arid rangelands of Central Australia. International Journal of Remote Sensing, 18, 1051–1058.

Honghui, L., Xiaohuan, Y. and Naibin, W. 1999. Remote sensing based estimation system for winter wheat yield in North China Plain. Chinese Geographical Journal, 9, 40–48.

Jupp, D.L.B., Strahler, A.H. and Woodcock, C.E. 1989a. Autocorrelation and regularization in digital images I. Basic theory. IEEE Transactions on Geoscience and Remote Sensing, 26, 463–473.

Jupp, D.L.B., Strahler, A.H. and Woodcock, C.E. 1989b. Autocorrelation and regularization in digital images II. Simple image models. IEEE Transactions on Geoscience and Remote Sensing, 27, 247–258.

Jupp, D.L.B. and Walker, J. 1996. Detecting structural and growth changes in woodlands and forests: The challenge for remote sensing and the role of geo-optical modelling. In: Gholz, H.L., Nakane, K. and Shimoda, H., eds, The Use of Remote Sensing in the Modeling of Forest Productivity. Dirdrecht, The Netherlands, Kluwer Academic Publications, 75–108.

Kaufman, Y.J. and Tanre, D. 1992. Atmospherically Resistant Vegetation Index (ARVI) for EOS-MODIS. IEEE Transactions on Geoscience and Remote Sensing, 30, 261–270.

Kustas, W.P. and Norman, J.M. 1996. Use of remote sensing for evapotranspiration monitoring over land. Hydrological Sciences Journal des Sciences Hydrologiques, 41, 495–516.

Lam, N. and Quattrochi, D.A. 1992. On the issues of scale, resolution, and fractal analysis in the mapping sciences. Professional Geographer, 44, 88–98.

Langran, G. 1992. Time in Geographic Information Systems. London, Taylor and Francis.

Lehmann, A. and Lachavanne, J.B. 1997. Geographic information systems and remote sensing in aquatic botany. Aquatic Botany, 58, 195–207.

Leprieur, C., Kerr, Y.H. and Pichon, J.M. 1996. Critical assessment of vegetation indices from AVHRR in a semi-arid environment. International Journal of Remote Sensing, 17, 2549–2563.

Liang, S. and Strahler, A.H. eds. 2000. Land Surface Bidirectional Reflectance Distribution Function (BRDF); Recent Advances and Future Prospects, Harwood Academic Publishers.

Lu, H., Raupach, M.R. and McVicar, T.R. 2001. Decomposition of Vegetation Cover into Woody and Herbaceous Components Using AVHRR NDVI Time Series. Canberra, Australia, CSIRO Land and Water, pp. 44.

Maracchi, G., Pérarnaud, V. and Kleschenko, A.D. 2000. Applications of geographical information systems and remote sensing in agrometeorology. Agricultural and Forest Meteorology, 103, 119–136.

Maselli, F., Conese, C., Petkov, L. and Gilabert, M. 1992. Use of NOAA-AVHRR NDVI data for environmental monitoring and crop forecasting in the Sahel. Preliminary Results. International Journal of Remote Sensing, 13, 2743–2749.

McVicar, T.R. and Bierwirth, P.N. 2001. Rapidly Assessing the 1997 Drought in Papua New Guinea using Composite AVHRR Imagery. International Journal of Remote Sensing, 22, 2109–2128.

McVicar, T.R. and Jupp, D.L.B. 1998. The current and potential operational uses of remote sensing to aid decisions on drought exceptional circumstances in Australia: a review. Agricultural Systems, 57, 399–468.

McVicar, T.R., Jupp, D.L.B., Reece, P.H. and Williams, N.A. 1996a. Relating LANDSAT TM vegetation indices to in situ leaf area index measurements. Canberra, ACT, CSIRO, Division of Water Resources, 80.

McVicar, T.R., Jupp, D.L.B. and Williams, N.A. 1996b. Relating AVHRR vegetation indices to LANDSAT TM leaf area index estimates. Canberra, ACT, CSIRO, Division of Water Resources, 33.

McVicar, T.R., Walker, J., Jupp, D.L.B., Pierce, L.L., Byrne, G.T. and Dallwitz, R. 1996c. Relating AVHRR vegetation indices to in situ leaf area index. Canberra, ACT, CSIRO, Division of Water Resources, 54.

McVicar, T.R., Zhang, G., Bradford, A.S., Wang, H., Dawes, W.R., Zhang, L. and Lingtao, L. 2000. Developing a spatial information system to monitor regional agricultural water use efficiency for Hebei Province on the North China Plain. Canberra, Australia, CSIRO Land and Water, 55.

Mesev, V. 1997. Remote sensing of urban systems: hierarchical integration with GIS. Computers, Environment and Urban Systems, 21, 175–187.

Mitasova, H., Mitas, L., Brown, W.M., Gerdes, D.P., Kosinovsky, I. and Baker, T. 1995. Modelling spatially and temporally distributed phenomena: new methods and tools for GRASS GIS. International Journal of Geographic Information Science, 9, 433–446.

Mitchell, R.M. 1999. Calibration status of the NOAA AVHRR solar reflectance channels: CalWatch Revision 1. CSIRO Atmospheric Research Technical Paper No. 42, Melbourne, 20.

Mowrer, H.T. and Congalton, R.G. 2000. Introduction: the past, present, and future of spatial uncertainity analysis. In: Mowrer, H.T. and Congalton, R.G., eds, Quantifying Spatial Uncertainty in Natural Resources: Theory and Applications for GIS and Remote Sensing. Chelsea, Michigan, Sleeping Bear Press, xv–xxiv.

Nemani, R.R. and Running, S.W. 1989. Testing a theoretical climate-soil-leaf area hydrologic equilibrium of forests using satellite data and ecosystem simulation. Agricultural and Forest Meteorology, 44, 245–260.

Peuquet, D.J. 1994. It's about time: a conceptual framework for the representation of spatial–temporal dynamics in geographic information systems. Annals of the Association of American Geographers, 84, 441–461.

Peuquet, D.J. 1995. An event-based spatial–temporal data model (ESTDM) for temporal analysis of geographical data. International Journal of Geographic Information Science, 9, 7–24.

Peuquet, D.J. 2001. Making space for time: issues in space-time data representation. GeoInformatica, 5, 11–32.

Prata, A.J., Caselles, V., Coll, C., Ottle, C. and Sobrino, J. 1995. Thermal remote sensing of land surface temperature from satellites: Current status and future prospects. Remote Sensing Reviews, 12, 175–224.

Quattrochi, D.A. 1993. The need for a lexicon of scale terms in integrating remote sensing data with geographic information systems. Journal of Geography, 92, 206–212.

Quattrochi, D.A. and Luvall, J.C. 1999. Thermal infrared remote sensing for analysis of landscape ecological processes: methods and applications. Landscape Ecology, 14, 577–598.

Rango, A. and Shalaby, A.I. 1998. Operational applications of remote sensing in hydrology: success, prospects and problems. Hydrological Sciences Journal des Sciences Hydrologiques, 43, 947–968.

Rasmussen, M.S. 1998a. Developing simple, operational, consistent NDVI-vegetation models by applying environmental and climatic information: Part I: Assessment of net primary productivity. International Journal of Remote Sensing, 19, 97–117.

Rasmussen, M.S. 1998b. Developing simple, operational, consistent NDVI-vegetation models by applying environmental and climatic information: Part II: Crop yield assessment. International Journal of Remote Sensing, 19, 119–139.

Roddick, J.F., Grandi, F., Mandreoli, F. and Rita Scalas, M. 2001. Beyond schema versioning: a flexible model for spatio-temporal schema selection. GeoInformatica, 5, 33–50.

Roderick, M.L., Chewing, V. and Smith, R.C.G. 2000. Remote sensing in vegetation and animal studies. In: 't Mennetje, L. and Jones, R.M., eds, Field and Laboratory Methods for Grassland and Animal Production Research. Wallingford UK, CABI, 205–225.

Santos, A.M.P. 2000. Fisheries oceanography using satellite and airborne remote sensing methods: a review. Fisheries Research, 49, 1–20.

Sellers, P.J. 1985. Canopy reflectance, photosynthesis and transpiration. International Journal of Remote Sensing, 6, 1335–1372.

Smith, R.C.G., Adams, J., Stephens, D.J. and Hick, P.T. 1995. Forecasting wheat yield in a Mediterranean-type environment from the NOAA Satellite. Australian Journal of Agricultural Research, 46, 113–125.

Sommer, S., Hill, J. and Mégier, J. 1998. The potential of remote sensing for monitoring rural land use changes and their effects on soil conditions. Agriculture, Ecosystems and Environment, 67, 197–209.

Stein, A., Staritsky, I.G., Bouma, J., Van Eijsbergen, A.C. and Bgegt, A.K. 1991. Simulation of moisture deficits and areal interpolation by universal cokriging. Water Resources Research, 27, 1963–1973.

Thenkabail, P.S., Ward, A.B., Lyon, J.G. and Merry, C.J. 1994. Thematic mapper vegetation indices for determining soybean and corn growth parameters. Photogrammetric Engineering and Remote Sensing, 60, 437–442.

Tian, G. 1989. Spectral Signatures and Vegetation Indices of Crops. Canberra, ACT, CSIRO Division of Water Resources.

Tucker, C.J. 1979. Red and photographic infrared linear combinations for monitoring vegetation. Remote Sensing of Environment, 8, 127–150.

Van Niel, T.G. and McVicar, T.R. 2001. Assessing positional accuracy and its effects on rice crop area measurement: an application at Coleambally Irrigation Area. Australian Journal of Experimental Agriculture, 41, 557–566.

Van Niel, T.G. and McVicar, T.R. 2002. Experimental evaluation of positional accuracy estimates of a linear network using point- and line-based testing methods. International Journal of Geographic Information Sciences, (Accepted).

Walker, J., Jupp, D.L.B., Penridge, L.K. and Tian, G. 1986. Interpretation of vegetation structure in Landsat MSS imagery: a case study in disturbed semi-arid eucalypt woodlands. Part 1. field data analysis. Journal of Environmental Management, 23, 19–33.

Woodcock, C.E. and Strahler, A.H. 1987. The factor of scale in remote sensing. Remote Sensing of Environment, 21, 311–332.

Woodcock, C.E., Strahler, A.H. and Jupp, D.L.B. 1988a. The use of variograms in remote sensing: I scene models and simulated images. Remote Sensing of Environment, 25, 323–348.

Woodcock, C.E., Strahler, A.H. and Jupp, D.L.B. 1988b. The use of variograms in remote sensing: II real digital images. Remote Sensing of Environment, 25, 349–379.

Zhang, W. and Hunter, G.J. 2000. Temporal interpolation of spatially dynamic objects. GeoInformatica, 4, 403–418.

17 The Duration of Soil Saturation: Point Measurements Versus a Catchment-Scale Method

Jim W. Cox* and Phil J. Davies*

Abstract

Almost two-thirds of the farms in southern Australia have a texture-contrast soil profile with sandy or loamy A and E horizons overlying clay B horizons. A common problem with some of these soils is the development of a perched watertable in winter, which causes severe reduction in crop yield and exacerbates land degradation. The aim of this study was to measure the extent of the variability in the duration of soil saturation in texture-contrast soils on slopes in a catchment in the Mount Lofty Ranges, South Australia. Furthermore, a method based on a topographic index was used to predict soil saturation at catchment scale, which was then compared to the conventional point-scale measurements.

In the relatively dry years of the study, water duration on the upper slopes was surprisingly higher than on the lower slopes but was rarely expressed at the soil surface. Furthermore, the cause of soil saturation on the mid- and upper slopes was different from that on the lower slopes. However, it was predicted that in wet years water would last longer on the lower slopes due to saturation by groundwaters. As the catchment-scale method was based on a topographic index, it should be useful for predicting the duration of saturation in wet years but not in dry years.

The information obtained on the variability and causes of waterlogging will be of benefit to farmers. It showed that the failure of some current management options to adequately control perched watertables on slopes is partly due to the lack of understanding of their causes and to inadequate prediction of their variability in catchments.

南澳几乎三分之二的农地土壤剖面质地不均，粘土层 B 之上有砂土或壤土层 A 和 E 覆盖。这类土壤的栖留水位冬天通常较高，导致作物大幅减产，加剧土地退化。本研究的目的是测量劳伏特山区一个坡地上土壤水分饱和状态持续时间的变动范围，采用地形指数法，预测整个流域范围内的饱和状况，然后将其与传统的点测结果相对比。

* CSIRO Land and Water, PMB 2, Glen Osmond, SA 5064, Australia. Email: jim.cox@.csiro.au

Cox, J.W. and Davies, P.J. 2002, The duration of soil saturation: point measurements versus a catchment-scale method. In: McVicar, T.R., Li Rui, Walker, J., Fitzpatrick, R.W. and Liu Changming (eds), *Regional Water and Soil Assessment for Managing Sustainable Agriculture in China and Australia*, ACIAR Monograph No. 84, 224–230.

在相对干旱的年份，坡地上部土壤饱和期竟然较下部的长，但在土壤表面很少表现出来。而且，坡地中上部和下部水分饱和的原因不同。不过在多雨年份，正如预期的那样，因地下水原因，坡地下部水分饱和最久。因流域尺度的方法基于地形指数，所以可对多雨年份的水分饱和期进行预测，但不适合干旱年份。

研究收集到的涝渍变动及成因材料对农户有用。这些材料也表明，现行的某些治理措施无法有效控制栖留地下水位，部分原因就在于对其成因缺乏了解，对其变化未能预报。

A COMMON morphological feature of texture-contrast (Chittleborough 1992) or duplex (Northcote 1979) soils of the agricultural lands of southern Australia (Fig. 1) is the strong contrast between the coarse textured A and E horizons and the fine textured B horizon. However, chemical, mineralogical and physical properties of the texture-contrast soils can vary (Tennant et al. 1992; McFarlane and Cox 1992). Texture-contrast soils are also common in other parts of the world (Chittleborough 1992). The B horizons of texture-contrast soils in catchments in Western Australia have been shown by Cox (1988) to have saturated hydraulic conductivities (*Ks*) as low as 0.002 m/day, whereas the A horizon is at least 10 times this value.

A common problem reported with some of these soils, due to a lack of vertical flow capacity in the B horizon, is the development of a perched watertable in winter (Cox and McFarlane 1995). On sloping land this results in significant throughflow to lower slopes, causing waterlogging (saturation of the root zone: see Fig. 2), reduction in crop yields and increased land degradation.

By comparison, the texture-contrast soils whose subsoils have a high *Ks* (up to 1.2 m/day in catchments in Western Australia; Cox 1988) have been termed 'leaky' (Cox and Fleming 1997); in these situations, throughflow in the A horizon is a minor component of the catchment water budget (Fleming and Cox 1998), with B horizon throughflow dominating (Stevens et al. 1999).

The aim of this study was to measure the causes and extent of waterlogging in texture-contrast soils on slopes in a catchment in the Mount Lofty Ranges, South Australia. A method based on a topographic index was used to predict waterlogging at the catchment scale, which was then compared to the conventional point-scale measurements. This information was necessary for advising farmers on better strategies to control waterlogging.

Figure 1. Location of texture-contrast soils in Australia (Chittleborough 1992).

Figure 2. Waterlogging of texture-contrast soils (Keynes catchment, Mount Lofty Ranges, 1993).

Materials and Methods

Site description

The study was carried out in the Keynes catchment near Keyneton in the Mount Lofty Ranges in South Australia. The Overview provides background information on the Mount Lofty Ranges. The climate is Mediterranean, with cool, wet winters and hot, dry summers. The long-term (91-year) average rainfall in Keyneton is 544 mm; evaporation is 839 mm.[1] Annual rainfall in the town is not significantly different from the catchment (Pritchard 1998). The long-term average data show that rainfall exceeds evaporation from April to October. During our study, monthly rainfall was measured by a tipping bucket pluviometer attached to a weather station (Monitor Sensors Pty Ltd). Potential evaporation was calculated using the Priestly–Taylor equation (Priestly and Taylor 1972).

Two toposequences with predominantly annual pastures (Cox and Pitman 2001) were chosen for this study: a 150 m convex toposequence (sites KH0 to KH9) and a 240 m concave toposequence (sites KV1–KV10). The sites were from flat (KH0, KV1) to crest (KH9, KV10) and thought to incorporate most soil types in the catchment and both diverging and converging water flow.

[1] Point patched meteorological data: see http://www.dnr.qld.gov.au/silo

Pedology and soil physics

Soil horizons along each toposequence were hand-textured and described according to McDonald et al. (1990); they were classified according to US taxonomy (Soil Survey Staff 1996). Soil toposequences were drawn according to the method of Rinder et al. (1994).

A constant head well permeameter (Talsma and Hallam 1980) and the equation of Reynolds and Elrick (1991) were used to measure *Ks* of the A, E and B horizons in triplicate. Bulk density (ρ_b) was measured with depth by taking duplicate soil cores (4.7 cm wide and 5 cm thick) from soil pits dug at the end of the project. All soils were analysed by the method of Rayment and Higginson (1992).

Measurement and quantification of perched watertables

To measure point-scale water duration, dipwells were installed at eight sites (KH1–KH8) along the convex toposequence and 10 sites (KV1–KV10) along the concave toposequence. At each site, a hole was dug with an auger to 0.5–0.6 m; the hole was lined with 50-mm diameter PVC pipe and capped on the top and bottom. All dipwells were fully slotted below ground level and sand packed. Dipwell water levels were manually measured every week in winter and less frequently at other times for five years (1 January 1994 to 31 December 1998). In addition, at three sites along each toposequence — lower slope (KH1 and KV1); mid-slope (KH5 and KV5); and upper slope (KH8 and KV10) — a data-logger and capacitance probe were installed to electronically measure water levels.

Water duration was quantified by accumulating, over the monitored period, the depth of water between the soil surface and 0.5 m (average depth to

the B horizon); this was termed the water duration index (WDI):

$$WDI_{50} = \sum_{i=1}^{n} S_i \qquad (1)$$

where n is the number of days in the analysis period and S_i is a statistic that is defined as:

$S_i = 50 - D_i$ *for* $D_i < 50$ cm

$S_i = 0$ for $D_i \geq 50$ cm

where D_i is the average depth (in centimetres) of the watertable below the soil surface on day i and $D_i > 50$ (the average depth of the B horizon in centimetres) means that the soil is not waterlogged. Cox et al. (1996) give a full explanation of the index.

Measurement and quantification of depth of saturation

Point scale

An aluminium access tube was installed to 2 m at five landscape positions on the convex slope — crest (KH9); upper slope (KH8); mid-slope (KH5); lower slope (KH1); and flat (KH0) — and three on the concave slope — upper slope (KV10); mid-slope (KV5); and lower slope (KV1) — using the method of Greacen (1981). Volumetric water content was measured every 15 cm (to 2 m) each 2 to 4 weeks for five years by a neutron moisture meter (NMM). Soil cores were taken on four occasions at each depth interval at each site and an NMM calibration was developed for each to determine volumetric water content and percentage saturation.

Catchment scale

To map the extent of soil saturation, a topographic index (Equation 2) was calculated for the study area to represent the geomorphic processes associated with soil water and its spatial distribution in the landscape. The variables of the index were evaluated on a cell-by-cell basis from a digital elevation model (DEM).

$$\ln (A_s/\tan \theta) \qquad (2)$$

where A_s = specific catchment area, and $\tan \theta$ = local slope angle.

Results and Discussion

Rainfall

Annual rainfall was below average (544 mm), except in 1996 (Table 1).

Topographic index

Figure 3 shows a three-dimensional representation of the topographic index. The index indicated that:

- permanent or long periods of soil saturation occur on the flats and lower slopes;
- infrequent to very infrequent saturation occurs on the mid-slopes; and
- short to long periods of saturation occur on the upper slopes and crests (for example, the mid-slopes have the darkest shading in Figure 3, and are the driest).

Point measured waterlogging

Table 1 shows three contrasting examples of the severity of water duration as measured in the dipwells. Figure 4 shows variations in perched watertables along the convex toposequence. A perched watertable rarely formed on some of the texture-contrast soils, but other such soils were very susceptible, even in dry years. The shortest water duration was measured on the mid-slopes, which agreed with the prediction from the topographic index. However, longer water duration was measured on the upper slopes than on the lower slopes. The lower slopes and flats probably have a long water duration when groundwaters are highest (when rainfall is above average).

Table 1. Rainfall (mm) and water duration.

	1994	1995	1996	1997	1998
Annual rainfall (mm)[a]	304	468	548	404	426
Water duration (WDI_{50} cm/day)[b]					
Lower slope	0	71	330	0	0
Mid-slope	0	0	2	0	0
Upper slope	485	345	850	289	134

[a] Long-term average annual rainfall is 544 mm
[b] Water duration at 50 cm depth (cm/day)

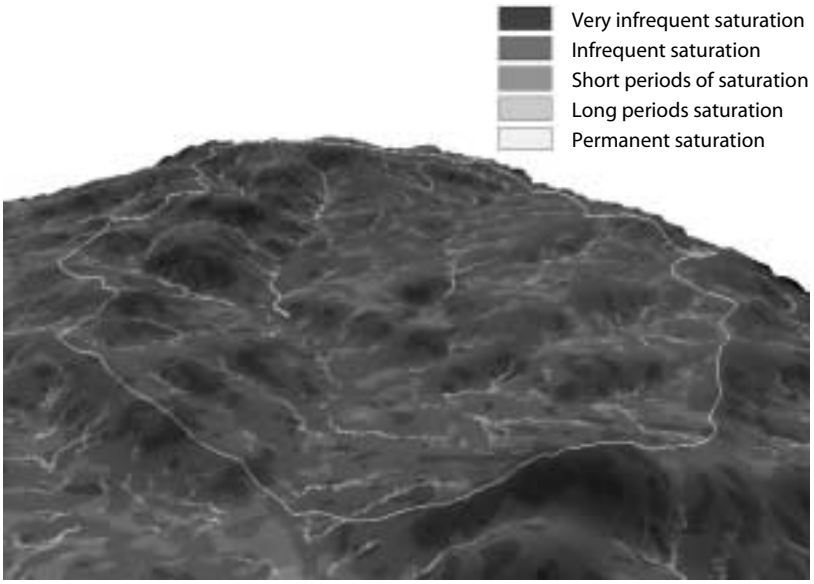

Figure 3. 3D representation of topographic index showing duration of saturation.

Figure 5 shows the relationship between the waterlogging and the annual rainfall less evaporation. Equation 3 expresses waterlogging as the average water duration severity over the hillslope:

$$WDI_{50} = 0.0072\ (R - E)^{2.0374},\ r^2 = 0.914 \quad (3)$$

where WDI_{50} is the water duration index (cm/day), R is rainfall (mm), and E is evaporation (mm).

Neutron moisture meter data

Figure 6 shows the water status of three soils as determined from the NMM data. Soil saturation was sometimes due to the development and persistence of perched watertables and at other times due to groundwaters each winter, depending on the position in the landscape. Soils on the lower slopes were wettest each winter below about 1.5 m. Saturation was due to saline groundwater; the duration and severity were due to the height the groundwater rose each winter. Although the degree of saturation increased in the A horizon each winter, a perched watertable never developed on the boundary between the A and B horizons on the flats and lower slopes. Saturation of the soils on the mid-slopes was due to a perched watertable developing either on or within the clay B horizon. In addition, groundwaters contributed to

saturation to within 1.0 m of the soil surface in 1995 and 1996. On the upper slopes, the lower A and B horizon soils became saturated each winter due to a perched watertable. In some soils the perching occurred at the boundary between the A and B horizons; in others it was deeper in the soil profile, nearer the boundary of the B and C horizons. In 1996, the wettest season, saturation extended into the upper C horizon.

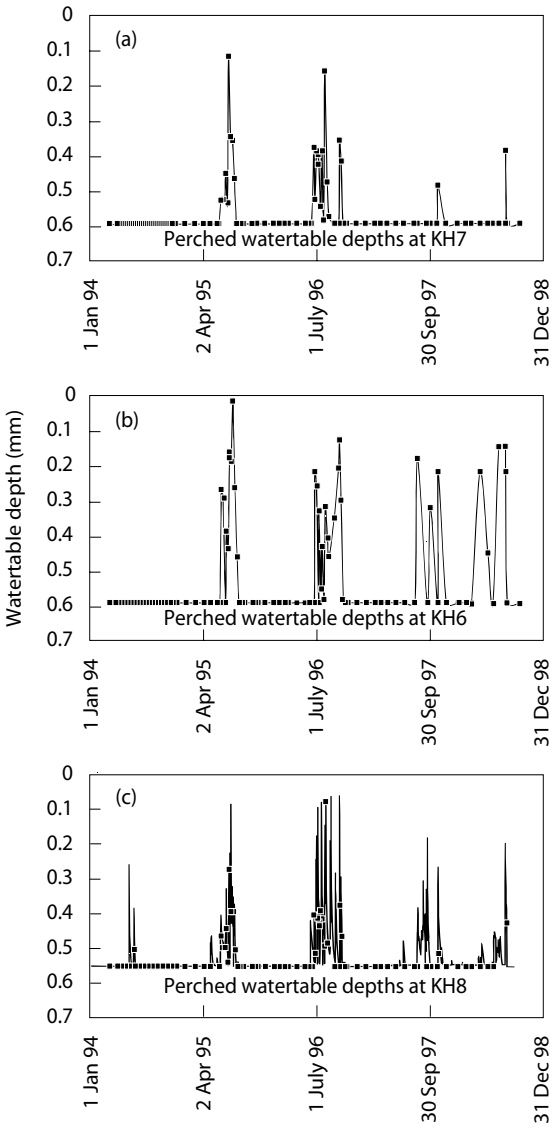

Figure 4. Examples of the development of a perched watertable along the convex toposequence.

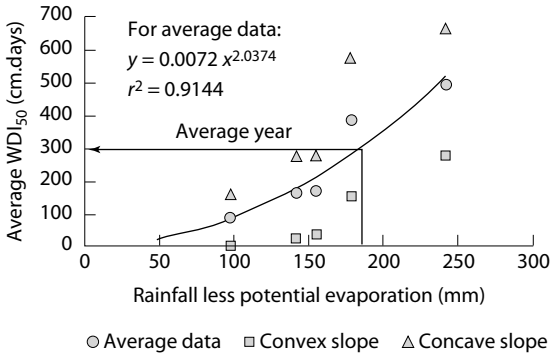

Figure 5. The relationship between rainfall less evaporation and waterlogging.

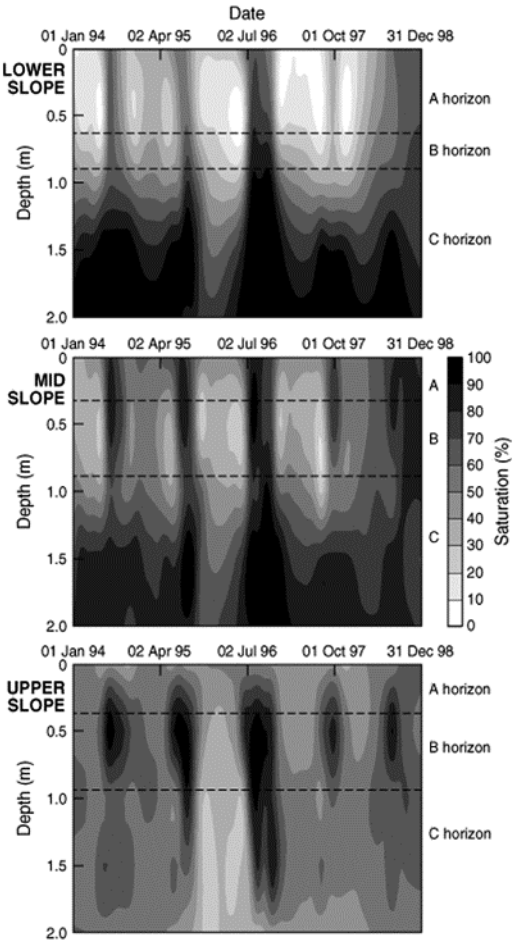

Figure 6. Examples of the degree of soil saturation at three positions in the landscape over five years.

Conclusions

In relatively dry years, water duration on the upper slopes of catchments in the Mount Lofty Ranges is higher than on the lower slopes. This is because the cause of soil saturation on the lower slopes is different from that on the mid- and upper slopes. It is predicted that the highest water duration on the lower slopes will occur in wet years (due to saturation by groundwaters); this is consistent with indications from a topographic index.

The failure of current management options to adequately control perched watertables on slopes is partly due to the lack of understanding of their causes and to inadequate prediction of their variability.

Acknowledgments

Mr Graham Keynes provided access to the land used in the study.

References

Chittleborough, D.J. 1992. Formation and pedology of duplex soils. Australian Journal of Experimental Agriculture, 32, 815–825.

Cox, J.W. 1988. Seepage interceptor drainage of duplex soils in south-western Australia. University of Western Australia, PhD Thesis.

Cox, J.W. and Ashley, R. 2000. Water quality of gully drainage from texture-contrast soils in the Mount Lofty Ranges in low rainfall years. Australian Journal of Soil Research, 38, 959–972.

Cox, J.W. and Fleming, N.K. 1997. Understanding landscape processes. Proceedings of an Australian Institute of Agricultural Science and Technology Symposium: Property and Catchment Planning, Issues Challenges and Professional Responsibilities, Waite Institute, Adelaide, 16 September 1997.

Cox, J.W., Fritsch, E. and Fitzpatrick, R.W. 1996. Interpretation of soil features produced by modern and ancient processes in degraded landscapes: VII. Water duration. Australian Journal of Soil Research, 34, 803–824.

Cox, J.W. and McFarlane, D.J. 1995. The causes of waterlogging in shallow soils and their drainage in southwestern Australia. Journal of Hydrology, 167, 175–194.

Cox, J.W. and Pitman, A. 2001. Chemical concentrations in drainage from perennials grown on sloping duplex soils. Australian Journal of Agriculture Research 52, 211–220.

Fleming, N.K. and Cox, J.W. 1998. Nutrient losses off dairy catchments located on texture contrast soils: carbon, phosphorus, sulphur and other chemicals. Australian Journal of Soil Research, 36, 979–995.

Greacen, E.L. 1981. Soil Water Assessment by the Neutron Method. Australia, CSIRO.

McDonald, R.C., Isbell, R.F., Speight, J.G., Walker, J. and Hopkins, M.S. 1990. Australian Soil and Land Survey, Field Handbook. Second edition. Melbourne, Inkata Press.

McFarlane, D.J. and Cox, J.W. 1992. Management of excess water in duplex soils. Australian Journal of Experimental Agriculture, 32, 857–864.

Northcote, K.H. 1979. A Factual Key for the Recognition of Australian Soils. Fourth edition. Glenside, Rellim Technical.

Priestly, C.H.B. and Taylor, R.J. 1972. On the assessment of surface heat flux and evaporation using large-scale parameters. Monthly Weather Review, 100, 81–92.

Pritchard, J. 1998. Modelling the water balance of duplex soils at Keyneton, Mt Lofty Ranges, SA. University of Adelaide, BSc Honours Thesis.

Rayment, G.E. and Higginson, F.R. 1992. Australian Laboratory Handbook of Soil and Water Chemical Methods. Sydney, Inkata Press.

Reynolds, W.D. and Elrick, D.E. 1991. Determination of hydraulic conductivity using a tension infiltrometer. Soil Science Society of America Journal, 55, 633–639.

Rinder, G.E., Fritsch, E. and Fitzpatrick, R.W. 1994. Computing procedures for mapping soil features at sub-catchment scale. Australian Journal of Soil Research, 32, 909–913.

Soil Survey Staff. 1996. Keys to Soil Taxonomy, 7th edition. Washington DC, United States Department of Agriculture, United States Government Printing Office.

Stevens, D.P., Cox, J.W. and Chittleborough, D.J. 1999. Pathways for phosphorus, nitrogen and carbon over and through texturally differentiated soils, South Australia. Australian Journal of Soil Research, 37, 679–693.

Talsma, T. and Hallam, P.M. 1980. Hydraulic conductivity measurement of forest catchments. Australian Journal of Soil Research, 18, 139–148.

Tennant, D., Scholz, G., Dixon, J. and Purdie, B. 1992. Physical and chemical characteristics of duplex soils and their distribution in the south-west of Western Australia. Australian Journal of Experimental Agriculture, 32, 827–843.

18 Monitoring Regional Water Use Efficiency Indicators on the North China Plain

Tim R. McVicar,[*] Guanglu Zhang,[†]
Andrew S. Bradford,[*] Huixiao Wang,[‡]
Warrick R. Dawes,[*] Lu Zhang[*] and Lingtao Li [*]

Abstract

Increasing competition for water in China, due to industrialisation of its economy and urbanisation of its population, has led to the introduction of water-saving agricultural practices to increase agricultural water use efficiency (Ag WUE). This study assessed whether changes in management practices increased regional Ag WUE for a focus area covering 20% of the 300,000 km^2 North China Plain (NCP). An 'input–output' definition of regional Ag WUE was used, where 'input' is the water available over the crop growing season and 'output' is grain yield. Regional databases of precipitation, irrigation and yield from 1984 to 1996 were established in a geographic information system (GIS) to calculate winter wheat and summer corn Ag WUE on a county basis. For wheat, the average Ag WUE was 7.0 kg/ha/mm in 1984, whereas in 1996 it was 14.3 kg/ha/mm. For corn, Ag WUE increased from 9.0 kg/ha/mm in 1984 to 10.1 kg/ha/mm in 1996, although values of more than 11.5 kg/ha/mm were obtained for both 1991 and 1992. Time series plots of the resulting Ag WUE and its components were generated to reveal spatial and temporal variability. Counties with a relatively high mean Ag WUE and a low year-to-year consistency were found to have the highest potential for improving Ag WUE management. Total county water resources (WR) were also calculated for the time series, and normalisation of Ag WUE and WR on a county basis also showed that there have been recent improvements in Ag WUE. For some counties in wet years, it may be possible to plant larger areas of crop to increase county-level Ag WUE. For the focus study site (and for the time series data available), it is most likely that recently introduced water-saving agricultural practices in the NCP region are associated with improvements to Ag WUE.

工业化和城市化的发展导致中国用水矛盾日益加剧，促使采取节水农业，以求提高水分利用效率（WUE）。本研究的目的是评估研究区农业经营方式的改变是否提高了 WUE。文中用到的区域农业 WUE“投入－产出”定义是：投入＝作物生长季节可利用的水分，产出＝作物产量。将该区从 1984 到 1996 年的降水、灌溉和产量数据储存在地理信息系统中，以县为单位计算

[*] CSIRO Land and Water, PO Box 1666, Canberra, ACT 2601, Australia. Email tim.mcvicar@csiro.au
[†] Shijiazhuang Institute of Agricultural Modernization, Chinese Academy of Sciences, Shijiazhuang 050021, PRC.
[‡] Beijing Normal University, Institute of Environmental Sciences, Beijing, PRC.

McVicar, T.R., Guanglu Zhang, Bradford, A.S., Huixiao Wang, Dawes, W.R., Lu Zhang and Lingtao Li. 2002. Monitoring regional water use efficiency indicators on the North China Plain. In: McVicar, T.R., Li Rui, Walker, J., Fitzpatrick, R.W. and Liu Changming (eds), *Regional Water and Soil Assessment for Managing Sustainable Agriculture in China and Australia*, ACIAR Monograph No. 84, 231–257.

各年度玉米和小麦的 WUE。结果表明，小麦的平均 WUE 值在 1984 年是 7.0 千克每公顷毫米，1996 年提高到 14.3，同期玉米的由 9.0 千克每公顷毫米提高到 10.1，尽管在 1991 和 1992 年曾超过了 11.5。WUE 按年份顺序生成，以表现其时间、空间变化过程。平均 WUE 相对较高而且年际变化大的县份，最有治理潜力。我们也计算了同期各县水资源总量（WR）。各县的农业 WUE 和 WR 正态分布也表明 WUE 在近年有所改善。在多雨年份，有些县份扩大作物种植面积有可能提高县级水平的农业 WUE。就研究区现有资料的年份而言，WUE 的提高很可能同近年实行的节水农业有关。

THERE is increasing competition for water in China due to industrialisation of its economy and urbanisation of its population (Brown and Halweil 1998; Rosegrant and Ringler 2000; Anderson and Peng 1998). This competition, coupled with the need for environmental river flows to ensure that aquatic and riparian ecosystems are sustainable, has placed increasing demands on the Chinese agricultural sector to maintain and increase production using less water. China depends on irrigation water to produce 70% of its grain supply (Brown and Halweil 1998; Zhang 1999). This water is obtained from surface and groundwater systems, at rates that are not sustainable (Jin et al. 1999; Zhang et al. 1998). Since 1978, the beginning of the post-Mao 'pragmatic period' (Muldavin 1997), water-saving agricultural practices and rural land tenure reforms (Wei 1997; Lin 1997; Xing 1997) were widely and proactively implemented by the Chinese central government to increase agricultural production. In North China, grain yield increased from 72 million tonnes in 1979 to 114 million tonnes in 1995 (Yang 1998), while the area of cultivated land decreased by 1.5 million ha (Yang and Li 2000). Currently, the area of arable land per capita in China is one-third the world average (Cao et al. 1995).

Achieving increased grain production with less land area has meant that agricultural systems have become intensively managed. Many agricultural practices designed to save water have been implemented (Wang et al. in press), and fertilisers have been widely used to overcome nutrient limitations, although overapplication has raised concerns about environmental degradation and pollution (Yong and Jiabao 1999; Rozelle et al. 1997).

Stanhill (1986) suggested three main components of water-saving agriculture: reducing delivery losses in irrigation systems; improving water transfer (from either irrigation or rainfall) to a depth where roots can access the water; and maximising water use efficiency (WUE) by crops. Minimising delivery losses is essentially an engineering problem. Water balance modelling can be used to ensure that water is applied at suitable times and in suitable amounts to optimise plant transpiration (Wang et al. 2001). Soil structure and fertility can be altered (for example, by increasing soil organic matter). Variations in regional WUE need to be monitored to assess the effectiveness of water-saving agricultural practices in the context of spatial and temporal variation of water resources. Different measurements and modelling approaches are required to determine agricultural WUE (abbreviated as Ag WUE hereafter) at different scales.

Stanhill (1986) defined WUE both hydrologically and physiologically. Hydrological WUE is the ratio of evapotranspiration to the water potentially

available for plant growth. It is expressed as a percentage or fraction (0–1). Physiological WUE measures the amount of plant growth for a given volume of water. Physiological WUE can be defined for different measures of 'plant growth' and 'volume of water'. Turner (1986) noted that care is needed when defining WUE. For example, in some studies 'plant growth' is measured in units of net biomass (including roots) (Ritchie 1983; Tanner and Sinclair 1983; Turner 1997) or crop grain yield (Tanner and Sinclair 1983; Turner 1997). In various previous studies, the units for 'volume of water' were total transpiration (Tanner and Sinclair 1983; Turner 1997; French and Schultz 1984a,b), total evapotranspiration (Ritchie 1983; Tanner and Sinclair 1983; Turner 1997), total water input (Sinclair et al. 1984), or total growing season precipitation plus initial soil water at the time of sowing (French and Schultz 1984a,b).

Sinclair et al. (1984) introduced different time scales for several definitions of WUE. Scales ranged from an instant to a day or a growing season that can be linked to a range of spatial scales, which in turn extend from a single leaf, through a canopy, field, farm or region (Table 1). The scales are linked: leaf WUE (in the order of tens of square centimetres) will usually be measured over a short time (e.g. from 1 second to 1 day); regional WUE (in the order of thousands of square kilometres) will usually be measured over a longer time (e.g. from a day to a growing season). To date, there has been very little research focusing on farm-level (Tuong and Bhuiyan 1999) or regional assessments of WUE.

Single-leaf WUE is commonly defined as the net carbon dioxide (CO_2) uptake per unit of transpiration. On a continuous basis — that is, at any instant within a day — it is expressed as the ratio of leaf net photosynthetic rate to leaf transpiration rate. On a daily basis it is expressed as the ratio of daytime CO_2 uptake to daytime transpiration. Canopy (or community) WUE is commonly defined as the ratio of the crop canopy's net CO_2 assimilation to its transpiration — that is, the ratio of the canopy's CO_2 flux to the water flux for transpiration. Canopy WUE can be expressed continuously and at a daily time scale, as above, and can also be calculated at specific plant growth stages. WUE can be defined as grain yield per unit of water transpired, measured in kilograms per hectare per millimetre (kg/ha/mm). It can be measured at field level or regional level but there are difficulties in measuring regional WUE because the region may support multiple land uses and multiple crops during the same season. We have therefore developed an 'input–output' definition of regional WUE (Zoebl 2000). 'Input' is the water available over the crop growing season (i.e. rainfall plus irrigation) and 'output' is grain yield. This 'input–output' approach takes into account spatial and temporal constructs of regionally available databases.

In this chapter we define agricultural WUE as grain yield per unit water available for crop growth. This definition ignores precipitation that falls on 'bare' soil (areas that are not sown to actively growing crops). We present the data as kilograms of crop

Table 1. Linkages between different spatial and temporal scales for physiological water use efficiency, and some common units by which they are measured.

Spatial scale	Temporal scale	Units
Single leaf	Second—day—growth stage	mg CO_2/g H_2O or µmol CO_2/mmol H_2O
Canopy	Second—day—growth stage	mg CO_2/g H_2O or µmol CO_2/mmol H_2O
Field	Day—growth stage—season	mg CO_2/gH_2O or kg/ha/mm
Farm	Growth stage—season—year	kg/ha/mm or t/km^2/GL
Region	Season—year	kg/ha/mm or t/km^2/GL

yield per hectare of crop area per millimetre of water available for crop growth (kg/ha/mm). To assess the link between Ag WUE and total county water resources, we have also mapped the volume of water available to a county over the growing season. This includes precipitation that falls on 'bare' soil, and is expressed as gigalitres (GL or 10^9 L). 'Water resources' is abbreviated to 'WR' hereafter. As total county WRs are a function of county area, they should be compared only for counties of a similar size or, more strictly, for the same county at different times.

The base unit of the region is the administrative county, which is the smallest geographic resolution that the available databases covered (Cao et al. 1995). Many variables influence Ag WUE, but data are not available for many of them. They include:

- species or crop varieties, comprising plant breeding (Li et al. 1995) and genetic modifications;
- soil conditions (Gong and Lin 2000), comprising soil erosion, sodicity, and salinisation (Rozelle et al. 1997);
- agricultural practices, involving the use of fertilisers (Garabet et al. 1998), efficient irrigation management (Zhang and Oweis 1999; Zhang et al. 1998; Liu et al. 1998), time of planting and crop rotation (Li et al. 2000), planting density (Karrou 1998), and the use of mulch (Tolk et al. 1999) or plastic film (Jin et al. 1999) to reduce soil evaporation; and
- climate change (Smit and Yunlong 1996; Loaiciga et al. 1996), including precipitation patterns (Thomas 2000) and CO_2 concentration (Hunsaker et al. 2000).

At the regional scale, the interactions are complex and unknown, making absolute measures of Ag WUE difficult. The spatial information system developed here to monitor regional Ag WUE is most suited to interpreting relative trends, both spatially and temporally. The aim of our research is to monitor regional Ag WUE on the North China Plain (NCP) using readily available data. The method developed for this purpose can be used in other agricultural regions. This work is a starting point for more detailed analyses to infer causal relationships between Ag WUE and agricultural practice.

Materials and Methods

Description of the study site

The study was carried out in Hebei Province on the NCP (Fig. 1) . The Overview describes the general characteristics of the NCP region. We selected the Hebei Province portion of the NCP because it allowed us to establish regional precipitation, yield and irrigation databases. The Hebei Plain is defined by longitudes 113.5–118.0°E and latitudes 36.0–40.0°N; it comprises 90 counties covering 61,636 km^2, or 20% of the NCP (see Fig. 1). Of these, 84 counties produce agricultural output; the average size is 710 km^2, with a standard deviation of 310 km^2. The largest county covers 1980 km^2 and the smallest 204 km^2. Most of the study area is essentially flat, with some of the western counties straddling the plains and foothills of the Taihang Mountains (McVicar et al. 2000).

In the study area, the main crops are winter wheat and summer corn. Most rain falls in the summer, so more irrigation is applied during the growth period of winter wheat, which is planted in early October. During winter, the growth of wheat is limited by low air temperatures, so grain development occurs during the following spring and summer. Farmers commonly apply fertiliser in late March to early April, and irrigate at the same time ('fertigate') to ensure that the fertiliser is dissolved. Wheat is harvested in early June the following year. A variety of crops are grown in summer, including corn, millet, soybeans and sorghum. In this chapter this season is denoted 'corn' as the crop dominates autumn harvests. Usually the monsoon period provides enough rainfall for summer crop growth; however, farmers commonly fertigate once during

the summer season. Peanuts, cotton and several other nongrain producing crops are also grown during this season. Most of these crops are planted in mid-June and harvested in late September.

Exact dates for planting and harvesting over the entire NCP vary slightly depending on latitude. The dates reported below were optimised for the study area; the numbers in parentheses refer to the day of the year (for nonleap years), a notation used throughout this chapter. We assume the wheat growing season is from 1 October (day 274) until 10 June (day 161) the following year, and that corn is planted on 15 June (day 166) and harvested on 20 September (day 263). Throughout the year, small plots of intensively managed market garden vegetables are also grown. Dual cropping is carried out over the entire NCP; however, some rice is grown in the southern portion of the NCP in Anhui and Jiangsu Provinces.

Available water for the growing seasons

For the wheat growing season, the 'volume of water' available for crop growth comprises precipitation ($P_{\_wheat}$), irrigation ($I_{\_wheat}$), and initial effective soil water storage (W_{o_wheat}). We used daily precipitation data (see below) from the day after harvest of the summer crops, in early autumn on day 264, until the harvest of wheat on day 161 the following year. All precipitation and irrigation in this period was assigned to the wheat growing season. W_{o_wheat}, defined as available soil water (to a depth of 1.5 m) minus wilting point moisture content, has been related to the cumulative precipitation from 1 July to 30 September (Yuan et al. 1992). Researchers at Luancheng Eco-Agro-

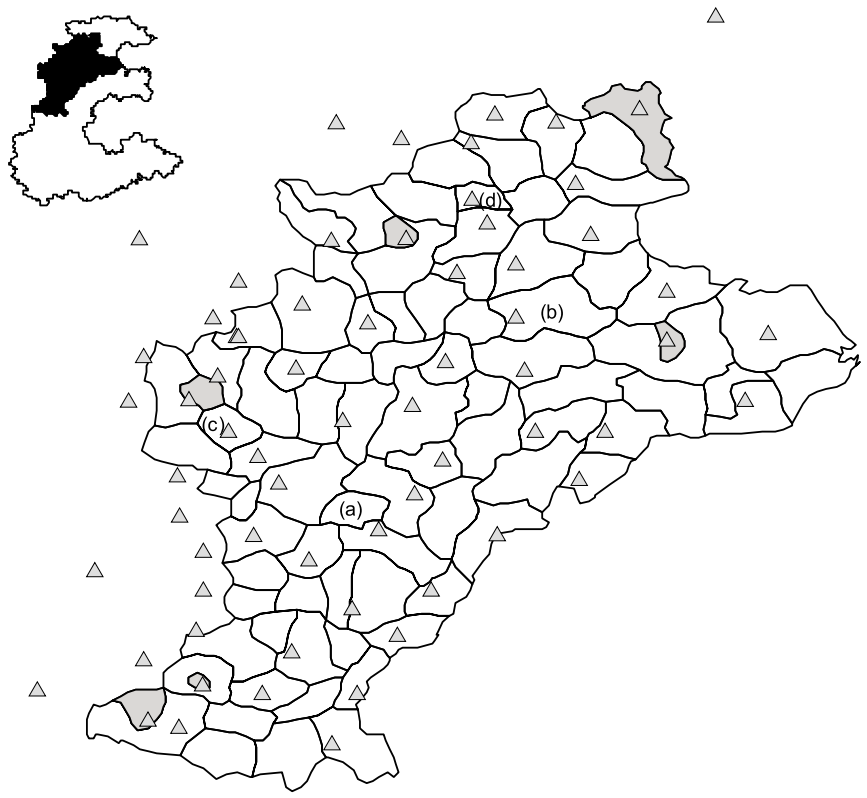

Figure 1. Location of counties and meteorological stations (△) in the Hebei Plain study area.The Hebei Plain area is shaded black in the inset map of the North China Plain. Four focus counties are identified: (a) Xinhe (132232); (b) Heijian (132922); (c) Luancheng (130124) and (d) Rongchen (132435). Nonagricultural counties, cities and industrial zones are shaded grey.

System Experimental Station used data over 16 years (1971–86) to develop the following relationship between the variables:

$$W_{o\_wheat} = -33.688 + 0.595 \sum P_{1\,July..30\,Sept},$$

with $r^2 = 0.837$.

Due to the summer-dominated rainfall, residual soil water (W_{o_wheat}) remaining after the summer corn growing season affects yields of the following wheat crop ($Y_{\_wheat}$).

The volume of water for the corn growing season also includes precipitation ($P_{\_corn}$) and irrigation ($I_{\_corn}$). The change in effective soil water storage from the start to the end of the corn growing season ($\Delta W_{\_corn}$) is of little importance to the final corn yield ($Y_{\_corn}$). This is because $P_{\_corn} + I_{\_corn} > \Delta W_{\_corn}$. The corn season is defined from the day after harvest of wheat on day 162 until the harvest of the autumn crops on day 263. Assuming that $\Delta W_{\_corn}$ is negligible results in a slight increase in wheat Ag WUE estimates and a slight decrease of corn Ag WUE.

Within a growing season, the amount and timing of rainfall and irrigation are obviously important for crop growth and final yields; however, due to the 'seasonal' resolution of the irrigation data (see below), we have integrated the precipitation data seasonally. This is the basis for our 'input–output' definition of Ag WUE, which used readily available regional data. To monitor Ag WUE regionally, we also assumed that capillary rise to the root zone, deep drainage from the root zone, and runoff were negligible. At the regional level, we defined Ag WUE as follows:

$$\text{Ag WUE}_{\_wheat} = \frac{Y_{\_wheat}}{P_{\_wheat} + I_{\_wheat} + W_{o\_wheat}} \text{ and}$$

$$\text{Ag WUE}_{\_corn} = \frac{Y_{\_corn}}{P_{\_corn} + I_{\_corn}}$$

with units of kg/ha/mm. The 'input–output' Ag WUE approach takes into account the spatial and temporal constructs of the regional databases that are available. The required databases, introduced below, were developed in a geographic information system (GIS) to calculate and map variations in Ag WUE regionally.

Precipitation data

Daily precipitation data were recorded from 1981 to 1996 at 65 stations in Hebei Province covering the study area. More than 50 stations are well distributed over the Hebei Plain; another 13 stations are located outside the NCP in the Taihang Mountains to the west. At each of the 65 stations $P_{\_wheat}$, W_{o_wheat} and $P_{\_corn}$ were calculated. Using ANUSPLIN (Hutchinson 1999), these three variables were then spatially interpolated over the entire study area at a resolution of $1/120^{th}$ of a degree. Selection of spline model parameters is fully documented in McVicar et al. (2000). For the three variables, the average for each county for each growing season was used in the calculations.

Irrigation data

The spatial irrigation database was established by contacting the relevant officials in each county, from the Agricultural Bureau, the Hydrological Bureau or the Agricultural Planning Bureau, depending on which organisation kept records. In the study area, all irrigation water is obtained from the regional groundwater aquifers by using electric pumps. The farmers pay the electricity costs twice a year (at the end of the wheat and corn growing seasons). Taking into account depth to watertable, the electricity costs are converted to electricity use, which translates into a volume of water extracted at each pump. This is aggregated to provide the amount of water used for irrigation at a county level. Seasonal irrigation amounts used for wheat and corn in 49 of the 84 agricultural counties were recorded from 1981 to 1996. Timing and location of individual irrigation events were not available. County-level irrigation amounts for the wheat season represent approximately nine months; for corn they represent approximately three months.

Yield data

The Hebei Province Agricultural Bureau recorded yield data for 84 counties (Fig. 1) from 1984 to 1996. The Chinese national standard, which has been used routinely over the last 20 years, was used to estimate county-level yield data. Briefly, the method relies on aggregating estimated yields from the village, to the township, to the county. Within the study area, 15–30 villages contribute to a township, and there are 10–20 townships within a county. For each village, the farmland is divided into three classes of productivity: good, medium and poor. At least 10% of the farmland of the entire village is sampled, with at least 3% being in each class. In the three classes, random sampling of grain yield is undertaken, calculated by seeds per spike multiplied by the number of spikes multiplied by the average seed weight. The three variables are determined for a 4 m^2 (2 m × 2 m) quadrat, repeated within a paddock two to five times depending on local variability. The average weight of a seed is determined from a 1000-seed sample in each quadrat. If the difference between all the variables is less than 2%, the average of the two samples is used to represent the paddock. If the difference is more than 2%, another sample is acquired and the difference between the new sample and the average of the previous samples is determined. This routine is continued until the difference is less than 2%. The average grain yield of the quadrat is then determined for each class. This value is then weighted by area, using the relative areas of the three classes of farmland productivity, to produce an estimate of yield for each village. These values are aggregated through the township level to the county level.

Data for both 1986 and 1988 were missing, and values for two counties were not recorded for one year[1] so there are 922 observations of yield and crop area for the main crop types, including wheat, corn, millet, sorghum and soybeans. We estimated the county yield for 1986 and 1988 using regional remotely sensed data; full technical details of this process are documented in McVicar et al. (2000). While the area of each crop in each county was known, the location was not. This restricted our analysis to an entire county level. Table 2 shows the yields and areas planted for summer and autumn harvested crops. For crops harvested in early June, wheat contributed more than 90% of the yield for all 922 observations. Sixty-four per cent of the counties had wheat planted to more than 30% of the county area. Corn was the most important autumn harvested crop, although millet, sorghum and soybeans were also important. For 63% of the 922 observations, the combined area planted with corn, millet, sorghum and soybeans within each county was more than 30% of the county area. For many counties, less than 50% of the county area was usually planted with crops.

County total water resources

We calculated (in GL) the total WR for both the wheat and corn growing periods for each county. The volume was obtained by summing [1] the product of crop area by the amount of irrigation water applied; and [2] the product of county area by average county precipitation. In the case of wheat, we added estimates of initial soil water content. For wheat, WR was calculated as:

$$\left(\text{crop area (ha)} \times I_{\_wheat}\,(\text{mm})\right)[1]$$
$$+\left\{\text{country area (ha)} \times \left(\begin{matrix} P_{\_wheat}\,(\text{mm}) + \\ W_{o\_wheat}\,(\text{mm}) \end{matrix}\right)\right\}[2]$$

As discussed previously, there is no corresponding W_o term for corn.

[1] Xincheng (132436) was missing in 1993 and Hengshui (133001) was missing in 1996 (figures in brackets represent the Chinese Central Government County Code Identification).

Table 2. Decile frequency distributions for both summer and autumn harvested crops (normalised by county yield and county area) for the 84 agricultural producing counties over 11 years (1984–96) for grains.

	Summer-harvested crops		Autumn-harvested crops[a]									
	Wheat		Corn		Millet		Sorghum		Soybean		Combined grains	
Per cent range	% by yield	% by area	% by yield	% by area	% by yield	% by area	% by yield	% by area	% by yield	% by area	% by yield	% by area
> 90	100 (922)	0 (0)	8(76)	0 (0)	0 (0)	0 (0)	0 (0)	0 (0)	0 (0)	0 (0)	56(524)	0 (0)
80–90	0 (0)	0 (0)	20(184)	0 (0)	0 (0)	0 (0)	0 (0)	0 (0)	0 (0)	0 (0)	31(287)	0 (0)
70–80	0 (0)	0 (0)	25(232)	0 (0)	0(1)	0 (0)	0 (0)	0 (0)	0 (0)	0 (0)	9(83)	0 (0)
60–70	0 (0)	2 (16)	21(196)	0 (0)	1(5)	0 (0)	0 (0)	0 (0)	0(2)	0 (0)	2(15)	0(3)
50–60	0 (0)	8 (72)	13(118)	0(1)	2(17)	0 (0)	0 (0)	0 (0)	0(2)	0 (0)	1(7)	4(39)
40–50	0 (0)	18 (171)	6(53)	5(47)	2(14)	0 (0)	0 (0)	0 (0)	0(2)	0 (0)	1(6)	21(194)
30–40	0 (0)	36 (333)	3(24)	18(162)	3(25)	0 (0)	0(3)	0 (0)	1(5)	0 (0)	0 (0)	38(344)
20–30	0 (0)	32 (293)	1(12)	34(312)	9(83)	0(1)	1(8)	0 (0)	4(36)	0(2)	0 (0)	34(316)
10–20	0 (0)	4 (35)	2(21)	35(326)	25(234)	10(88)	4(32)	0 (0)	21(194)	12(107)	0 (0)	3(25)
< 10	0 (0)	0 (2)	1(6)	8(74)	58(543)	90(833)	95(879)	100(922)	74(681)	88(813)	0 (0)	0(1)

[a] Harvested mid-September

Note: Wheat yield was calculated as the percentage of the total summer grain harvest. Wheat area was the percentage of each county planted to wheat. The percentage of the total autumn grain harvest was calculated for corn, millet, sorghum, and soybean. Autumn crop areas are the percentage of county planted with each crop. Combined grains are corn, millet, sorghum, and soybean. Numbers in brackets are the number of observations

Results and Discussion

Agricultural water use efficiency

Figures 2 and 3 show the Ag WUE from 1984 until 1996 for the wheat and corn growing seasons, respectively; they also show the components used for the calculation of Ag WUE. The data are presented for the year of harvest. The use of the county average from the interpolated surfaces for $P_{\_wheat}$, W_{o_wheat} and $P_{\_corn}$ introduces uncertainty into the final Ag WUE calculation. To understand the potential uncertainty introduced, we divided the average county range by the average mean for $P_{\_wheat}$, W_{o_wheat}, and $P_{\_corn}$. For $P_{\_wheat}$, for the 1092 observations (84 counties over 13 years), the average range (12.43 mm) divided by the average mean (147.70 mm) was 8.42%. For W_{o_wheat}, the average range (24.18 mm) divided by the average mean (165.35 mm) was 14.63%. For $P_{\_corn}$, the average range (48.11 mm) divided by the average mean (386.01 mm) was 12.46%. These statistics illustrate that taking the county average interpolated output introduced less than 15% uncertainty into the seasonal county-based Ag WUE calculation.

For both wheat and corn in 1986 and 1988, county yields estimated from regional remote sensing appeared to be erroneous (Figs 2 and 3). Comparing these two years with all other yield data revealed that the relative spatial variability across the study site for these two years was dampened. That is, the yield estimated for counties in the east (with low measured yields) appears to be overestimated; for counties in the west (with high measured yields), it appears to be underestimated. The poor performance of the remotely sensed estimates of yield is probably caused by resampling on the satellite to produce global area coverage data (McVicar et al. 2000). The data for 1986 and 1988 for both wheat and corn have been ignored in all subsequent analysis of Ag WUE.

For the 538 valid measurements (49 counties over 11 years), Ag WUE for wheat had a mean value of 9.6 kg/ha/mm, with a standard deviation of 3.8 kg/ha/mm and a range of 21.5–1.2 kg/ha/mm. During the corn growing season, the mean Ag WUE was 9.5 kg/ha/mm, with a standard deviation of 5.1 kg/ha/mm and a range of 39.0–1.7 kg/ha/mm. Table 3 shows the average annual Ag WUE for both the wheat and corn growing seasons for the 49 counties. For wheat, the average Ag WUE was 7.0 kg/ha/mm in 1984; in 1996 it was 14.3 kg/ha/mm. For corn, Ag WUE increased from 9.0 kg/ha/mm in 1984 to 10.1 kg/ha/mm in 1996, although values of more than 11.5 kg/ha/mm were obtained in both 1991 and 1992. Figures 2 and 3 show the temporal and spatial variation for the wheat and corn growing seasons. If data were not available, the map is shaded grey and internal county boundaries are dissolved; this convention is used throughout the chapter.

Table 4 shows the frequency distributions for Ag WUE for both the wheat and corn growing seasons. For wheat, Ag WUE for 482 of the 538 observations (89%) was in the range 0–15 kg/ha/mm. Two previous studies conducted on the NCP, both using a seasonal evapotranspiration (ET) WUE definition, reported wheat Ag WUE values similar to those presented here. In the first, Zhang et al. (1999) assessed four different experimental sites, and reported values of 9.8–12.2 kg/ha/mm for rainfed conditions, and 11.8–14.0 kg/ha/mm for irrigated wheat. In the second, Jin et al. (1999) studied the impact of mulch, fertiliser and irrigation scheduling and reported values of 14.9–23.0 kg/ha/mm. The range of values presented in Table 4 is consistent with WUE values for wheat presented for other areas in China (9.3–15.5 kg/ha/mm, Zhang et al. 1998; 6.5–12.1 kg/ha/mm, Li et al. 2000), and for other locations, including Australia (2.5–10.4 kg/ha/mm, O'Leary et al. 1985; 5.5–16.5 kg/ha/mm, Regan et al. 1997), West Asia and North Africa (4.1–8.9 kg/ha/mm, Karrou 1998; 2.5–16.0 kg/ha/mm, Zhang and Oweis 1999; 8.1 to 11.0 kg/ha/mm, Oweis et al. 2000).

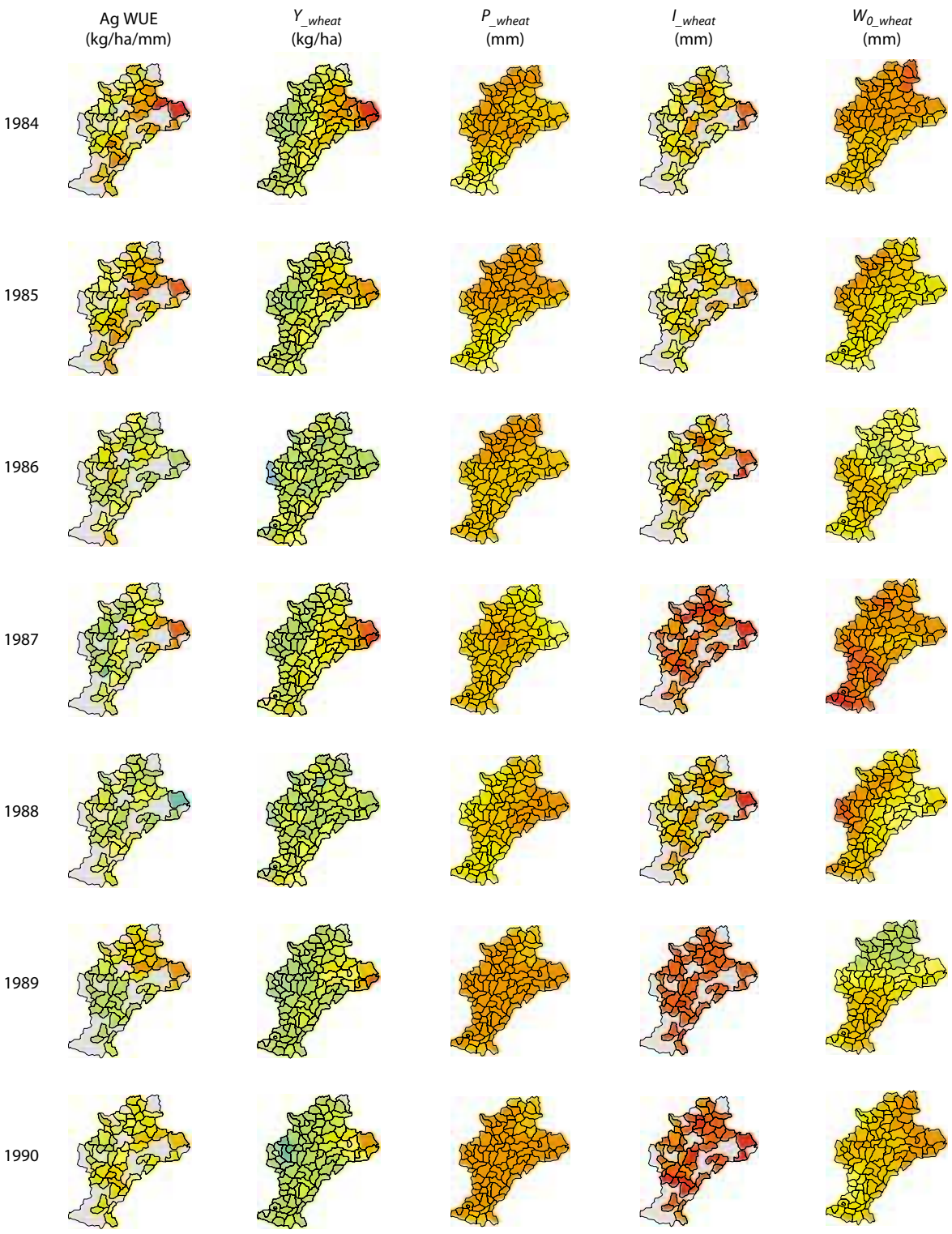

Figure 2. Agricultural water use efficiency for wheat grown on the Hebei Plain study area, 1984–96.
The figure shows agricultural water use efficiency (AgWUE) in kg/ha/mm and its components: $Y_{\_wheat}$ (kg/ha), $P_{\_wheat}$ (mm), $I_{\_wheat}$ (mm) and W_{o_wheat} (mm).

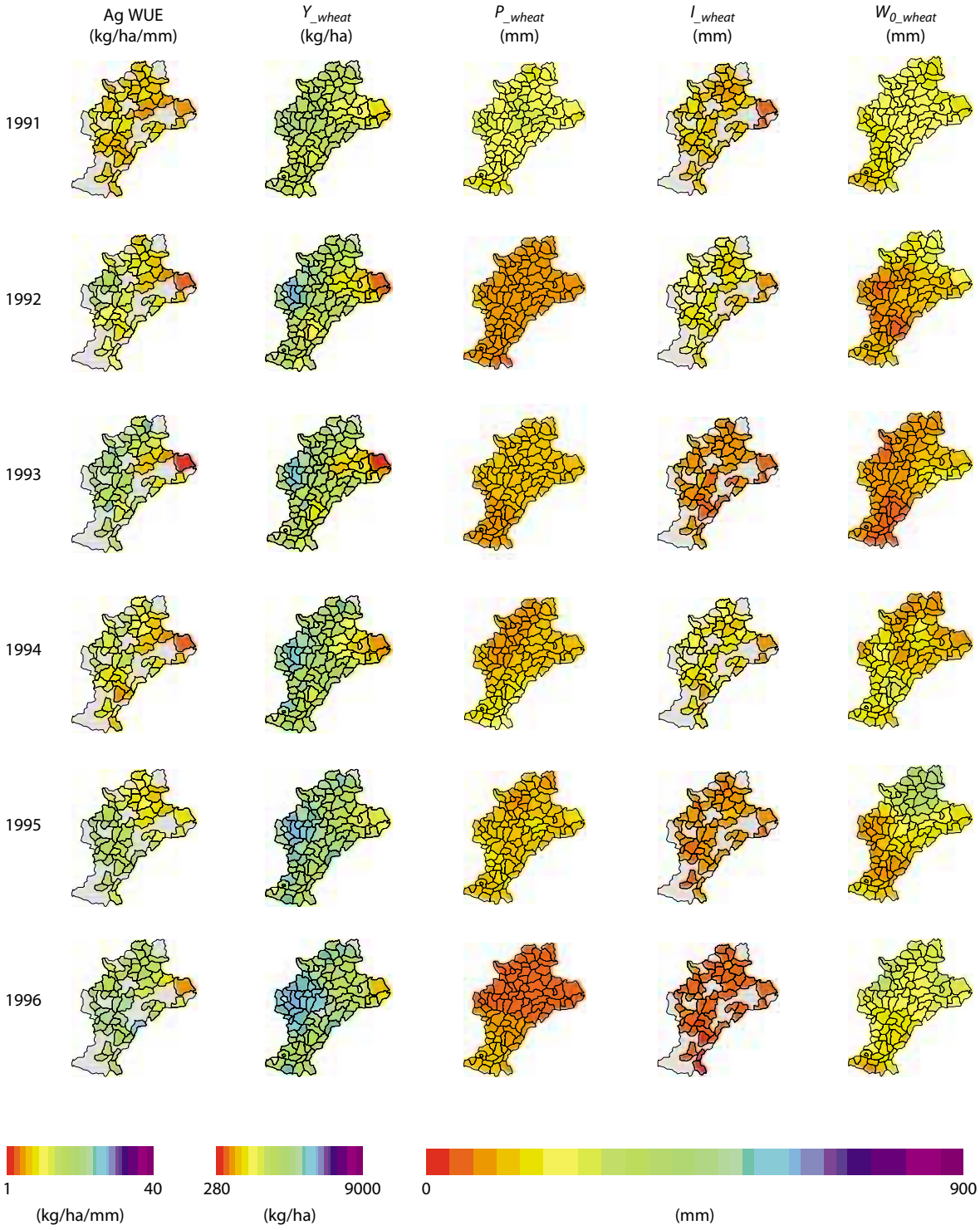

Figure 2. (cont'd) Agricultural water use efficiency for wheat grown on the Hebei Plain study area, 1984–96.
The figure shows agricultural water use efficiency (AgWUE) in kg/ha/mm and its components: $Y_{\_wheat}$ (kg/ha), $P_{\_wheat}$ (mm), $I_{\_wheat}$ (mm) and W_{o_wheat} (mm).

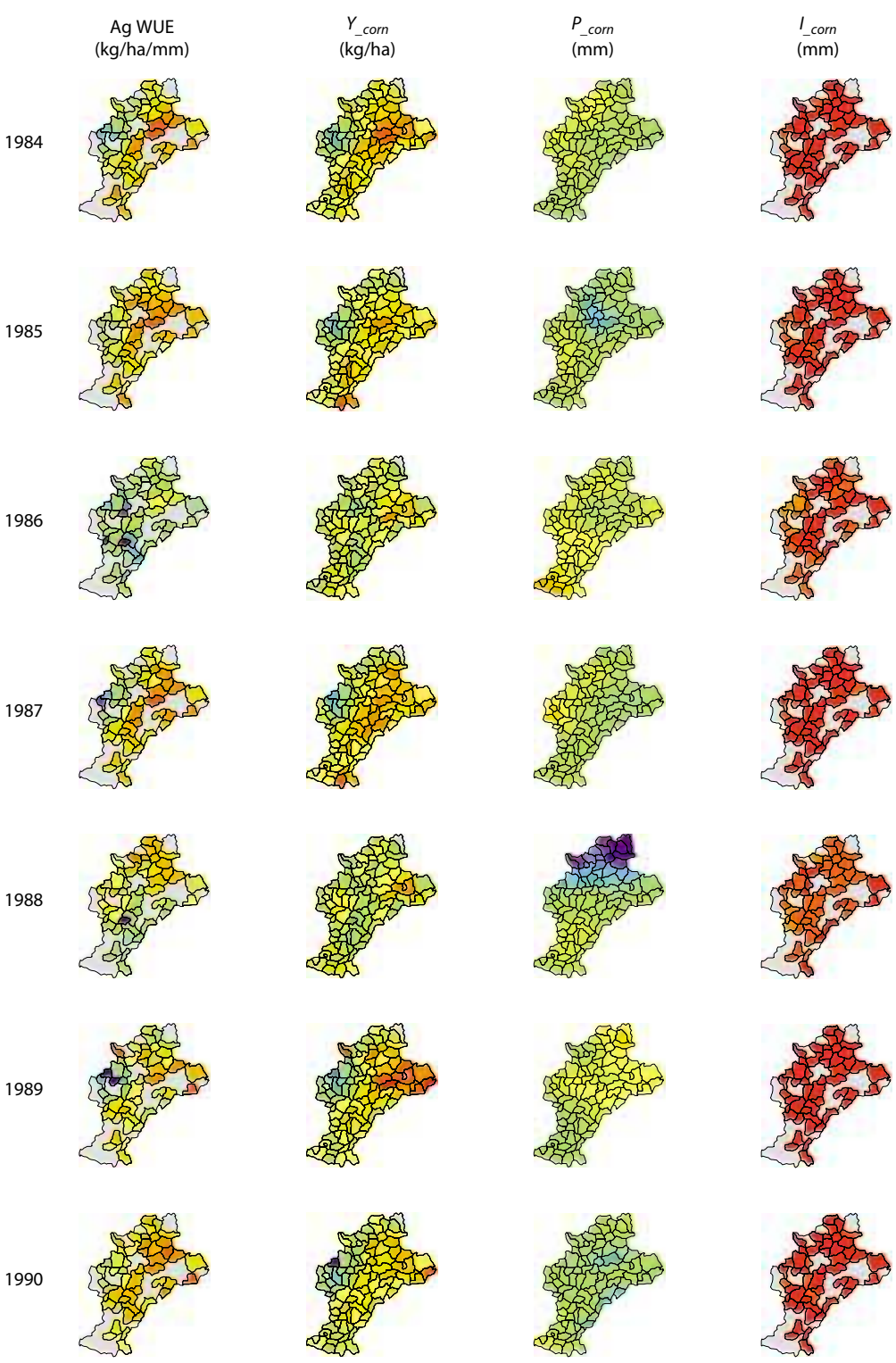

Figure 3. Agricultural water use efficiency for corn grown on the Hebei Plain study area, 1984–96.
The figure shows agricultural water use efficiency (AgWUE) in kg/ha/mm and its components: $Y_{\_corn}$ (kg/ha), $P_{\_corn}$ (mm) and $I_{\_corn}$ (mm).

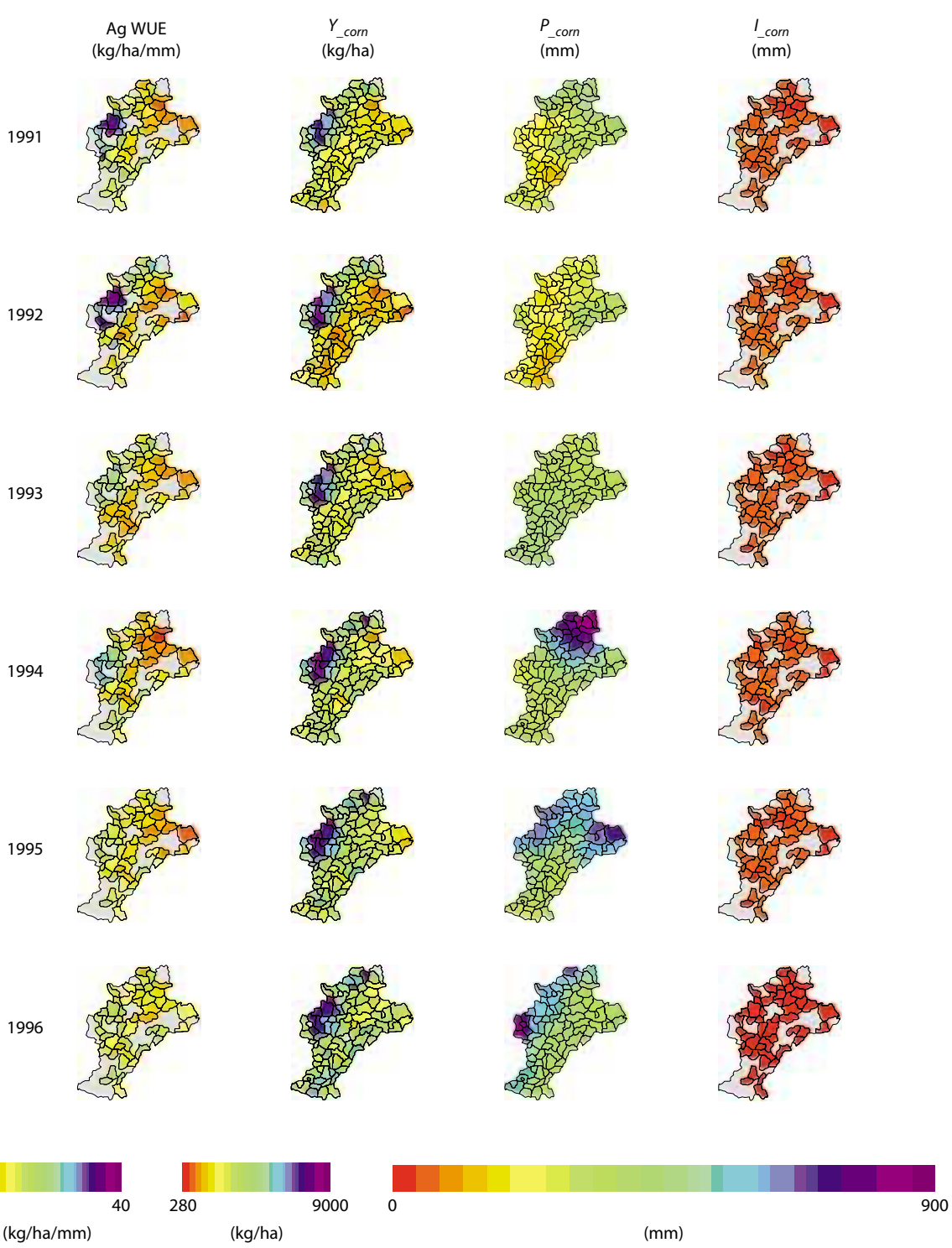

Figure 3. (cont'd) Agricultural water use efficiency for corn grown on the Hebei Plain study area, 1984–96.
The figure shows agricultural water use efficiency (AgWUE) in kg/ha/mm and its components: Y_corn (kg/ha), P_corn (mm) and I_corn (mm).

Table 3. Annual agricultural water use efficiency mean and standard deviations for all 49 counties for both the wheat and corn growing seasons (units are kg/ha mm).

	Wheat		Corn	
Year[a]	Mean	SD	Mean	SD
1984	7.0	2.7	9.0	4.4
1985	6.7	2.1	7.7	3.3
1987	10.7	3.6	8.9	5.0
1989	10.0	3.6	10.9	5.4
1990	8.6	1.9	7.4	3.0
1991	6.4	1.1	11.6	6.8
1992	9.5	3.1	12.4	8.1
1993	12.7	4.3	8.9	4.3
1994	8.7	2.5	9.2	5.2
1995	11.3	3.5	8.5	2.8
1996	14.3	3.1	10.1	2.5

SD = standard deviation
[a] There are no data for 1986 and 1988

Table 4. Frequency distribution of agricultural water use efficiency for all 538 observations (49 counties by 11 years) for both the wheat and corn growing seasons.

	Wheat		Corn	
Range (kg/ha/mm)	No. of observations	%	No. of observations	%
0–5	43	8	71	13
5–10	270	50	285	53
10–15	169	31	111	21
15–20	53	10	46	9
20–25	3	1	13	2
25–30	0	0	10	2
30–35	0	0	1	0
35–40	0	0	1	0

Note: There are 538 observations, not 539 (11 times 49), as there are no yield data for Xincheng County in 1993.

Table 4 shows that 467 of the 538 corn Ag WUE observations (87%) are also in the range 0–15 kg/ha/mm. In 25 cases, the corn Ag WUE is more than 20 kg/ha/mm, compared to only three cases for wheat (Table 4). It is expected that crops with a C_4 photosynthetic pathway will have higher Ag WUE than C_3 crops[2] (Beale et al. 1999). However, two cases recorded Ag WUE greater than 30 kg/ha/mm with no obvious errors. Hu (1998), responding to comments from Hill (1997), discussed the issue of China's agricultural statistics, which may be unreliable for individual counties in some years; as a result, the calculated corn Ag WUE is likely to be greater than 30 kg/ha/mm.

Most Ag WUE values for corn presented here are similar to those reported in other studies. In the northwest of China, Ag WUE was 12.6–23.1 kg/ha/mm for corn, 7.5–20.9 kg/ha/mm for millet, 15.5–15.7 kg/ha/mm for sorghum, and 4.1–5.7 kg/ha/mm for soybeans (Li et al. 2000). These results are similar to those reported for other locations. In the semiarid central and southern high plains of the United States, Tolk et al. (1999) reported values of 12.6–15.8 kg/ha/mm for corn; Stone et al. (1996) reported values of 8.3–15.7 kg/ha/mm for corn and 15.2–16.0 kg/ha/mm for sorghum. In the semiarid Sahel, transpiration WUE for pearl millet was 4.5–16.6 kg/ha/mm (Rockström et al. 1998). For sorghum grown within agroforestry sites along a rainfall gradient ranging from 350 to 2640 mm in Africa, Cannell et al. (1998) reported transpiration WUE of 1.5–9.0 kg/ha/mm. For sorghum in central Queensland, values were 3.4–11.2 kg/ha/mm (Armstrong et al. 1999).

For both the wheat and corn growing seasons, several strong spatial trends can be seen (Figs 2 and

[2] 'C_3' and 'C_4' refer to the number of carbon atoms in the first stable product formed during photosynthesis. C_3 plants, including winter wheat on the NCP, are usually active in cooler months. C_4 plants, such as corn on the NCP, are usually active in summer.

3). The Ag WUE and yield data are higher in the western counties than in the east (Fig. 4). The main reason for this is assumed to be that the irrigation water quality and soil conditions in the west are more favourable. For the 11 years of valid wheat yield data (Fig. 2), a gradual increase in Ag WUE from 1984 to 1996 can be seen; this is summarised in Table 3. The increase is most likely to be the result of water-saving agricultural practices; however, no definite conclusions can be reached, because of the lack of regional data.

The relationship between $P_{\_corn}$ and W_{o_wheat} is illustrated by the similar spatial patterns for $P_{\_corn}$ in 1984 (Fig. 3) and W_{o_wheat} in 1985 (Fig. 2). For the 13 years of W_{o_wheat} data, temporal and spatial changes that mimic the preceding $P_{\_corn}$ can be seen. $P_{\_wheat}$ shows a high degree of temporal and spatial variability, as would be expected (Fig. 3). In 1989, 1990, 1992 and 1996, rainfall was low over most of the study area during the wheat growing seasons. However, in 1989 and 1996, relatively high W_{o_wheat} suggests that there was adequate water to obtain near-average yields, and near-average Ag WUE were recorded in both years. In 1992, irrigation amounts were high, so yields were slightly above average, resulting in a slightly lower than average Ag WUE. Moreover, since 1986, the amount of irrigation applied during the wheat growing season has been reduced, with no loss of grain yield, so Ag WUE has increased (Fig. 2). It is interesting to note that there has been a steady increase of $Y_{\_wheat}$ in the central western counties of the study area since 1991.

Subtle interactions of the various components contributing to Ag WUE are revealed by close inspection of data for the wheat growing seasons of 1991 and 1992 (Fig. 2). In 1991, W_{o_wheat} was moderate (due to a relatively high $P_{\_corn}$ in 1990), $I_{\_wheat}$ was applied at slightly above average rates, and $P_{\_wheat}$ was also above average. Harvested yields for 1991 were about average; however, Ag WUE was low due to the relatively plentiful supply of water. In comparison, irrigation water was necessarily high in

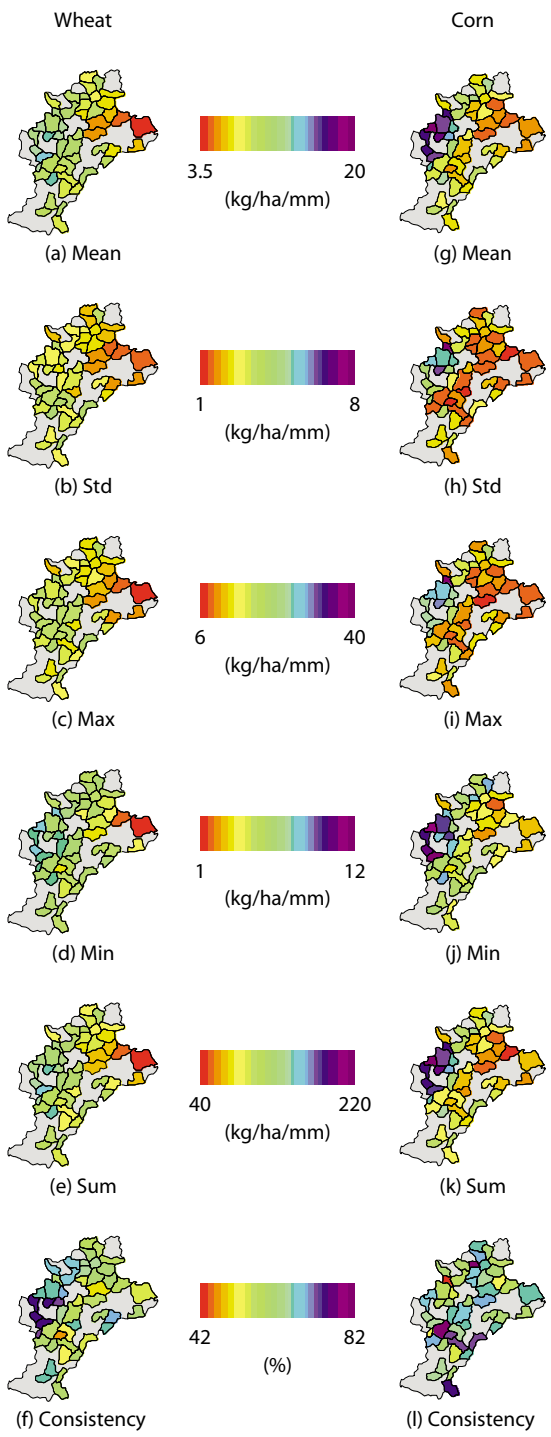

Figure 4. County summary statistics of agricultural water use efficiency for wheat (a–f) and corn (g–l) grown on the Hebei Plain study area, 1984–96.
Max = maximum, Min = minimum, Std = standard deviation. Consistency is a measure of year-to-year consistency for each county.

1992, as both P_{wheat} and W_{o_wheat} were relatively low (Fig. 2). However, irrigation timing and amounts were probably optimised for crop growth; this resulted in average yields, so higher Ag WUEs were achieved in 1992 compared to 1991 (Fig. 2).

Figure 4 shows summary maps of Ag WUE for both wheat and corn. For wheat the maximum mean was 14.1 kg/ha/mm, while the minimum mean was 3.7 kg/ha/mm (Fig. 4a). Standard deviations ranged from 1.4 to 4.7 kg/ha/mm (Fig. 4b). The highest maximum was 21.5 kg/ha/mm and the lowest was 6.7 kg/ha/mm (Fig. 4c); the highest minimum was 8.2 kg/ha/mm and the lowest was 1.1 kg/ha/mm (Fig. 4d). Over the 11 years of valid data, the cumulative Ag WUE ranged from 40.3 to 154.8 kg/ha/mm (Fig. 4e). A measure of consistency (C) was developed as:

$$C = \sum_{i=1}^{11} \mathrm{AgWUE}_{country} / 11 \ * \ \max \mathrm{AgWUE}_{country}$$

where 11 is the number of valid years of data available. This scales the cumulative Ag WUE for each county by 11 times the maximum Ag WUE for each county and is expressed as a percentage. For wheat, this value ranges from 48 to 76% (Fig. 4f). Counties with a high mean Ag WUE (green to purple) (Fig. 4a) and a low consistency (red to yellow) (Fig. 4f) are those with the highest potential for improving Ag WUE management. A relatively low consistency might be due to variables such as frosts, pests or disease affecting crops. For example, in Figure 4f some of the counties with a low consistency are in a similar location; the reasons for the low consistency need to be better understood before any management action is instigated.

The relative value of Ag WUE consistency is an important measure, but the timing of the maximum Ag WUE used in the calculation must also be taken into account. Figure 5 shows time series plots of Ag WUE and WR for four representative counties (Fig. 1) for the wheat growing season. In Xinhe county (Fig. 5a), the maximum wheat Ag WUE of more than 18 kg/ha/mm occurred in 1996. This was associated with relatively low county WR (Fig. 5e). However, in other years with relatively low county WR (1987, 1989, 1992 and 1993), Ag WUE did not exceed 14 kg/ha/mm.

One challenge for agricultural managers is to maintain the improvement recorded in 1996 for future dry years by optimising local management practices. For Xinhe County, the generally complementary nature of WR and Ag WUE can be seen by comparing Figures 5a and 5e: years that have a low WR usually have a high Ag WUE. Moving along the time series, improvements can be seen; for example, in 1984, 1985 and 1995, similar WRs were calculated (approximately 150 GL), yet in 1995 Ag WUE was more than 10 kg/ha/mm, whereas in 1984 and 1985 it was less than 3 kg/ha/mm (Fig. 5a). Agricultural practices have probably improved over these 10 years.

From 1984 until 1995, wheat Ag WUE in Heijian county (Fig. 5b) was approximately 6 kg/ha/mm. In 1996, when less than 400 GL was available to this county (Fig. 5f), Ag WUE doubled to 12 kg/ha/mm. However, in other dry years (1984, 1985, 1987, 1992 and 1993), county-level Ag WUE was less than 8 kg/ha/mm. Again, this probably illustrates a general improvement in agricultural practices.

The generally complementary relationship between WR and Ag WUE is seen for most years at Luancheng County. Since 1993, Luancheng County (Fig. 5c) has recorded Ag WUE values of about 18 kg/ha/mm, except in 1994 when there was a sharp decrease to about 11 kg/ha/mm, associated with a local WR maximum (Fig. 5g). However, in 1992 and 1993, which had similar WR values (Fig. 5g), there was not always a similar Ag WUE (Fig. 5c). Differences may be due to seasonal rainfall distribution and management practices such as the timing and amount of irrigation applied at different crop-growth stages (Zhang et al. 1999). Other

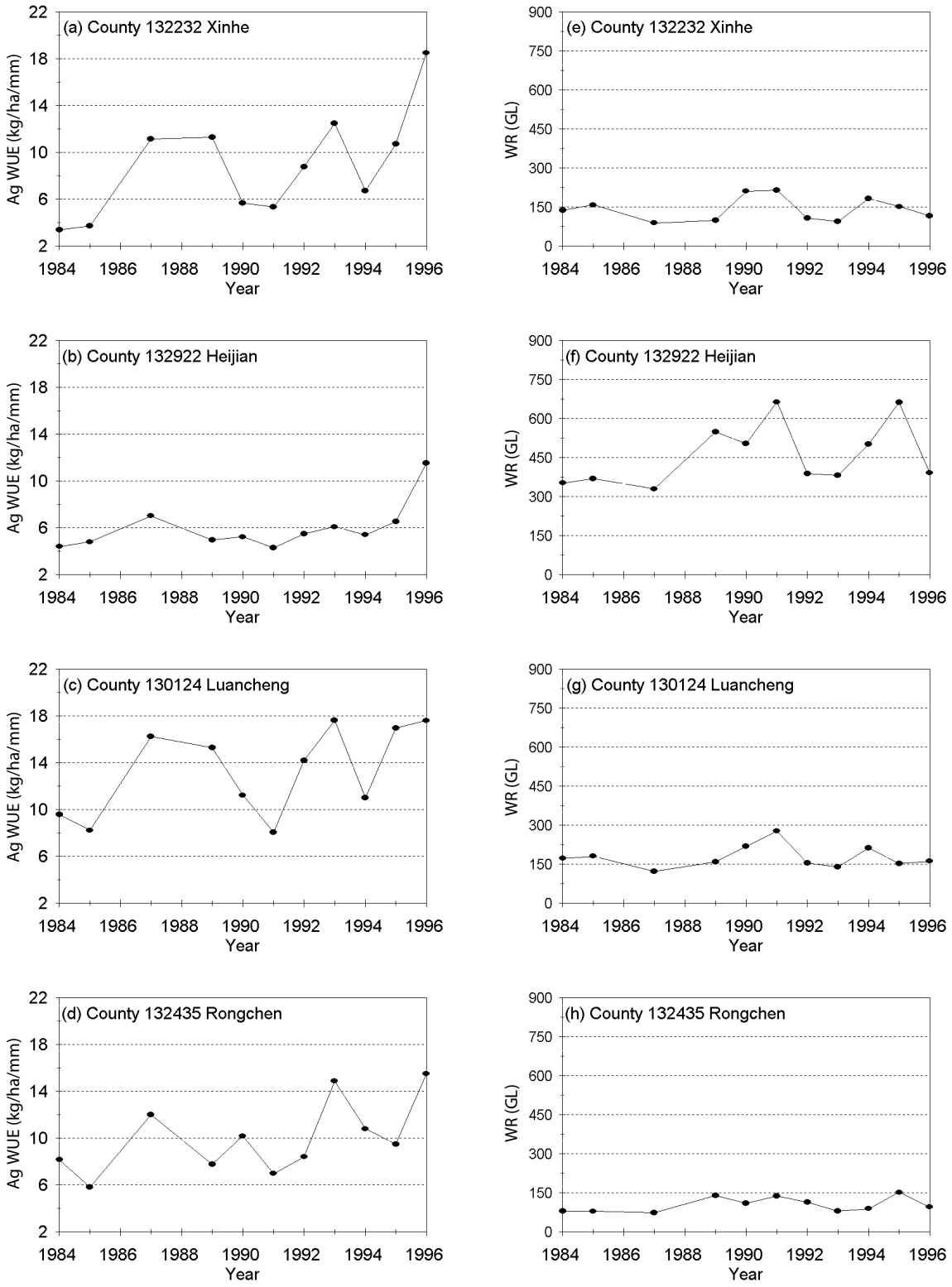

Figure 5. Time series plots for the wheat growing season in Xinhe, Heijian, Luancheng and Rongchen counties: agricultural water use efficiency (Ag WUE) (a–d) and corresponding water resources (WR) (e–h). The location of each county is shown in Figure 1.

constraints on grain yield include the incidence and severity of frosts, disease or pests. At the regional scale there are no figures for these factors, which impact on final yields. In Rongchen, there was a steady increase in Ag WUE (Fig. 5d), modified by the county WR figure (Fig. 5h). The question for local agricultural and water management agencies is whether management practices can be optimised consistently to decrease local variability.

For corn, the mean Ag WUE varied from 20.0 to 4.2 kg/ha/mm (Fig. 4g). Standard deviations ranged from 1.0 to 7.9 kg/ha/mm (Fig. 4h). The highest maximum was 39.0 kg/ha/mm and the lowest 6.3 kg/ha/mm (Fig. 4i); the highest minimum was 11.8 kg/ha/mm and the lowest 1.7 kg/ha/mm (Fig. 4j). Over the 11 years of valid data, the cumulative Ag WUE ranged from 46.4 to 219.5 kg/ha/mm (Fig. 4k). Fig. 4l illustrates that, for corn, the measure of consistency ranged from 43% to 82%. Counties with a high mean Ag WUE (green to purple) (Fig. 4g) and a low consistency (red to yellow) (Fig. 4l) are those with the highest potential for improved management of Ag WUE.

During the corn growing season, the estimates of Ag WUE and WR were generally complementary (Fig. 6). However, sometimes Ag WUE and WR are 'in phase'. For example, for Xinhe county in 1992, low WRs were available (Fig. 6e), a condition associated with low Ag WUE (Fig. 6a). In 1992, Xinhe and several surrounding counties suffered severe drought during the corn season and consequently produced low yields (see Figure 3 for details). In Heijian county, Ag WUE was estimated to be less than 8 kg/ha/mm for the time series (Fig. 6b), but in several years WR was above 600 GL (Fig. 6f). This suggests that there are opportunities for planting larger areas with summer crops. In Luancheng county in 1992 (Fig. 6c), there was a low rainfall during the corn season (Fig. 3), though it may have fallen at optimal times for summer crop growth, leading to high yields. This combination of factors resulted in an estimated Ag WUE of more than than 25 kg/ha/mm. From 1993 to 1996, high average yields were recorded (Fig. 3), while WR increased (Fig. 6g) due to above-average P_corn (Fig. 3); consequently Ag WUE for these years was estimated to be lower than the 1992 season. This suggests that when more water is available, its use is less efficient. In Rongchen county (Fig. 6d), the Ag WUE varied from 7 to 14 kg/ha/mm; again there was a general complementary relationship with WR (compare Figure 6d with 6h). There may be little scope to increase Ag WUE at the paddock level in counties like Luancheng; however, increasing county-level Ag WUE may be possible by either planting larger areas of crop or reducing the volume of water used for irrigation.

County total water resources

Figure 7 shows the time series of WR from 1984 to 1996 for both the wheat and corn seasons for each county. To better understand interactions with Ag WUE, both 1986 and 1988 were removed from any subsequent analysis of WR. For the 538 valid observations (49 counties over the 11 years), WR for wheat had a mean of 263.3 GL, with a standard deviation of 130.9 GL. The maximum and minimum wheat WR values were 856.7 and 47.5 GL, respectively. During the corn season the mean WR was 299.6 GL, with a standard deviation of 168.5 GL; the maximum and minimum were 1431.7 and 46.6 GL, respectively.

Table 5 shows the annual WR for both the wheat and corn growing seasons for the 49 counties, including the variability in total WR. For wheat, the maximum occurred in 1991 and can be associated with above-average summer rains in 1990 (Fig. 3), which extended into the 1991 wheat growing season (Fig. 2). For the corn season, the three wettest years were 1994, 1995 and 1996 (Table 5). WR is a function of county area, so variance in WR should be assessed mainly temporally, though counties of approximately equal areas may be loosely compared.

During the wheat season in 1991, many of the northeastern counties had near maximum WR

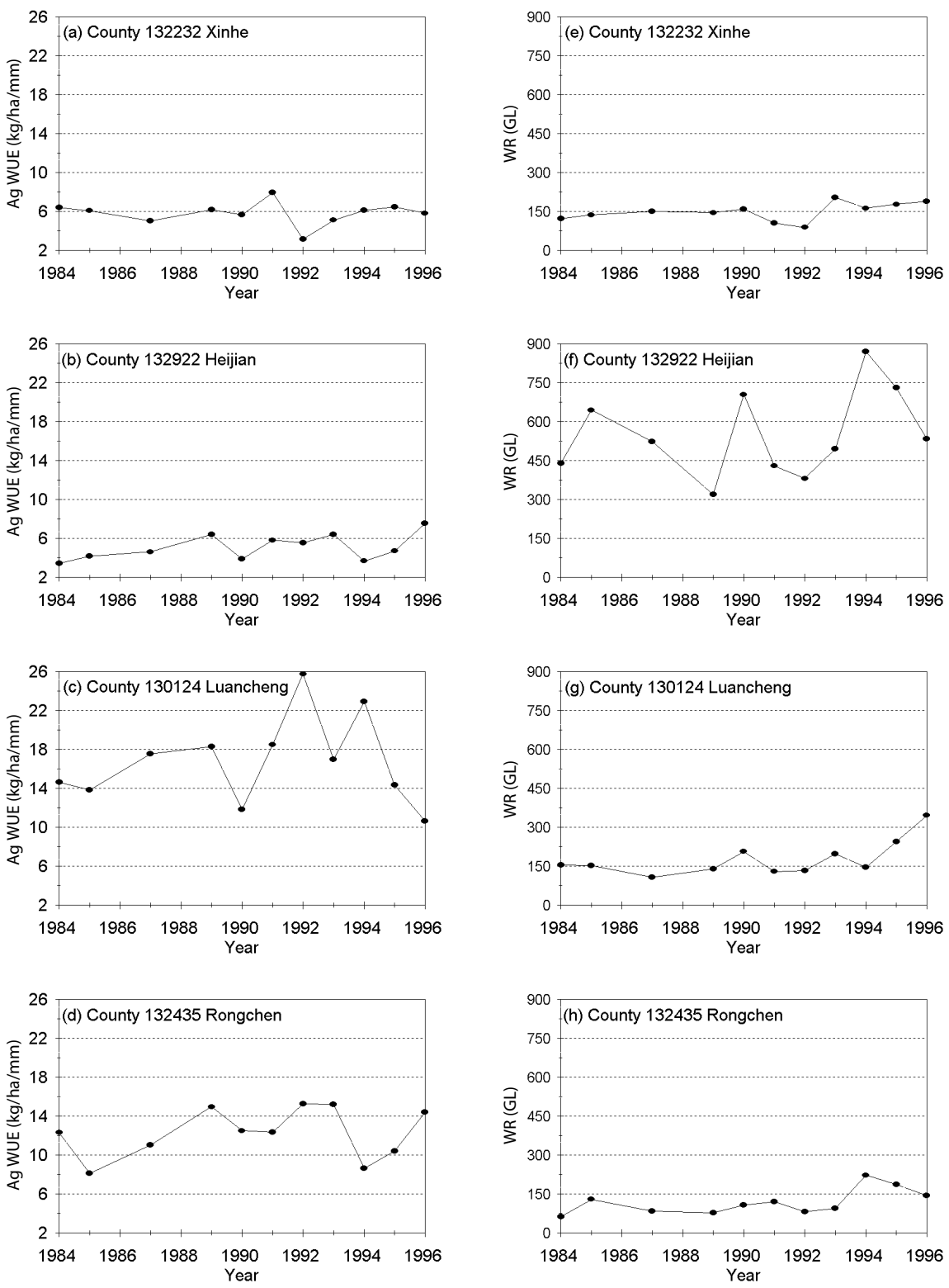

Figure 6. Time series plots for the corn growing season in Xinhe, Heijian, Luancheng and Rongchen counties: agricultural water use efficiency (Ag WUE) (a–d) and corresponding water resources (WR) (e–h). The location of each county is shown in Figure 1.

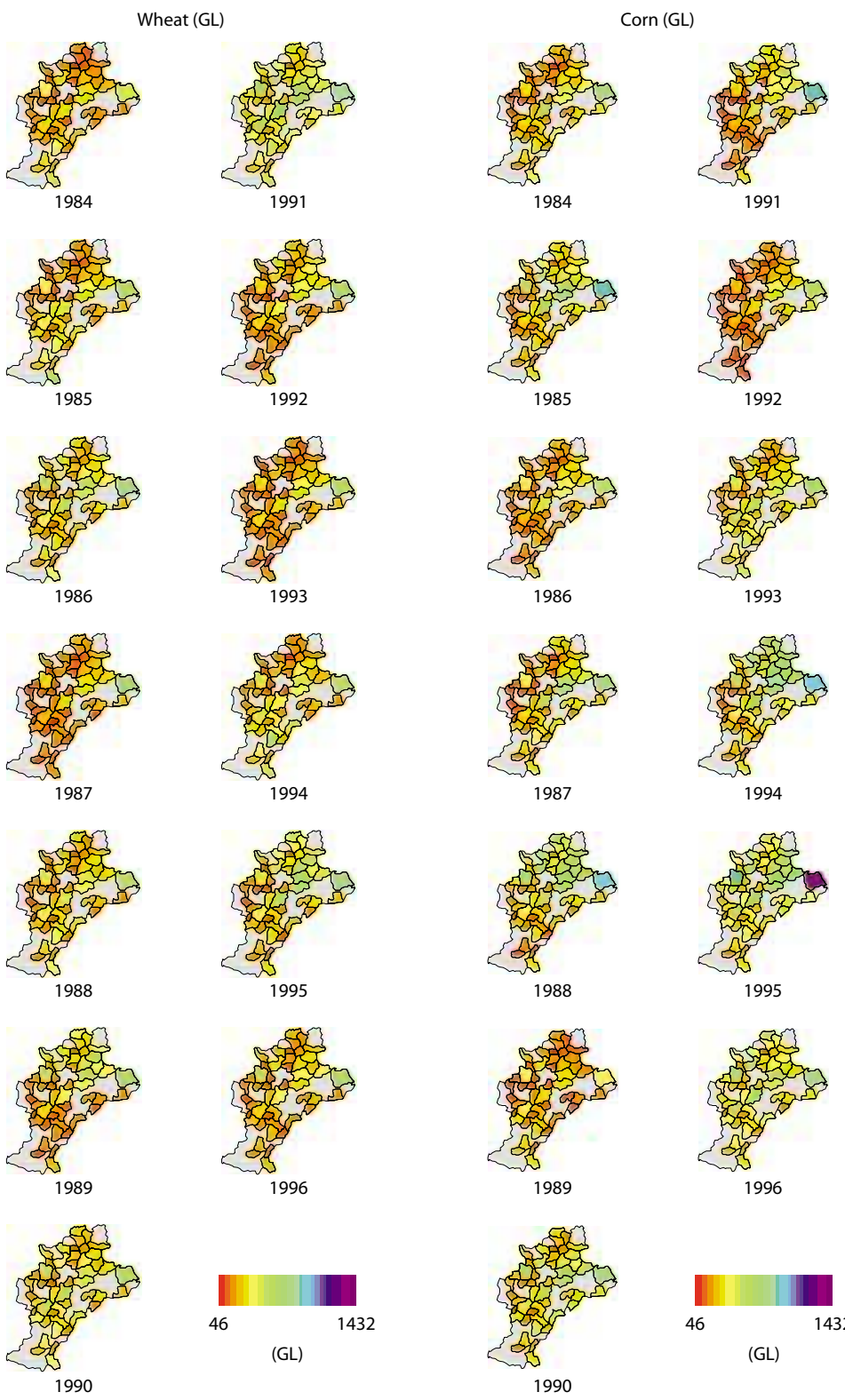

Figure 7. County total water resources for the counties of the Hebei province study area for the wheat and corn growing seasons, 1984–96.
Counties of different sizes should not be compared, because water resources values are a function of county area.

(Fig. 7). This was associated with the high rainfall during the 1991 wheat growing season and a moderate 1991 W_0, which is related to the preceding high P_{corn}. However, in 1991, I_{wheat} was relatively high (Fig. 2). Combining these water sources meant that the resulting WR was high, so a low Ag WUE was estimated during the 1991 wheat season. Two management actions might have been implemented to increase the county-level Ag WUE for the northeastern counties in 1991: a larger area could have been planted with wheat or less irrigation could have been applied. However, it should be noted that we do not know the timing of the irrigation events. Retrospective analysis of irrigation volumes is of some interest, but to actually decide to reduce the amount of irrigation applied during a growing season requires the ability to reliably predict future rainfall events for the entire growing season. Evans (1996) suggests it is not advisable to base such decisions on current short-term climate prediction models of precipitation. A decision to plant larger areas of crop (or to increase the planting density of areas currently planted) also depends on economic factors (Yang 1998; Yang and Li 2000; Anderson and Peng 1998); political factors (Allan 1999; Frankenstein 1995); environmental factors (e.g. reducing applications of fertilisers or enhancing river flows); and having the capacity to store and process an anticipated increase in grain production.

Table 5. Annual water resources mean and standard deviations for all 49 counties for the wheat and corn growing seasons (GL).

	Wheat		Corn	
Year[a]	Mean	SD	Mean	SD
1984	225	95	250	130
1985	254	113	307	162
1987	198	105	265	136
1989	275	139	210	88
1990	307	119	334	151
1991	375	154	251	149
1992	229	106	198	103
1993	200	96	304	129
1994	275	118	393	218
1995	310	155	421	223
1996	246	110	366	142

SD = standard deviation
[a] There are no data for 1986 and 1988

Figure 8 shows summary maps for both wheat and corn WRs. For wheat, the maximum mean was 660.5 GL, while the minimum mean was 75.1 GL (Fig. 8a). The standard deviations ranged from 18.7 to 119.8 GL (Fig. 8b). Figure 8c indicates that the highest maximum was 856.7 GL and the lowest 108.9 GL, while the highest minimum was 507.0 GL and the lowest 47.5 GL (Fig. 8d). Over the 11 years of valid data, the cumulative WR ranged from 826.1 to 9423.5 GL (Fig. 8e), with a measure of consistency of 49–77% (Fig. 8f).

For corn WR, the maximum mean was 830.0 GL and the minimum mean was 74.2 GL (Fig. 8g). Standard deviations ranged from 23.0 to 240.2 GL (Fig. 8h). The highest and lowest maxima were 1431.7 GL and 121.4 GL, respectively (Fig. 8i) while the highest and lowest minima were 423.5 GL 46.6 GL, respectively (Fig. 8j). Over the 11 years of valid data, the cumulative WR ranged from 815.9 to 9130.5 GL (Fig. 8k). For corn, the measure of consistency ranged from 51 to 77% (Fig. 8l). Several counties located in the northwestern portion of the study area had low consistency values for WR, associated with high maximum WR recorded in both 1988 and 1994 (Fig. 7), a direct result of the high P_{corn} during these two corn growing seasons (Fig. 3).

Normalisation and cross-plotting Ag WUE and WR

Relationships between Ag WUE and WR were generally complementary (Fig. 5 and 6), but there were differences, as discussed above. The relationships were normalised as follows using the county mean and county standard deviation for

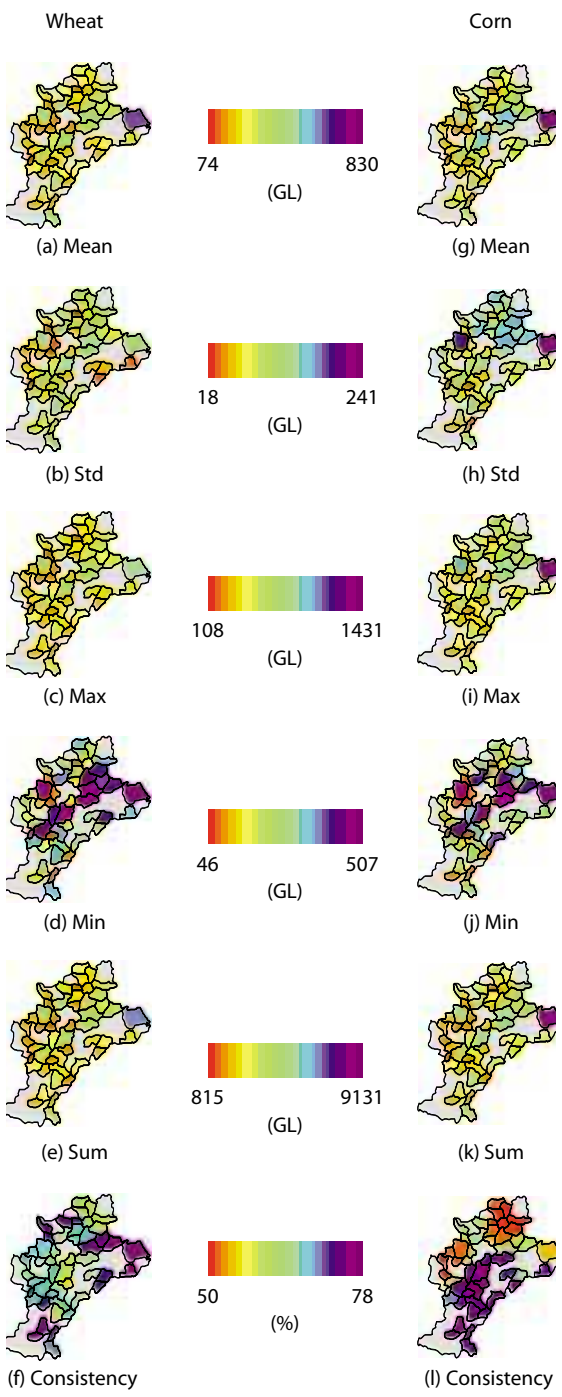

Figure 8. County summary statistics of total water resources for the counties of the Hebei Province study area for wheat (a–f) and corn (g–l).
Max = maximum, Min = minimum, Std = standard deviation.

each of the 49 counties (denoted, respectively, NAg WUE and NWR):

$$\text{NAgWUE} = \frac{\text{AgWUE}_{\text{county}} - \overline{\text{AgWUE}_{\text{11 years, county}}}}{\text{Std AgWUE}_{\text{11 years, county}}}$$

and

$$\text{NWR} = \frac{\text{WR}_{\text{county}} - \overline{\text{WR}_{\text{11 years, county}}}}{\text{Std WR}_{\text{11 years, county}}}$$

Differences in county size inherent in the WR calculation were normalised. For both wheat and corn, data from 1986 and 1988 were excluded from this analysis. NAg WUE and NWR have been cross-plotted for the wheat and corn growing periods (see Fig. 9a and 9b, respectively). For wheat, the lowest NWR is –1.75 (Fig. 9a), whereas for corn it is –2.5 (Fig. 9b); this indicates that there is less variability during the wheat season than the corn season. Figure 9c provides an indicative schematic explanation for the data plots. Timing of rainfall events and management practices, including the timing and amount of irrigation applied (Zhang et al. 1999), and many other variables (for example, the incidence and severity of frosts, disease or pests) may impact on final yields, so the schematic explanations are indicative only. Observations with both a near-zero NWR and NAg WUE are regarded as 'near normal'. Counties with both negative NWR and NAg WUE have experienced 'poor practice and dry' conditions, whereas a negative NWR and positive NAg WUE implies 'good practice and dry' conditions. When county NWR is above average, NAg WUE tends to become negative, suggesting that with more than average water available the water was used inefficiently. This is because WUE becomes less critical in obtaining high yields.

For both wheat and corn, there were few cases when both NWR and NAg WUE were greater than 1.0. The quadrant with both positive NWR and NAg WUE has been deemed 'good practice and wet' conditions, whereas when NWR was positive and NAg WUE negative the quadrant was denoted

'poor practice and wet' conditions. The NAg WUE and NWR data plots have been stratified and colour coded (Fig. 9d). The stratified cross-plots were then mapped over the time series for both the wheat and corn growing seasons (Fig. 10).

In the wheat growing season of 1984 there was severe drought in the northeast of the study area (Fig. 10); several counties recorded below-average NAg WUE and NWR (yellow). For these counties, it seems likely that the irrigation delivery system did not supply adequate water to the entire county or over the entire growing season. This may also be the reason why one county was located in this stratum during the 1994 wheat season. In 1984, five other northern counties received below-average NWR but recorded near-average NAg WUE (orange). For the 1984 wheat season, many counties had near-average NWR, but some had low NAg WUE (yellow/green) compared to others that recorded near-average NAg WUE (beige). This pattern also existed in the 1985 wheat season. For the remainder of the wheat time series, only isolated counties fell into the strata coded yellow or yellow/green, probably indicating an improvement of agricultural management practices.

During dry years, irrigation was applied in adequate amounts, at near optimal times, to produce yields that suggest the water resources were used efficiently. For example, in 1987 many counties experienced below-average NWR, yet recorded near-average NAg WUE (orange) or above-average NAg WUE (red), indicating good management practices. For the wheat season of 1991, and to a lesser extent in 1989, several counties were located in the low NAg WUE and high NWR strata (green). These years were extremely wet, and opportunities may have existed to plant a larger area with wheat or to irrigate less. Given that when water is plentiful it is usually used less efficiently than when it is scarce, and that it is difficult to predict wet years, it may be difficult to implement these management options. The 1995 wheat growing period was extremely wet, especially in the north; however most counties recorded near-average NAg WUE (cyan), while two eastern counties recorded above-average NAg WUE (blue). For all northern counties, little irrigation was applied in 1995 (Fig. 2). In these two eastern counties (shaded blue for wheat in 1995 in Figure 10), poor quality groundwater (Zhang et al. 1999), due to the proximity to the Bohai Sea (see Figure 3 of the Overview), would usually be used to irrigate wheat. However, for these two eastern counties in 1995, there was above-average NAg WUE because little, poor-quality groundwater was applied. In 1995 and 1996, many counties recorded above-average NAg WUE and near-average NWR (pink), indicating that good agricultural management was practised during the wheat growing season.

During the corn season, it appears that management practices have improved since the 1990 season, as few counties in particular years have recorded below-average NAg WUE with near-average NWR (yellow/green). In 1989 and 1992, one county each year recorded below-average NAg WUE and NWR (yellow), suggesting that irrigation scheduling (both in timing and amount) may not have been managed optimally. In 1984, 1989, 1991 and 1992, many counties experienced below-average NWR, yet recorded near-average NAg WUE (orange) or above-average NAg WUE (red), indicating good management practice. As with wheat, when above-average water resources were available they were usually used less efficiently, resulting in many counties falling within the low NAg WUE and high NWR strata (green). In the north, corn management practices for wet years have improved, with several counties falling within the green strata in 1994 moving into the cyan strata (near-average NAg WUE and high NWR) in 1995. Only in 1995 and 1996 did any counties record both above-average NAg WUE and NWR (blue). This again indicates that improved management practices have been adopted during wet corn growing seasons. In 1996, most eastern counties received near-average NWR (beige and pink), yet many recorded above-average NAg WUE (pink). This indicates the adoption of improved management practices during these corn seasons.

Conclusions

We have developed a spatial information system that allows water-saving agricultural practices to be assessed. The system is based on the spatial and temporal constructs of the available regional databases, which partly determined our 'input–output' Ag WUE approach, For the wheat growing season, the average Ag WUE for the 49 counties was 7.0 kg/ha/mm in 1984, whereas in 1996 it had risen to 14.3 kg/ha/mm. It is most likely that these improvements in Ag WUE for wheat are the result of farmers adopting water-saving agricultural practices. For the corn growing season, Ag WUE increased from 9.0 kg/ha/mm in 1984 to 10.1 kg/ha/mm in 1996, although values of more than 11.5 kg/ha/mm were obtained in 1991 and 1992. For both wheat and corn, we have identified counties that have a relatively high mean Ag WUE and yet are somewhat inconsistent from year to year. These counties have the highest potential to achieve improvements in Ag WUE.

The spatial mapping of the time series data for the 'NAg WUE and NWR' stratified data space also showed where recent improvements in Ag WUE had been achieved. For some counties in wet years, there may be opportunities for planting larger areas of crop and thereby increasing county-level Ag WUE. For the study site and the time series of data available, recently introduced water-saving agricultural practices on the NCP seem to have

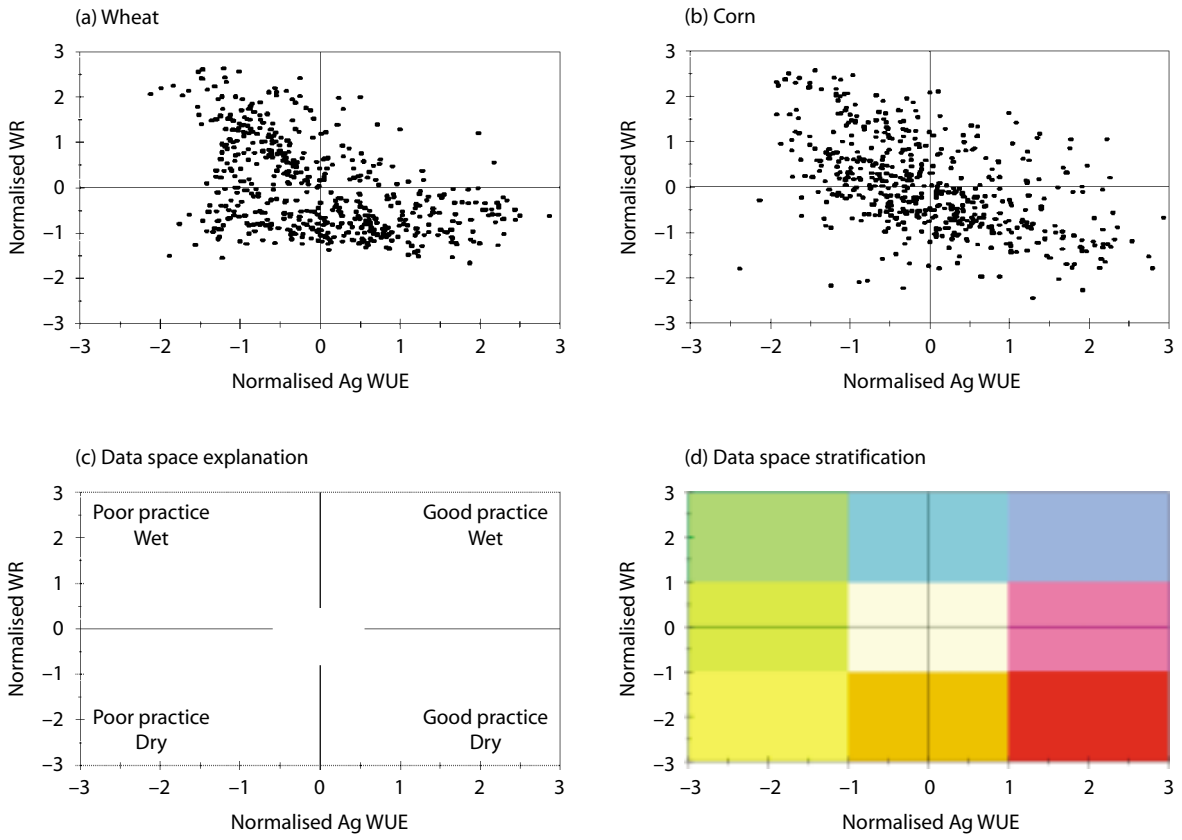

Figure 9. Cross-plots of normalised agricultural water use efficiency (Ag WUE) and normalised water resources (WR) for the wheat and corn growing seasons.
Figure shows (a) wheat; (b) corn; (c) a schematic explaining the data space; and (d) the stratification and colour codes used in Figure 10. Starting at the bottom-right corner of (d) and progressing clockwise, the colours are described as: red, orange, yellow, yellow/green, green, cyan, blue, and pink, with beige in the centre.

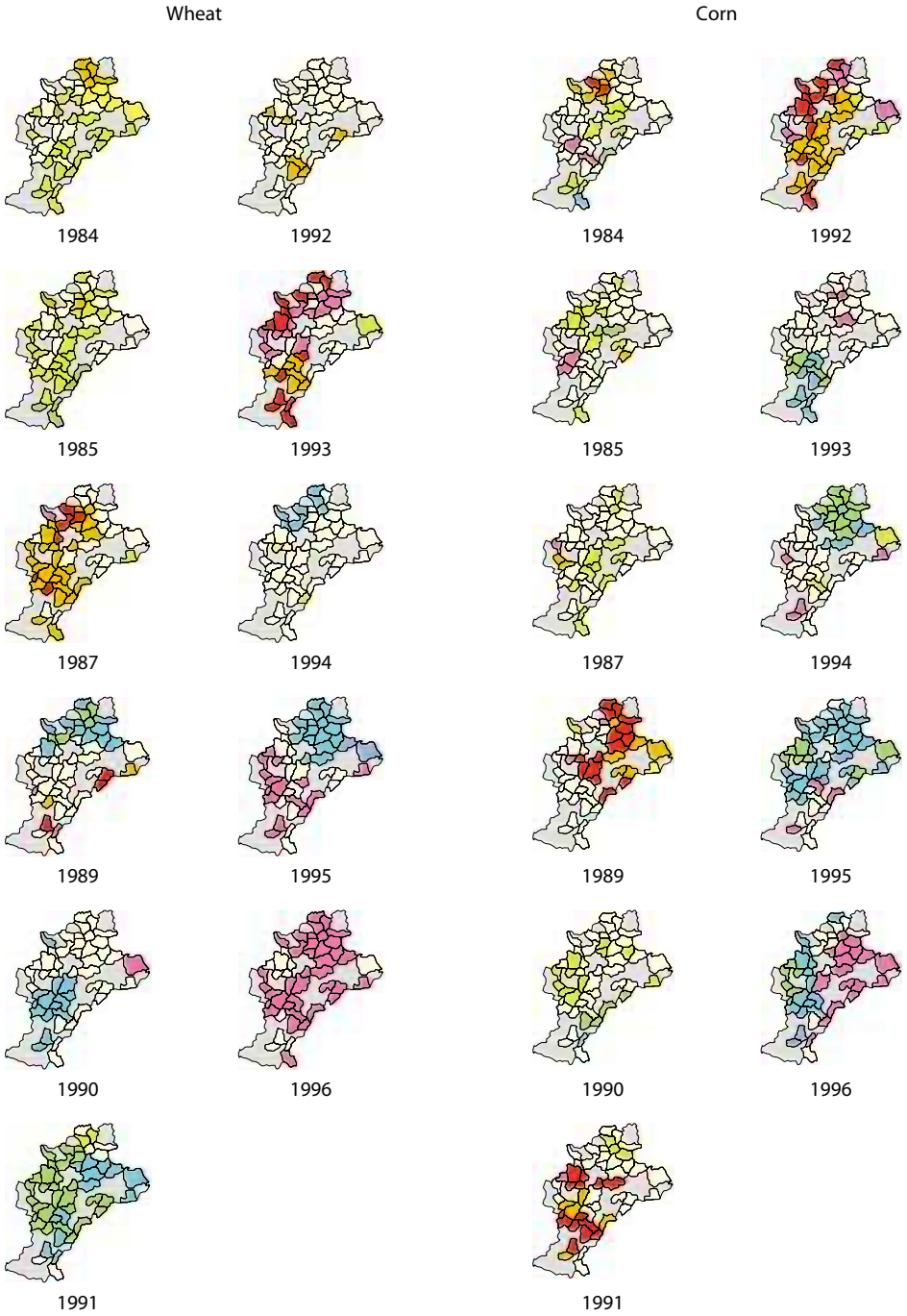

Figure 10. Time series of the cross-plotted stratified normalised agricultural water use efficiency and normalised water resources data space. Figure 9 shows the basis of the colour selection.

resulted in an increase in Ag WUE. This increase may have occurred, in part, due to the widespread application of fertilisers. In this intensively managed agricultural region, it is important to assess the impact of fertiliser on environmental pollution of both land and water (including surface and ground) resources. Also, if regional groundwater levels are available at appropriate spatial and temporal resolutions, the effects of various agricultural practices (including recent

improvements made to Ag WUE) on the sustainability of regional groundwater can be assessed.

The methods developed here can be used to monitor regional Ag WUE from 1997 onwards and could eventually be extended to the entire NCP, all of China, or other countries. For all geographic regions, spatial and temporal trend analysis of Ag WUE (and other variables) obviously needs to be based on data. It is difficult to infer the causal relationships between Ag WUE and detailed agricultural practices for large areas over long periods, because there is currently a mismatch between available and required data. The collection, quality and availability of such data are major issues facing regional agricultural operational and research organisations. These issues need to be addressed by organisations involved in managing agricultural, water and land resources.

Acknowledgments

This research has been supported by contributions from ACIAR to Project LWR1/95/07 conducted by CSIRO Land and Water and the Chinese Academy of Sciences. Thanks to Liu Jianhua from Shijiazhuang Institute of Agricultural Modernization for entering much of the data used in this study. More details can be found at <http://www.eoc.csiro.au/aciar/>.

References

Allan, T. 1999. Productive efficiency and allocative efficiency: why better water management may not solve the problem. Agricultural Water Management, 40, 71–75.

Anderson, K. and Peng, C.Y. 1998. Feeding and fueling China in the 21st Century. World Development, 26, 1413–1429.

Armstrong, R.D., McCosker, K., Millar, G., Kuskopf, B., Johnson, S., Walsh, K., Probertd, M.E. and Standley, J. 1999. Legume and opportunity cropping systems in central Queensland. 2. Effect of legumes on following crops. Australian Journal of Agricultural Research, 50, 925–936.

Beale, C.V., Morison, J.I.L. and Long, S.P. 1999. Water use efficiency of C4 perennial grasses in a temperate climate. Agricultural and Forest Meteorology, 96, 103–115.

Brown, L.R. and Halweil, B. 1998. China's water shortage could shake world food security. World Watch, 11, 10–21.

Cannell, M.G.R., Mobbs, D.C. and Lawson, G.J. 1998. Complementarity of light and water use in tropical agroforests. II. Modelled theoretical tree production and potential crop yield in arid to humid climates. Forest Ecology and Management, 102, 275–282.

Cao, M., Ma, S. and Han, C. 1995. Potential productivity and human carrying capacity of an agro-ecosystem: an analysis of food production potential of China. Agricultural Systems, 47, 387–414.

Evans, T.E. 1996. The effects of changes in the world hydrological cycle on availability of water resources. In: Bazzaz, F.A. and Sombroek, W.G., eds, Global Change and Agricultural Production. Chichester, Wiley, pp. 15–48.

Frankenstein, J. 1995. The Beijing Rules: contradictions, ambiguities and controls. Long Range Planning, 28, 70–80.

French, R.J. and Schultz, J.E. 1984a. Water use efficiency of wheat in a Mediterranean-type environment. I. The relation between yield, water use and climate. Australian Journal of Agricultural Research, 35, 743–64.

French, R.J. and Schultz, J.E. 1984b. Water use efficiency of wheat in a Mediterranean-type environment. II. Some limitations to efficiency. Australian Journal of Agricultural Research, 35, 765–775.

Garabet, S., Ryan, J. and Wood, M. 1998. Nitrogen and water effects on wheat yield in a Mediterranean-type climate. I. Growth, water-use and nitrogen accumulation. Field Crops Research, 57, 309–318.

Gong, J. and Lin, H. 2000. Sustainable development for agricultural region in China: case studies. Forest Ecology and Management, 128, 27–38.

Hill, R.D. 1997. Questions for Chinese agriculture. Land Use Policy, 14, 335–336.

Hu, W. 1998. Issues for sustaining Chinese agriculture. Land Use Policy, 15, 167–170.

Hunsaker, D.J., Kimball, B.A., Pinter, P.J.J., Wall, G.W., LaMorte, R.L., Adamsen, F.J., Leavitt, S.W., Thompson, T.L., Matthias, A.D. and Brooks, T.J. 2000. CO2 enrichment and soil nitrogen effects on wheat evapotranspiration and water use efficiency. Agricultural and Forest Meteorology, 104, 85–105.

Hutchinson, M.F. 1999. ANUSPLIN Version 4.0 User Guide. Canberra, The Australian National University.

Jin, M., Zhang, R., Sun, L. and Gao, Y. 1999. Temporal and spatial soil water management: a case study in the Heilonggang region, PR China. Agricultural Water Management, 42, 173–187.

Karrou, M. 1998. Observations on effect of seeding pattern on water-use efficiency of durum wheat in semi-arid areas of Morocco. Field Crops Research, 59, 175–179.

Li, F., Zhao, S. and Geballe, G.T. 2000. Water use patterns and agronomic performance for some cropping systems with and without fallow crops in a semi-arid environment of northwest China. Agriculture, Ecosystems and Environment, 79, 129–142.

Li, J., Liu, X., Zhou, W., Sun, J., Tong, Y., Liu, W., Li, Z., Wang, P. and Yao, S. 1995. Technique of wheat breeding for efficiently utilizing soil nutrient elements. Science in China, 38, 1313–1320.

Lin, J.Y. 1997. Institutional reforms and dynamics of agricultural growth in China. Food Policy, 22, 201–212.

Liu, Y., Teixeira, J.L., Zhang, H.J. and Pereira, L.S. 1998. Model validation and crop coefficients for irrigation scheduling in the North China Plain. Agricultural Water Management, 36, 233–246.

Loaiciga, H.A., Valdes, J.B., Vogel, R., Garvey, J. and Schwarz, H. 1996. Global warming and the hydrologic cycle. Journal of Hydrology, 174, 83–127.

McVicar, T.R., Zhang, G., Bradford, A.S., Wang, H., Dawes, W.R., Zhang, L. and Lingtao, L. 2000. Developing a spatial information system to monitor regional agricultural water use efficiency for Hebei Province on the North China Plain. Canberra, CSIRO Land and Water, 55.

Muldavin, J. 1997. The limits of market triumphalism in rural China. Geoforum, 28, 289–312.

O'Leary, G.J., Connor, D.J. and White, D.H. 1985. A simulation model of the development, growth and yield of the wheat crop. Agricultural Systems, 17, 1–26.

Oweis, T., Zhang, H. and Pala, M. 2000. Water use efficiency of rainfed and irrigated bread wheat in a Mediterranean environment. Agronomy Journal, 92, 231–238.

Regan, K.L., Siddique, K.H.M., Tennant, D. and Abrecht, D.G. 1997. Grain yield and water use efficiency of early maturing wheat in low rainfall Mediterranean environments. Australian Journal of Agriculture Research, 48, 595–603.

Ritchie, J.T. 1983. Efficient water use in crop production: generality of relations between biomass production and evapotranspiration. In: Taylor, H.M., Jordan, W.R. and Sinclair, T.R., eds, Limitations to Efficient Water Use in Crop Production. Madison, American Society of Agronomy, 29–44.

Rockström, J., Jansson, P.-E. and Barron, J. 1998. Seasonal rainfall partitioning under runon and runoff conditions on sandy soil in Niger. On-farm measurements and water balance modelling. Journal of Hydrology, 210, 68–92.

Rosegrant, M.W. and Ringler, C. 2000. Impact on food security and rural development of transferring water out of agriculture. Water Policy, 1, 567–586.

Rozelle, S., Huang, J. and Zhang, L. 1997. Poverty, population and environmental degradation in China. Food Policy, 22, 229–251.

Sinclair, T.R., Tanner, C.B. and Bennett, J.M. 1984. Water-use efficiency in crop production. BioScience, 34, 36–40.

Smit, B. and Yunlong, C. 1996. Climate change and agriculture in China. Global Environmental Change, 6, 205–214.

Stanhill, G. 1986. Water use efficiency. Advances in Agronomy, 39, 53–85.

Stone, L.R., Schlegel, A.J., Gwin Jr., R.E. and Khan, A.H. 1996. Response of corn, grain sorghum, and sunflower to irrigation in the High Plains of Kansas. Agricultural Water Management, 30, 251–259.

Tanner, C.B. and Sinclair, T.R. 1983. Efficient water use in crop production: research or re-search ? In: Taylor, H.M., Jordan, W.R. and Sinclair, T.R., eds, Limitations to Efficient Water Use in Crop Production. Madison, American Society of Agronomy, 1–28.

Thomas, A. 2000. Climatic changes in yield index and soil water deficit trends in China. Agricultural and Forest Meteorology, 102, 71–81.

Tolk, J.A., Howell, T.A. and Evett, S.R. 1999. Effect of mulch, irrigation, and soil type on water use and yield of maize. Soil and Tillage Research, 50, 137–147.

Tuong, T.P. and Bhuiyan, S.I. 1999. Increasing water-use efficiency in rice production: farm-level perspectives. Agricultural Water Management, 40, 117–122.

Turner, N.C. 1986. Crop water deficits: a decade of progress. Advances in Agronomy, 39, 1–51.

Turner, N.C. 1997. Further progress in crop water relations. Advances in Agronomy, 58, 293–338.

Wang, H., Liu, C. and Zhang, L. In press. Water-saving agriculture in China: An overview. Advances in Agronomy.

Wang, H., Zhang, L., Dawes, W.R. and Liu, C. 2001. Improving water use efficiency of irrigated crops in the North China Plain—measurements and modelling. Agricultural Water Management, 48, 151–167.

Wei, H. 1997. Household land tenure reform in China: its impact on farming land use and agro-environment. Land Use Policy, 14, 175–186.

Xing, Q.Z. 1997. Urban land reform in China. Land Use Policy, 14, 187–199.

Yang, H. 1998. Trends in China's regional grain production and their implications. Agricultural Economics, 19, 309–325.

Yang, H. and Li, X. 2000. Cultivated land and food supply in China. Land Use Policy, 17, 73–88.

Yong, L. and Jiabao, Z. 1999. Agricultural diffuse pollution from fertilisers and pesticides in China. Water Science and Technology, 39, 25–32.

Yuan, X., Wang, H., Zhang, X. and You, M. 1992. The relationship between winter wheat yield and water consumption. In: Xie, X. and Yu, H., eds, The Study of Relationship Between Crop and Water. Beijing, Beijing Science and Technology Press, 10–18.

Zhang, C. 1999. Problems on water saving agriculture in China: background issues. In: Problems on Water Saving Agriculture in China. Beijing, China Hydrology and Hydroelectric Press, 5–10.

Zhang, H. and Oweis, T. 1999. Water-yield relations and optimal irrigation scheduling of wheat in the Mediterranean region. Agricultural Water Management, 38, 195–211.

Zhang, H., Wang, X., You, M. and Liu, C. 1999. Water-yield relations and water-use efficiency of winter wheat in the North China Plain. Irrigation Science, 19, 37–45.

Zhang, J., Sui, X., Li, B., Su, B., Li, J. and Zhou, D. 1998. An improved water-use efficiency for winter wheat grown under reduced irrigation. Field Crops Research, 59, 91–98.

Zoebl, D. 2000. Patterns of input-output relations in agro-ecosystems. Agriculture, Ecosystems and Environment, 79, 233–244.

19 A 'Calculate then Interpolate' Approach to Monitoring Regional Moisture Availability

Tim R. McVicar* and David L.B. Jupp†

Abstract

This chapter describes a method to estimate moisture availability in the 1.1 million km^2 Murray–Darling Basin (MDB) in southeast Australia. Remotely sensed data from the advanced very high resolution radiometer (AVHRR) are combined with meteorological data to estimate the normalised difference temperature index (NDTI). The NDTI provides a measure of moisture availability, the ratio of actual to potential evapotranspiration. Eighty-five per cent of variation in the modelled NDTI could be explained by surface temperature minus air temperature, per cent vegetation cover and net radiation. These three covariates can be used across the network of meteorological stations to calculate NDTI images, which map changes in moisture availability across the MDB. The method uses a 'calculate then interpolate' (CI) approach: the per-pixel variation present in the AVHRR data is used as the backbone for the spatial interpolation. Using the spatially dense AVHRR-based covariates in a CI approach avoids errors that occur between measurement points when interpolating variables for regional hydrological modelling, most significantly the spatial pattern of rainfall. The NDTI provides a link into regional water balance modelling that does not require spatial interpolation of daily rainfall. Assessing spatial and temporal interactions between the NDTI and the normalised difference vegetation index (NDVI) provides useful information about regional hydroecological processes, including agricultural management, within the context of Australia's highly variable climate and sparse network of meteorological stations.

本文估算了澳大利亚东南部默里达令盆地（MDB）一百一十万平方公里土地的可利用水分。标准差值温度指数（NDTI）系由气象台站资料和AVHRR遥感数据运算而来，用以计算有效水分，即水分蒸发蒸腾实际总量与潜在总量的比例。用地表温度和空气温度的差值、植被覆盖度和净辐射三个变量，可以较好地解释数值变动（决定系数 r^2=85%）。通过气象网络各台站的这三种数据，可以计算得到 NDTI 图象，显示 MDB 可利用水分的变化情况。该方法计算后再插值（CI），以逐像元变化的 AVHRR 数据为主干，作

* CSIRO Land and Water, PO Box 1666, Canberra, ACT 2601, Australia. Email: tim.mcvicar@csiro.au

† CSIRO Earth Observation Centre, PO Box 3023, Canberra, ACT 2601, Australia.

McVicar, T.R. and Jupp, D.L.B. 2002. A 'calculate then interpolate' approach to monitoring regional moisture availability. In: McVicar, T.R., Li Rui, Walker, J., Fitzpatrick, R.W. and Liu Changming (eds), *Regional Water and Soil Assessment for Managing Sustainable Agriculture in China and Australia*, ACIAR Monograph No. 84, 258–276.

空间插值运算。因为在 AVHRR 图像上，变量的空间分布稠密，使用 CI 法，可以避免区域水文模型变量插值测点之间的误差，作降雨空间分布插值时尤其明显。由于澳大利亚的气候多变，气象台站分布稀疏，评估 NDTI 和 NDVI（标准差值植被指数）间的时空相互作用，可以提供包括农业活动在内的区域性水文－生态过程的有用信息。

HYDROLOGICAL and plant growth models are often developed at points. One way of extending the models to regions is to interpolate the relevant data and then perform calculations on the interpolated measurements. For example, Cole et al. (1993), Kittel et al. (1995), Carter et al. (1996), Nalder and Wein (1998) and Thornton et al. (1997) interpolated the input parameters and driving variables, and then calculated the values at each location. The interpolation can be a daunting task, depending on the complexity of the model, the spatial and temporal resolution and the extent of the modelling. Chapter 16 discusses the idea of 'data construct'. Another way of extending the models to regions is to use some remotely sensed variables with interpolated meteorological variables and then perform the calculations. Moran et al. (1996), Pierce et al. (1993) and Zhang et al. (1995) have used this approach. Raupach et al. (1997) used output from a general circulation model (GCM) as input to a coupled carbon, water and energy flux model. In this approach the GCM is viewed as an 'interpolator' of the required input meteorological variables for the spatially distributed process model. Prince et al. (1998) use high frequency advanced very high resolution radiometer (AVHRR) data to provide estimates of some of the variables needed for a regional plant growth model, which is run at every point. The approach used in all of these methods can be summarised as 'interpolate then calculate' (IC).

A less frequently used approach is to 'calculate then interpolate' (CI). Stein et al. (1991) first introduced CI procedures to simulate the moisture deficit for a 404-hectare (ha) area in the Netherlands. They used 399 observations in the modelling framework, where seven procedures (four CI and three IC) were performed. Subsequently, the results for each of the seven were compared with another 100 observations, and a mean squared error (MSE) for each was calculated. Overall, the CI procedures provided lower MSE results than the IC procedures, which led Stein et al. (1991) to state that 'in short, CI procedures are to be preferred over IC procedures'. Bosma et al. (1994) simulated the three-dimensional flow of a heavy metal contaminant and used both IC and CI methods, using ordinary point kriging, to predict a parameter for a 20 m^2 field. They analysed the influence of sample size and concluded that, for the smallest samples, CI procedures performed better than IC procedures. These previous papers provide support for the use of CI in comparison to IC.

Our study integrated data types with very different spatial and temporal scales. AVHRR data are spatially dense, with an at-nadir 1.1 km^2 resolution, and are recorded over large areas in a matter of seconds, at a specific time, for specific wavelengths. Remotely sensed data are therefore a 'census' at a particular spatial scale, recorded at a specific time. Depending on the amount of cloud coverage and the repeat characteristics of the satellite, optical remotely sensed data may be available only weekly or monthly. Meteorological data are recorded sparsely, with the points often separated by tens to hundreds of kilometres. The variables measured at

these points represent a certain area. However, the exact area being represented by a given point measurement is unknown because the spatial autocorrelation is unknown. Meteorological data from standard long-term, large-area surface networks are usually daily integrals (e.g. rainfall (P) and wind run (U)) or daily extremes (e.g. maximum (T_x) and minimum (T_n) air temperatures) acquired regularly over decades. Thus, remotely sensed data are spatially dense but temporally sparse, while meteorological data are spatially sparse but temporally dense. One aim of our research was to combine the high temporal density of meteorological data with the high spatial density of remotely sensed data. The inherent spatial density of remotely sensed data may be compromised by the IC approach. As a result, geographic information system (GIS) boundaries may lead to artefacts in the final modelled images.

We used covariates derived mainly from spatially dense AVHRR data to spatially interpolate the normalised difference temperature index (NDTI). The approach is very similar to using a digital elevation model (DEM) as a covariate to interpolate surfaces of air temperature. Various numerical approaches can be used to spatially interpolate point data (Lam 1983); two of the most popular are splines and kriging. Several recent papers (e.g. Dubrule 1983; Dubrule 1984; Hutchinson 1993; Hutchinson and Gessler 1994; Laslett 1994; Borga and Vizzaccaro 1997) have compared the outputs from splines and kriging and found little difference between the two in most circumstances, provided the interpolation parameters were selected carefully. Incorporating regular gridded data, usually a DEM, but in this case AVHRR-based variables, as a covariate can be performed routinely using ANUSPLIN (Hutchinson 1997), a commercially available software package. Any spline or kriging package that can utilise covariates can be used to spatially interpolate NDTI.

The Normalised Difference Temperature Index

Jackson et al. (1977) developed the following empirical model to estimate daily actual evapotranspiration (λE_{a_DAY}):

$$\lambda E_{a\_DAY} - R_{n\_DAY} = A - B\left(T_s - T_a\right)$$

where R_{n_DAY} is the daily net radiation in watts per square metre (W/m^2), T_s is the surface temperature (K), T_a is the air temperature (K), and A and B are empirical coefficients. Seguin et al. (1982a, 1982b) extended this approach. Lagouarde (1991) described how the approach could be implemented and noted that the effect of changes in surface cover type and amount (especially roughness length) on the coefficient B were not addressed by the model. Courault et al. (1996) extended the work and provided alternative parameterisations for B. In principle, A and B should be consistent over areas with similar land cover structure.

The crop water stress index (CWSI) was originally developed at the agricultural field and daily time scale (Jackson et al. 1981). AVHRR-based estimates of actual evapotranspiration (λE_{a_AVHRR}) to λE_{a_DAY} are usually related using the approximation of Jackson et al. (1983), which has been extended by Xie (1991). Both are in the context of agricultural field-scale experiments.

There is an alternative to using spatial variance in remotely sensed data to map λE_{a_DAY}. T_s can be linked with meteorological variables if the meteorological data have the same temporal resolution as the remotely sensed data. High temporal resolution (e.g. every minute) meteorological data usually require intensive field campaigns for small, well-instrumented catchments. However, McVicar and Jupp (1999a) have recently shown that meteorological variables at the time of remotely sensed data acquisition can be adequately estimated from daily meteorological data for use with a resistance energy balance model

(REBM). This allows the development of a 'dual' approach to the well-known CWSI. Consequently, large regions in an operational framework can be monitored to derive a spatially varying index of moisture availability (m_a, the ratio of actual evapotranspiration to potential evapotranspiration (λE_p)) from daytime T_s. The development of the NDTI undertakes this dual approach. The NDTI is defined as:

$$NDTI = \frac{(T_\infty - T_s)}{(T_\infty - T_0)} \quad (1)$$

The two bounding temperatures, T_0 and T_∞, are derived by inverting an REBM. T_0 is an REBM inverted surface temperature when r_s (the composite surface resistance) = 0 s/m — that is, when it is assumed $\lambda E_a = \lambda E_p$. T_∞ is an REBM inverted surface temperature when $r_s = \infty$ s/m — that is, when it is assumed $\lambda E_a = 0$ W/m^2. The methods and assumptions used here are discussed fully in Jupp et al. (1998). In our study, daytime T_s is derived from the AVHRR sensor; however, it could be derived from any other space, or airborne, thermal sensor. If the REBM and the meteorological data — T_a vapour pressure (e_a), shortwave radiation (R_s) and wind speed (u) — estimated at the time of AVHRR data acquisition, are well defined, a time series of T_s should fall within the envelope defined by the limits T_0 and T_∞. McVicar and Jupp (1998) presented this relationship for five years of AVHRR T_s data recorded at Cobar, Australia.

The NDTI can be regarded as a specific time-of-day version of the CWSI. The NDTI brings the concept of mapping m_a from T_s onto a regional basis and is generic across different land surfaces by using the per-pixel variation present in the AVHRR data as the backbone for the spatial interpolation. This is achieved by developing suitable spatial covariates that incorporate AVHRR per-pixel variation. Both $T_s - T_a$ and R_n are potential covariates (Jackson et al. 1977). Vegetation cover (*VegCov*) is a potential covariate if changes in surface cover type and amount are to be incorporated.

Data Sets

Our requirements for daily meteorological data are modest: only T_n, T_x and P are essential. However, in the 1.1 million km^2 Murray–Darling Basin (MDB), only 63 Australian Bureau of Meteorology (ABM) stations have measured this data continuously from 1980 until the present. Figure 1 shows the location of the MDB and of the relevant meteorological sites. If available, daily U (km/day) was used to estimate u (m/s) (McVicar and Jupp 1999a). The northwest cloudband is a synoptic scale feature of the Australian region (Colls and Whitaker 1990), so 13 additional ABM stations to the north and west of the MDB were included in the meteorological database. Within the extended NDTI study area, there are 70 ABM stations, of which 57 are in the basin and an additional 13 are to the north and west of the basin.

Remotely sensed data were acquired by the AVHRR sensor on board the NOAA-9 and NOAA-11 satellites. Cracknell (1997) provides an extensive overview of the AVHRR sensor, the NOAA series of satellites and some previous applications of AVHRR data. The data archive that focuses on the MDB consists of 97 AVHRR single overpass afternoon images from June 1986 to January 1994, recorded at approximately monthly time intervals.

Selecting the Spatial Covariates

At Cobar (Fig. 1) daily meteorological data T_n, T_x, P and U were linked using the procedures described in McVicar and Jupp (1999a) to estimate T_a, e_a, R_s and u at the times of AVHRR data acquisition. The data were used with variables routinely derived from AVHRR data (T_s, *VegCov* and albedo (α)) in the REBM (Jupp et al. 1998) to model NDTI and λE_a. This was performed only for the 73 cloud-free AVHRR overpasses at Cobar.

The utility of each of the three potential covariates ($T_s - T_a$; *VegCov*; and R_n) was evaluated by linearly regressing them against the REBM outputs of NDTI

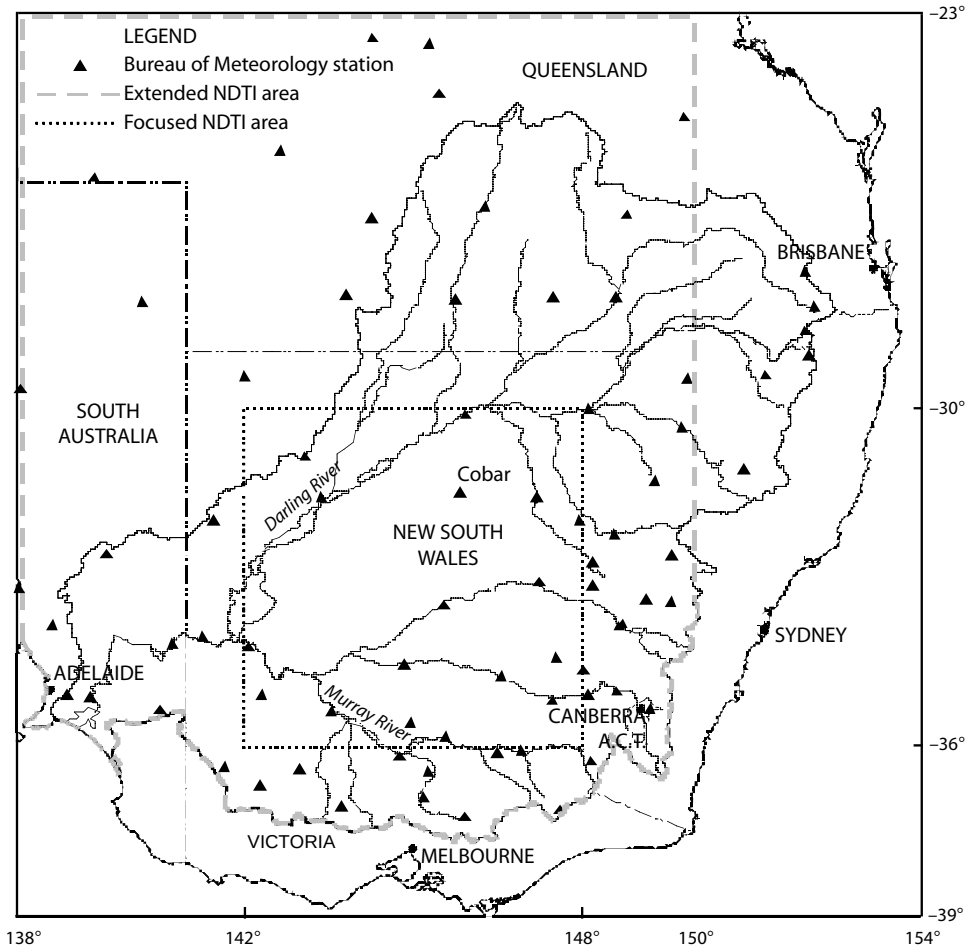

Figure 1. Location of sites in the Murray–Darling Basin, Australia.
The sites of the 76 Australian Bureau of Meteorology (ABM) stations are indicated. The focus and extended normalised difference temperature index (NDTI) study areas are shown.

or λE_a. Multiple linear regression was used as required. Table 1 shows the results. Only data with r_s greater than 0 s/m and R_n greater than 125 W/m^2 were used in the analysis. Increasing the R_n threshold increased the r^2 statistic but reduced the number of observations in the analysis, and vice versa. The threshold of $R_n > 125$ W/m^2 was a pragmatic balance between the strength of the relationship between the three potential covariates and the REBM NDTI, and the number of observations used (McVicar and Jupp 1999b).

Table 1 shows the results of the regression analysis between the REBM NDTI and one potential covariate in turn. $T_s - T_a$ had the largest r^2 and lowest standard error of the estimate of Y on X (SEY). Multiple linear regression analysis showed that $T_s - T_a$ and R_n were able to explain 79% of the variance within the NDTI, while $T_s - T_a$ and *VegCov* were able to explain only 60% (Table 1). When all three potential covariates were used, 85% of the variance within the NDTI was explained and the SEY was less than 0.1.

It is interesting to note that when we regressed λE_a against each potential covariate in turn, R_n provided the highest r^2 and the lowest SEY (Table 1). The r^2 and SEY values when both $T_s - T_a$ and R_n were used

were almost identical to the values when $T_s - T_a$, R_n and *VegCov* were used (Table 1). This indicates that, if interpolating λE_a rather than m_a, *VegCov* is not as important as $T_s - T_a$ and R_n.

We calculated regression model estimates of the NDTI and λE_a — denoted NDTI' and λE_a' respectively — based on one covariate ($T_s - T_a$), two covariates ($T_s - T_a$ and R_n) or three covariates ($T_s - T_a$, R_n and *VegCov*). We then cross-plotted them against the REBM NDTI or REBM λE_a, respectively. Figures 2a–c show the results for NDTI when three covariates were used for the modelling. The use of three covariates explained most of the variance of the REBM NDTI (Fig. 2a–c). This confirms that all three potential covariates should be developed as spatial surfaces to interpolate the NDTI. This is not necessary for spatially interpolating λE_a by comparing λE_a' with REBM λE_a: Figures 2d–f show that this regression can be performed adequately using only $T_s - T_a$ and R_n as spline model covariates.

Developing the Spatial Covariates

We used the CI approach to interpolate the NDTI, which was calculated at the ABM stations (considered points in the MDB) and then spatially interpolated. We used the following data to develop continuous grids, to be used as covariates, or in the modelling of R_n:

- interpolated meteorological data (T_a, e_a and effective beam transmittance at 0 m (τ_0));
- remotely sensed data (T_s and α);
- supervised classification of AVHRR reflective data used as a GIS stratum with the time series of AVHRR reflective data (*VegCov*); and
- R_n modelled using all of the above six variables as inputs.

Figure 3 illustrates the development of the six input variables required to generate R_n; Figure 4 shows how R_n is calculated. $T_s - T_a$ and *VegCov* are developed from some of the six variables. The following discussion provides further details of the methods used to develop the spatial covariates and intermediate variables, and the results we obtained.

Air temperature (T_a)

Continuous grids of T_a for the specific times of AVHRR data acquisition were calculated in a two-step process. First, T_a was temporally interpolated from T_n and T_x to provide estimates of T_a at the 70

Table 1. Regression analysis using REBM NDTI or REBM λE_a as the dependent variable and the potential covariates as the independent variable(s).

	Dependent variable					
	REBM NDTI			REBM λE_a		
Independent variable(s)	r^2	SEY	df	r^2	SEY	df
T_s–T_a	0.42	0.17	47	0.01	67.1	47
R_n	0.00	0.23	47	0.38	53.0	47
VegCov	0.31	0.19	47	0.21	59.7	47
T_s–T_a and R_n	0.79	0.11	46	0.95	15.4	46
T_s–T_a and *VegCov*	0.60	0.14	46	0.21	60.3	46
T_s–T_a, R_n and *VegCov*	0.85	0.09	45	0.97	12.5	45

df = degrees of freedom; NDTI = normalised difference temperature index; r^2 = coefficient of determination; REBM = resistance energy balance model; SEY = standard error of the estimate of Y on X. See text for an explanation of the other symbols. There were 49 observations.

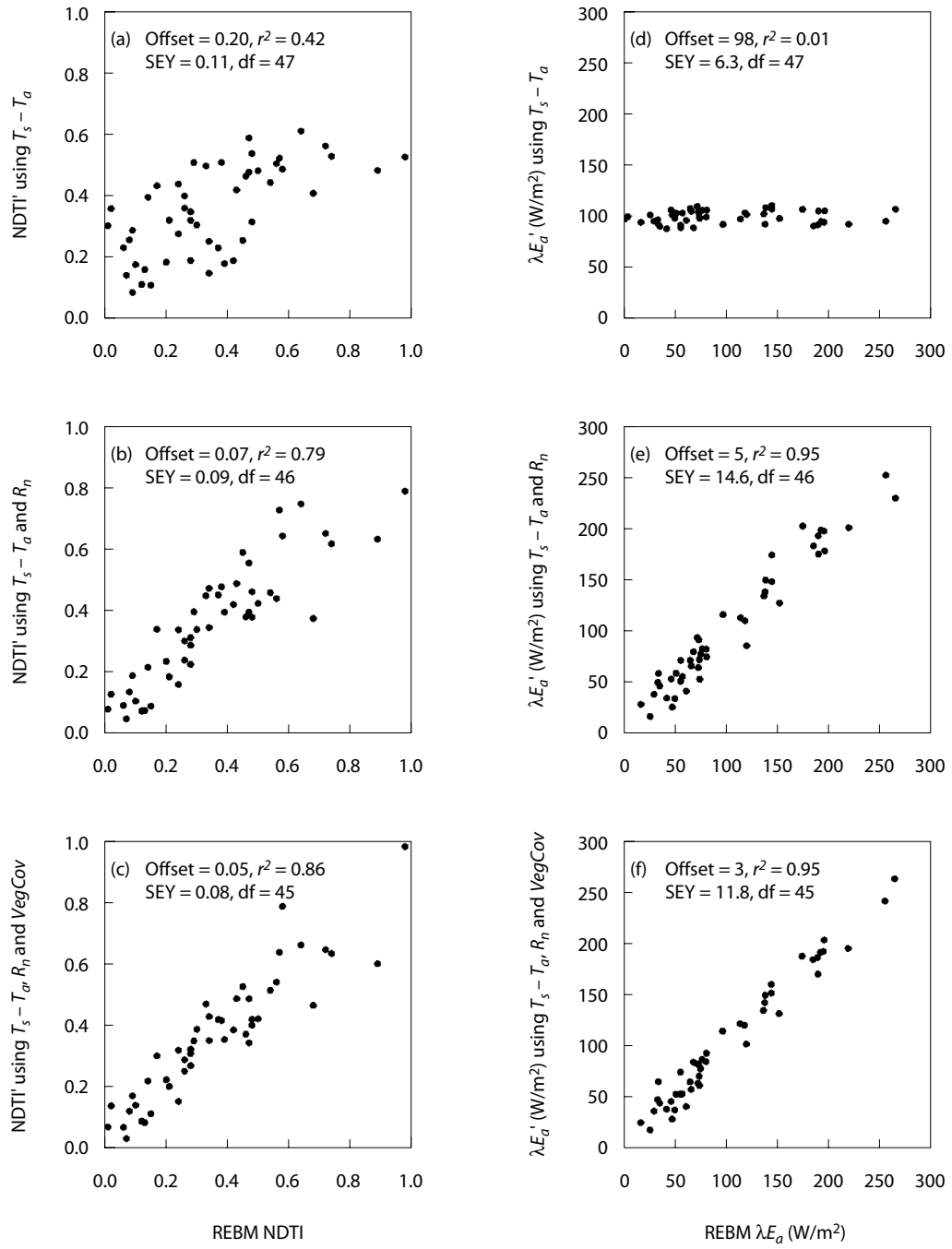

Figure 2. Cross-plots of resistance energy balance and regression models.
(a) to (c) show resistance energy balance model (REBM) normalised difference temperature index (NDTI) with regression model NDTI'; (d) to (f) show REBM λE_a with regression model λE_a'. The regression models are based on (a) and (d) T_s–T_a,; (b) and (e) T_s–T_a and R_n,; (c) and (f) T_s–T_a, R_n and *VegCov*. SEY = standard error of the estimate of Y on X. See text for an explanation of the terms used.

ABM stations, denoted $T_{a\_AVHRR\_PT}$ in Figure 3. Second, the values of $T_{a\_AVHRR\_PT}$ were spatially interpolated to generate continuous grids of T_a for the extended NDTI study site (Fig. 1), denoted $T_{a\_AVHRR\_GD}$ in Figure 3.

To select the spline model parameters, we undertook a detailed analysis using $T_{a\_AVHRR\_PT}$ supporting the AVHRR overpass acquired by NOAA-9 Orbit Number 14301, 22 September 1987 at 1629 local time. The influence of elevation was incorporated into the thin plate spline (TPS) by fitting the data with four variations:

- bivariate TPS function of longitude and latitude;
- trivariate partial thin plate spline (PTPS), incorporating a bivariate TPS function of longitude and latitude and a constant linear dependence on elevation;
- trivariate TPS function of longitude, latitude and elevation, in the units of metres; and
- trivariate TPS function of longitude, latitude and elevation, in the units of kilometres.

When using elevation (or any other variable) as an independent spline variable in a TPS, the units can influence the output surface. Hutchinson (1995) explored the scaling of elevation when interpolating mean monthly rainfall: elevation data expressed as

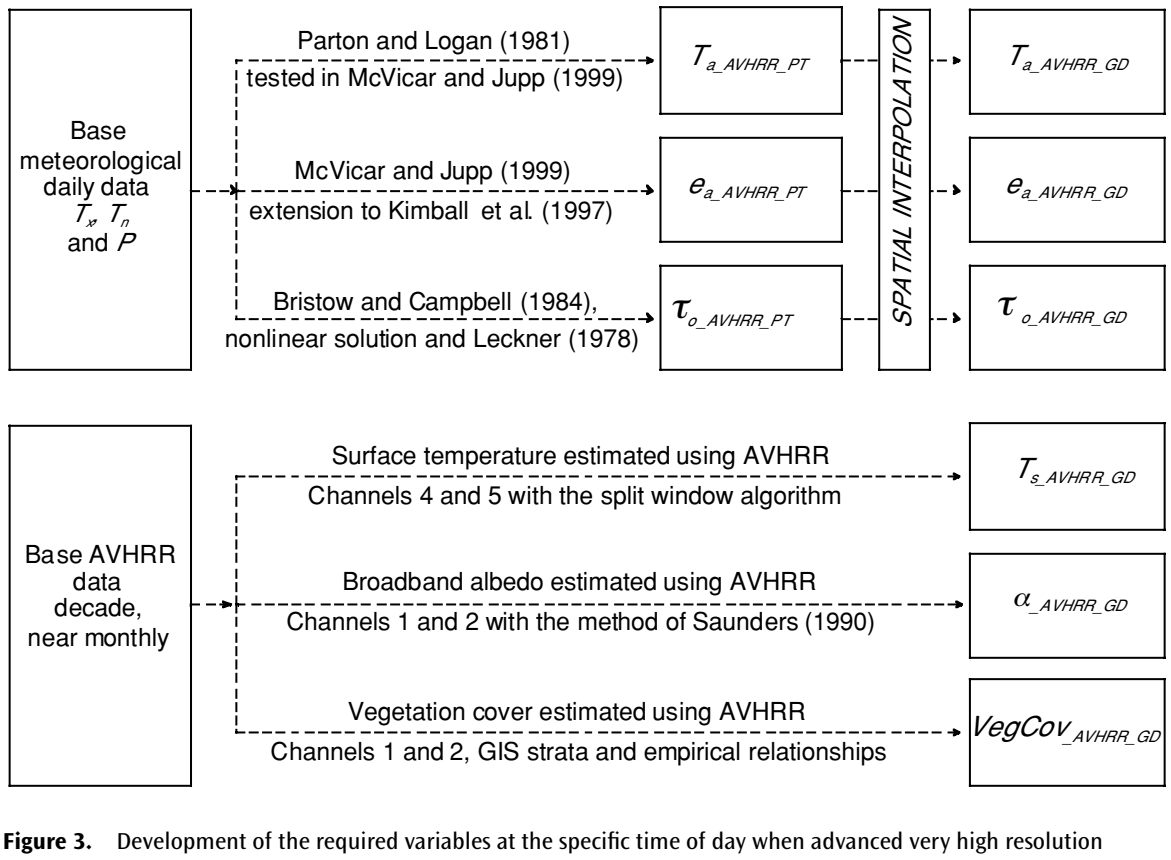

Figure 3. Development of the required variables at the specific time of day when advanced very high resolution radiometer (AVHRR) data are acquired.
The six variables are derived from two main sources. Daily meteorological data (T_n, T_x and P) are used to estimate T_a, e_a and τ_0. Then these three variables are spatially interpolated. AVHRR data are used to estimate T_s, α and *VegCov*. T_s–T_a and *VegCov* are used as covariates. All six variables are used in modelling the third covariate R_n (see Fig. 4). The subscript *AVHRR* refers to the specific time of day that AVHRR data are acquired; the subscript *PT* refers to measurements made at a 'point'; the subscript *GD* refers to measurement, or interpolated output, which is a continuous 'grid'.

kilometres were both convenient and in the range of units that provided a minimal validation residual. For TPS, the range of all independent variables should be approximately equal. However, scaling of elevation does not influence the output statistics if the TPS is extended to a PTPS by including elevation as a linear parametric submodel. This is the case for all covariates. As shown above, we scaled the elevation in metres or kilometres when using a trivariate TPS. The order of the partial derivate (m) was varied from 2 to 4 (three cases) for each of the four cases shown in the above bullet points, resulting in a total of 12 options.

For all 12 spline models, the smoothing parameter (λ) was automatically selected by minimising the generalised cross-validation error, denoted as $GCV(m,\lambda)$. McVicar and Jupp (1999b) present full statistics for all 12 options. The trivariate TPS with elevation in kilometres $m = 3$ had the lowest $\sqrt{GCV(m,\lambda)}$ (0.792°C) and this spline model was used to spatially interpolate the 97 surfaces of $T_{a\_AVHRR\_GD}$, using $T_{a\_AVHRR\_PT}$ as input data (Fig. 3).

Figure 5a shows the output for 22 September 1987. T_a gradually increases from the southeast to the northwest, but this trend is modified by local changes in elevation. The northwest portion is considered semiarid; in the southeast during September (the southern hemisphere spring), if drought conditions are not experienced, there is a spring growth flush of cereal crops (wheat, barley and oats). The 97 continuous grids of T_a were calculated and used with the other variables as required to develop the covariates (Fig. 4).

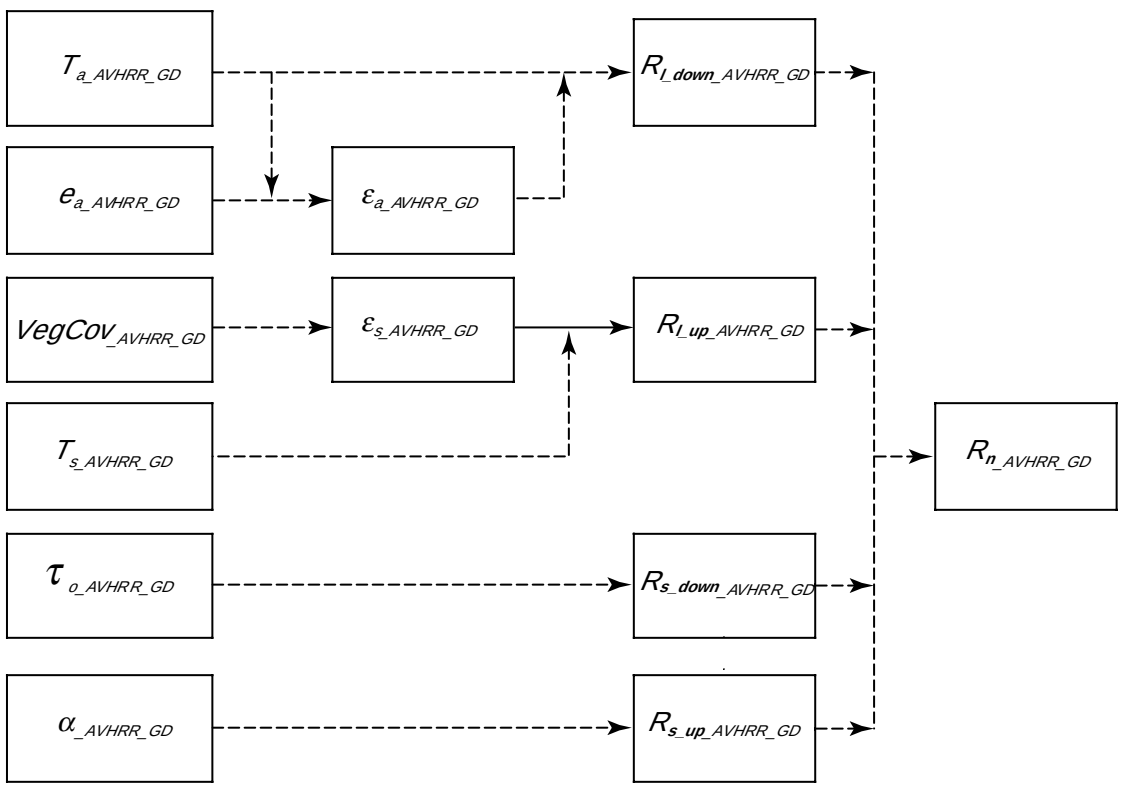

Figure 4. Development of R_n.
R_l and R_s refer to longwave and shortwave radiation, respectively; the subscript 'down' refers to radiative fluxes from the atmosphere towards the land surface; the subscript 'up' refers to radiative fluxes from the land surface toward the atmosphere. Refer to Figure 3 for the development of the six input variables.

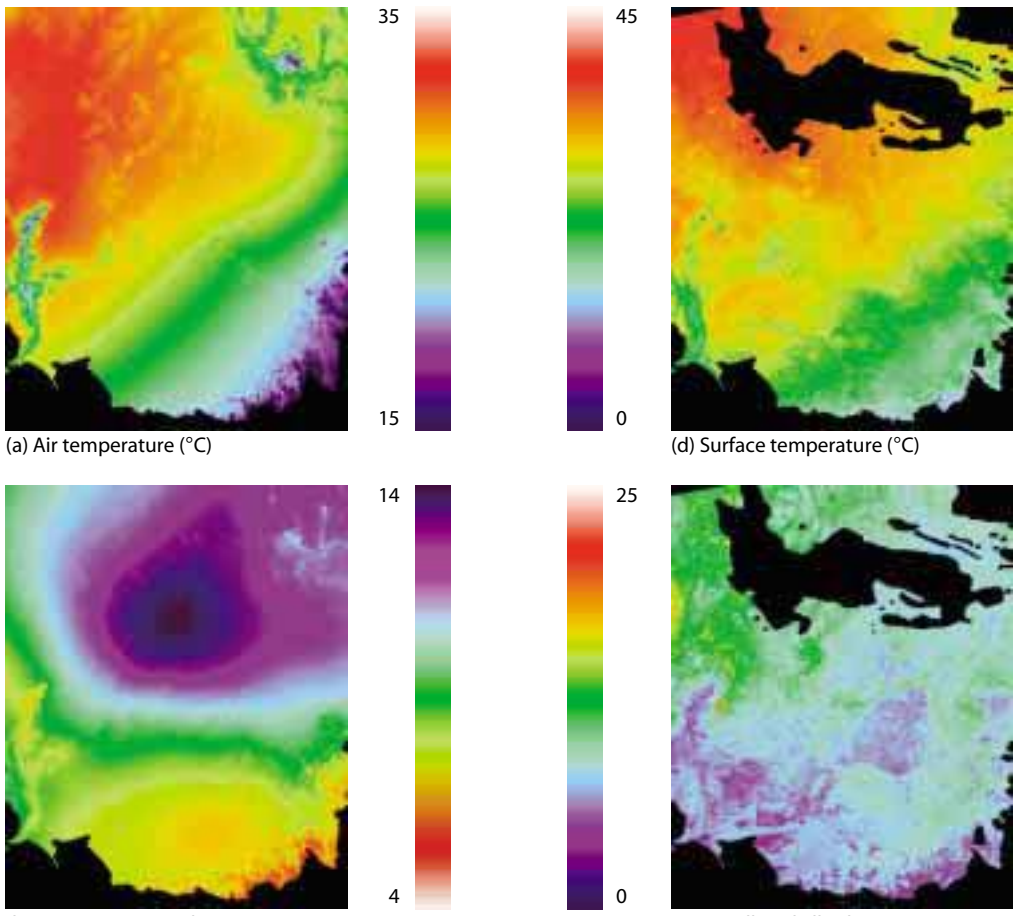

Figure 5. Continuous grids of the six required variables.
The required variables are (a) T_a (°C); (b) e_a (hPa); (c) τ_0 (%); (d) T_s (°C); (e) α (%); and (f) *VegCov* (%) for the extended normalised difference temperature index (NDTI) area shown in Figure 1. Variables (a), (b) and (c) are derived from spatial interpolation based on data recorded at the 70 ABM stations. Variables (d), (e) and (f) are derived from advanced very high resolution radiometer (AVHRR) data, some of which are not reliable because they are cloud affected; these data have been nulled and are shown in black. Note the difference in the smoothness of the output based on the source of the data. Refer to Figure 3 for the development of the six variables.

Vapour pressure (e_a)

Continuous grids of e_a for the specific times of AVHRR data acquisition were calculated using two steps. The first was to temporally estimate e_a. Recently Kimball et al. (1997) estimated dew point temperature based on empirical regressions between T_x and T_n, and an introduced term 'EF', which is the ratio of Priestly–Taylor λE_{p_DAY} divided by annual precipitation. The assumption that e_a remains constant throughout the day was improved upon by linearly interpolating e_a between the times of sunrise for consecutive days, denoted K97 'interpolation' in McVicar and Jupp (1999a). The K97 interpolation method was used to develop $e_{a\_AVHRR\_PT}$ (Fig. 3) estimates at the 70 ABM stations (Fig. 1). In the second step, the values of $e_{a\_AVHRR\_PT}$ were spatially interpolated to generate continuous grids of e_a for the extended NDTI study site (Fig. 1), denoted $e_{a\_AVHRR\_GD}$ in Figure 3. To test the sensitivity of m and the use of and units of elevation as a covariate (Jackson et al. 1985) in developing $e_{a\_AVHRR\_GD}$, we used the same 12 spline models used for T_a.

For all 12 spline models, λ was again automatically selected by minimising $GCV(m,\lambda)$. The model with the lowest $\sqrt{GCV(m,\lambda)}$ is the trivariate PTPS m = 2 (1.11 hPa). McVicar and Jupp (1999b) provide full statistics for all 12 spline models. Figure 5(b) shows the output for 22 September 1987. The area of high e_a in the northern portion of Figure 5(b) approximately conforms to the area identified as cloud in the AVHRR data (Fig. 5d–f). The 97 continuous grids of e_a were calculated and used to model atmospheric emissivity (ε_a)(Fig. 4).

Atmospheric transmittance (τ_0)

Calculating continuous grids of τ_0 for the specific days of AVHRR data acquisition is a two-step process. First, we calculated $\tau_{0\_AVHRR\_PT}$ (Fig. 3), for each of the 97 AVHRR days at each of the 70 ABM stations. McVicar and Jupp (1999b) present full details. Second, we spatially interpolated $\tau_{0\_AVHRR\_PT}$ to provide continuous grids of τ_0, denoted $\tau_{0\_AVHRR\_GD}$ (Fig. 3), using a TPS. Detailed results for the spatial interpolation of $\tau_{0\_AVHRR\_GD}$, using $\tau_{0\_AVHRR\_PT}$ as the input data, for the bivariate TPS varying m from 2 to 4 were examined. As with T_a, λ was automatically selected by minimising $GCV(m,\lambda)$. The bivariate TPS m = 2 has the lowest $\sqrt{GCV(m,\lambda)}$ (0.0157%). McVicar and Jupp (1999b) provide the complete listing of output statistics. Elevation was not incorporated in this spline model as the relationship between τ_0 and elevation is implicitly defined by using a DEM in the calculation of downward short-wave radiation (R_{s_down}). $\tau_{0\_AVHRR\_GD}$ is assumed constant over the day; the specific time of day, day of year and geographical position of each resampled AVHRR pixel centre are used to determine transmission path length (p) and cosine of the solar zenith angle ($\cos\theta_s$).

Figure 5c shows this output for 22 September 1987; the area of lower τ_0 approximately conforms to the area of higher e_a (shown in Fig. 5b) and is identified as cloud in Figure 5d–f. The 97 continuous grids of τ_0 are used to calculate R_{s_down} (Fig. 4).

Surface temperature (T_s)

$T_{s\_AVHRR\_GD}$ is calculated using a split-window approach, which takes advantage of the differential atmospheric absorption observed in AVHRR channels 4 and 5. The radiance measured by AVHRR channels 4 and 5 is converted to brightness temperatures, denoted *T4* and *T5* respectively, using Plank's law. An estimate of brightness T_s, denoted Tb_s, has then been developed using the formula $Tb_s = T_5 + 3\,\Delta T_{4,5} + 0.5$, where $\Delta T_{4,5}$ is $T_4 - T_5$. The split-window coefficients were determined by simulating the absorption coefficients for the AVHRR channel 4 and 5 bandwidths using Australian atmospheric data (Maher and Lee 1977) and the LOWTRAN6 package (Kneizys et al. 1983). T_s estimates were obtained by correcting the data for emissivity, based on pixel fractional *VegCov* using 0.98 for vegetation emissivity (ε_v) and 0.96 for ground (or soil) emissivity (ε_g) (Wan and Dozier 1996). Generating $T_{s\_AVHRR\_GD}$ does not require any spatial interpolation.

Figure 5d shows the increase in T_s toward the semiarid area in the northwest; lower T_s values to the southeast are associated with an increase in m_a. The increases in λE_a are associated with an increase in *VegCov* due to the spring growth flush of cereals crops (Fig. 5f). Cloud clearing means that AVHRR data are available only when there was no cloud. The 97 images of T_s were calculated and used with the other variables as required to develop the covariates (Fig. 4).

Broadband albedo (α)

$\alpha_{\_AVHRR\_GD}$ was calculated using the Saunders (1990) model with AVHRR channels 1 and 2 (Fig. 3). Sensor drift degradation was taken in account using the methods provided by Mitchell (1999). The resulting effective reflectance factor is used in the Saunders model to estimate $\alpha_{\_AVHRR\_GD}$ for all 97 AVHRR images. Figure 5e is an example of α; the high albedo area to the west is Lake Frome, a salt lake; the very small area to the southeast is snow cover on the Australian Alps. Remnant forests and woodlands have the lower albedos. The 97 images of α were calculated and used to model the shortwave radiation reflected upward by the surface (R_{s_up}) (Fig. 4).

Vegetation cover

$VegCov_{\_AVHRR\_GD}$ is calculated as continuous grids for the specific days of AVHRR data acquisition in a two-step process. Firstly, we defined a stratum of woody and nonwoody vegetation by classifying reflective AVHRR data from several dates throughout 1987 into a woody/nonwoody vegetation stratum. Secondly, we developed empirical relationships between in situ leaf area index (LAI) and AVHRR channels 1 (Red) and 2 (NIR). For nonwoody vegetation, LAI = –1.15 + 0.96 × (NIR/Red) (McVicar et al. 1996a); for woody vegetation, LAI = –4.65 + 4.22 × (NIR/Red) (McVicar et al. 1996b). Finally $LAI_{\_AVHRR\_GD}$ were converted into estimates of *VegCov* using the relationship $VegCov = 100.0 \times (1.0 - \exp^{(-LAI/2)}$, assuming random distribution of foliage above the soil and uniform leaf-angle distribution (Choudhury 1989).

Figure 5f illustrates this output for 22 September 1987. The areas of higher amounts of *VegCov* are remnent forests and woodlands; the large expanse of moderate values across the southern portion of the image (Fig. 5f) is due to the spring growth flush of cereal crops. The large expanse with 0% *VegCov* toward the northwest is semiarid (Fig. 5f) and corresponds to the area of high T_s in Figure 5d. *VegCov* is used as a covariate and is also used to calculate surface emissivity (ε_s).

Net radiation (R_n)

R_n can be expressed as the sum of its four components:

$$R_n = R_{s\_down} - R_{s\_up} + R_{l\_down} - R_{l\_up} \qquad (2)$$

where R_s is short-wave radiation and R_l is longwave radiation. The components can be calculated from the six variables introduced above (see Fig. 4). An IC approach is used for R_n because R_n is strongly influenced by α and T_s, which can be discontinuous due to land use (e.g. when agricultural land is adjacent to remnant forest). Information about α, T_s and *VegCov* is obtained directly from the spatially dense AVHRR data (Fig. 3). This means that changes in α, T_s and *VegCov* are accounted for in space — at $1/64^{th}$ of a degree, the spatial resolution of the resampled AVHRR data — and in time, near monthly, the temporal resolution in the AVHRR data base.

The methods used to model the radiation components are fully documented in McVicar and Jupp (1999b) and are briefly documented below. R_{s_down} is modelled by:

$$R_{s\_down} = \tau_0^{\frac{P_z}{P_0} p/2} \cos\theta_s Q_0' \qquad (3)$$

where P is the total pressure (the subscripts denote the altitude above a zero height surface) and Q_0' is

the exoatmospheric normal solar irradiance modified for sun–earth distance. The input variables required are:

- a continuous raster of τ_0 (see above);
- the specific time of day, day of year and geographical position of the pixel centre of resampled AVHRR data (used to determine p and $\cos\theta_s$);
- a continuous raster of height, obtained from AUSTDEM Ver 4.0; and
- slope and aspect, derived from the DEM (used to modify the calculation) (Iqbal 1983).

R_{s_up} is the fraction of R_{s_down} reflected by the surface; this is controlled by α. R_{l_down} is calculated using the method described in Kustas et al. (1989), in which ε_a and T_a are variables. The estimate of ε_a relies on e_a and T_a (Brutsaert 1975). To calculate R_{l_up}, both ε_s and T_s are required (Kustas et al. 1989). ε_s is calculated from *VegCov*, using 0.98 for ε_v and 0.96 for ε_g (Wan and Dozier 1996). The relatively small component of outgoing longwave radiation by reflected sky radiation is ignored (Jackson et al. 1985).

We developed the components of R_n using the methods described above and summarised in Figure 4. In Figure 6a the longitudinal banding of R_{s_down} is due to changes in p and $\cos\theta_s$ when the AVHRR data were acquired at 1629 local time. Modification by elevation, slope and aspect are shown. Figure 6b illustrates the influence of α and banding of R_{s_down} on R_{s_up}. The spatial pattern of R_{l_down}, shown in Figure 6c is dominated by T_a. R_{l_up} (Fig. 6d) follows the spatial variability present in T_s. The components have been added together (Equation 2) to provide continuous rasters of R_n, denoted $R_{n\_AVHRR\_GD}$, which is used as a covariate. $R_{n\_AVHRR\_GD}$ for 22 September 1987 is illustrated in Figure 7c.

Applying the Spatial Covariates to the Murray–Darling Basin

We used the CI approach to develop the 97 surfaces of the NDTI for the focus area of the MDB. The NDTI (Equation 1) was calculated at the ABM stations shown in Figure 1. To generate continuous NDTI surfaces, we used a quintvariate PTPS, incorporating a bivariate TPS function of longitude and latitude with constant linear dependencies on $T_s - T_a$, *VegCov* and R_n (see Figures 7a, b and c respectively). To select the spline model, we varied m from 2 to 4 and assessed its influence (McVicar and Jupp 1999b). We examined detailed results for the spatial interpolation of NDTI for the three options $m = 2$ to 4; full results are presented in McVicar and Jupp (1999b). As with T_a above, λ was automatically selected for the spline models by minimising $GCV(m,\lambda)$. The model with the lowest $\sqrt{GCV(m,\lambda)}$ was the quintvariate PTPS with three covariates $m = 2$.

The high spatial density of AVHRR data is seen in the resulting NDTI images. Figure 8a shows the NDTI image for spring (22 September 1987) and Figure 8b shows the NDTI image for summer (25 December 1987). Changes in the NDTI between the two dates are shown in Figure 8c, where blue is an increase, green fairly constant and red a decrease between the two dates. Figure 8a shows that the Menindee Lakes system is the only area where NDTI is greater than 0.8, with the southern portion of the wheatbelt in the southeast having an NDTI of about 0.5. Some areas around the Menindee Lakes also have an NDTI of about 0.5; these are assumed to have received scattered rainfall. Figure 5d shows the larger extent of this pattern, confirmed by a decrease in T_s. In Figure 8b some areas with an NDTI greater than 0.8 are lakes while others are associated with flood irrigation of crops and remnant river red gum forests (Barham and Gulpa State Forests) along the Murray River. On the Cobar peneplain there are scattered areas with NDTI values of approximately 0.5, which corresponds to

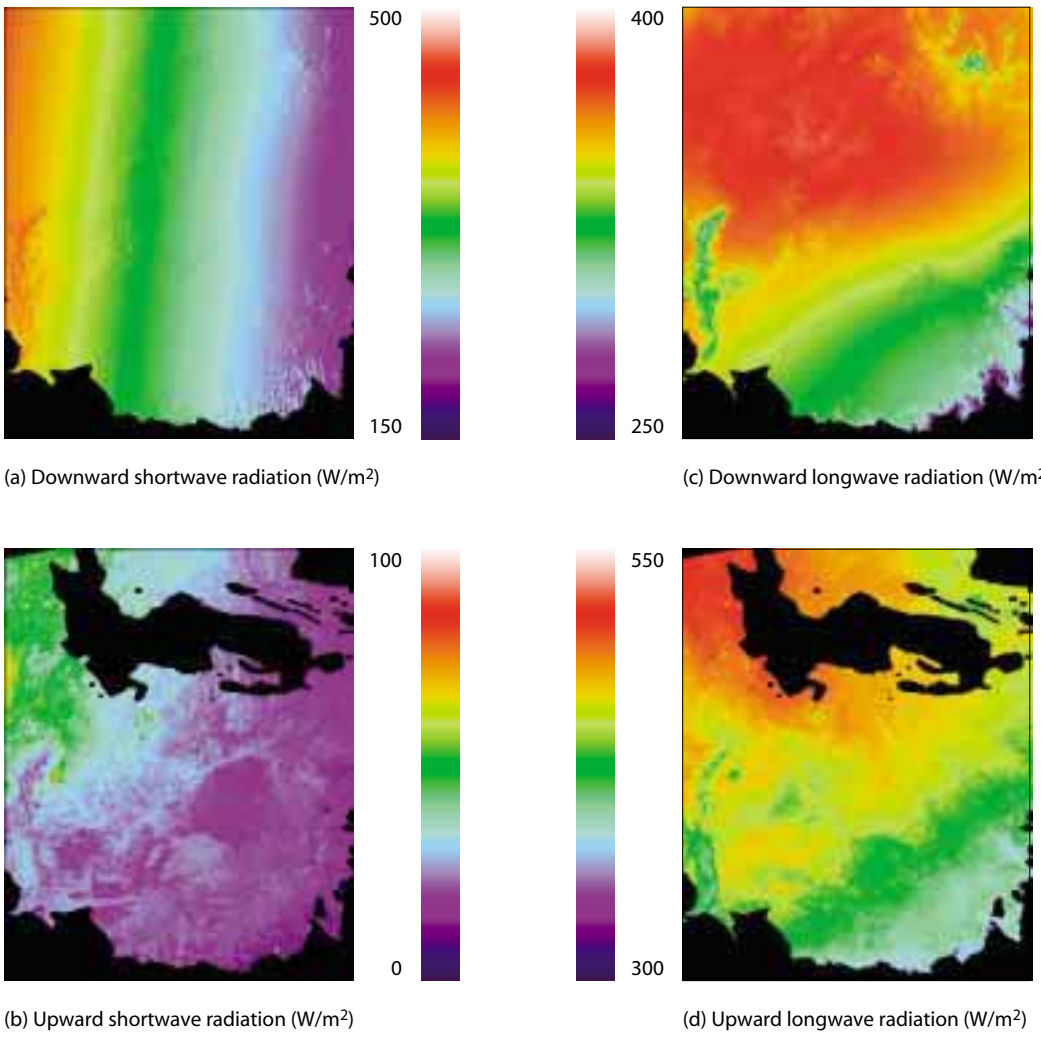

(a) Downward shortwave radiation (W/m^2)

(c) Downward longwave radiation (W/m^2)

(b) Upward shortwave radiation (W/m^2)

(d) Upward longwave radiation (W/m^2)

Figure 6. Continuous grids of the four radiation components.
The figure shows (a) R_{s_down} (W/m^2); (b) R_{s_up} (W/m^2); (c) R_{l_down} (W/m^2) and (d) R_{l_up} (W/m^2) for the extended normalised difference temperature index (NDTI) area shown in Figure 1 used to calculate R_n. Variables (b) and (d) require input variables from advanced very high resolution radiometer (AVHRR) data (see Fig. 4). Consequently the areas cloud affected in the AVHRR data (see Fig. 5) are nulled and are shown as black for these variables. Refer to Figure 4 for the development of the four components.

areas where the NDTI has increased between the two dates (Fig. 8c); these areas have probably received scattered rainfall.

Figures 8d and 8e show the AVHRR derived estimates of *VegCov* for spring and summer, respectively. The remnant deep-rooted forests are identified by having a stable *VegCov* between the two seasons. This is especially seen for the remnant river red gum forests along the Murray River. In the woodlands of the Cobar peneplain, *VegCov* is mainly stable. However, there are some areas on the Cobar peneplain — the blue areas in Fig. 8f — where *VegCov* has increased between the two periods. These areas are associated with an increase in the NDTI (Fig. 8c). This increase in *VegCov* is probably associated with an increase in the amount of grass cover. The grasses have adapted to respond to short-term changes in available moisture and will be observable through the relatively open overstorey canopy (10–20%).

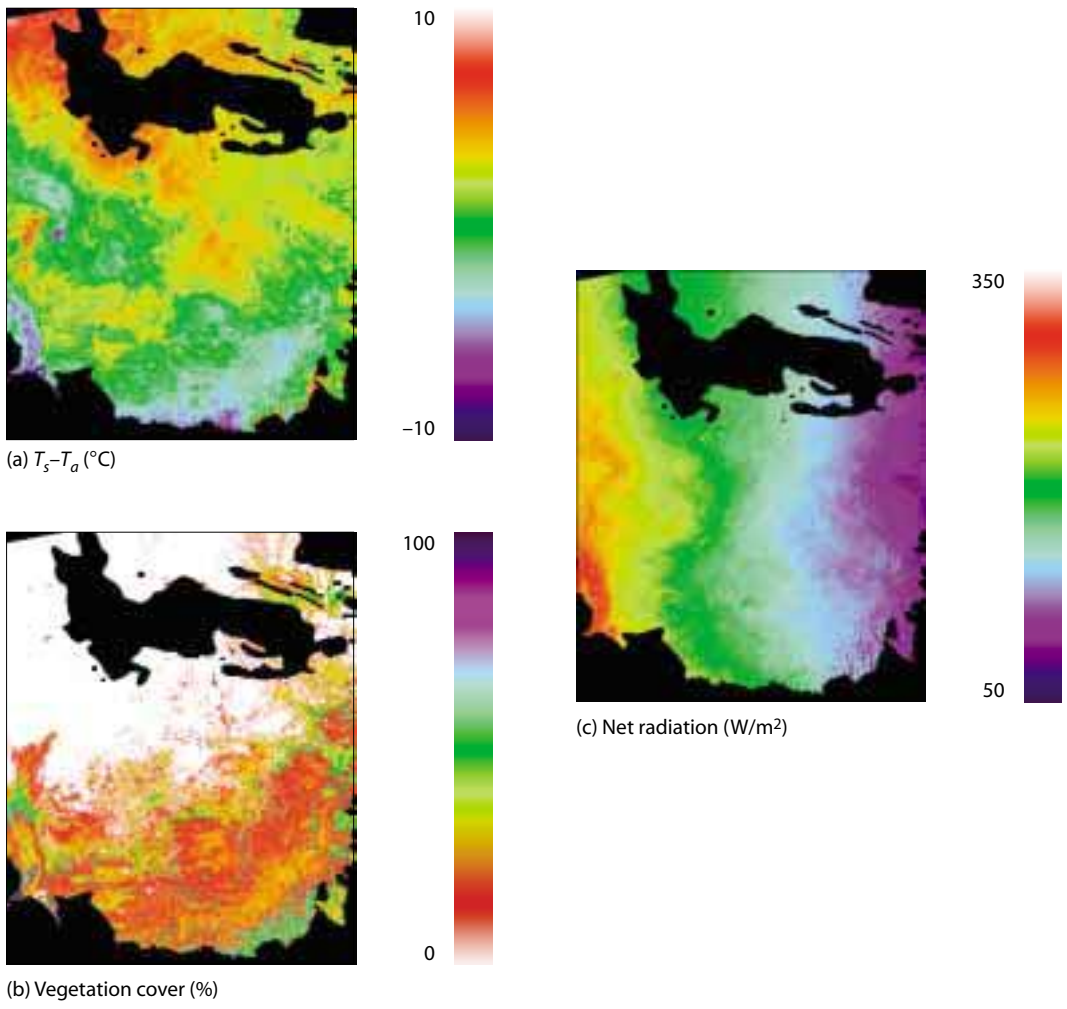

Figure 7. Continuous grids of the three covariates.
The figure shows (a) $T_s - T_a$ (°C); (b) *VegCov* (%) and (c) R_n (W/m^2) for the extended normalised difference temperature index (NDTI) area shown in Figure 1. All three covariates use advanced very high resolution radiometer (AVHRR) data; consequently areas cloud affected in the AVHRR data (see Fig. 5 and 6) are nulled and are shown as black for each of the covariates.

The changes between the two dates in NDTI (Fig. 8c) and *VegCov* (Fig. 8f) are similar, though not identical. For example, along the northeastern border of the two images, there is a large negative change in *VegCov* due to harvesting of cereal crops, whereas in this area the NDTI remains fairly constant (it is less than 0.2 for both dates). To assist in regional agricultural management, including drought assessment, the resulting NDTI images and reflective-based images, such as *VegCov* or the normalised difference vegetation index (NDVI), and their interactions, need to be analysed in a spatial–temporal context. If the NDTI is viewed as an indicator of moisture availability, and the NDVI is thought of as an indicator of moisture utilisation, there is an opportunity to separate variability induced by climate from that induced by management (McVicar and Jupp 1998). For example, in cropping or pasture agricultural systems, if the NDTI reduces during a growing

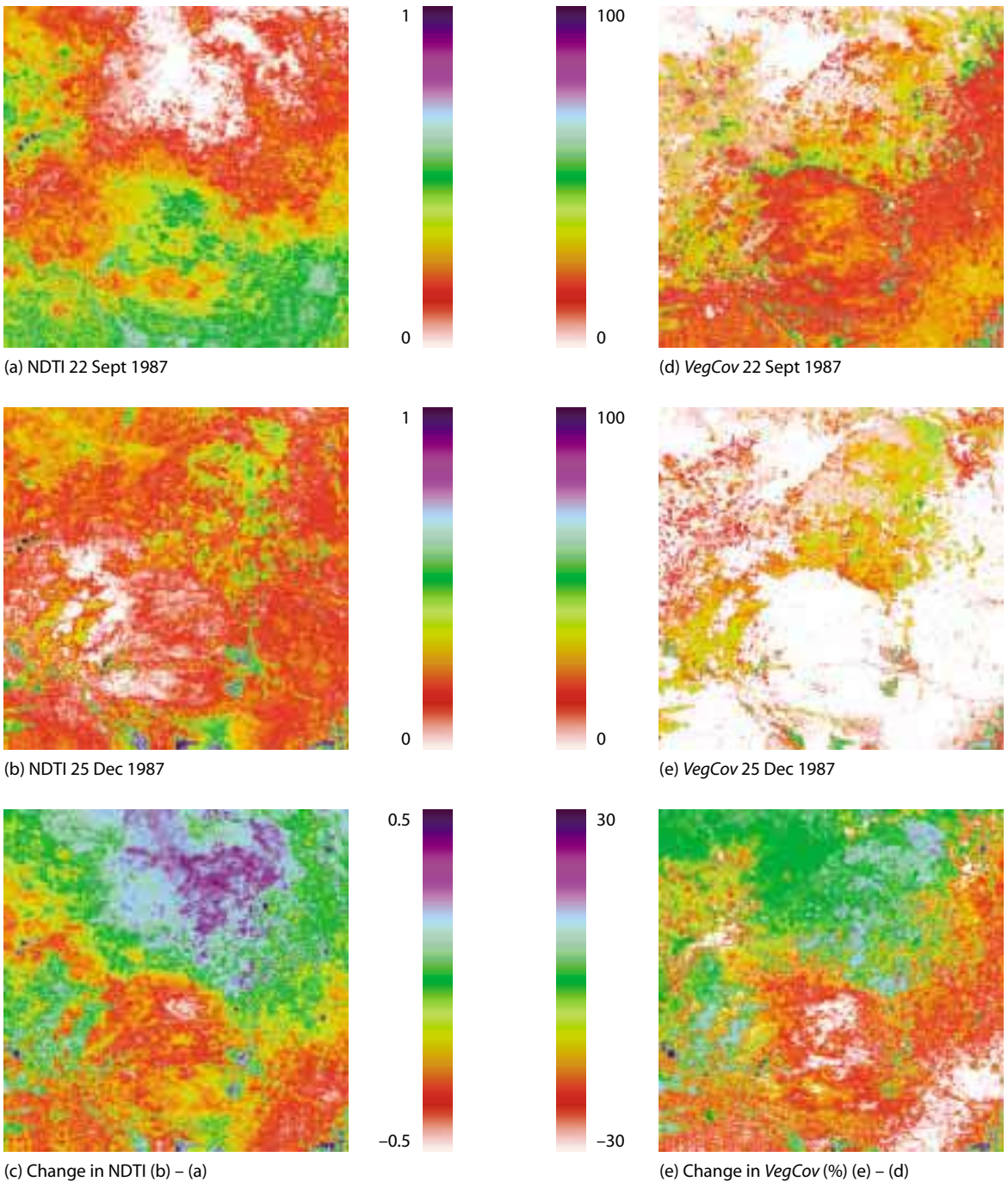

(a) NDTI 22 Sept 1987

(d) *VegCov* 22 Sept 1987

(b) NDTI 25 Dec 1987

(e) *VegCov* 25 Dec 1987

(c) Change in NDTI (b) – (a)

(e) Change in *VegCov* (%) (e) – (d)

Figure 8. Images of the focus NDTI area shown in Figure 1.
The figure shows (a) normalised difference temperature index (NDTI) for 22 September 1987; (b) NDTI for 25 December 1987 and (c) the difference of NDTI between these two dates, calculated as (b) – (a). (d) to (f) as for (a) to (c), except that *VegCov* is shown.

season while the NDVI increases, this would indicate that some of the decrease in moisture availability was due to transpiration. However, there may be cases where the NDTI reduces during the growing season and the NDVI fails to show any response. Such a case could be the result of disease or insect damage early during the crop growing season and the resulting decrease in moisture availability may be attributable only to soil evaporation. During crop growing seasons these interactions may be best analysed by calculating the integrals under a time series of NDTI and NDVI images. The timing of the maximum NDTI and NDVI during crop growth periods would probably have to be included. McVicar and Jupp (2002) provide a formal sensitivity analysis of the variables used in developing the covariates to interpolate the NDTI.

Conclusions

The NDTI, which can be considered a specific time-of-day version of the CSWI, is calculated using an REBM at the ABM stations where meteorological data are acquired. We have used a CI approach to spatially interpolate the NDTI from these isolated stations to generate a continuous surface in the MDB. Three covariates were required: $T_s - T_a$, *VegCov*, and R_n. They were obtained mainly from AVHRR data and spatial interpolation of selected meteorological variables, with R_n modelled using an IC approach. We are not advocating CI in preference to IC; the underlying issues determine which is most useful in a given situation. We are advocating, and have presented, a CI method that inherently uses the high spatial density of AVHRR data as the backbone for the spatial interpolation.

The NDTI provides a link into regional water balance modelling that does not require spatial interpolation of daily rainfall. Assessing spatial and temporal interactions between the NDTI and *VegCov* or NDVI will provide useful information about regional hydroecological processes, including agricultural management, in the context of Australia's highly variable climate.

Acknowledgments

This research has been supported in part with contributions by ACIAR and CSIRO Land and Water. We had helpful discussions with Dr Michael Hutchinson (Australian National University, Centre of Resources and Environmental Studies) while conducting this research.

References

Borga, M. and Vizzaccaro, A. 1997. On the interpolation of hydrologic variables: formal equivalence of multiquadratic surface fitting and kriging. Journal of Hydrology, 195, 160–171.

Bosma, W.J.P., Marinussen, M.P.J.C. and van der Zee, S.E.A.T.M. 1994. Simulation and areal interpolation of reactive solute transport. Geoderma, 62, 217–231.

Brutsaert, W.H. 1975. On a derivable formula for longwave radiation from clear skies. Water Resources Research, 11, 742–744.

Carter, J., Flood, N., Danaher, T. et al. 1996. Development of a National Drought Alert Strategic Information System. Volume 3. Development of data rasters for model inputs. Final Report to Land and Water Resources Research and Development Corporation, Queensland Department of Primary Industries, 20, Brisbane, 76.

Choudhury, B.J. 1989. Estimating evaporation and carbon assimilation using infrared temperature data: vistas in modelling. In: Asrar, G., ed., Theory and Applications of Optical Remote Sensing. New York, John Wiley and Sons, 628–690.

Cole, C.V., Paustian, K., Elliott, E.T., Metherell, A.K., Ojima, D.S. and Parton, W.J. 1993. Analysis of agroecosystem carbon pools. Water, Air and Soil Pollution, 70, 357–371.

Colls, K. and Whitaker, R. 1990. The Australian Weather Book. Sydney, Child and Associates.

Courault, D., Lagouarde, J.P. and Aloui, B. 1996. Evaporation for maritime catchment combining a meteorological model with vegetation information and airborne surface temperatures. Agricultural and Forest Meteorology, 82, 93–117.

Cracknell, A.P. 1997. The Advanced Very High Resolution Radiometer (AVHRR). London, Taylor and Francis.

Dubrule, O. 1983. Two methods with different objectives: splines and kriging. Mathematical Geology, 15, 245–257.

Dubrule, O. 1984. Comparing splines and kriging. Computers and Geosciences, 10, 327–338.

Hutchinson, M.F. 1993. On thin plates splines and kriging. In: Tarter, M.E. and Lock, M.D., eds, Computing and Science in Statistics, Vol. 25. University of California, Berkeley: Interface Foundation of North America, 55–62.

Hutchinson, M.F. 1995. Interpolating mean rainfall using thin plate smoothing splines. International Journal of Geographic Information Science, 9, 385–403.

Hutchinson, M.F. 1997. ANUSPLIN Version 3.2 User Guide. Canberra, ANU.

Hutchinson, M.F. and Gessler, P.E. 1994. Splines—more than just a smooth interpolator. Geoderma, 62, 45–67.

Iqbal, M. 1983. An Introduction to Solar Radiation. Vancouver, Academic Press.

Jackson, R.D., Hatfield, J.L., Reginato, R.J., Idso, S.B. and Pinter Jr., P.J. 1983. Estimation of daily evapotranspiration from one-time-of-day measurements. Agricultural Water Management, 7, 351–362.

Jackson, R.D., Idso, S.B., Reginato, R.J. and Pinter Jr., P.J. 1981. Canopy temperature as a crop water stress indicator. Water Resources Research, 17, 1133–1138.

Jackson, R.D., Pinter Jr., P.J. and Reginato, R.J. 1985. Net radiation calculated from remote multispectral and ground station meteorological data. Agricultural and Forest Meteorology, 35, 153–164.

Jackson, R.D., Reginato, R.J. and Idso, S.B. 1977. Wheat canopy temperature: a practical tool for evaluating water requirements. Water Resources Research, 13, 651–656.

Jupp, D.L.B., Tian, G., McVicar, T.R., Qin, Y. and Fuqin, L. 1998. Soil Moisture and Drought Monitoring Using Remote Sensing. I: Theoretical Background and Methods. Canberra, CSIRO Earth Observation Centre, 96.

Kimball, J.S., Running, S.W. and Nemani, R.R. 1997. An improved method for estimating surface humidity from daily minimum temperature. Agricultural and Forest Meteorology, 85, 87–98.

Kittel, T.G.F., Rosenbloom, N.A., Painter, T.H. and Schimel, D.S. 1995. The VEMAP integrated database for modelling United States ecosystem/vegetation sensitivity to climate change. Journal of Biogeography, 22, 857–862.

Kneizys, F.X., Shettle, E.P., Abreu, L.W., Anderson, G.P., Chetwynd, J.H., Gallery, W.O., Selby, J.E. and Clough, S.A. 1983. Atmospheric transmittance/radiance: computer code LOWTRAN 6. Technical Report AFGL-TR-83-0187. Massachusetts, United States Air Force Geophysics Laboratory, 200.

Kustas, W.P., Jackson, R.D. and Asrar, G. 1989. Estimating surface energy-balance components from remotely sensed data. In: Asrar, G., ed., Theory and Application of Optical Remote Sensing. New York, John Wiley and Sons, 604–627.

Lagouarde, J.-P. 1991. Use of NOAA AVHRR data combined with an agrometeorological model for evaporation mapping. International Journal of Remote Sensing, 12, 1853–1864.

Lam, N.S. 1983. Spatial interpolation methods: a review. The American Cartographer, 10, 129–149.

Laslett, G.M. 1994. Kriging and splines: an empirical comparison of their predictive performance in some applications. Journal of the American Statistical Association, 89, 391–409.

Maher, J.V. and Lee, D.M. 1977. Upper Air Statistics Australia. Surface to 5 mb 1957 to 1975. Canberra, Department of Science, Bureau of Meteorology.

McVicar, T.R. and Jupp, D.L.B. 1998. The current and potential operational uses of remote sensing to aid decisions on drought exceptional circumstances in Australia: a review. Agricultural Systems, 57, 399–468.

McVicar, T.R. and Jupp, D.L.B. 1999a. Estimating one-time-of-day meteorological data from standard daily data as inputs to thermal remote sensing based energy balance models. Agricultural and Forest Meteorology, 96, 219–238.

McVicar, T.R. and Jupp, D.L.B. 1999b. Using AVHRR data and meteorological surfaces to spatially interpolate moisture availability in the Murray–Darling Basin. Canberra, CSIRO Land and Water, 45.

McVicar, T.R. and Jupp, D.L.B. 2002. Using covariates to spatially interpolate moisture availability in the Murray–Darling Basin: a novel use of remotely sensed data. Remote Sensing of Environment, 79, 199–212.

McVicar, T.R., Jupp, D.L.B. and Williams, N.A. 1996a. Relating AVHRR vegetation indices to LANDSAT TM leaf area index estimates. Canberra, CSIRO Division of Water Resources, 33.

McVicar, T.R., Walker, J., Jupp, D.L.B., Pierce, L.L., Byrne, G.T. and Dallwitz, R. 1996b. Relating AVHRR vegetation indices to in situ leaf area index. Canberra, CSIRO Division of Water Resources, 54.

Mitchell, R.M. 1999. Calibration status of the NOAA AVHRR solar reflectance channels: CalWatch Revision 1. Melbourne, CSIRO Atmospheric Research Technical Paper No. 42,. 20.

Moran, M.S., Rahman, A.F., Washburne, J.C., Goodrich, D.C., Weltz, M.A. and Kustas, W.P. 1996. Combining the Penman-Monteith equation with measurements of surface temperature and reflectance to estimate evaporation rates of semi-arid grassland. Agricultural and Forest Meteorology, 80, 87–109.

Nalder, I.A. and Wein, R.W. 1998. Spatial interpolation of climatic Normals: test of a new method in the Canadian boreal forest. Agricultural and Forest Meteorology, 92, 211–225.

Parton, W.J. and Logan, J.A. 1981. A model for diurnal variation in soil and air temperature. Agricultural Meteorology, 23, 205–216.

Pierce, L.L., Walker, J., Dowling, T.I., McVicar, T.R., Hatton, T.J., Running, S.W. and Coughlan, J.C. 1993. Ecohydrological changes in the Murray–Darling Basin. III. A simulation of regional hydrological changes. Journal of Applied Ecology, 30, 283–294.

Prince, S.D., Goetz, S.J., Dubayah, R.O., Czajkowski, K.P. and Thawley, M. 1998. Inference of surface and air temperature, atmospheric precipitable water and vapor pressure deficit using Advanced Very High-Resolution Radiometer satellite observations: comparison with field observations. Journal of Hydrology, 212, 230–249.

Raupach, M.R., Finkele, K., Briggs, P.B., Cleugh, H.A., Coppin, P.A., Leuning, R. and Graetz, R.D. 1997. Water and carbon dynamics of the Australian biosphere. In: Munro, R.K. and Leslie, L.M., eds, Climate Prediction for Agricultural and Resource Management: Australian Academy of Science Conference, Canberra, 6–8 May 1997. Canberra, Bureau of Resources Sciences, 211–229.

Saunders, R.W. 1990. The determination of broad band surface albedo from AVHRR visible and near-infrared radiances. International Journal of Remote Sensing, 11, 49–67.

Seguin, B., Baelz, S., Monget, J.M. and Petit, V. 1982a. Utilisation de la thermographie IR pour l'estimation de l'evaporation regionale. I: Mise au point methodologique sur le site de la Crau. Agronomie, 2, 7–16.

Seguin, B., Baelz, S., Monget, J.M. and Petit, V. 1982b. Utilisation de la thermographie IR pour l'estimation de l'evaporation regionale. II: Resultats obtenus a partir de donnees de satellite. Agronomie, 2, 113–118.

Stein, A., Staritsky, I.G., Bouma, J., Van Eijsbergen, A.C. and Bgegt, A.K. 1991. Simulation of moisture deficits and areal interpolation by universal cokriging. Water Resources Research, 27, 1963–1973.

Thornton, P.E., Running, S.W. and White, M.A. 1997. Generating surfaces of daily meteorological variables over large regions of complex terrain. Journal of Hydrology, 190, 214–251.

Wan, Z. and Dozier, J. 1996. A generalized split-window algorithm for retrieving land-surface temperature from space. IEEE Transactions on Geoscience and Remote Sensing, 34, 892–905.

Xie, X. 1991. Estimation of daily evapotranspiration (ET) from one-time-of-day remotely sensed canopy temperature. Remote Sensing of Environment (China), 6, 253–260.

Zhang, L., Lemeur, R. and Goutorbe, J.P. 1995. A one-layer resistance model for estimating regional evapotranspiration using remote sensing data. Agricultural and Forest Meteorology, 77, 241–261.

20 Application of a Mean Annual Water Balance Model to the Murray–Darling Basin: Past, Present and Future

Andrew S. Bradford* and Lu Zhang*

Abstract

Catchment water balance is strongly affected by land-use and vegetation characteristics; generally, trees use more water than pasture and crops. As a result, forested catchments yield less stream flow (water yield). In the Murray–Darling Basin (MDB) there are plans to convert large areas of pasture to forestry plantations in the coming decades; a range of commercial and environmental considerations motivates these plans. This chapter describes how a simple water balance model in a geographic information systems (GIS) framework can be used to assess average annual stream flow under different land-use scenarios. The model only requires percentage forest cover of a catchment and mean annual rainfall. The method is well suited for regional-scale assessment of the impacts of change in land use on water yield.

The case study described here is based on average rainfall data for 1980–95, and vegetation cover data under different land-use conditions obtained from the MDB Commission, the Australian Land Information Group (AUSLIG), and CSIRO Forestry and Forest Products. Estimated mean annual catchment water yields agreed well with measured stream flow data for catchments with medium to high rainfall in the MDB but tended to overestimate water yield for low-rainfall catchments. The model showed that clearing native vegetation in the MDB is likely to significantly increase water yield from most of the catchments within the basin. It also predicted that afforestation in the basin may reduce mean annual water yield by up to 40 mm/year.

土地利用方式和植被类别影响流域水量平衡。一般情况下树木比牧草、农作物消耗更多的水分，因而森林覆盖的流域产生的径流较少。出于环境和商业的考虑，计划在未来的几十年里，把默里达令盆地（MDB）的草地大面积改造成林地。本文介绍了一个简单的水量平衡模型在地理信息系统里如何评估不同土地利用方式产生的径流量。该模型只要求输入流域的森林覆盖率

* CSIRO Land and Water, PO Box 1666, Canberra, ACT 2601, Australia. Email: lu.zhang@csiro.au

Bradford, A.S. and Lu Zhang. 2002. Application of a mean annual water balance model to the Murray–Darling Basin: past, present and future. In: McVicar, T.R., Li Rui, Walker, J., Fitzpatrick, R.W. and Liu Changming (eds), *Regional Water and Soil Assessment for Managing Sustainable Agriculture in China and Australia*, ACIAR Monograph No. 84, 277–290.

和年均降雨量，可用于评估区域范围土地利用变化对产水量的影响。

本项研究基于 1980－1995 年的平均降雨量和不同土地利用下的植被覆盖度。对 MDB 里降雨量高或适中的流域所估算的产水量与实测值吻合很好，但对降水少的流域的估算值偏高。该模型显示原始森林的砍伐很可能使得 MDB 多数流域的产水量大增。它也预测 MDB 完成造林后，年均产水量可减少多达 40 毫米。

LAND use in the Murray–Darling Basin (MDB) has undergone massive changes following European settlement. These changes have significantly modified the hydrological regime of the catchment. The replacement of perennial deep-rooted native vegetation with shallow-rooted vegetation such as perennial grasses, annual grasses and crops has resulted in major changes to catchment-wide evapotranspiration and stream flow (Zhang et al. 1999, 2001; Vertessy and Bessard 1999). These changes to the water balance and vegetation have in turn had major effects on the salt balance and stream salinity within the catchments (Jolly et al. 1997, 2001; Natural Heritage Trust 2001).

There are plans to convert large areas of pasture in the MDB to forestry plantations in the coming decades (e.g. Department of Primary Industries and Energy 1997). A range of commercial and environmental considerations, including the management of dryland salinity, motivates these plans. As this paper demonstrates, the spatial distribution of plantations within catchments greatly influences the resulting change in hydrology.

A number of studies have shown that evapotranspiration from a forested catchment is generally greater than that from a grassed catchment with the same climatic conditions (Holmes and Sinclair 1986; Turner 1991; Zhang et al. 2001). Thus, land-use management strategies will impact on catchment water balance. The key factors controlling evapotranspiration include rainfall interception, net radiation, advection, turbulent transport, leaf area and plant available water capacity. The relative importance of these processes is likely to depend on climate, soil and vegetation conditions. Zhang et al. (2001) have developed a simple water balance model to assess impacts of land-use changes, which requires only vegetation, annual total streamflow and rainfall data. The model agreed with independent water balance estimates from more than 250 catchments. This paper describes how the model was used within a GIS framework to estimate catchment water yield under different vegetation conditions in the MDB.

Mean Annual Water Balance Model

Zhang et al. (2001) developed the catchment balance model used in this study, based on an examination of annual rainfall and evapotranspiration relationships. It is assumed that, under very dry conditions, potential evapotranspiration exceeds precipitation and actual evapotranspiration equals precipitation; under very wet conditions, water availability exceeds potential evapotranspiration and actual evapotranspiration equals potential evapotranspiration. Based on these assumptions, mean annual evapotranspiration (*ET*)

can be calculated from mean annual rainfall (P) and potential evapotranspiration (E_0):

$$ET = P\left\{\frac{1+w\left(\frac{E_0}{P}\right)}{1+w\left(\frac{E_0}{P}\right)+\left(\frac{E_0}{P}\right)^{-1}}\right\} \quad (1)$$

where w is the plant available water coefficient.

Following Eagleson (1982), we assumed that mean annual evapotranspiration from a catchment is the sum of the evapotranspiration from herbaceous vegetation ($ET_{nonforest}$) (including soil evaporation) and from forest (ET_{forest}), weighted linearly according to their percentage areas. The general equation can be expressed as:

$$ET_{total} = f \times ET_{forest} + 1(1-f) \times ET_{nonforest} \quad (2)$$

where f is percentage area of a catchment forested. The nonforest part of a catchment could be further divided into woodland and grasses if such data were available.

To simplify the calculation, the parameters in Equation 1 were established for forested and nonforested catchments:

$$ET_{forest} = \left\{\frac{1+2.0\times\frac{1410}{P}}{1+2.0\times\frac{1410}{P}+\frac{P}{1410}}\right\}\times P \quad (3)$$

$$ET_{nonforest} = \left\{\frac{1+0.5\times\frac{1100}{P}}{1+0.5\times\frac{1100}{P}+\frac{P}{1100}}\right\}\times P \quad (4)$$

These relationships are shown in Figure 1, together with observed evapotranspiration from the catchments listed in Zhang et al. (1999). The size of these catchments varied from less than 1 km^2 to 6×10^5 km^2, and they span a variety of climates. The vegetation varies from same-aged plantation trees to native woodlands, open forest, rainforest, eucalypt forest, native and managed grassland, and agricultural cropping.

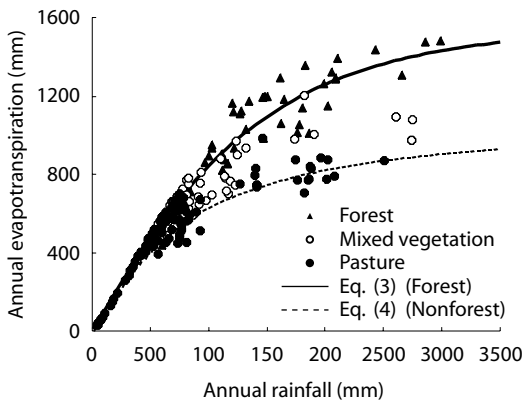

Figure 1. Relationships between annual evapotranspiration and rainfall (Zhang et al. 1999).

It is clear from Figure 1 that most of the forested catchments plot within the upper curve described by Equation 3, nonforested catchments plot around the lower curve described by Equation 4 and mixed vegetation catchments plot in the middle. The relationships described by Equations 3 and 4 are very similar to the empirical curves proposed by Holmes and Sinclair (1986) for catchments in Victoria.

Assuming that the change in catchment water storage over a long period is zero, catchment average water yield is calculated as the difference between long-term average rainfall and evapotranspiration. Figure 2 shows the resulting relationship between water yield and rainfall.

Case Studies

Estimation of the impact of land-use changes on catchment water yield for the main drainage divisions within the MDB (Fig. 3) required spatial data sets of rainfall, catchment boundaries and forest cover. We considered three land-use scenarios—pre-European vegetation, current vegetation and potential future forest plantation. We describe the sourcing and manipulation of these data, which were obtained from various government agencies and

captured for different purposes, and the methods and procedures used to estimate catchment area rainfall and percentage forest cover from these data.

We characterised forest cover for a given catchment using pre-European, current and potential future plantation forest areas of different temporal and spatial scales. Problems associated with initial vegetation classification were overcome by reclassifying the data into two main categories. This process allowed us to compare past, present and potential future vegetation coverage. We wrote ArcInfo programs (ARC macro languages; AMLs) to automate the resampling, the reprojecting of data and the model itself.

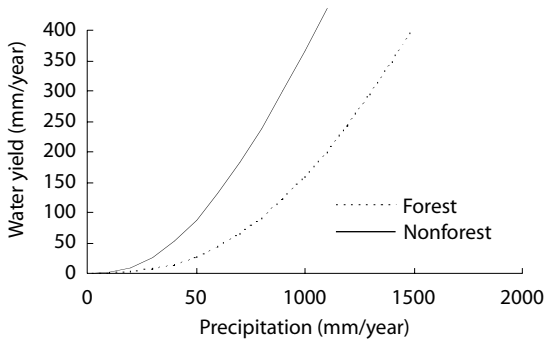

Figure 2. Relationship between catchment water yield and rainfall.

Rainfall surface

Monthly interpolated rainfall surfaces were combined to give a mean annual rainfall surface for 1980–95. Each grid cell is 0.05°, or approximately 25 km^2 (Jolly et al. 1997). The grid point analysis technique used to derive surfaces provides an objective average for each grid cell and useful estimates of rainfall in data-sparse areas. However, in data-rich areas such as southeast Australia or in regions with a strong rainfall gradient, 'data smoothing' will occur, resulting in values at point locations which may differ slightly from the exact rainfall recorded. Figure 4 shows the range and spatial distribution of long-term mean annual rainfall across the MDB.

Catchment boundaries

This project is based on 26 drainage divisions of the MDB with catchments ranging in size from 700 km^2 to 130,000 km^2 (Fig. 5). These catchment boundaries were taken from a previous salt load study (Jolly et al. 1997), which delineated catchments using a watershed analysis. Table 1 lists catchment areas and mean annual rainfall.

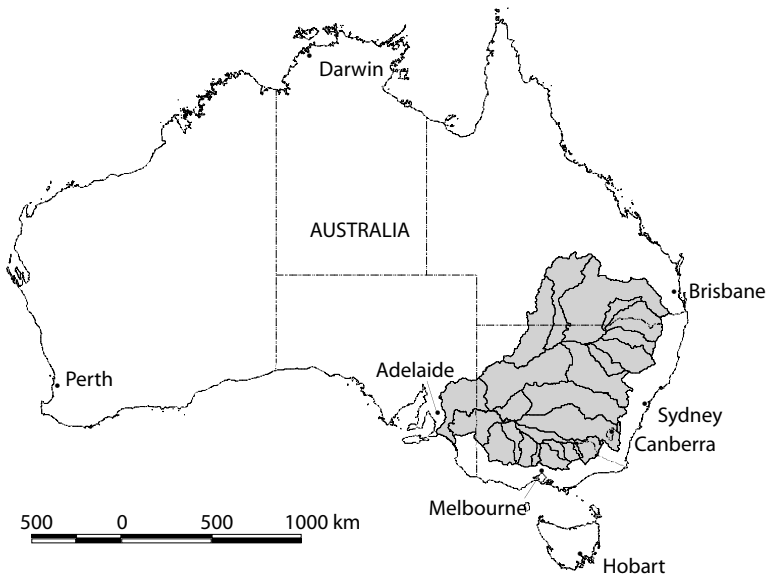

Figure 3. Location of the Murray–Darling Basin (grey area).

M305 vegetation dataset

The m305 multistructured vegetation data set contains attributes characterising land cover and vegetation (Ritman 1995). This study focuses on the woody vegetation component of the land cover class. The woody vegetation was mapped from Landsat Thematic mapper (TM) imagery at a 30 m ground resolution with six bands per scene from as many cloud-free days as possible. Between late 1989 and 1991, images were chosen to maximise the

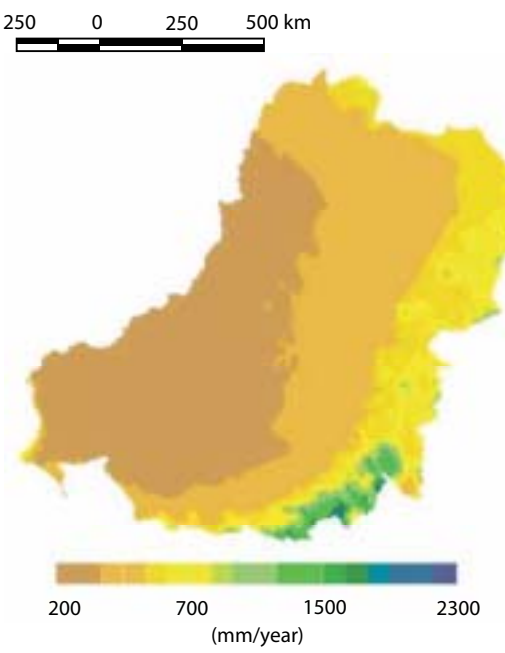

Figure 4. Distribution of mean annual rainfall throughout the Murray–Darling Basin.

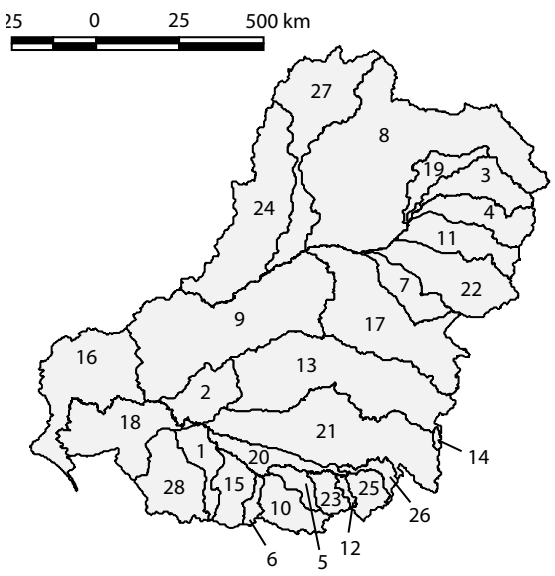

Figure 5. Location of the main drainage divisions within the Murray–Darling Basin (Jolly et al. 1997).

Table 1. Catchment area and mean annual rainfall for the 26 catchments within the Murray–Darling Basin.

ID No.	Catchments	Mean annual rainfall (mm)	Area (km^2)
1	Warrego River	408	62,940
2	Condamine-Culgoa	482	162,597
3	Paroo River	281	73,953
4	Moonie River	519	14,342
5	Border Rivers	621	48,041
6	Gwydir	620	26,586
7	Namoi	617	42,000
8	Macquarie	523	74,792
9	Darling River	295	112,832
10	Castlereagh River	537	17,423
11	Lower Murray	281	58,274
12	Lachlan River	470	90,880
13	Benanee	291	21,345
14	Murrumbidgee River	556	81,643
15	Mallee	301	41,488
16	Avoca River	365	14,201
17	Lake George	701	942
18	Wimmera-Avon	405	30,367
19	Murray–Riverina	395	15,039
20	Loddon River	461	15,655
21	Upper Murray River	1,105	15,342
22	Broken River	593	7,099
23	Ovens River	992	7,981
24	Goulburn	829	16,857
25	Campaspe River	590	4,048
26	Kiewa	1,190	1,912

number of cloud-free days. The imagery was initially resampled from 30 m to 25 m. An unsupervised classification into 100 classes was performed on the imagery to derive the woody vegetation. Each map sheet required resampling from 25 m to 250 m because the final mosaic grid would otherwise have been too data intensive. The resulting woody vegetation layer was filtered to minimum clusters of 0.25 ha. Woody vegetation is represented as land cover class 7 and defined as vegetation that has 20% crown cover and is over 2 m in height. A consolidated grid surface was created from the 472 1:100,000 scale map sheets and each map sheet was reprojected from the Australian map grid (AMG) to latitudes and longitudes. New South Wales, Queensland and Victoria had three AMG zones and South Australia had one. The Albers equal area coordinate system (Ritman 1995) is recommended for the basin-wide area statements. However, the model framework discussed does not require any absolute measured areas; it needs only the proportion of catchment under forest.

Carnahan pre-European vegetation data

The Carnahan pre-European settlement vegetation mapping is stored as a 1:5,000,000 scale map covering all of Australia in a geographic projection. The polygon coverage is based on the AUSLIG present vegetation that was created from Landsat multispectral scanner (MSS) imagery at the 1:1,000,000 scale between 1980 and 1985. We derived the pre-European vegetation by modifying current vegetation polygons using historical information, including the diaries of explorers and camel drivers, and soil and vegetation reports that date to the latter part of the nineteenth century. The Carnahan source data are an estimation of what vegetation could have existed prior to European settlement.

The classification attributes of the 1980–85 data were carried across to the Carnahan data set. It was therefore possible to compare the AUSLIG base vegetation data set (1980–85 MSS data) and m305 vegetation data set. Although there are large differences between the spatial scale of the current m305 and the Carnahan pre-European vegetation data sets, the Carnahan data is the best that is available at this time. From a temporal perspective, the AUSLIG current vegetation coverage (1980–85) and the m305 vegetation data set (1989–91) are comparable. The comparison was undertaken to set classification rules for the polygon attributes when compared to the tree areas of the m305. Finally, these rules were transferred to the Carnahan pre-European data set to model a possible scenario. Three attribute fields were analysed from the current AUSLIG vegetation data set: 'tallest stratum', 'density' and 'species growth form'.

Vegetation density foliage cover is expressed in terms of the proportion of the ground that is shaded by the tallest stratum at midday (McDonald et al. 1990). The AUSLIG vegetation data set expresses this in four classes, from < 10% to > 70%. Class 1 is 0–10% (crowns well separated), class 2 is 10–30% (crowns clearly separated), class 3 is 30–70% (crowns touching or slightly separated) and class 4 is 70% or greater (crowns touching to overlapping). The density of foliage cover of the lower stratum is not recorded in the code.

We chose classes 2 to 4 from the foliage cover attribute field. Classes 2 and 3 contain the greatest source of potential error of commission because they cover a broad range of vegetation types and are therefore difficult to compare with the 20% crown cover of the m305 data set. Foliage density was the first class to be investigated, so class 2 was included on the grounds that vegetation height and species would sufficiently discriminate the tree areas for comparison with the m305 vegetation cover. Moreover, when class 2 was omitted, significant areas that were considered 'tree' by the m305 data set were not accounted for. In short, more class 2 was considered as 'tree' than as 'no tree' when comparing to the woody m305 data set.

Species growth form is primarily classified into three vegetation groups: grasses, shrubs and trees.

These three groups are further broken down by vegetation height. Grasses and shrubs less than 2 m high were considered to be nonwoody vegetation and were excluded from the classification because they did not fit the m305 woody vegetation criteria. Table 2 shows which classes were chosen from the AUSLIG present vegetation classes and used in the analysis of the Carnahan pre-European vegetation. Figure 6 shows how the comparison is represented spatially between the two vegetation data sets based on the rules in Table 2.

The tallest stratum is defined as the uppermost stratum in which most of the incoming solar radiation is intercepted (McDonald et al. 1990).

Table 2. The rules used in the vegetation classification of forest for the AUSLIG vegetation data sets.

Rule	Class	Vegetation type
1	Tallest stratum (TS_SD)	Eucalyptus Conifers
2	Density (TS_D)	10–30% 30–70% 70% >
3	Species growth form (GF)	Low trees < 10 m (L) Medium trees 10–30 m (M) Tall shrubs > 2 m (S) Tall trees > 30 m (T)

When the data were tested, the tallest stratum data field was tested against the m305 vegetation data set. Conifers and eucalyptus were found to have the best correlation with the woody component of the m305 data set.

We generated a new grid by merging the m305 vegetation data set and the AUSLIG 'present vegetation' cover. With such estimations, there is a chance that errors of omission from the original data will occur. The correlation matrix shown in Table 3 illustrates an 8% error of omission where m305 has forest present and AUSLIG 'present vegetation' does not, and an 8% error of commission where m305 has no forest present and AUSLIG 'present vegetation' shows forest. This comparison is encouraging, particularly because the m305 vegetation data set was generated from a classification on a cell-by-cell basis and the AUSLIG vegetation is a polygon data set of grouped like-vegetation classes.

Table 3. Correlation matrix of the m305 vegetation data set and the AUSLIG present vegetation data set with regard to tree and no-tree areas.

		AUSLIG present	
		No tree	Tree
m305	No tree	72%	8%
	Tree	8%	12%

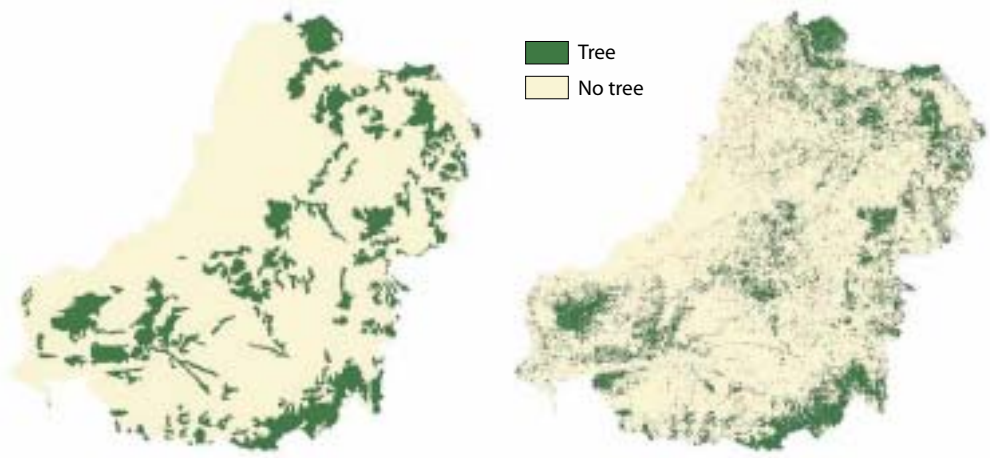

Figure 6. M305 vegetation and AUSLIG present vegetation shown as tree and no tree.

The rules described in Table 2 were applied to the Carnahan vegetation data set. Figure 7 shows the final classified Carnahan pre-European vegetation data set of tree and no tree.

Potential afforestation data

The potential afforestation data set was designed to predict areas suitable for hardwood plantation timbers across Australia. The main source data set used in this analysis considered the environmental factors that favour plantation hardwoods, including precipitation, topography, soils, pests and diseases (Booth and Jovanovic 1991). The potential forest plantation data set involved only the transformation of points to grids and reprojection from AMG coordinates to geographic coordinates. The cell size was 0.05° in latitude and longitude (approximately 25 km^2). The resolution was chosen on the basis of the complexity of the analysis, storage requirements and the similarly coarse resolution of other data sets used in the suitability analysis. The attributes of the point data set were carried across to the grid surface. All areas suitable for plantation (i.e. low, medium or high suitability) were considered as the potential afforestation areas (Fig. 8); this represents the total areas currently under forest and the areas that can be reforested.

Results and Discussion

Catchment water yield under current vegetation conditions

The m305 woody vegetation data set of the MDB provides a coherent data set across the basin. Evapotranspiration from each catchment was calculated by combining the vegetation data with the annual rainfall data. In order to compare the results with stream flow measurements, catchment water yield was obtained by subtracting evapotranspiration from rainfall. Figure 9 shows estimates of the catchment water yield in relation to rainfall for all 26 catchments. The calculated catchment-scale water yields ranged from 14 to 335 mm/year, and were within the mean annual water yield relationships defined by Equations 3 and 4. It is clear from Figure 9 that the difference in catchment water yield between forested and nonforested catchments is small (up to 700 mm/year). However, the difference becomes larger as rainfall increases, suggesting that changes in vegetation cover will have a relatively large impact on catchment water yield in high-rainfall areas. This is an important relationship because areas of high rainfall are of great importance for water supply and stream salinity dilution.

Figure 7. Classified tree/no tree data from the Carnahan pre-European vegetation data set.

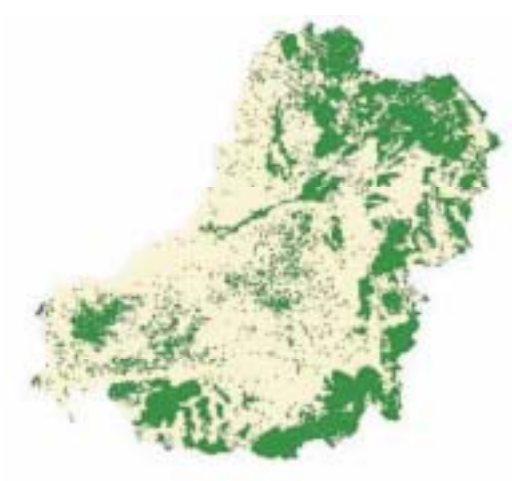

Figure 8. Potential plantation areas and the m305 vegetation data set combined.

Figure 10 shows the modelled catchment-scale water yields compared with long-term stream flow measurements reported by the Department of Natural Resources (1976) and Jolly et al. (1997). The best-fit slope through the origin was 1.03 and the model estimates were statistically consistent with the measurements. However, there were relatively large scatters in the results, and the model tended to overestimate water yield in low-rainfall catchments. When expressed as a percentage of mean annual rainfall, the error in the estimated water yield ranged between 16% and –5%.

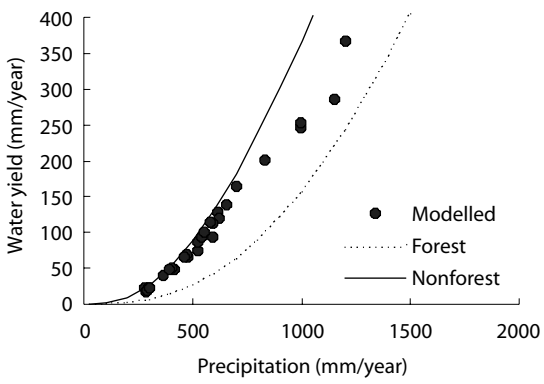

Figure 9. Estimates of water yield under current vegetation cover for the 26 catchments in the Murray–Darling Basin.

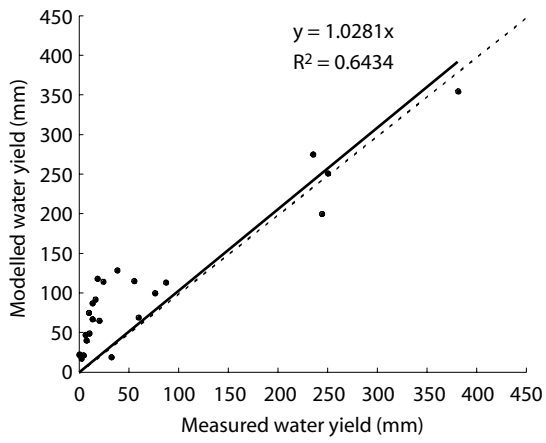

Figure 10. Comparison of calculated and measured catchment water yield for the major catchments in the Murray–Darling Basin. The dashed line is the 1:1 line and the solid line the regression line.

A number of factors could have contributed to the errors in the results. First, estimates of percentage forest cover could affect evapotranspiration modelled by Equation 3. In low rainfall catchments, average percentage forest cover was a small fraction of the total catchment area and some open woodlands were classified as nonforests. This would result in underestimates of evapotranspiration or overestimates of water yield. Second, rainfall distribution could also affect estimates of evapotranspiration and hence water yield. By using mean annual rainfall, the model is likely to underestimate evapotranspiration in catchments with summer dominant rainfall. Examination of the results shows that the model underestimated evapotranspiration in catchments such as Condamine–Culgoa, Moonie and Namoi. Rainfall in these catchments is summer dominant, with 35% of rain falling from December to February. The results from the model can be improved by introducing a seasonality index; this will be investigated in a future study. Finally, diversion of water occurs in many of the catchments in the MDB and it is extremely difficult to account for the effects of diversions on stream flow measurements. This shortcoming will also be investigated in a future study.

The estimated catchment water yields show significant spatial variation (Fig. 11). In the Benanee and Lower Murray catchments, mean annual water yield was less than 20 mm per year; in the eastern catchments, such as the Ovens and Upper Murray catchments, mean annual water yield was above 250 mm per year.

Catchment water yield under pre-European vegetation conditions

We used the model to try to evaluate the effect of clearing native vegetation on mean annual water yield based on current and pre-European vegetation data. Catchment water yields under pre-European vegetation conditions were calculated from the Carnahan pre-European vegetation data

set. We assumed that mean annual precipitation during that time was the same as the mean annual rainfall for the period 1980–95. The results are shown in Figure 12. The large-scale AUSLIG data set estimated average forest cover as 69% before European settlement. This value is significantly higher than the current forest cover of 20%, taken from the m305 woody vegetation data set. Table 4 illustrates the loss in forest cover for each catchment, using the above data set. As a result of loss of vegetation, estimated water yield under pre-European vegetation conditions was consistently lower than that under current vegetation conditions (Figs 9 and 12). Water yield increased from 0 to 80 mm/year with the most significant changes occurring in the catchments east of the Darling River (Fig. 13). On average, estimated water yield in the MDB has increased from 46 to 69 mm/year.

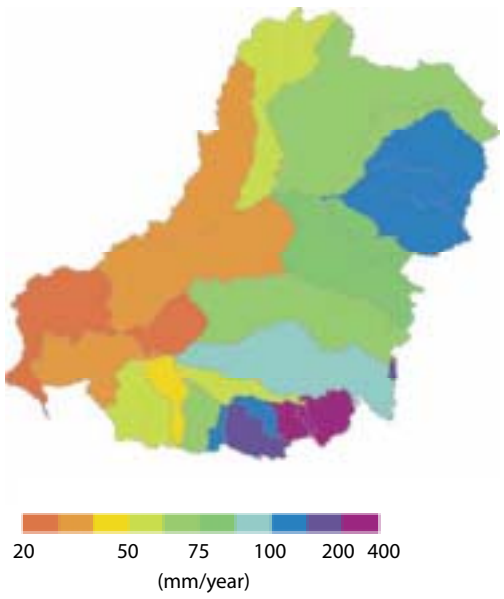

Figure 11. Predicted mean annual water yield distribution across the Murray–Darling Basin under current vegetation cover.

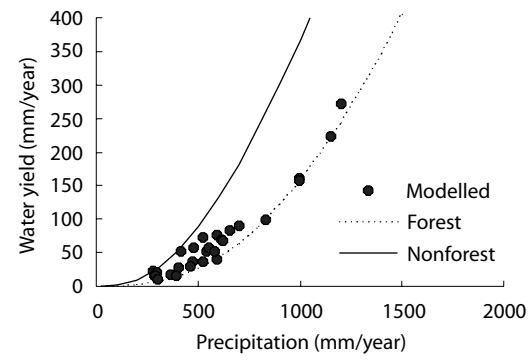

Figure 12. Catchment water yield under pre-European vegetation conditions.

These results are indicative only and may not represent the actual water yield under pre-European vegetation conditions. However, they provide some estimates of likely changes in catchment water yields resulting from the clearing of native vegetation. There are no gauged stream flow data under pre-European vegetation conditions; the only descriptive information available is written records left by explorers, travellers and settlers. Their view of streams, based on European experience, may be subjective but it provides a qualitative picture of the streams under pre-European conditions. For example, in the Upper Murrumbidgee, 'It seems the small streams of the catchment were swampy at the time of European exploration, and many were chains-of-ponds.' (Starr et al. 1999). This information suggests that stream flow under pre-European vegetation conditions would be less than the current stream flow.

Impact of potential afforestation on catchment water yield

Increased groundwater recharge has been identified as a major factor causing dryland salinity in the MDB. A number of land management options have been considered to reduce groundwater recharge; one is forest plantations. Forest can use more water than pasture and hence reduce recharge to groundwater systems. Afforestation can also affect water yield (Vertessy and Bessard 1999). A forest plantation capability scenario was mapped for the purpose of investigating potential commercially viable plantation areas (Booth and Jovanovic 1991). Plantation areas in the MDB were calculated from numerous factors, one of which was the absence of existing forests, which meant that a future scenario of

forested areas could only be estimated by combining the potential afforested areas with the m305 vegetation data set. The vegetation scenario was based on the potential implementation of eucalyptus, acacia and pine as commercial plantations. Table 5 lists the criteria on which each species was chosen.

Table 4 illustrates the potential rise in forest cover given full adoption of potential plantation areas. There is opportunity for a significant increase in plantation area in some catchments — such as Condamine–Culgoa Rivers, Moonie River, Border Rivers, Goulburn River, and Wimmera–Avon

Table 4. Current forest cover compared to pre-European forest cover and potential plantation forest cover for the 26 catchments of the Murray–Darling Basin.

Catchment	Current forest (%)	Pre-European forest (%)	Decrease (%)	Potential plantation (%)	Increase (%)
Warrego River	21	21	0	38	17
Condamine-Culgoa	25	40	15	55	30
Paroo River	4	4	0	7	3
Moonie River	31	34	2	70	36
Border Rivers	29	64	35	49	19
Gwydir	14	75	61	32	18
Namoi	24	78	54	38	14
Macquarie	16	88	72	29	13
Darling River	13	23	10	13	0
Castlereagh	16	72	56	37	21
Lower Murray	28	39	12	29	1
Lachlan River	14	71	57	21	7
Benanee	27	48	21	27	0
Murrumbidgee	16	70	54	26	10
Mallee	23	80	57	24	1
Avoca River	8	76	69	46	39
Lake George	17	76	59	36	19
Wimmera–Avon	13	66	53	53	40
Murray–Riverina	10	92	83	14	4
Loddon River	16	84	68	46	30
Upper Murray	69	99	30	85	16
Broken River	18	100	82	24	7
Ovens River	54	99	45	65	11
Goulburn	36	100	64	61	25
Campaspe	15	86	71	20	6
Kiewa	56	89	33	69	13

Rivers. Such plantations would increase catchment evapotranspiration and hence reduce water yield (Fig. 14).

Figure 15 shows changes in water yield from the current vegetation and the potential plantation for all catchments. The southeastern catchments of the MDB would have a low to moderate change in water yield as a result of the afforestation; the catchments at the headwaters of the Murray River, where annual rainfall is relatively high, would experience a reduction in water yield of 20–40 mm/year. Minimal changes in water yield would occur in other catchments that are not considered to be suited for sustainable plantations. Although these changes are not as dramatic as those under the pre-European vegetation conditions, they may have significant impacts on water supply and salinity

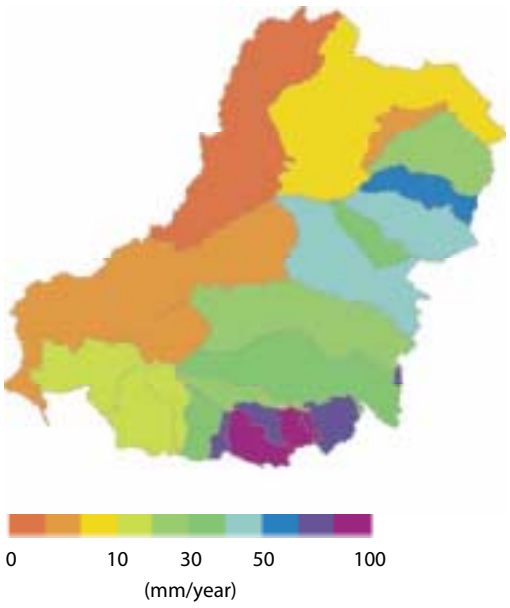

Figure 13. Increase in water yield from pre-European vegetation cover to current vegetation cover.

Table 5. Criteria for the selection of suitable forest plantation areas by species.

Species	Mean rainfall (mm/year)	Rainfall regime	Dry season length (months)	Mean max temp (°C)	Mean min temp (°C)	Mean annual temp (°C)	Soil
Eucalyptus globulus	600–1500	Winter/ uniform	0–5	19–30	2–12	9–18	Fertile loams
Eucalyptus grandis	800–2500	Summer	0–5	25–34	3–16	14–25	Alluvial, volcanic
Eucalyptus nitens	750–1500	All	0–4	20–28	–3–5	7–14	Granite, basalt
Eucalyptus pilularis	750–2000	Summer/ uniform	0–2	22–31	5–12	15–22	Sandy loams
Eucalyptus regnans	900–2000	Winter/ uniform	0–3	17–27	–2–6	7–14	Deep moist
Eucalyptus saligna	700–1800	Uniform/ summer	0–5	22–32	1–14	14–21	Sandy loams
Acacia mangium	1150–3700	Summer	0–5	29–33	12–30	23–28	Acid volcanic
Acacia mearnsii	800–1600	Uniform				16–20	Sands, loams
Acacia melanoxylon	480–2950			19–34	–3–16	9–25	Volcanic soils
Pinus elliottii	750–1700	Summer	0–5	26.5–31	5–12.5	18–23	Phosphorus soils
Pinus radiata	650–1600	Winter/ uniform	0–4	20–30	–2–12	11–18	Mixed

Source: Booth and Jovanovic (1991).

control. Vertessy and Bessard (1999) applied a similar relationship — developed by Holmes and Sinclair (1986) — to the Murrumbidgee catchment and concluded that afforestation in the catchment may significantly reduce mean annual runoff. Reduction in water yield not only imposes costs on users downstream but also affects stream salinity dilution. An important issue is the tradeoff between recharge control and water yield reduction, as these are likely to vary with rainfall. Such information can help us to make responsible management decisions about land-use changes in the MDB.

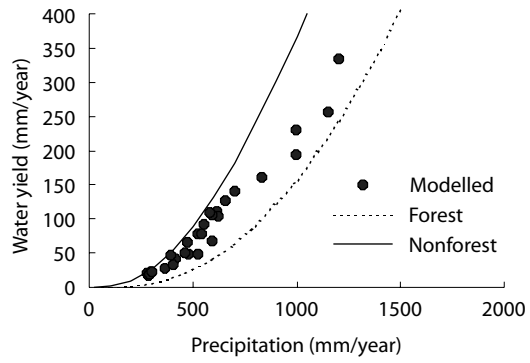

Figure 14. Estimates of water yield under the potential afforestation scenario.

Figure 15. Change in water yield from current vegetation to potential afforested areas.

Conclusions

This chapter demonstrates how the simple water balance model developed by Zhang et al. (2001) can be used in a GIS framework to estimate the impacts of vegetation changes on mean annual average water yield in a catchment. The model considers the effects of available energy and water on evapotranspiration and requires only mean annual rainfall and vegetation-cover measurements. Comparison between predicted and measured water yield under current land-use conditions agreed reasonably well for catchments with high rainfall; however, the model tended to overestimate water yield for low-rainfall catchments. The model may be improved by introducing a rainfall seasonality index and this will be further investigated. To evaluate the impact of clearing of the native vegetation in the MDB, we estimated water yield under pre-European vegetation conditions. The results showed significant reduction in water yield from most of the catchments within the basin. Although there are no direct stream flow data with which to compare these estimates, some descriptive information seems to indicate that there would be less runoff under pre-European vegetation conditions from the basin. We also attempted to evaluate the impact of afforestation on future catchment water yields and our analysis suggests that broad-scale afforestation in the basin may reduce mean annual water yield by up to 40 mm/year. This may be desirable from a point of view of recharge reduction but its impact on downstream water supply needs to be considered.

Large-scale afforestation affects not only mean annual stream flow, but also flow regime. Results from some paired catchment studies have shown significant changes in flow regime following clearing of forests (Burch et al. 1987; Jones 2000). Further studies are necessary to model these hydrological responses in large catchments.

Acknowledgments

This study was supported by a Land and Water Australia through the National Dryland Salinity Program grant 'Predicting the Combined Environmental Impact of Catchment Management Regimes on Dryland Salinity' (CLW29), the Cooperative Research Centre for Catchment Hydrology and ACIAR (LWR 1/95/07). We gratefully acknowledge the Murray–Darling Basin Commission, the Australian Land and Information Group and the CSIRO Division of Forestry for providing data for this study. Dr Kim Ritman, Environmental Systems Research Institute (ESRI) Defence, Dr Tim McVicar and Susan Cuddy, CSIRO Land and Water assisted with review and structure of this chapter and we thank them for their contribution.

References

Booth, T.H. and Jovanovic, T. 1991. Identification of Land Capable of Private Plantation Development. Report of the National Plantations Advisory Committee. Canberra, Department of Primary Industries and Energy, Appendix B, 1–86.

Burch, G.J., Bath, R.K., Moore, I.D. and O'Loughlin, E.M. 1987. Comparative hydrological behaviour of forested and cleared catchments in southeastern Australia. Journal of Hydrology, 90, 19–42.

Department of Natural Resources 1976. Review of Australia's Water Resources (1975). Canberra, Australian Government Publishing Service.

Department of Primary Industries and Energy (DPIE) 1997. The 2020 Vision Statement. Canberra, ACT, DPIE.

Eagleson, P.S. 1982. Ecological optimality in water-limited natural soil vegetation systems. 1. Theory and Hypothesis. Water Resources Research, 18, 325–340.

Holmes, J.W. and Sinclair, J.A. 1986. Water Yield from Some Afforested Catchments in Victoria.

Jolly, I.D., Dowling, T.I, Zhang, L, Williamson, D.R. and Walker, G.R. 1997. Water and Salt Balances of the Catchments of the Murray–Darling Basin. Adelaide, CSIRO Land and Water Technical Report 37/97.

Jolly I.D., Williamson D.R., Gilfedder M., Walker G.R., Morton R., Robinson G., Jones H., Zhang L., Dowling T.I., Dyce P., Nathan R.J., Nandakumar N., Clarke R., and McNeill V. 2001. Historical stream salinity trends and catchment salt balances in the Murray–Darling Basin, Australia. Marine and Freshwater Research, 52 (1): 53-63.

Jones, J.A. 2000. Hydrologic processes and peak discharge response to forest removal, regrowth, and roads in 10 small experimental basin, western Cascades, Oregon. Water Resources Research, 36, 2621–2642.

McDonald, R.C., Isbell, R.F., Speight, J.G., Walker, J. and Hopkins, M.S. 1990. Australian Soil and Land Survey Field Handbook, 2nd edition.

Natural Heritage Trust. 2001. Australian Dryland Salinity Assessment 2000. National Land and Water Resources Audit, Land and Water Australia, Canberra ACT.

Ritman, K.T. 1995. Structural Vegetation Data: a specification manual for the Murray Darling Basin Project M305.

Starr, B.J. 1999. The catchment at the time of European settlement. In: Wasson, R.J. and Caitcheaon, G., eds, Soil Erosion, Phosphorous and Dryland Salinity in the Upper Murrumbidgee: Past Change and Current Findings.

Turner, K.M. 1991. Annual evapotranspiration of native vegetation in a Mediterranean-type climate. Water Resources Bulletin, 27, 1–6.

Vertessy, R.A. and Bessard, Y. 1999. Anticipating the Negative Hydrologic Effect of Plantation Expansion: Results From a GIS-Based Analysis on the Murrumbidgee Basin.

Zhang, L., Dawes, W.R. and Walker, G.R. 1999. Predicting the Effect of Vegetation Changes on the Catchment Average Water Balance. CSIRO Land and Water Tech Report 99/12.

Zhang, L., Dawes, W.R. and Walker, G.R. 2001. The response of mean annual evapotranspiration to vegetation changes at catchment scale. Water Resources Research, 37, 701–708.

21

Land Degradation Assessment in the Mount Lofty Ranges: Upscaling from Points to Regions via a Toposequence

Phil J. Davies,* Rob W. Fitzpatrick,* David A. Bruce,†
Leonie R. Spouncer* and Richard H. Merry*

Abstract

Natural resource assessment at regional scales is often time consuming, expensive and reliant upon the local knowledge and judgment of the surveyor. In this chapter we describe the development of an efficient method to assess land degradation (specifically waterlogging and saline and acid soils) at a regional scale. We developed spatial models by integrating knowledge of landscape processes with remotely sensed, terrain and field data, within a geographic information system (GIS). The key to this approach was the linkage of soil and hydrological processes (identified at the point scale) to mapped soil units via toposequences, and the allocation of land degradation classes to each of the units. The data were aggregated to catchment and regional scale to produce maps of land degradation. The results obtained from the modelling were validated by random ground assessments of sites across the region. The method described here could be applied to the assessment of other types of land degradation, and to other regions with comparable landscapes and vegetative covers, where similar soils, terrain and remotely sensed data exist.

区域尺度的自然资源评价既费时又耗资，常常不现实，而且也依赖于评估人员的知识水平、对该地区的了解程度和个人判断能力。本研究提出了评估土地退化（尤其是酸化、盐碱化和渍涝状况）更有效方法，给研究区劳伏特山地各流域的健康状态排名。我们将景观信息、遥感数据、野外数据与地理信息系统相结合，开发出空间模型。该方法的关键在于由布点测量的土壤和水文数据，推算坡面数据，与土壤地图单元联系，确定各单元土壤退化程度。将这些数据再汇总得到流域和区域范围的土地退化图。模型给出的结果

* CSIRO Land and Water, PMB 2, Glen Osmond, SA 5064, Australia. Email: phil.davies@csiro.au
† University of South Australia, GPO Box 2471, Adelaide, SA 5001, Australia.

Davies, P.J., Fitzpatrick, R.W., Bruce, D.A., Spouncer, L.R. and Merry, R.H. 2002. Land degradation assessment in the Mount Lofty Ranges: upscaling from points to regions via a toposequence. In: McVicar, T.R., Li Rui, Walker, J., Fitzpatrick, R.W. and Liu Changming (eds), *Regional Water and Soil Assessment for Managing Sustainable Agriculture in China and Australia*, ACIAR Monograph No. 84, 291–303.

和在整个地区野外随机检验结果一致。该方法可评估其他不同形式的土地退化，也可以应用到那些具有相似的景观和植被覆盖、存在类似的土壤地形和遥感数据的地区。

IN THE high-rainfall catchments of the Mount Lofty Ranges, South Australia, land degradation and poor quality of stream water contribute to losses in farm production and to off-site environmental impacts. The replacement of native vegetation by pastures and cereals that use less water has led to the development of salinity throughout the southern Australian agricultural zone. This change in land use increases the amount of water recharging to deeper groundwaters, which then rise and mobilise salt stored in soil profiles. The extent of waterlogged saline scalds is increasing. Such scalds are an early indicator of the formation of saline, structureless soils that are prone to water erosion. This land degradation has serious potential impacts on the supply and quality of Adelaide's drinking water, because the region contributes approximately 50–60% of the city's total supply.

There is no consistent method for assessing waterlogging and soil acidification or alkalinisation in catchments at regional scale. Organisations or individuals assessing land degradation have developed techniques and expertise best suited to the particular task, adopting methods that are subjective, not clearly defined and often only applied to one particular type of land degradation. This lack of consistency is a major obstacle to the reliable assessment of degradation caused, for example, by poor drainage, salinity and erosion.

Our aim was to develop appropriate methods for assessing potential land degradation at the regional level, by upscaling data from point to catchment scale and using it for spatial modelling in a geographic information system (GIS).

Study Area

The region studied is centred east of the township of Mount Torrens in the Mount Lofty Ranges of South Australia and is approximately 80 km^2 in extent (Fig. 1). The climate is Mediterranean and representative of the eastern Mount Lofty Ranges, with a mean annual rainfall of 680 mm and a mean annual evaporation of 1170 mm. The generalised topography of the area consists of valley floors surrounded by rolling hills, with Mount Torrens lying to the west and a major faultline range defining the eastern extent of the area. A regional northeast to southwest topographic high, east of Mount Torrens township, bisects the area. Catchments to the west of this high drain into the Onkaparinga and Torrens catchment systems; catchments to the east of it form part of the Murray–Darling Basin catchment system. The topographic morphology of the area is strongly related to the underlying geology of near vertical dipping, north–south trending lineament features associated with Precambrian and Cambrian metamorphic formations.

Soils of the area are typical of the eastern Mount Lofty Ranges, being mostly Xeralfs (Soil Survey Staff 1998), formed from strongly weathered micaceous sandstones and schists of the underlying metasediments. These soils are characterised by abrupt textural boundaries between sandy and loamy textured surface horizons (A and E horizons) and clayey subsurface horizons (B horizons) with mottled and/or sodic properties. The land cover of the area is predominantly pasture, most native tree vegetation having been cleared by the end of the

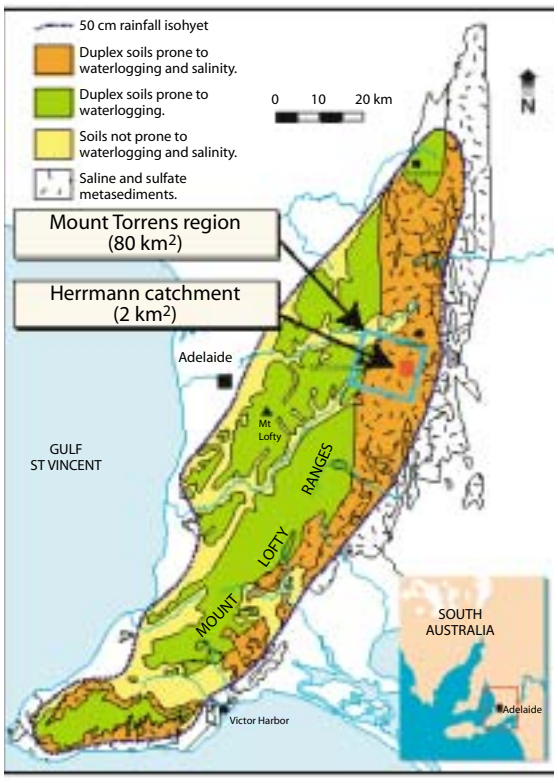

Figure 1. The Mount Torrens study area.

1800s. The remaining areas of remnant vegetation are associated mainly with topographic high points, roadways and watercourses.

To facilitate the process of upscaling, we selected a number of areas within the region for which data on soil, landscape, water quality and remote sensing were available. Detailed information on these studies is reported by Fritsch and Fitzpatrick (1994), Bruce (1996), Cox et al. (1996), Fitzpatrick et al. (1996) and Davies et al. (1998).

Scales and Nature of the Data

This chapter lists and briefly describes some of the various data sets that were used in the analysis. Table 1 summarises the data sets used at each of the various scales within the 80 km^2 regional area. A more comprehensive discussion of these data and how they were derived can be found in Fitzpatrick et al. (1999).

Herrmann toposequence (~400 m) and key area (~0.2 km^2)

Measurements were taken at strategic soil sample points along a 400 m long toposequence within a 0.2 km^2 key area. They include:

- soil morphology, chemistry and mineralogy
- topography (landform)
- vegetation
- hydrology (perched and groundwater fluctuations)
- geomorphology
- multitemporal aerial photography
- airborne thermal infrared (IR) video.

Herrmann catchment (~2.0 km^2)

- 1:5000 scale soil survey mapping
- soil pH measurements
- grid digital elevation model (DEM) and derived topographic index
- airborne synthetic aperture radar (SAR) and derived soil dielectric constant
- airborne thermal IR video
- Landsat Thematic mapper
- airphoto-derived vegetation index
- EM31 derived apparent electrical conductivity (ECa) and discharge index.

Mount Torrens region (~80 km^2)

- 1:50,000 scale landscape unit (SLU) mapping and derived aquic index
- 1:50,000 SLU derived acidity classes
- 1:50,000 scale geology and derived geosalinity classes
- DEM and derived topographic index
- airborne SAR and derived soil dielectric constant
- Landsat Thematic mapper.

Description of derived data sets

The vegetation index for the catchment was linked to soil drainage conditions. We developed a computerised classification of multitemporal aerial photography corresponding to the late winter and late summer seasons using information collected for the toposequence and key areas. Native and introduced grass species found in different soil drainage and salinity conditions respond in different ways during these seasons. Thermal IR airborne video showed potential for assessing groundwater discharge sites and remnant stream channels. However, the poor geometry of this imagery only permitted interpretation at the key area scale.

Topographic index ($\ln(A_s/\tan\beta)$) is a secondary terrain attribute. It represents the geomorphic processes associated with soil moisture and its spatial distribution in the landscape. To determine the topographic index for the study area, we created a hydrologically correct, grid DEM using the method of Hutchinson (1989), and evaluated the variables of the index using the procedure of Hutchinson and Dowling (1992).

A soil dielectric constant was derived using data from the National Aeronautics and Space Administration Jet Propulsion Laboratory's airborne synthetic aperture radar. We related the constant to soil moisture status by modelling the radar backscatter. For this study we used the empirical approach of Dubois et al. (1995) to derive a dielectric constant for the entire 80 km^2 region.

We used ECa, derived from the EM31 survey,[1] to determine the relative distribution of soluble salts in the landscape and preferred pathways of solute and water flow in the subsurface region. ECa was also a quick and efficient means to interpolate between sites of known soil properties.

A discharge index, used to partition the landscape into zones of recharge or discharge (Cook and Williams 1998), was also derived from EM31 survey data. This index adds an extra dimension to salinity hazard mapping; it provides a numerical value ranging from strongly negative for low salinity/strongly recharging soils to strongly positive for high salinity/strongly discharging soils.

We derived an aquic index from the land classification attributes associated with the digital 1:50,000 scale SLU data mapped by Primary Industries and Resources South Australia (PIRSA). These attributes or land qualities include drainage, water erosion potential, scalding, salinity and recharge potential. The classification ranks each of these qualities on a numeric scale according to eight generically defined class limits. We considered salinity and drainage to be indicative of aquic conditions (i.e. soil landscape units prone to waterlogging).

We constructed geosalinity classes from the digital geology 1:50,000 scale coverage from PIRSA and classified representative units on the basis of inferred landscape salinity effect. Unit classifications ranged from no significant effect, to acting as a potential source of cyclic salt, to being a source of pyritic materials capable of causing aggressive acid weathering and salt generation (sulfate, chloride, magnesium, sodium, calcium and iron).

To predict the distribution of acidity classes over the region, we consolidated the acidity attribute of the 1:50,000 SLU data from the catchment survey into five classes that represent the progression from extreme profile alkalinity (and sodicity) to extreme profile acidity. These classes are associated with susceptibility to dispersion, salinity and erosion in the case of extreme alkalinity and acidification.

[1] EM31-D is an electromagnetic induction instrument (manufactured by Geonics Ltd, Mississauga, Ontario, Canada), used to measure the apparent electrical conductivity of the ground.

Methodology

Upscaling and spatial modelling

Our approach was to extrapolate soil and hydrological process patterns recognised in the field from point scale to catchment and region by aggregating them. Such upscaling is generally difficult due to the lack of relevant and precise data at the broader scale (Wood et al. 1988; King et al. 1998). The problem can be overcome by linking process patterns to mapped soil units via the toposequence and allocating land degradation classes to each of the units. This approach integrates broader-scale soil, geology, terrain and remotely sensed data within a GIS modelling environment.

Most of the nonpoint data used for this study consists of multiclass raster (regular grid cell) coverages. As the objective was to assess potential land degradation at the regional level, we decided to use a weighted index overlay as the spatial modelling technique (Bonham-Carter 1994). This model is linear, additive and suitable for ranking areas according to potential for degradation (i.e. it is predictive). We evaluated each coverage according to a weighted criterion, based on both trial data and expert knowledge, and scaled the results of the model by applying a classification table of breakpoints to the ranking. The resulting classified data set provided an estimate of potential land degradation that could be verified by limited, random field survey.

The modelling procedures for waterlogged, saline and acid soil conditions are described below for each of the scales. To illustrate the approach we give examples of data models and results for estimates of drainage/waterlogging at each scale. Full details of the procedures and results are reported in Fitzpatrick et al. (1999).

Toposequence/key area

For the toposequence/key area, we analysed a range of detailed point data. The steps outlined below were used to select, describe, distinguish and construct the soil layers in the toposequence. Using this data we could map soil profiles in the key area surrounding the toposequence and thus extrapolate landscape degradation patterns to the catchment and regional level.

Table 1. Summary of data sets used at different scales for different types of land degradation.

	Scale											
	Toposequence			Key area			Catchment			Region		
Data	D/W	SAL	A/A	D/W	SAL	A/A	D/W	SAL	A/A	D/W	SAL	A/A
Soil samples	■	■	■	■	■	■	■	■	■			
Hydrology	■	■	■									
Topography	■	■	■	■	■	■	■	■	■	■	■	■
Vegetation	■	■	■	■	■	■	■	■	■			
EM31							■	■				
Soil dielectric							■	■		■	■	
SLU										■		■
Geology										■	■	

Note: shaded boxes indicate data used for that scale; if boxes are not shaded, data were not used at that scale. A/A = acidity/alkalinity; D/W = drainage/waterlogging; EM31 = conductivity; SAL = salinity; SLU = scale landscape unit

Steps in the process

Select representative catchments and toposequences

- Collate existing information on soil, geology and vegetation.

Describe morphological features in toposequences

- Describe morphological features in soil layers (e.g. soil colour and stone lines).
- Identify soil horizons (e.g. E or Btg) to compare with common scientific terminology.

Group and map morphological features in toposequences

- Group similar morphological features into a smaller number of soil layers (soil systems) using the structural analysis approach (Fritsch et al. 1992), which groups soil features by nested or concordant relationships.
- Develop cross-sections of toposequences for the combined soil layers.

Match soil layers to pedohydrological processes

- Monitor watertable fluctuations (using piezometers and dipwells), soil redox potentials (using Eh probes) and geochemical changes such as EC.
- Link soil and hydrological processes, such as water flow paths and salinity, to each soil layer.

Identify soil mapping units in a key study area surrounding the toposequence

- Collect field survey data from boreholes and representative soil profiles down several toposequences, and analyse soil samples in the laboratory.
- Define landscape and soil mapping units in the key study area using 1:5000 scale aerial photography.
- Determine a range of diagnostic variables for each mapping unit from field observations and soil profile analysis.

Link soil and hydrological processes to the soil mapping units

- Allocate drainage/waterlogging, salinity and acidity/alkalinity classes to each map unit by linking to soil and hydrological processes.

For each type of land degradation (drainage/waterlogging, salinity and acidity/alkalinity), eight classes were allocated to soil layers in the toposequence and five to soil profiles for the key area. Figure 2 illustrates the model used to estimate soil drainage/waterlogging at both scales.

Results—toposequence/key area

Table 2 illustrates the relationships that were developed for each of the three types of land degradation from the toposequence and key area studies. Figure 1 of Chapter 9 shows the estimate of soil drainage/waterlogging for the toposequence and Figure 3 of this paper shows the estimate for the key area. The types of land degradation were verified using soil survey and hydrological data (Cox et al. 1996; Fitzpatrick et al. 1996).

Catchment

Before data modelling and mapping, we developed a GIS for the catchment area to integrate and analyse field and remote sensing data. We digitised the soil survey data at 1:5000 scale, derived from aerial photography and borehole investigations (Fig. 4) and attributed it to the classes defined in Table 2. This information helped us to rank potential drainage/waterlogging, salinisation and acidification at the catchment scale.

We estimated soil drainage/waterlogging from the weighted overlay of vegetation index, topographic index, soil dielectric and EM31-derived discharge index (Fig. 5); salinity from the weighted overlay of topographic index, soil dielectric and EM31-derived EC; and acidity/alkalinity from the weighted overlay of topographic index, geology and soil pH measures.

Table 2. Soil mapping units and associated drainage/waterlogging, salinity and acidity/alkalinity classes for the Herrmann toposequence and key area.

Map unit	Landform elements	Soil description	Drainage/waterlogging	Acidity/alkalinity[a]	Salinity (ECse)/ depth to saline water (m)
1a	Flat	Grey sandy loam surface layer over yellow-grey mottled clay	Poorly drained Strongly waterlogged	Moderately acidic (pHw=<6.5) surface, neutral to alkaline at depth	Slightly saline 1–4 dS/m; 1–1.5 m
2n	Flat	Salt efflorescence (halite and gypsum) on surface with grey sandy loam surface over yellow-grey clay	Poorly drained Strongly waterlogged	Mostly alkaline throughout (pHw >7.5)	Very saline >8–16 dS/m < 1 m
3s	Flat/lower slope seepages	Salt efflorescence (halite and gypsum) on surface with loamy black sulfidic material overlying yellow-grey clay	Very poorly drained Strongly waterlogged	Mostly alkaline throughout (pHw >7.5): sporadic occurrences of highly acidic (pHw <5.5) near-surface layers (<5cm), which develop due to oxidation of sulfidic materials	Extremely saline >16 dS/m; < 1 m
4a	Lower slope, open depression	Grey sandy loam surface layer over yellow-red-grey mottled clay	Poorly drained Periodic waterlogging	Neutral throughout (pHw 6.5–7.5)	Slightly saline 1–4 dS/m 1.5–3 m
5s	Lower slope, open depression	Deep grey sand over yellow-grey mottled clay	Poorly drained Periodic waterlogging	Acidic throughout (pHw=<6.5) (low buffer capacity)	Nonsaline <1 dS/m; 1.5–3 m
6l	Crest	Shallow sandy loam over red uniform coloured clay over weathered rock	Freely drained Infrequently waterlogged	Very acidic throughout (pHw <5.5)	Nonsaline <1 dS/m > 3 m
7a	Mid-slope	Brown loam over red and yellow uniform coloured clay. Deep.	Freely drained Infrequently waterlogged	Moderately acidic (pHw <6.5) throughout	Nonsaline <1 dS/m > 3 m
7ag	Crest, upper-slope	Deep well-drained red and yellow soils	Freely drained Infrequently waterlogged	Moderately acidic (pHw <6.5) surface, neutral to alkaline at depth	Nonsaline <1 dS/m > 3 m
7b	Crest, upper-slope	Deep well-drained red and yellow soils	Freely drained Infrequently waterlogged	Very acidic throughout (pHw <5.5)	Nonsaline <1 dS/m > 3 m
7bg	Crest, upper-slope	Shallow well-drained red yellow soils	Freely drained Infrequently waterlogged	Moderately acidic (pHw <6.5) throughout	Nonsaline <1 dS/m > 3 m
7c	Lower slope, open depression	Shallow well-drained yellow soils	Moderately drained Infrequently waterlogged	Neutral throughout (pHw 6.5–7.5)	Nonsaline <1 dS/m 1.5–3 m
Rq	Crest, upper-slope	Shallow well-drained yellow and red soils with quartz fragments	Freely drained Infrequently waterlogged	Moderately acidic (pHw <6.5) throughout	Nonsaline <1 dS/m > 3 m
Rf	Crest, upper-slope	Shallow well-drained yellow and red soils with ferricrete fragments	Freely drained Infrequently waterlogged	Very acidic throughout (pHw <5.5)	Nonsaline <1 dS/m > 3 m
Rs	Mid-slope	Shallow well-drained red soils with micaceous rock fragments	Freely drained Infrequently waterlogged	Moderately acidic (pHw <6.5) surface, neutral at depth, high buffer capacity	Slightly saline 1–4 dS/m > 3 m
E	Flat/stream channel	Gully, tunnel and rill erosion	Very poorly drained Strongly waterlogged	Mostly alkaline throughout (pHw >7.5)	Extremely saline >16 dS/m; < 1 m

[a] pHw means that the pH measurement was taken in water

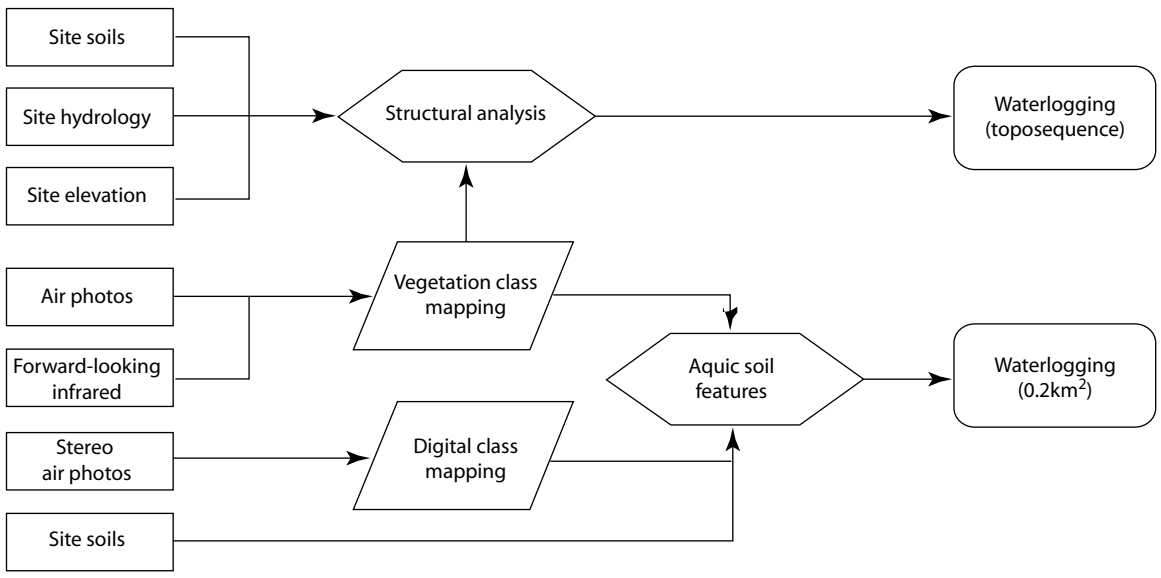

Figure 2. Drainage/waterlogging data model for the toposequence and key area.

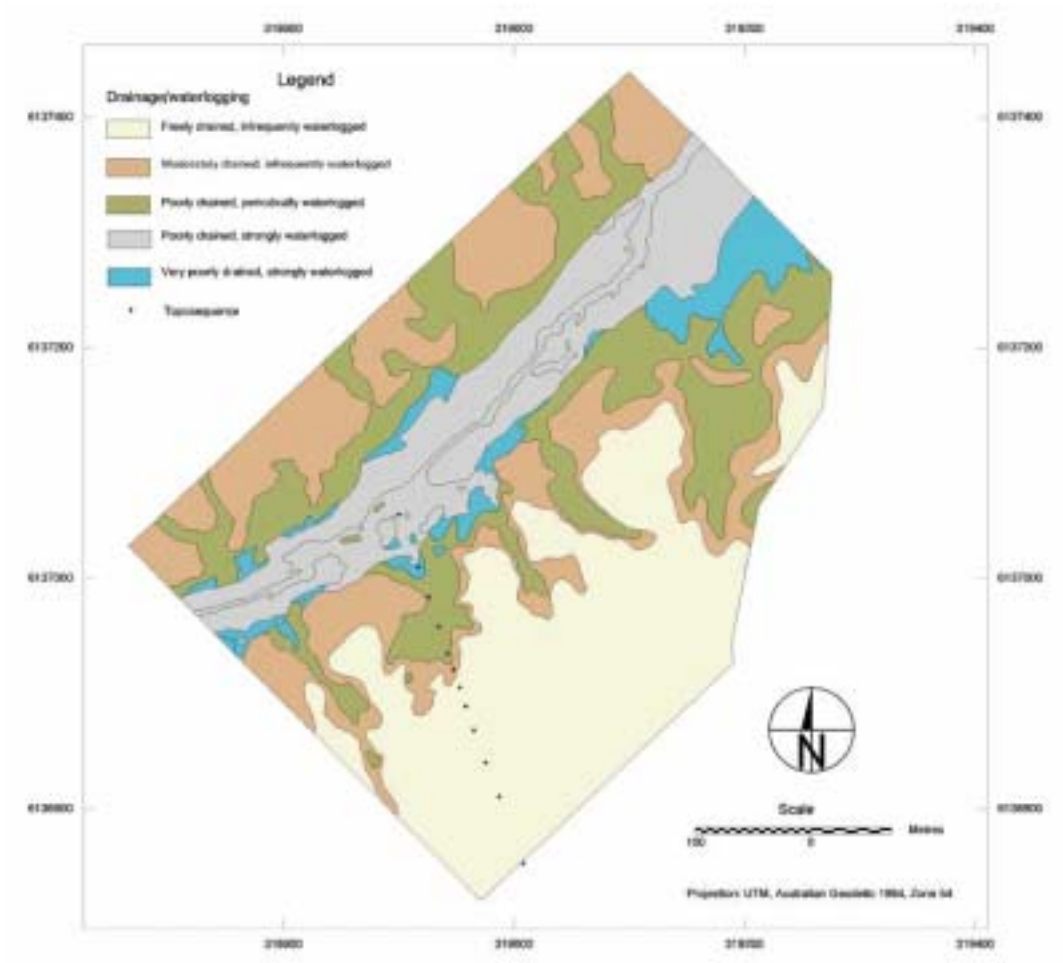

Figure 3 Estimate of drainage/waterlogging for the key area.

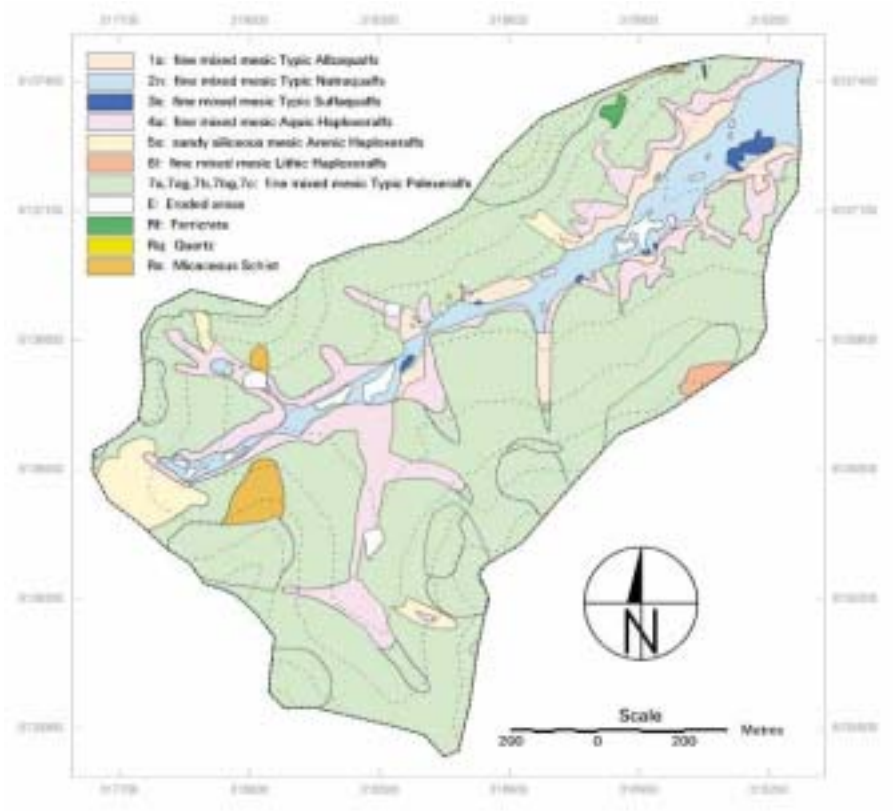

Figure 4. 1:5000 scale soil survey of the Herrmann catchment.

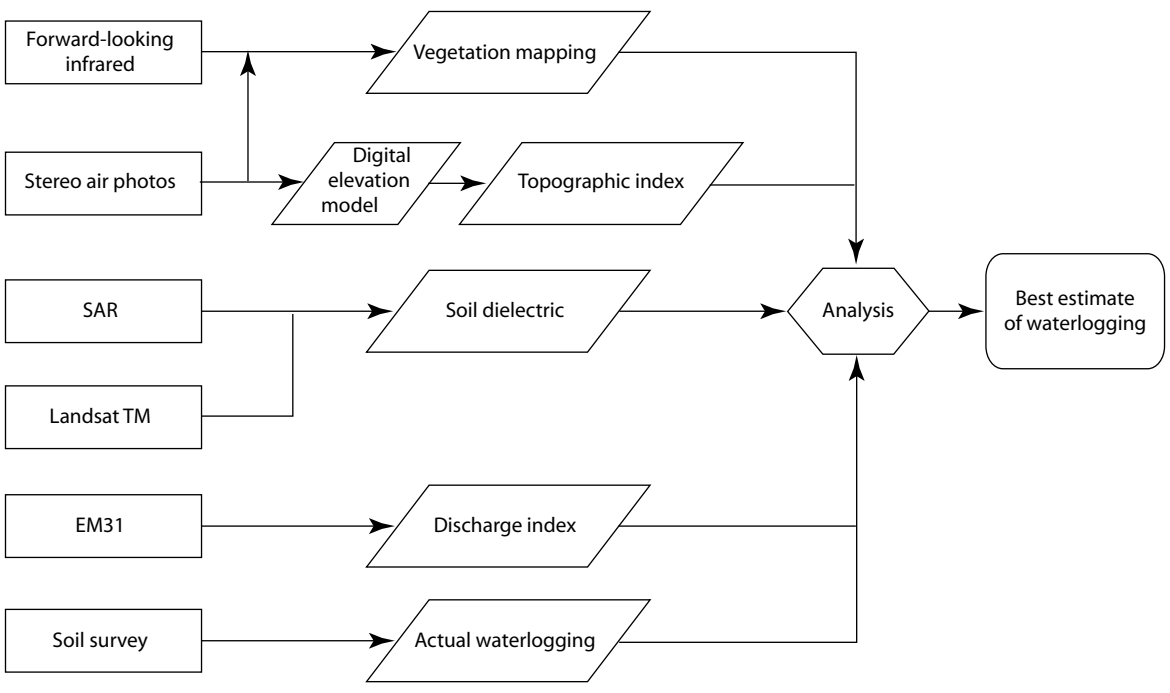

Figure 5. Drainage/waterlogging data model for the catchment. SAR is airborne synthetic aperture radar; Landsat TM is Landsat Thematic mapper; EM31 is derived apparent electrical conductivity.

Results—catchment

Each of the three estimates for the catchment was classified according to the relevant types of land degradation mapped by the 1:5000 scale soil survey. Figure 6 compares the estimate of drainage/waterlogging to mapped information. In general, the estimated results show a positive relationship with the field mapping (Davies et al. 2000). The results of the weighted overlay modelling are affected by any anomalies in the input data. For example, the discharge index showed an area of discharge in the catchment that does not correlate with drainage/waterlogging as mapped by survey. This was explained by field investigations, which indicated an area of clay-rich soil (not previously mapped) that was being incorrectly sensed by the EM31 survey as an area of high ECa.

Region

Some of the higher resolution data used for catchment modelling are not available at regional scale. The weighted overlay model provided a means to aggregate the appropriate broader scale data with suitable higher resolution data, to allow ranking of the potential for land degradation.

At a regional scale, drainage/waterlogging was estimated from the weighted overlay of topographic index, soil dielectric and SLU-derived aquic index (Fig. 7); salinity from the weighted overlay of geology, soil dielectric and topographic index; and acidity/alkalinity from the weighted overlay of topographic index and SLU-derived acidity index.

Results—region

Figure 8 shows the results of modelling to estimate drainage/waterlogging at the regional scale. Thirty-five independent historical sites and five recently sampled random sites were used to verify the three land degradation estimates at regional scale. The estimates from the model correlated well with the site samples. More detailed analyses of the acidity estimates are included in Merry et al. (2000).

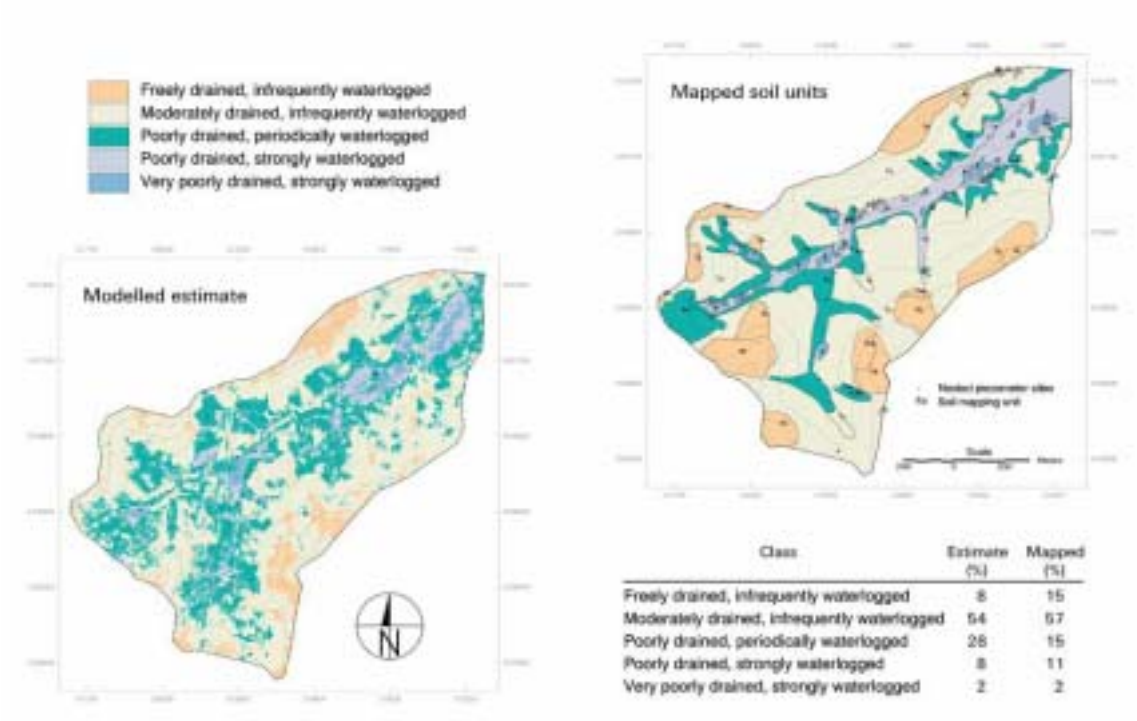

Class	Estimate (%)	Mapped (%)
Freely drained, infrequently waterlogged	8	15
Moderately drained, infrequently waterlogged	54	57
Poorly drained, periodically waterlogged	28	15
Poorly drained, strongly waterlogged	8	11
Very poorly drained, strongly waterlogged	2	2

Figure 6. Potential waterlogging in the Herrmann catchment: comparison of map of best estimate data with mapped soil units.

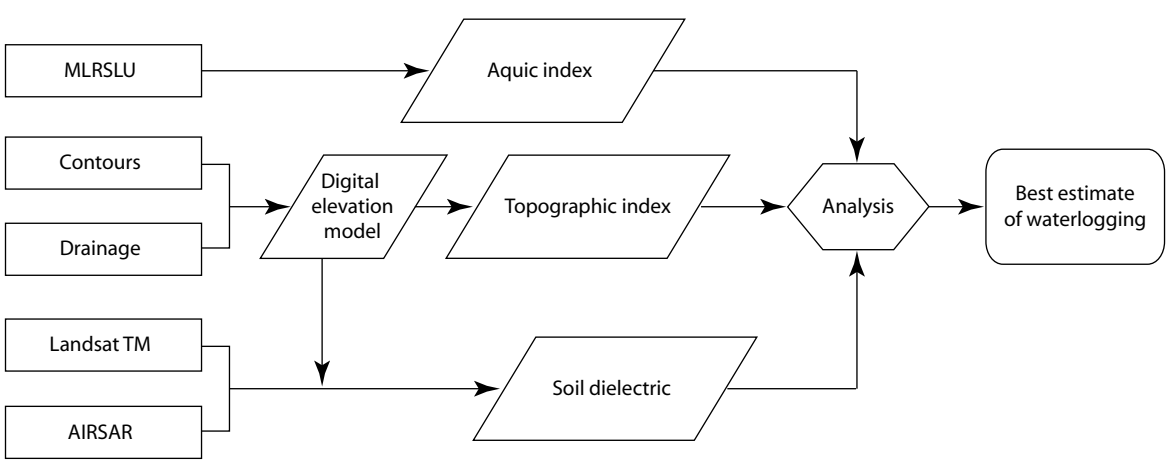

Figure 7. Drainage/waterlogging data model for the Mount Torrens region. MLRSLU = Mount Lofty Ranges scale landscape unit; TM = Thematic mapper.

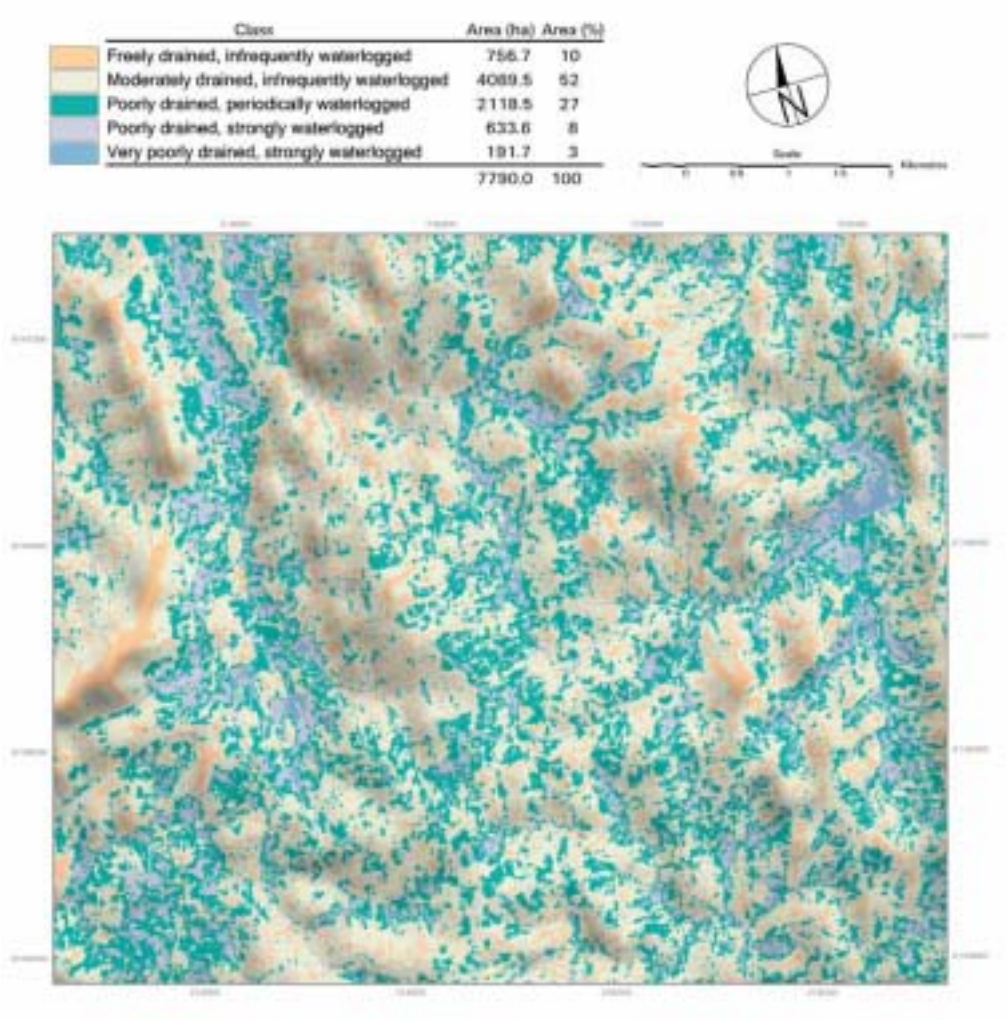

Figure 8. Estimate of drainage/waterlogging for the Mount Torrens region.

Discussion

Using relationships developed from detailed toposequence studies we were able to classify each type of land degradation for the 1:5000 scale soil survey. This classification allowed us to explore the value of broader-scale spatial data in weighted overlay modelling.

Using the models, we could aggregate many of the data sets at the regional scale and rank the potential for land degradation. These rankings could then be classified at the catchment scale using mapped areas and at the regional scale using information obtained from random sites. The extensive use of topography in the form of a grid-based DEM at all scales was a major factor in the ability to aggregate many of the data sets at the regional scale.

The linear, additive nature of the weighted index overlay technique has some disadvantages — any anomalies in the input data tend to modify the results. In such cases, a fuzzy logic method with more flexible combination rules would be advantageous. In this study, anomalies were partially resolved by obtaining appropriate field samples.

The classified ranking provided estimates of waterlogged, saline and acid soils at the regional scale. Although the results have only been analysed qualitatively and have not undergone spatial statistical analyses, they show good agreement with data from independent site checks across the region.

Conclusions

We successfully used a number of different sets of data to upscale assessment of land degradation. The key to translating between scales is to link point-scale process patterns to mapped soil units and allocate land degradation classes to each of the units. We were able to extrapolate point observations to the catchment and regional scale by integrating broader-scale data through weighted overlay modelling within a raster GIS environment.

Using models, we could characterise and assess natural resource status and condition at a scale appropriate for ranking the relative quality of catchments. Regional assessment of land degradation can be used in conjunction with a soil assessment manual (Fitzpatrick et al. 1997) to map problem sites and develop strategies for property management. This approach can help Landcare groups and government agencies to make decisions on resource management based on the knowledge of soil conditions.

The approach described here could be applied to other types of land degradation, and could be used in other regions with comparable landscapes and vegetative covers, where there are similar soils, terrain and remotely sensed data.

Acknowledgments

The authors gratefully acknowledge funding support and assistance: The research was funded by ACIAR and in part by the National Heritage Trust through the National Land and Water Resources Audit. Dr Emmanual Fritsch (pedology) and Mr David Maschmedt (pedology, interpretation of SLU data) contributed substantially to this study. The Tungkillo Landcare Group provided encouragement and assistance with site access. PIRSA kindly provided the 1:50,000 scale soil landscape unit and geology data.

References

Bonham-Carter, G.F. 1994. Computer Methods in the Geosciences: geographic information systems for geoscientists: modelling with GIS. Oxford, Pergamon.

Bruce, D.A. 1996. Soil moisture from multi-spectral, multi-polarising SAR. In: Proceedings of 8th Australasian Remote Sensing Conference, Canberra, March.

Cook, P.G. and Williams, B.G. 1998. Basics of Recharge and Discharge: Part 8 Electromagnetic induction techniques. Collingwood, CSIRO Publishing.

Cox, J.W., Fritsch, E. and Fitzpatrick, R.W. 1996. Interpretation of soil features produced by ancient and modern processes in degraded landscapes: VII. Water duration. Australian Journal of Soil Research, 34, 803–824.

Davies, P.J., Bruce, D.A., Fitzpatrick, R.W., Cox, J.W., Maschmedt, D. and Bishop, L. 1998. A GIS using remotely sensed data

for identification of soil drainage/waterlogging in southern Australia. Proceedings of the International Soil Science Society Congress, Montpellier, France. 20–26 August, 1998.

Davies, P.J., Fitzpatrick, R.W., Bruce, D.A., Spouncer, L.R. and Merry, R.H. 2000. Use of spatial analysis techniques to assess potential waterlogging in soil landscapes. In: Adams, J.A. and Metherell, A.K., eds, Soil 2000: New Horizons for a New Century. Australian and New Zealand Second Joint Soils Conference. Volume 3: Poster Papers. 3–8 December 2000, Lincoln University. New Zealand Society of Soil Science.

Dubois, P.C., van Zyl, J.J. and Engman, E.T. 1995. Measuring soil moisture with imaging radars. IEEE Transactions on Geoscience and Remote Sensing, 33, 4, 510–516.

Fitzpatrick, R.W., Fritsch, E. and Self, P.G. 1996. Interpretation of soil features produced by ancient and modern processes in degraded landscapes: V. Development of saline sulfidic features in non-tidal seepage areas. Geoderma, 69, 1–29.

Fitzpatrick, R.W., Cox, J.W. and Bourne, J. 1997. Managing waterlogged and saline catchments in the Mount Lofty Ranges, South Australia: a soil-landscape and vegetation key with on-farm management options. Catchment Management Series. CRC for Soil and Land Management. CSIRO Publishing, Melbourne. 36 pp. ISBN 1 876162 30 9.

Fitzpatrick, R.W., Bruce, D.A., Davies, P.J., Spouncer, L.R., Merry, R.H., Fritsch, E. and Maschmedt, D.J. 1999. Soil Landscape Quality Assessment at Catchment and Regional scale: Mt Lofty Ranges Pilot Project, final technical report. CSIRO Land and Water Technical Report No. 28/1999, 50 p.

Fritsch, E., Peterschmitt, E. and Herbillon, A.J. 1992. A structural approach to the regolith: Identification of structures, analysis of structural relationships and interpretations. Sciences Géologiques, 45, 2, 77–97.

Fritsch, E. and Fitzpatrick, R.W. 1994. Interpretation of soil features produced by ancient and modern processes in degraded landscapes: I. A new method for constructing conceptual soil–water–landscape models. Australian Journal of Soil Research, 32, 889–907 (colour figs. 880–885).

Hutchinson, M.F. 1989. A new procedure for gridding elevation and stream line data with automatic removal of spurious pits. Journal of Hydrology, 106, 211–232.

Hutchinson, M.F. and Dowling, T.I. 1992. A continental hydrological assessment of a new grid-based digital elevation model of Australia. In: Beven, K.J. and Moore, I.D., eds, Terrain Analysis and Distributed Modelling in Hydrology. Chichester, John Wiley.

King, D., Fox, D.M., Daroussin, J., Le Bissonnais, Y. and Danneels, V. 1998. Upscaling a simple erosion model from small area to a large region. Nutrient cycling in Agroecosystems, 50, 143–149.

Merry, R.H., Spouncer, L.R., Fitzpatrick, R.W., Davies, P.J. and Bruce, D.A. 2000. Prediction of soil profile acidity and alkalinity—from point to region. In: Adams, J.A. and Metherell, A.K., eds, Soil 2000: New Horizons for a New Century. Australian and New Zealand Second Joint Soils Conference. Volume 3: Poster Papers. 3–8 December 2000, Lincoln University. New Zealand Society of Soil Science.

Soil Survey Staff 1998. Keys to Soil Taxonomy, 8th edition. Washington, US Government Printing Office: USDA, Natural Resources Conservation Service.

Wood, E.F., Sivapalan, M., Bevan, K.J. and Band, L.E. 1988. Effects of spatial variability and scale with implications to hydrological modelling. Journal of Hydrology, 102, 28–47.

22 Regional Evaluation of Soil Erosion by Water: a Case Study on the Loess Plateau of China

Yang Qinke,* Li Rui,* Xiaoping Zhang* and Liangjun Hu*

Abstract

This chapter discusses how spatial information techniques can be used to predict and evaluate regional soil erosion. The study, carried out in central China, identified sediment discharge, precipitation, soil composition, gully density and land use as the controlling factors of regional erosion. The authors found that soil erosion can be assessed and predicted quantitatively at a regional scale; that quantitative evaluation can be used to study and describe the soil erosion mechanism at the macro scale; and that soil erosion at the national or provincial scale can be rapidly surveyed using remote sensing, geographic information systems (GIS) and erosion modelling.

本研究以黄土高原为例，在分析了区域水土流失过程、类型和分布特点的基础上，拟订了区域水土流失评价指标体系，包括：沟壑密度、汛期降雨量、土壤团粒含量、植被盖度、坡地面积比等。根据遥感影象划分编制了评价单元图并在 GIS 环境下集成各评价因子建立了评价数据库。根据地理统计方法建立了评价模型。研究表明：区域水土流失宏观趋势的定量评价预测是可能的，基于水土保持类型区的定量评价，可以揭示区域水土流失的宏观规律，进而实现区域水土流失快速调查是可能的。最后对于模型进一步改进方法和途径进行了讨论。

* Institute of Soil and Water Conservation, Chinese Academy of Sciences and Water Resources Ministry, Yangling, Shaanxi 712100, PRC.
Email: qkyang@ms.iswc.ac.cn

Yang Qinke, Li Rui, Xiaoping Zhang and Liangjun Hu. 2002. Regional evaluation of soil erosion by water: a case study on the Loess Plateau of China. In: McVicar, T.R., Li Rui, Walker, J., Fitzpatrick, R.W. and Liu Changming (eds), *Regional Water and Soil Assessment for Managing Sustainable Agriculture in China and Australia*, ACIAR Monograph No. 84, 304–310.

CHINA suffers severe soil erosion (Xianmo Zhu et al. 1999; Qinke Yang 1994). As the country's economy has developed, soil conservation and ecological rehabilitation have been increasingly taken into account and land-use policy has shifted its focus from small watersheds to large regions (China's Agenda 21 1994; Posen et al. 1996). As a result, policy makers and those responsible for planning soil conservation and environmental rehabilitation measures are demanding systematic information about the current situation and trend of soil erosion, and the benefits of soil conservation and ecological rehabilitation practices. This information is required urgently and will need to be continually updated.

Regional soil erosion and conservation are not just local effects; they also affect the surrounding region, including rivers downstream. Widespread events such as floods, sediment deposition in rivers and reservoirs, dust storms, land degradation and water shortages may result from localised erosion events. Consequently, we must quantify and predict the degree and effects of soil erosion at the regional, national and even global scales.

Spatial information sciences and techniques — including remote sensing, geographic information systems (GIS), global positioning systems (GPS) and related internet technology — have been widely applied to soil erosion monitoring and surveying since the 1980s. In China, the technology for modelling and predicting soil erosion has been developed and applied at the regional scale using GIS and remote sensing (Rui Li et al. 1998; Qinke Yang and Rui Li 1998; Feng Jiao et al. 1998). Usually the study area is divided into several integrated spatial units, so the heterogeneous characteristics or spatial differentiation of the units can be taken into account. Most research into erosion evaluation and prediction has been carried out at the scale of the slope or plot (Renard et al. 1997); there have been relatively few regional studies. Where studies have been carried out, they have usually been based on small areas, with scaling up and/or aggregation being used to extrapolate soil erosion data to a regional or even global scale (Posen et al. 1996; Kirkby et al. 1996; Qinke Yang and Rui Li 1998).

China has been divided into eight soil erosion areas and the soil erosion trend in each has been predicted by relating sediment discharge to factors such as annual runoff, daily maximum runoff and control area (%) (Peihua Zhou 1988). Soil erosion data can also be obtained by the aggregation method using plot data from the United States Department of Agriculture (USDA) monitoring network (Rui Li et al. 1998). However, the problems of evaluating and predicting soil erosion regionally are not entirely solved.

Methodology

Study area

The study area was the 623,700 km^2 Loess Plateau, in central China. The plateau includes the southern part of Ninxia Autonomous Region, the whole of Shanxi Province, northern Shaanxi Province, the eastern and central parts of Gansu Province, the southern part of the Inner Mongolia Autonomous Region, and the western part of Henan Province. It borders the Riyue Mountains to the west and the Taihang Mountains to the east; and it extends from Qinling Mountains in the south to the Yingshan Mountains in the north. Figure 1 in the Overview shows the general location of the area.

The Loess Plateau is located in the second of the three grand relief landform terraces in China. The basic geomorphological types include loess hills, sand–loess hills and loess tableland; the gully density is 4–6 km/km^2 and 40–60% of the area has gullies. The climate is continental monsoonal, with mean annual temperature between 6.6 and 14.3°C and mean annual precipitation between 250 and 700 mm. Rain falls mainly in summer (50–70% of the annual total) and is most intense from July to October. The dominant soils are widely eroded, especially in northern Shaanxi Province, central eastern Gansu Province and western Shanxi Province. Secondary vegetation is limited to only a

few stony hills. For over 2000 years, crop growing has been the main form of land use in the area. The population density is 40–270/km^2. The relationship between the agricultural activities of people and the natural environment is not harmonious.

Figure 1 shows how erosion can be subdivided according to erosive intensity. According to this classification, the Loess Plateau has three erosion regions: the water erosion region, the wind–water erosion region and the wind erosion region.

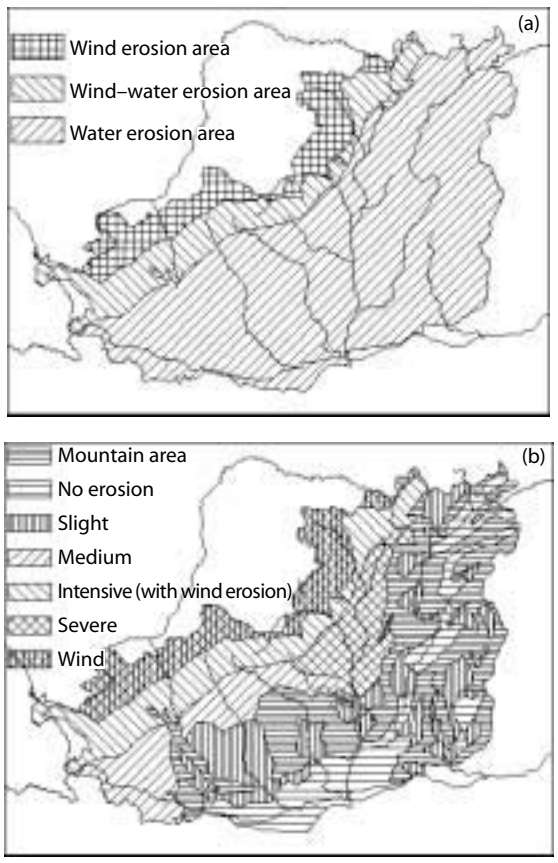

Figure 1. Soil erosion map of the Loess Plateau, showing (a) the types of erosion and (b) the major regions of erosion.

Data and materials

Field surveys and cartographic research by Xianmo Zhu (1981a, b; 1982a, b) show that regional soil erosion is a very complicated process that is affected by many factors, including geomorphology, soil conditions, meteorology, hydrology, land use, vegetation coverage and soil conservation measures. By analysing these environmental factors and how they affect erosion, we describe the processes of regional erosion and quantitatively evaluate the interactions of the factors and the ability to semi-empirically model the spatial distributions of erosion intensity. In this study, we use the following data.

- **Sediment discharge data** were obtained from the records of 250 hydrological stations covering the period from 1959 to 1986.
- **Precipitation data** measured from 1955 to 1986 at 178 meteorology stations were used to calculate the mean rainfall in the rainy season (July to October).
- **Soil classification data** were obtained from the 1:2,000,000 Loess Plateau soil map produced in 1991 by the Institute of Soil and Water Conservation (ISWC), the Chinese Academy of Sciences and the Ministry of Water Resources. Soil organic matter content data were extracted from monographs that reported the results of the second national soil survey.
- **Gully density data** were determined from gully density annotation points from a 1:500,000 soil erosion map of the Loess Plateau that was produced in 1991.
- **Land-use data.** We estimated the ratio of cropland to forest/grassland from a 1:250,000 land-use map in ArcInfo format, produced by ISWC in 1993 based on the interpretation of Landsat Thematic mapper (TM) data (see Chapter 16 for further details).

Precipitation, sediment and gully density data were in coordinate format (x,y,z) and were spatially interpolated and contoured using ArcInfo. All data were transformed into the Albers projection.

Parameters and database

Table 1 shows the parameters selected for the evaluation. Their choice was dictated by what was needed for prediction and by what was available over the entire study area.

The characteristics of regional soil erosion vary over space and time. Consequently, multilevel areas and classes of erosion can be identified. The study of erosion on a regional scale is based on experimentation and observation at plot and watershed scales, but the data cannot simply be extrapolated from a slope surface or other small area to a larger area using spatiotemporal modelling of the environment (Burough 1998).

To adequately describe the study, the study area must be discretised in space and time. Conventionally, geoentities in space are described by vector data such as points, lines and polygons and other common factors. We divided our study area into 3380 spatial units of uniform map area (UMA) according to Landsat TM imagery.

The parameters were processed into map format and integrated into each of the UMAs, based on the theory and method of the georelationship model. During the process of integration, the data for location and topology were based on the UMA map or base map. The number of data entities on the base map remained constant during data integration.

Results and Analysis

Modelling regional erosion

The general format of the model of regional erosion is:

$$A = f(Q, S, g, v, c) \quad (1)$$

where A is the erosion intensity, Q is a hydrological/climate factor, S is a soil factor, g is a landform factor, v is a vegetation factor, and c is a conservation measure factor.

There is an exponential correlation between the amount of erosion, the amount of rainfall in the rainy season, the gully density, the proportion of slope cropland, the coverage of vegetation and the content of aggregate (≥ 0.25 mm) (JunJie Ma 1990; JiYang Liang 1992; QiuSheng Wang 1991). The relationship can be expressed as:

$$L = 0.4735P^{0.9282} S^{-0.08855} \times G^{2.2666} M^{0.07254} e^{-0.00047C} \quad (2)$$

where L is the erosive intensity (tonnes/km^2/year), P is the precipitation in the wet season (mm), S is aggregate content (g/kg), G is the gully density (km/km^2), M is the ratio of slope cropland (%), and C is vegetation cover (%).

The highly significant regression result ($r = 0.937$, $F = 2984.64 >> F_{0.05} = 2.21$ where F is the F-statistic, which is much higher than the level for 5%) indicates that the erosive intensity is positively correlated with rainfall quantity in the wet season, gully density, and the proportion of slope cropland. It is negatively correlated with the content of aggregate and vegetation cover. In other words, the higher the rainfall in the wet season, the greater the erosion intensity; the higher the aggregate content and vegetation covering, the lower the erosion intensity. This accords with general principles of soil erosion, and with other research in this field.

Evaluating the erosion factors

We have identified five variables controlling erosion regionally. These variables can be converted into

Table 1. Parameters used in the evaluation.

Erosion factor	Soil erosion	Climate	Soil	Plant	Land use	Relief
Parameter	Sediment intensity	Rainfall in wet season	The fraction of soil (g/kg) with a diameter > 0.25 mm	Plant cover	Slope to area ratio	Gully density

specific units and extracted from existing survey or remote sensing information. The variables are suitable for a macro study to evaluate trends, as in our study. Land-use data provide some indication of the extent to which soil and water conservation are practised in the region. For the purpose of analysing erosion potential, the landscape can be categorised into plains, terraces, hills and mountains. There are obvious differences between the categories in patterns of erosion, measures and patterns of soil conservation and types of reasonable land use. Topographic maps and TM imagery have made it possible to determine locations with a high degree of accuracy. As the UMA map has 2230 polygons and the 1:500,000 Loess Plateau erosion map has only 1100 polygons, each UMA can contain values derived from different thematic layers. Thus, erosion levels can differ within UMAs for the same landscape zone.

We applied several algorithms for attribute values from the maps (in digital format) to the databases. We used a flexible method to calculate the relationship between location and descriptive data. Consequently, all variables in the model can be integrated into the UMA map, and a database with multi-items can be built to satisfy the demands of multifactor evaluation (Qinke Yang 2001).

Figure 2 is a GIS map showing soil erosion calculated using Equation 2; it shows the relationships among the different factors affecting soil erosion and accords with the spatial differentiation pattern of soil erosion observed on the Loess Plateau. The result is useful in macro policy making.

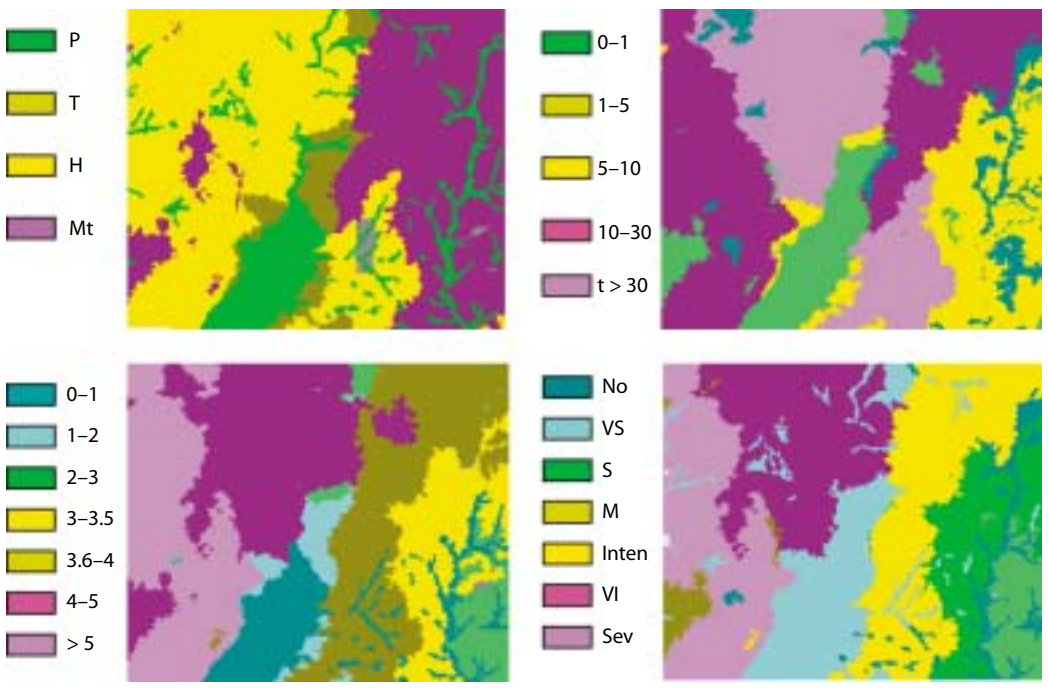

Figure 2. An example of factors influencing regional erosion modelling for a 127 km × 117 km portion of the Loess Plateau situated in Shaanxi Province. The top left image is of landform; P is plain; T is tableland; H is hill; and Mt is mountains. The top right image is the percentage slope of cropland for each polygon. The lower left image shows the density of gullies (km/km^2). The lower right image illustrates erosion intensity (t/km^2/year), which can be used for regional decision making on soil erosion control and ecorehabilitation; No is none, VS is very slight, S is slight, M is medium, Inten is intensive, VI is very intensive and Sev is severe.

Modelling regional soil erosion

Equation 1 allows runoff modulus (kL/km^2/year) to be used as a measure of relevant hydrology factors (Q) and soil antiscourability (kg/kL) as a measure of soil factors (S). Information for the landform factor (g) can be derived from regional DEMs, where the relative relief — the maximum elevation difference in a specified area — is used (Xinhua Liu et al. 2001). The remaining two factors, the vegetation index and soil conservation index, can be derived from advanced very high resolution radiometer (AVHRR) data (see Chapter 16 for further details) and soil conservation statistics, respectively.

Discussion

It is possible and practical to quantitatively assess and predict macro trends in soil erosion at the regional scale, using the theory and methodologies of regional soil conservation and GIS. The methodology involves:

- dividing the study area into discrete units in space and time with homogeneous factors and erosion types based on the analysis of processes and the spatial differentiation of soil erosion and related environmental factors at the regional scale;
- using research on the factors affecting regional erosion and the results of erosion evaluation studies, coordinated with the characters of GIS modelling methods, to identify the relevant parameters of the model;
- extracting the parameters one by one from many kinds of approaches, including field tests, thematic maps, descriptions of observed materials and remote sensing imagery/DEM analysis, and integrating all the parameters into the basic unit map to build up a parameter database; and
- establishing a statistical model for the sediment discharge (the sediment yield from erosion) and each relevant factor using geostatistical and correlative analysis methods.

Our study supports unpublished work of the national soil erosion survey that suggests that remote sensing, GIS and erosion modelling can be used to efficiently survey soil erosion at the national or provincial scale. In the 1980s, it took about 10 years to map soil erosion in China at the national scale using mainly manual methods; in 1998–2000, it took only two years to do the same using a combination of manual and computer methods. When we have all the basic information at the national scale, we will be able to survey erosion quantitatively and annually. The increased timeliness in providing a nationwide overview by performing this massive task in temporal GIS (TGIS, see Chapter 16) will allow cost–benefit analysis of soil conservation and ecological rehabilitation practices to feed back more quickly into policy decisions and directions. The development of this TGIS will not only allow monitoring of the environmental response, but also allow central government officials to determine the effectiveness of money spent in different regions.

Conclusions

This study has shown that soil erosion can be assessed and predicted quantitatively at a regional scale; and that soil erosion at the national or provincial scale can be rapidly surveyed using remote sensing, GIS and erosion modelling. The information so provided will assist macro policy making at the national and provincial levels. The accurate evaluation and prediction of regional soil erosion should be based on systematic research on the genesis and evolution of erosion at the macro scale, and on the factors that cause erosion. The current situation is far from perfect; we are doing more work on this topic.

References

Burrough, P.A. 1998. Dynamic modeling and geo-computation. In: Karssenberg, D. and Burrough, P.A., eds, Environmental Modeling in GIS. Utrecht University, The Netherlands, Faculty of Geographical Sciences.

China's Agenda 21. 1994. White Paper on China's Population, Environment, and Development in the 21st Century. Beijing.

Feng Jiao, Xiaoping Zhang and Rui Li 1998. Application of GPS in soil and water conservation. Bulletin of Soil and Water Conservation, 18(5), 32–34.

Jiyang Liang 1992. Analysis and simulation of storm, runoff and sediment on the Loess Plateau. Journal of Soil and Water Conservation, 6(2), 12–16.

Junjie Ma 1990.The regression analysis of soil erosion on loess hill and tableland in the middle of Shaanxi. Journal of Soil and Water Conservation, 4, 21–28.

Kirkby, M.J., Imeson, A.G., Bergkamp, G. and Cammeraat, L.H. 1996. Scaling up processes and models from the field plot to the watershed and regional areas. Journal of Soil and Water Conservation, 391–396.

Peihua Zhou 1988. The prediction and prevention of soil erosion in China in 2000. Memoir of the Institute of Soil and Water Conservation, Academia Sinica, 1988(7), 57–71.

Posen, J.W., Boardman, J., Wilcox, B. and Valentin, C. 1996. Water erosion monitoring and experimentation for global change studies. Journal of Soil and Water Conservation, 386–390.

Qinke Yang 1994. The classes and regions of soil erosion in China. In: Soil Science Study in Modern Time. Beijing, Agriculture, Science and Technology Publishing House.

Qinke Yang 2001. Study on overlay and its application of digital map overlay analysis. In Rui Li and Qinke Yang, eds, Study on Rapid Survey of Region Soil Erosion and Soil Conservation Information System. Zhengzhou, Huanghe Water Resources Press, 126–134.

Qinke Yang and Rui Li 1998. Review of quantitative assessment on soil erosion in China. Bulletin of Soil and Water Conservation, 18 (5), 13–18.

Qinke Yang and Rui Li 1999. Application of GIS. In: Li Rui and Yang Qinke, eds, Research on the Rapid Survey and Management Information System at Regional Scale. Zhengzhou, Huanghe Water Resources Press, 19–24.

QiuSheng Wang 1991.The mathematical model for vegetation control of soil erosion and its application. Journal of Soil and Water Conservation, 5(4), 68–72.

Renard, K.G., Foster, G.R., Weesies, G.A., McCool, D.K. and Yoder, D.C. 1997. Predicting Soil Erosion by Water: a guide to conservation planning with the revised universal soil erosive (RUSLE). Washington DC, United States Department of Agriculture, Agriculture Handbook, 703.

Rui Li, Qinke Yang and Yong'an Zhao 1998. Application of spatial information technology in soil and water conservation of China. Bulletin of Soil and Water Conservation, 18(5), 1–5.

Xianmo Zhu 1981a. The main types of water erosion and their related factors in the Loess Plateau (1). Bulletin of Soil and Water Conservation, 1981(3), 1–9.

Xianmo Zhu 1981b. The main types of water erosion and their related factors in the Loess Plateau (2). Bulletin of Soil and Water Conservation, 1981(4), 13–18.

Xianmo Zhu 1982a. The main types of water erosion and their related factors in the Loess Plateau (3). Bulletin of Soil and Water Conservation, 1982(1), 25–30.

Xianmo Zhu 1982b. The main types of water erosion and their related factors in the Loess Plateau (4). Bulletin of Soil and Water Conservation, 1982(3), 40–44.

Xianmo Zhu, Daizhong Cheng and Qinke Yang 1999. 1:15000,000 soil erosion map of China. In: Atlas of Physical Geography of PRC (2nd edition). Beijing, Cartographic Publishing House, 200.

Xinhua Liu, Qinke Yang and Rui Li 2001. Extraction of relief roughness and its application in regional erosion prediction in China. Bulletin of Soil and Water Conservation,. 21(1), 57–59.

23 Assessing Cropland Using Geographical Information Systems and Land Survey Data: an Example from China

Yang Qinke,* Tim R. McVicar,† Li Rui* and Xiaoping Zhang*

Abstract

China's current cropland taxation policy is based on the results of a land survey carried out in the 1950s. There is an urgent need to evaluate cropland quality so that land can be taxed and managed using up-to-date information. In China, different agricultural areas are taxed at different rates, based on land evaluation assessment. Farmers on more favourable land pay higher levels of tax. This chapter describes how 15 parameters were integrated into basic polygons to create a database for use in land evaluation. The parameters were obtained mainly from the national land survey and included accumulated annual temperature, annual precipitation, soil organic matter, elevation, slope and soil erosion. We evaluated cropland for each of the polygons using ArcInfo and Foxbase, integrated the database with an aggregated model produced from cropland evaluation of Shaanxi Province and created maps of cropland classes and related tables of statistics.

中国的农业税率因土地质量而异，好地课税率高。现行的税率是根据 50 年代土地详查结果而定的，目前亟需对农地的质量重新评价，以便采用最新数据来征税和管理。本文将 15 个参数集成于地块单元以建立耕地评价数据库。这些参数主要来源于国土详查资料，也包括相关研究中积累的年气温、降水、土壤有机质、海拔、坡度和土壤侵蚀数据。在 ArcInfo 和 Foxbase 环境下评价每个地块的质量等级，将数据库与陕西省农地评价所生成的模型结合，得到农地质量等级图以及有关的统计图表。

* Institute of Soil and Water Conservation, Chinese Academy of Sciences and Ministry of Water Resources, Yangling, Shaanxi 712100, PRC. Email: qkyang@ms.iswc.ac.cn

† CSIRO Land and Water, PO Box 1666, Canberra, ACT 2601, Australia.

Yang Qinke, McVicar, T.R., Li Rui and Xiaoping Zhang. 2002. Assessing cropland using geographical information systems and land survey data: an example from China. In: McVicar, T.R., Li Rui, Walker, J., Fitzpatrick, R.W. and Liu Changming (eds), *Regional Water and Soil Assessment for Managing Sustainable Agriculture in China and Australia*, ACIAR Monograph No. 84, 311–320.

THE QUALITY and quantity of cropland in China was surveyed in the 1950s, soon after the creation of the People's Republic of China. The cropland taxation policy used today is based on the results of this 1950s survey, which evaluated land according to its type (e.g. hills, tablelands and plains) and features (e.g. soil organic matter content, bulk and porosity). In China, farmers pay different tax rates depending on the land evaluation assessment. For example, farmers located on fertile soils close to water sources pay a higher tax rate than those located on relatively infertile soils with lower rainfall or less access to irrigation. Hence, land assessment plays a critical role in agricultural economies at both micro (farmer) and macro (all China) levels.

Since the original survey, farmers and/or government have introduced land improvement measures such as capital works, irrigation networks and improvements to low-quality soils. Because productivity of the land has changed greatly over the intervening years, the 1950s-based land taxation criteria are no longer appropriate. Consequently, it has become necessary to reassess the land in order to adjust the taxation regime in a rational and balanced way that takes into account regional land conditions.

In the early 1990s, aerial photographs were used to construct a nationwide land survey at a scale of 1:10,000 in agricultural areas and 1:50,000 in forest and grassland areas. To date, only the areas of land parcels have been mapped; land quality has not been evaluated. There is an urgent need to evaluate cropland quality so that land can be taxed and managed using up-to-date information.

Three classification systems have been used for nationwide land evaluation in China:

- the land capability classification of the United States Department of Agriculture (USDA) (Klingebiel and Montomery 1961) (this system was used in 1982 by the central Chinese Government Office of the Second Soil Survey);
- the Food and Agriculture Organization land evaluation system (FAO 1976) (this system has been used to assess the suitability of the land for different purposes); and
- a hybrid system, based on the USDA and FAO methods, modified to suit Chinese conditions (Shi Yulin 1982) (this system was used to report at a scale of 1:1,000,000 for all China).

These systems of land evaluation are designed primarily to help set policies that use land resources sustainably at a regional and national scale, or to gain maximum benefit from land improvement practices (e.g. establishing an irrigation area) for minimal cost. Our aim was to improve the basis for land taxation by using land survey data and geographic information systems (GIS). Two key steps are reported here. First, we identified and mapped the land evaluation units using GIS overlay techniques and readily available regional databases. Second, we developed a land evaluation model in a GIS environment.

Methodology

Land resources are affected by geographical factors (e.g. geomorphology, soil, vegetation, climate and hydrology) and socioeconomic factors (e.g. the infrastructure associated with agronomy, transportation and location). The quality of the land can be represented generally by the following equation:

$$Lq = f(c, g, s, p, e) \qquad (1)$$

where Lq is a measure of land quality, c is a measure of climate, g is a measure of geomorphology, s is a measure of soil type, p is a measure of cropland infrastructure and e is a measure of economic conditions.

Land evaluation requires identification and mapping of the evaluation unit (the basic polygon), development of databases to be used in the analysis, and construction of a model to score the land with

respect to different (either real or potential) land uses. Additionally, maps and statistical summaries must be produced for the end user.

In this study, the parameters used, their ranking and their weight were taken from the guide for cropland evaluation of Shaanxi Province (Zhang Qifan 1994). The approach used was based on research from the West and from China. In the light of the information we have accumulated, our data handling capacity and trials in northern, central and southern Shaanxi Province (Zhang Qifan 1994), we believe that 15 parameters are required (Table 1). These parameters cover climate, geomorphology, soil, agricultural infrastructure and economic factors. Cropland quality maps are generally at a scale of 1:10,000, which is suitable for use in the field. The parameters and classes are listed in Tables 1and 2 and can be expressed as:

$$P = \sum_{i=1}^{n} A_i K_i \qquad (2)$$

where P is the score for the evaluation unit, A_i is a measure of the score for the specified factor, K_i is a measure of the weight of the specified factor, and n is the serial number of the evaluation unit (polygon).

Study Area

The study was performed in Changwu County, which is located in western Shaanxi Province, in the south of the Loess Plateau and covers an area of 565.9 km^2. Figure 1 shows the location of the study area. The dominant geomorphological types in the Loess Plateau are loess tablelands, loess hills and river plains. Background information about the plateau is contained in the Overview. Mean annual rainfall is 584.1 mm, mean annual temperature is 9.1°C and total annual sunshine is 1659.9 hours. A detailed land survey was completed in 1992 at a scale of 1:10,000 and the information has been upgraded yearly since 1995. The maps, tables and other related data are all managed in paper format and must be accessed manually (Office of the Land Detail Survey of Changwu County 1994; Committee of the Land Detail Survey of Shaanxi Province 1987).

The six data sets used in this study, and the general data constructs, are described below.

- *Land-use maps* (1:10,000). These were produced from the detailed survey of land resources (Committee of the Land Detail Survey of Shaanxi Province 1987). Each polygon has two items of data: the land-use code, and the number of the polygon. Items recorded in the map table associated with each land-use polygon were the map-sheet code; the administrative region (village, township, county); the type of land use; the area of the polygon and lines (roads, canals, etc.); and the ownership of land. The map also shows a third class of land use classified mainly by environmental factors such as landform, soil type and slope.
- *Cropland slope maps* (1:10,000). These are based on the land-use map and contain data about the cropland slope for each polygon.
- *Land-use change maps* (1:10,000). These are based on the land-use update. Where land use has changed, the old land use, the new land use, and the date of change are recorded for each polygon.
- *Climate condition maps* (1:100,000). These include contour maps of annual precipitation and annual cumulative mean daily air temperature when the air temperature is greater than 10°C. Both were produced by the Meteorological Bureau of Changwu County, based on 40 years data.
- *Soil maps* (1:50,000). These include soil type and soil organic matter maps, based on soil survey data produced in 1980 by the Agricultural Bureau of Changwu, Shaanxi Province.
- *Topographic maps* (1:10,000). These maps are produced by the Survey and Mapping Bureau of Shaanxi Province and are based on aerial photographs from flights conducted in 1976. The contour interval is 10 m.

Table 1. The 15 parameters (bold numbers) used in the land evaluation model, and the weighting factor (Wt), criteria and score used.

Factor		Wt (%)	Criteria	Marks
Climate	**1** ≥10°C accumulated temp	8	> 4600	9
			4600–4300	8
			4300–4000	7
			4000–3700	6
			3700–3400	5
			3400–3100	4
			3100–2800	3
			2800–2500	2
			< 2500	1
	2 Precipitation (mm)	10	> 640	9
			640–600	8
			600–560	7
			560–520	6
			520–480	5
			480–440	4
			440–400	3
			400–360	2
			<360	1
Geomorphology	**3** Elevation (m)	4	<400	9
			400–500	8
			500–600	7
			600–700	6
			700–800	5
			800–900	4
			900–1000	3
			1000–1100	2
			> 1100	1
	4 Slope (°)	10	< 2	9
			2–6	7
			6–15	5
			15–25	3
			> 25	1
Soil	**5** Erosion	6	None	9
			Slight	7
			Medium	5
			Strong	3
			Severe	1
	6 Depth (cm)	4	> 100	9
			100–70	7
			70–50	5
			50–30	3
			< 30	1
	7 Texture	5	Fine sand	9
			Clay/fine sand	7
			Clay	5
			Sandy/stone	3
			Stone	1

Factor		Wt (%)	Criteria	Marks
Soil (continued)	**8** Organic (%)	5	> 1.8	9
			1.8–1.6	8
			1.6–1.4	7
			1.4–1.2	6
			1.2–1.0	5
			1.0–0.8	4
			0.8–0.6	3
			0.6–0.4	2
			< 0.4	1
	9 Saline or wet	5	No/no	9
			0.6	6
			Slight	
			0.6–1.0	3
			Seasonal	
			> 1.0	0
			water < 0.5	
	10 Pollution	4	None	9
			Slight	6
			Medium	3
			Strong	0
Condition of irrigation	**11** Irrigation	12	Irrigation if needed	9
			20% need	7
			Three times	5
			Twice	3
			Once	1
			Not possible[a]	0
	12 Contain water	8	Best	9
			Better	7
			OK	5
			Poor	3
			Worse	1
	13 Distance	7	< 1 km	9
			1–2 km	7
			2–3 km	5
			3–4 km	3
			> 4 km	1
Economic condition	**14** Transport	6	Fair	9
			OK	5
			Poor	1
	15 Location	7	Very large city	9
			Large city	7
			Medium city	5
			Small city	3
			County	1
			Rural area	0

[a] There is no infrastructure to irrigate the crops

Generation of Parameters and Integration of Data

The spatial map unit is the basic polygon of the digital map. Each polygon has uniform attributes of land use, land management, cropping practice and related environmental factors. Figure 1 of Chapter 16 shows this stratification overlay concept. Additionally, each basic polygon has a definite boundary and area (Yang Qinke et al. 1985). In the field, the polygons are bounded by field engineering or clear line entities such as roads, canals, gullies or cliffs (Zhang Qifan 1994). Research and mapping of these units provided the basis for the scientific and practical evaluations in this study.

We used the land-use map as a basis for identifying and mapping the units, taking into consideration environmental factors and their relationship with land quality. Each unit has a unique identity and is related to one record in the attribute database; Table 3 shows an example of the database for 10 polygons. The overlaying and merging of the polygon attribute table (PAT) and ArcInfo (boundary of polygons) attributes table (AAT) were automated in order to manage the data. In the overlay process, the basic polygon map was used as a base map, with all the other maps overlaid in GIS. For integration, we added an item or parameter into the attribute table of the base map one or more times, as required. Figure 2 shows the steps in this process.

Figure 1 Shaanxi Province counties (Changwu County is shaded grey).

The data were manipulated in three ways:

- Attribute data with ArcInfo were used to map basic polygons and integrate them into multithematic maps. In this way, a database of parameters in the georelational data structure was developed, with multiple items describing each of

Table 2. Stratification of the land evaluation score into classes calculated from the 15 parameters and weighting factors, both introduced in Table 1, using Equation 2.

Class	Subclass	Score	Potential yield (kg/ha)	Class	Subclass	Score	Potential yield (kg/ha)
I	1	900–855	7500–7050	V	10	495–450	3450–3000
	2	855–810	7550–6600	VI	11	450–405	3000–2625
II	3	810–765	6600–6150		12	405–360	2625–2250
	4	765–720	6150–5700	VII	13	360–315	2250–1875
III	5	720–675	5700–5250		14	315–270	1875–1500
	6	675–630	5250–5175	VIII	15	270–225	1500–1125
IV	7	630–585	5175–4350		16	225–180	1125–750
	8	585–540	4350–3525	IX	17	180–135	750–225
V	9	540–495	3525–3450		18	135–0	<225

the basic polygons. Thematic management of data is easier than manual management.

- Cropland evaluation was scripted with SML (simple micro language of ArcInfo) and Foxbase, to calculate the cropland classes automatically.
- A cropland classes map was created by programming with SML according to the guide to cropland evaluation issued by Shaanxi Province. Three categories and 25 types of table were also created automatically.

In order to avoid creating many erroneous new small polygons due to 'gaps' and 'slivers' (Burrough 1986) when overlaying two, or more, vector GIS data sources, we developed a new method, which is based on the selection of primary, secondary and

Table 3. An example set of the database for 10 polygons. The score of the 15 parameters (here called A1 to A15) results from the criteria and weighting introduced in Table 1. The final score, class and subclass are derived from Table 2.

Bnd	Poly#	LU	A1	A2	A3	A4	A5	A6	A7	A8	A9	A10	A11	A12	A13	A14	A15	Score	Class-Subclass
403	38-2	146	3200	530	1150	3	3	55	5	7	9	9	0	0	4500	1	0	289	VII-14
403	51-0	144	3200	530	1150	5	5	80	9	8	9	9	0	0	4500	1	0	349	VII-13
402	37-1	145	3100	540	1150	9	9	95	7	8	9	9	0	0	4500	1	0	395	VI-12
403	1-4	145	3300	530	1150	9	9	95	7	9	9	9	0	0	4500	1	0	408	VI-11
403	7	145	3300	530	1150	9	9	95	7	10	9	9	0	0	4500	1	0	408	VI-11
401	60	145	3200	540	1150	9	9	95	7	12	9	9	0	0	4500	1	0	413	VI-11
401	61-1	145	3200	540	1150	9	9	95	7	12	9	9	0	0	4500	1	0	413	VI-11
402	39	145	3200	540	1150	9	9	95	7	12	9	9	0	0	4500	1	0	413	VI-11
402	15-1	211	3200	540	1150	7	7	95	7	8	9	9	0	0	1000	1	0	413	VI-11
401	25	135	3200	540	1150	7	7	95	7	10	9	9	0	0	500	1	0	432	VI-11

bnd = administrative area code; poly# = no of the polygon of the parcel map; LU = code of land use

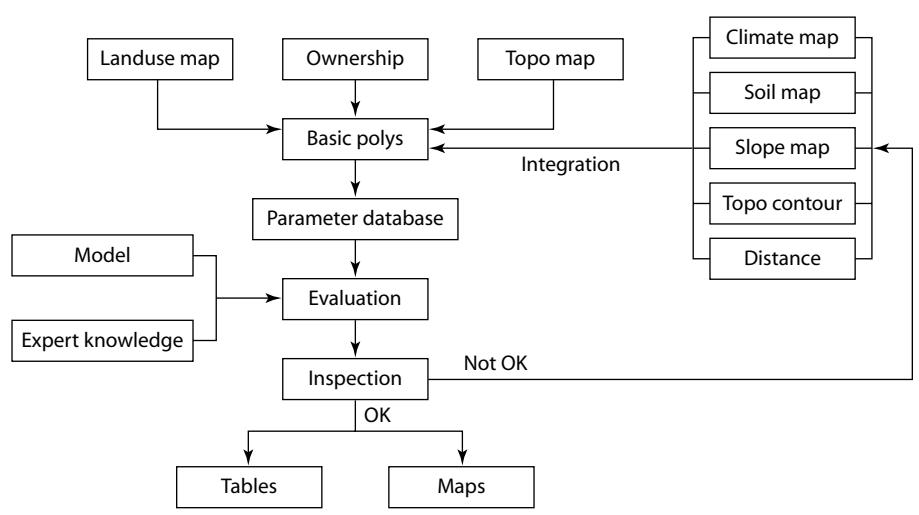

Figure 2. Flow chart of the development of the basic map unit for the land evaluation, the data used in generating the score and the inspection decision point. If the GIS-based land evaluation score, and hence the resulting class and subclass stratification, is deemed not okay, then the process cycles to reviewing the input data.

subsequent data layers in the GIS overlay process. In Figure 3, the upper two data layers are inputs to be overlapped, the primary layer is the top layer and the secondary layer the one below. The top layer has two attributes (A and B); the second layer also has two attributes (a and b). The attributes and areas are shown in 1.pat and 2.pat, respectively. The third layer is the result of overlaying the two input layers; this results in four polygons, which have attributes Aa, Ab, Ba and Bb, as shown in 3.pat. In 3.pat the spurious new polygons (Ab and Ba) are probably the result of slight misregistration of the vectors used in the two input data sets. In the lower data layer, the boundary from the primary data and the area of the resulting sliver polygons are used to assign the slivers to one of the two primary map units (see 4.pat). In addition to misregistration, there are instances where it is unnecessary or impossible for cartographers to locate the same geo-entity with the same geographic coordinates. This may be due to different input data layers being produced by different mapping programs having slightly different, though related, thematic classes and these having different positional accuracies.

We extracted the parameters from a group of thematic maps, including those for slope, cumulative air temperature, precipitation, soil, soil organic matter, topographic shape, road network and village boundary. After entering the values into ArcInfo, we mapped the field data and other parameters, such as soil depth, texture, salinity, water-holding capacity and pollution, the state of irrigation and the location. The data were inserted into a common GIS, and each of the digital maps was projected using the Gauss–Krug projection — the official projection used in China for scales between 1:10,000 and 1:500,000. The land evaluation was programmed according to the method shown in Tables 1 and 2, with Equation 2,

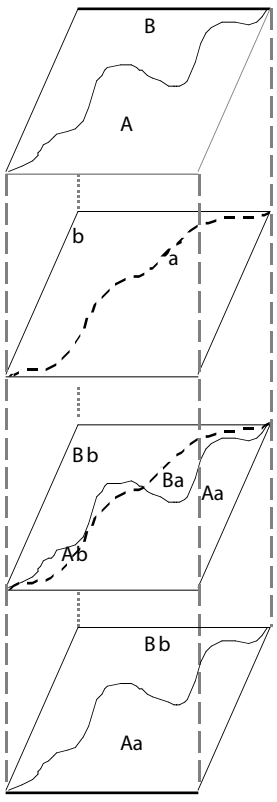

1.pat

1_ID	ATTa	AREA
1	A	20
2	B	20

2.pat

2_ID	ATTb	AREA
1	a	23
2	b	17

3.pat

3_ID	1_ID	ATTa	2_ID	ATTb	AREA
1	1	A	1	a	19
2	1	A	2	b	1
3	2	B	2	b	18
4	2	B	1	a	2

4.pat

4_ID	ATTa	ATTb	AREA
1	B	b	20
2	A	a	20

Figure 3. A schematic diagram illustrating the overlay procedure (see text for full details). The spatial data are denoted 1 to 4 from top to bottom.

using an extension developed in ArcInfo to deal with slivers (Figure 3).

The reliability of the land evaluation was verified by comparing the land evaluation map generated by GIS with the actual situation. The local government land surveyor helped to build a simple expert system, through their independent in situ databases. This allowed us to validate the quality of the data ingested and the approach used (specifically, the weighting values selected) for modelling the GIS-based land evaluation.

Analysis

When assessing cropland for local government, the results should be repeatable, should be practical, and should be obtained using the methods specified by local government. This study meets these three criteria. The need for the assessment to be repeatable and transparent is particularly important in China, because land evaluation is used as the basis for tax rates for farming communities. Thus, farmers on high-quality fertile land adjacent to rivers, possibly with access to irrigation water, are taxed at a higher rate than farmers situated on lands with greater slopes or less fertile soils, and relying on rainwater or water that they haul to their farms.

We found that evaluating cropland using GIS gave results that were both theoretically and technically valid. The results of the evaluation, in either map or tabular format, were consistent with the actual situation for more than 95% of the polygons and are accepted by the farmers and local cadastral recorders. The method, the parameterisation, the mapping and the tabular data all closely followed the Shaanxi Province guide. All results, including maps, tables, and related documents, have been approved by scientists and officers of the Bureau of Land Management and Finance of Shaanxi Province. It is important to note that the results from this study have been endorsed by both the taxpayers (the farmers) and the tax collectors (government officers).

Land evaluation can be used not only for taxation management, but also for estimating grain yields, creating policies for cropland building and improvement, land management, and designing and building a practical land information system.

Discussion

To build a parameter database for a region of China, it is more practical to use a spatial unit than to use soil series or land-type data. This is because China has more traditional cropping systems and technologies than the West, and a much greater degree of spatial, physical and socioeconomic variation. For example, the status of fertiliser use, field management and infrastructure is highly dependent on the distances between the land and the owners, and on transport conditions.

Multithematic map data can be integrated automatically by using GIS overlays and database manipulation. This can be achieved without generating spurious polygons, which can be an issue for GIS research and application (Burrough 1986; McAlpine and Cook 1971; Goodchild 1978; Arbia et al. 1998; Smith and Campbell 1989). A parameter database with multiple items for each polygon can be built efficiently using integration processes. The results of the integration reflect the macro features of environmental factors; errors in the land-evaluation GIS-based model were about 2% of the total number of base polygons (Table 4). Producing maps of 98% accuracy is acceptable to policy makers involved in land-evaluation assessment to decide farmer taxation levels. Parameterisation and evaluation can be programmed and integrated with GIS; the evaluation method has been automated and is hence repeatable.

Conclusion

Information technology can be useful in managing land resources, but is in the early stages of development. It is time consuming to digitise land data (maps), and problems with raw data must be

Table 4. Differences in overlaying, shown as both m^2 and % area of the base map.

	Area (m^2)		Difference	
Accumulated temperature	In base map	In attribute map	Area (m^2)	%
3300	7,944,437	7,797,598	146,839	1.85
3400	11,547,616	11,488,230	59,386	0.51
3500	5,596,422	5,480,886	445,536	2.06

overcome when entering them into the GIS. These include maintaining accurate metadata, geometrically matching maps from different data sources; and keeping track of the temporal changes in GIS data sets. Many of these issues are areas of active research, and practical tools are starting to become available to operational users of GIS technology.

More research is needed on how to handle errors introduced during overlay processing through the removal of spurious polygons. There is also a need to assess the sensitivity of the final results by reducing the number of input GIS data layers from 15 to about four or five (hence simplifying the model). If the results are similar, then the method developed here can be more easily translated to other counties in the Loess Plateau, as the input data requirements will better match the regional data availability.

Acknowledgments

Financial support was provided by ACIAR and by the Bureau of Land Managment of Xian Yang City, Shaanxi Province, PRC.

References

Arbia, G., Griffith, D. and Haining, R. 1998. Error propagation modelling in raster GIS: overlay operations. International Journal of Geographical Information Science, 12, 2, 145–167.

Burrough, P.A. 1986. Principles of Geographical Information Systems for Land Resources Assessment. Oxford, Clarendon Press.

Committee of the Land Detail Survey of Shaanxi Province 1987. Guide of the land detail survey of Shaanxi Province, Xi'an.

FAO (Food and Agriculture Organization) 1976. A framework for land evaluation. Soils Bulletin 32, FAO, Rome.

Goodchild, M.F. 1978. Statistical aspects of the polygon overlay problem. In: Dutton, G., ed., Harvard Papers on Geographic Information Systems, 6, Addison-Wesley Reading, Mass.

Klingebiel, A.A. and Montomery, P.H. 1961. Land-capability Classification of the United States Department of Agriculture (USDA) Agriculture Handbook 210. Soil Conservation Service. USDA, Washington, DC.

McAlpine, J.R. and Cook, B.G. 1971. Data reliability from map overlay. In: Proceedings of the Australian and New Zealand Association for the Advancement of Science, 43rd Congress, Brisbane, May. Section 21—Geographical Science.

Office of the Land Detail Survey of Changwu County 1994. The land resources in Changwu County. Changwu, 1994–6.

Shi Yulin 1982. Guide of the land resources mapping at 1:1,000,000 in China. Journal of Natural Resources.

Smith, J.W.F. and Campbell, I.A. 1989. Error in polygon overlay processing of geomorphic data. Earth Surface Processes and Landforms, 14, 703–717.

Yang Qinke, Song Guiqin, and Li Rui 1985. The mapping and discussion of basic polygon—a case study in Chang area. Bulletin of Soil and Water Conservation, 13, 5, 34–38.

Zhang Qifan (ed.) 1994. The theory and practice of the cropland evaluation. Xi'an Map Press, Xi'an.

24 Environmental Indicators and Sustainable Agriculture

Joe Walker*

Abstract

This chapter looks at how indicators can be used to assess agricultural sustainability. Indicators are biophysical, economic and social attributes that can be measured and used to assess the condition and sustainability of the land from the farm to the regional level. Reliable indicators provide signals about the current status of natural resources and how they are likely to change. They can be used to confirm that current farming practices and land-use systems are effective in maintaining the resource base or economic status, identify problems and highlight potential risks. Indicators provide useful information for initiating change or deciding on future on-ground investments.

本文论述健康诊断指标如何应用于农业持续能力的评价。诊断指标是可以量测的生物物理和社会经济特征，用来评价从单个农场到整个地区不同尺度的土地状况和持续发展能力。可靠的诊断指标能体现自然资源的当前状态，及其可能产生的变化。可用于辨别现行的农业生产活动和土地利用系统能否有效维持资源或经济发展水平，确认存在的问题，突出潜在的危机。它能为土地利用方式的修正和未来的土地投资决策提供有用信息。

FARMING practices are changing the environmental resource base. Some changes are for the better (e.g. organic farming), but many are deleterious and could endanger future agricultural activities. Rural and urban environmental changes caused by various human activities, not just farming, are increasingly felt, raising perceptions of the environmental costs of these activities. For example, in the cities, people experience poor air quality; some rivers and beaches are no longer fit for recreational use; and valued natural areas have been lost to suburban and industrial development. Farmers and rural inhabitants have seen soil loss through wind and water erosion; they are aware of areas that can no longer be farmed because of crop and pasture decline, and gully development in saline areas.

Observation of environmental deterioration in farmed areas is not a recent phenomenon.

* CSIRO Land and Water, PO Box 1666, Canberra, ACT 2601, Australia. Email: joe.walker@csiro.au

Walker, J. 2002. Environmental indicators and sustainable agriculture. In: McVicar, T.R., Li Rui, Walker, J., Fitzpatrick, R.W. and Liu Changming (eds), *Regional Water and Soil Assessment for Managing Sustainable Agriculture in China and Australia*, ACIAR Monograph No. 84, 323–332.

Australian farmers in the early 20th century noticed changes that were detrimental to productive agriculture such as an increase in unpalatable grasses and weeds, the advent of saline flows in previously fresh creeks and streams, the need for increased ploughing to retain a tilth in fallowed paddocks and a decline in crop yields and animal production. The signs were there, both visually and in quantifiably reduced yields.

Visible undesirable changes in the condition of the atmosphere, land and water are 'indicators' of degradation brought about through changes in environmental processes resulting from human activity. The changes may be due to the introduction of new processes (e.g. the addition of pesticides to the soil) or to increases or decreases in existing processes (e.g. more recharge leading to rising watertables in Australia and reduced recharge leading to falling watertables in parts of China). Visual indicators such as soil surface crusting, sheet and gully erosion, and stream and river turbidity have alerted us to problems. Thus, we have been using environmental indicators in agriculture for a long time and the concept is nothing new. However, there has recently been greater recognition of the role that indicators of environmental change could have in assessing and monitoring the effect of land use on natural resources. Indicators can be a powerful means for those managing the land to identify potential problems and assess the effect of their management practices on ecosystems (Walker and Reuter 1996; SCARM 1993; US National Research Foundation 2000; Pykh et al. 1999). Provided that indicators are meaningful to a range of users, from farmers to policy makers, they can help to achieve sustainable agriculture. However, indicators must be selected and used carefully if they are to be effective.

Farmers have long used indicators to decide on changes to farm practice. An obvious next step is to develop a more standard, yet simple, way of recording and assessing environmental change that can have immediate application at the farm and catchment levels. Farmers are already 'production literate' but they also need to be 'environmentally literate'. The two literacies working together can help ensure a sustainable future for agriculture.

How Can We Define Indicators?

Indicators are a subset of the many possible attributes that could be used to quantify the condition of a particular landscape, catchment or ecosystem (Walker 1998). They can be derived from biophysical, economic, social, management and institutional attributes, and from a range of measurement types. Indicators have been defined as 'measurable attributes of the environment that can be monitored via field observation, field sampling, remote sensing or compilation of existing data' (Meyer et al. 1992). Ideally, each indicator is precise and accurate in describing a particular process within the environment and will serve to signal undesirable changes that have occurred or that may occur (Landres 1992).

Researchers distinguish several types of indicators. For example, 'compliance indicators' identify deviation from previously defined conditions, 'diagnostic indicators' identify the specific cause of a problem and 'early warning indicators' signal an impending decline of conditions (Cairns and McCormick 1992). It is important to define the purpose of indicators and to select them on the basis of how well they can fulfil the required role.

Indicators are perhaps best viewed as communication tools that can turn scientific knowledge into a form better understood by a range of community groups, policy makers and others (Walker et al. 1996). Questions have been raised about the credibility of indicators for resource assessments, but this applies only if indicators are poorly selected. In selecting indicators it is necessary to look at certain criteria such as reliability, interpretability, data availability, established threshold values (needed to set class boundaries) and known links to processes (Walker and Reuter 1996;

Jackson et al. 2000). There are better grounds to question the aggregation of indicators into an index (e.g. catchment health rating) or subindex (water quality), since this involves the addition of disparate measures, usually in a simplistic way. Fuzzy approaches (Roberts et al. 1997) offer a possible means to be mathematically correct, but the interpretation of any given index is still an issue.

Steps in Using Environmental Indicators

Indicator development starts with defining a problem — identifying the issues and their value to society. We then ask questions to specify the issues more clearly. This involves making balanced and integrated judgments on the economic, social and environmental condition of a region's rural enterprises (SCARM 1998). The next step is to choose attributes to use as indicators; for example, current condition (or status) and the direction and magnitude of any change in condition. Certain indicators will be influenced by changes in other indicators, and these interactions must be taken into account.

Questions that could be used to determine the specific issues, for example for the grains industry, are:

- Where is farm productivity falling and the natural resource base declining?
- Where is farm productivity increasing or stable and the resource base stable?
- Where is farm productivity improving and the natural resource base declining?

These questions can be asked at individual paddock, catchment and region scales. By using different sets of indicators to answer these questions and by analysing the responses, an assessment report can be produced. If the report shows that current farming practices are having detrimental impacts on the resource base, it can be used as the basis for remedial action. Indicators can then be used to monitor the outcomes of whatever action is taken. These steps are depicted in Figure 1.

Many of the chapters in this book illustrate the use of indicators in summarising research knowledge. This section examines various issues involved in selecting suitable indicators of catchment and farm health, and in developing appropriate monitoring programs.

Interpreting Indicators at Different Scales

Different spatial scales often require different questions to be asked, requiring different indicator sets and thresholds (Walker et al. 2001). Table 1 illustrates the different kinds of questions asked at different scales. Table 2 lists some of the indicators that are relevant at particular scales. They include single indicators (e.g. soil nitrogen), composite indicators (e.g. cropping on steep slopes as an estimate of erosion risk) and aggregated indexes (e.g. soil moisture index or soil fertility indexes).

Data collected in farm surveys can be aggregated and reported at regional and even national level, provided that sampling intensity and measurement quality are adequate and the indicators reflect regional or farm diversity.

At the national and State scale (Table 1) the interest is mainly on policy development and identifying 'hot spots' that require immediate attention. 'State of environment' reporting at the national and State levels are examples. The approach is 'top-down': the initiative is taken by people from State and national bodies and the results handed over for implementation. The data used are generally readily available data with little attempt to collect detail. These issues are discussed more fully in Chapter 26.

Indicators for regional or local government/ provincial scales could also refer to a particular sector, reflecting concerns about the production and

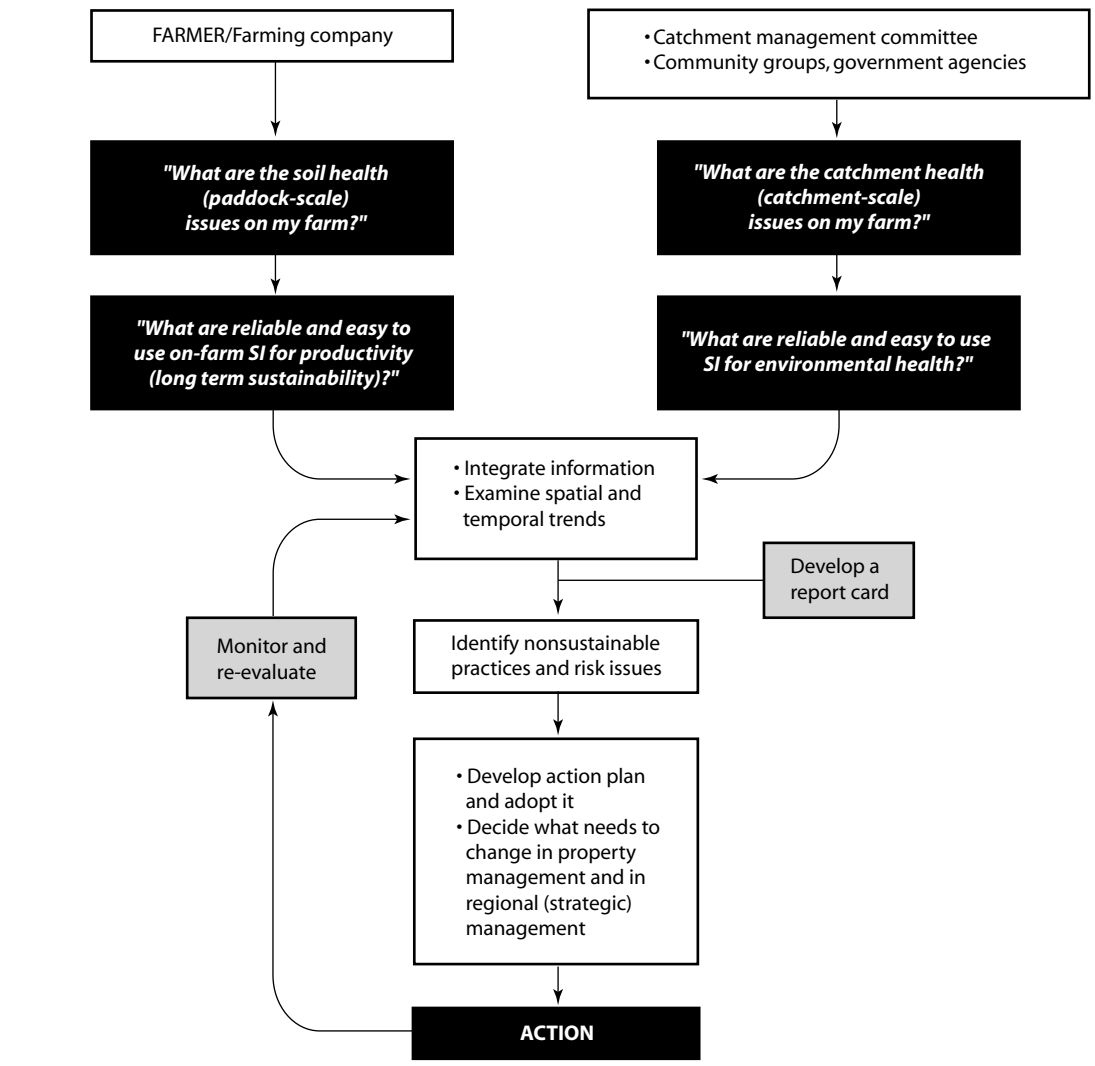

Figure 1. A logical decision tree for using sustainability indicators (SI).

economic future of a region. Examples of the kind of information available for indicator development at this scale are given in Section 3 of this Volume.

At the farm level, questions refer to specific management problems — how to identify undesirable changes and what action to take. The approach is 'bottom-up', with emphasis on self-help. The focus is on changing practices at the paddock scale in a way likely to improve farm and catchment health. Examples in this book are found in Chapters 21 and 28.

A Structured Approach to Using Sustainability Indicators

Indicators must be relevant, robust and scientifically defensible. There is little point in using indicators that have known weaknesses or that cannot be interpreted reliably. For example, mean soil worm density is difficult to interpret because of regional and seasonal variability; mean soil pH has little meaning at a catchment scale but is useful at a farm scale or for a particular soil landscape. We need to set criteria against which the merits of an indicator can be judged — for example, by rating

Table 1. The categories of questions asked at different scales.

National scale	Regional/catchment scale	Farm/site scale
Top-down approach	Top-down approach	Bottom-up approach
Purpose of indicators		
National/State assessment	← Two-way linking process → Social–economic–natural resources	Site assessment
Socioeconomics (resource economics)		Socially acceptable economic choices
Policy development		On-ground action
Agricultural sustainability		Condition of the land (paddock)
State of environment (SoE) reporting		Assessing trends for a farm
Agricultural production		Whole environment/conservation urban/rural links
Indicator programs or groups interested in using them		
• DEST (SoE reporting) • State SoE reporting • SCARM (sustainability program) • ABARE (Outlook conference) • ABS (national statistics) • Research and development corporations such as LWRRDC, GRDC and RIRDC • State EPAs	• CALP boards • Regional land management boards • MDBC • State water/land/agriculture departments • NLP • Indicators of catchment health developed by CSIRO • ALGA • ABARE	• Farmer groups • Farm planning groups • Land care groups • Providers of extension services • ACF/SAWCAA • Streamwatch • Waterwatch • Farm 500
Questions		
1. How degraded are Australia's natural resources? 2. Where are the urgent problems? 3. How sustainable are our agricultural practices? 4. What are the broad trends in costs versus profits for agricultural enterprises? 5. What policies can be developed to encourage sustainable agriculture?	1. How can production, quality of life and profits be increased? 2. What methods need to be developed to better manage natural, social and economic resources? 3. What effects are agricultural practices having on natural, social and economic resources? 4. What impacts are social and economic events having on resource management?	1. How can I best manage my farm? 2. How can I make a living on my farm? 3. What sort of life can I have? 4. How can I assess land and water health on my farm? 5. How much will it cost to fix a biophysical/resource depletion problem?

ABARE = Australian Bureau of Agriculture and Resource Economics; ABS = Australian Bureau of Statistics; ACF = Australian Conservation Foundation; ALGA = Australian Local Government Association; CALP boards = catchment and land protection boards; DEST = Department of the Environment, Sport and Territories; EPA = environmental protection agency; GRDC = Grains Research and Development Corporation; LWRRDC = Land and Water Resources Research and Development Corporation; NLP = National Landcare Program; MDBC = Murray–Darling Basin Commission; RIRDC = Rural Industries Research and Development Corporation; SAWCAA = Soil and Water Conservation Association of Australia; SCARM = Standing Committee on Agriculture and Resource Management; SoE = State of environment

Table 2. Examples of linkages between issues, sustainability indicators and scales.

Scale	Issue	Sustainability indicator
National	Average real net farm income Access to key services	Farmer's terms of trade Distance to regional centres
State	Health of river basins	Trends in water quality
Agricultural industry	Meeting commodity market specifications Farmer's skills	Trends in silo protein levels for wheat % farmers using property management plans
Region	Health of rural environments	% land affected by salinity Condition and extent of native vegetation
Catchment	Meeting water quality targets	Trends in water quality % area with protected riparian vegetation
Farm	Optimising farm returns Planning the annual farm business	Disposable income per family Forecast trends in commodity prices
Paddock	Yield performance Soil health assessment	% potential yield or $ water use efficiency Reliable soil tests

each indicator in terms of relevance, ease of capture and reliability. Table 3, which broadly follows Jackson et al. (2000) and Walker et al. (2000), summarises the criteria for selecting reliable sustainability indicators.

Threshold guidelines for resource condition

Figure 2 shows how a hypothetical resource indicator in an agroecosystem might change with time. Initially, sample values vary within accepted thresholds. For example, even if a system has been changed from a natural to a managed agroecosystem, it may be performing within acceptable limits. Such a system is considered stable (e.g. not leaking nutrients or water to streams or groundwater systems) within the set thresholds. This is the concept of 'conditional stability' developed by Walker (1999). In later years, values may move outside threshold limits. For example, increased electrical conductivity could signal increasing salinity in soil or streams, or decreased soil nitrogen levels could indicate nutrient depletion under intensive cropping regimes. The main problem is in setting threshold values that apply nationally. Some thresholds are well defined (e.g. some water quality measures are related to human health), but values are more difficult to set in landscapes and catchments. Values are known to vary regionally and thresholds vary with spatial scale. This variability makes the idea of setting environmental targets difficult to define absolutely.

A suite of indicators is needed to examine changes in resource condition. For example, commercial soil sampling services offer clients multiple tests on each sample submitted. The results can then be

Table 3. Challenges for selecting reliable sustainability indicators (SIs).

Criteria	Challenges
Reliability	Is a standard method available to measure the SI?
	Are low errors associated with measurement?
	Is the SI measurement stable?
	Can the SI be interpreted and ranked reliably?
	Does the SI respond to change or disturbance?
	Is the SI accepted by farming communities?
Data capture and cost	Can SI data be easily captured?
	Is the data capture at low cost?
	Does the SI need to be monitored regularly?
Ranking and assessment	Can the SI data be mapped or graphed?
	Can SI assessments be integrated soundly in space and time?
	Do previous SI data exist?

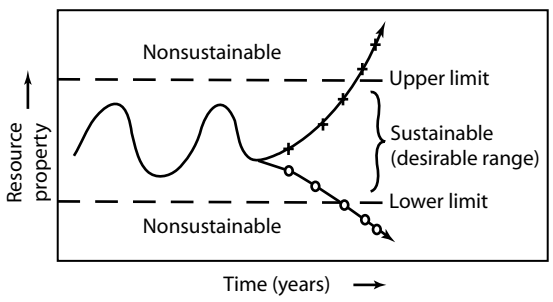

Figure 2. Conceptual diagram showing the requirement for validated upper and lower limits to assess temporal trends (A, B) in a resource property (indicator values) (Reuter 1998).

compared to relevant guidelines[1] and used to summarise trends. Farmers and their advisers can carry out these tests themselves at relatively low cost using practical 'do-it-yourself' test kits. Kits are available through the Western Australian Farm Management Society and Charles Sturt University. Rengasamy and Bourne (1997) have also developed a kit for assessing soil salinity, acidity and sodicity.

[1] For example, there are Australian guidelines for interpreting soil (Peverill et al. 1999), plant (Reuter and Robinson 1997) and water quality tests for assessment of stream condition (Ladson and White 1999).

Benchmarking farm business health

The Australian Bureau of Agricultural and Resource Economics (ABARE) has defined economic indicators of farm performance (ABARE 1999). These are derived as complex national or industry indexes, or estimated from aggregated data from various sources such as annual ABARE farm surveys, the Australian agricultural census and agricultural financial surveys from the Australian Bureau of Statistics (ABS). ABARE and ABS publish regular updates showing trends for economic indicators.

Dealing with large annual variations

When there are large annual variations in indicator values, it is important to know the trends over time. Many economic indicators, such as disposable income per family or profit at full equity, vary greatly from year to year through the combined effects of seasonal weather conditions, shifts in commodity prices and other market forces (e.g. interest rates). For these indicators, trends in data, acquired annually, should be assessed at constant dollar value over several years or decades to understand the magnitude and direction of longer term changes. The impact of rainfall on economic indicators can be partly circumvented by expressing data in units of

rainfall received in any given season — the so-called dollar water use efficiency ($WUE) indicator.

National assessments of sustainable agriculture

The Standing Committee on Agricultural Resource Management (SCARM) published a series of reports during the 1990s. These culminated in a pioneering but incomplete report on the assessment of sustainable agriculture in Australia's 11 agroecological zones. Initially, 'sustainable agriculture' was defined and guiding principles were developed for assessing the level of sustainability achieved by the agricultural sector (SCA 1991). Subsequently, an indicator framework was devised for making these assessments (SCARM 1993). A pilot feasibility study was undertaken to evaluate the validity and availability of data for these indicators (SLWRMC 1996). A final report (SCARM 1998) documented the data and trends. Table 4 lists the indicators used by SCARM to assess sustainability in Australian agriculture. It also lists possible indicators that were not identified in the report but are now acknowledged to be important for a complete assessment of sustainable agriculture in Australia. Some of these indicators are now used in the National Land and Water Resources Audit.

Comparing Different Condition or Sustainability Assessments

It is often useful to compare agricultural performance with catchment condition or with other indexes (e.g. economic or social indexes). Figure 3 shows a cross-comparison matrix of ranked assessments of farm production and ranked assessments of catchment condition. The focus in the figure is on combinations that do not conform to expected (i.e. the diagonal). For example, if a

Table 4. Composite indicators and attributes used by SCARM (1998) to assess sustainability in Australian agriculture, together with some additional attributes required for a more complete assessment.

SCARM indicators	Attributes assessed by SCARM (1998)	Attributes not assessed by SCARM (1998)
Long-term real net farm income	• Real net farm income • Total factor productivity • Farmer's terms of trade • Average real net farm income • Debt servicing ratio	• Costs of land degradation • Costs and benefits from remediating degraded resources • $ water use efficiency (for rainfed and irrigated farms)
Natural resource condition	• Phosphate and potassium balance • Soil condition: acidity and sodicity • Rangeland condition and trend • Diversity of agricultural plant species • Water use by vegetation	• Nitrogen and sulfur balances • Extent of soil structural decline • Level of groundwater reserve exploitation • Extent of land salinisation • Assessment of catchment condition
Off-site environmental impacts	• Chemical residues in products • Salinity in streams • Dust storm index • Impact of agriculture on native vegetation	• Impacts of soil erosion on river water quality • Extent of nonreserve native vegetation on farms
Managerial skills	• Level of farmer education • Extent of participation in training and Landcare • Implementation of sustainable practices	• Adoption by industry of best management practices • Extent of farmer access to the internet
Socioeconomic impacts	• Age structure of the agricultural workforce • Access to key services	• Capacity of rural communities to change • Extent of diversification within rural regions • Extent to which current infrastructure, policies and laws support sustainable agriculture

catchment is biophysically in poor condition and production is high, the system is probably maintained by high inputs of fertiliser and may not be environmentally sustainable. The matrix, which was developed by Walker et al. (2000), is not meant to show causal relationships, but suggests where more investigation is needed. It is particularly useful in broadly comparing biophysical indexes with production, economic and social indexes and in interpreting sustainability at catchment and regional scales. The matrix is based on a list of core indicators for benchmarking economic and resource health within catchments (Walker and Reuter 1996). The initial list was drawn up in 1996; other indicators were added following a national workshop (see Table 3 in Reuter 1998).

Conclusion

Most programs involved in monitoring and assessing environmental condition are ultimately associated with issues of sustainability. The word 'sustainability' has many connotations, including longevity, continuity, function and stability. There are thus different questions to ask and different approaches available. Process-based models have a place and also have limitations; so do indicators. Process-based models, as illustrated in other chapters in this book, can be useful to develop a range of scenarios, but in the context of indicators they can be particularly useful in setting workable threshold values. Unfortunately, many process modellers and reductionist scientists have relegated environmental indicators to the soft sciences, little

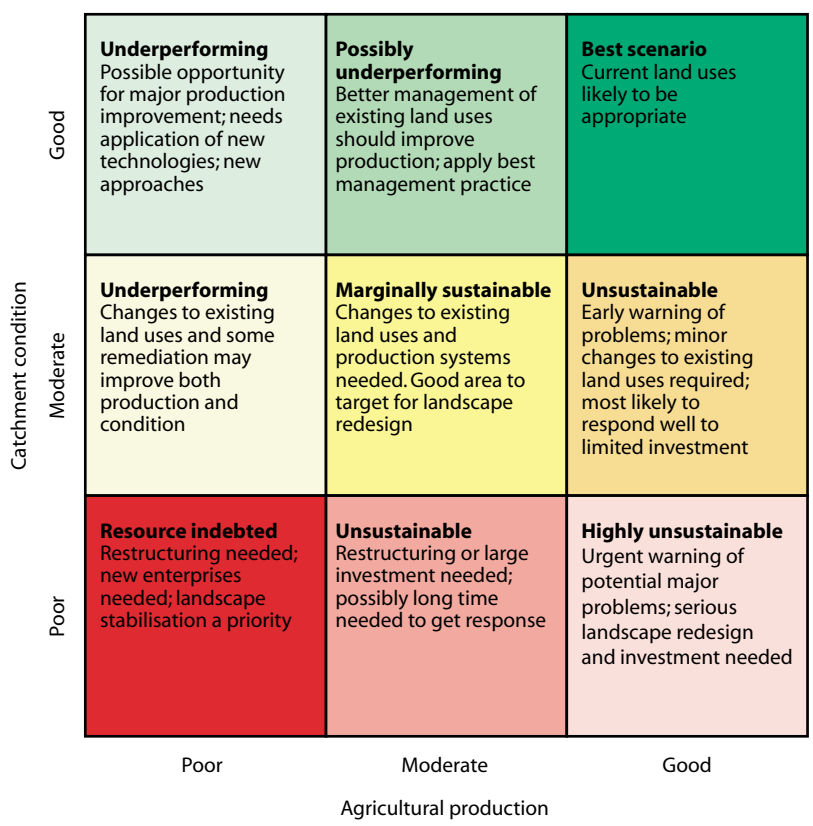

Figure 3. Possible interpretation of the catchment condition–agricultural production cross-comparison matrix.

realising that indicators have a process base. This attitude is usually based on ignorance about the derivation and use of indicators. The establishment of the new journal *Environmental Indicators*[2] will help to establish indicators as a credible systems approach to sustainability issues.

References

ABARE (Australian Bureau of Agricultural and Resource Economics) 1999. Performance indicators for the grains industry. In: Australian Grains Industry Performance by Grains Research and Development Corporation Agroecological Zones, 15–21.

Cairns, J. and McCormick, P.V. 1992. Developing an ecosystem-based capability for ecological risk assessments. The Environmental Professional, 14, 186–96.

Jackson, L.A., Kuartz, J.C. and Fisher, W.S. 2000. Review of EPA evaluation guidelines for ecological indicators. EPA/600/3-90/060.

Ladson, A.R. and White, L. 1999. An index of stream condition: reference manual. Victoria, Waterways Unit Department of Natural Resources and Environment.

Landres, P.B. 1992. Ecological indicators: panacea or liability? In: McKenzie, D.H., Hyatt, D.E. and McDonald, V.J., eds, Ecological Indicators, Vol. 2. New York, Elsevier Applied Science, 1295–318.

Meyer, J.R., Cambell, C.L., Moser, T.J., Hess, G.R., Rawlings, J.O., Peck, S. and Heck, W.W. 1992. Indicators of the ecological status of agroecosystems. In: McKenzie, D.H., Hyatt, D.E. and McDonald, V.J., eds, Ecological Indicators, Vol. 2. New York, Elsevier Applied Science, 628–58.

Peverill, K.I., Sparrow, L.A. and Reuter, D.J. 1999. Soil Analysis: an Interpretation Manual. Melbourne, CSIRO Publishing.

Pykh, Y.A., Hyatt, D.E. and Lenz, R.J.M., eds 1999. Advances in Sustainable Development: Environmental Indices Systems Analysis Approach. Oxford, EOLSS Publishers.

Rengasamy, P. and Bourne, J. 1997. Managing sodic, acid and sodic soils. Co-operative Research Centre for Soil and Land Management SAS 8/97, Adelaide.

Reuter, D.J. 1998. Developing indicators for monitoring catchment health: the challenges. Australian Journal of Experimental Agriculture, 38, 637–48.

Reuter, D.J. and Robinson J.B. 1997. Plant Analysis: An Interpretation Manual, 2nd edition. Melbourne, CSIRO Publishing.

Roberts, D.W., Dowling, T.I. and Walker, J. 1997. FLAG: A Fuzzy Landscape Analysis GIS Method for Dryland Salinity Assessment. CSIRO, Land and Water Technical Report 8/97, Canberra, July 1997.

SCA (Standing Committee on Agriculture). 1991. Sustainable Agriculture. SCA technical report series No. 36. Melbourne, CSIRO Publishing.

SCARM (Standing Committee on Agricultural and Resource Management) 1993. Sustainable Agriculture: Tracking the Indicators for Australia and New Zealand. Melbourne, CSIRO Publishing.

SCARM 1998. Sustainable Agriculture: Assessing Australia's Recent Performance. Melbourne, CSIRO Publishing.

SLWRMC (Sustainable Land and Water Resource Management Committee) 1996. Indicators for Sustainable Agriculture: Evaluation of Pilot Testing. SLWRMC, April.1996, CSIRO Publishing.

US NRC (National Research Council). 2000. Ecological Indicators for the Nation. Washington, DC, National Academy Press, 180 pp.

Walker, J. 1998. Environmental indicators of catchment and farm health. In: Williams, J., Hook, R.A. and Gascoigne, H.L., eds, Farming Action Catchment Reaction: the Effects of Dryland Farming on the Natural Environment. Melbourne, CSIRO Publishing, 99–117.

Walker, J. 1999. Conditional health indicators as a proxy for sustainability indicators. In: Pykh, Y.A., Hyatt, D.E. and Lenz, R.J.M., eds, Advances in Sustainable Development: Environmental Indices a Systems Analysis Approach. Oxford, UK, EOLSS Publishing Co. Ltd, 349–362.

Walker, J. and Reuter, D.J. (eds) 1996. Indicators of Catchment Health: A Technical Perspective. Collingwood, Victoria, CSIRO Publishing.

Walker, J., Alexander, D., Irons, C., Jones, B., Penridge, H. and Rapport, D. 1996. Catchment health indicators: an overview. In: Walker, J. and Reuter, D.J., eds, Indicators of Catchment Health: A Technical Perspective. Melbourne, CSIRO Publishing, 3–18.

Walker, J., Veitch, S., Braaten, R., Dowling, T., Guppy, L. and Herron, N. 2000. Catchment Condition in Australia: an Assessment at the National Scale. A discussion paper for the National Land and Water Resources Audit (Project 7/8).

Walker, J., Veitch, S., Braaten, R., Dowling, T., Guppy, L. and Herron, N. 2001. Catchment Condition in Australia. Final Report to the National Land and Water Resources Audit, November, 2001.

[2] www.elsevier.com/locate/ecolind

25 Testing Readily Available Catchment-Scale Indicators as Measures of Catchment Salinity Status

Joe Walker,[*] Trevor I. Dowling,[*] Bruce K. Jones,[†] D. Peter Richardson,[*] Kurt H. Riitters[‡] and James D. Wickham[§]

Abstract

This study compares a biophysical index of catchment salinity status based on readily available indicators with field measures of stream salinity. It also looks at the time required to compile a data set from readily available data, and whether meaningful results can be obtained from averaged data for third-order catchments. The catchments studied form the entire Upper Murrumbidgee catchment (approximately 12,000 km^2).

The study outlines a systematic approach to selecting relevant, appropriate and readily available indicators. The indicators selected were per cent forest cover, forested areas greater than 50 ha, road density per unit area, per cent agriculture on slopes greater than 5%, number of roads crossing streams/rivers per unit area and the hypsometric integral per catchment. The indicators were compiled and collated in 10 days. The field data comprised stream salt concentration, salt load and two measures of macroinvertebrate group richness—the number of families of macroinvertebrates and the number of families observed compared to the number expected (O/E). The field work required nine months to complete. The biophysical and field indexes were calculated using a simple additive model. The data were placed in three classes using threshold values equivalent to best, intermediate and worst, weighted as 3, 2 and 1 respectively.

Significant relationships were detected between stream salinity and the biophysical index, and between the biophysical and field indexes. A lesser but significant relationship was detected between O/E biota and the biophysical index. These relationships suggest that the readily available data ranked the salinity status of the catchment in a credible way. We suggest that coarse-scale data are grossly undervalued in developing comparative scenarios; indicators carefully selected from readily available data can be used to quickly derive big picture scenarios.

[*] CSIRO Land and Water, PO Box 1666, Canberra, ACT 2601, Australia. Email: joe.walker@csiro.au

[†] Environmental Sciences Division, US Environmental Protection Agency, EMSL, Las Vegas, Nevada, United States.

[‡] Biological Resources Division, US Geological Survey, Knoxville, Tennessee, United States.

[§] Environmental Research Center, Tennessee Valley Authority, Historic Forestry Building, Norris, Tennessee, United States.

Walker, J., Dowling, T.I., Jones, B.K., Richardson, D.P., Riitters, K.H. and Wickham, J.D. 2002. Testing readily available catchment-scale indicators as measures of catchment salinity status. In: McVicar, T.R., Li Rui, Walker, J., Fitzpatrick, R.W. and Liu Changming (eds), *Regional Water and Soil Assessment for Managing Sustainable Agriculture in China and Australia*, ACIAR Monograph No. 84, 333–341.

本文对比了反映流域盐化状况的生物物理指标和反映河流盐分状况的野外量测指标，前者基于从现有资料中选择出来的环境指标，后者由野外测量得到。也讨论了从现有资料中收集整理出一套指标数据所用的时间，以及平均数据能否得到对第三级流域有用的结果。此项研究覆盖了整个默如比基流域的上游地区（约一万两千平方公里）。

作者概述了从现有资料中选择相关、适当的诊断指标的一个系统化的方法。选择的指标有森林覆盖率，面积大于 50 公顷的林地，单位面积的道路密度，坡度大于 5% 的农地比例，单位面积内跨越河流的道路数量，以及每个流域的高程积分。健康诊断指标数据在十天内完成编辑汇总。野外数据包括河流盐分浓度，排盐量和反映大型无脊椎动物群丰度的两个值－－大型无脊椎动物门数及其调察值与预期值的（O/E）的比值。野外作业需九个月完成。生物物理指标和野外量测指标由简单的加法模型计算得出。数据被分为三个等级，其阈值分别相当于好、中、差，权重分别是 3、2、1。

研究发现河流盐分和生物物理指标之间以及生物物理指标与野外量测指标之间有着明显关联。O/E 和生物物理指标间的关联比它们稍弱但仍很明显。这些联系表明简单易得的诊断指标对流域盐分状况的反映可信度很高。我们认为写意式粗线条数据的价值总的来说被低估，在作对比项目中，采用认真挑选的诊断指标，能够快速反映总体轮廓特征。

THE PRIMARY purpose of this study was to investigate the credibility of a stream salinity index based on a small set of easily obtained landscape indicators, by comparing the index with independent measures of stream salinity. The study was also designed to look at the time needed to compile a data set from readily available data, and whether meaningful results could be obtained from averaged data for third-order catchments.

Why use a set of landscape metrics to rate relative salinity risk across a group of catchments when the measurement of salt concentrations in streams is relatively simple? The answer is that there is a major dilemma with salt measurements from streams. The problem is illustrated by Figure 1, in which stream salinity — electrical conductivity (EC) in microSiemens per cm — is plotted against sample time. Figure 1 shows that EC is extremely variable and is related to stream flows: high flows tend to have low salt concentrations and vice versa. The range in salt concentrations can be important; for example, for stream biota and for livestock drinking the water. Given that most streams lack sample points, establishing catchment stream salinity status would require regular sampling over years or even decades.

An alternative measure of salinity risk is salt loads in streams (concentration × volume). In Australian streams, water volumes can vary quickly following rainfall, often in a timespan of hours; stream volume is therefore much more difficult to measure than EC. Sampling across a region can take several days, so it is difficult to sample similar parts of the stream hydrograph (plot of volume against time).

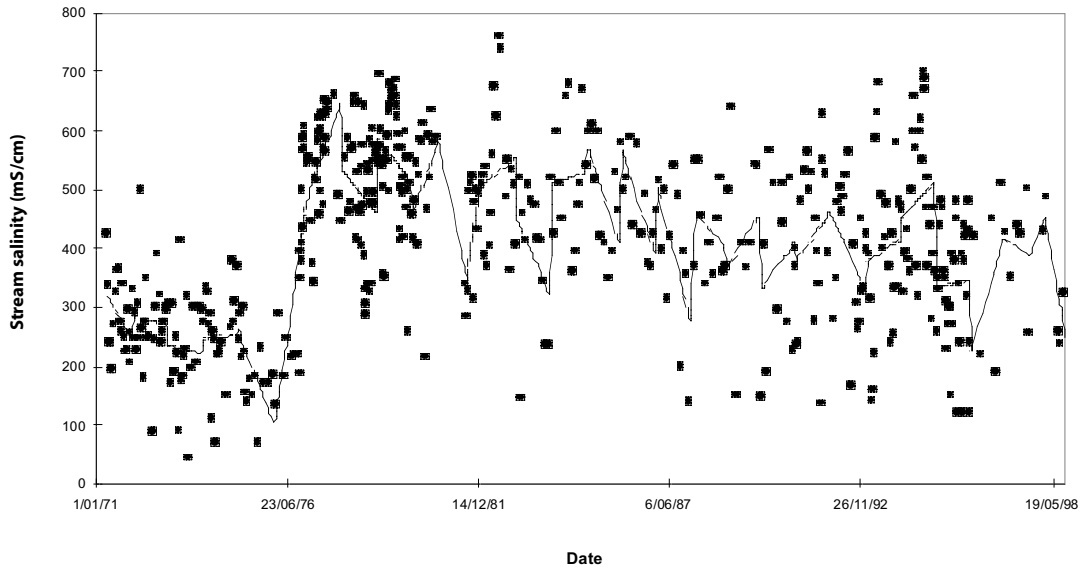

Figure 1. Stream salinity (electrical conductivity, EC) plotted with time for a stream in the Gininderra catchment, Australian Capital Territory (data from Environment ACT).

Accurate measuring of stream EC and volume requires permanent sampling stations and frequent (at least every hour) sampling. Such stations occur primarily on research sites or at the outlets of very large catchments, providing sparse but high-quality data. Dividing a large catchment into contributions from subcatchments can be a problem in the absence of sampling sites in the subcatchments.

We believe that stream salinity status can be assessed with appropriate landscape indicators. In this way, sparse, high-quality data can be complemented by poorer-quality, dense sampling. If the measures selected are the main drivers of the systems, the values obtained can act as benchmarks for further monitoring.

Study Area, Data Collection and Indicators

Figure 2 of the Overview shows the location of the Upper Murrumbidgee catchment. The catchment has a total area of approximately 12,000 km^2 and includes the national capital, Canberra (population 300,000), and the rural centres of Yass and Cooma, each with a population of less than 10,000. Land uses include cropping, extensive livestock grazing, forestry, viticulture, water catchments for the supply of town drinking water, national parks and many small hobby farms. Many areas have been cleared of native forest and woodland vegetation, and this contrasts with other areas that are in pristine condition. Issues identified by local Landcare groups and the Upper Murrumbidgee Catchment Committee include weeds, feral animals, waterlogging, salinity, stream turbidity, soil erosion and water quality.

Walker et al. (2001) and Jones et al. (1997) have suggested a series of steps in developing an indicator approach to resource assessment. These are:

- first identify *societal values*;
- then identify the *specific issue* to examine;
- frame an *assessment question* to address the issue; and
- select *indicators* that address the assessment question.

In this study of the Upper Murrumbidgee catchment, the societal value was good-quality water; the issue was the risk of increasing stream salinity; and the assessment question was 'What is the relative salinity status of catchments in the Upper Murrumbidgee?'

In order to gain an indication of how long it would take to complete a national assessment, a time limit for the study was set at 10 days. Another aim of the study was to determine whether a catchment size of about 500 km^2 could be used to assess catchment condition. The size is typical of catchments used by Landcare groups and as management units for regional planning and management. At an Australia-wide scale, catchments approximately 500–1000 km^2 in area are often third-order catchments and can be explicitly defined from appropriate digital elevation models (DEMs).

The strategy adopted to address the assessment question was as follows:

- identify and collate readily available spatial environmental attributes for the region;
- select indicators from the available attributes according to the criteria (reliability, interpretability, data availability, known thresholds and links to biophysical processes);
- use a simple additive model to calculate an index of salinity status for each catchment (a relative ranking from best to worst (good to bad)); and
- collect independent data on stream salinity and examine the relationship with the catchment condition values (the expectation is that a relationship should exist).

Figure 2 shows the subcatchments used in the study. The Upper Murrumbidgee region was divided into 13 third-order stream catchments defined by the New South Wales Department of Land and Water Conservation from previous and current gauging stations. Catchment No. 8 was larger than the others and subdivision would be desirable. However, only 13 catchments were gauged.

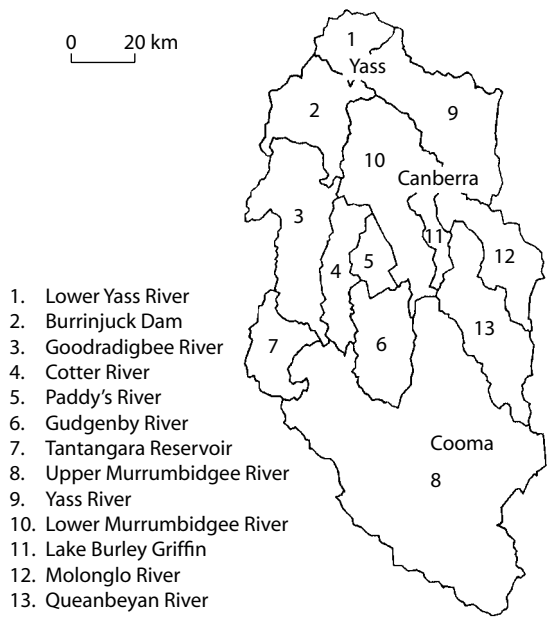

Figure 2. Subcatchments in the Upper Murrumbidgee Region of New South Wales.

Indicators of Catchment Condition

The processes driving salinisation in this region are well understood; they include urban development, tree removal for agriculture, destruction of the riparian buffer and shallow, salty groundwaters. We selected indicators that were linked with these processes and were readily available. The data sources were Thematic mapper satellite imagery,[1] a DEM at 250 m resolution (AUSLIG 1994), and cadastral and land-use information (AUSLIG 1996). The imagery enabled us to identify the major vegetation/land-use types — treed areas (woodland and forest with a projected cover of more than 20%), improved pastures, cropping areas and urban areas. The DEM allowed slope classes and catchment areas to be derived. From the DEM data we calculated two landscape indexes — catchment area and a hypsometric integral. Strahler (1952) defined a hypsometric integral as an area–altitude curve that relates horizontal cross-sectional area of

[1] Provided by Dr Tim McVicar and Lingtao Li, CSIRO Land and Water. See Chapter 16 for specifications of Landsat Thematic mapper.

a drainage basin to relative elevation about the basin mouth. The measure was considered to be related to several catchment processes, including hydrological regime, soil erosion, landscape age and sedimentation. It has seldom been applied or used to interpret catchment processes.

Six indicators collected were used in the analysis. Indicators used were per cent forest cover, per cent forested areas of more than 50 ha, road density per unit area, per cent agriculture on steep slopes (slopes of more than 5%), number of roads crossing streams per unit area and the hypsometric integral. Table 1 shows values for the biophysical indicators.

Classification

The individual indicator values were placed into three classes (thresholds), representing poor, medium and good (red, yellow and green), as illustrated in the example shown in Table 2. For four of the six indicators, the range in values was simply divided into three equal parts. For per cent forest cover, evidence from other studies suggested that classes at < 20%, 20–60% and > 60% were correlated with stream salinity (high to low). The three classes for the hypsometric integral were determined as equal areas under the frequency/value curve obtained from a more extensive study in the region. This classification gave approximately equal numbers of catchments in each class for each indicator (more by chance than design). Maps of classes for individual indicators were drawn using individual indicator values but are not presented here.

Class weightings

Weightings can be carried out in several different ways; similarly, the means to recognise class boundaries and to develop an index can have several variants. Weightings were applied to each of the classes as 1, 2 or 3 (poor, medium or good) and summed for each catchment to give an aggregated

Table 1. Biophysical attributes (indicators) for the catchments.

Catchment number	Road density per unit area	% Forest cover	% Forested > 50 ha	Roads crossing streams	% Agriculture on steep slopes	Hypsometric integral	Biophysical index
1	0.0165	2.99	0.00	0.3181	38.07	0.3787	7
2	0.0136	21.51	1.53	0.1443	46.64	0.2393	9
3	0.0137	72.41	32.20	0.1890	23.46	0.3995	14
4	0.0174	81.75	46.16	0.2695	16.05	0.4312	14
5	0.0169	54.79	17.68	0.1793	37.18	0.3836	12
6	0.0100	61.55	20.58	0.1780	33.41	0.4495	16
7	0.0108	60.99	8.12	0.2059	21.57	0.2916	12
8	0.0156	46.15	14.26	0.1449	28.81	0.3200	12
9	0.0152	13.63	0.17	0.0442	37.13	0.3578	8
10	0.0210	14.91	0.39	0.0598	46.02	0.3028	8
11	0.0282	17.89	0.26	0.0514	34.87	0.2195	9
12	0.0157	35.35	7.45	0.1130	27.96	0.3342	11
13	0.0144	48.57	15.04	0.1618	34.47	0.3853	13

value for its condition, as illustrated in Table 2. Thus, values for catchment biophysical condition ranged from 6 (all indicators poor) to 18 (all indicators good). These catchment ratings were then compared with independent field measures of stream salinity.

Table 1 shows the biophysical index values for the catchments using these threshold values and weightings.

Field Sampling for Stream Salinity and the Biotic Response

We selected four independent measures (termed field indicators) to reflect changes in stream salinity:

- salt concentration (measured as EC at base flow/ discharge);
- salt load (salt concentration × stream base flow); and
- two measures of macroinvertebrate group richness (number of families of macroinvertebrates, and observed over expected number of families).

The measures were for an autumn sample and were taken at the exits of the 13 catchments during a period of base flow some 10 days after a rainfall event. The assessment team collected the data for EC. The Co-operative Research Centre for Freshwater Ecology (University of Canberra) and Environment ACT supplied the data for macroinvertebrates. These data are part of a national study that defined expected values and determined methods for sampling and analysis. One field site was omitted from the analyses (site 2 was sampled at the outlet rather than the inlet of Lake Burley Griffin), because the lake acted as a salt buffer.

The field sampling had to be deferred several times because of variable stream base flows across the catchments, and the need to coincide with the macroinvertebrate sampling. Sampling for EC required two field days, so we had to wait for the right conditions. Table 3 gives the values for the field measures and the field index.

Table 2. Classification of indicators using threshold values. Green indicates good; yellow indicates medium; and red indicates poor. Classes are weighted 1, 2 and 3, respectively (good to poor) and the weightings added to give an index score. The minimum score is 6 (all poor); the maximum is 18 (all good). Three examples are shown to introduce the working.

	Threshold values for the 13 site analysis						
Weighting	Forest cover (%)	% Forested areas > 50 ha	Road density per unit area	% Agriculture on steep slopes	No. of roads crossing streams per unit area	Hypso-metric integral	
1 (poor) (red)	< 20	< 5	> 0.015	> 36.0	> 0.2	< 0.31	
2 (medium) (yellow)	20–60	5–10	0.015–0.010	22.0–36.0	0.1–0.2	0.31–0.4	
3 (good) (green)	> 60	> 10	< 0.010	< 22.0	< 0.1	> 0.4	
Catchment no.							Field index
1	2.9	0.00	0.0165	38.1	0.318	0.3787	7
2	21.5	1.5	0.0136	46.6	0.146	0.2393	9
3	72.4	32.2	0.0137	23.5	0.189	0.3995	14

Relationships Between Catchment Condition and Field Measures

The four field data sets and the field index were plotted against the catchment biophysical index. Figure 3 shows the plots that had a significant linear relationship (note that some points are plotted on top of each other, giving apparently different numbers of catchments). The relationship between stream salinity (measured as EC) and the biophysical index (Fig. 3a) was negative and the correlation strong ($r^2 = 0.75$, $P < 0.001$). This suggests that the index is predicting the salinity status of the streams very well.

The relationship between the biophysical index (based on indicators) and the field index (which includes biological and stream salt measures) (Fig. 3b) was likewise strong and positive ($r^2 = 0.74$, $P < 0.001$). The relationship between the macroinvertebrate data (observed number of macroinvertebrate families over expected number) and the biophysical index (Fig. 3c) was positive but weak ($r^2 = 0.34$ P < 0.05). This suggests that at the scale of catchments used in the study (500–1000 km^2), the influence of landscapes and changes in land use is reflected in the stream fauna. Although weak, this relationship is encouraging, given the limited nature of the field data and the potential for large variability. The relationship between salt load and the biophysical index (not shown) was very weak ($r^2 = 0.04$). An examination of the biophysical data set suggested that the measure dominating the results is per cent tree cover remaining in the catchment.

Discussion and Conclusion

This study set out to compare readily available landscape biophysical data, which can be collected quickly, with stream measurements, which take much longer to collect and also require specialist

Table 3. Field measurements of salinity and biota in the catchments.

Catchment Number	Conductivity (EC)	Salt load (concentration × flow)	Macro-invertebrates (observed mean)	Macro-invertebrates O/E	Field index
1	974	1.412	8.50	0.86	7
2	406	0.128	2.00	0.21	7
3	102	2.239	14.00	1.11	10
4	64	0.077	10.50	0.83	11
5	99	0.072	12.20	1.08	12
6	140	0.057	11.20	0.97	12
7	30	0.777	13.00	0.89	11
8	494	0.401	11.00	0.97	11
9	1081	0.954	8.00	0.79	6
10	970	0.085	5.15	0.57	6
11	456	0.133	5.33	0.55	7
12	505	0.504	8.20	0.88	9
13	314	0.412	7.80	0.78	9

O/E = number of families of macroinvertebrates observed compared to the number expected

expertise. The strong correlation between the biophysical landscape data and the field data suggests that, at least for the area examined, the index performed very well.

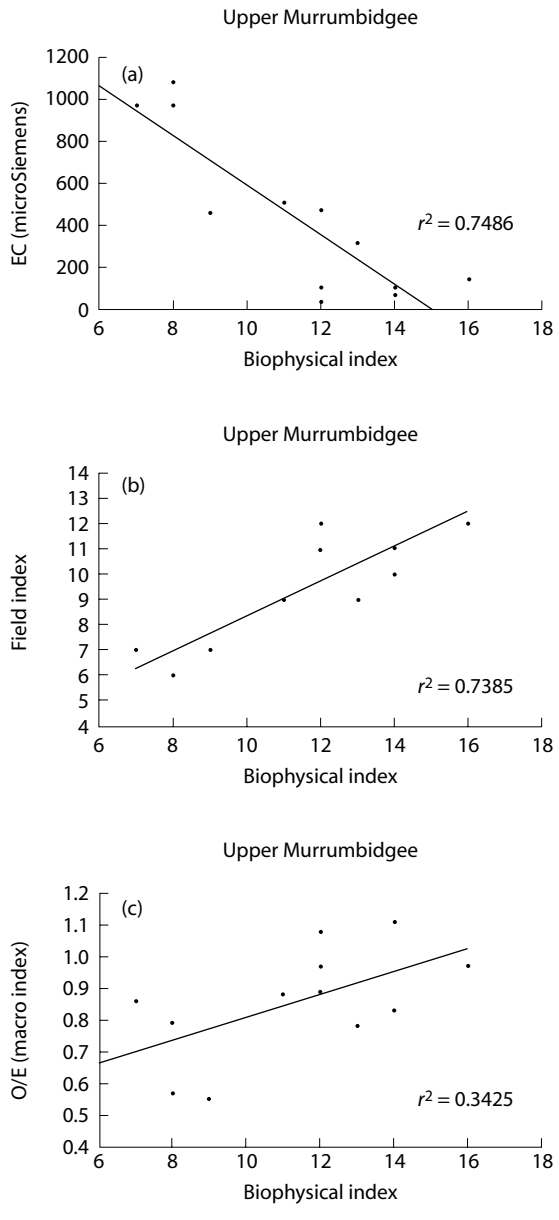

Figure 3. Relationships between catchment condition and stream measurements: (a) plot of stream salinity versus the catchment condition biophysical index; (b) plot of the biophysical versus field catchment condition indexes; and (c) plot of observed/expected macroinvertebrate groups versus the biophysical index of catchment condition.

The mechanisms controlling salinity in the study area were reasonably well known and the question arises as to whether the same indicators can be used in other areas to rate salinity status. Sufficient research has been carried out across Australia to suggest that different mechanisms are at work in different regions (e.g. seasonality of rainfall, magnitude and mobility of salt stores and different kinds of groundwater flow systems contributing to dryland salinity). Recent groundwater mapping as part of the National Land and Water Resources Audit (Coram et al. 2000) shows the areas with local, intermediate and regional groundwater flow systems. Inspection of the maps suggests that the indicator set could apply to the southeast temperate areas of Australia on the western side of the Great Dividing Range, mapped as local or intermediate groundwater flow systems.

The catchment size used approximated third-order catchments, with the majority ranging in size from 500 to 1000 km^2. Subsequent studies over smaller and larger areas suggest that size does influence the results, particularly threshold values, and the indicators that are appropriate (Walker et al. 2001). There could be many different reasons for this effect, but the most obvious with respect to stream salinity are that:

- as size increases, varying inputs of high-quality versus salty water along the length of the river will affect the relationships, and
- at smaller scales, the impacts of good management practices can reduce salt inputs from the land (e.g. repairs to the riparian zone can reduce overland flows).

Data for these parameters are generally not available at the broader scales. Therefore, it is advisable to use sizes of around 500 km^2. Nevertheless, the indicator approach described can be useful as context information at the more detailed scale, and detailed data can be added when available.

The collation of the data sets was carried out within a week, suggesting that application at a national level is possible within a realistic timeframe. Regional differences are important in such an exercise, and it would be advisable to identify the local mechanisms controlling salinity inputs.

Because the study was confined to 13 catchments it has statistical limitations. The next stage, before a national study, involved collecting data from 169 subcatchments in the Upper Murrumbidgee and more intensive field sampling. Some results of this work are reported in Chapter 26.

The results raise an interesting question about the use of coarse-scale data as opposed to detailed measurements to carry out 'big-picture' assessments. It may well be that detailed measurements will not perform any better, and past experience suggests that spatial density is a major consideration. Perhaps continental-scale data have been undervalued and a top-down approach will suffice for most applications relevant to planning or policy development.

References

AUSLIG (Australian Land Information Group) 1994. Topo 250k Series 1, 1:250,000 Digital Topographic map data of Australia. AUSLIG, Canberra (digital data).

AUSLIG 1996. Geodata 9 second DEM, Total Relief in 9 seconds, A national digital elevation model of Australia with a grid spacing of 9 seconds in latitude and longitude. AUSLIG, Canberra (digital data).

Jones, K.B., Ritters, K.H., Wickham, J.D., Tankersley Jr, R.D., O'Neill, R.V., Chaloud, D.J., Smith, E.R. and Neale, A.C. 1997. An ecological assessment of the United States mid Atlantic region: a landscape atlas. United States Environmental Protection Agency, EPA/600/R-97/130.

Strahler, A.N. 1952. Hypsometric analysis of erosional topography, Bulletin of the Geological Society of America, 63, 1117–1142.

Walker, J., Veitch, S., Braaten, R., Dowling, T., Guppy, L. and Herron, N. 2001. Catchment Condition in Australia: Final Report to the National Land and Water Resources Audit, November 2001.

26 Using Indicators to Assess Environmental Condition and Agricultural Sustainability at Farm to Regional Scales

Doug J. Reuter,* Joe Walker,† Rob W. Fitzpatrick,* Graham D. Schwenke‡ and Philip G. O'Callaghan§

Abstract

In this chapter we review recent experiences in using soil, terrain, landscape and catchment indicators to assess the condition of the resource base underpinning agricultural activities. We describe the use of indicators in three case studies, and suggest potential indicators for assessing and monitoring system sustainability in the northern grains region of Australia.

本文回顾了近些年来使用诊断指标对土地和流域健康状况进行评价的经验，介绍了三个具体的研究实例，并提出了可评估和监测澳大利亚北部产粮区生态系统持续能力的一套指标。

IT IS IMPORTANT to choose indicators that match predetermined regional needs and priorities, be they for farm production or environmental issues. In choosing indicators, current knowledge about their strengths and weaknesses needs to be consolidated (see Chapter 24). For example, publications such as SOILpak (Daniells et al. 1994) or Soil Matters (Dalgliesh and Foale 1998) deal with

* CSIRO Land and Water, PMB 2, Glen Osmond, SA 5064, Australia. Email: dreuter@bigpond.com
† CSIRO Land and Water, PO Box 1666, Canberra, ACT 2601, Australia.
‡ NSW Agriculture, Tamworth Centre for Crop Improvement, Tamworth, NSW 2340, Australia.
§ Neil Clark and Associates, PO Box 540, Bendigo, Vic 3552, Australia.

Reuter, D.J., Walker, J., Fitzpatrick, R.W., Schwenke, G.D. and O'Callaghan, P.G. 2002. Using indicators to assess environmental condition and agricultural sustainability at farm to regional scales. In: McVicar, T.R., Li Rui, Walker, J., Fitzpatrick, R.W. and Liu Changming (eds), *Regional Water and Soil Assessment for Managing Sustainable Agriculture in China and Australia*, ACIAR Monograph No. 84, 342–357.

the management of soils in the northern grain belt. In southern Australia, PADDOCKCARE (McCord et al. 2000) consolidates information on 51 farm indicators. PADDOCKCARE, which is available as a CD-ROM, allows farmers to record and graph indicator data over time and to progressively rank and integrate the status of a range of issues assessed by indicators. Dalal et al. (1999) provide an example of selecting indicators for the central Queensland grain region.

Whilst industry and regional benchmarks for assessing economic indicators are available, our focus is on the sustainability of the resource base. The following case studies show how data sets can be integrated and visualised at catchment to regional scale, using biophysical indicators. In each study, we used geographic information systems (GIS) to produce interpolated surfaces of risk. In the Upper Murrumbidgee region, we used surrogate indicators (indirect measures) to assess catchment conditions. In the Mount Lofty Ranges of South Australia, we determined risks for soil salinity, sodicity and acidity by extrapolating from a subcatchment to a subregion using detailed point source data and knowledge of landscape processes. In the Young area of southern New South Wales, we assessed several catchments using report cards based on easily measured indicators. At a regional scale, we developed indicators to assess the sustainability of the northern grains industry. The Overview provides background information about these areas and shows their location (Figure 2 of the Overview).

Case Study 1: The Upper Murrumbidgee Catchment

To construct maps of catchment condition, we focused on readily available rather than high quality data, as the latter are often not available for the whole region. We identified key regional issues, then refined the assessment questions and sampling strategy for a small group of indicators, generally surrogates, relevant at the catchment scale. The study area was the Upper Murrumbidgee catchment (Canberra–Yass–Cooma), comprising 169 subcatchments in an area of approximately 12,000 km^2. The main environmental issues were salinity and sediment movement. The preliminary study of 13 large catchments in this area is described in Chapter 25.

We used seven readily available biophysical indicators (all surrogate indicators):

- percentage of forest cover (surrogate for estimating departures from the original condition and also related to stream salinity);
- percentage forest cover greater than 50 hectares (habitat);
- agriculture on steep slopes (potential erosion);
- road density (human impact);
- roads crossing streams (correlated with sediment input to streams); and
- intact forest along streams (a riparian zone/habitat and sediment filter).

The data were obtained from satellite imagery, AUSLIG[1] road information and digital elevation model (DEM) information, all of which is readily available and can be assembled within one week. We estimated each indicator for a total of 169 catchments and placed the value in one of three classes: (1) good, (2) intermediate and (3) poor.[2] Catchment condition scores were obtained by summing the weightings for each indicator per catchment to get an aggregate catchment condition value. These values ranged from 8 to 16 and were divided into three catchment classes: 8–10 (good),

[1] Australian Surveying and Land Information Group.

[2] The use of good and poor raises semantic issues, and some prefer to use best to worst when the analysis gives a relative ranking. However, in this case we had a reasonable idea of the threshold values and used good to poor ranking. See Chapter 24 for details on weightings and aggregation.

11–13 (intermediate) and more than 13 (poor). Figure 1 shows the distribution of these classes in the Upper Murrumbidgee catchment.

This condition map is best considered a risk map. Catchments in poor condition are most likely to contain areas with evident or likely future environmental degradation, those in intermediate condition are likely to have some problems or to develop problems in the future, and those in good condition are likely to have few biophysical condition problems.

Figure 1. A preliminary catchment condition assessment for the Upper Murrumbidgee basin.

Case Study 2: Mount Lofty Ranges

We integrated soil, vegetation and terrain indicators using a GIS framework and assessed variability in drainage/waterlogging, salinity and acidity/alkalinity using remotely sensed data. Based on the results we developed an index of catchment health and a field manual. The purpose of the manual is to enable landholders and regional advisers to identify problems on properties and plan remedial action.

Study site

The regional study area in the Mount Lofty Ranges of South Australia covers approximately 80 km^2, including the town of Mount Torrens and an area to the east of the town (Fitzpatrick et al. 1999). The climate is Mediterranean and representative of the eastern part of the Mount Lofty Ranges, with a mean annual rainfall of 650–700 mm. A northeast to southwest topographic high east of Mount Torrens bisects the area: small catchments to the west drain into the Onkaparinga and Torrens catchment systems; catchments to the east form part of the Murray–Darling Basin system. Based on morphological, chemical and physical soil data (Fritsch and Fitzpatrick 1994), landscape DEM data (Davies et al. 1998), and water quality and remote sensing data (e.g. AIRSAR/TOPSAR; Bruce 1996), four focus areas were selected:

- a toposequence (~400 m in length) from the Herrmann area;
- the Herrmann area (~0.20 km^2);
- the Herrmann focus catchment (~2.0 km^2); and
- the Mount Torrens regional area (~80 km^2), comprising 55 smaller catchments.

Soil degradation index

We constructed a best-estimate map for each type of soil degradation data and used the maps to develop a soil degradation index (SDI), which itself is part of the broader catchment health indicator (see below).

In the Herrmann focus catchment, the processes by which drainage/waterlogging, salinisation and acidification/alkalisation occur are well understood (Fritsch and Fitzpatrick 1994; Fitzpatrick et al. 1996). We extrapolated spatial patterns of soil

degradation processes at toposequence scale (400 m within a 0.2 km^2 key area) to catchment (2 km^2) and regional (80 km^2) scales (Fitzpatrick et al. 1999). By integrating data obtained on the ground with remotely sensed, DEM and vector GIS data, we created best-estimate maps for soil salinity (Fitzpatrick et al. 2000; see Figure 2), waterlogging/drainage (Davies et al. 2000) and acidity/alkalinity (Merry et al. 2000) for the 80 km^2 regional area. A prediction that 3% of the soils of the region would be extremely saline or very saline and that 10% would be slightly saline was validated by data from 50 randomly selected sites and other observations across the 80 km^2 region (see Chapter 21).

Index of catchment health

The United States Environmental Protection Authority (Jones et al. 1977) ranked catchments at large regional scales to obtain an index of relative condition. Our approach is similar in that we ranked attribute values from best to worst for soil salinity, waterlogging/drainage and acidity/alkalinity, and then summed rankings across all three categories to give an aggregated score. Thus, the method differs from the aggregation approach used in the Upper Murrumbidgee study. This method has also been applied to smaller catchments and fewer categories of indicators (Bruce et al. 2000; Fitzpatrick et al. 1999).

Most of the 55 small catchments or watersheds lie totally within the rectangular regional boundary. Catchment subdivisions were based on general surface water flows interpreted from topographic shapes and stream flow patterns (Bruce et al. 2000).

We constructed an SDI by ranking each of the 55 catchments according to the area of degradation due to soil salinity, waterlogging/drainage and acidity/alkalinity and then summed the rankings for each catchment to derive new SDIs (Bruce et al.

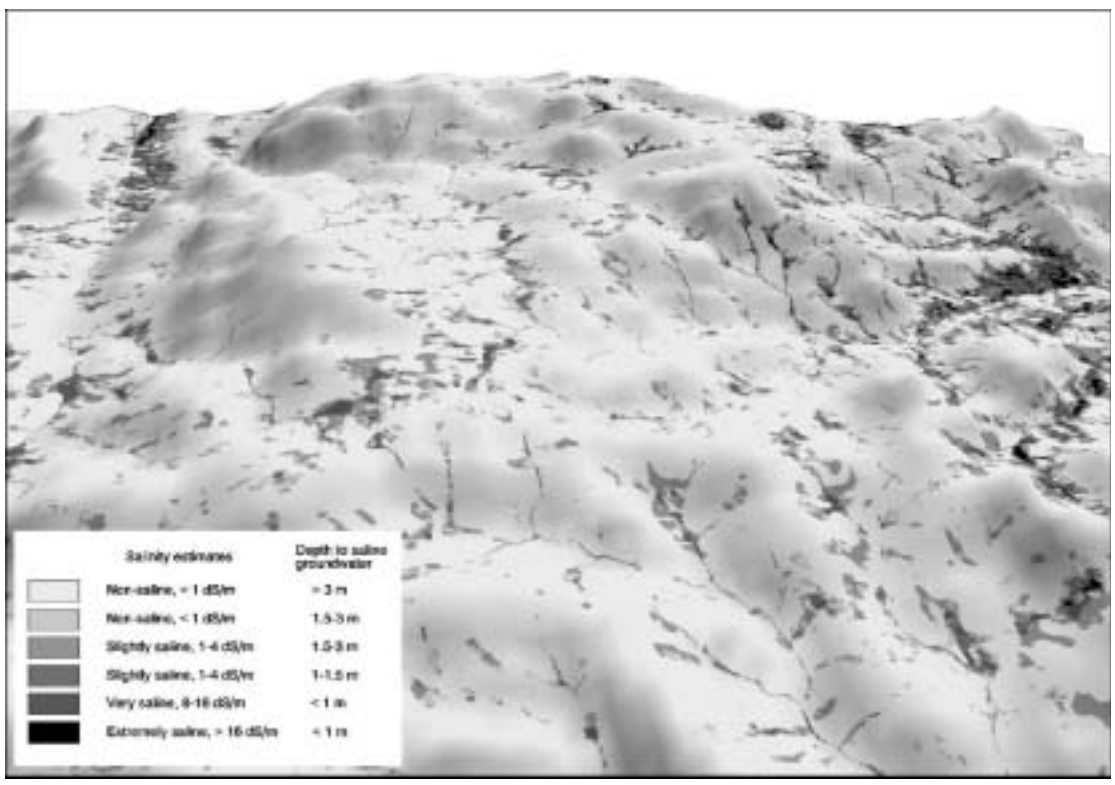

Figure 2. Three-dimensional representation showing six classes of salinity for part of the 80 km^2 study area (from Fitzpatrick et al. 2000).

2000). We used regional maps for best estimates of these three categories to produce a composite, regional-scale assessment of soil degradation.

As illustrated in Figure 3, we used the following indexes to rank the 55 catchments in terms of landscape processes and subsequent environmental effects such as stream water quality:

- SDI — developed from the best estimates of salinisation, drainage/waterlogging and acidity/alkalinity;
- land cover index (LI) — developed from land cover and DEMs;
- riparian land cover index (RLI) — developed from the intersection of buffered streams and land cover; and
- road index (RI) — developed from a summation of the weighted lengths of roads.

Using these indexes, catchments were ranked based on the zonal summation of raster GIS attributes per vector subcatchment polygon. To normalise for different catchment areas, the index value was divided by the area of the catchment.

We combined the rankings by summing each ranking for all catchment characteristics. The final

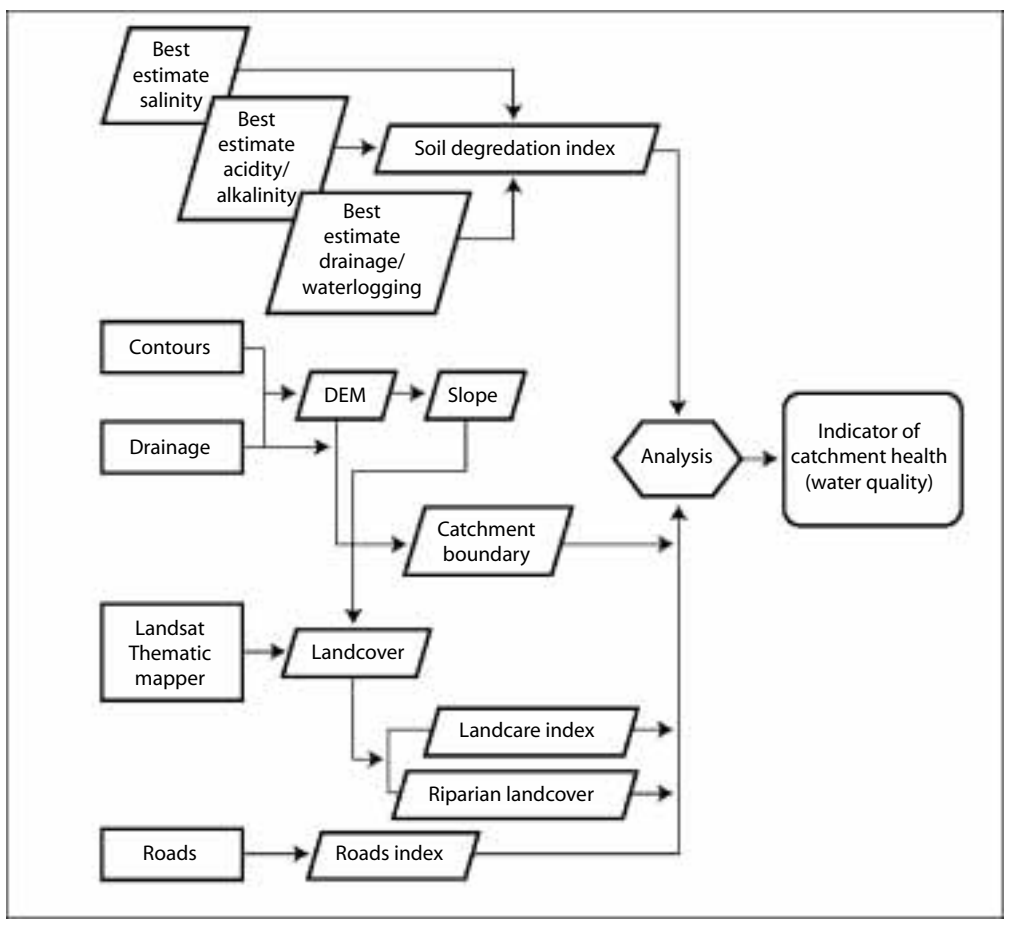

Figure 3. Data model used for the generation of catchment indices (from Fitzpatrick et al. 1999). DEM is digital elevation model.

catchment indicator (CI) of health was calculated using the following model:

CI = SDI + RI + LI + RLI

We then grouped catchments into quintiles, and rated soil and surface water quality.

To give land managers graphic tools on which to base management decisions, we produced maps such as the final CI map, which used different colours to indicate differences in quality (e.g. catchments with red tones were considered to have poor quality soil and water). The Herrmann focus catchment in the Mount Torrens region fell in the poorest category. Our knowledge of the area suggested that other catchment rankings were valid, but they require validation on the ground.

In the 'Catchment Condition' project of the National Land and Water Audit, Walker et al. (2001) developed a decision system called CatCon that enables indicator aggregations and spatial scenarios to be produced easily.[3]

Availability of data

Most data sets that are needed to aggregate from point measurements in focus catchments to regions are readily available throughout Australia; for example, there are regional data sets for most Australian agricultural regions. Although radar data (used here to refine the drainage/waterlogging and salinity maps) are not readily available for the whole country, the data sets that are readily available still allow for very robust analysis. The key data sets used in this case study need to be combined with knowledge from a representative key study area ('training area'). A hydrologically correct DEM (obtained by editing contour and stream data for the terrain analysis of the region) is needed, as is expert knowledge of the soil hydrological processes for a small key area.

[3] http://www.brs.gov.au/mapserv/catchment/

Application of the approach to other areas

Information gained through use of indicators has been used to help landholders better assess problem sites and develop property management plans. The approach can help Landcare groups, government agencies and others to make resource management decisions and assess the social and economic viability of a region.

Case Study 3: Catchment Condition Report Card for the Young Area

A great strength of an indicator approach is that it can identify individual activities that are causing specific problems, which is useful in planning and implementing remedial actions. Walker et al. (1996) applied landscape indicators to a mixed farming area around Young in the Upper Murrumbidgee catchment. The outputs were presented in a report card that summarised the indicator values, classes and trends (see Table 1 for an example of a report card).

Table 1 shows a report card for two groups of paddocks — one with annual pastures (low capital input), the other with improved perennial pastures (lucerne established after lime and phosphate fertiliser application) — with each indicator giving a measure of some aspect of system health. Standards to rank each indicator from very good to very poor were established using locally collected data. The table shows that the condition of annual pastures was generally poor and deteriorating: weeds and bare soil were high, plant rooting depth was shallow and the saline watertable had stayed at a constant level.

For perennial pastures, the trends were generally good and improving. Depth to the watertable had increased (the watertable was saline and needed to be well below rooting depth). The rooting depth was greater than in the annual pastures and was expected to improve water use efficiency (WUE); the higher percentage yield implied that the pastures were making better use of the available

Table 1. A trend report card for paddocks with annual pastures and perennial pastures.

Indicator	Very good	Good	Fair	Poor	Very poor
Bare soil				●→	
Root depth				●→	
Soil pH				●→	
Soil EC		←●			
Weeds					●→
Stream pH		●→			
Stream EC				●→	
Turbidity		←●			
Macroinvertebrates				←●	
Watertable depth			←●		

Perennial pastures (mean for four paddocks on similar soils)

Indicator	Very good	Good	Fair	Poor	Very poor
Bare soil			←●		
Root depth		←●			
Soil pH		●→			
Soil EC		←●			
Weeds		←●			
Stream pH		●→			
Stream EC				●→	
Turbidity		←●			
Macroinvertebrates				←●	
Watertable depth		←●			

EC = electrical conductivity

rainfall; and stream water quality, especially turbidity, was satisfactory for most indicators.

There were some negative signs for the perennial pasture system. The trend in pH indicated that liming was necessary to maintain production, and the low macroinvertebrate biodiversity counts in nearby streams implied a higher than acceptable level of salinity in water moving from paddocks. An increase in stream electrical conductivity (EC) could indicate that more areas might be affected by salinisation in the future; therefore, a more detailed examination, such as mapping EC with appropriate equipment, could be warranted.

Overall, the health of the landscape had slowly degenerated. The following actions were suggested to reverse the downward trend:

- changes in crop rotations (generally wheat in this area) towards longer periods of permanent pasture to improve soil and water health (these improvements at the farm scale would have flow-on effects in improving the general health of the landscape);
- possibly tree planting across the contours and above evident discharge areas (salinity levels have been partially stabilised under the perennial pasture system but are still of some concern); and
- closer monitoring of streams, because their poor biological condition implies that pollution other than salinity is a problem.

The report card approach gives landholders sufficient information to decide on positive actions. Decisions about what to do in any specific example will depend on commodity prices versus continuing slow declines in the health of the landscape.

Application to the Northern Grains Region

The northern grains region lies on the subtropical slopes and plains of eastern Australia (SCARM 1998) between latitudes of 21°30' (north of Clermont, Queensland) and 33° (south of Dubbo, New South Wales). It comprises three agroecological zones: western, eastern and central Queensland (Fig. 4). The region is bounded on the east by the Great Dividing Range (152°E at its eastern extremity) and on the west by rainfall isohyets suitable for dryland cropping (146°E at its western extremity). Agriculture is the dominant land use. In 1997–98, 25% of the region was cropped and 25% was sown to pastures (ABARE 1999). The remaining land was used for extensive grazing or nonagricultural uses such as state forests, national parks and mining. Between 1995 and 1999, 17.5% of the Australian grain crop was harvested from this region, of which 65% was produced in the eastern zone (Knopke et al. 2000).

Land use

The region incorporates a variety of farm enterprises; the ratio of cropped land to pasture land ranges from 0 to 1. The cropping–pasture mix tends to ebb and flow according to commodity prices and farmers' aspirations, but the following general types of farms can be identified in the region:

- *Mixed farming*. Livestock and cropping enterprises are integrated and use the same land. This form of land use is usually practised more in the older, eastern areas of the region.
- *Cropping only*. Intensive, continuous cropping is mostly undertaken on the more fertile lands of the region and where there are small areas of irrigation. Few, if any, livestock graze these areas.
- *Separate cropping and livestock industries on the same farm*. Cropping and livestock enterprises are undertaken on the same farm, but each is located in a separate area, often determined by factors such as soil type and slope. On the fertile Darling Downs of Queensland and the Liverpool Plains of New South Wales, cropping is practised on flat to undulating alluvial plains, while livestock graze the steep nonarable slopes. In the western part of the region, traditional livestock farms are gradually changing into mixed, but nonintegrated, farming enterprises.
- *Livestock only*. Much of the region is used only for cattle and sheep grazing, as the land is unsuitable for cropping or the landowner does not wish to produce crops.

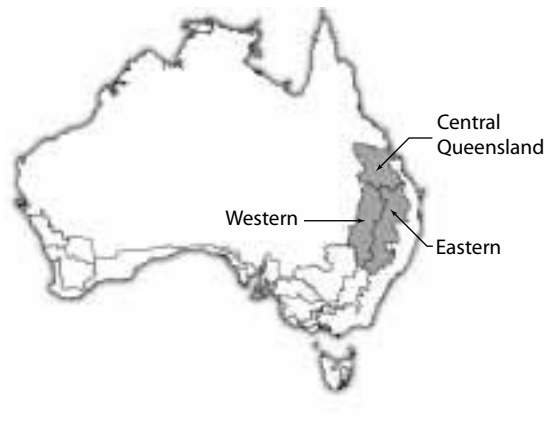

Figure 4. The northern grains region of Australia consists of three subregions: western, eastern and central Queensland.

Areas of dryland and irrigated cotton growing fall into the first three categories. Dryland grain cropping in the region is dominated by winter and summer production of cereals (chiefly wheat, sorghum, barley and corn). The dominant soil types for cropping are Vertosols (black, grey and brown cracking clays), Sodosols (solodised solonetz and solodic), Chromosols (red-brown earths) and Ferrosols (Krasnozems and Euchrozems) (Webb et al. 1997). The moderate to high water-holding capacity of the Vertosols is important for the production of winter crops because most rain falls in the summer, particularly in the north. Webb et al. (1997) provide more information about the region, its soils and the characteristics of its climate.

Sustainability issues for the northern grains region at various scales

The first step in using indicators is to identify the key sustainability issues facing the region. These vary at paddock, farm, catchment and regional level, as shown in Tables 2–4.

At the paddock and farm scale, soil health is a key issue. Soil erosion causes loss of surface structure, decreased storage of plant available water, and loss of soil nutrients in eroded sediments. Other issues include increased risk of salinisation, sodicity, soil acidification and structural damage, crop pests and weeds and diseases; and reduced diversity and abundance of soil fauna. These issues are related to site-specific factors such as soil type, climate, agronomic management and farm history. In some cases, the problems may not be recognised by land managers because they are relatively insidious or not well understood (e.g. subsoil compaction, deep drainage, vertical and lateral leakage of solutes, and the conservation of beneficial soil organisms).

Most catchment-scale issues relate to water quality. Catchment-scale issues tend to have downstream and offsite impacts on whole communities, affecting towns, cities, forests, national parks, beaches, estuaries and coral reefs as well as agriculture. For example, widespread soil erosion in the Fitzroy River catchment, which drains much of the central Queensland agricultural area, has led to high levels of suspended sediments, nutrients and pesticides in streams and groundwater (Noble et al. 1997). For many local towns, this in turn impacts upon their sole water supply. In the Liverpool Plains in northern New South Wales, six key natural resource management issues pertinent to the sustainability of the catchment have been identified: dryland salinity (and groundwater recharge),

Table 2. Performance indicator levels in Queensland showing the number of businesses in each category.

	Performance targets				Queensland sample (% of farms in each category)			
Farm indicators	Weak	Medium	Strong	Dynamic	Weak	Medium	Strong	Dynamic
Disposable income Per family ($'000)	< 30	30–60	60–100	> 100	33	29	24	14
Farm input costs Operating costs/farm income (%)	> 60	60–50	50–45	< 45	65	21	10	4
Land productivity Operating surplus/land value (%)	< 8	8–15	15–20	> 20	31	43	16	10
Farm size Land value per family ($'000)	< 400	400–800	800–1200	> 1200	6	55	18	21
Debt servicing Financing costs/total income (%)	> 15	15–7	7–3	< 3	29	37	16	18
Machinery Machinery market value/farm income (ratio)	> 1.2	1.2–0.8	0.8–0.6	< 0.6	53	21	18	8
Nonfarm income Net nonfarm income per family ($'000)	< 5	5–15	15–30	> 30	63	16	17	4

flooding, soil erosion, water quality and quantity, biodiversity and riparian zone degradation (Dames and Moore 2000).

At the regional level, most sustainability issues relate to soil nutrient depletion, soil structural degradation, soil erosion, diseases, pests, weeds and chemical contamination of food and the environment (Clarke and Bridge 1997). Until recently, cropping in the region was often characterised by nutrient 'mining', as nutrients (particularly nitrogen) removed through harvested grain, stubble removal (either hay-baling or burning) and soil erosion were not replaced (Dalal and Probert 1997). Although many farmers now replace 'harvested' nutrients with fertiliser inputs, the regional balance is still negative (Knopke et al. 2000). SCARM (1998) found phosphorus and potassium balances for broadacre industries in the subtropical slopes and plains to be consistently negative during the period 1986–95, with no indication of improvement. Another regional issue is stream eutrophication and turbidity (Knopke et al. 2000).

Table 3. Business health indicators.

Indicators	Performance targets				Qld median
	Weak	Medium	Strong	Dynamic	
Business health					
Disposable income/family ($'000)	< 30	30–60	60–100	> 100	46
Net worth—Net assets/family ($'000)	< 500	500–1000	1000–1500	> 1,500	971
Income drivers					
Production system Farm income per hectare per 100 mm annual rainfall ($/ha/100 mm rain)					
• Intensive cropping	< 60	60–70	70–80	> 80	51
• Mixed farms	< 40	40–50	50–60	> 60	51
Farm input cost—Operating costs/farm income (%)	> 60	60–50	50–45	< 45	62
Farm size—Land value/family ($'000)	< 400	400–800	800–1200	> 1200	656
Debt servicing—Financing costs/total income (%)	> 15	15–7	7–3	< 3	11
Machinery—Machinery market value/farm income (ratio)	> 1.2	1.2–0.8	0.8–0.6	< 0.6	1.2
Nonfarm income					
Net nonfarm income/family($'000)	< 5	5–15	15–30	> 30	2
Resource use					
Land productivity—Operating surplus/land value (%)	< 8	8–15	15–20	> 20	10
Labour—Income per labour unit ($'000)	< 100	100–150	150–200	> 200	115
Return on capital—Return on farm capital (%)	< 2	2–7	7–12	> 12	3

Table 4. Associating farm productivity issues in the northern grains region with commonly advocated indicators.

Sustainability issue / component	Scale	Suggested sustainability indicators	Possible action to take	Investor (who pays?)	Likely time to achieve benefit
Declining productivity					
Poor WUE by crops (declining crop yields)	P, F	• % of potential yield • WUE	• Adopt improved agronomy • Identify yield limiting constraints including subsoil factors • Use water balance / push probe to better target yields	• Farmer • Farmer / advisory companies / research funds • Farmer / adviser	• Within season • Few years • Within season
Declining profitability	P, F	• $WUE • Disposable income per family • Net profit per hectare	• Optimise inputs and rotation sequence (opportunity cropping) • Be aware of commodity price shifts	• Farmer / adviser / researchers • Farmer / cooperatives / commodity markets	• Few years • Within season
Declining product quality					
Declining protein in cereals	P, F	• % protein of crop	• Attend N budgeting workshop • Increase N applications • Rotate annual cereal crops with legumes	• Farmer / agriculture departments / cooperatives / grain boards / grain companies	• Within season
	R	• % protein at local silo	• As above	• As above	• Few years
	P, F, R	• Nonlegume:legume ratio in rotations	• Grow pulses or legume-based pastures	• Farmer	• Season after pulse crop
	P, F, R	• % legume in pasture	• Increase pasture legume composition	• Farmer	• Season after pasture removal (effect may last several seasons)

F = farm; N = nitrogen; P = paddock; R = region; WUE = water use efficiency

Suggested indicators for the northern grains region

Tables 4 and 5 list potential sustainability indicators at paddock to farm scale; Table 4 shows those more relevant at the catchment to regional scales. Some indicators are common to different scales. The tables also describe actions that could be taken in order to solve problems, suggest who is likely to invest in solving either farm or environmental problems, and provide estimates of how long after remedial treatment benefits are likely to accrue. Clearly, not all indicators will be used simultaneously. Individual farmers or rural communities need to determine the most pressing issues.

A popular and effective means for creating a greater knowledge base for targeting local issues are programs such as 'Farming for the Future', where farmers learn together in facilitated action-learning groups. A recent survey by Lobry de Bruyn (1999) found that farmers across northwestern New South Wales monitored soil health through soil tests, crop performance (yield and protein), visual observation of plants and soil, and the structure and workability of soil (by a soil 'feel' test).

Where more than one problem is identified, combined corrective measures often produce a synergistic response. For example, some 16% (195,000 ha) of the Liverpool Plains catchment is considered to be at risk from salinisation, with 50,000 ha currently exhibiting symptoms of dryland salinity (LPLMC 2000). This is a significant local issue and one worth monitoring and addressing, because farm profit and environmental outcomes are linked. Soil tests (EC), piezometer monitoring (watertable height and EC), observations of salt scalds, dominance of pastures by salt-tolerant plant species and permanently waterlogged areas within paddocks are all useful indicators for identifying salinity. Where salinisation is identified or where the risk of salinisation is high, farmers may fence off salt-affected land, plant deep-rooted perennials, use salt-tolerant species, or use reverse interceptor banks (especially on sloping duplex soils) to divert lateral subsoil water. Landowners usually pay for these actions, but Landcare funding is sometimes available. It is important to realise that where changes to groundwater hydrology are sought, the results of these actions may not be manifest for several years or even decades.

The above example of salinity deals with farm and paddock-scale remedial actions. Broader-scale solutions are typically required to prevent salinity in the first place. At a catchment scale, indicators of salinity include soil, groundwater and streamwater EC, electromagnetic surveys (mapping of EC within the landscape), and DEM (inferring and mapping likely areas of salinity hazard based on landscape position). Catchment management strategies are typically funded by federal or State governments. An example at a State level is the New South Wales Salinity Strategy (August 2000), which set interim end-of-valley salinity targets for salt load and EC to be achieved by 2010. An example of a catchment-scale response is the Liverpool Plains Catchment Investment Strategy, which proposes an environmental management system to be used as a tool for sharing the cost of implementing solutions to problems such as dryland salinity (LPLMC 2000). One recommended action is to cease cropping in designated land management units where deep drainage is most likely, and instead establish and maintain tree cover (farm forestry).

Future directions

Farming and rural communities will adopt sustainability indicators only if they believe they will improve the short-term benefits and long-term viability of their enterprises. It is worth remembering that the farming community has always used broad indicators in farming practice and management. This is often thought of as 'experience' and it extends to reading the likely weather, knowing when to fertilise, examining trends in commodity prices and exchange rates and

Table 5. Associating soil health issues in the northern grains region with commonly advocated indicators).

Sustainability issue / component	Scale	Suggested sustainability indicators	Possible action to take	Investor (who pays?)	Likely time to achieve benefit
Soil health					
Poor surface structure / reduced water infiltration	P, T	• Dispersion / slaking tests • Exchangeable sodium percentage • Soil organic carbon • Soil consistency • Water intake rate • Surface crusting / sealing / pugging	• Grow pastures • Apply gypsum • Reduce tillage • Increase organic matter	• Farmer	Few years up to a decade
Subsurface compaction	P, T	• Effective rooting depth • Soil consistency • Visual assessment • Push probe measurement	• Avoid trafficking (machinery or grazing animals) on wet soils • Practise controlled traffic	• Farmer	Few years up to a decade
Soil erosion	P, T, C	• % bare soil • Slope class • Exchangeable sodium percentage • Presence of rill/gully erosion • Soil movement under fences	• Maintain groundcover • Reduce tillage • Stubble retention • Grassed waterways • Contour banks	• Farmer • Landcare groups • Catchment management committees	Straight after introduction of most actions
Sodicity	P, F, C?	• Dispersion tests • Exchangeable sodium percentage • Sodicity meter	• Apply gypsum • Use low sodium irrigation water • Plant pastures instead of crops	• Farmer	Within first season after application

Table 5. (cont'd) Associating soil health issues in the northern grains region with commonly advocated indicators).

Sustainability issue / component	Scale	Suggested sustainability indicators	Possible action to take	Investor (who pays?)	Likely time to achieve benefit
Soil health					
Salinisation	P, F, C, R	• Electrical conductivity • Electromagnetic surveys • Digital elevation modelling • Salt scalds observed • Areas dominated by salt-tolerant species • Permanently waterlogged areas within paddocks	• Fence off salt-affected land • Plant deep-rooted perennials • Use salt-tolerant species • Use reverse interceptor banks (especially on sloping duplex soils) to divert lateral subsoil water	• Farmer • Landcare	Years to decades
Nutrient deficiencies	P, F	• Soil and plant tests • Nutrient balance sheet (inputs x efficiency / outputs)	• Match projected and actual nutrient exports with fertiliser application • Use regular soil/plant testing	• Farmer • Fertiliser industry	Within first season after action (effects may last for several years)
Acidification	P, F, C	• Trends in soil pH	• Adopt liming practices • Use less acidifying practices	• Farmer • Agribusiness	Several years
Crop diseases	P, F, C	• Crop rotation index • Plant diagnosis • Soil DNA probes • Climate prediction model	• Identify disease problem • Alter tillage practices • Adopt better crop rotations • Use disease-resistant varieties	• Farmer • Plant breeders • Plant pathologists	Within season or within new rotation

C = catchment; DNA = deoxyribonucleic acid; F = farm; P = paddock; R = region; T = toposequence

so on. Making the effort to collect relevant environmental data beyond soil tests should not be a major shift in attitude, provided the tests can be interpreted in a way that is meaningful to the productivity of the farm or region. The adoption of environmental measures in Farm 500 (a group of 500 Australian farmers collecting environmental and production indicators) and the collection of information in 'precision farming' demonstrate that many farmers believe that benefits can be obtained.

If farmers are to adopt the indicators, they must first be shown how to collect, store and interpret the data. After that, the greatest success is likely to come from self-help groups.

Conclusions

Several packages to help land managers to address sustainability issues at the paddock, farm and catchment scale have now been developed and implemented in some of Australia's southern farming regions. A common feature of the cases discussed in this chapter is the incorporation of knowledge about the soil and landscape characteristics with various direct and indirect (surrogate) indicators, and the conversion of this information to a regional scale using technologies such as DEM, GIS and remote sensing. This level of complexity is not always necessary; the message here is to encourage farmers to clearly identify the issues to be assessed, to ask assessment questions likely to provide the information they need, to identify the best indicators, and then to record the indicators consistently and accurately.

Australia's northern grains region, where soil and catchment degradation are recognised as significant issues, would benefit from the kind of knowledge and decision-support packages that we have described for southern Australia. We have assembled a suite of sustainability indicators to help identify paddock, farm and catchment health issues and to monitor the situation after remedial action. We hope these may form the beginning of wider recognition of soil and catchment sustainability issues in the north.

Acknowledgments

Case study research was funded in part by ACIAR, the Land and Water Resources Research and Development Corporation (LWRRDC), the National Soil Conservation Program , the Natural Heritage Trust (NHT) and the National Land and Water Resources Audit. We are grateful to members of the Tungkillo Landcare Group for their encouragement and assistance. We thank the many colleagues in CSIRO Land and Water, the Bureau of Rural Sciences and NSW Agriculture who contributed to these studies. Thanks are also due to Greg Rinder and Trevor Dowling from CSIRO Land and Water for graphics.

References

ABARE 1999. Performance indicators for the grains industry. In: Australian Grains Industry Performance by Grains Research and Development Corporation Agroecological Zones. 15–21.

Bruce, D.A., Fitzpatrick, R.W., Davies, P.G., Spouncer, L., Merry, R.H. and Phillips, J. 2000. Catchment indicators: the use of remote sensing, vector and raster GIS in sub-catchment assessment. Proceedings of the 10th Australasian and Remote Sensing Conference, Adelaide, August.

Bruce, D.A. 1996. Soil moisture from multi-spectral, multi-polarising SAR. In: Proceedings of 8th Australasian Remote Sensing Conference. Canberra, March.

Clarke, A.L. and Bridge, B.J. 1997. Constraints in perspective. Clarke, A.L. and Wylie, P.B., eds, Sustainable Crop production in the Sub-Tropics: and Australian Perspective. Queensland Department of primary Industries, 170–178.

Dalal, R.C., Lawrence, P., Walker, J., Shaw, R.J., Lawrence, G., Yule, D., Doughton, J.A., Bourne, A., Duivenvoorden, L., Choy, S., Moloney, D., Turner, L., King, C. and Dale, A. 1999. A framework to monitor sustainability in the grains industry. Australian Journal of Experimental Agriculture, 39, 605–702.

Dalal, R.C. and Probert, M.E. 1997. Soil nutrient depletion. In: Clarke, A.L. and Wylie, P.B., eds, Sustainable Crop Production in the Sub-Tropics: and Australian Perspective. Queensland, Department of Primary Industries, 42–63.

Dalgliesh, N. and Foale, M. 1998. Soil matters: monitoring soil water and nutrients in dryland farming. Toowoomba, Queensland, Agricultural Production Systems Research Unit.

Dames and Moore 2000. Natural resource management report to Liverpool Plains Land Management Committee.

Daniells, I., Brown, R. and Deegan, L. 1994. Northern wheat-belt SOILpak: a soil management package for dryland farming in the summer rainfall zone. Tamworth, New South Wales Agriculture.

Davies, P.J., Bruce, D., Fitzpatrick, R.W., Cox, J.W., Maschmedt, D. and Bishop, L. 1998. A GIS using remotely sensed data for identification of soil drainage/waterlogging in southern Australia. In: Proceedings of the International Soil Science Society Congress. 20–26 August, Symposium No. 17. France, Montpellier, 8.

Davies, P.J., Fitzpatrick, R.W., Bruce, D.A., Spouncer, LR. and Merry, R.H. 2000. Use of spatial analysis techniques to assess potential waterlogging in soil landscapes. In: Adams, J.A. and Metherell, A.K., eds, Soil 2000: New Horizons for a New Century. Australian and New Zealand Second Joint Soils Conference, Volume 3: Poster papers. 3–8 December 2000, Lincoln University. New Zealand Society of Soil Science. 49–50.

Fitzpatrick, R.W., Davies, P.J., Merry, R.H., Cox, J.W., Spouncer, L.R. and Bruce, D.A. 2000. Using soil-landscape models to assess and manage salinity in the Mt Lofty Ranges. In: Adams, J.A. and Metherell, A.K., eds, Soil 2000: new horizons for a new century. Australian and New Zealand Second Joint Soils Conference Volume 2: Oral papers. 3–8 December 2000, Lincoln University. New Zealand Society of Soil Science, 107–108.

Fitzpatrick, R.W., Fritsch, E. and Self, P.G. 1996. Interpretation of soil features produced by ancient and modern processes in degraded landscapes: V. Development of saline sulfidic features in non-tidal seepage areas. Geoderma, 69, 1–29.

Fitzpatrick, R.W., Bruce, D.A., Davies, P.J., Spouncer, L.R., Merry, R.H., Fritsch, E. and Maschmedt, D. 1999. Soil Landscape Quality Assessment at Catchment and Regional Scale. Mount Lofty Ranges Pilot Project: National Land & Water Resources Audit. CSIRO Land & Water Technical Report, 28/99, 69. www.clw.csiro.au/publications/technical99/tr28-99.pdf

Fritsch, E. and Fitzpatrick, R.W. 1994. Interpretation of soil features produced by ancient and modern processes in degraded landscapes: I. A new method for constructing conceptual soil-water-landscape models. Australian Journal of Soil Research, 32, 889–907. (colour figs. 880–885).

Knopke, P., O'Donnell, V. and Shepherd, A. 2000. Productivity growth in Australian grains industry. ABARE Research report 2000.1, Canberra, ABARE.

LPLMC (Liverpool Plains Land Management Committee) 2000. Liverpool Plains Catchment Investment Strategy.

Lobry de Bruyn, L.A. 1999. Farmers' perspective on soil health: capturing and adapting intuitive understanding of soil health to monitor land condition. In: Proceedings of `Country Matters', 20–21 May Canberra 1999. Canberra, Bureau of Rural Science.

McCord, A., Reuter, D.J., van Gaans, G., Davies, K. and Fisher, F. 2000. PADDOCKCARE: a software tool to identify and rank key sustainability issues. (A CD-ROM product).

Merry, R.H., Spouncer, L.R., Fitzpatrick, R.W., Davies, P.J. and Bruce, D. 2000. Prediction of soil profile acidity and alkalinity—from point to region. In: Adams, J.A. and Metherell, A.K., eds, Soil 2000: new horizons for a new century. Australian and New Zealand Second Joint Soils Conference Volume 3: Poster papers. 3–8 December 2000, Lincoln University. New Zealand Society of Soil Science. 145–146.

Noble, R.M., Duivenvoorden, L.J., Rummenie, S.K., Long, P.E. and Fabbro, L.D. 1997. Downstream Effects of Land Use in the Fitzroy Catchment. A Summary Report. Biloela, Queensland Department of Natural Resources.

SCARM (Standing Committee on Agricultural Resource Management) 1998. Sustainable Agriculture: Assessing Australia's Recent Performance. Melbourne, CSIRO Publishing.

Walker, J., Richardson, P.B. and Gardiner, T. 1996. The report card: a case study. In: Walker, J. and Reuter, D.J., eds, Indicators of Catchment Health: A Technical Perspective. Melbourne, CSIRO Publishing.

Walker, J., Veitch, S., Braaten, R., Dowling, T., Guppy, L. and Herron, N. 2001. Catchment Condition in Australia: Final Report to NLWRA, November 2001.

Webb, A.A., Grundy, M.J., Powell, B. and Littleboy, M. 1997. The Australian sub-tropical cereal belt: soils, climate and agriculture. In: Clarke, A.A. and Wylie, P.B., eds, Sustainable Crop Production in the Sub-Tropics. Brisbane, Queensland Department of Primary Industries, 8–23.

27 Ecosystem Rehabilitation on the Loess Plateau

Li Rui,* Guobin Liu,* Yongsheng Xie,* Yang Qinke* and Yinli Liang*

Abstract

The Loess Plateau is well known for its deep loess deposits and serious soil erosion. The region covers five provinces and 0.62 million km^2; 45% of the area is eroded and there is an average soil loss of 3720 tonnes/km^2/year. Since 1985, the comprehensive reclamation of the Loess Plateau has been listed as a key science and technology project in China. Eleven small catchments have been selected as experimental and demonstration areas for ecosystem rehabilitation in different regions of the plateau. After 15 years, each of the 11 catchments has formed a good model for local areas. A set of technologies to control land degradation has been developed. The average yield of farmland has increased by 100–300%, the area under crops has decreased by 30–70%, perennial vegetation cover has increased by 70–150% and soil erosion has decreased by 60–80%. The economic structure of the region has undergone major changes, with income from grain down from 80% to 30%. Other sources indicate that farmers' incomes are 5–10 times greater than previous levels.

The key task in the region is to improve land use. In the loess hill region, cultivated land occupies more than 40% of the total area, most of which is on steep slopes (more than 15°) and about 20–30% of which is on slopes of more than 25°. Only 12% of the region is forested, and only half of that forested area effectively controls soil erosion. Only 30.5% is grassland, of which almost 69% has deteriorated from overgrazing. Land use should consist of flat area cropping for subsistence; forestry in gullies to protect the local ecology; and fruit growing and animal husbandry on sloping land for income.

Results from the 11 trial areas indicate that small catchments can be ecologically rehabilitated, but that they must pass through three stages—restoration, stabilisation and sustainable development—taking 15–20 years. The prospects for the Loess Plateau are bright, but there is a long way to go.

黄土高原以其深厚的黄土沉积和严重的水土流失著称于世。黄土高原地区涉及 5 个省（区），62 万平方公里。其中水土流失面积占 45%，每平方公里平均每年有 3720 吨的土壤流失掉。从 1985 年开始，国家把黄土高原的水土保持综合治理列为重点科技攻关项目，在不同类型区选择了 11 个小流域作为国家生态恢复重建试验示范区。经过 15 年连续治理，这 11 个小流域均成为当地的先进样板。研究开发了一套防治土地退化的技术。农田的单位面积

* Institute of Soil and Water Conservation, Chinese Academy of Sciences and Ministry of Water Resources, NWSUAF, Yangling, Shaanxi 712100, PRC. Email: lirui@ms.iswc.ac.cn

Li Rui, Guobin Liu, Yongsheng Xie, Yang Qinke and Yinli Liang. 2002. Ecosystem rehabilitation on the Loess Plateau. In: McVicar, T.R., Li Rui, Walker, J., Fitzpatrick, R.W. and Liu Changming (eds), *Regional Water and Soil Assessment for Managing Sustainable Agriculture in China and Australia*, ACIAR Monograph No. 84, 358–365.

产量提高了 1-3 倍，林草植被覆盖度增加了 70-150%。土壤侵蚀减少了 60-80%，农民收入提高了 5-10 倍。土地利用和经济结构发生了根本变化，农耕地面积减少了 30-70%，种植业的收入在总收入的比例由过去的 80%以上变为 30%左右。

15 年的研究结果表明：调整土地利用结构是首要而关键的任务。黄土丘陵区农耕地面积占总面积的 40%，大部分是 15 度以上的坡耕地，20-30%的耕地的坡度大于 25 度。有林地面积只占总面积的 12%，其中能起到控制水土流失作用的林地只有 6.5%。草地面积只占总面积的 30.5%，其中 68.8%的草地由于超载放牧严重退化。根据 11 个试验示范区的研究结果，黄土高原的土地利用和产业调整的基本原则为平地为农耕地，实现粮食基本自给；沟壑坡地宜发展生态保护型林业；在坡地上发展草业和果，这将是该区商品经济潜力所在。

11 个试验示范区的实践表明，一个退化的小流域生态系统是可以通过有序治理达到恢复重建的，但要经过 3 个阶段，即恢复阶段、稳定发展阶段和良性循环阶段。一般需要 15-20 年时间。所以，黄土高原的治理前景是美好的，但需要付出时间和投入。

THE Loess Plateau, located in the middle reaches of the Yellow River, is the cradle of Chinese civilisation. Cultivation in this region started 6000 years ago. The national economy relies on the energy base of the Loess Plateau for its heavy and chemical industries. The plateau is rich in sunlight and heat energy, the soil layer is thick, and there are vast areas of land suitable for forestry, fruit trees and grass. However, predatory exploitation, wanton deforestation, overgrazing and other forms of malpractice caused by a population explosion have caused degeneration of the ecosystems on the plateau. As a result, local economies are underdeveloped. The Overview provides background information about the region; Figure 1 of the Overview shows its location.

People in the Loess Plateau region have struggled long and hard against soil and water loss. The government has increasingly paid attention to the region, especially in the past 50 years, and has made great efforts to improve conditions. Since 1985, state authorities have listed the control of water and soil losses on the Loess Plateau as key research topics.

The Study Areas

Eleven experimental and demonstration areas (EDAs) were set up on the Loess Plateau on the basis of natural and social differences. Figure 1 shows the location of the experimental and demonstration areas; Table 1 shows the main environmental characteristics of the sites.

All EDAs represent seriously depleted ecosystems on the Loess Plateau. We have developed a set of technologies to control land degradation, as a result of which each EDA is expected to develop as a

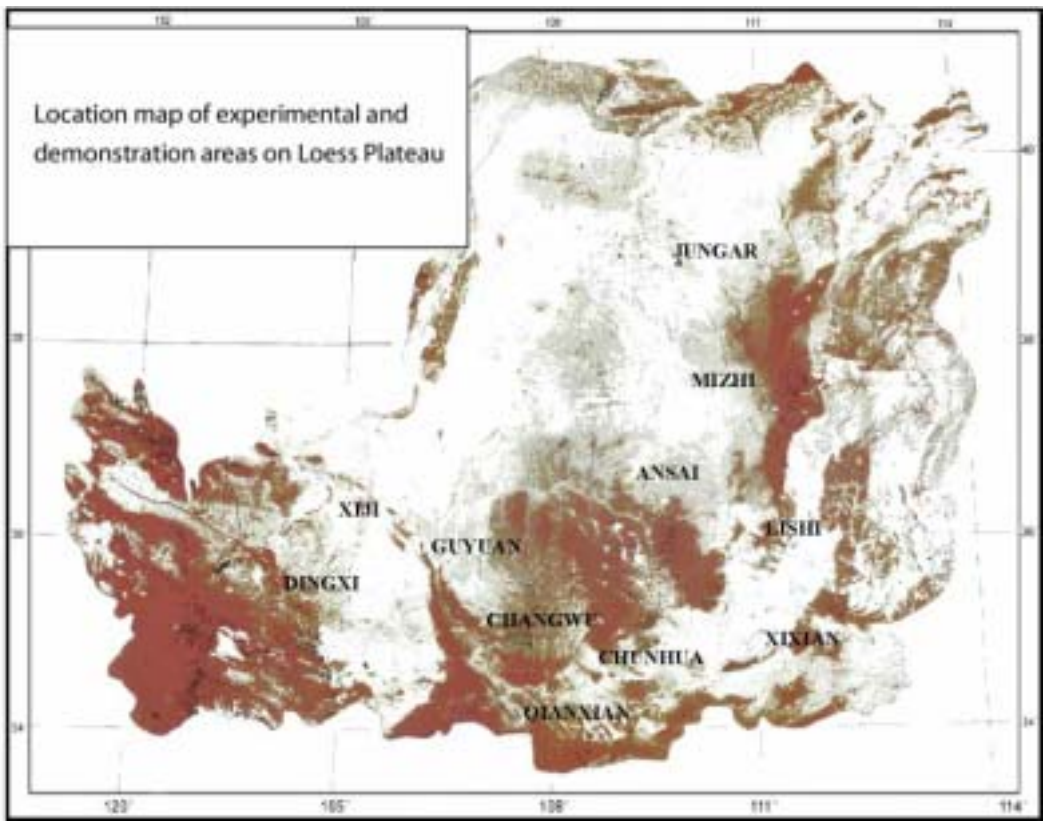

Figure 1. Location of experimental and demonstration areas on the Loess Plateau.

Table 1. Main environmental characteristics of experimental and demonstration areas (EDAs) on the Loess Plateau.

Type of region	Name of EDA	Area (km^2)	Annual rainfall (mm)	Annual average temperature (°C)	Population (persons)	Density of gully (km/km^2)
Windy and sandy	Jungar	7.7	344.2	5.3	330	2.37
Loess hill	Mizhi	5.6	422.0	8.4	586	3.00
	Ansai	8.3	497.6	8.8	407	3.06
	Lishi	9.1	484.7	9.0	1235	3.81
	Guyuan	15.1	472.0	7.0	785	2.16
	Xiji	5.7	402.0	5.3	491	3.32
	Dingxi	9.2	415.0	6.3	1564	1.57
Loess tableland	Changwu	8.3	584.0	9.7	1815	2.76
	Chunhua	9.2	600.0	9.8	2708	2.13
	Qianxian	8.5	590.0	10.8	1806	1.89
	Xixian	10.9	510.6	8.8	1211	1.46

Source: Database of the office of EDA project, Bureau of Resources and Environment, Chinese Academy of Sciences

sustainable farming zone on a large scale. Each EDA has formed a good model for the local region.

Main Achievements of the Program

During the past 15 years, the 11 EDAs have undergone great change. The average yield of farmland has increased by 100–300%. Grain yield has increased from 5737.5 kilograms per hectare (kg/ha) to 8196 kg/ha; average personal income has risen from 218 yuan/year to more than 2000 yuan/year (US$1 = 8.0 yuan). The amount of reclaimed land has increased from 46.1% to 80.2%. Research achievements have been applied to up to 10 million hectares of farmland, with some 5.55 billion yuan in increased crop value.

The project has not only improved the regional economy and farming practice on the Loess Plateau, but also promoted rehabilitation of the regional ecosystem. Some 150,000 km^2 of eroded land has been controlled by various conservation measures. The flow of sediments into the Yellow River has been reduced by about 300 million tonnes/year. By the end of 1995, reclamation had already led to an increase of 53.9 million tonnes in the aggregate grain yield over the previous 10 years. Increases in crop yield through the prevention of soil erosion and flood containment have resulted in economic returns of 180 billion yuan according to 1995 prices. Statistics from more than 2000 small watersheds showed that in each of the past 20 years, more than 4% of the eroded area has been controlled by soil and water conservation engineering on the Loess Plateau (before the 1980s, the figure was less than 1%) (Li Yushan 1996; Yang Wenzhi et al. 1992).

Land Use

Improving the land-use structure

The Loess Plateau has a long history of cultivation but natural and social factors have resulted in severe land-use problems, in particular a low proportion of vegetation cover and severe soil erosion and desertification.

Proportion of cultivation and vegetation cover

In loess hill areas, cultivated land occupies more than 40%, most of which is on steep slopes, with about 20–30% on slopes of more than 25°. There is little vegetation cover and the grassland is severely degraded, with less than 50% grass cover in most areas. For example, in south Nixia, grass yield is less than 500 kg/ha. Recent investigations have suggested that forested areas account for 12% of the whole region, of which only 6.5% can effectively control soil erosion. Most regions have only 30.5% grassland, of which 68.8% has deteriorated to some extent from overgrazing (Yang Wenzhi et al. 1992; Li Rui et al. 1992).

Soil erosion and desertification

The Loess Plateau suffers severe soil erosion and desertification. The long-term average sediment load of the Yellow River is about 1.6 billion tonnes per year, most of which comes from the plateau. Table 2 shows the main types of soil erosion on the Loess Plateau; Table 3 shows the intensity of the erosion.

Principles of rational land use

Experience, environmental characteristics and the nature of the land-use problems on the Loess Plateau suggest that the following principles should be considered for land-use planning in this region.

Table 2. Types of soil erosion on the Loess Plateau.

Soil erosion type	Area (km^2)	Proportion of total area (%)
Water erosion	289,300	46.36
Wind erosion	156,500	25.08
Water and wind erosion	178,200	28.56

Source: Tang Keli (unpublished lecture notes on soil erosion and conservation in China for the 2nd International Training Course on Soil and Water Conservation, September 1993).

Consider the economic benefits and ecological effects together

Human impact on the environment is continually increasing as the population increases and more demands are placed on land resources. If ecological effects are neglected during cultivation, land degradation and environmental deterioration will be more severe. Considering the economic benefits and ecological effects together will bring land reclamation and cultivation into ecological balance. On the other hand, soil conservation measures are unlikely to be followed by farmers if economic benefits are neglected.

Look at the integrated structure of land use

We must look at the overall regional economic arrangements as well as comprehensive land use. As mentioned above, semiarid regions have a variety of land-use types, which tend to be distributed in regular patterns. For example, in the hilly area, land types are in the following order: hilltop; land with a gentle slope (< 8°); steeply sloping land (15–35°); gully slope land (< 30°); gully terrace land (< 5°); and gully bed. Land-use arrangements must match the structure of the land type.

Remember that the overall function is bigger than the sum of the parts

This is one of the principles of systems engineering. Land use must match local conditions and there are mutual benefits between different land uses. For example, imagine that there are three hills to be used for planting crops, grass and trees. There are at least two ways to proceed. One is to plant crops on one hill, grasses on another and trees on another; the other is to plant grasses on the top, crops on the middle part (with gently sloping terraces), and trees on the lower part (the gully slope) of each hill. The first method means that one hill will produce grain, another forage and another wood. The results are the sum of the parts: 1 + 1 + 1 = 3. In the second method, the three kinds of uses can provide mutual benefits: the grassland on the top can protect cropland from water and soil erosion; trees on the lower part can control gully erosion. The results are more than the sum of the parts: 1 + 1 + 1 > 3. The second method is known as the integrated (or 'inlaid') method (Ju Ren et al. 1992; Song Guiqing and Quan Zhijie 1996). The key to realising this principle is to correctly handle the relationships between the subsystems and to establish a coordinated environment.

Table 3. Intensity of soil erosion on the Loess Plateau.

Grade of erosion	Amount of soil lost through erosion (t/km^2/year)	Area (km^2)	Proportion of total (%)
Very slight	< 1,000 (500)[a]	99,434	15.94
Slight	1,000 (500)–2,500	192,348	30.83
Moderate	2,500–5,000	40,622	6.51
Severe	5,000–10,000	111,384	17.85
Very severe	10,000–15,000	94,162	15.00
Extreme	> 15,000	86,049	13.79

[a] The figure in brackets refers to rocky mountain regions, not the loess region
Source: Tang Keli (unpublished lecture notes on soil erosion and conservation in China for the 2nd International Training Course on Soil and Water Conservation, September 1993).

Combine land use with land construction

Land degradation — soil erosion, desertification, salinity, soil deterioration and so on — occurs easily on the Loess Plateau. The situation is exacerbated because the poor economic situation means that there is little input to the land. We recommend the following techniques to reduce soil degradation.

- *To transform steeply sloping land into level land.* Steeply sloping lands are widespread in the Loess Plateau. They are known as 'three losses land' because they tend to lose water, soil and fertiliser . Terracing and dam lands[1] are effective in improving conditions. Some problems can be solved by conservation measures such as reduced ploughing.
- *To enrich the soil.* Loess soil is a young soil with low fertility, so it must be enriched in order to get higher yields. We recommend rotation cropping (for example, grass–crop–grass–crop or grain–beans–grain–beans, etc.) and increasing the amount of farm manure and chemical fertiliser.
- *To develop limited irrigation*. In arid and semiarid areas, water is an important limiting factor for agricultural development. Water conservation and optimal water use are key measures for increased agricultural production.

Techniques for Maximising Land Productivity

Grain is essential for people's survival. In the past, people have resorted to every possible means to provide farmland to obtain grain, including deforestation. Deforestation has led to the destruction of ecosystems, causing chronic and increasing impoverishment. To change this scenario, we must increase grain output per unit area, and transform the primitive practice of extensive cultivation — and its concomitant notorious low productivity — into intensive cultivation. Yields will increase and the environment will be rehabilitated if all land resources on the plateau are used rationally in the balanced development of various farming undertakings, including crop plantation, fruit production, forestry and animal husbandry. Increasing grain yield is the main objective of our work on the plateau, in order to eliminate poverty among the local inhabitants and boost the rural economy. The grain production target on the Loess Plateau is 400–500 kg per capita, at which level the local people will have a slight surplus of grain. Our experiences in the experimental zones prove that such a target may be reached within five years if input is increased sufficiently and if key agronomic instructions are available at the right time (Li Yushan 1996).

Any increase in grain yield depends on the planted crop strain, the amount of good basic farmland, agronomic measures taken for crop cultivation, etc. In order to cope with natural conditions and the current grain-planting situation on the Loess Plateau, the key to increasing grain yield lies in an improved water supply for farmland irrigation and in fertiliser application.

Increasing the amount of applied fertiliser and farmyard manure is especially important. The level of fertiliser application on the plateau is about 32% of the national average. Initially, chemical fertiliser was used to increase yields from medium (0.75 t/ha) to high (1.5–2.25 t/ha) levels. In the experimental areas, yields doubled or tripled when chemical fertiliser and farmyard manure were applied together. At a demonstration point in Dingxi Prefecture, for example, yield increased by 79.9% when the amount of chemical fertiliser was increased by 166%. Similarly, when the amount of chemical fertiliser at a demonstration point in Changwu County was increased by 144%, a yield of 5.25 t/ha was achieved, an increase of 99.5%. On average, the application of 1 kg of impurity-free

[1] Dam land is a kind of flat land at the bottom of a gully, formed by the deposited soils eroded from the slope.

fertiliser to Loess Plateau farmland will increase grain yield by 6–10 kg (Li Yushan 1996).

For nonirrigated farmland, yields are increased primarily by collecting water from seasonal rainfall. When there is sufficient water, fertiliser plays a key role in increasing yield up to a certain point, but above this point water is again the decisive factor for further increases in yield. Over many years, our work has shown that it would be impossible to break the ceiling of 3 t/ha for dryland wheat yield by simply increasing the amount of fertiliser applied. It is also necessary to increase the water supply; for example, by collecting runoff from seasonal rainfall, using plastic film to suppress evaporation from the ground surface and making more effective use of available water. Farmland tests in the demonstration zones in Luochuan, Guyuan and Changwu counties showed that these measures could be both feasible and effective. For example, in Guyuan County, when 40 m^3 of water (one-quarter to one-third of the amount of water required for the whole crop) was applied to spring wheat just before the tillering stage, the yield increased from 2.175 to 3.915 t/ha, three-quarters of the yield in fully irrigated crops. In this case, the water use efficiency is about 42 kg/ha using 1 m^3 irrigation water. On the other hand, there is considerable potential to make better use of local precipitation. In semiarid areas of the plateau, 25–30% of natural precipitation is absorbed by individual crops in transpiration, 10–20% becomes runoff on the ground surface and flows away, and the remaining 55–65% evaporates. Rainwater can be used more effectively by collecting runoff and reducing surface evaporation with plastic film.

Stages of Ecosystem Rehabilitation of Catchments

In Ansai County in northern Shaanxi Province, we restored a tiny watershed to its original state by mending and rebuilding the depleted ecosystem and ensuring that any further development would be sustainable. The watershed was a barren and depopulated gully in Zhi Fanggou in the hilly heartland of the plateau that had been plagued by serious water loss and soil erosion. From the 1940s to the 1990s Zhi Fanggou underwent 40 years of land degradation followed by 20 years of restoration. Before the drive, farming was a primitive kind of extensive cultivation; the grain yield was 0.6 t/ha and income as pitifully low as 222.1 yuan (about $27.80) per person per year. After the reclamation drive, the proportion of uncultivated land went down from 51.5% to 18%. The proportion of forest and meadow increased to 41.2%. By 1995, there was 0.18 ha/person of farmland, 0.47 ha/person of woodland, and 0.14 ha/person of artificially created pastureland; the average per capita income was 1658 yuan. Almost all peasant households now have their own television sets; 40% own colour television sets. Every village has its own ground-based equipment for receiving satellite-relayed television signals. Hence the countryside has undergone a radical change in appearance (Lu Zongfan et al. 1997). The experimental zones have become high-level models for comprehensive reclamation of the plateau; they also provide a base for theoretical exploration and an exemplary agrotechnological system for water and soil preservation.

The Loess Plateau is a backwater of the Chinese hinterland, plagued by poverty, underdevelopment, and serious water loss and soil erosion. Our work in Zhi Fanggou for the past 20 years suggests that in order to ensure that the Loess Plateau has a bright future it is best to focus efforts on sustainable ecological development rather than just on economic return. In line with this approach, in the context of stability and progress in the local farming system, we recommend the following three stages to develop ecoagriculture on the plateau while maximising water and soil preservation (Lu Zongfan et al. 1997).

Restoring the ecosystem

The main task of restoration is to increase vegetation cover by returning some cultivated land

to forest. The ecological benefits are likely to be seen earlier than economic benefits, although the gap between the two is decreasing and the effectiveness of the investment increases as the original vegetation is gradually restored. At present, restoration is hampered by the difficulty of communicating the complex technological information that forms the basis of any restoration to the local people who carry it out.

Making sure the ecosystem is stable

The newly restored ecosystem is weak and relative unstable. It may revert to its previous state unless care is taken. It is therefore very important to maintain a balance between ecological benefits and economic return. A timeframe of 5–10 years is usually practical for both ecological and economical benefits.

Making sure the ecosystem is sustainable

As the ecosystem becomes sustainable, people's natural and social attributes reach harmony. Both family planning and the rational exploitation of natural resources become conscious actions, with well-defined goals among the local inhabitants. The ecoagricultural system will be more complicated but will function more efficiently. Farming practice and business management are based on scientific and technological data and information resources. Our studies at Zhi Fanggou suggest that the following parameters should be regarded as standardised targets for appraising the three stages in developing an ecosystem rehabilitation in a small catchment: the area of controlled land, the basic amount of farmland and cropland per capita, and the yield (see Table 4).

Table 4. Stages and targets of ecosystem rehabilitation of a small catchment.

Stages	Time (years)	Area controlled (%)	Basic farmland (ha/person)	Cropland (ha/person)	Yield (t/ha)
Restoration	10–15	40	0.07–0.1	0.5–0.8	0.6–0.975
Stabilisation	5–10	60	0.1–0.13	0.4–0.53	0.96–1.35
Sustainable development		80	> 0.17	0.27–0.4	1.875–2.25

Acknowledgments

This article reports a number of research results by Mrs Li Yushan, Lu Zongfan and other scientists.The authors are greatly indebted to them as well as to Wang Lizhi, Wu Pute, Zhao Hongxing and other scholars for their generous contributions to this paper.

References

Ju Ren, Song Guiqing and Li Rui. 1992. Land resources and the principles of rational use in the Loess Plateau. Memoir of the Northwestern Institute of Soil and Water Conservation, 16.

Li Yushan 1996. The new position of the Loess Plateau in the development of the national economy. Chinese Academy of Sciences Bulletin, 11(2), 118–121.

Li Rui, Zhao Yongan, Song Guiqing et al. 1992. Land resources information system of Shanghuang in Guyuan County. Memoir of the Northwestern Institute of Soil and Water Conservation, 16.

Lu Zongfan et al. 1997. Research on Eco-agriculture on China's Loess Plateau. Xi'an, Shaanxi Science and Technology Press.

Song Guiqing and Quan Zhijie. 1996. Theory and Practice on the Land Resources of the Loess Plateau. Beijing, China Hydropower Press.

Yang Wenzhi et al. 1992. The Regional Reclamation and Appraisal of the Loess Plateau. Beijing, The Science Press.

28 Reclaiming the Saline Soils of Nanpi County: Turning Knowledge into Practice

Xiaojing Liu,* Renzhao Mao,* Pujun Bai† and Chungda Luo†

Abstract

Through studies over five years the authors assessed the health of a catchment in a saline region of Nanpi County in Hebei Province, China using a set of key indicators. The indicators chosen included groundwater table level, electrical conductivity in groundwater, soil colour, pH and consistency. From this assessment they constructed a knowledge transfer network involving the Nanpi Eco-Agricultural Experimental Station, local government, a technical extension station, scientists, technicians and key users.

根据区域农业发展存在的环境问题，利用环境质量评价指标体系，建立了南皮县盐碱地环境质量评价体系。体系的构成包括地下水水位、水质、土壤颜色、土壤 pH 值、土壤紧持度等一系列指标。在指标建立的同时，建立了指标的推广体系。这一体系包括中国科学院南皮生态农业试验站、南皮县政府、南皮县技术推广站、直至农民用户。通过努力，一个持续健康发展的农业体系必将在盐碱地环境下建立。

NANPI County is located in the east of Hebei Province, which is near Beijing and Tianjin on the North China Plain (NCP). The county is 70 km west of the Bohai Sea, at an elevation of 6–13 m. It covers 690 km^2 and has a population of 320,000. Annual mean temperature is 11.3°C and mean precipitation is 500–600 mm. Over 70% of annual rainfall occurs in July, August and September. The shallow groundwater table is about 5–8 m below the

* Shijiazhuang Institute of Agricultural Modernization, Chinese Academy of Sciences, 286 HuaiZhong Road, Shijiazhuang, Hebei 050021, PRC. Email: xliu@ms.sjziam.ac.cn

† People's Government of Nanpi County, Hebei 050021, PRC.

Xiaojing Liu, Renzhao Mao, Pujun Bai and Chungda Luo. 2002. Reclaiming the saline soils of Nanpi County: turning knowledge into practice. In: McVicar, T.R., Li Rui, Walker, J., Fitzpatrick, R.W. and Liu Changming (eds), *Regional Water and Soil Assessment for Managing Sustainable Agriculture in China and Australia*, ACIAR Monograph No. 84, 366–370.

surface; about two-thirds of the shallow groundwater is saline. The deep groundwater table is 60 m below the surface and is declining. Wheat, corn, cotton and Chinese dates are the main cultivated crops of the region. The Overview provides further details about the NCP region; Figure 1 of the Overview shows its location.

The lower reaches of many rivers are located in Nanpi County, so it is a region of salt deposit and accumulation, with a history of problems due to saline soils. Chapter 13 describes the chemical properties of some of the soils in the region. It has been said that in wet seasons the region has only frogs, in dry seasons only locusts and in normal seasons only salt. Until the 1960s, about 30% of the land area was saline. With water shortages, better water engineering and better reclamation of saline soils, the area affected by salinity is rapidly decreasing and now accounts for less than 5% of the land area.

Problems for sustainable agriculture in saline areas of Nanpi County

Although the area of saline soil in Nanpi County has been reduced, the remaining saline area will be more difficult to reclaim because of water deficit and secondary salinity (because the salt in the reclaimed soils has not moved out of the region). In 1995, the Dalangdian reservoir was constructed to provide water from the Yellow River for domestic and industry use in Cangzhou city. This development will affect the groundwater table and may lead to further soil salinisation. Thus, drought, water deficiency and soil salinity are major problems for the development of sustainable agriculture in Nanpi County. Methods to assess catchment health are needed in order to achieve sustainable agriculture.

Long-term studies on the reclamation of saline soil have provided much knowledge, which should be shared not only with scientists but also with end users such as landholders and local officers. To do this, the knowledge must be converted into simple, transferable environmental indicators. This approach will benefit Nanpi County and adjoining regions such as Huanghua and Haixing, where there are about 100,000 ha of saline soil (Liu and Tian 2000).

Selection of Key Indicators and Saline Soil Reclamation

Table 1 shows the key indicators selected for assessing soil salinity in Nanpi County based on the criteria developed by Walker and Reuter (1996) and on the theory and experience of saline soil reclamation (Mao and Liu 2000).

In Nanpi County, soil salinity and soil formation are controlled mainly by groundwater and water quality. The groundwater table itself is affected by

Table 1. Threshold guideline for soil salinity indicators in Nanpi County.

Indicator	Very good	Good	Fair	Poor	Very poor
Groundwater table (m)	4.5–6	3.5–4.5	2.5–3.5	1.5–2.5	< 1.5
Electrical conductivity in groundwater (dS/m)	<0.5	0.5–1	1–1.5	1.5–3	> 3
Soil colour	–	–	Grey brown	White	Grey black brown
Soil pH	7–7.5	7.5–8	8–8.5	8.5–9	> 9
Soil consistency	Loose	Soft	Firm	Very firm	Rigid

dS/m (deciSiemens per metre) = mS/cm (milliSiemens per centimetre)

climate, topography, irrigation and drainage, and is thus an important indicator of trends in water and salt balance. Based on a study at the Nanpi Eco-Agricultural Experimental Station (NPEES) of the Chinese Academy of Sciences, the groundwater table is declining by about 2–3 m each year (NPEES 1996,1997,1998,1999). The reduction in the depth of the groundwater table helps to remove salt from the soil, but if it is too extensive it will result in seawater entering the watertable, increasing salinity.

Groundwater electrical conductivity (EC) is an indicator for irrigation water quality and soil alkalinisation during soil desalination. Soil colour is an important attribute for assessing soil quality, and in Nanpi County, soil colour can easily be used as an indicator of soil salinity. For example, saline soil containing chloride is grey, black or brown; saline soil containing sulfate is white. The pH value of soil can easily be measured with pH paper; the consistency of the soil can be tested by hand.

We used the indicators and methods of saline soil reclamation to construct a diagram for guiding saline soil reclamation (Fig. 1). The model indicates that controlling the groundwater table is the most important aspect of saline soil reclamation. Rainwater, irrigation and the construction of drainage systems are important in the adjustment of the groundwater table. Fertilisers and biological methods can also be used in soil reclamation (e.g. to supply N to raise the bioproductivity and grow salt-tolerant plans such as lucerne for fodder production).

Knowledge Transfer

In order to turn this knowledge into practice, we developed a knowledge transfer network and built several testing plots (Fig. 2). The network included NPEES, local government, a technical extension station, scientists, technicians and key users.

- *NPEES.* The station is a centre for knowledge creation and transfer, where scientists study indicators of salinity, assess trends in soil

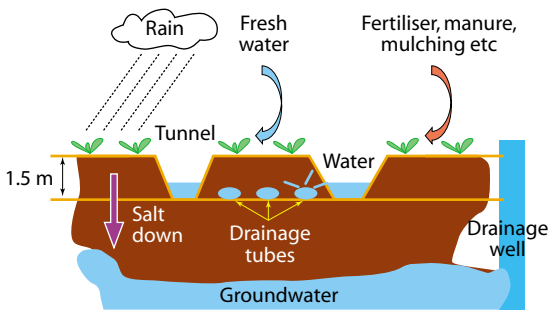

Figure 1. Diagram of saline soil reclamation in Nanpi County.

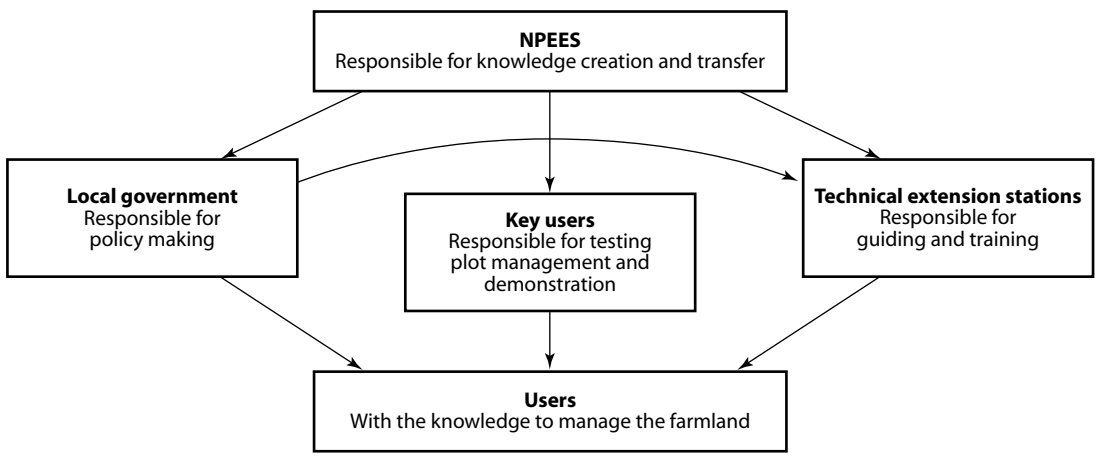

Figure 2. Knowledge transfer network in Nanpi County. NPEES is the Nanpi Eco-Agricultural Experimental Station.

salinity and monitor changes in the groundwater table. Twice a month, technicians from NPEES measure the groundwater table and electrical conductivity, and take water samples. In alternate months, starting in January, soil samples are also taken, to measure salt content and electrical conductivity. Scientists use the results to write proposals for local government and provide technical support for technical extension stations and users.

NPEES has built five trial plots to demonstrate research results directly to end users. For example, in a trial plot close to the Dalangdian reservoir, vegetables are grown in greenhouses in winter. Groundwater is recharged mainly between November and January, when the introduction of fresh water improves the quality of the shallow groundwater and raises its level. Farmers can pump irrigation water and obtain a good income while improving groundwater use and controlling soil salinisation. Other trial plots demonstrate the irrigation of winter wheat and the use of cotton fields to grow pasture in winter.

- *Local government.* At least twice each year the local government in Nanpi County formulates policies based on technical reports and proposals from NPEES for managing regional agriculture. Local government asks extension stations and technical departments to use the research results, and it assists with knowledge transfer by providing some funding for publishing technical reports and holding meetings.

- *Technical extension stations.* Nanpi County has several technical extension stations, including an agricultural technical service and a soil and fertiliser technical station. Technicians at these stations are familiar with the needs and practices of the end users and are well placed to transfer knowledge to them. Therefore, NPEES asks the local government to send five technicians from different technical extension stations to NPEES, to act as a bridge between the institution and end users during the growing seasons. Funds are available from local or higher levels of government for technology transfer.

- *Key users.* Key users are the landholders who use the indicators first and then demonstrate the results to other users. In China, landholders are often poorly educated; in order to be successful in implementing new practices, they need a good understanding of the changes they are being asked to make. Key users play an important role in knowledge transfer. Several well-educated users are taught how to use indicators to assess plot health and make rational decisions about plot management. Once these key users have obtained acceptable results, several site meetings are held on their plots, with other landholders invited to attend. Generally, these meetings are jointly organised by NPEES, local government and technical extension stations. In a meeting, a key user tells other landholders about the results he has obtained and how he has achieved them. Through this process, knowledge is transferred easily and quickly.

- *Users.* In a family unit in China, each landholder has only a small area of land: in Nanpi County this is about 0.8 ha/family. To see an effect of the indicators on catchment health, all the landholders in a village must be involved, which is difficult to achieve. Administrative measures and site meetings can be useful in organising landholders.

Results and Discussion

Over the past five years, we have made progress in using indicators to assess health in a saline environment. The area of saline soil in Nanpi County has continually decreased and there is no secondary salinity around Dalangdian reservoir. The mean income of landholders increased from 1100 yuan/person in 1996 to 2400 yuan/person in 2000 (US$1 = 8.0 yuan). In certain areas where trial plots were located, such as Dalangdian, the net

income per hectare increased from 6000 yuan to 30,000 yuan. The groundwater table has been maintained at around 5 m and water quality is improving. The local government has formulated three policies for catchment health:

- building greenhouses around the Dalangdian reservoir;
- irrigation of winter wheat in spring; and
- using cotton fields in winter to grow pasture.

More than 3500 indicator report cards have been sent out. Eight site meetings have been held and more than 1000 landholders attended.

Although much has been achieved in assessing catchment health using indicators of salinity, much remains to be done because this is a new technique for China. Indicator research on a regional scale with remote sense techniques and a computer-based transfer network is needed.

References

Liu, X. and Tian, K. 2000. Preliminary discussion on the distribution of agricultural resources and sustainable agriculture development patterns in saline region of Huan Bohai Sea. Chinese Journal of Eco-Agriculture Research, 8(4), 67–70.

Mao, R. and Liu, X. 2000. Study on the indicators for assessment of agro-ecoenvironmental quality in saline region of Lower Haihe Plain. Chinese Journal of Eco-Agriculture Research, 8(3), 59–62.

Nanpi Eco-Agricultural Experimental Station Annual Report. 1996, 1997, 1998, 1999.

Walker, J. and Reuter, D.J. 1996. Key indicators to assess farm and catchment health. In: Walker, J. and Reuter, D.J., eds, Indicators of Catchment Health: A Technical Perspective. Melbourne, CSIRO Publishing, 21–33.

29 Transferring Scientific Knowledge to Farmers

Rob W. Fitzpatrick,* Jim W. Cox,* Bruce Munday,† John Bourne‡ and Chunsheng Hu§

Abstract

This study describes the development of a systematic approach to identifying important soil morphological and vegetation field indicators. The objective was to use the indicators to target land management in degraded landscapes in a specific region. The authors linked soil–landscape features to the main soil and water processes operating within the landscape. In Australia, they used this information to develop a set of field indicators (e.g. soil colour) within a user-friendly soil classification key that was linked to land-use options to form the basis of a manual. Information written in this format helped farmers and regional advisers to identify options for remediation of waterlogged and saline areas and to improve planning at property and catchment scales. The authors identified a series of steps to be taken in producing the manual. Steps 1 to 5 describe the soil layers and construct them in toposequences, which are then used to map soil types in key surrounding areas. Steps 6 to 9 involve the local community in developing the manual.

This chapter describes how manuals were produced for two badly degraded areas in southern Australia (the Mount Lofty Ranges in South Australia and an area in western Victoria) and suggests how they can be applied elsewhere. Descriptive soil information and pictures taken along toposequences are used to identify key soil features. The use of coloured cross-sectional diagrams and photographs of soil and vegetation helps local groups to understand complex scientific processes and terminology, and see how best management practices can be used to advantage. A similar approach using indicators such as soil colour and morphology was developed in Luancheng County on the North China Plain. Scientists in this region linked their data to farmers' observations to provide a set of indicators to help farmers manage their land more effectively.

本章介绍了确定重要的野外土地形态和植被诊断指标的系统方法，目的在于应用这些指标对特定区域退化的土地进行治理。作者将土地景观与其上面的主要土壤与水文过程结合为一体，形成一套野外诊断指标（如土壤颜色），置于一个简单易懂的、与土地利用方式相联系的土壤类别比照图内，制作成应用指南。此种形式的信息可帮助农民与有关人员选择渍涝与盐碱地

* CSIRO Land and Water, PMB 2, Glen Osmond, SA 5064, Australia. Email: rob.fitzpatrick@csiro.au

† PO Box 375, Mount Torrens, SA 5244, Australia.

‡ Primary Industries and Resources, South Australia, PO Box 752, Murray Bridge, SA 5253, Australia.

§ Shijiazhuang Institute of Agricultural Modernization, Chinese Academy of Sciences, 286 Huaizhong Road, Shijiazhuang, Hebei 050021, PRC.

Fitzpatrick, R.W., Cox, J.W., Munday, B., Bourne, J. and Chunsheng Hu. 2002. Transferring scientific knowledge to farmers. In: McVicar, T.R., Li Rui, Walker, J., Fitzpatrick, R.W. and Liu Changming (eds), *Regional Water and Soil Assessment for Managing Sustainable Agriculture in China and Australia*, ACIAR Monograph No. 84, 371–384.

的改良措施，改进农场和区域的利用规划。作者总结了制作此应用指南的一系列步骤，包括土层及其在坡面的构成，土壤类型图的生成等，也涉及当地社区在此过程中所起的作用。

文章具体讲解了南澳两个土地严重退化地区应用指南的制作以及如何将该指南用于其它区域。描述性的土壤信息和沿坡面拍摄的照片用来辨明土壤的主要特点。彩色的截面土壤和植被照片及图表可以最大程度地帮助当地居民和团体了解复杂的科学知识和专业术语，了解可以采取的措施。太行脚下的栾城县也采用了一种相似的、以土壤颜色或地貌特征作为指标的方法。该地区的科学家将他们的数据跟农民的观察结合起来，提供了一套指标系统来帮助农民更有效的管理他们的土地。

MUCH has been published on the general application of soil indicators and tests, and on the causes and remediation of land degradation in Australia (e.g. Hunt and Gilkes 1992; Charman and Murphy 1991; Dalgliesh and Foale 1998; Moore 1998; NSW DLWC 2000). Most of these publications provide a good general overview of the major issues but are not designed to address land-use and degradation issues for a specific region, although there are exceptions like SoilPak (McKenzie 1998), which is specific for irrigated cotton in New South Wales. The objective of the studies described in this paper was to develop some tools to communicate scientific knowledge to farmers and regional advisers in order to help them to identify land degradation in specific regions. In Australia, the approach was to produce a manual to help landholders to identify and remedy degradation. The study focused initially on two regions in southern Australia where dryland salinity and waterlogging cause major land degradation — the Mount Lofty Ranges of South Australia and an area in southwestern Victoria. In Luancheng County on the North China Plain, the approach was to show farmers how they could better manage their lands using easily observable soil indicators.

Field indicators linked to landform elements help landholders and regional advisers to identify areas of soil degradation. Indicators used for characterising 'soil quality' can be descriptive or analytical (Fitzpatrick et al. 1999). Standard descriptive soil indicators such as visual indicators (e.g. colour) and consistency are often used by farmers, regional advisers and scientists in the field to identify and report attributes of soil quality (Fitzpatrick 1996). For example, soil colour can provide a simple means to recognise or predict salt-affected, waterlogged wetlands caused by poor drainage (Fitzpatrick et al. 1996), providing an alternative to the difficult and expensive process of documenting watertable depths to estimate water duration in soils (Cox et al. 1996). Visual indicators may be obvious (e.g. white salt accumulations on soil surfaces) or subtle (e.g. subsoil mottling patterns). Analytical indicators include electrical conductivity (salinity) and dispersion (sodicity). Combining descriptive and analytical indicators can provide vital information about soil–water processes to improve land management and remediation of degraded land (Fitzpatrick et al. 1994). The challenge is to communicate this information to landholders and agricultural advisers.

Fitzpatrick et al. (1994, 1998) have previously shown that complex scientific processes and terminology can be effectively communicated to local groups using coloured cross-sectional diagrams and photographs of soil and vegetation. By combining this approach with community advice, the authors developed easy-to-follow manuals that incorporated soil–landscape and vegetation keys. The manuals could be used as a simple decision-making tool for land management based on recommendations in the scientific literature.

Developing a Manual: a Systematic Approach Used in Australia

Topography strongly affects the physical and chemical characteristics of soils, because landform influences the flow of water both through and over the soil surface. For example, excessive runoff on sloping ground reduces plant growth by decreasing the availability of soil water, increasing erosion (leading to reduced soil depth) and causing loss of nutrients. On flat land at the bottom of slopes, severe waterlogging can have a pronounced effect on plant production. A specific type of landscape or catchment is generally characterised by a particular succession of soils down the slope of the topo-sequence, associated with changes in soil moisture (Milne 1934; Sommer and Schlichting 1997).

To understand the lateral linkages and relationships between soil profiles down landscape slopes, we developed a systematic approach for studying the morphological (e.g. colour and textural patterns), chemical and mineralogical characterisics of soils and their underlying weathered bedrock or saprolite (Fritsch and Fitzpatrick 1994; Fitzpatrick et al. 1996). We linked these soil–landscape features to the main soil and water processes operating within the landscape and developed a set of field indicators, described in easy-to-follow practical manuals. The manuals help farmers and regional advisers to identify options for remediation of waterlogged and saline catchments and to improve planning at the property and catchment level.

Box 1 shows the sequence of steps used to develop the manuals. Steps 1 to 5 describe the soil layers and construct them in toposequences, which are then used to map soil types in key surrounding areas. Steps 6 to 9 involve the local community in developing the manual. Figure 1 summarises the steps involved.

The steps were identified and evaluated during work at a study site in the Mount Lofty Ranges of South Australia (Fitzpatrick et al. 1997) and in western Victoria (Cox et al. 1999). Both regions have 500–600 mm annual rainfall; in both, the problem of land degradation is worsening and farmers are concerned about the rapid increase in saline scalds. Figure 2 shows the location and some characteristics of the Mount Lofty Ranges. Figures 3–5 show some of the tools used in developing and applying the manual: Figure 3 shows an example of a key; Figure 4 shows how major soil types are linked to on-farm management options; Figure 5

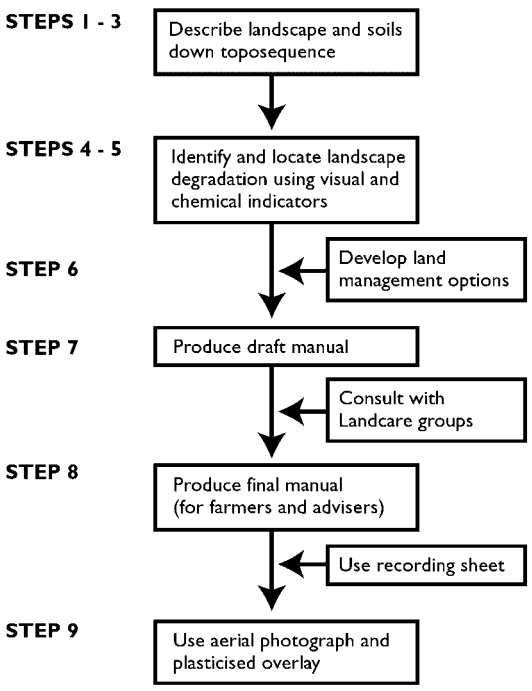

Figure 1. Flow diagram showing the main steps involved in developing a pictorial manual to aid property and catchment planning.

Box 1. Steps in developing an Australian manual

This box summarises the main steps involved in developing a pictorial manual to aid property and catchment planning. These steps are described in detail below and summarised in Figure 1.

Step 1. Select representative focus catchments and landscape sequences

Two tasks are required for this step:

- *Collate soil, geological and climatic information.* Using published broad-scale (e.g. regional) soil, geological and climatic maps such as the one shown in Figure 2a; the first task is to select a representative focus catchment such as the one shown in Figure 2b (Fitzpatrick et al. 1997).
- *Reconnaissance survey soil in the focus catchment.* Establish the most common succession of soil types within the representative catchment, using aerial photographs, road cuttings (if available), random soil augering and soil pits along toposequences. Then select a suite of the most commonly found soils along an idealised toposequence (X–Y shown in Figure 2b).

Step 2. Describe in detail soils along the selected toposequence

This step requires two tasks:

- *Describe soil layers in detail.* This step involves three stages:
  - identify and photograph the complete sequence of soil profiles down the toposequence (X–Y, Figures 2b and c);
  - identify and describe, by depth interval only, all similar soil features (i.e. soil components with similar consistency, colour, textural and structural patterns, and chemical and mineralogical properties) using conventional soil description handbooks (e.g. McDonald et al. 1990; Soil Survey Division Staff 1993); and
  - draw boundaries around the similar soil features within the soil profiles and record them (Boulet et al. 1982; Fritsch et al. 1992, Fritsch and Fitzpatrick 1994).
- *Describe soil horizons and classify soil profiles.* Identify standard soil horizons in order to classify the soils according to soil taxonomy (Soil Survey Division Staff 1998) or the Australian Soil Classification System (Isbell 1996).

Step 3. Group and map similar soil features in the toposequence

This step requires two tasks:

- *Group similar soil features into fewer soil layers using structural analysis.* Structural analysis of the soil involves three stages:
  - use nested or concordant relationships to group soil features, and discordant relationships to separate them;
  - draw boundaries around similar features between the soil profiles to link them down the toposequence, and map them at toposequence scale in cross-sections (Boulet et al. 1982) (Note: soil horizons are not used to demarcate these boundaries because the features used to define soil horizons are too strictly grouped to allow accurate lateral linking between profiles along toposequences); and
  - group similar soil features into a smaller number of soil layers based on concordant and discordant relationships.
- *Display the combined soil layers of the toposequence graphically in cross-section.* Using computer software, display the soil layers graphically in cross sections down toposequences (Rinder et al. 1994). The colour patterns down the X–Y toposequence in Figure 2c display the soil layers.

Step 4. Match soil layers to hydrological processes

- *Field monitoring and laboratory analyses.* Monitor rainfall, watertable fluctuations (in piezometers and dipwells), soil water content, soil redox (Eh electrodes) and chemical changes (e.g. electrical conductivity, cations and anions) (Cox et al. 1999; Fitzpatrick et al. 1996). To select representative sites and determine soil depths where field instrumentation should be placed, monitoring

Box 1. (cont'd)

must focus on identifying changes in soil layers along the entire length of the toposequence.

- *Link soil and hydrological processes to soil layers.* Link soil and hydrological processes (e.g. water flow paths and salinity) to each soil layer displayed in cross-sections. In Figure 2c hatching represents soil salinity and arrows indicate water flow.

Step 5. Develop vegetation and soil–landscape keys

- *Develop easy-to-follow vegetation keys.* Photograph and list groups of plants that identify high, moderate and low levels of salting (e.g. Matters and Bozon 1995). Also record features such as plant density, vigour, health and abundance for each category of plant.
- *Develop simple soil–landscape keys.* Identify up to 10 soil types that best represent the soils in the study region (which could contain 100 or more soil series), based on topography, simple morphological features and chemical tests. Construct a taxonomic key to enable the reader to easily identify these soil types. The key comprises a colour photograph of the typical soil type, an indication of where the soil is usually found (e.g. crest, mid-slope, lower slope, footslope) and drainage characteristics (well drained, poorly drained). Each soil layer (e.g. top, bottom layer 1, bottom layer 2) is clearly demarcated using a thick black dotted line. Alongside each layer, easily observable (e.g. colour, white salt crystals, vegetation) or measurable (e.g. soil consistency and dispersion) features can be recorded. The key is ordered so that the reader moves systematically through the identification of the soils in a stepwise progression, answering 'yes' or 'no' to the question of whether the features shown for each soil are present. Selected portions from a key are shown in Figure 3.

Step 6. Link major soil types to on-farm management options

For each soil type, identify appropriate management options based on input from a wide range of technical experts, including pasture agronomists, salt land agronomists, livestock advisers, specialists in woody perennial revegetation, soils and drainage specialists, and key community members. Summarise management options in a box above a colour photograph of the soil type located along the generalised toposequence. This process is illustrated in Figure 4.

Step 7. Draft the manual

- *Develop a framework.* Set up a framework for the spiral-bound manual, including:
  - soil keys based on colour photographs of soils and plants;
  - an idealised cross-section of a toposequence sketched in colour compiled from the features found in most of the major toposequences of the region (Figs. 2 and 4); and
  - recording sheets for use in the field.

Figure 5 illustrates a recording sheet.

- *Consult with community groups.* Work with potential users of the manual to obtain feedback.

Step 8. Produce the final manual

Revise the manual in the light of feedback from potential users. Recommendations following the field trials described above included expanding the number of photographs of indicator plants, using high-grade graphics for production of all photographs and constructing a water-resistant summary sheet or insert. The quality of the diagnostic photographs was improved so that that they could be more easily recognised by landholders, and the text was revised with input from both the Northern Hills Soil Conservation Board and local officers of Primary Industries and Resources South Australia.

Step 9. Obtain aerial photographs

Obtain aerial photographs for the paddocks (fields) and overlay with clear plastic, on which field observations and management options can be marked. Figure 6 illustrates aerial photographs for the selected catchment.

shows one of the recording sheets used in the field. At present, salinity affects only about 1500 ha in the Mount Lofty Ranges but it has a serious impact on Adelaide's water resource and the expanding wine grape industry. A similar approach was subsequently used in Luancheng County, on the North China Plain. The Overview provides some background information about the study areas in China and Australia; Figures 1 and 2 of the Overview show their location.

The Northern Hills Soil Conservation Board, in South Australia's Mount Lofty Ranges, expressed an interest in developing a manual based on recommendations in the scientific literature and incorporating a soil–landscape and vegetation key

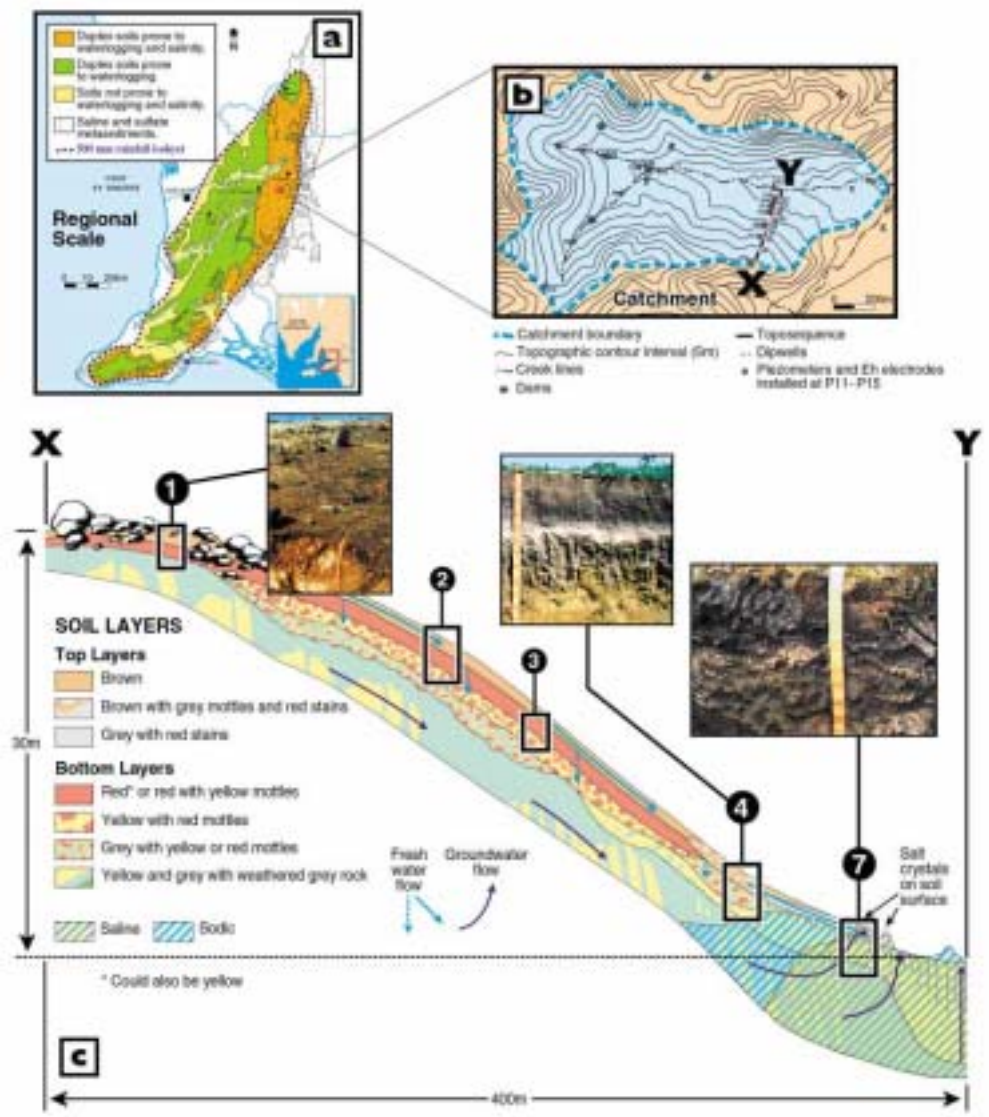

Figure 2. Diagram showing (a) a regional map of the Mount Lofty Ranges with generalised rainfall, geology, and soil pattern, (b) selected focus catchment, (c) toposequence with soil features and water flow paths and three selected soil profiles (modified from Fitzpatrick et al. 1997).

(Fitzpatrick et al. 1994). The board thought that the key described in this work used too much scientific terminology and could be improved if it were made more practical and written in a language and style that would engage landholders. Although the board accepted the need for a simple decision-making tool, it wanted to avoid the approach of 'glossy' booklets that are seldom used because they are written in obscure language, involve impractical tests or advocate unrealistic options. The board also required the manual to be 'road tested' to demonstrate that it would provide accurate interpretation and lead to realistic management options.

Applying the manual to a farm

To use the manual on a particular property, a landholder selects several transects across a paddock (usually down a slope) likely to have waterlogging or salinity problems, and marks them on a plastic overlay on an aerial photograph of the property. Starting at the top of the hillslope (observation point a1, Fig. 5), observations are made on the recording sheet at several points down the slope (observation points a2 – a7, Fig. 5). Where needed, soil samples are collected for measuring dispersion and pH in the field, using methods described in the manuals.

From the information on the recording sheet, the boundaries between soil types and the soil type number (1 – 7) are marked (Fig. 6a), making use of the landholder's personal knowledge of the paddock, contours and vegetation differences to improve the accuracy of the boundaries. Finally,

Figure 3. Examples of two pages from the taxonomic key for identifying soil features that indicate degrees of waterlogged and saline conditions, and management options (modified from Cox et al. 1999). Magnified areas appear in bold text to give an indication of the nature of the key.

management options associated with each of the soil types listed in the key are selected and recorded using a set of symbols (Fig. 6b).

Evaluating the manual in the field

Members of the Woorndoo Landcare Group in western Victoria tested the key developed for their area. Some profiles were found to lie between one standard profile in the key and the next, a situation that has implications for determining appropriate management options. The group had a pre-conception about the sequence of soils they would find in the landscape, based on surface features such as slope, but discovered that their estimate of the location of profiles was often inaccurate.

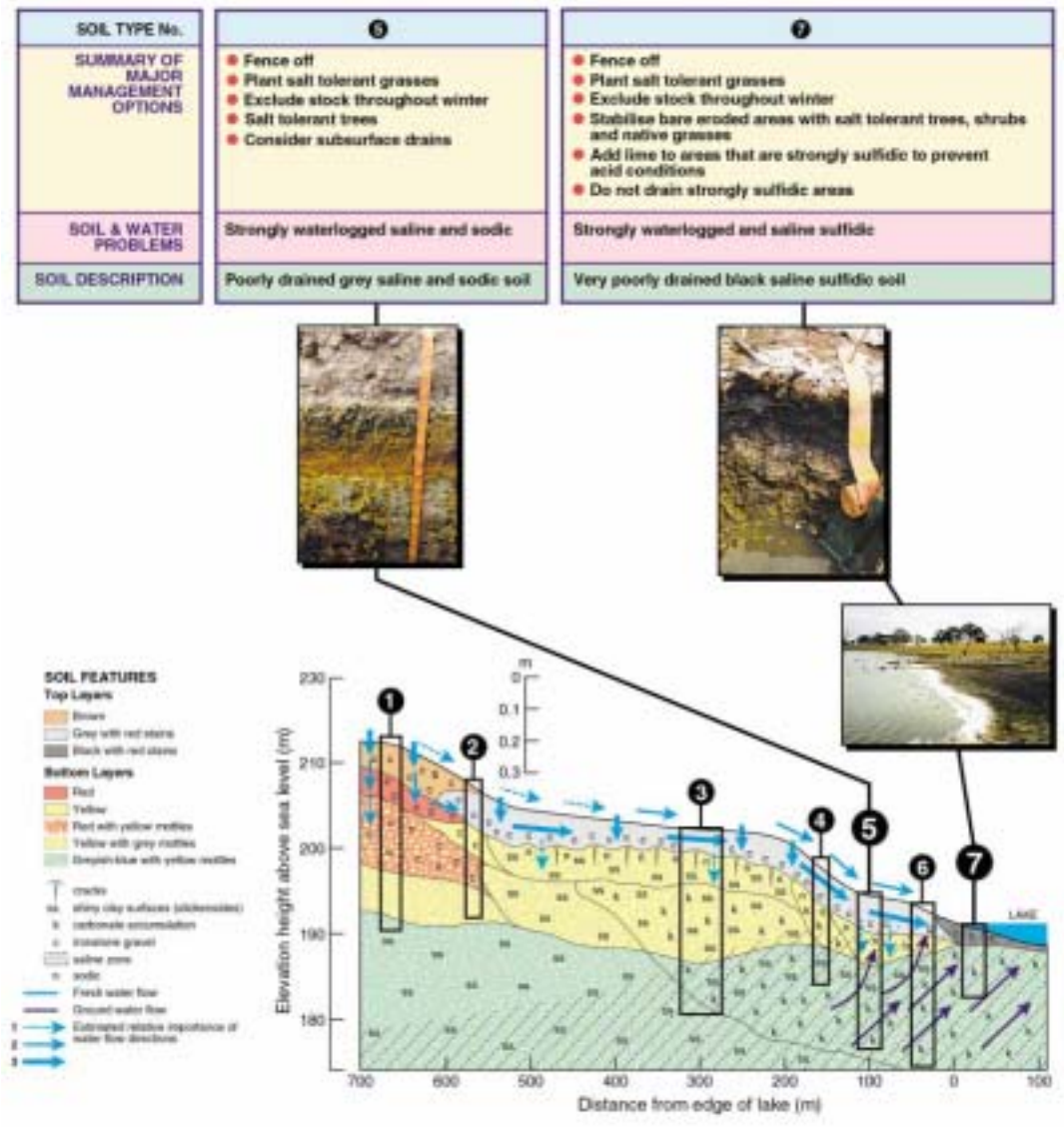

Figure 4. Sequence of soils down a slope to a lake (two of the seven soils are illustrated) with brief summaries of management options associated with each of the soil types (modified from Cox et al. 1999).

Observation point	a1	a2	a3	a4	a5	a6	a7
Plants indicating low level salting (Class 1)	✔	✔					
Plants indicating moderate level salting (Class 2)				✔	✔		

Bottom layer 1							
– red with ironstone gravel	✔						
– yellow		✔			✔		
– yellow with grey mottles, columns, cracks and shiny clay surfaces				✔			
– dark grey with yellow mottles						✔	✔ ✔
Bottom layer 2							
–							

d. Soil tests – bottom layers							
Sodicity (1:5 soil in water suspension)							
Partly cloudy (not sodic)	✔	✔				✔	✔
Cloudy (medium)					✔		
Very cloudy (highly sodic)			✔	✔			
Salinity							
Not saline	✔	✔	✔	✔			
EC of top layer is above 0.7 dS/m					✔	✔	✔
Acidity (pH in water)							
pH less than 5.5 (highly acidic)							
pH between 5.5 and 8.5	✔	✔	✔	✔	✔	✔	✔
pH greater than 8.5 (highly alkaline)							
e. Soil type number (1-8) from soil key.							
Could be transitional between 2 soil type numbers	1	2	3	4	5	6	7

Figure 5. Three sections from the field recording sheet, which consists of three A4 pages (modified from Cox et al. 1999).

Figure 6. (a) Soil type number marked and boundaries demarcated along a single transect on a portion of an aerial photograph, (b) management decisions marked on the aerial photograph showing perennial pastures, fencelines and areas to plant with salt-tolerant shrubs and trees (modified from Cox et al. 1999).

Developing Indicators at an Appropriate Scale: the Chinese Approach

Indicators are measurable attributes of the environment that can be monitored via field observation, field sampling, remote sensing or the compilation of existing data. Each indicator describes a particular function of the environment and can signal desirable or undesirable changes that have occurred or that may occur in the future (Walker and Reuter 1996). Different users have different concerns and objectives, and different indicators may be required for different scales of land use (farmland, county, region). For example, soil colour, soil texture and leaf colour are suitable indicators for farmers but measured data may be more useful for people working on a county scale. Figure 7 shows how soil colour and texture are suitable soil health indicators for farmers. Chinese scientists have developed a set of indicators at farm scale based on measurements of soil properties (Hu Chunsheng and Wang Zhiping 1999; Hu Chunsheng 1999). Box 2 shows how indicators were selected and verified to assess soil health on the NCP.

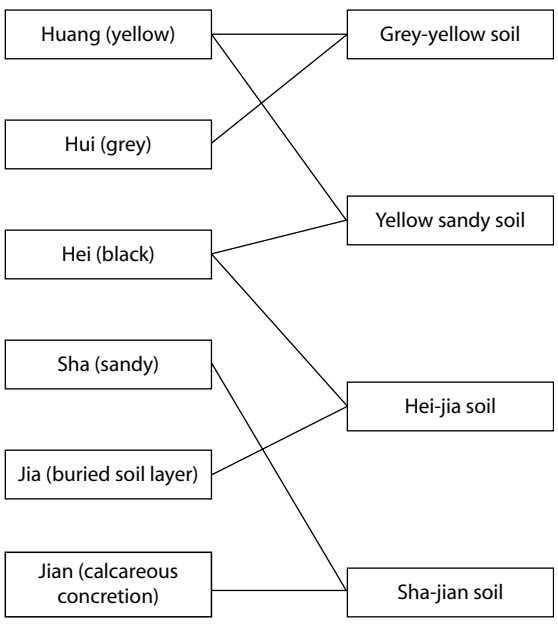

Figure 7. Example of soil classification used by Chinese soil scientists (right) and equivalent categories recognised by farmers (left).

Discussion

The key was a crucial component of the Australian manual. Local advisory officers from Primary Industries and Resources South Australia (PIRSA) and members of the community-based Northern Hills District Soil Conservation Board tested the key developed for the case study area in the Mount Lofty Ranges. A typical subcatchment on a local property was selected at random, and groups of advisory officers each completed separate transects down a toposequence. Surface observation down one transect suggested saline conditions because saline-tolerant plant species dominated much of the area. By exposing the soil profile at a number of points along the transect (Fig. 6a) and comparing it to the standard profiles outlined in the key, it became clear that waterlogging was the major problem, with salinity present only in the lowest part of the subcatchment. Along a second transect there were no plant indicators of saline conditions, and the area was not saline. The group was surprised to find that the profile at the top of the transect was waterlogged rather than well drained, meaning that the pasture species being grown at this location was not ideal.

Trialling the manual in the case study areas confirmed the value of the key. It also emphasised the need to look beyond surface soil and plant factors, and to consider additional soil observations and measurements to better understand and manage local situations. Combining the manual with observations of subsurface soil features can improve management decisions. For example, the pasture species most appropriate for well-drained areas on upper and mid-slopes would be different from those selected for areas that are periodically waterlogged, but it would be difficult to distinguish well-drained areas from waterlogged areas by surface observation alone. Similarly, surface

Box 2. Selecting key indicators to assess soil health on the North China Plain

At the farmland scale, the main soil indicators should include soil colour, texture, bulk density, field capacity, wilting point, total organic material, total nitrogen, available phosphorus and available potassium. Morphological properties such as soil colour, soil texture and the structure of soil profiles are very useful indicators for farmers to assess the health of the land.

In Luancheng County on the piedmont plain of Mount Taihang, farmers can identify six categories of soil that can be used to indicate the degree of soil fertility, the soil tilth index, the degree of porosity and the degree of conservation of soil water and nutrients. These categories are:

- Huang (yellow soil colour), which is associated with good water drainage and good tilth;
- Hei (black soil colour), associated with a high organic matter content;
- Hui (grey soil colour), associated with an even higher soil organic matter content than Hei;
- Sha (sand), associated with good drainage capacity but a low nutrient content and a poor ability to conserve soil water and nutrients;
- Jia, which is soil with a 'buried' soil layer, indicating clay, with poor-quality tilth restricting the growth of seedlings but suitable for older shoots; and
- Jian, which is soil with calcareous concretion or a calcium horizon, which restricts root growth.

These categories are the easiest and most practical way for farmers to assess soil health.

Soil in Luancheng County is typical cinnamon soil with a thin humus layer and middle or thick solum. The buried layer, clay course, calcareous concretion layer, sand soil layer and ploughed layer are the standard diagnostic horizons for soil species classification. Soils can be divided into 17 soil types. The boxes on the right side of Figure 7 show four examples of the soil classification used by soil scientists; those on the left indicate the equivalent categories recognised by farmers.

Case study: grey–yellow soil

From the name of the soil, farmers can judge that this kind of soil has good soil structure, tillage properties and moisture capacity, but that there is a plough pan with high bulk density where the soil becomes lighter in colour (Tables 1 and 2). Measurement of root density, consistency and texture confirms farmer perceptions based on soil colour.

Table 1. Morphology and root density of grey–yellow soil in Luancheng County.

Layer	Thickness (cm)	Consistency	Colour	Texture	Root density (cm/cm^3)	
					Corn	Wheat
A_1	0–17	Soft	Grey brown	Sandy loam	3.49	1.12
A_1B	17–30	Very hard	Light brown	Sandy loam	1.63	0.48
B_1	30–65	Firm	Dark brown	Loam	0.51	0.26
B_2	65–90	Firm	Dark brown	Loam	0.34	0.25
BK	90–145	Very hard	Light yellow	Light clay	0.16	0.12
B_3	145–170	Very hard	Gray yellow	Light clay	0.18	–
BC	170–190	Very hard	Light yellow	Medium clay	–	–

Box 2 (cont'd)

Table 2. Physical indicators of grey–yellow soil in Luancheng County.

Layer	Thickness (cm)	Field capacity (%)	Wilting point (%)	Plant available water (%)	Bulk density (g/cm^3)	Total porosity (%)	Air-filled porosity (%)
A_1	0–17	36.35	9.63	26.73	1.41	46.42	10.07
A_1B	17–30	34.86	11.37	23.49	1.51	42.62	7.76
B_1	30–65	33.25	13.92	19.33	1.47	44.14	10.89
B_2	65–90	34.28	13.91	20.37	1.51	42.62	8.34
BK	90–145	34.36	12.95	21.41	1.54	41.48	7.12
B_3	145–170	38.98	13.87	25.11	1.64	37.68	1.42
BC	170–190	38.05	16.44	21.61	1.59	39.58	1.53

(reverse interceptor) drains are sometimes installed to remove water to improve pasture establishment (e.g. Cox and McFarlane 1995); in sodic subsoils they are likely to fail due to dispersion of soil particles, but this condition is difficult to determine simply from surface soil observations.

The manual helps users to make good decisions, improves their understanding of the processes of dryland salinity and waterlogging, and offers solutions to improve the quality of their properties. Where the manual has been applied in the Mount Lofty Ranges area, degraded saline wet areas have been rehabilitated and erosion has been halted through measures such as realigning fencelines and revegetation.

The manual developed for the Mount Lofty Ranges has been used as a standard text in the small farms land management course that is run four times a year by the local soil board. Bruce Munday, a farmer near Mount Torrens, during an interview with Pyper and Davidson (2001), stated:

> The publication of the CRC–CSIRO manual on waterlogged, saline and acid sulfate soils in the Mount Lofty Ranges has also made land management that much easier for farmers … The manual is very much a do-it-yourself kit that has enabled us to manage these things properly, rather than by trial and error ... Trial and error has always been a great standby for farmers, but it sometimes has dire consequences.

Conclusions

We have summarised a set of procedures for identifying the best set of soil–landscape and vegetation field indicators for a region. Farmers, catchment groups and natural resource management agencies can use the approach to achieve the following outcomes.

- Knowledge of soil and hydrological processes and production systems can be brought together and used as the basis for recommendations for appropriate management options.

- Viable land-use options and management systems (including mosaic farming) that are more resource efficient than current 'trial and error' practices can be adopted.

- Significant impetus for land-use change based on sound scientific knowledge and community involvement and an understanding of community needs.

- Effective extension mechanisms that can be used to transcend institutional boundaries (e.g. the Commonwealth Scientific and Industrial Research Organisation (CSIRO); PIRSA; catchment boards; Landcare groups). The mechanisms provide a model for other multiagency interdisciplinary research.

The following procedures are used to identify the best set of soil–landscape and vegetation field indicators:

- identifying easily recognised landform elements and soil morphological features, such as soil colour and consistency, down an idealised slope sequence (toposequence);

- using an idealised toposequence to encompass a compilation of the main features present within most of the major toposequences of a specific region;

- linking the soil and vegetation indicators to a pictorial soil–landscape and vegetation key and thereby matching to locally practised on-farm management options;

- using, where needed, simple tests for soil electrical conductivity (salinity), dispersion (sodicity) and pH (acidity); and

- packaging information in an easy-to-follow pictorial manual with input from Landcare groups.

The approach has generic application.

Acknowledgments

The research was funded in part ACIAR, Land and Water Australia, the National Landcare Program and the Natural Heritage Trust. We are grateful to members of the Tungkillo Landcare Group for their assistance. Scientists who contributed substantially to the study include Dr E. Fritsch (ORSTOM), Dr P. Self, Mr G. Rinder, Dr D. Reuter, Ms Mary-Anne Fiebig (CSIRO) and Dr H. Cadman (Biotext).

References

Boulet, R., Humbel, F.X. and Lucas, Y. 1982. Analyse structural et cartographie en pédologie: II Une méthode d'analyse prenant en compte l'organisation tridimensionnelle des couvertures pédologiques. Cahiers ORSTOM, série Pédologie 19, 323–339.

Charman, P.E.V. and Murphy, B.W. (eds). 1991. Soils: their properties and management—a soil conservation handbook for New South Wales. Sydney University Press and Oxford University Press.

Cox, J.W., Fritsch, E. and Fitzpatrick, R.W. 1996. Interpretation of soil features produced by ancient and modern processes in degraded landscapes: VII. Water duration. Australian Journal of Soil Research, 34, 803–824.

Cox, J.W. and McFarlane, D.J. 1995. The causes of waterlogging in shallow soils and their drainage in southwestern Australia. Journal of Hydrology, 167, 175–94.

Cox, J.W., Fitzpatrick, R.W., Mintern, L., Bourne, J. and Whipp, G. 1999. Managing waterlogged and saline catchments in south-west Victoria: a soil–landscape and vegetation key with on-farm management options. Woorndoo Land Protection Group Area Case Study. Melbourne, CSIRO Publishing, Catchment Management Series No. 2.

Dalgliesh, N. and Foale, M. 1998. Soil matters: monitoring soil water and nutrients in dryland farming. Toowoomba, Queensland, Agricultural Production Systems Research Unit.

Fitzpatrick, R.W. 1996. Morphological indicators of soil health. In: Indicators of Catchment Health: a technical perspective, eds J. Walker and D.J. Reuter. Melbourne, CSIRO Publishing, 75–88.

Fitzpatrick, R.W., Cox, J.W. and Bourne, J. 1997. Managing waterlogged and saline catchments in the Mt. Lofty Ranges, South Australia: a soil–landscape and vegetation key with on-farm management options. Melbourne, CSIRO Publishing, Catchment Management Series No. 1.

Fitzpatrick, R.W., Cox, J.W. and Bourne, J. 1998. Soil indicators of catchment health: tools for property planning. In: Proceedings of the International Soil Science Society Congress, Montpellier, France. Montpellier, International Soil Science Society, Symposium No. 37, CD-ROM, 8.

Fitzpatrick, R.W., Cox, J.W., Fritsch, E. and Hollingsworth, I.D. 1994. A soil-diagnostic key for managing waterlogging and dryland salinity in catchments in the Mt Lofty Ranges, South Australia. Soil Use and Management, 10, 145–152.

Fitzpatrick, R.W., Fritsch, E. and Self, P.G. 1996. Interpretation of soil features produced by ancient and modern processes in degraded landscapes. V. Development of saline sulfidic features in non-tidal seepage areas. Geoderma, 69, 1–29.

Fitzpatrick, R.W., McKenzie, N.J. and Maschmedt, D. 1999. Soil morphological indicators and their importance to soil fertility. In: Soil Analysis: an interpretation manual, eds K. Peverell, L.A. Sparrow and D.J. Reuter. Melbourne, CSIRO Publishing, 55–69

Fritsch, E. and Fitzpatrick, R.W. 1994. Interpretation of soil features produced by ancient and modern processes in degraded landscapes. I. A new method for constructing conceptual soil–water–landscape models. Australian Journal of Soil Research, 32, 889–907 (colour figures 880–885).

Fritsch, E., Peterschmitt, E. and Herbillon, A.J. 1992. A structural approach to the regolith: identification of structures, analysis of structural relationships and interpretations. Sciences Géologiques, 45(2), 77–97.

Hunt, N. and Gilkes, R. 1992. Farm monitoring handbook. Perth, University of Western Australia.

Hu Chunsheng. 1999. Physical and chemical indicators of soil health diagnostics and its application. Eco-Agriculture Research (in Chinese), l.7(3).

Hu Chunsheng and Wang Zhiping. 1999. The soil nutrient balance and fertilizer use efficiency in farmland ecosystems in Taihang Mountain Piedmont. Progress in Geography, 17 (supp.), 131–138.

Isbell, R.F. 1996. The Australian soil classification system. Melbourne, CSIRO Publishing.

Matters, J. and Bozon, J. 1995. Spotting Soil Salting: a Victorian field guide to salt indicator plants. Victoria, Department of Natural Resources and Environment.

McDonald, R.C., Isbell, R.F., Speight, J.G., Walker, J. and Hopkins, M.S. 1990. Australian Soil and Land Survey Field Handbook, 2nd edn. Melbourne, Inkata Press, 87–183.

McKenzie, D. 1998. SOILpak for cotton growers, 3rd edn. Orange, New South Wales Agriculture.

Milne, G. 1934. Some suggested units of classification and mapping particularly for east African soils. Soil Research, 4(2), 183–198.

Moore, G (ed). 1998. Soil Guide: A handbook for understanding and managing soils. Perth, Agriculture Western Australia, Bulletin No. 4343.

NSW DLWC (New South Wales Department of Land and Water Conservation). 2000. Soil and Landscape Issues in Environmental Impact Assessment, 2nd edn. Sydney, NSW Department of Land and Water Conservation, Technical Report No. 34.

Pyper, W., Davidson, S. 2001. Bubble bubble—Uncovering the true nature and severity of acid sulfate soil in inland Australia. Ecos, 106, 28–31.

Rinder, G., Fritsch, E., Fitzpatrick, R.W. 1994. Computing procedures for mapping soil features at sub-catchment scale. Australian Journal of Soil Research, 32, 909–913 (colour figures 886–887).

Soil Survey Division Staff. 1993. Soil Survey Manual. United States Department of Agriculture Handbook No. 18. Washington DC, US Government Printing Office.

Soil Survey Division Staff. 1998. Keys to Soil Taxonomy, 8th edn. Washington DC, US Government Printing Office.

Sommer, M. and Schlichting, E. 1997. Archetypes of catenas in respect to matter—a concept for structuring and grouping catenas. Geoderma, 76, 1–33.

Walker, J. and D.J. Reuter (eds). 1996. Indicators of catchment health—A technical perspective. Melbourne, CSIRO Publishing.